UNIVERSITÉ PARIS-SUD 11

FACULTÉ DE PHARMACIE DE CHÂTENAY-MALABRY

ECOLE DOCTORALE :

INNOVATION THÉRAPEUTIQUE : DU FONDAMENTAL A L'APPLIQUÉ

PÔLE : PHARMACOTECHNIE ET PHYSICO-CHIMIE

ANNÉE 2010   SÉRIE DOCTORAT N° 1057

THÈSE

Présentée

À L'UNITÉ DE FORMATION ET DE RECHERCHE

FACULTE DE PHARMACIE DE CHATENAY-MALABRY

UNIVERSITÉ PARIS-SUD 11

Pour l'obtention du grade de

DOCTEUR DE L'UNIVERSITÉ PARIS-SUD 11

par

Mlle Selma Čorović

Titre de la thèse :

Modélisation et visualisation de l'électroperméabilisation dans des tissus biologiques exposés à des impulsions électriques de haut voltage

soutenue le : 19 Avril 2010

JURY: M. Claude MALVY (Professeur, Université Paris-Sud XI, Villejuif, France), Président

M. Justin TEISSIÉ (Directeur de recherche DR1 CNRS, IPBS Toulouse, France), Rapporteur

M. Tadej KOTNIK (Assist. Professeur, Université de Ljubljana, Slovénie), Rapporteur

M. Janez BEŠTER (Professeur, Université de Ljubljana, Slovénie), Examinateur

M. Clair POIGNARD (Chargé de recherche CNRS, INRIA Bordeaux, France), Examinateur

M. Lluis M. MIR (Directeur de recherche DR1 CNRS, Villejuif, France), Codirecteur de thèse

M. Damijan MIKLAVČIČ (Professeur, Université de Ljubljana, Slovénie), Codirecteur de thèse

Preface

The present PhD thesis is the result of realistic numerical modeling, *in vivo* research and web based application development performed at the Laboratory of Biocybernetics, University of Ljubljana and at the Institut Gustave-Roussy, Villejuif, CNRS (Centre National de la Recherche Scientifique), University of Paris XI, Paris, France. The results of these studies were published in the following papers:

Paper I: Corovic S, Pavlin M, Miklavcic D. Analytical and numerical quantification and comparison of the local electric field in the tissue for different electrode configurations. *Biomed. Eng. Online* 6(37): 1-14, 2007.

Paper II: Corovic S, Zupanic A, Miklavcic D. Numerical modeling and optimization of electric field distribution in subcutaneous tumor treated with electrochemotherapy using needle electrodes. *IEEE Trans. Plasma Sci.* 36: 1665-1672, 2008.

Paper III: Corovic S, Al Sakere B, Haddad V, Miklavcic D, Mir LM. Importance of contact surface between electrodes and treated tissue in electrochemotherapy. *Technol. Cancer Res. Treat.* 7: 393-399, 2008.

Paper IV: Corovic S, Bester J, Miklavcic D. An e-learning application on electrochemotherapy. *Biomed. Eng. Online* 8(26): 1-15, 2009.

Paper V: Corovic S, Mir LM, Miklavcic D. *In vivo* muscle electroporation threshold determination - realistic numerical models and *in vivo* experiments. Submitted to the *Comptes rendus de l'Académie des Sciences, Physique*

Paper VI: Corovic S, Zupanic A, Kranjc S, Al Sakere B, Leroy-Willig A, Mir LM, Miklavcic D. Influence of skeletal muscle anisotropy on electroporation: *in vivo* study and numerical modeling. *Med. Biol. Eng. Comput.* 48:637–648, 2010.

Paper VII: Zupanic A, **Corovic S**, Miklavcic D. Optimization of electrode position and electric pulse amplitude in electrochemotherapy. *Radiol. Oncol.* 42: 93-101, 2008.

Paper VIII: Rebersek M, **Corovic S**, Sersa G, Miklavcic D. Electrode commutation sequence for honeycomb arrangement of electrodes in electrochemotherapy and corresponding electric field distribution. *Bioelectrochemistry* 74: 26-31, 2008.

Paper IX: Pavselj N, Cukjati D, **Corovic S**, Jarm T, Sersa G, Miklavcic D. Spremljanje, modeliranje in analiza dogajanja med elektroporacijo celičnih membran in vivo ter njena uporaba. *Med. Razgl.* 47: 177-191, 2008.

Paper X: Mali B, Jarm T, **Corovic S**, Paulin-Kosir MS, Cemazar M, Sersa G, Miklavcic D. The effect of electroporation pulses on functioning of the heart. *Med. Biol. Eng. Comput.* 46: 745-757, 2008.

Paper XI: Rebersek M, Faurie C, Kanduser M, **Corovic S**, Teissie J, Rols MP, Miklavcic D. Electroporator with automatic change of electric field direction improves gene electrotransfer *in vitro. Biomed. Eng. Online* 6(25): 1-11, 2007.

Paper XII: Miklavcic D, **Corovic S**, Pucihar G, Pavselj N. Importance of tumour coverage by sufficiently high local electric field for effective electrochemotherapy. *Eur. J. Cancer Suppl.* 4: 45-51, 2006.

Paper XIII: Corovic S, Pavlovic I, Sersa G, Miklavcic, D. Elektroporacija ćelije i njena primena u medicini. *Sanamed*, 2007, 2:99-107, 2007.

Paper XIV: Pavlovic I, Kramar P, **Corovic S**, Cukjati D, Miklavcic D. A web-application that extends functionality of medical device for tumor treatment by means of electrochemotherapy. *Radiol Oncol*, 38:49-54, 2004.

Paper XV: Puc M, **Corovic S**, Flisar K, Petkovsek M, Nastran J, Miklavcic D. Techniques of signal generation required for electropermeabilization. Survey of electropermeabilization devices. *Bioelectrochemistry* 64: 113-124, 2004.

Acknowledgement

I'm deeply indebted to my teacher and my supervisor Prof. Dr. Damijan Miklavcic for his inspiring guidance throughout my study and my work. I'm especially grateful to him for supporting and understanding me in the most difficult moments.

It is a great pleasure for me to express my gratitude also to my French supervisor, Dr. Lluis M. Mir, for his guidance, support and advices through my research work and results publication.

Thanks to all colleagues in the Laboratoriy of Biocybernetics and the Institute Gustave-Roussy for fruitful and pleasant collaboration. I'm deeply indebted to all those who become my valuable friends.

Thanks to my parents, my brother, my sister, Katarina, Benjamin and all other friends.

Selma Corovic

Ljubljana, February 11th, 2010

TABLE OF CONTENTS

Abstract

Electroporation is a phenomenon of cell membrane permeability increase due to local delivery of short and sufficiently intense voltage pulses to the target cells and tissues. *In vivo* electroporation is used as an effective and safe tool for administration tool for administration of a variety of extracelular agents such as chemotherapeutic drugs, DNA or other molecules, which in normal conditions do not cross the cell membrane, into many different target tissue cells. *In vivo* electroporation, is widely used for various applications in biology, medicine and biotechnology. The main focus of the present doctoral theses is the analysis of *in vivo* electroporation and corresponding local electric field distribution used in electrochemotherapy and electroporation based gene therapy and vaccination.

The appropriate local electric field distribution in the treated tissue is one of the most important conditions that need to be met for an effective electroporation based therapy or treatment to be successful as well as in vivo experiments in both humans and animals to be adequately designed. Currently, local electric field distribution can not be visualized during the electroporation based therapy or treatment. Therefore it is of outmost importance to a priori select the appropriate parameters and to 'design' the appropriate local electric field distribution for each particular therapy, treatment or experiment. Visualization of the spatial distribution of local electric field distribution can be effectively carried out with numerical calculations using realistic numerical models (i.e. numerical or analytical models of biological tissues validated on corresponding *in vivo* experiment). Development of realistic mathematical models thus plays an important role in the prediction of successful outcome of an electroporation based therapy, treatment or experiment.

In order to develop a good realistic model the knowledge and experience exchange from different scientific fields, involved in electroporation based therapies and treatments, is needed, which can be successfully assisted by using web-based e-learning systems.

The aims of this doctoral thesis cover three important issues in the development of electroporation based technologies and treatments:

1. development of realistic numerical models of different tissues (i.e. muscle, tumor and skin) and calculations and visualization of local electric field distribution in the models;

2. validation of the realistic numerical models by in vivo experiments; and

3. development of a web-based interactive e-learning application on electroporation based technologies and treatments such as electrochemotherapy.

The general conclusion of our study is that calculation and visualization of local electric field distribution in realistic numerical models allows for the selection of parameters, such as electrode configuration, electrode positioning and amplitude of electroporation pulses, so that the optimal permeabilisation of a treated tissue is achieved (i.e. electroporation of all cells within the target tissue by exposing them to the local electric field between reversible and irreversible threshold values $(E_{rev} < E < E_{irrev})$, while minimizing the total electric current flowing through the tissue and the electrically-induced damage to the healthy tissue) .

Our results can significantly contribute to more efficient tissue electroporation used in electroporation based therapies and treatments (e.g. clinical electrochemotherapy of tumors and gene electrotransfer) by the selection of electric parameters based on calculation and visualization of local electric field.

We developed an e-learning application on electroporation based therapies and treatments, hhich provides an easy and rapid approach for information, knowledge and experience exchange among the experts from different scientific fields, which can facilitate development and optimization of electroporation based therapies and treatments.

Résume de thèse en français

Modélisation et visualisation de l'électroperméabilisation dans des tissus biologiques exposés à des impulsions de haut voltage

Sous l'action d'impulsions de haut voltage, le champ électrique local se distribue dans les tissus biologiques, ce qui peut mener à une grande l'augmentation de la perméabilité des membranes cellulaires et à une grande augmentation de la conductivité électrique de la membrane des cellules. L'augmentation réversible de la perméabilité membranaire nécessite que soit dépassée une valeur critique du champ électrique local et elle permet aux substances, pour lesquelles la membrane cellulaire n'est pas perméable (telles que les ions, des petites molécules et même des macromolécules comme l'ADN), d'entrer à l'intérieur de la cellule. Dans la littérature l'augmentation de la perméabilité de la cellule à l'aide d'un champ électrique est décrite par un changement structural de la membrane cellulaire voire par l'apparition de pores dans la membrane. Ce phénomène est nommé électroporation ou électroperméabilisation [Mir *et al.*, 1988, Neumann et al., 1989, Maček-Lebar et al., 2001]. Les impulsions de haut voltage, qui induisent le champ électrique local nécessaire pour électroporer les cellules des tissus biologiques ou les cellules en suspension sont produites par des générateurs (électroporateurs) et délivrées aux cellules ou aux tissus à traiter par des électrodes d'une géométrie appropriée [Puc *et al.*, 2004, Marty *at al.*, 2006, Mir *et al.*, 2006]. Afin d'électroporer les cellules des tissus ou des cellules en suspension l'amplitude des impulsions électriques délivrées doit dépasser une certaine valeur critique. Si l'amplitude, la durée, et le nombre d'impulsions ne sont pas trop élevés la membrane récupère son intégrité initiale après la fin de l'exposition aux impulsions. Ainsi les substances internalisées restent encapsulées a l'intérieur de la cellule pour pouvoir exercer leur activité. Dans ce cas on parle d'une electroporation réversible induite par un champ électrique local dépassant une valeur

Résume de thèse en français

---

critique réversible ($E \geq E_{rev}$) mais qui ne dépasse pas une valeur critique irréversible ($E < E_{irrev}$). Pour le champ électrique local dépassant la valeur seuil irréversible ($E \geq E_{irrev}$) les cellules sont détruites de façon permanente. L'électroperméabilisation ne se produit pas à la même valeur de l'amplitude d'impulsion et à la même valeur du champ électrique local pour toute la population cellulaire et tissulaire. Le champ électrique local nécessaire pour l'électroporation des cellules ou des tissus dépend de leur propriétés électriques et géométriques, aussi bien que des conditions du traitement (e.g. *in vivo* ou *in vitro*).

Au niveau de la membrane cellulaire, l'électroperméabilisation est basée sur la modification du voltage transmembranaire induite par le champ électrique externe appliqué. Dans des conditions physiologiques, un potentiel de repos entre -90 mV et -40 mV est toujours présent à la surface de la membrane des cellules (Cole, 1972). Ce voltage est produit par un petit déficit en ions positifs dans le cytoplasme par rapport aux ions négatifs, qui est une conséquence du transport spécifique d'ions à travers la membrane. Alors que le voltage transmembranaire de repos est présent sur la membrane cellulaire à tout moment, l'exposition de la cellule à un champ électrique induit une composante additionnelle : un voltage transmembranaire induit, qui se superpose au voltage de repos. Pour faire en sorte que la membrane cellulaire soit électroperméabilisée le voltage transmembranaire doit être supérieur à une valeur seuil critique. Le voltage transmembranaire critique, au dessus duquel l'électroperméabilisation se produit se situe entre 0.2 V et 1 V [Neumman *et al.*, 1982, Mir *et al.*, 1988, Mir *et al.*, 1991, Weaver et al., 1996]. Le phénomène de l'électroporation a été étudié plus intensivement au niveau des cellules en suspension qu'au niveau des tissus *in vivo*, cependant cette connaissance peut être, au moins partiellement, utilisée aussi pour l'analyse du tissu biologique qui n'est qu'un ensemble de plusieurs cellules [Pavlin *et al.*, 2002]. Le but du travail de recherche dans ma thèse est d'etudier l'électroperméabilisation des tissus *in vivo*

Résume de thèse en français

par la visualisation du champ électrique local à l'aide d'expériences *in vivo*, de calculs mathématiques numériques résultant dans des modèles réalistes, ainsi qu'à l'aide d'une application internet que j'ai développé pour l'enseignement à distance sur les connaissances récupérées par les expériences *in vivo* et la modélisation mathématique.

L'électroperméabilisation est appliquée dans divers domaines de la médecine, biologie, biotechnologie etc. Les applications basées sur cette méthode dépendent de la valeur du champ électrique local dans le tissu ou les cellules cibles. La Figure 1 illustre les différents régimes de l'électroperméabilisation en fonction du champ électrique local, et ses applications.
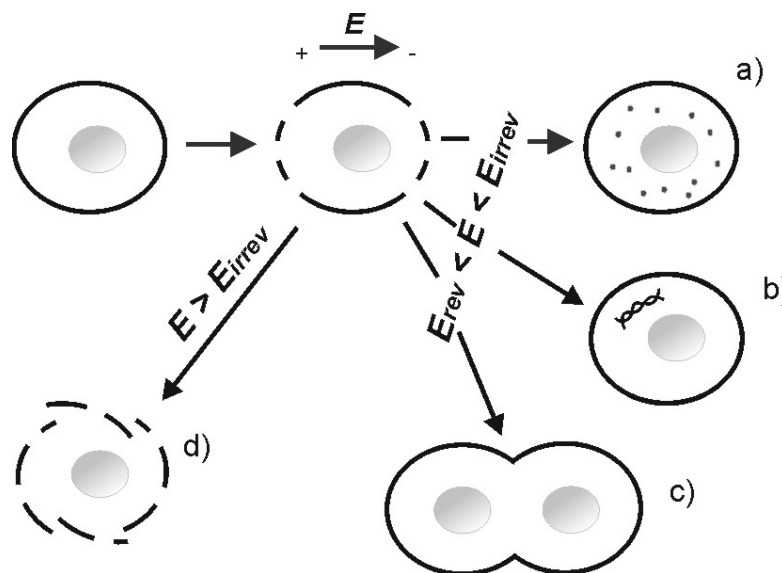
Figure 1: Les applications de l'electroporation: l'electroporation réversible $E_{rev} < E < E_{irrev}$ a) pour l'administration des petites molécules (électrochimiothérapie), b) l'administration des macromolécules (électrotransfer de gènes – thérapie genique et vaccination de l'ADN), c) l'electrofusion des cellules et d) l'électroporation irréversible $E > E_{irrev}$: pour l'ablation des tissus, stérilisation d'aliments, traitement de l'eau [Kanduser and Miklavcic, 2008]

L'électropermeabilisation permet l'internalisation de différents types de molécules dans les cellules. Parmi ces molécules il y a les médicaments cytotoxiques utilisés dans la chimiothérapie, ainsi que les molécules d'ADN. A cause de cela, l'électroperméabilisation est utilisée dans beaucoup d'applications expérimentales et cliniques dans plusieurs domaines de

Résume de thèse en français

la médecine, biologie, biotechnologie etc. Dans la clinique et la recherche l'électroperméabilisation est utilisée dans l'électrochimiothérapie antitumorale, l'électrotransfert de gènes et l'administration de médicaments à travers la peau. L'électroperméabilisation peut être également utilisée pour l'internalisation de différentes molécules dans les cellules des plantes. L'électroperméabilisation réversible peut-être aussi utilisée pour l'electrofusion de cellules. Les possibilités des applications de l'électroperméabilisation irréversible sont également explorées dans plusieurs domaines tels que l'ablation des tissus, la stérilisation d'aliments et le traitement de l'eau [Kanduser and Miklavcic, 2008]. Dans cette thèse j'ai étudié le rôle des paramètres du champ électrique local dans l'efficacité de l'électroperméabilisation au niveau des tissus, un paramètre très important dans l'électrochimiotherapie et dans l'électrotransfert de gènes.

L'électrochimiothérapie est un traitement anticancéreux associant l'administration d'un médicament cytotoxique, tel que la bleomycine ou le cisplatine, et l'application locale, au niveau du site tumoral à traiter, d'impulsions électriques potentialisant les effets antimoraux de ce médicament [Mir et *al.*, 1999]. L'efficacité de l'électrochimiothérapie est due à l'électroperméabilisation des cellules constituant les tissus ciblés. Ce mécanisme électrique est basé sur l'augmentation transitoire de la perméabilité de la membrane plasmique de ces cellules lorsqu'elles sont soumises à un champ électrique local (E) d'intensité supérieure à une valeur seuil réversible ($E \geq E_{rev}$). Une cellule électroperméabilisée est ainsi plus sensible à un médicament cytotoxique. Une fois à l'intérieur de la cellule, les médicaments utilisés brisent l'ADN des chromosomes, causant une mort cellulaire localisée, ce qui constitue la base de l'électrochimiothérapie. À ce jour, l'électrochimiothérapie est limitée au traitement des nodules tumoraux de surface (des tumeurs cutanées et sous-cutanées), étant aisément accessibles par les électrodes [Marty et al., 2006]. Le phénomène électrique régissant

Résume de thèse en français

l'électroperméabilisation n'est pas spécifique à un type de tumeur, mais universellement applicable sur tous les types de tissus. Pour qu'une électrochimothérapie soit efficace, il faut utiliser les électrodes adéquates et appliquer le voltage optimal de manière que le champ électrique local (E) dans la totalité de tumeur soit supérieur à une valeur seuil réversible ($E \geq E_{rev}$) en épargnant le tissu sain environnant la tumeur [Mir et *al.*, 2006]. Grâce à des simulations numériques réalisées par la méthode des éléments finis, il est possible de calculer la distribution du champ électrique dans le tissu tumoral, ce qui permet d'optimiser le choix du type d'électrodes à utiliser et l'amplitude du voltage à appliquer de telle sorte que l'électrochimiothérapie soit la plus efficace possible.

L'électrotransfection génique est une méthode pour l'administration des gènes dans les cellules ciblées qui utilise l'électroperméabilisation [Neumann *et al.*, 1982, Mir *et al.*, 1999]. Pour qu'une thérapie genique, aussi bien qu'une vaccination génique à l'aide d'électroperméabilisation, soient efficaces il est très important que la viabilite des cellules du tissu ciblé reste intacte, ce qui nécessite une électroperméabilisation réversible (i.e. un champ électrique local E tel que ($E_{rev} < E < E_{irrev}$). Un tel régime d'électroperméabilisation nécessite un choix approprie de la géométrie des électrodes et des paramètres des impulsions de haut voltage. La méthode fait actuellement l'objet de recherches précliniques et cliniques, mais grâce à ses nombreux avantages nous nous attendons à ce qu'elle commence à s'appliquer à la clinique [Daud *et al.*, 2008].

L'efficacité des technologies et traitements basés sur l'électroporation est directement liée à l'efficacité de l'électroperméabilisation des tissus exposés aux impulsions de haut voltage, ce qui dépend de l'intensité du champ électrique local induit dans les tissus cibles. Le rapport entre un champ électrique local et l'électroperméabilisation a déjà été montré au niveau de la cellule et au niveau du tissu par les résultats des traitements basés sur

Résume de thèse en français

l'électroperméabilisation [Sale and Hamilton, 1968, Neumann *et al.*, 1982, Mir *et al.*, 1988, Mir *et al.*, 1991, Sersa *et al.*, 1995, Gabriel et Teissie, 1997, Miklavcic *et al.*,1998, Mir *et al.*, 1998, Ramirez *et al.*,1998, Mir *et al.*, 1999, Gehl *et al.*, 1999, Kotnik et al.,2000, Pavlin et al, 2000, Leroy-Willig *at al.*, 2005, Mir *et al.*, 2005, Marty *et al.*,2006, Mir, 2006, Andre *et al.*, 2008, Campana *et al.*, 2008, Daud *et al.*, 2008, Snoj *et al.*, 2009].

Le tissu ciblé peut être électroperméabilisé de manière optimale à condition que les paramètres du champ électriques local soient adéquats. Ces paramètres sont les suivants :

- l'amplitude du voltage appliqué sur les électrodes;

- la géométrie des électrodes;

- la distance entre les électrodes;

- la position des électrodes par rapport au tissu à cibler.

Le champ électrique local est influencé par la géométrie et la position du tissu ciblé, la géométrie et la position de tissu voisin ainsi que par les caractéristiques électriques des tissus ciblés et des tissus voisins. Pour la détection de l'efficacité de l'électroperméabilisation les E_{rev} et E_{irrev} du tissu ciblé et des tissus voisins doivent être déterminés *à priori* par des expériences *in vivo*.

Les seuils E_{rev} et E_{irrev} sont à déterminer pour chaque type de cellule et de tissu, car la distribution du champ électrique local et les seuils du champ électrique local E_{rev} et E_{irrev} dépendent de: la géométrie des cellules, la distribution des cellules, l'orientation des cellules, la fréquence, le nombre et la durée des impulsions.

Pour localiser la région de tissu étant électroperméabilisée il faut utiliser des méthodes pour la détection de l'électroperméabilisation en visualisant le tissu électroperméabilisé. Plusieurs méthodes *in vivo*, *in vitro* et *in silico* existent pour déterminer l'efficacité de

Résume de thèse en français

l'électroperméabilisation des cellules et des tissus à cibler. Les méthodes expérimentales *in vivo* et *in vitro* déjà utilisées pour détecter l'électroperméabilisation sont basées sur la détection de l'efficacité de l'internalisation dans les cellules ciblées de substances ayant des propriétés fluorescentes, luminescentes ou radioactives [Gabriel *et al.*, 1997, Engstrom *et al.*, 1998, Gehl *et al.*, 1999, A. Leroy-Willig *et al.*, 2005]. Plusieurs inconvénients de ces méthodes existent *in vivo* : d'une part elles prennent beaucoup de temps pour déterminer le résultat de leur internalisation dans les cellules et d'autre part les expériences doivent être répétées sur un grand nombre d'animaux, ce qui nécessite une mise en œuvre dans des laboratoires spécialisés. Parmi les méthodes pour détecter la perméabilisation des tissus *in vivo* il y a aussi les mesures de changement de la conductance du tissu ciblé, par des mesures du courant électrique I [A] et du voltage appliqué U [V], (couplées à des mesures d'incorporation de ^{51}CrEDTA) [Cukjati *et al.*, 2007]. Cette méthode est très efficace dans la detection de l'électroperméabilisation, mais elle ne permet pas localisation exacte du tissu electropermeabilisé. En 2000, dans le laboratoire de Dr. Lluis M. Mir à l'IGR (Villejuif) un modèle simple numérique a été développé par [Miklavcic *et al,* 2000] pour localiser l'électroperméabilisation dans des tissus (le foie), par la visualisation du champ électrique *in silico* couplée à la visualisation de la région électroperméabilisée *in vivo*. Cela a été le début du développement des modèles 3D réalistes où les calculs numériques sont validés par des expériences *in vivo*.

Le but principal de ma thèse est le développement des modèles réalistes en 3D du tissu musculaire, tumoral et de la peau en considérant les changements de leurs propriétés électriques dû à l'électroperméabilisation, aussi bien que la géométrie des tissus à traiter. Le but principal des modèles réalistes est la localisation de efficacité de l'électroperméabilisation des tissus par la visualisation du champ électrique local dans les modèles, ce qui a une grande

Résume de thèse en français

importance dans le choix des électrodes et de l'impulsion appropriée pour chaque tissu à traiter.

Objectifs de la thèse

La première partie de la thèse s'est intéressée aux modèles mathématiques des tissues ciblés afin de visualiser la distribution du champ électrique local par des simulations numériques, ce qui permet d'optimiser le choix du type d'électrodes à utiliser et l'amplitude du voltage à appliquer de telle sorte qu'une thérapie (électrochimiothérapie par exemple) basée sur l'électro-perméabilisation soit la plus efficace possible.

La deuxième partie expérimentale a consisté à valider ces modèles mathématiques par des expériences *in vivo* chez les animaux.

La troisième partie de la thèse concerne le développement d'une application internet pour l'enseignement/apprentissage à distance sur les mécanismes de l'électroperméabilisation au niveau des cellules et des tissus.

Dans la première partie de ma thèse les résultats de la recherche visaient donc à explorer les différents paramètres qui pouvaient avoir un effet sur la distribution du champ électrique local dans les tissus à traiter. Dans un premier temps j'ai étudié l'influence des différents paramètres sur la distribution du champ électrique par le biais de modèles 2D et 3D que j'ai développé dans cette thèse afin de tenter de comprendre quels paramètres sont importants et quels paramètres il faut optimiser pour obtenir une électroperméabilisation efficace. J'ai étudié l'influence de la géométrie des électrodes, de la position des électrodes, des propriétés électriques du tissu ciblé, et du voltage appliqué sur les électrodes, sur la distribution du champ électrique local a l'aide de la visualisation du champ électrique local par la modélisation en 2D et en 3D [**Publication I**, **Publication II**]. J'ai effectué une comparaison et

Résume de thèse en français

une quantification systématique du champ électrique local dans les modèles que j'ai développés pour les électrodes qui sont déjà le plus souvent utilisées en clinique et en recherche. J'ai analysé le champ électrique de façon analytique et numérique. Les résultats des calculs analytiques et numériques montrent que le champ électrique local au sein d'un tissu n'est pas homogène (E local $\neq U/d$) et que E change en fonction de:

- la géométrie des électrodes (plaque, aiguilles, nombre des électrodes)

- de l'activation des électrodes

- la position des électrodes par rapport au tissu ciblé

- de l'insertion des électrodes dans le tissue à traiter

- des propriétés électriques (conductivité) de tissu ciblé.

Vu que l'efficacité de l'électroperméabilisation est directement liée a l'intensité du champ électrique local, tous ces paramètres doivent être pris en considération dans le 'treatment planning' des thérapies basées sur l'électroperméabilisation

La deuxième étape de ma thèse a été consacrée au développement des modèles réalistes de la tumeur, du muscle et de la peau et à la validation des modèles par des expériences *in vivo* chez les animaux.

Dans le cadre de traitement des tumeurs cutanées je présente une étude d'optimisation de la distribution du champ électrique dans le cadre de l'électrochimiothérapie des tumeurs cutanées avec des électrodes en plaque, basée sur la modélisation mathématique et les expériences *in vivo* chez les animaux. En effet, j'ai développé un modèle numérique réaliste de la tumeur cutanée afin de montrer l'influence de la surface de contact entre les électrodes et la tumeur sur l'efficacité de l'électrochimiothérapie. L'idée est de pouvoir proposer une l'électrochimiothérapie des tumeurs cutanées encore plus sûre et efficace en traitant uniquement le tissu ciblé (les cellules de la tumeur) et en diminuant le risque

Résume de thèse en français

d'électroperméabilisation irréversible des tissus sains environnant la tumeur. J'ai comparé l'efficacité de l'électrochimiothérapie obtenue avec deux placements des électrodes ayant une surface de contact différente entre les électrodes et la tumeur. Parallèlement un troisième groupe d'animaux avec des tumeurs ayant les mêmes dimensions, a servi comme témoin, car les tumeurs dans ce dernier groupe n'ont pas été traitées par l'électrochimiothérapie. Les résultats de l'étude montrent que l'intensité du champ électrique dans la tumeur est d'autant plus élevée et d'autant plus homogène que la surface de contact augmente. Les résultats de cette étude, que j'ai réalisé pour ma thèse, permettent d'effectuer une électroperméabilisation du tissu cible de manière plus précise, ce qui permet de couvrir la totalité de la tumeur par un champ électrique local au-delà de la valeur seuil réversible $E > E_{rev}$. En même temps les tissus sains sont moins exposés au champ électrique au-delà du seuil irréversible ($E > E_{irrev}$). Les résultats montrent qu'une électrochimiothérapie plus efficace peut être réalisée à condition que la tumeur soit bien placée entre des électrodes fournissant une surface de contact la plus grande possible. En conclusion, à l'aide de la visualisation du champ électrique local dans les modèles réalistes des tumeurs sous-cutanées j'ai montré qu'à l'aide des calculs numériques l'efficacité de l'électroperméabilisation du tissu cible et donc l'efficacité de l'électrochimiothérapie peuvent être prévues à priori [**Publication III**].

Dans le cadre du développement des modèles réalistes du muscle j'ai étudié l'influence de l'orientation du champ électrique appliqué sur l'électroperméabilisation du muscle et l'influence de la peau sur l'électroperméabilisation du muscle.

J'ai étudié le phénomène d'électroperméabilisation du tissu musculaire, qui est grâce à ses propriétés physiologiques une cible de choix pour le transfert de gènes, utilisée pour la thérapie génique et la vaccination génique. Le tissu musculaire peut être grossièrement décrit comme un faisceau de cellules musculaires ou de fibres qui sont entourées par une membrane

Résume de thèse en français

moins perméable. Entre les fibres musculaires il existe du liquide extracellulaire, qui est plus conducteur que les membranes des fibres musculaires. Grâce à sa structure spécifique le tissu musculaire montre une forte anisotropie : dans le sens des fibres le tissu musculaire est beaucoup plus conducteur que dans la direction perpendiculaire aux fibres.

En raison de la forme et de l'orientation spécifique des cellules musculaires, j'ai prévu que la valeur seuil de l'électroperméabilisation dans le sens longitudinal (le champ électrique étant orienté de façon longitudinale par rapport à l'axe des fibres musculaires) est moins importante que la valeurs seuil de l'électroperméabilisation dans le sens transversal (lorsque le champ électrique est orienté perpendiculairement à l'axe des fibres musculaires) (E_{rev} (parallèle) < E_{rev} (perpendiculaire)). Dans ma thèse cette hypothèse de l'influence de l'orientation du champ électrique par rapport aux fibres musculaires sur l'électroperméabilisation du tissu musculaire a été confirmée de façon numérique et expérimentale *in vivo* [**Publication VI**]. J'ai développé un modèle numérique réaliste du muscle et des électrodes en plaque. Parallèlement, j'ai étudié l'électroperméabilisation du muscle par des expériences *in vivo*. La comparaison entre les résultats numériques et les résultats obtenus *in vivo* a validé mes modèles. Les expériences *in vivo* on été réalisées dans le laboratoire à l'Institut Gustave-Roussy selon les règles institutionnelles et les exigences imposées par la loi française.

Afin d'étudier l'influence de la peau sur l'électroperméabilisation du muscle j'ai aussi développé une modèle réaliste du muscle sans la peau et avec la peau [**Publication V**]. Pour valider ces modèles réalistes, j'ai utilisé les résultats d'expériences *in vivo* sur la peau et le muscle chez des rats (mesures de I (U) et de la rétention de ^{51}CrEDTA), effectuées par Cukjati et collègues [Cukjati *et al.* 2007] dans le même laboratoire, avant ma thèse. Les résultats du travail de ma thèse montrent que l'électroperméabilisation dans le tissu musculaire a lieu à la même valeur seuil E_{rev} que le muscle soit électroporé directement (sans peau) ou

Résume de thèse en français

indirectement (à travers la peau). En conclusion, la peau n'a pas d'influence sur la valeur E_{rev} du muscle. Cependant, dans le cadre du muscle avec peau il faut appliquer un voltage externe plus élevé que dans le cadre du muscle sans peau pour atteindre la valeur seuil de perméabilisation réversible (E_{rev}) du muscle.

Les résultats de la modélisation réaliste en 3D que j'ai réalisé dans cette thèse peuvent être utilisés pour optimiser l'électroperméabilisation des tissus biologiques, ce qui a une grande importance dans le 'treatment planning' des thérapies basées sur l'électroperméabilisation telles que l'électrothérapie génique et la vaccination, l'électrochimiothérapie, et l'administration de médicaments à travers la peau. Ainsi, le 'treatment planning' des thérapies basées sur électroperméabilisation représente la perspective future de la recherche que j'ai effectué dans le cadre de ma thèse.

Il est important de souligner que les traitements basés sur l'électroperméabilisation tels que l'électrochimiothérapie et l'électrotransfert de gènes demandent une multidisciplinarité et des connaissances dans différents champs thématiques. L'efficacité de ces thérapies nécessite des collaborations entre des experts de plusieurs domaines tel que la médicine, la biologie, la physique, la chimie, la pharmacie, l'électronique, l'informatique etc. Dans le but de standardiser les protocoles d'électrochimiothérapie et de thérapie par électrotransfert de gènes et d'introduire cette méthode dans un environnement clinique, un projet européen a été effectué dans le cinquième programme-cadre [www.cliniporator.com]. Les essais cliniques de l'électrochimiothérapie et de la thérapie par électrotransfert de gènes ont eu lieu dans plusieurs centres anticancéreux en Europe. Dans le cadre de ce projet une application internet a été développée pour récupérer /rassembler les résultats des traitement réalisés dans les différents centres anticancéreux [Pavlović et *al.*, 2004]. Malgré les très bons résultats des essais cliniques [Marty *et al.* 2006], la plupart des protocoles pour l'électroperméabilisation ont été définis par le rapport entre le voltage appliqué et la distance entre les électrodes (*U/d*),

Résume de thèse en français

ce qui ne prend pas en compte le champ électrique local dans le tissue traité. Les résultats de la visualisation du champ électrique par modélisation et les expériences *in vivo* ont montré que le champ électrique local dans le tissu ciblé est hétérogène et inférieur à la valeur *U/d*. L'hypothèse de ma thèse est qu'il est possible d'améliorer l'efficacité de l'électrochimiothérapie avec une bonne connaissance des paramètres clés du champ électrique local qui ont une influence directe sur l'efficacité de l'électroperméabilisation et par conséquence sur l'efficacité des thérapies basées sur l'électroporation. Une étape clé pour la réussite de électrochimiothérapie représente l'éducation des personnes qui préparent ou effectuent le traitement. Les technologies web représentent un outil efficace pour le rassemblement et la dissémination de la connaissance en vue de la formation à distance [Day *et al.*, 2006, Humar *et al.*, 2005]. Dans le cadre de cette thèse de doctorat j'ai développé une application internet pour la dissémination de la connaissance sur l'importance de la distribution du champ électrique local pour l'électroperméabilisation des cellules et des tissus et par conséquence sur l'efficacité des thérapies basées sur l'électroperméabilisation. Le contenu de l'application que j'ai développé est basé sur des résultats des recherches et des données cliniques déjà publiées dans la littérature scientifique. Le programme a été développé de façon modulaire, ce qui permet une mise à jour facile de nouveaux contenus obtenus en clinique et/ou par la recherche, ce qui est l'une des perspectives futures du travail de ma thèse. Cette application est destinée aux utilisateurs venant de divers domaines tels que la clinique (les médecins, le personnel médical, les patients), la recherche (les biologistes, les chimistes, les ingénieurs) et les étudiants. J'ai réalisé une analyse de l'efficacité pédagogique et de la facilité d'utilisation de ce programme. Les résultats du test de l'efficacité d'utilisation montrent que ce programme est facile à prendre en main et intuitif [**Publication IV**].

Modeliranje in vizualizacija elektropermeabilizacije bioloških tkiv izpostavljenih visokonapetostnim kratkotrajnim pulzom

Ob izpostavitvi biološkega tkiva visokonapetostnim kratkotrajnim pulzom se v tkivu ustvari lokalno električno polje, ki lahko povzroči strukturne spremembe na celičnih membranah. V primeru ko lokalno električno polje preseže kritično vrednost se te strukturne spremembe kažejo kot povečanje prepustnosti celičnih membran za ione, molekule in makromolekule za katere je membrana sicer neprepustna. Povečanje prepustnosti membrane v literaturi opisujejo z nastankom tako imenovanih por v lipidnem dvosloju, skozi katere ioni in molekule prehajajo v notranjost celic. Zato tak pojav pri katerem dovolj visoko električno polje v celični membrani povzroči nastanek por oziroma strukturnih sprememb v lipidnem dvosloju imenujemo elektroporacija ali elektropermeabilizacija [Neumann *et al.*, 1989, Maček-Lebar et *al.*, 2001]. Visokonapetosne kratkotrajne pulze katerim izpostavimo biološko tkivo imenujemo elektroporacijski pulzi. Elektroporacijske pulze generiraramo s pomočjo napetostnega generatorja za izvajanje elektroporacije, do ciljnih celic pa jih dovedemo preko prevodnih elektrod ustrezne oblike [Puc et *al.*, 2004].

Strukturne spremembe v celični membrani so posledica visokega električnega polja in vodijo do povečanja prepustnosti membrane, glede na koncentracijski gradient pa opazovana snov teče v ali iz celice. Z matematičnega vidika povečanje prepustnosti celične membrane obravnavamo kot presežek kritične vrednosti transmembranske napetosti, ta pa je seštevek mirovne transmembranske napetosti in vsiljene transmembranske napetosti. Mirovna transmembranska napetost je na celični membrani vseskozi prisotna, vsiljena

transmembranska napetost pa se ustvari zaradi delovanja zunanjega električnega polja. Za uspešno permeabilizacijo celic je torej ključen parameter kritična transmembranska napetost. Vrednosti kritične transmembranske napetosti, ki jih v literaturi navajajo so v območju od 200 mV do 1 V [Neumman *et al.*, 1982, Weaver *et al.*, 1996, Miklavcic *et al.*, 2000]. Proces elektroporacije je sicer bolj raziskan na nivoju celic, vendar pridobljeno znanje lahko vsaj deloma uporabimo tudi na biološkem tkivu kot skupku celic [Pavlin *et al.*, 2002]. V okviru doktorske disertacije se osredotočamo na preučevanje uspešnosti *in vivo* elektropermeabilizacije tkiv na podlagi numeričnih modelov in poskusov *in vivo*, ter na razvoj spletne aplikacije za poučevanje na daljavo o pridobljenemu znanju na podlagi eksperimentov in numeričnega modeliranja.

Uspešna elektropermeabilizacija ciljnega tkiva pomeni izpostavitev tkiva takšnemu električnemu polju, da so vse celice znotraj ciljnega področja uspešno elektropermeabilizirane. Bistveno vlogo pri uspešnosti elektropermeabilizacije igra lokalno električno polje, ki se v tkivu vzpostavi kot odziv na vzbujanje z zunanjim električnim poljem. Za uspešno elektropermeabilizacijo, v tkivu moramo zagotoviti lokalno električno polje, ki mora preseči kritično vrednost, ki je značilna za vsako vrsto tkiva. Omenjeno kritično vrednost lokalnega električnega polja imenujemo reverzibilni prag elektropermeabilizacije (E_{rev}), ki celic oziroma tkiva ne poškoduje, po izklopu električnih pulzov pa se membrane celic zacelijo, tkivo pa povrne v normalno stanje. Povečevanje vrednosti lokalnega električnega polja do irevezibilnega praga elektropermeabilizacije (E_{irrev}) pa celične membrane trajno poškoduje in celice odmrejo.

Uporaba elektroporacije je odvisna od vrednosti lokalnega električnega polja, ki ga ustvarimo v obravnavanem ciljnem vzorcu (na celicah ali tkuvih). Na sliki 1 so prikazane različne

uporabe electroporacije glede na ustvarjeno vrednost lokalnega električnega polja na obravnavanem vzorcu celic ali tkiva.
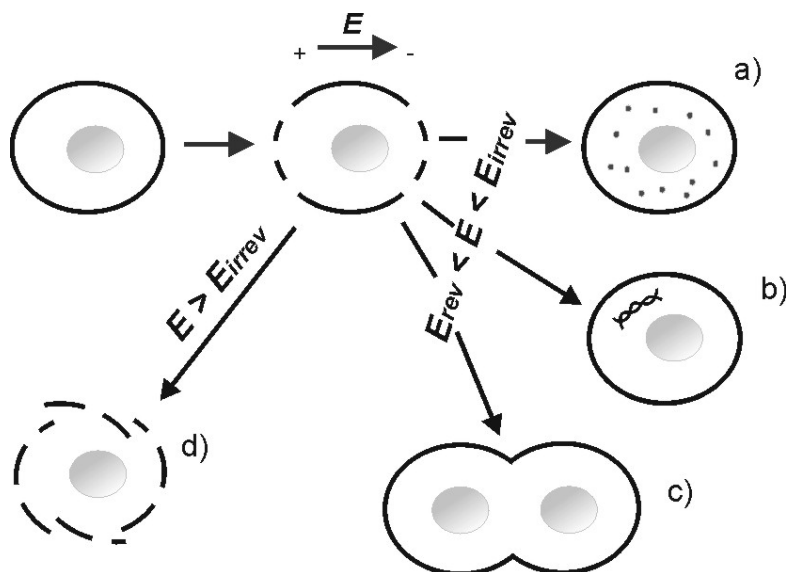
Slika 1: Različne uporabe elektroporacije glede na ustvarjeno vrednost lokalnega električnega polja na ciljnem vzorcu: reverzibilna elektroporacija $E_{rev} < E < E_{irrev}$ za ustavljanje majhnih molekul (kot so na primer kemoterapevtiki in razna barvila) (a), za vstavljanje makromolekul (kot je DNK) (b) ter za elektrofuzijo celic (c) in ireverzibilna elektroporacija $E > E_{irrev}$ ki celice nepovratno poškoduje (d) [Slika je objavljena v znanstvenem prispevku Kanduser and Miklavcic, 2008]

Snov, ki jo z elektroporacijo/elektropermeabilizacio lahko vnesemo v celice je lahko zdravilna učinkovina, kot so na primer nekateri kemoterapevtiki in DNK. Elektroporacijo uspešno uporabljamo na različnih področjih medicine in biologije: kot na primer v kliniki in raziskavah na področjih elektrokemoterapije tumorjev, v genski elektrotransfekciji ter vnosu zdravilnih učinkovin preko kože. Elektroporacijo uporabljajo tudi kot metodo za vnos različnih snovi v rastlinske celice. Možnost uporabe elektroporacije preučujejo tudi na področjih obdelave živil ter prečiščevanju pitne vode, kot metodo za uničevanje škodljivih mikroorganizmov [Kanduser and Miklavcic, 2008]. V doktorski disertaciji smo se osredotočili na uporabo elektroporacije na nivoju biološkega tkiva na področjih elektrokemoterapije in vnosa genov z elektroporacijo oziroma genske elektrotransfekcije.

Elektrokemoterapija kot metoda za zdravljenje rakastih bolezni združuje metodo kemoterapije in elektropermeabilizacije tkiv [Mir et *al.*, 1999]. Pri elektrokemoterapiji je ključnega pomena, da jakost električnega polja v ciljnem/tumorkem tkivu preseže reverzibilno pragovno vrednost elektropermeabilizacije. Zelo pomembno je poudariti, da z ustreznim izborom elektrod in ustreznimi električnimi pulzi, električno polje omejimo le na ciljno/tumorsko tkivo in tako preprečimo oziroma minimiziramo poškodbe zdravega tkiva. Prednost elektrokemoterapije pred samo kemoterapijo je povečano učinkovanje kemoterapevtika tako, da za enak učinek pri zdravjenju potrebujemo manjše koncentracije kemoterapevtikov, kar pomeni manj stranskih učinkov pri zdravljenju. Ker se zdravilna učinka kemoterapevtikov in električnega polja med sabo dopolnjujeta, pri elektrokemoterapiji potrebujemo nižje električno polje kot bi ga sicer bilo potrebno zagotoviti brez delovanja kemoterapevtikov. Elektrokemoterapija se že uspešno uporablja v kliniki kot učinkovita metoda za lokalno zdravljenje kožnih in podkožnih tumorjev [Marty *et al.*, 2006].

Genska elektrotransfekcija je metoda za vnašanje genskega materiala v celice z elektroporacijo [Neumann *et al.*, 1982, Mir *et al.*, 1999]. Pri genski terapiji želimo, da celice ciljnega tkiva ostanejo nepoškodovane zato je ključnega pomena, da v ciljnem tkivu jakost električnega polja ohranjamo v reverzibilnem področju elektropermeabilizacije t.j. od reveribilnega do ireverzibilnega praga ($E_{rev} < E < E_{irrev}$). Takšen režim elektropermeabilizacije tkivu lahko zagotovimo z ustreznim izborom elektrod ter ustreznimi električnimi pulzi. Metoda je trenutno predmet predkliničnih raziskav, vendar zaradi številnih prednosti pričakujemo, da jo bodo začeli uporabljati tudi v kliniki [Daud *et al.*, 2008].

Uspešnost metod, ki temeljijo na elektroporaciji je odvisna od uspešnosti elektropemeabilizacije ciljnega tkiva, ta pa je v neposredni povezavi z jakostjo lokalnega

električnega polja, ki se v tkivu porazdeli ob dovajanju elektroporacijskih pulzov. Ciljno tkivo lahko uspešno elektroporiramo/elektropermeabiliziramo le ob pravilni izbiri ključnih parametrov lokalnega električnega polja, kot so

- pritisnjena napetost na elektrodah;

- oblika in velikost elektrod;

- razdalja med elektrodami;

- postavitev in orientacija elektrod glede na ciljno tkivo in

- kontaktna površina med tkivom in elektrodo.

Ustrezne parametre lokalnega električnega polja za vsako ciljno tkivo lahko uspešno določimo na podlagi izračunov in vizualizacije na realističnih numeričnih modelih, ki so potrjeni z ustreznimi poskusi na realnem tkivu [Miklavcic *et al.*, 1998, Miklavcic *et al.*, 2000, Sel *et al.*, 2005, Pavselj *et al.*, 2005, Miklavcic *et al.*, 2006]. Nujno potrebni parametri za razvoj učinkovitega realističnega numeričnega modela so kritične reverzibilne E_{rev} in ireverzibilne E_{irrev} vrednosti lokalnega električnega polja obravnavanih tkiv, ter električne in geometrične (velikost, oblika in lega) lastnosti ciljnega in okoliškega, ki jih je potrebno določiti z meritvami *in vivo*.

Uspešnost elektropermeabilizacije tkiv v *in vivo* pogojih je možno spremljati z metodami ki temeljijo na uporabi indikatorskih snovi s fluorescenčnimi, luminescenčnimi ter radioaktivnimi lastnostmi, kot so: propidijev jodid s fluorescenčnimi lastnostmi [Gabriel *et al.*, 1997], fluorescenčni protein GFP [Pavšelj *et al.*, 2005], protein luciferaza [Pavšelj *et al.*, 2005], pri katerem izkoriščamo lastnost bioluminescence, radioktivne molekule 111In-Bleomycin [Engstrom *et al.*, 1998], ^{51}Cr-EDTA [Ghel *et al.*, 1999] ter Gd-DTPA [A. Leroy-Willing *et al.*, 2005]. Ena izmed glavnih pomanjkljivosti eksperimentalnih *in vivo* metod je

njihova časovna zamudnost, saj pri večini informacijo o elektropermeabilizaciji lahko pridobimo šele po nekaj dneh, glede na število parametrov, ki pogojujejo uspešnost elektropermeabilizacije, pa je poskuse potrebno ponoviti na velikem številu živali. Poleg tega poskuse v *in vivo* pogojih lahko izvajamo le v posebej specializiranih laboratorijih. Zato je nujen korak k pridobitvi informacije o tem kolikšen delež ciljnega tkiva je bil izpostavljen ustrezni jakosti električnega polja vizualizacija porazdelitve jakosti električnega polja v 3D numeričnih modelih.

Cilji doktorske disertacije so naslednji:

1. razvoj realističnih numeričnih modelov različnih tkiv (t.j. mišice, tumorja in kože) ter izračun in vizualizacija lokalnega električnega polja v modelih;

2. vrednotenje numeričnih modelov validation na in *in vivo* poskusih

3. razvoj spletne izobraževalne aplikacije o terapijah in postopkih, ki temeljijo na procesu elektroporacije.

Za zagotavljanje uspešnosti elektrokemoterapije smo se osredotočili na preučevanje vpliva ključnih parametrov lokalnega električnega polja na numeričnih modelih kožnih in podkožnih tumorjev. Izhajali smo iz predpostavke, da je za uspešno elektrokemoterapijo tumorjev kot ciljnega tkiva potrebno uporabiti elektrode primerne oblike glede na obliko in položaj t.j oblike in lego tumorja v koži, ter električne lastnosti tumorja.

Naredili smo sistematčno primerjavo in kvantifikacijo lokalnega električnega polja v modelih tkiva za elektrode, ki so v uporabi v kliniki in raziskavah. Porazdelitev lokalnega električnega polja smo analizirali na podlagi analitičnih modelov v dveh dimenzijah ter numeričnih modelov v dveh in treh dimenzijah [**Paper I**, **Paper II**]. Pokazali smo, da učinkovito elektroporacijo ciljnega tkiva lahko zagotovimo z izbiro naslednjih parametrov lokanega

električnega polja: amplituda pritisnjene napetosti, geometrija in pozicija elektrod glede na pozicijo ciljnega tkiva, število elektrod, razdalja med elektrodami ter globina elektrod v tkivu. Omenjeni parametri so relevantni parametri za postopek optimizacije in morajo biti določeni za vsako ciljno tkivo posebej. Izbor ustreznih parametrov na podlagi izračunov in vizualizacije lokalnega električnega polja v realističnih numeričnih modelih tkiv predstavlja pomemben korak v načrtovanju terapij in postopkov ki temeljijo na elektroporaciji ter ustreznih raziskovalnih poskusov.

Razvili smo 3D realistični numerični model kožnega tumorja in pokazali vpliv kontaktne površine med elektrodo in tumorskim tkivom na rezultat zdravljenja z elektrokemoterapijo. Večja kontaktna povšina prispeva k večji homogenosti lokalnega električnega polja v tumorju in omogoča bolj učinkovito zdravljenje kožnih tumorjev. Naši rezultati lahko prispevajo k natančni elektroporaciji ciljnega tumorskega tkiva, zaščiti okoliškega zdravega tkiva pred ireverzibilno elektroporacijo ($E > E_{irrev}$) ter k zmanjšanju občutka bolečine, ki sicer lahko nastane zaradi penetracije premočnega električnega polja v globja tkiva. Na osnovi vizualizacije lokalnega električnega polja v modelih kožnih tumorjev smo pokazali, da z numeričnimi izračni lahko napovemo uspešnost elektropermeabilizacije ciljnega tkiva in s tem uspešnost elektrokemoterapije [**Paper III**].

Proces elektropermeabilizacije smo preučili tudi na mišičnem tkivu, ki zaradi svojih fizioloških lastnosti predstavlja najbolj učinkovito ciljno tkivo za lokalno in sistemsko gensko terapijo in vakcinacijo z elektroporacijo. Mišično tkivo v grobem lahko opišemo kot skupek mišičnih celic oziroma vlaken, ki so obdane z manj prepustno membrano, med vlakni pa se pretaka bolj prevodna zunajcelična tekočina. Zaradi svoje specifične zgradbe tkivo mišice izkazuje izrazito anizotropijo, v smeri vlaken je mišica bistveno bolj prevodna kot v smeri pravokotno na vlakna. Zaradi oblike in orientacije mišične celice smo pričakovali, da je

pragovna vrednost elektropermeabilizacije v longitudinalni smeri, ko je električno polje orientirano v smeri mišičnih vlaken, nižja v primerjavi s pragovnimi vrednostmi v transverzalni smeri, ko je električno polje orientirano pravokotno na mišična vlakna. To hipotezo vpliva orientacije električnega polja glede na mišična vlakna smo potrdili numerično in eksperimentalno [**Paper VI**]. Zgradili smo namreč realistični numerični model mišičnega tkiva in uporabljenih ploščatih elektrod. Na podlagi primerjave rezultatov pridobljenih *in vivo* in numeričnih izračunov smo ovrednotili naše numerične modele. Uspešnost elektropermeabilizacije smo raziskali še eksperimentalno v *in vivo* pogojih. Poskusi so bili izvedeni v živalskem laboratoriju inštituta IGR (Institut Gustave-Roussy, 39 Rue C. Desmoulins F-94805 Villejuif Cédex - France) v skladu z institucionalnimi pravili in zahtevami, ki jih postavlja francoska zakonodaja. Na podlagi realističnih modelov mišice smo raziskali tudi vpliv kože na elektroporacijo mišičnega tkiva in ugotovili, da prisotnost kože ne vpliva na pragovno vrednost lokalnege električnega polja, ki je potrebna za elektroporacijo mišičnega tkiva [**Paper V**]. Za ovrednotenje realističnih modelov mišice s in brez kože smo uporabili rezultate *in vivo* poskusov na mišici pogane, ki jih je opravil Cukjati s sodelavci [Cukjati *et al.*, 2007].

Potrebno je poudariti, da področji elektrokemoterapije in elektrogenske terapije zahtevata interdisciplinarnost, kar pomeni, da je za uspešnost terapije ključnega pomena sodelovanje ekspertov z različnih področij kot so medicina, biologija, elektrotehnika. S ciljem standardizacije protokolov za elektrokemoterapijo in elektrogenskoterapijo in vpeljavo te metode v klinično okolje je potekal evropski projekt v petem okvirnem programu [www.cliniporator.com]. Preizkušanje klinične uporabe elektrokemoterapije in elektrogenske terapije je potekalo v več onkoloških centrih po Evropi. V okviru znanstvega projekta pa je razvita spletna aplikacija za zbiranje podatkov o poteku in rezultatih poskusov in terapij

[Pavlović *et al.*, 2004]. Kljub izredno dobrim dosežkom [Marty *et al.*, 2006], večina trenutnih protokolov za izvajanje elektroporacije temelji na fenomenološkem podatku *U/d* (razmerje pritisnjene napetosti in razdalje med elektrodama), kot oceni o porazdelitvi jakosti električnega polja v tkivu. Zaradi specifične zgradbe in električnih lastnosti bioloških tkiv, še zlasti tumorskega tkiva, je električno polje, ki se v tkivu porazdeli, kot odziv na vzbujanje s napetostnimi pulzi, nehomogeno in običajno nižje od vrednosti *U/d*. Naša predpostavka je, da je uspešnost elektrokemoterapije možno izboljšati z dobrim poznavanjem ključnih parametrov lokalnega električnega polja, ki vplivajo na uspešnost elektropermeabilizacije in posledično terapij ki temeljijo na elektroporaciji. Ključen korak k uspešnosti elektrokemoterapije predstavlja izobraževanje oseb, ki terapijo načrtujejo ali izvajajo. Zelo učinkovito orodje za podajanje znanja je spletna tehnologija za namene izobraževanja na daljavo [Day *et al.*, 2006, Humar *et al.*, 2005]. V okviru doktorske disertacije smo razvili spletno izobraževalno aplikacijo, s katero naj bi podali pridobljeno znanje o vplivu ključnih parametrov lokalnega električnega polja na uspešnost elektropermeabilizacije ciljnega tkiva. Naša izobraževalna aplikacija je namenjena podajanju znanja ciljnim uporabnikom z različnih področij, kot so: klinika (zdravniki, zdravniško osebje, pacienti), raziskave (biologi, kemiki, inženirji) in študentje [**Paper IV**].

1. INTRODUCTION

The effect of high voltage pulses that causes cell membrane electroporation has been extensively studied for almost four decades since the early studies [Sale and Hamilton, 1967, Hamilton and Sale, 1967, Sale and Hamilton, 1968, Zimmermann *et al.*, 1974]. The electroporation can be used in all types of cells and tissues to render cell membranes permeable to substances that otherwise would not be able to effectively enter the cell interior [Tsong, 1991]. If the parameters for reversible electroporation are selected the cell membrane is able to reseal after the application of pulses so that the viability of the electroporated cell is preserved [Neumann *et al.*, 1982, Rols and Teissie, 1990], as schematically shown in Figure 1.
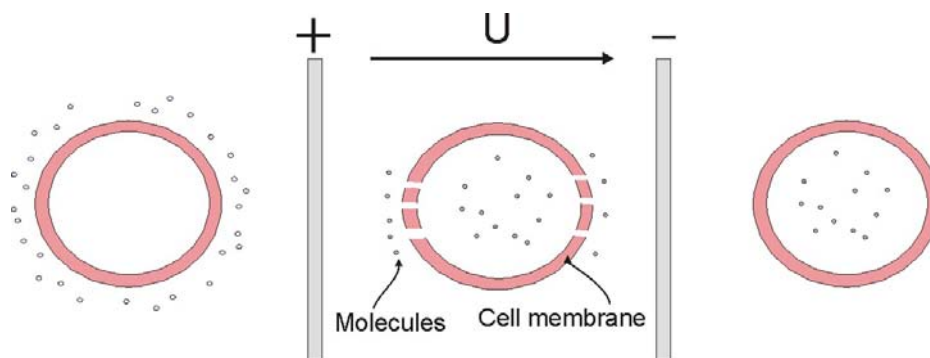
Figure 1: Illustration of a reversible cell electroporation, where *U* is the applied voltage pulse

Nowadays reversible electroporation, as an effective and safe tool for administration of different extracelular agents into targets cells, is widely used for various applications in biology, medicine and biotechnology. The most advanced electroporation based therapy and treatment in medical field are electrochemotherapy, gene electrotransfer for gene therapy and vaccination and transdermal drug delivery. New medical applications of reversible electroporation (such as intravascular delivery of drugs and genes with electroporation catheters, electroinsertion of molecules into membranes, intraocular delivery of drugs and genes, electrofusion) are emerging at increasing rate. In the last decade also destructive

applications relying on irreversible electroporation found its way in different medical and biotechnological fields such as minimally invasive tissue ablation [Davalos *et al.*, 2005, Al-Sakere *et al.,* 2007], water treatment [Teissie *et al.*, 2002], where efficacy of chemical treatment is enhanced with electroporation, and food sanitization [Heinz *et al.*, 2002, Sampedro *et al.*, 2007] where the electroporation is used to inactivate different microorganisms.

The main focus of the present doctoral theses is the analysis of *in vivo* electroporation and corresponding local electric field distribution used in electrochemotherapy and electroporation based gene therapy and vaccination.

1.1 Basic principles of electroporation

Electroporation is a phenomenon of cell membrane permeability increase (i.e. electropermeabilization) due to local delivery of short and sufficiently intense voltage pulses (electroporation pulses) to the target cells and tissues [Sale and Hamilton, 1967, Mir *et al*, 1988, Rols and Teissie, 1989, Neumann *et al*, 1989, Rols and Teissie, 1990, Miklavcic *et al.*, 2000]. The application of sufficiently high electric pulses creates an induced potential difference ($V_{induced}$) across the cell membrane which is superimposed on the resting membrane potential ($V_{resting}$). The increase in cell membrane permeability occurs when the total transmembrane potential difference ($\Delta V = V_{induced} + V_{resting}$) exceeds the critical breakdown value of the applied electroporation pulses.

The standard model of electroporation (i.e. model of pore formation) defines the phenomenon of electroporation as formation of aqueous pores in the presence of transmembrane voltage [Weaver and Chizmadzhev, 1996]. According to this model, transmembrane voltage induces a transition from the hydrophobic to the hydrophilic state. The hydrophilic pores are stable, due to a local minimum of free energy, which explains the experimentally observed durability of the electropermeabilized state. This state is reversible until the applied voltage above the

critical value causes an irreversible breakdown of the membrane [Tadej Kotnik, Doctoral thesis, 2000].

The cell membrane becomes successfully electropermeabilized if the transmembrane voltage ΔV reaches critical values ranging from 200 mV to 1 V, as reported in the literature [Neumman *et al.*, 1982, Zimermann 1982, Neumann *et al.*, 1989, Weaver *et al.*, 1996, Miklavcic *et al.*, 2000].

The induced transmembrane potential difference ΔV for a spherical cell is given by Schwan's equation (Schwan, 1957) (Eq.1):

$$\Delta V = 1.5\ r\ E \cos(\varphi) \qquad \text{(Eq.1)},$$

where *r* is the radius of the cell, *E* is external electric field, and φ is the angle between the direction of the electric field and the selected point on the cell surface (Figure 2a). The model of a spherical cell with radius *r* is illustrated in Figure 2a. The transmembrane voltage depends on the position on the cell membrane as shown in Figure 2b. It is the highest at the cell poles facing the electrodes for $\varphi=0$ and $\varphi=\pi$. However, in case of a very low conductive external media this simplified equation leads to considerable errors and the original equation has to be used, where all three conductivities influence the induced transmembrane voltage [Kotnik *et al.*, 1997].

Experiments *in vitro* on CHO cell in suspension (by using propidium iodide and ethidium bromide dyes, both naturally relatively membrane impermeant [Sixou and Teissie, 1993], showed that the membrane breakdown first occurs at the anodic hemisphere for $\varphi=\pi$, which was shown to be due to the resting potential which is superimposed on the induced transmembrane voltage [Gabriel and Teissie, 1997].
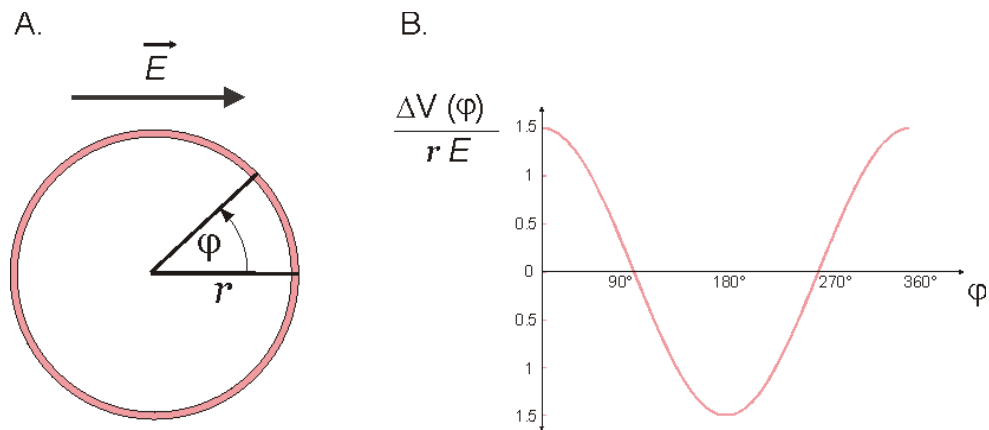
Figure 2: The model of a spherical cell (A) and the dependence of the transmembrane potential on the position on the cell membrane (B)

For some geometrical shapes of cells, such as spheroids [Kotnik and Miklavcic, 2000a] and cylinders, the transmembrane potential can be derived analytically, while for more complicated cell geometries the numerical methods are to be used [Pucihar *et al.*, 2006].

1.1.1 Important parameters for effective cell and tissue electroporation

The effectiveness of cell and tissue electroporation, and thus the effectiveness of electroporation based therapies, depends on one hand on the parameters of the applied pulses such as amplitude, duration, number and repetition frequency, type of electrodes used, and on the other hand on the characteristics of the cell and tissues to be electroporated (such as cell shape, cell orientation, cell density in the tissue) [Susil *et al.*, 1998, Valic *et al.*, 2003]. Namely, the increase in the electroporation pulse amplitude and subsequently the external electric field results in a larger area of membrane permeabilised (as shown in Figures 3a-d), while increase in pulse number or duration does not affect the membrane area but increases the extent of electroporation (number and size of pores) [Gabriel and Teissie, 1997], as illustrated in Figure 3e. The value of induced transmembrane voltage and thus the electroporation of a cell within a tissue also depends on geometrical and electrical properties of the cell (i.e. on the cell size, shape, electric conductivity), the orientation of the cell with respect to the direction of applied electric field [Valic *et al.*, 2003], as well as of cell density,

arrangement and cell position inside a cell system or tissue [Susil *et al.*, 1998, Pavlin *et al.*, 2002].
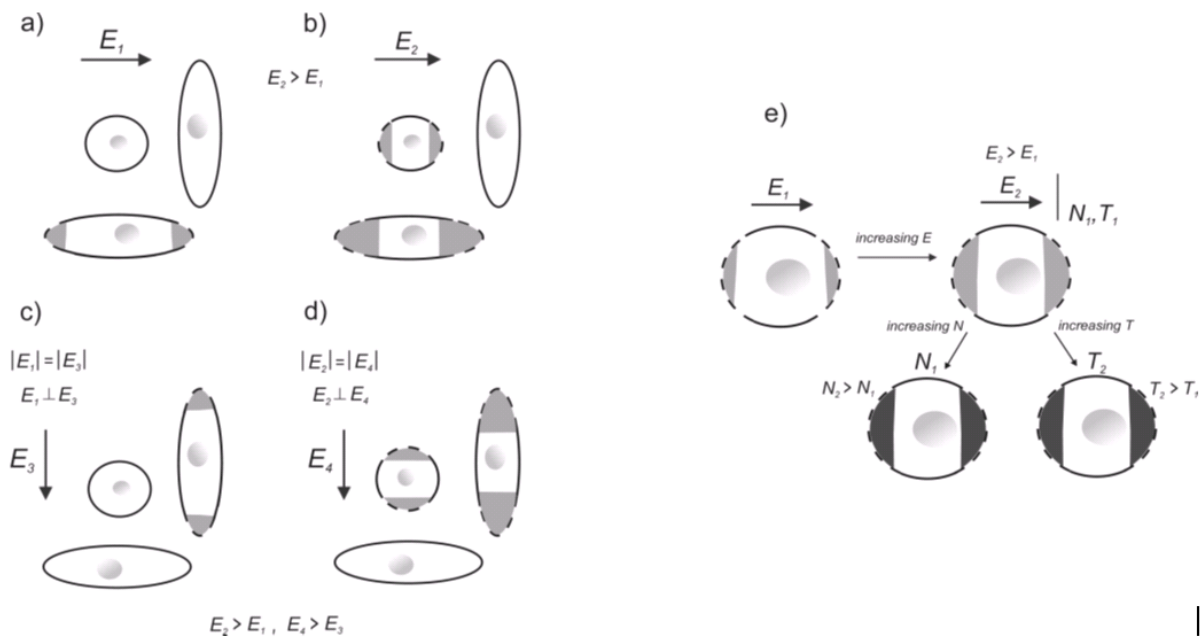
Figure 3: (a) Electric field parallel to elongated cell, (b) electric pulse amplitude is increased, (c) orientation of electric field is changed, (d) electric pulse amplitude is increased and (e) increasing the pulse amplitude results in larger area of membrane with smaller extent of electroporation, while increase in pulse number or duration does not affect the membrane area but increases the extent of electroporation. [Figure originally published in Kanduser and Miklavcic, 2008]

1.1.2 From the cell to the tissue electroporation detection

Although the electoporation process on a microscopic level can be very complicated the experimental and analytical studies on cell suspensions and *in vivo* studies in tissue demonstrated that electroporation process can be followed also on a macroscopic level. Namely, Kinosita and Tsong experimentally showed in cell suspensions that structural changes in cell membrane cause increased membrane conductivity, which consequently leads to a change in bulk conductivity [Kinosita and Tsong, 1979]. By impedance measurements the authors observed an increase of the effective conductivity of erythrocytes suspension. These changes depended on the field strength, pulse duration and conductivity of the extracellular medium. Similarly, Abidor and colleagues measured changes of the resistance of cell pellets due to the electroporation and drop in the effective resistance was observed after the

application of electroporation pulses [Abidor *et al.*, 1993]. Indirectly, by measuring the transmembrane potential, changes in membrane conductivity of sea urchin due to the electroporation was observed [Hibino *et al.*, 1991]. Analytical and numerical analysis by Pavlin and Miklavcic [Pavlin and Miklavcic, 2003] suggested that it was possible to estimate the changes of the membrane conductivity from the measurements of the effective conductivity of a cell suspension. The authors derived the equation, which connects cell membrane conductivity with the effective conductivity of the cell suspension. *In vivo* studies in tissue showed that the increase in tissue conductivity can be used for *in vivo* monitoring of tissue permeabilization by tissue conductance measurements during the application of electroporation pulses [Davalos *et al.*, 2000, Davalos *et al.*, 2002, Davalos *et al.*, 2004]. In an extensive *in vivo* study performed on several types of tissues (muscle, tumor, liver and skin) by Cukjati and colleagues tissue permeabilization was detected by tissue conductivity measurements [Cukjati *et al.*, 2007]. In 2000 Miklavcic and colleagues showed that the permeabilizated region of tissue *in vivo* can be determined by visualization of local electric field distribution by means of direct comparison of numerical calculation and *in vivo* observations in liver tissue [Miklavcic *et al.*, 2000]. Sel and colleagues developed a 3D numerical model of liver tissue based on *in vivo* measurements [Cukjati *et al.*, 2007] and first demonstrated that tissue permeabilization can be described as a functional dependency of tissue conductivity on the local electric field distribution [Sel *et al.*, 2005]. Namely, the authors showed that the increase in tissue conductivity occurred if the electroporation threshold of local electric field in tissue was exceeded. Both studies [Miklavcic *et al.*, 2000] and [Sel *et al.*, 2005] demonstrated importance of local electric field distribution in numerical models for detection of permeabilized tissue region *in vivo*.

1.2 Local electric field distribution – importance of modelling and visualization

When the electroporation pulses (U) are applied, local electric field (E) is established within the treated tissue. In order to cause structural changes in cell membrane, the magnitude of the local electric field needs to achieve the critical reversible threshold value (E_{rev}). The phenomenon is reversible until the magnitude of the local electric field reaches the irreversible threshold value E_{irrev}, which causes permanent damages of the cell membrane. Depending on the electric pulse parameters used, electroporation can be reversible or irreversible.

Possible applications of electroporation process, depending on parameters of the electric pulses applied, are illustrated in Figure 4: the introduction of small molecules (Figure 4a), of macromolecules (Figure 4b), and cells electrofusion (Figure 4c) require reversible electroporation regime ($E_{rev} < E < E_{irrev}$), while the permanent cell damaging requires irreversible electroporation parameters (Figure 4d), thus local electric field exceeding irreversible threshold ($E > E_{irrev}$). The critical threshold values (E_{rev} and E_{irrev}) are specific for each type of cells and tissues and need to be determined experimentally. The E_{rev} and E_{irrev} thresholds depend also on pulse characteristics such as the number, duration and repetition frequency of the applied voltage pulses.
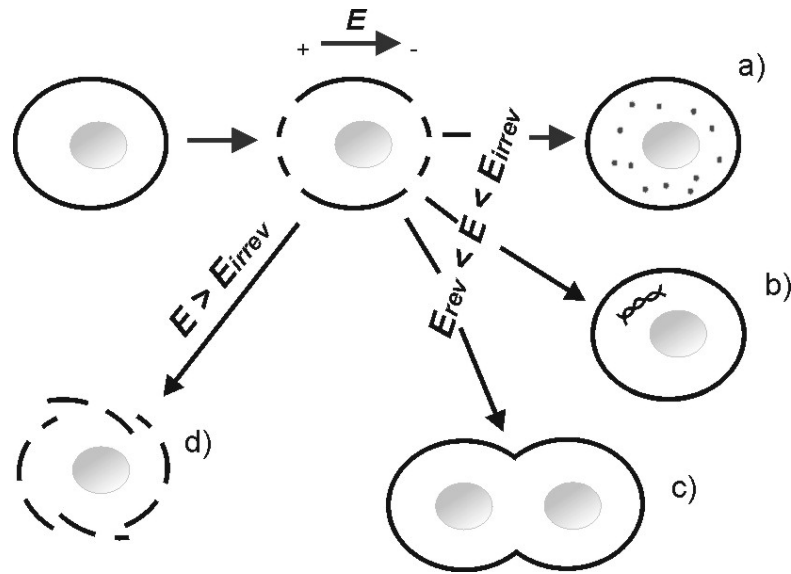
Figure 4: Different electroporation regimes depending on the local electric field strength E: reversible electroporation $E_{rev} < E < E_{irrev}$ needed for the introduction of small molecules (a), the introduction of macromolecules (b) and cells' electrofusion (c) and irreversible electrop oration $E > E_{irrev}$ needed for the permanent cell damaging (d) [Figure originally published in Kanduser and Miklavcic, 2008]

For efficient planning of electroporation based applications visualization and determination of local electric field distribution within the target tissue for given electrodes and parameters of the applied electroporation pulses is needed. This information needs to be known a priori for the entire region of the target tissue as well as of its surrounding tissues. Realistic numerical models of tissues that are based on 3D numerical modeling in combination with *in vivo* experiments are an efficient tool for analysis of local electric field distribution and its control within the body [Miklavcic *et al.* 1998, Miklavcic *et al.*, 2000, Sel *et al.*, 2005, Pavselj *et al.*, 2005, **Paper III**: **Corovic** *et al.*, 2008, **Paper V**: **Corovic** *et al.*, 2009-submited, **Paper VI**: **Corovic** *et al.*, 2009-submited].

The local electric field distribution within the treated tissue can be controlled by appropriate selection the following electric parameters:

- applied voltage on the electrodes;

- the shape and size of electrodes;

- distance between electrodes;

- placement of electrodes with respect to the target tissue and

- contact surface between the treated tissue and the electrode.

When selecting the abovementioned parameters one should also consider that local electric field is influenced by the following tissue parameters:

- size, shape and position of the target tissue;

- geometry of the tissue surrounding the target tissue and

- electric properties of the target and its surrounding tissues

In electroporation based therapy and treatment planning the critical reversible E_{rev} and irreversible E_{irrev} threshold values of the local electric field for both the target tissue and the surrounding tissues also have to be considered.

1.3 Knowledge exchange and collaboration among the experts involved in electroporation based therapies and treatments

In electroporation based therapies development, a multidisciplinary expertise is required. For example in electrochemotherapy a close collaboration, knowledge and experience exchange among experts in the fields of oncology, biology, biophysics, physical chemistry and electrical, biomedical engineering and informatics is needed (Table 1).

Table 1: Scientific fields and the corresponding expertise needed in electroporation based therapies and treatments

Field	Expertise
oncology	tumor cells and tissues, cancer
biology	cells, normal tissues
biophysics	physics of biological cells and tissues
physical chemistry	chemistry, membrane electroporation
electrical engineering	devices, electrodes
biomedical engineering	application of engineering principles in medicine and biology
computer engineering	database systems, interactive web applications

The efficacy of an electroporation based therapy or treatment can be assured with the knowledge of parameters of the local electric field (i.e. pulse parameters and electrode geometry and their positioning), being crucial for successful tissue electroporation and subsequently for the best treatment outcome. Another condition that has to be met for the therapy of treatment to be efficient is that a sufficient amount of the administered extracellular agent has to be present in the target tissue when the electric pulses are applied. Realistic mathematical models validated by corresponding experimental observations are valuable tool in designing and optimizing local electric field distribution. To develop a good mathematical model allowing for therapy outcome prediction the engineers need to possess knowledge about biological mechanisms involved in electrochemotherapy. On the other hand, to make the therapy as efficient as possible it is of great importance to transfer the knowledge from basic science to the field of biomedical engineering and further to the practicing clinicians who then perform the treatment.

Information and communication technology can be successfully used for efficient interdisciplinary collaboration and knowledge exchange. Internet technology has already been successfully used to support clinical trials of electrochemotherapy by establishing a central database and the Web application system for electronic data collection [**Paper XIV:** Pavlovic

_et al._, 2004, Pavlovic _et al._, 2007, Pavlovic _et al._, 2009]. Users from distant medical centers across Europe have been entering the data (such as treatment parameters used and treatment efficiency follow up), which reduces costs and improves data quality and control. Based on a comprehensive analysis of collected data, performed by the developed system, the standard operating procedures for clinical electrochemotherapy of cutaneous and subcutaneous tumor in patients have been defined [Marty _et al._, 2006, Mir _et al._, 2006].

1.4. History and basic principles of electrochemotherapy and electroporation based gene therapy and vaccination

Electrochemotherapy

Electrochemotherapy is a non-thermal antitumor treatment employing locally applied high voltage electric pulses (i.e. electroporation pulses) in combination with chemotherapeutic drugs [Mir _et al._, 1991, Mir, 2006, Sersa and Miklavcic, 2008].

The results of _in vivo_ experiments with electrochemotherapy were first reported by Okino and Mohri in 1987 [Okino and Mohri, 1987]. The therapy of subcutaneous tumors in rats was performed by application of a single high voltage pulse following intramuscular injection of bleomycin. Okino and Mori found that the combined treatment of an electric pulse and bleomycin had a strong antitumor effect, and neither the electrical pulse nor bleomycin administration alone had such an inhibitory effect on the tumor growth. In parallel systematic _in vitro_ studies on the cytotoxicity of bleomycin combined with electroporation pulses were performed by Orlowski and colleagues [Orlowski _et al._, 1988] and Mir and colleagues [Mir _et al._, 1988].

Since then numerous studies have shown the efficiency of the combined treatment of electroporation and antitumor drugs in treatment of subcutaneous and cutaneous malignancies

[Mir *et al.*, 1991, Sersa *et al.*, 1998, Heller *et al.*, 1998]. Several studies on the electrochemotherapy of orthotopic tumors, such as the brain [Salford *et al.*, 1993], the liver [Jaroszeski *et al.*, 1997, Chazal *et al.*, 1998, Ramirez *et al.*, 1998] and the pancreas [Jaroszeski *et al.*, 1999a] have also shown promising results.

Two non-permeant chemotherapeutic drugs (bleomycin and cisplatin) were found to be the most suitable candidates for combined use with electroporation pulses [Orlowski *et al.*, 1988, Sersa *et al.*, 1995]. *In vitro* experiments showed that the cytotoxicity of bleomycin is potentiated by several hundred times [Poddevin *et al.*, 1991] and the cytotoxicity of cisplatin up to 70 times [Sersa *et al.*, 1995]. *In vivo*, anti tumor effectiveness of bleomycin and cisplatin after electropermeabilization of cells is increased several-fold [Mir *et al.*, 1991, Heller *et al.*, 1995, Sersa *et al.*, 1995]. First clinical trial in patients (on head and neck tumor nodules) was performed in France (Institute Gustave-Rroussy, Villejiuf) and the results were published in 1991 by Mir and colleagues [Mir *at al.*, 1991]. This study was thereafter followed by other clinical trials in patients that demonstrated high efficiency in antitumor treatment of tumors with different histologies, such as head and neck squamous cell carcinoma, melanoma, basal cell carcinoma and adenocarcinoma [Rudolf *et al.*, 1995, Heller *et al.*, 1998; Sersa *et al.* 1998, Heller *et al.*, 1999, Rols *et al.*, 2000, Rodrigez-Cuevas *et al.*, 2001, Gothelf *et al.*, 2003, Sersa *et al.*, 2003, Rebersek *et al.*, 2004, Snoj *et al.*, 2005].

Clinical studies have been paralleled by the design of new electroporation pulse generators and electrodes [Puc *et al.*, 2004] aided by the development of the numerical models of tissues exposed to electroporation pulses [Miklavcic *at al.*, 1998, Gehl *et al.*, 1999, Miklavcic *et al.*, 2000, Semrov and Miklavcic, 2000, Sel *et al.*, 2005, Pavselj *et al.*, 2005]. Based on these knowledge obtained from the numerical models the electrochemotherapy treatment protocols have been continuously improved and refined.

In 2006 electrochemotherapy standard operating procedures (SOP) have been defined for the treatment of cutaneous and subcutaneous tumor nodules of different histologies as a conclusion of a multy-institutional study, which was conducted by a consortium of four European centers gathered in the ESOPE project funded under the European Commission's 5th Framework Programme [Marty *et al.*, 2006]. The timeline illustrating the evolution of *in vivo* studies on electrochemotherapy from the first report from the first report by Sale and Hamilton [Sale and Hamilton, 1967] to the definition of SOP in 2006 [Marty *et al.*, 2006] and the first clinical electrochemotherapy of liver tissue is shown in Figure 5a.

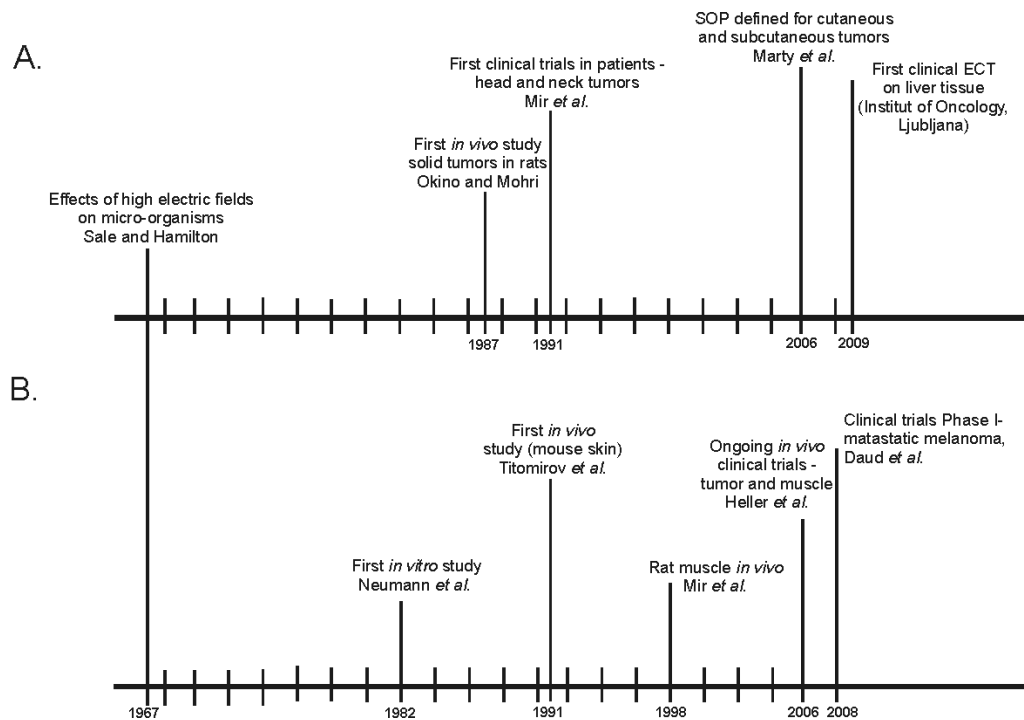**Figure 5**: The timeline illustrating the evolution of *in vivo* studies: a. on electrochemotherapy b. on gene electrotransfer

In the ESOPE study, the treatment response was tested according to tumor type, drug used, route of administration and type of electrodes was tested. The study confirmed previous reports on the effectiveness of electrochemotherapy and following results were obtained during the study:

1. An objective response of 85% (73.7% complete response rate) was achieved for tumor nodules regardless of tumor histology, drug or route of administration used;

2. At 150 days after treatment, the local tumor control rate for electrochemotherapy was 88 % with bleomycin given intravenously, 73 % with bleomycin given intratumorally and 75 % with cisplatin given intratumoraly, demonstrating that all three approaches were equally effective in local tumor treatment, with a preference for the intravenous administration of the bleomycin;

3. Side effects of electrochemotherapy (such as muscle contractions and pain sensation) were minor and tolerable.

In addition, several advantages of the electrochemotherapy treatment have been reported, such as:

1. Easy and effective treatment of single or multiple tumor nodules of any histology in cutaneous and subcutaneous tissue;

2. Treatment that increases quality of life in patients with progressive disease;

3. Treatment of choice for tumors refractory to conventional treatments;

4. Neoadjuvant treatment in the form of cytoreductive therapy before conventional treatment;

5. Organ sparing and function saving treatment;

6. Treatment of hemorrhagic or painful nodules, since it reduces bleeding and in some cases pain level and

7. After electrochemotherapy good cosmetic effects are obtained due to a selective cell death mechanism that primarily affects the dividing tumor cells.

In the ESOPE study electrochemotherapy with plate electrodes has been proven to be very suitable for treatment of protruding cutaneous tumors, where entire volume can be held between the electrodes, while in cases where tumor is seeded more deeply in the skin and underlying tissues the needle electrodes are to be used [Miklavcic *et al.*, 2006, Mir *at al.*,

2006, Marty *et al.*, 2006]. For electroporation, square wave electric pulses with an amplitude over distance ratio of 1000-1300 V/cm, duration of 100 µs, frequency of 1 Hz or 5 kHz were used.

In addition, to the efficacy and safety, the electrochemotherapy is a cost-effective method, which has recently been demonstrated by Colombo and colleagues in a cost-effectiveness analysis of electrochemotherapy compared to other methods (such as radiotherapy, hyperthermia associated with radiotherapy and chemotherapy, interferon-alpha, and isolated limb perfusion) for the control and treatment of cutaneous and subcutaneous tumors [Colombo *et al.*, 2008].

The clinical electrochemotherapy is currently used as a palliative treatment of cutaneous and subcutaneous tumor nodules of different malignances. Namely, after ESOPE study several clinical studies using the defined SOP protocols [Mir, 2006] were published confirming the results obtained during the ESOPE study [Campana *et al.*, 2008, Curatolo *et al.*, 2008, Fantini *et al.*, 2008, Quaglino *et al.*, 2008, Snoj *et al.*, 2009].

In order to further improve and refine the protocols of electrochemotheray of cutaneous and subcutaneous tumor nodules and to broaden the clinical electrochemotherapy to other types of tumors (i.e. orthotopic tumors: brain, liver and other) the needed equipment (i.e. generators, electrodes, software) and the treatment planning methods are being developed. Numerical models of local electric field distribution in tumors and its surrounding healthy tissue can serve as an important tool in optimization of parameters (i.e., applied voltage, the shape, size and placement of electrodes with respect to the target tissue) needed for the successful therapy outcome and can play an important role in treatment planning of electrochemotherapy.

Gene electrotransfer – electroporation based gene therapy and vaccination

Gene therapy is a technique for correcting defective genes responsible for disease development. Gene vaccination is a vaccine approach used to induce an immune response to an antigen protein expressed *in vivo*, which can be used against infectious agents such as hepatitis B virus or human immunodeficiency virus-1.

The delivery of genes to the target tissue can be carried out by viral or non-viral transfection. In spite of the high efficiency viral methods have several disadvantages. Namely, vector interacts with the immune system, which can cause fatal consequences, such as premature death or incidences of leukemia [Ferber, 2001]. Electroporation has been shown to be one of the most efficient and simple non-viral methods for gene transfer into target tissue provided appropriate electrical parameters are chosen [Mir, 1999; Mir, 2001].

The first studies showing an efficient *in vitro* gene transfection by electroporation pulses were published in 1982 [Neumann *et al.*, 1982; Wong and Neumann, 1982]. Since then a large body of evidence was collected showing that the gene electrotransver is efficient in both *in vitro* and *in vivo* systems [Gehl, 2003, *Mir at. al.* 2005, Prud'homme *et al.*, 2006, Andre *et al.*, 2008]. First *in vivo* studies on gene electrotransfection were published in 1991 by Totimirov and colleagues [Titomirov et al, 1991]. In 1996 *in vivo* studies on gene electrotransfection were reported by Heller and colleagues (liver tissue) [Heller *et al.*, 1996] and by Nishi and colleagues (brain tumor) [Nishi *et al.*, 1996]. Two years later high gene transfection level using trains of long pulses (5 to 50 ms) was demonstrated in muscle [Mir *et al.*, 1998, Aihara and Myazaki, 1998], in melanoma tumors [Rols *et al.*, 1998], and in liver [Suzuki *et al.*, 1998].

Since than, efficient *in vivo* gene electrotransfer has been shown in a wide variety of tissues (e.g., tumors, muscle, liver, skin and other organs such as retina, kidney, lung, brain etc.) [Gehl and Mir, 1999; Jaroszeski *et al.*, 1999; Mir *et al.*, 1999; Bettan *et al.*, 2000; Payen *et al.*,

2001; Zhang *et al.*, 2002; Kesmodel and Spitz, 2003; Khan *et al.*, 2005; Zampaglione *et al.*, 2005]. The majority of studies have used trains of several pulses (3 to 10) of milliseconds to tens of milliseconds duration. Several studies on muscle tissue proposed the use of a pulsing protocol, consisting of a high-voltage, permeabilizing pulse, followed by a low-voltage, electrophoretic pulse [Mir *et al.*, 1998; Mir *et al.*, 1999; Bureau *et al.*, 2000; Satkauskas *et al.*, 2002; Satkauskas *et al.*, 2005, Hojman *et al.*, 2008].

Experiments on disease models showed that gene electrotransfer can be equally applicable to small and large animals (e.g. rodents, dogs, farm animals and primates). Gene electrotransfer has also been performed in humans and it seems likely it could be applied clinically for nonviral gene therapy and vaccination [Prud'homme *et al.*, 2006]. The results of the first clinical trials with gene electrotransfer to tumors and muscle tissue have been published in 2006 [Heller *et al.*, 2006]. The most recent results obtained in ongoing clinical trials (Phase I) in patients with metastatic melanoma were published in 2008 by Daud and colleagues [Daud *et al.*, 2008].

Since the electroporation based gene therapy and vaccine are cost-effective and easily implementable methods of administration they can be useful for treatment of cronic diseases where patients must be treated for years of even for their whole lifetime. These two methods might especially be of great help in developing countries also for treatment of severe viral diseases such as HIV or HCV and malaria infections, which currently represent major health concerns [Perez *et al.*, 2004].

Numerous preclinical studies in various species (including mice, guinea pigs, rabbits and rhesus macaques) reported promising results of electroporation based DNA vaccination for AIDS, Hepatitis B and C, herpes virus, tuberculosis, and malaria [Otten et al., 2004, Rosati et al., 2008, Golzio, 2009 [www.cliniporator.com/ect/proceedings]] and several clinical trials are currently under way [http://clinicaltrials.gov].

The timeline illustrating the evolution of *in vivo* gene electrotransfer from the report by Sale and Hamilton [Sale and Hamilton, 1967] and the first *in vitro* gene electrotransfection report by Neumann and colleagues [Neumman *et al.*, 1982] to the latest clinical trial report by Daud and colleagues [Daud et al, 2008] is shown in Figure 5b.

In order to assure optimal conditions for electroporation based gene therapy and vaccination (i.e. reversible and safe electroporation just above the reversible threshold value E_{rev}) the electrical parameters (such as applied voltage, electrode shape and position) need to be carefully selected [Gehl and Mir, 1999, Gehl *et al.*, 1999, Miklavic *et al.*, 2000]. Namely, for successful gene electrotransfer and expression the target muscle tissue need to be permeabilized so as not to affect the viability of the cells – target muscle tissue need to be reversibly permeabilised with local electric field just above E_{rev}. Analysis of tissue electroporation by means of numerical modeling (i.e. calculation and visualization of local electric field distribution) is reported to be of great importance in also the selection of the appropriate electrical parameters for gene electrotransfer [Gehl *et al.*, 1999, Miklavic *et al.*, 2000].

1.5 Aims-Objectives of doctoral theses

The appropriate local electric field distribution in the treated tissue is one of the most important conditions that need to be met for an effective electroporation based therapy or treatment to be successful as well as *in vivo* experiments in both humans and animals to be adequately designed. Currently, local electric field distribution can not be visualized during the electroporation based therapy or treatment. Therefore it is of outmost importance to *a priori* select the appropriate parameters and to 'design' the appropriate local electric field distribution for each particular therapy, treatment or experiment. Visualization of the spatial distribution of local electric field distribution can be effectively carried out with numerical calculations using realistic numerical models (i.e. numerical or analytical models of biological tissues validated on corresponding *in vivo* experiment). Development of realistic mathematical models thus plays an important role in the prediction of successful outcome of an electroporation based therapy, treatment or experiment.

In order to develop a good realistic model the knowledge and experience exchange from different scientific fields, involved in electroporation based therapies and treatments, is needed, which can be successfully assisted by using web-based e-learning systems.

The aims of this doctoral thesis cover three important issues in the development of electroporation based technologies and treatments:

1. development of realistic numerical models of different tissues (i.e. muscle, tumor and skin) and calculations and visualization of local electric field distribution in the models;

2. validation of the realistic numerical models by *in vivo* experiments; and

3. development of a web-based interactive e-learning application on electroporation based technologies and treatments such as electrochemotherapy.

1.5.1 Calculations and visualization of the local electric field distribution in realistic numerical models of cutaneous and subcutaneous tumors

According to the Standard Operating Procedures [Mir, 2006] the protocol for electrochemotherapy is the delivery of electroporation pulses (square wave electric pulses, duration of 100 µs, frequency of 1 Hz or 5 kHz) by parallel plate to the superficial cutaneous tumors and by needle electrodes (needle row for small tumors and hexagonal centered for larger tumors) to the more deeply seeded tumors, which was defined based on results of ESOPE clinical trials [Marty *et al.*, 2006]. However, the amplitude to be applied on the electrodes is defined as amplitude over distance ratio: 1300 V/cm for plate and 1000 V/cm for needle electrodes, both regardless of tumor properties (its shape, position and electric properties). Moreover the geometry of electrodes (electrode dimensions, number of electrodes, distance between electrodes) currently used in clinics also can not be changed.

The goals of further development of clinical electrochemotherapy are the therapy of tumors of internal organs (i.e. brain, liver and other), as well as the refinement of the existing protocols for the improvement of the response rate of cutaneous and subcutaneous tumor treatment (including bigger – larger than 3 cm in diameter and thicker than 0.5 cm) by treatment planning for each individual case of tumor.

In addition to a sufficient amount of chemotherapeutic drug, for successful electrochemotherapy, it is of crucial importance to create a local electric field sufficiently strong (above E_{rev}) to induce electropermeabilisation of the entire tumor volume and consequently allow the chemotherapeutic drug to enter all tumor cells, without damaging the surrounding healthy tissue ($E > E_{irrev}$) and without causing painful sensations. In order to achieve the effective therapy treatment outcome, an appropriate placement and shape of electrodes and amplitude of voltage pulses need to be selected with respect to the position, shape and electric properties of target/tumor tissue as well as with respect to the properties of

surrounding tissue. Our hypothesis is that the precise targeting of the tumor cells with a sufficient amount of chemotherapeutic drugs can be assured with the appropriate parameters selected based on calculation of local electric field distribution within the treated tissue. Namely, tumors can be seeded in different layers of the skin and can be arbitrarily shaped. In addition, electric conductivities of tumor tissue are usually higher compared to the surrounding tissues.

The aim of our study is to develop realistic numerical models of cutaneous tumor in order to investigate the influence of different placements of parallel plate electrode against the cutaneous tumor tissue on the electrochemotherapy outcome. The development of the models is based on *in vivo* experiments in animals using bleomycin. Based on this we demonstrate that the electrode placement for successful electrochemotherapy outcome can be determined in advance based on calculation and visualization of local electric field in a realistic tumor model. We further systematically compare local electric field distribution for different electrode geometries and voltage applied used in clinics and research in the past years with the aim to show which parameters are important for further refinement of protocols used in electroporation based therapies and treatments (such as electrochemotherapy). One of the aims of this thesis was also to build 3D finite element numerical models of differently shaped and positioned tumors tissues. The results of our study are aimed to provide guidance to practitioners as to choose the most sutable electric parameters (such as the amplitude of electroporation pulses and electrode configuration – plate or needle, electrode placement, number and insertion) in order to perform the treatment as precisely as possible: to target the tumor with $E > E_{rev}$ and destroy all tumor cells, while minimizing electrically induced damage to the healthy tissue and avoiding pain sensations. Our results are also aimed to provide relevant parameters needed in treatment planning development of realistic tumors based on calculation and visualization of local electric field in realistic numerical models.

1.5.2 Calculations and visualization of the local electric field distribution in realistic numerical models of muscle tissue

Skeletal muscle is one of the most attractive tissues for administration of therapeutic genes by electroporation for both local and systemic gene therapy, for genetic vaccination against infectious agents as well as for basic research of muscle physiology, due to a number of its biological properties such as relatively easy access the skeletal muscles, long term stable transgene expression and excellent vascularisation [Mathiesen, 1999; Umeda, 2004; Perez *et al.,* 2004; Hojman *et al.*, 2007; Tevz *et al.*, 2008]. In order to assure optimal conditions for gene therapy and genetic vaccination, the electrical parameters (such as applied voltage, electrode shape and position) need to be chosen to assure reversible and safe muscle electroporation just above the reversible threshold value [Gehl and Mir, 1999, Gehl *et al.*, 1999, Miklavcic *et al.*, 2000]. For successful gene electrotransfer and expression, the target muscle tissue need to be electropermeabilized so as not to affect the viability of the cells. Therefore, the critical electroporation thresholds (E_{rev} and E_{irrev}) are necessary parameters for the selection of appropriate electric parameters and design of local electric field distribution. So far, the electroporation thresholds (E_{rev} and E_{irrev}) of local electric field for muscle have not been detected based on realistic 3D models of muscle and only a few studies have dealt with detection of the threshold as applied voltage U divided by distance between electrodes d (U/d). Gehl and colleagues experimentally determined threshold of the ratio U/d *in vivo* using ^{51}Cr-EDTA electroporation indicator and numerical calculations of the electric field distribution in two dimensions [Gehl *et al.*, 1999]. Cukjati and co-workers experimentally determined the threshold values of the U/d ratio needed for electropermeabilization of the muscle tissue employing ^{51}Cr-EDTA electroporation indicator and electric current measurements [Cukjati *et al.*, 2007]. Pavselj and colleagues compared the experimental results obtained in [Cukjati *et al.*, 2007] to the numerical calculations with a 3D numerical

model of cutaneous tumor by using parallel plate electrodes, so that the electric field was parallel to the muscle fibers and determined the thresholds for muscle being tumor underlying tissue [Pavselj *et al.*, 2005].

The aim of the doctoral thesis was to develop realistic numerical models of skeletal muscle and to numerically and experimentally study muscle tissue electroporation for two different orientations of the electric field with respect to the muscle fibers: parallel and perpendicular. Namely, our aims were to determine electroporation thresholds (E_{rev} and E_{irrev}) of local electric field of the muscle tissue needed for both orientations, to detect successfully electroporated region of muscle tissue and to determine the influence of muscle tissue structure and electrode placement on muscle electroporation.

One of the aims was also the development of realistic numerical models of muscle in order to examine the influence of skin on muscle electroporation. For the model validation we used *in vivo* experiments performed with ^{57}CrEDTA and by total electric current measurements [Cukjati *et al.*, 2007]. The results obtained in this part of our study are aimed to help defining protocols for selection of electrical parameters, based on local electric field distribution, which is needed in gene electrotransfer.

1.5.3 Development of a web-based e-learning application on electroporation based therapies and treatments such as electrochemotrapy and gene electrotransfer

Development of a realistic mathematical model, designing an *in vivo* experiment or performing of an electroporation based therapy and treatment require a complete understanding of the tissue electroporation mechanisms. For example in order to assure a successful electrochemotherapy or gene electrotransfer a suficient amount of chemotherapeutic drug or therapeutic gene need to be provided, decisions on route of administration, anesthesia, and eligibility of patients need to be made and appropriate electric parameters need to be chosen, which requires a complete knowledge from different scientific

fields: biology, medicine, chemistry and biomedical engineering. Web based technologies and e-learning systems are useful tool for the knowledge dissemination, which can very effectively provide the knowledge and experience flow within the scientific fields involved.

Our aim in this part of doctoral thesis was to develop a web based learning application to provide and support collaboration, knowledge and experience exchange among experts involved in electrochemotherapy and to apply the acquired knowledge to other electroporation based therapies and treatments. The aim of this part was also to evaluate the pedagogical efficiency and usability of the developed e-learning application.

Our web-based distance learning application brings together the educational material providing basic mechanisms underlying electroporation process on the levels of cell membrane, cells and tissues and the basic background of electrochemotherapy and gene electrotransfer. The application is especially aimed at providing the knowledge about the parameters of local electric field being important in electroporation based therapies and treatments.

1.6. Methodology and background theory

1.6.1 Calculation and visualization of the local electric field distribution in biological tissue

1.6.1.1 Experimental methods

In order to detect cell electroporation *in vivo* it is necessary to use a non-permeant marker (i.e. an electroporation marker) that will enter and label the successfully electroporated cells. For a successful electroporation detection the viability of the electroporated cells needs to be preserved, thus a local electric field (E) between reversible and irreversible electroporation thresholds ($E_{rev} < E < E_{irrev}$) needs to be established. If the E does not exceed E_{rev} the electroporation marker does not enter the cells (as the cell membrane is not electroporated), while an E above E_{irrev} permanently damages the cells, thus the electroporation marker leaks out of the cells (as the cell membrane do not reseal). Several electroporation markers have been used as marker molecules for *in vivo* electroporation detection such as: Bleomycin [Belehradek *et al.*, 1994], [51]CrEDTA [Gehl *et al.*, 1999, Cukjati *et al.*, 2007], (99m)Tc-DTPA [Engstrom *et al.*, 1999], PI - Propidium Iodide [Rols *et al.*, 1998], and Gd-DTPA [Leroy-Willig *et al.*, 2005]. The electroporation *in vivo* can be detected also by impedance spectroscopy measurements [Ivorra and Rubinsky, 2007] and *in vivo* measurements of voltage applied and total electric current flowing through tissue (i.e. the *I/U* measurements) [Cukjati *et al.*, 2007].

In order to determine the electroporation threshold values based on direct comparison of local electric field distribution visualized in the realistic numerical models to the *in vivo* observations, the tissue geometry in *in vivo* experiments need to be preserved, otherwise the information about the local electric field distribution (i.e. electroporated tissue region) in the tissue is lost. In our study of muscle tissue electroporation we used two *in vivo* methods which enabled us to preserve the tissue geometry during the experiment: i. propidium iodide uptake

detection [Rols *et al.*, 1998] and ii. magnetic resonance imaging of contrast agent Gd-DOTA internalized into the electroporated cells [Leroy-Willig *et al.*, 2005]. Propidium iodide fluorescence observed under the microscope allows the determination of successfully permeabilized region of the treated tissue, which in turn allows us to locate the local electric field distribution above the critical reversible threshold value E_{rev} in the tissue and to compare the obtained results to the numerical calculations. Similarly, magnetic resonance imaging of a contrast agent Gd-DOTA that selectively enters only the electroporated cells allows the determination of successfully electroporated volume of the treated muscle. The *in vivo* experimental methods and determination of the electroporation thresholds for skeletal muscle tissue based on our realistic numerical models are described in **Paper VI**. We also used *in vivo* experimental data of skeletal muscle electroporation obtained with [51]CrEDTA and the *I/U* measurements for determination of electroporation threshold values based on our numerical models described in the **Paper V**. For validation of our models of cutaneous tumor tissue and *in vivo* confirmations of numerically predicted electrochemotherapy outcome we used bleomycin molecule [**Paper III**].

1.6.1.2 Analytical methods

The analytical solution of electric field distribution in biological tissues is only possible for regularly shaped geometries. The most important limitation of the analytical approach are that the problem to be solved often need to be restricted to two dimensions. In addition, analytical models assume uniform electric tissue properties (i.e. tissue electric conductivity), while most tissue exhibit some degree of inhomogeneity. However, the analytical solutions can provide a convenient, rapid, but approximate method for a pre-analysis of electric field distribution in treated tissue [**Paper I**].

Analytical calculations – plate electrodes

Analytical solution for the electric field between two infinite parallel plate electrodes gives a trivial solution $E = U/d$, where d is the distance between the electrodes and U is the applied voltage on the electrodes. The electric field strength E is constant in the entire region between infinite electrodes.

Analytical calculations – needle electrodes

Krasowsska and colleagues [Dev *et al.*, 2003] showed that for electrostatic problem analytical solution for the potential and the electric field also around the needle electrodes in 2D can be obtained by solving Laplace equation, if the needle penetration depth is larger than the distance between the electrodes. If we consider Laplace equation of a complex analytic function for a given region:

$$\Delta\phi(z) = 0$$

where $z = x + iy$, we obtain that the real part of this function Re $(\Phi(z))$ is also a solution of the Laplace equation. The potential can be written as a sum of multipoles of all electrodes, details are given in reference [Dev *et al.*, 2003]. If higher terms in multipole series are neglected we can write the potential as a sum of the leading terms of all n electrodes:

$$\phi(z) = \sum_{n=1}^{N} C_N \log \frac{a}{z - z_n} + C_0$$

where a is the radius of an electrode, z_n is the position of the n-th electrode and the coefficients Cn are determined from the boundary conditions. The above approximation can be used when $a << d$ (needle electrodes are not too thick compared to typical inter-electrode

distance). From Eq. 2 we can obtain the electric field strength from calculating the gradient of the potential:

$$E(z) = \sum_{n=1}^{N} C_N \frac{1}{z - z_n}$$

1.6.1.3 Numerical methods

Most biological systems have intricate geometries, along with material nonhomogeneities and anisotropies, which means numerical methods are a more suitable option for studying the effects of electromagnetic fields on cells, tissues and organs.

Numerical calculations (by using finite element method) of electric field distribution in realistic mathematical models, validated by adequate experimental results, can be used as an effective approach for 3-dimensional visualization of electric field distribution and thus, for detection of the level of tissue electropermeabilisation, as reported in numerous studies [Miklavcic *et al.*, 1998, Miklavcic *et al.*, 2000, Sel *et al.*, 2005, Pavselj *et al.*, 2005, Miklavcic *et al.*, 2006]. The *in vivo* experiments are necessary for development of realistic numerical models, however once the model is built experimenting and electroporation outcome planning is easier and faster than performing *in vivo* experiments (when they are not necessary). In order to investigate the influence of all the parameters on the effectiveness of electroporation process *in vivo* experiments need to be carried out on a large number of animals. In addition, most of experimental methods can be time-consuming since the results can only be collected after several days. Moreover, *in vivo* experiments are permitted to be performed only in specialized laboratories. When experimenting on the models, we can easily change the parameters such as distance between electrodes, number and arrangement of electrodes by modifying geometry parameters of the model or the amplitude of the applied electroporation pulses by applying different boundary conditions of the model.

Finite element method

For the numerical calculations we used finite element method [Chandrupatla and Belegundu, 1997]. The finite elements method turned out to be a very useful method for solving partial differential equations when studying electric field distributions inside biological systems. The essence of the method is the discretization of the geometry into smaller elements – finite elements – where the quantity of interest is approximated with a simple function or is assumed to be constant throughout the element. Material properties inside a finite element are homogeneous. Mathematically, the finite element method is used for finding an approximate solution of partial differential equations as well as of integral equations.

We built our numerical models by using COMSOL Multiphysics® simulation environment which is based on finite element method and facilitates all steps in the modeling process such as defining geometry, specifying physics, meshing, solving and post-processing of the obtained results [COMSOL Multiphysics 3.5a].

1.6.2 Modeling of electrical response and electric properties of tissues exposed to electroporation pulses

1.6.2.1 Calculation of electric field distribution in biological tissue

Electrical response of biological tissue exposed to high voltage electroporation pulses can be theoretically described with equations for constant direct electric field (DC) conductive media.

Namely, for any material whose electric properties are in the range of those of biological tissues or organs and its dimensions do not exceed 1 m and the frequency of the electric field stays below 1 kHz, the electrical behavior in any given moment as a response to electric current can be described with a set of equations describing stationary fields (i.e. quasi-stationary analysis). The electric current field thus induced is not a source field (has no sources nor drains), which can be described with the following equation [Sinigoj, 1996]:

$$\oint_A \vec{J} \cdot d\vec{A} = 0 , \qquad \text{(Eq. 2.1)}$$

where A is a closed surface enclosing the volume V and J represents the current density vector (in units: A/m^2).

Ohm's law applies, and can be written in differential equation as:

$$\vec{J} = \sigma \cdot \vec{E} \qquad \text{(Eq. 2.2)}$$

where E is the vector of the electric field (in units: V/m), inducting the electric current in the material (free charge displacement).

Electric field is defined as a negative gradient of the potential u (in units: V):

$$\vec{E} = -\nabla u \qquad \text{(Eq. 2.3).}$$

As in the case of electrostatic conservative field the potential u (T) in any point of space T (x,y,z) is equal to the path integral of the electrostatic field from an arbitrary reference point

T_0 until the point $T(x,y,z)$). Voltage difference U_{12} between two points T_1 and T_2 in space can be defined as a difference of potentials V defined in these two points:

$$U_{12} = u(T_1) - u(T_2) = \int_{T_1}^{T_2} \vec{E} \cdot d\vec{l} \quad \text{(Eq. 2.4)}$$

The conductivity of the material (in units: S/m) can in general (in the case of an anisotropic conductor) be represented with a tensor:

$$\vec{J}_i = \sum \sigma_{ij} \cdot \vec{E}_j \quad \text{(Eq. 2.5)}$$

$$\sigma_{ij} = \begin{bmatrix} \sigma_{xx} & \sigma_{xy} & \sigma_{xz} \\ \sigma_{yx} & \sigma_{yy} & \sigma_{yz} \\ \sigma_{zx} & \sigma_{zy} & \sigma_{zz} \end{bmatrix} \quad \text{(Eq. 2.6)}$$

The equation 2.1 can be written as:

$$\nabla \cdot \vec{J} = 0 \quad \text{(Eq. 2.7).}$$

Using Ohm's law, it transcribes into:

$$\nabla \cdot \left(\sigma \cdot \vec{E} \right) = 0 \quad \text{(Eq. 2.8)}$$

Combining equation 2.8 with the definition of the electric field (equation 2.3), we get:

$$\nabla \cdot \left(\sigma \cdot \left(-\nabla u \right) \right) = 0 \quad \text{(Eq. 2.9)}$$

In the case of a homogeneous isotropic material (constant σ) we get a Laplace differential equation:

$$\nabla^2 u = 0 \quad \text{(Eq. 2.10),}$$

or:

$$\nabla^2 u = \frac{\partial^2 u}{\partial x^2} + \frac{\partial^2 u}{\partial y^2} + \frac{\partial^2 u}{\partial z^2} \quad \text{in the volume } V \quad \text{(Eq. 2.11).}$$

The equation 2.11 is an elliptic partial differential equation that in combination with the boundary conditions:

$$u = \bar{u} \quad \text{on the surface } S_1 \quad \text{(Eq. 2.12)}$$

and the derivation u in the direction of the normal vector:

$$q = \frac{\partial u}{\partial n} = \overline{q} \text{ on the surface } S_2, \quad \text{(Eq. 2.13)}$$

defines the mixed or Robin's problem, where:

$$S = S_1 + S_2, \quad \text{(Eq. 2.14)}$$

is the surface enclosing the volume V. When only the first boundary condition is given (the equation (2.12)), we are dealing with the Dirichlet boundary condition, while, when we know the derivation from the equation 2.13, we have the Neumann boundary condition.

1.6.2.2 Electric properties of modeled tissues and their response to electroporation pulses

In order to study the response of biological tissues to electrical stimulus, data on their electric properties are needed. In practice, biological materials exhibit characteristics of both, insulators and conductors, because they contain dipoles as well as charges which can move. On a microscopic level electric properties of the tissues can be described with their passive electric properties such as electric conductivities and relative permittivity. The electrical properties can depend on several factors such as the tissue orientation relative to the applied field (directional anisotropy), the frequency of the applied field (the tissue is neither a perfect dielectric nor a perfect conductor), or they can be time and space dependent (e.g., changes in tissue conductivity during electroporation). The results of electric conductivity measurements that have been published indicate that the impedance at frequencies less than 100 Hz is almost entirely resistive and that the capacitive component accounts for only around 10% in most tissues; between 100 Hz and 100 kHz most tissues show almost no frequency-dependence. [Miklavcic *et al.*, 2006]

An extensive *in vivo* study on animal tissue response to electroporation pulses showed that the capacitive component of the tissue is present only at the beginning of the pulse while after the

transient the electroporated tissue exhibit only the ohmic behavior [Cukjati *et al.*, 2007]. The typical responses (by the electric current measured) of the target tissue to the applied electroporation pulses is shown in Figure 6. If the amplitude of the applied voltage is not high enough to permeabilize the tissue (i.e. the local electric field in the tissue does not exceed E_{rev}) after the transient the electric current decreases and stabilizes at the constant value Figure 6a. When an EP voltage pulse is applied, sufficient to permeabilize the tissue (i.e. the local electric field in the tissue exceeded E_{rev}) after the transient the electric current start to increase indicating tissue permeabilization has been occurred (Figure 6b).
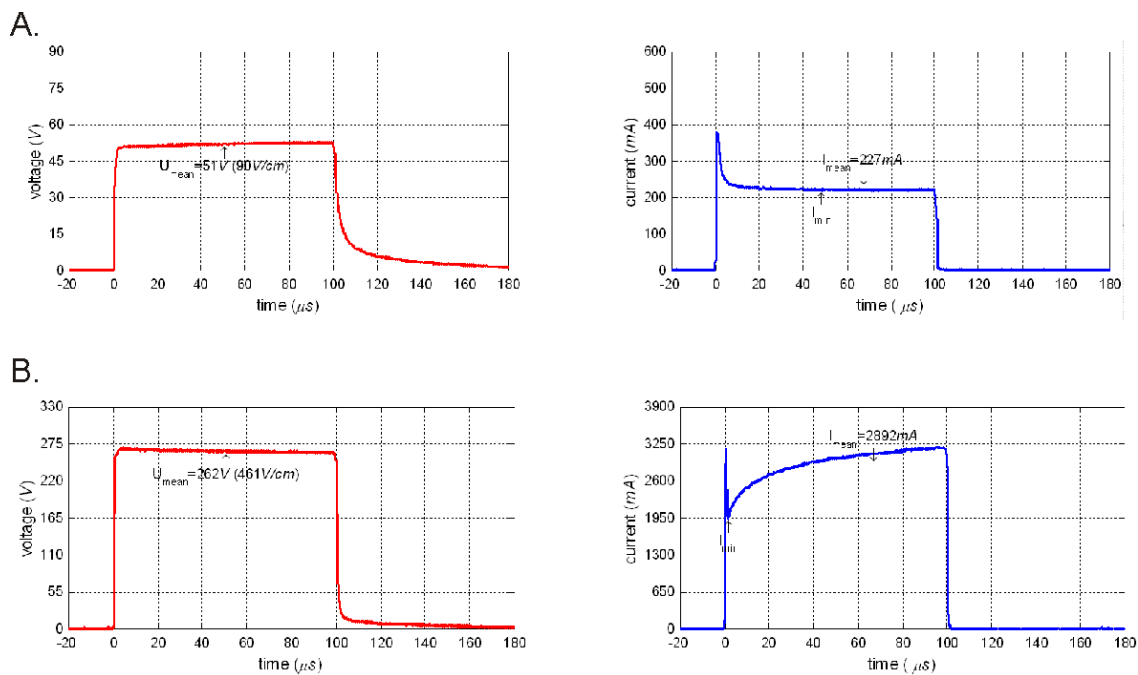

Figure 6: A. Applied voltage pulse and the measured electric current in the situation when the permeailization was not achieved; B. Applied voltage pulse and measured electric current flowing through permeabilized tissue

In our numerical models ohmic tissue behavior was analyzed i.e. tumor, muscle and skin electric conductivities σ [S/m] of these tissues were analyzed. In our present study only ohmic behavior of biological tissues exposed to electroporation pulses was analyzed, i.e. only electric conductivities σ [S/m] of tumor, muscle and skin tissue were taken into account.

In the following subsection we briefly present the electric properties of the modeled tissues: skeletal muscle, tumor, and skin.

Electric properties of skeletal muscle tissue

Muscle tissue is composed of fibers (i.e. very large individual cells aligned in the direction of muscle contraction). Muscle tissue exhibits typical anisotropic electric properties since the electric current flows more easily along the muscle fibers than through the extracellular space between the muscle fibers due the poor conductivity of the muscle cell membranes. Therefore measured electric properties at low frequencies depend on the position of electrodes on the muscle tissue and subsequently on the orientation of the electric field with respect to the long axis of the muscle fibers. Parallel and transversal position of the electrodes and corresponding orientation of the electric field with respect to the orientation of the long axis of the muscle fibers is illustrated in Figure 7. Muscle tissue is considered anisotropic conductor, being more conductive along the muscle fibers compared to the directions perpendicular to the muscle fiber. The results of electric conductivity measurements at low frequencies in the literature are usually presented separately for the transverse and longitudinal directions. The longitudinal electric conductivity of the muscle is significantly higher then the transverse conductivity (Table 2).
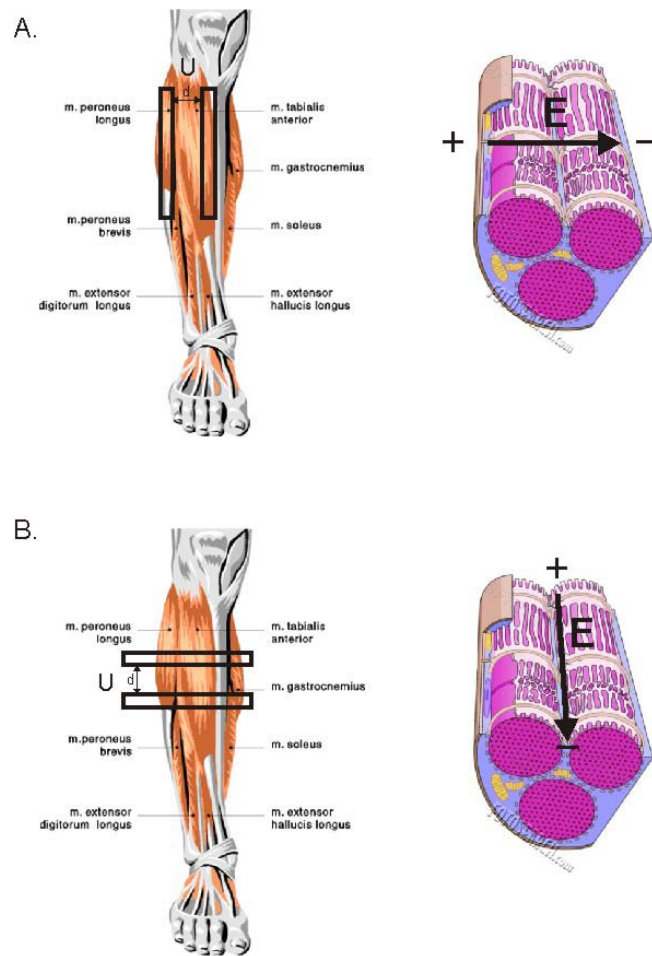
Figure 7: Muscle tissue anisotropy: A. electrodes are placed parallel to the long axis of the muscle fibers (electric field is oriented perpendicularly to the muscle fibers) and B. electrode are placed perpendicularly to the long axis of the muscle fibers (electric field is oriented parallel to the muscle fibers).

Electric properties of tumor tissue

Tumor tissue is an abnormal tissue surrounded by one or more healthy tissues. Tumors usually have higher water content than normal cells due to the cellular necrosis and irregular vacsularisation, which contributes to significantly different electrical properties from the surrounding healthy tissues. Electric conductivity of tumor tissue is usually higher then the conductivity of the surrounding healthy tissue [Smith *et al.*, 1986, Surowiec *et al.*, 1988, Haemmerich *et al.,* 2009]. For example, a study by Smith et al. on tumors in liver tissue showed that tumor electric conductivity is 6–7.5-fold higher than the liver conductivity. In addition, large differences in electric conductivities exist between different tumor types (i.e.

carcinoma, sarcoma, melanoma, teratoma) and even between tumors of the same type, as electrical properties of tumor tissue depend on its structure (portion of necrotic cells, water content, vascularisation), on the size and geometry or the development stage of the tumor. An example of a mastectomy specimen containing a very large cancer of the breast (in this case, an invasive ductal carcinoma) is shown in Figure 8. In spite of the tumor inhomogeneities at the microscopic level the macroscopic properties of tumors can be analyzed as a bulk homogeneous structure [Pavselj *et al.*, 2005]. In the literature measured bulk electric properties of the tumor tissues are given as single values.

Figure 8: Breast cancer: A large invasive ductal carcinoma in a mastectomy (the surgical removal of one or both breasts, partially or completely) specimen. [http://en.wikipedia.org/wiki/File:BreastCancer.jpg]

Electric properties of skin tissue

Skin is composed of three primary layers: the epidermis, dermis, and subcutis. Skin tissue anatomy is illustrated in Figure 9. The epidermis is the outer layer of skin and contains different layers. This layer provides waterproofing and serves as a barrier to infections. The top part of the epidermis (i.e. *stratum corneum*) is composed of dead, flat skin cells which are constantly shed (about every two weeks). Although the *stratum corneum* is very thin (typically around 20 mm) it contributes a great deal to the dielectric properties of the skin due to its very high electric resistivity (i.e. very low electric conductivity). Its main function is protection of the body from the external environmental factors. Underneath the dead cells are

live squamous cells, and under these are basal cells which are constantly reproducing. Below the epidermis is the dermis which contains tiny blood and lymph vessels and gives firmness and elasticity, and the subcutis, hence subcutaneous tissue composed of fat, connective tissue, larger blood vessels, and nerves. The dermis and subcutis have much lower resistivities compared to the epidermis. Especially in the low-frequency range (under 10 kHz); the impedance of skin is dominated by the *stratum corneum* even though this layer is very thin. Studies show that, for frequencies less than 10 kHz, the share of *stratum corneum* in the total impedance of skin is around 50%, but at 100 kHz drops to around 10%.

In our models skin tissue was considered isotropic and homogeneous. Since the skin tissue was not primary target of our investigation different layers of skin were not modeled; instead the average conductivity was assigned to the modeled skin. Namely, large differences in skin layers geometry would unnecessarily increase the computational time of numerical simulations while not contributing to the accuracy of the electric field distribution in the muscle and tumor tissue [Pavselj *et al.*, 2005].
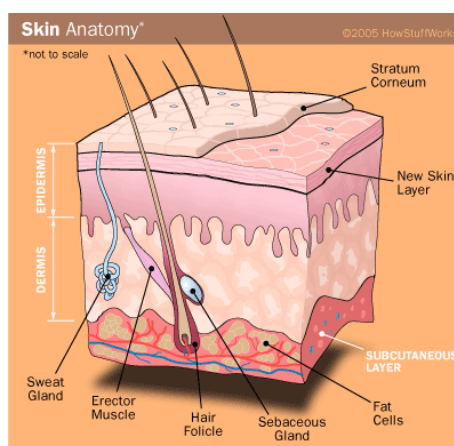

Figure 9: The illustration of skin tissue anatomy

1.6.2.3 Modeling of electroporation process in biological tissue - sequential analysis

In our numerical models ohmic tissue behavior was analyzed i.e. tumor, muscle and skin electric conductivities σ [S/m] of these tissues were analyzed. Before applying EP pulses or if the amplitude of the applied EP pulses was too low to produce the local electric field above the reversible electroporation threshold ($E < E_{rev}$) the tissues were modeled as linear conductors with linear current-voltage $I\ (U)$ relationships due to the constant tissue conductivities. The initial prepulse values of conductivities (corresponding to $E < E_{rev}$ condition) used in numerical models were selected from the available literature [Miklavcic *et al.*, 2006] (Table 2).

Table 2: Electric conductivities of muscle tumor and skin tissue found in the literature [Miklavicic *et al.*, 2006]

biological tissue		electric conductivity [S/m]
muscle	transversal	0.04 - 0.14
	longitudinal	0.3 - 0.8
tumor		0.22 - 0.4
skin (dry)		0.00002 - 0.0002
skin (wet)		0.0003 - 0.2
skin - stratum corneum		0.0000125
skin - lower layers		0.227

If the local electric field in the tissues exceeded the E_{rev} value the tissue electric properties change i.e. tissue conductivity increases due to the electroporation process. During the application of electroporation pulses the tissue conductivity increases according to the functional dependency of the tissue conductivity on the local electric field distribution $\sigma(E)$, which in our study describes the dynamics of the electroporation process. This subsequently results in nonlinear electric current of the applied voltage $I(U)$. From the deviation of $I(U)$ from the linear relationship $I = U / R$ (where R [Ohm] is tissue electric resistance), due to the change of σ, we detected the threshold electroporation E_{rev}.

The tissue electroporation dynamics in our models was modeled based on the sequential permeabilization model, proposed by Sel and colleagues [Sel *et al.*, 2005], where changes in tissue conductivity were used as an indicator of tissue permeabilization. For this purpose, a sequence analysis subprogram was developed to model the dynamics of electroporation as a discrete process with sequence of static finite element models, where each of them describes process at one discrete interval (each of the discrete intervals relates to a real discrete, but undetermined time interval). In each static model in sequence the tissue conductivity was determined based on electric field distribution from previous model in sequence, as described by equation 3:

$$\sigma\ (k) = f\ (E(k\text{-}1))\ , \qquad\qquad (Eq.3)$$

where k stands for number of static finite element models in sequence.

Model input is the applied voltage pulse and model outputs are the electric field distribution E and total electrical current I in each specific sequence k. The modeled tissue behavior during the electroporation pulse delivery is illustrated in Figure 10. The increase of electrical current I from I_0 to I_k simulates the tissue response during the delivery of the electroporation pulses U, in each discrete interval k (static finite element model in sequence), to the tissue electroporation (i.e. due to the functional dependency of the σ on the electric field distribution E). If the electroporation does not occur σ remains constant, thus $I = I_0$. The sequence analysis subprogram gives us a choice of different $\sigma(E)$ relationships.
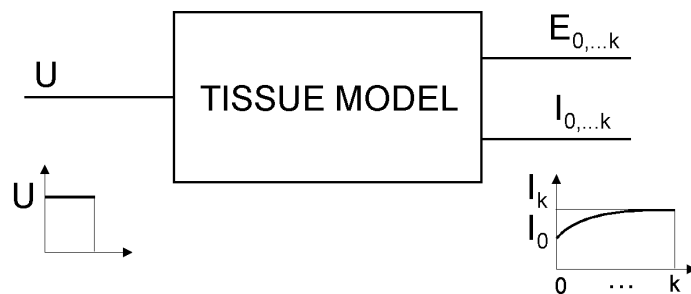

Figure 10: The modeled tissue behavior during the eletroporation pulse delivery, where U is the amplitude of the electroporation pulses delivered to the tissues. E is the electric field strength and I is the total electric current calculated in each sequence, where k is the number of the sequences corresponding to the duration of the electroporation pulses.

1.6.2.4 Electric properties of complex tissues and their changes during electroporation

The target tissue in the body is surrounded by one or more tissues having different electric conductivities and geometries. When *U* is applied*,* the local electric field is distributed within the complex tissue according to its specific electric properties (acting as a voltage divider), meaning that the electric field is highest in the layer with the highest electric resistivity (i.e. lowest conductivity) [Pavselj *et al.*, 2008]. When the skin becomes permeabilized, its conductivity increases according to the function *σ(E)*, which leads to the electric field redistribution in the skin and its underlying more conductive tissues (in our case muscle tissue). If *U* is too low, the highest electric field remains in the skin layer and does not reach the muscle Figure 11a. Due to the skin electroporation, an increase of skin conductivity reduces its electric resistance and consequently reduces electric field intensity in the skin which results in increased electric field intensity in the muscle, provided that a sufficient voltage is applied, as shown in Figure 11b.
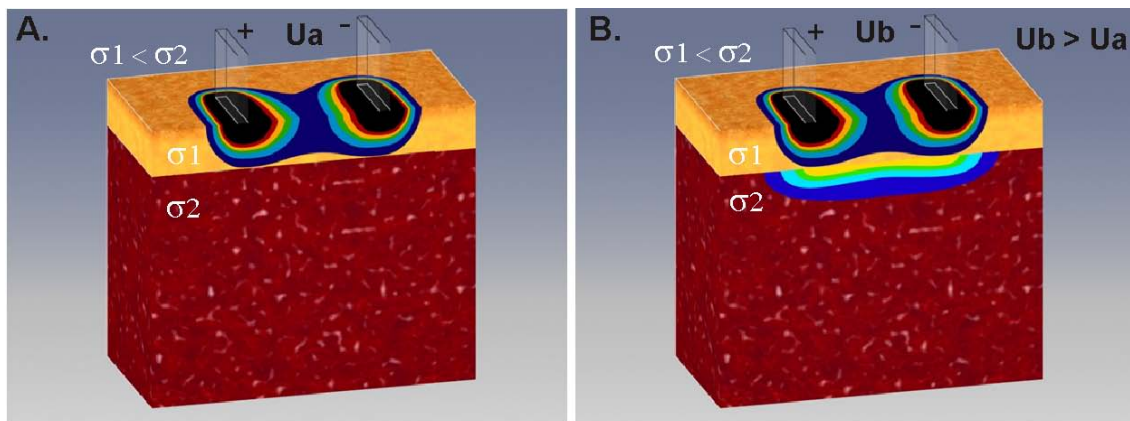
Figure 11: Local electric field distribution E in a complex tissue (skin with a conductivity σ_1 and underling more conductive tissue with σ_2 ($\sigma_1 < \sigma_2$)): A. the local electric field above E_{rev} remains only in the skin- the applied *Ua* is too low to allow the penetration of the sufficient E into deeper tissue below the skin and B. higher applied voltage (*Ub > Ua*) increases the local electric field in the tissue below the skin

1.6.3 Development of a web-based learning application

The e-learning programs that incorporate computer based simulations and visualization tools enable educationally most effective learning and teaching method such as hands-on learning (named also learning by doing or action-learning) as demonstrated by educationist Edgar Dale [Dale, 1969]. During the 1960s, Dale's research led to the development of the Cone of Experience, a widely cited model related to instructional design and learning processes, showing that learners retain more information by what they "do" as opposed to what is "heard", "read" or "observed". The average retention rate for various methods of teaching is given in Figure 12 (left).
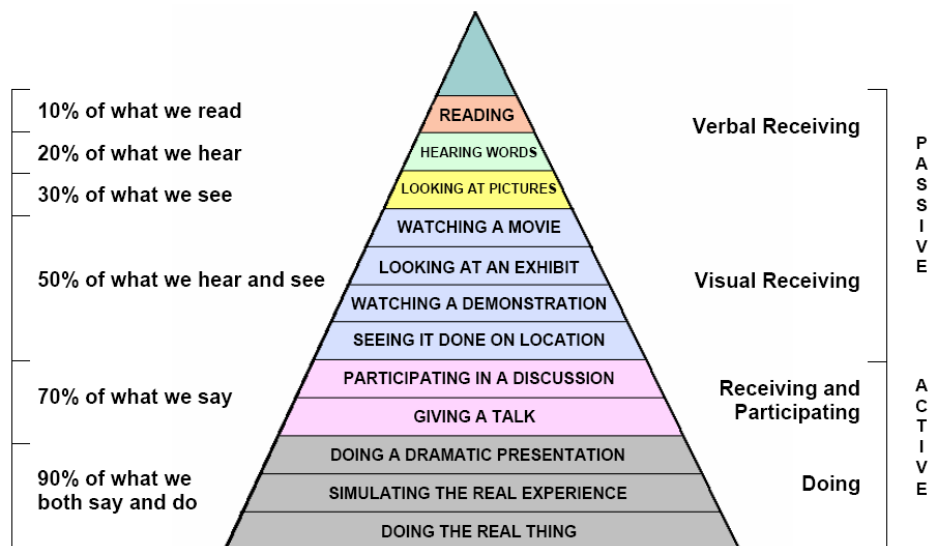
Figure 12: The Cone of Experience [Dale, 1969]

According to Dale's research (Figure 12), the least effective method at the top, involves learning by reading and learning from information presented through verbal symbols, i.e., listening to spoken words (resulting in 10% - 20% retention). The further the learners progress down the cone, the greater the learning and the more information is likely to be retained. The most effective methods at the bottom, involve direct, purposeful learning experiences, such as hands-on experience (doing the real thing). It reveals that "hand-on learning" techniques

result in up to 90% retention. It also suggests that when choosing an instructional method it is important to remember that involving learners in the process strengthens knowledge retention. Accordingly, in our the e-learning application, we developed an interactive module for visualization of local electric field distribution in treated tissues for different parameters such as voltage applied, electrode' dimension, geometry and position, treated tissue geometry and its electric properties (i.e. electric conductivity). We used computer graphics such as model-based visualization (i.e. 3D numerical modelling using finite element method) and 3D computer animations and graphical illustrations to facilitate the representation of complex biological and physical aspects in electrochemotherapy. The interactive content allows for hands-on learning on how the aforementioned parameters can modify the local electric field distribution within the treated tissue. The application also provides a tool to help practitioners make decisions about electrochemotherapy treatment.

The e-learning application is integrated into an interactive e-learning environment developed at our institution, enabling collaboration and knowledge exchange among the users. We evaluated the designed e-learning application at the International Scientific workshop and postgraduate course (Electroporation Based Technologies and Treatments [www.cliniporator.com/ect]). The evaluation was carried out by testing the pedagogical efficiency of the presented educational content and by performing the usability study of the application. The e-learning application and results of pedagogical efficiency and usability study are described in [**Paper IV**: Corovic *et al.*, 2009]

2. Results

In this chapter we outline the results on the three important aspects in the development of electroporation based technologies and treatments, according to the aims of our study:

i)   development of realistic models of different tissues (i.e. muscle, tumor and skin) and calculations and visualization of local electric field distribution in the models;

ii)   validation of the models by *in vivo* experiments and

iii)   development of a web-based interactive e-learning application on electroporation based technologies and treatments.

The detailed results will be presented in the form of published papers in SCI (Science Citation Indexed) journals in the same order as listed in the Preface chapter of the doctoral thesis.

The results of modeling and visualization of local electric field distribution presented in the **Papers I**, **II**, **VII**, **XII** demonstrate the importance of relevant parameters that has to be taken into account for development of realistic tissue models and optimization of local electric field in the models. In **Papers III**, **V** and **VI** we present results of realistic numerical modeling validated on experimental *in vivo* results according to first two aims of our study (tumor model-**Paper III**, muscle model with and without skin-**Paper V**, muscle model-**Paper VI**). In **Papers VIII** and **XI** we demonstrate that calculation and visualization of local electric field distribution in 3D can be successfully used in electrode design for *in vivo* and *in vitro* settings, respectively. In the **Paper X** we built 3D numerical models of cutaneous and subcutaneous tumors and calculated local electric field and total electric current in order to evaluate safety level of electroporation when electrochemotherapy is performed on tumors

localized on the torso close to the heart muscle. For the muscle electroporation thresholds we used the values we determined in the **Papers V** and **VI**. And in **the Paper IV** we present a web-based learning application we developed according to the third aim of our study.

In the **Paper XIV** we present developments of the digital clinical report file (CRF) that were integrated in the web-application allowing for collection of the results of the clinical trials to the central database. The clinical trials were performed in four approved medical centers in Europe, funded by European Community in a frame of ESOPE project (2003-2004) with the aim to define Standard Operating Procedures (SOP) for electrochemotherapy. In the **Paper XV** we review commercially available electrodes and electroporators with their parameters and biological applications as suggested by manufacturers.

In the **Paper IX** we review electroporation assessment methods; we describe basic principles of modeling and analysis of cell and tissue electroporation *in vivo* and list its applications (The paper is written in Slovenian with an abstract in English language).

In the **Paper XIII** we describe basic principles of cell and tissue electroporation and importance of numerical modeling in electroporation based therapies and treatments. We review main applications of electroporation in medicine with special emphases on clinical electrochemotherapy (The paper is written in Serbian language with an abstract in English language).

To briefly summarize the results related to the goals of the doctoral thesis:

In **Paper I** we present results of systematic quantification and comparison of local electric field in the tissue for most widely used electrode configurations (plate and needle) in electrochemotherapy and gene electrotransfer in past years. We analytically and numerically calculate and visualize local electric field distribution inside an example of modeled treated tissue (spherical target tissue and its surroundings) in 2D for the plate and needle electrode

configurations and compared the local electric field distribution to parameter *U/d*, which is widely used parameter in currently defined electroporation protocols. We show that the parameter *U/d* can differ significantly from the actual calculated values of the local electric field inside both homogeneous tissue and in tissue with more conductive target tissue compared to its surroundings. We showed dependency of local electric field distribution on the electrical parameters such as applied voltage on the electrodes, electrode placement with respect to the target tissue, electrode shape (plate or needle), number of electrodes, and distance between electrodes. We demonstrated that the local electric field in the treated tissue can be successfully controlled by the aforementioned electrical parameters. Furthermore, our results also demonstrate that local electric field is influenced by electric properties of the target tissue and its surroundings.

In the **Paper II** we extend the 2D numerical study to 3D numerical study i.e. calculation, visualization and optimization of local electric field distribution in spherical subcutaneous tumor treated with needle electrodes' configuration used in clinics and research in past years. The results show that voltage applied, distances between electrodes and depth of electrode insertion are all relevant for the control of local electric field distribution in the model and all four parameters were chosen for the optimization procedure. Our results have show that parallel array electrodes are the most suitable for the spherical tumor geometry, because the whole tumor volume is subjected to sufficiently high electric field while requiring the least electric current and causing the least tissue damage. However, the tumor needs to be completely encompassed between the electrodes.

In the **Paper VII** we performed calculation, visualization and optimization in 3D numerical models of subcutaneous tumors models of different shapes and sizes (a sphere and two ellipsoids) and a realistic brain tumor model acquired from medical images. In all tumor cases, parallel needle electrode arrays were a better choice than hexagonal needle electrode

arrays, since their utilization required less electric current and caused less healthy tissue damage.

In the **Paper XII** we demonstrate the importance of tumour coverage by sufficiently high local electric field for succsesful electrochemotherapy ($E > E_{rev}$). We namely compare the results of numerical calculation and visualization we obtained in 3D models of cutaneous and subcutaneous tumors when using plate and needle electrodes, for the same amplitude applied. The results show that by using plate electrodes better coverage by sufficiently high local electric field is achieved in models of protruding cutaneous tumors, and that the needle electrode configurations were more suitable for sufficient coverage of subcutaneous tumors.

In **Paper III** we develop a realistic 3D numerical model of cutaneous protruding tumor and showed the importance of contact surface between parallel plate electrodes and the treated tissue. Larger contact surface resulted in complete coverage of target tumor tissue with local electric field above reversible electroporation threshold. The predicted numerical results were confirmed with *in vivo* results using bleomycin: the placement of electrodes giving larger electrode-tissue contact surface leads to improved electrochemotherapy outcome (i.e. higher complete response rate).

In **Paper V** we present realistic numerical models of skeletal muscle tissue electroporated directly and transcutaneously, which we developed in order to investigate influence of skin on muscle electroporation. The numerical calculations are validated on *in vivo* experimental results using [51]CrEDTA indicator. We found the functional dependency of tissue conductivity on electric field intensity $\sigma\ (E)$ to be exponential for skin with electroporation thresholds E_{rev} = 480 V/cm and E_{irrev} = 1050 V/cm and sigmoid for muscle tissue with E_{rev} = 240 V/cm and E_{irrev} = 430 V/cm. The same electroporation threshold values E_{rev} and E_{irrev} were found for both muscle electroporated directly and transcutaneously, demonstrating that the skin layer has no influence on the thresholds that the local electric field intensity itself is important for

successful muscle tissue electroporation. But it does require higher voltage to be applied between the electrodes when muscle is electroporated transcutaneously.

In **Paper VI** we present a realistic 3D numerical model of the mouse *tibialis cranialis* muscle (electroporated directly i.e. with skin removed) that we developed in order to experimentally and numerically investigate muscle electroporation for parallel and perpendicular orientation of the applied electric field with respect to the muscle fibers using parallel plate electrodes. The agreement between numerically calculated results and experimental observations validated our 3D model. The electroporated muscle regions were visualized with two *in vivo* methods: magnetic resonance (Gd-DOTA) and fluorescence imaging (propidium iodide). We present the first results of different electroporation thresholds with respect to electrode vs. tissue orientation for the tissue with anisotropic electric properties; we determined the electroporation threshold values (pulse parameters: 8 x 100 μs, 1 Hz) to be 80 V/cm and 200 V/cm for parallel and perpendicular orientation, respectively.

In **Paper VIII** we present results of numerical calculations of local electric field distribution for the electrode commutation sequence for multiple needle electrodes developed for electrochemotherapy of larger tumours. For this an electrode commutation circuit was developed, which commutates to multiple electrodes the usual electroporation single output signal from an electroporator. We used seven-needle electrodes, for which we suggested and tested an effective electrode commutation sequence for tissue electroporation. We developed a 3D finite-elements model of tumour tissue with inserted seven-needle electrodes (honeycomb arrangement) according to specifications of *in vivo* electrochemotherapy experiment in order to model local electric field distribution and electric conductivity changes in tumour tissue during the electroporation process. We calculated the corresponding local electric field distribution in 3D model of tumour tissue by taking into account the increase of tissue conductivity due to electroporation in order to demonstrate also theoretically that the

entire tumour volume is exposed to sufficiently high electric field leading to tissue permeabilization and efficient electrochemotherapy. Electrochemotherapy, performed by multiple needle electrodes and tested pulse sequence on large subcutaneous murine tumours resulted in tumour growth delay and 57% complete responses, thus demonstrating that the tested electrode commutation sequence is efficient and confirming the results we predicted by numerical modeling.

Numerical calculation and visualization of local electric field distribution in 3D can also be successfully used in electrode design for *in vitro* settings, as we demonstrated in **Paper XI**. The results obtained with our numerical modeling supported design of new electrodes for *in vitro* gene electrotransfection integrated into the new system allowing for automatic changing of electric field direction. The aim of the research was to develop and test a new system and protocol that would improve gene electrotransfer by the automatic change of electric field direction between electrical pulses. We used finite-elements method to calculate and evaluate the electric field homogeneity between these new electrodes. Namely, we designed new electrodes made of four cylindrical rods that provides as homogeneous electric field distribution as possible. We calculated the distribution of electric field numerically for given electrode design and electric field protocol. New system and protocols were tested experimentally on Chinese Hamster Ovary cells. In-vitro gene transfection and cell survival were evaluated for different electric field protocols by fluorescence microscopy. The results showed that the new system can be used in *in vitro* gene electrotransfer to improve cell transfection by changing electric field direction between electrical pulses, without affecting cell survival. Changing the electric field direction between electrical pulses therefore improves the efficiency of gene electrotransfer indirectly by increasing the area of successful electropermeabilized membrane, or directly by interaction of DNA molecules with the cell membrane on both sides. In addition to the *in vitro* applications, the automatic change of

electric field direction between electrical pulses could be also useful in *in vivo* applications for successful electropermeabilization of the treated samples.

In **Paper X** the results of the study on the effect of electroporation pulses on functioning of the heart are presented. We built 3D numerical models of cutaneous and subcutaneous tumors and calculated local electric field and total electric current considering safety level of electoporation when electrochemotherapy is performed on tumors localized on the torso close to the heart muscle. The modeled conditions (i.e. needle row array, needle hexagonal array and plate configurations and voltages applied) were the same as actually used in clinical electrochemotherapy. We proposed safety protocols of depth of insertion of needle electrodes and distance between plate electrodes for reversible and irreversible electroporation and fibrillation of cardiac muscle. We also calculated the critical depth for electric field of 200 and 450 V/cm (value for reversible and irreversible electroporation of the muscle, respectively), and the critical depth for current of 100 mA (threshold for ventricular fibrillation for 500 μs-long electrical stimulus). Of the total electric current flowing through the tissue during the EP pulse delivery, no more than 100 mA (the threshold value for fibrillation) is allowed to flow through the heart. Therefore we defined the critical depth as a distance from the surface of the body (at the site of EP delivery) below which the total electric current flowing is equal to this threshold value.

In **paper IV** we present a web-based learning application on electroporation based therapies and treatments. We developed, implemented and tested an e-learning application by using web based e-learning technologies to support collaboration, knowledge and experience exchange among experts involved in electrochemotherapy and to also apply the acquired knowledge to other electroporation-based technologies, according to the objective of the doctoral thesis. The educational content on electrochemotherapy and cell and tissue electroporation was based on previously published studies from molecular dynamics, lipid

bilayers, single cell level and simplified tissue models to complex biological tissues and research and clinical results of electrochemotherapy treatment. We evaluated the pedagogical efficiency and usability of the developed e-learning application and presented the obtained results.

In **Paper XIV** a web-application that extends functionality of medical device for tumor treatment by means of electrochemotherapy is presented. The web-application was developed in order to collect, store and allow the analysis of electrochemotherapy clinical trials performed during the testing period of medical device Cliniporator™. The clinical trials were performed in four approved medical centers in Europe, funded by European Community in the frame of ESOPE project (2003-2004) with the aim to define Standard Operating Procedures (SOP) for electrochemotherapy. The developed web-application allowed for collection of the results of the clinical trials to the central database through the digital clinical report file (CRF) we developed based on web technologies such as ASP, HTML, Flash, JavaScript, XML and others. Namely, through digital clinical report file (CRF) clinicians from all four centers submitted general data about the patient (demography, medical history, physical examination...etc.), the tumor treatment protocol and tumor treatment response data to the central database. Based on the data (i.e. results of the clinical trials) collected a detailed analysis was performed, which contributed to the definition of the standard operating procedures (SOP) for clinical electrochemotherapy of cutaneous and subcutaneous tumors.

In the **Paper XV** we present an overview of commercially available electroporators and electroporation systems that were described in accessible literature. Namely, efficiency of electroporation based applications strongly depends on parameters of electric pulses that are delivered to the treated object using specially developed electrodes and electronic devices — electroporators. Our results are presented as:

i)   a list of commercially available electrodes with their properties and biological applications suggested by manufacturer and

ii)   a list of commercially available electroporators with their parameters, biological applications and possible signal generation technique.

Paper I

BioMedical Engineering OnLine

Research

Analytical and numerical quantification and comparison of the local electric field in the tissue for different electrode configurations

Selma Čorović, Mojca Pavlin and Damijan Miklavčič*

Address: University of Ljubljana, Faculty of Electrical Engineering, Ljubljana, Slovenia

Email: Selma Čorović - selma.corovic@fe.uni-lj.si; Mojca Pavlin - mojca.pavlin@fe.uni-lj.si; Damijan Miklavčič* - damijan.miklavcic@fe.uni-lj.si

* Corresponding author

Abstract

Background: Electrochemotherapy and gene electrotransfer are novel promising treatments employing locally applied high electric pulses to introduce chemotherapeutic drugs into tumor cells or genes into target cells based on the cell membrane electroporation. The main focus of this paper was to calculate analytically and numerically local electric field distribution inside the treated tissue in two dimensional (2D) models for different plate and needle electrode configurations and to compare the local electric field distribution to parameter *U/d*, which is widely used in electrochemotherapy and gene electrotransfer studies. We demonstrate the importance of evaluating the local electric field distribution in electrochemotherapy and gene electrotransfer.

Methods: We analytically and numerically analyze electric field distribution based on 2D models for electrodes and electrode configurations which are most widely used in electrochemotherapy and gene electrotransfer. Analytical calculations were performed by solving the Laplace equation and numerical calculations by means of finite element method in two dimensions.

Results: We determine the minimal and maximal *E* inside the target tissue as well as the maximal *E* over the entire treated tissue for the given electrode configurations. By comparing the local electric field distribution calculated for different electrode configurations to the ratio *U/d*, we show that the parameter *U/d* can differ significantly from the actual calculated values of the local electric field inside the treated tissue. By calculating the needed voltage to obtain *E > U/d* inside the target tissue, we showed that better electric field distribution can be obtained by increasing the number and changing the arrangement of the electrodes.

Conclusion: Based on our analytical and numerical models of the local electric field distribution we show that the applied voltage, configuration of the electrodes and electrode position need to be chosen specifically for each individual case, and that numerical modeling can be used to optimize the appropriate electrode configuration and adequate voltage. Using numerical models we further calculate the needed voltage for a specific electrode configuration to achieve adequate *E* inside the target tissue while minimizing damages of the surrounding tissue. We present also analytical solutions, which provide a convenient, rapid, but approximate method for a pre-analysis of electric field distribution in treated tissue.

Background

Electroporation, also termed electropermeabilization, is a phenomenon where increased permeability of cells exposed to an external electric field is observed. The induced transmembrane voltage presumably leads to the formation of aqueous pores in the phospholipid bilayer, which increases the permeability of the cell membrane for water-soluble molecules and ions [1-4]. Electropermeabilization is currently widely used in vivo and in vitro in many biological and medical applications including electrochemotherapy of tumors (ECT) [5-7], transdermal drug delivery [8,9] and gene electrotransfer [5,10-14].

Electropermeabilization is a phenomenon, where the membrane becomes permeable after the magnitude of the electric field (E) exceeds reversible threshold value (E_{rev}), while E below E_{rev} does not significantly affect the cell membrane. When the magnitude of local electric field E reaches irreversible threshold value (E_{irrev}), electric field causes permanent damages on the cell membrane leading to cell death. The threshold values, E_{rev} and E_{irrev} vary for different tissues in range from 200–400 V/cm and 450–900 V/cm, respectively [15-19]. Electropermeabilization with E in the range of $E_{rev} \leq E < E_{irrev}$ reversibly permeabilizes the cell membrane and at the same time does not affect the viability of a biological cell. Reversible electropermeabilization has been proven to be successful in electrochemotherapy, where electric field enables chemotherapeutic drug to enter into tumor cells, and for gene electrotransfer, which can be used for gene therapy, where electric field enables DNA to enter the target cells. Irreversible electroporation with $E > E_{irrev}$ was suggested for water treatment and food preservation as a method for destruction of the cell membrane of noxious microorganisms and for tissue ablation [20-22].

In this paper we focus on the importance of calculating the local electric field distribution for successful electrochemotherapy tumor treatment and gene electrotransfer of target cells. Namely, for successful electrochemotherapy it is crucial that all clonogenic cells forming tumor tissue are exposed to the local electric field above the threshold value E_{rev} and preferably below irreversible threshold E_{irrev}. Similarly, successful gene electrotransfer also requires local electric field in the range of reversible electroporation regime ($E_{rev} \leq E < E_{irrev}$). It was previously shown by combining numerical modeling and experimental approaches that the efficacy of the electrochemotherapy and gene electrotransfer treatment depends on the magnitude of the local electric field inside the target tissue [17,18,23-28].

However, both threshold values (E_{rev}, E_{irrev}) differ for electrochemotherapy and gene electrotransfer as well as they depend on pulse parameters and the type of treated tissue.

From the theoretical principles it follows that the local electric field inside the tissue is in general a function of time and place $E(x, y, z, t)$. However, since most often electric pulses used in electrochemotherapy and gene electrotransfer are usually long (0.1 – 10 ms) compared to the typical constant for the polarization of the cell membrane (around 1 μs), we can assume steady-state conditions for our analysis [29,30]. The local electric field distribution $E(x, y, z)$ in the tissue is a complex function of several parameters. It depends on the applied voltage on the electrodes, the geometry and position of the electrodes, and on the non-homogeneous properties and geometry of the tissue. For this reason electric field distribution during electroporation can not be solved analytically except for the most simple cases [31] and therefore numerical methods have to be used [16,25].

In principle there are two complementary approaches to determine the optimal electrode configuration and applied voltage to achieve appropriate local electric field inside the target tissue ($E \geq E_{rev}$). Ideally one should calculate E for each individual case taking into account all geometric details and electric properties of the treated tissue in order to assure appropriate local E inside the target tissue (i.e. pretreatment planning). However, this requires sophisticated numerical modeling for each individual problem and is in many cases not realistic. Alternatively some approximate estimates of E inside the target tissue are used, where usually a gross approximation U/d "electric field intensity" as defined and reported in a number of different reports [8-10,12,15,32-36] is used as an approximate value of E for plate as well as for needle electrodes.

Most of the experimental and clinical studies on electrochemotherapy were performed with the treatment protocol (applying eight 100 μs long pulses at the repetition frequency 1 Hz) using the parameter (U/d) from 1300–1500 V/cm to select applied voltage on the electrodes [26,37]. However, despite the fact that the parameter U/d is widely used in order to determine the applied voltage, this parameter alone does not give the information about the actual electric field inside the target tissue. It also makes difficult the comparison between different studies reported, especially since exact geometry is usually not given.

In this study we present an approach of local electric field evaluation, by means of 2D numerical and analytical models which can be used to determine the appropriate electrodes and electrode configurations and applied voltage in electrochemotherapy and studies of gene electrotransfer. We numerically and analytically compare $E(x,y)$ in 2D for different electrodes and electrode configurations which are used for in vivo electrochemotherapy and gene electrotransfer. We demonstrate that the calculated local

electric field inside the target tissue strongly depends on the chosen electrodes and electrode configuration and can be significantly different than the value U/d. In order to quantify and compare different electrode configurations we visualized the regions inside the treated tissue exposed to the local electric field exceeding the value U/d ($E \geq U/d$) keeping the value U/d for all configurations constant so that the electric field distribution can be directly compared between electrode configurations. In addition, we calculate the necessary voltage for a given electrode configuration in order to achieve adequate electric field distribution in the target tissue. We also demonstrated that changing electrodes' orientation and electrode arrangement with respect to the target tissue leads to better exposure of the target tissue to the adequate electric field distribution.

Methods
Numerical calculations
Numerical calculations were performed by means of finite element method (FEM) [38] using FEMLAB software packages Femlab 2.3 and 3.0 (Comsol, Sweden). The numerical calculations were performed on the personal computer Intel Pentium 4, 2.40 GHz CPU and 1 GB RAM. The electric field distribution in 2D models was calculated using the steady current module. We analyzed $E(x,y)$ for two parallel plate electrodes (Fig. 1) and different number (2, 4, 6 and 7) and configurations of needle electrodes as shown in Fig. 2. These configurations were chosen based on different reports [15,25,26,33,39–41] where such electrodes and electrode configurations were used in electrochemotherapy and gene electrotransfer in vivo experiments.

In all models the electrodes were positioned inside a square representing homogeneous tissue having a constant conductivity. A constant voltage was assigned to the grid points in regions where electrodes were placed, while insulation boundary conditions were set on the remaining boundaries. In all cases the constant voltage was applied between the electrodes giving U/d = 1.15 V/cm. The radius a of all needle electrodes was 0.215 mm. The distance d, defined as the distance between the positive
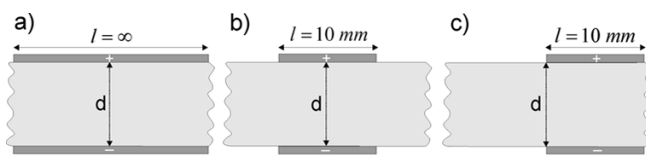
and the negative electrode, was $d = 5\sqrt{3}$ mm for configurations shown in Figs. 2a–2e, whereas in configurations shown in Figs. 2f and 2g we set $d = l = 5$ mm. The dimension of the outer square was 20 mm > $2d$ in all models, since it was already shown [31] that for model size (boundaries of the outer square) being $2d$ the error due to the finite size of the model is negligible.

Model geometries were meshed by triangular finite elements. The final mesh models were obtained refining the mesh until the discrepancies of the mean and maximum relative difference between numerical solutions, obtained with two different meshes were negligible. For example, for electrode configuration 2c the final mesh consisted of 86 944 elements. The results of this model were compared to the results obtained with the same electrode configuration but coarser mesh which consisted only of 21 736 elements. The relative difference of the mean and the maximum value of the electric field between the two models were 2.14 * 10^{-6} and 4.22*10^{-3}, respectively.

Analytical calculations – plate electrodes
Analytical solution for the electric field between two infinite parallel plate electrodes (Fig. 1a) gives a trivial solution $E = U/d$, where d is the distance between the
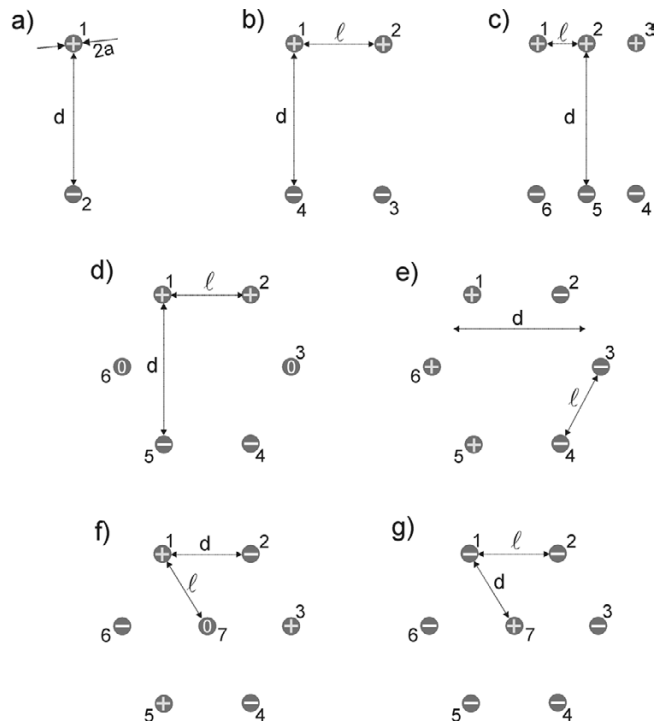

Figure 2
Different needle electrode configurations analyzed in this study.

Figure 1
Three geometries with parallel plate electrodes analyzed in this study (d = 8.66 mm).

electrodes and *U* is the applied voltage on the electrodes. The electric field strength *E* is constant in the entire region between infinite electrodes.

Analytical calculations – needle electrodes

As already shown [31], for electrostatic problem analytical solution for the potential and the electric field also around the needle electrodes in 2D can be obtained by solving Laplace equation, if the needle penetration depth is larger than the distance between the electrodes. If we consider Laplace equation of a complex analytic function for a given region:

$$\Delta\phi(z) = 0, \tag{1}$$

where $z = x + iy$, we obtain that the real part of this function Re $(\Phi(z))$ is also a solution of the Laplace equation. The potential can be written as a sum of multipoles of all electrodes, details are given in reference [31]. If higher terms in multipole series are neglected we can write the potential as a sum of the leading terms of all *n* electrodes:

$$\phi(z) = \sum_{n=1}^{N} C_n \log \frac{a}{z - z_n} + C_0, \tag{2}$$

where *a* is the radius of an electrode, z_n is the position of the n-th electrode and the coefficients C_n are determined from the boundary conditions. The above approximation can be used when $a \ll d$ (needle electrodes are not too thick compared to typical inter-electrode distance). From Eq. 2 we can obtain the electric field strength from calculating the gradient of the potential:

$$E(z) = \sum_{n=1}^{N} C_n \frac{1}{z - z_n}. \tag{3}$$

Results

The results of our study are organized in five subsections. The first and second subsections show the numerical and analytical results of the electric field distribution, respectively, for plate and needle electrodes as shown in Figs. 1 and 2. In the third subsection we present the comparison of the numerical and analytical results. In the next subsection we quantify the local electric field for given electrode configurations. Finally, in the last subsection we analyze the effect of tissue inhomogeneities on the local electric field distribution for the needle electrode configurations.

In order to compare and quantify the influence of geometry, number and position of different electrode configurations on the electric field distribution we used the same parameter $U/d = 1.15$ V/cm in all models. We present the calculated electric field with equal scale of *E* from 0 to 1.15 V/cm. The values of electric field strength are shown by colour scale legend (see Figs. 3 and 4) with the maxi-
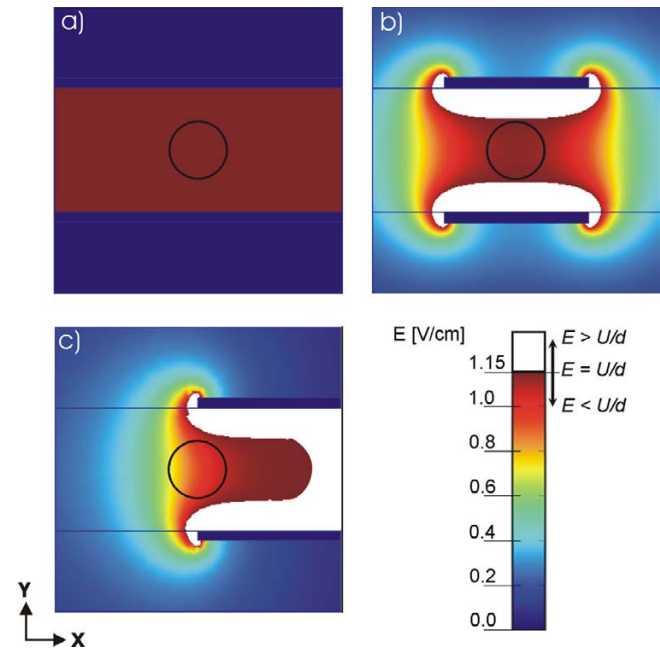

Figure 3
Calculated electric field distribution for the geometries with parallel plate electrodes. Numerical results of the electric field distribution for geometries defined in Fig. 1: a) the infinite plate electrodes case, b) the target tissue symmetrically placed between the finite plate electrodes and c) the non-symmetrical example when the target tissue is not entirely in-between the finite plate electrodes. The circle represents the target tissue e.g. tumor tissue and the white region represents part of tissue where $E \geq U/d$.

mal value representing the ratio $U/d = 1.15$ V/cm in order to demonstrate the region below (color scale) and above the value U/d (white region). The encircled region in Figs. 3a–3c and Figs. 4a–4e represent one of the possible geometries and positions of the target tissues. It is within this target tissue that the electric field needs to be sufficiently high ($E > E_{rev}$).

Electric field distribution between plate and needle electrodes – numerical results

All models were calculated for the voltage between two electrodes $U = (1$ V, 0.575 V) giving the value of parameter $U/d = 1.15$ V/cm, but values of *E'* for any other voltage can be obtained just by multiplying all values with given voltage *U'* divided by applied voltage *U* (1 V, 0.575 V). Namely, since our models are linear all results for *E* can be scaled for any arbitrary applied voltage *U'*: $E' = E U'/U$. In the following subsections we will present results obtained for $U/d = 1.15$ V/cm and scaled results for $U/d = 1300$ V/cm.
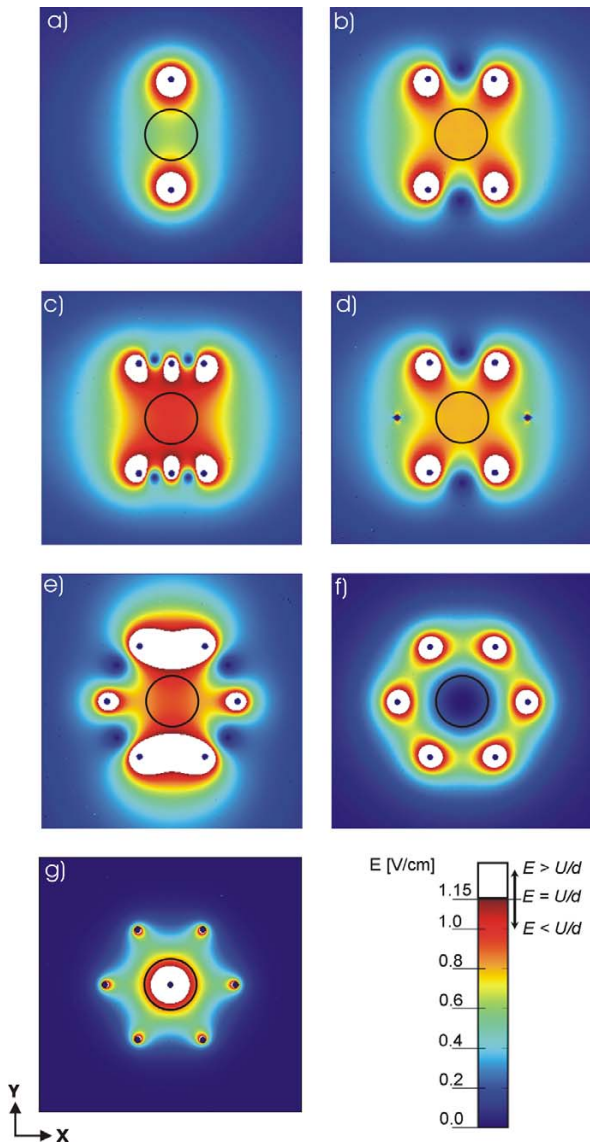
Figure 4
Calculated electric field distribution for different needle electrode configurations. Numerical results of the electric field distribution for the geometries defined in Fig. 2: a) two needle electrodes, b) four needle electrodes, c) six needle electrodes in two rows, d) six electrodes placed in a circle with polarities as shown in Fig. 2d, e) six needle electrodes placed in a circle with polarities as shown in Fig. 2e, f) seven needle electrodes placed in a circle – using alternating polarities seven needle electrodes placed in a circle – with central positive and surrounding electrodes having negative polarities and g) seven needle electrodes placed in a circle – with central positive and surrounding electrodes having negative polarities. In all cases the applied voltage was set in such a way that U/d = 1.15 V/cm, where d = 8.66 mm for Figs. 4a, 4b, 4c, 4d and 4e and d = 5 mm for Figs. 4f and 4g. The circle represents the target tissue and the white region represents part of tissue where $E \geq U/d$.

I.) Plate electrodes
Fig. 3 presents the comparison of electric field distribution of three different configurations of parallel plate electrodes for U = 1 V and d = 8.66 mm (U/d = 1.15 V/cm). For an ideal case with infinite parallel plate electrodes (Fig. 3a) we obtained constant electric field in the entire region between the electrodes. In Fig. 3b we can see that for a more realistic geometry, where finite electrodes are considered, the electric field between the electrodes is not constant and is decreased towards the central region. Furthermore, if we change the position of electrodes with respect to the target tissue (encircled region), as presented in Fig. 3c, the electric field inside the target tissue is further reduced. Only in the case of the infinite parallel plate electrodes, one can use the expression $E = U/d$, and only in this ideal case E is constant in the entire region between the electrodes (provided that the tissue between the electrodes is homogeneous).

II.) Needle electrodes
In Fig. 4 numerically calculated electric field distribution for different needle electrode configurations and different polarities are shown. The values of the distances between the needle electrodes d and l are shown in Table 1, and were chosen in a way to correspond to values of Dev et al. [31]. The applied voltage for all configurations was U = 1 V (d = 8.66 mm), except for configurations shown in Fig. 2g and Fig. 2f where U = 0.575 V (d = 5 mm) keeping the ratio U/d constant.

In Fig. 4 it can be clearly seen that the electric field distribution in the tissue strongly depends on the number, position and polarities of the electrodes. As expected the highest values of E are obtained in the vicinity of the electrodes. With increasing the number of electrodes the electric field strength inside the target tissue becomes higher. It can be seen that by using six or seven electrodes we can achieve a better distribution of E than by using only two or four electrodes. One can also observe that only a smaller part of the tissue is exposed to $E \geq U/d$ (white region), whereas in the other regions of tissue E is smaller then U/d.

In Figs. 4d and 4e we compare the distribution of E for two different sets of polarities for electrode configuration of six electrodes arranged in the circle as used by Gilbert and co-workers [26]. We obtained higher electric field inside the target tissue with electrode configuration shown in Fig. 4e (3 positive, 3 negative electrodes) compared to the electric field inside the target tissue with the electrode configuration shown in Fig. 4d (2 positive, 2 negative electrodes). For both configurations the specific electrodes' positions enables rotation of the electric field direction (by rotating the polarities of the electrodes for a given angle) thus achieving better coverage of the target

Table 1: The distances *d* and *l* between the needle electrodes as defined in Fig. 2.

Electrodes configuration	2 Fig. 2a	4 Fig. 2b	6 Fig. 2c	6 Fig. 2d, e	7 Fig. 2f, g
d [mm]	8.66	8.66	8.66	8.66	5
l [mm]	/	5	2.5	5	5

tissue with needed electric field. Comparing Figs. 4d to 4b we can also see that both electrode configuration results in equal electric field distribution, since the two electrodes with zero potential do not contribute to *E* distribution.

Figures 4f and 4g represent two examples of seven electrodes arranged in a circle with a central electrode having different polarities. We can see that in the first case (Fig. 4f) we obtain high intensity of the electric field in the ring around the electrodes surrounding the central region, whereas in the second case (Fig. 4g) we obtain high intensity of the electric field in the central region between the electrodes. Therefore by using combinations of these two different possibilities of setting the polarities of the electrodes we can successfully electropermeabilize all the tissue between the electrodes. However, by using only the configuration as shown in Fig. 4d the target tissue is not permeabilized.

Electric field distribution between plate and needle electrodes – analytical results
I.) Plate electrodes
Analytical solution for the electric field between two infinite parallel plate electrodes (Fig. 1a) gives a trivial solution $E = U/d$, where *E* is constant in entire region. In all other cases *E* between the electrodes is not constant: for finite dimensions of the electrodes (Fig. 1b) or if the target tissue is not set entirely between the plate electrodes as shown in Fig. 1c.

II.) Needle electrodes
Since the derivation using the leading-order solution for a problem with electrodes positioned as shown in Fig. 2b is already given in detail in [31] we present here the final solutions for different geometries as shown in Fig. 2. In all geometries we set the applied voltage *U* by setting the potential on the electrodes to $V_0 = \pm U/2$. Using the equation for the potential Eq.2 (leading order approximation)

$$\phi(\bar{r}) = \sum_{n=1}^{N} C_n \log \frac{a}{|\bar{r} - \bar{r}_n|} + C_0, \qquad (4)$$

and applying appropriate boundary condition (potential on the electrodes) we obtained the coefficients C_n, which are given in Appendix section. Taking the real part of Eq. 3 and solutions for C_n (Eqs. A.1-A.6) we obtained analyti-

cal expressions for the electric field strength for different geometries as shown in Fig. 2:

$$E(\bar{r}) = \sum_{n=1}^{N} C_n \frac{1}{|\bar{r} - \bar{r}_n|}. \qquad (5)$$

The presented analytical results are extensions of the analytical expression given by Dev et al. [31] for geometries given in Fig. 2 for arbitrary values of *d* and *l*, as well as for different polarities in case of seven electrodes, where $\bar{r}_n$ is the position of the *n*-th electrode as shown Fig. 2. Using the analytical expression for the electric field (Eq.5 and Eqs. A.1-A.6) we calculated electric field distribution *E* for different electrode configurations. These analytical results arevery similar to numerical results of electric field distribution shown in Fig. 4.

Comparison of the analytical and the numerical results
In our study both numerical results as well as analytical results were obtained. The analytical results were validated with the numerical calculations for given electrode configurations. In Fig. 5 we compare the analytical and numerical solutions for the geometry of six electrodes (Fig. 2c) of the electric potential $V(x,y)$ (a) and the electric field distribution $E(x,y)$ (b) along *y* axis (*x = 0*). We can see that a good agreement between numerical and analytical solution is obtained in the area between the electrodes, whereas the discrepancy between numerical and analytical solution increases outside the electrodes |y| > 4. The mean and maximal relative difference between numerical and analytical solutions of electric field strength inside the electrode array calculated between the electrodes (over all nodes within the area: |x| < 4 and |y| < 4) were less than 0.7 % and 3.9 %, respectively. Similarly, we obtained a good agreement for both, the potential and the electric field also for other presented geometries (results are not shown).

Since the differences between analytical and numerical results were negligible only numerical results are further analyzed and presented in figures.

Quantification of the local electric field
In order to further quantify and compare local electric field distribution within the tissue for different electrodes
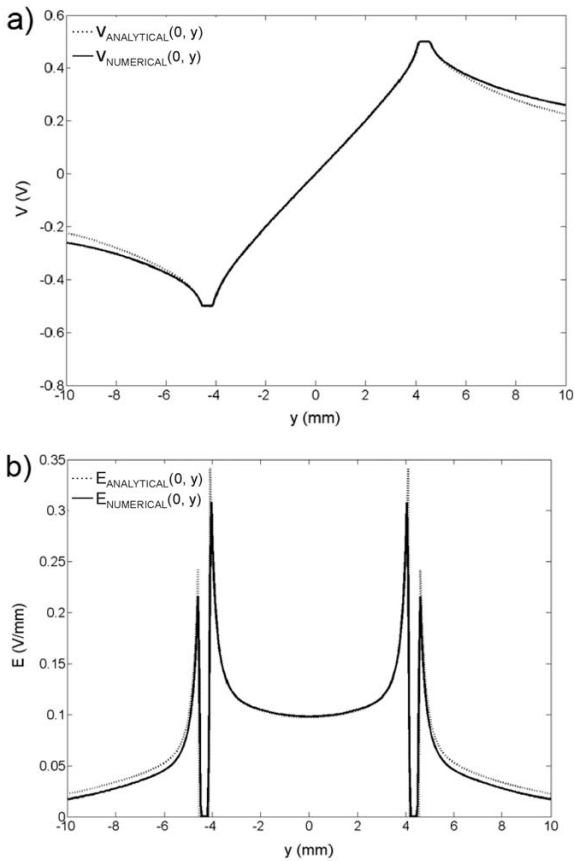
Figure 5
Comparison of the analytical and the numerical solution. The analytical and the numerical solutions of a) the electric potential and b) electric field distribution along *y* axis (*x* = 0) for applied voltage *U* = 1 V (*V_+* = 0.5 V, *V_-* = - 0.5 V) are given for the configuration defined in Fig. 2c.

and electrode configurations, as defined in Fig. 1 and Fig. 2, we calculated minimal Ett_{min} and maximal electric field strengths Ett_{max} inside the target tissue, as well as the high-

est value of *E* within entire tissue – E_{max}. These parameters are important for the optimization of electrochemotherapy and gene electrotransfer, namely Ett_{min} should be above E_{rev} while E_{max} should be as low as possible to prevent excessive damages of the surrounding tissue. Furthermore, we calculated the necessary voltage U_c which has to be applied to the electrodes in order to achieve successful electropermeabilization in the target tissue $Ett_{min} \geq E_{rev}$, where we used $E_{rev} = U/d$. Here we have to stress that we set the value $E_{rev} = U/d$ in order to compare our results of the local electric field distribution to the previously published studies which used the approximation U/d as an estimate of the local electric field in the treated tissue. The results of quantification of the parameters Ett_{min}, Ett_{max} and E_{max} for given electrode configurations are listed in Tables 2, 3, 4, 5.

I.) Plate electrodes
From Fig. 1 and Table 2 it can be seen that electric field is homogeneous ($Ett_{max}= Ett_{min}= E_{max}= U/d$) only for the model with infinite plate electrodes and can be calculated as the ratio $E = U/d$. As soon as we use more realistic electrodes having finite length *l* (see Fig. 1b), or realistic electrodes position with the respect to the treated tissue (see Fig. 1c), the electric field intensity within the tissue between the electrodes is no longer homogeneous. The values of Ett_{min} and Ett_{max} inside the target tissue have lower values from U/d whereas the E_{max} in the near proximity of the plate electrodes increases and are higher than ratio U/d (see Table 2). In Table 3 we give the results of necessary voltage U_c in order to obtain the condition $Ett_{min} > U/d$, needed for successful target tissue permeabilization. Based on this we can conclude that in realistic cases (see Figs. 1b and 1c) the value of U_c has to be higher compared to the value U_c in the homogeneous model (Fig. 1a) in order to effectively treat the entire target tissue.

II.) Needle electrodes
In Fig. 4 we compare electric field distributions calculated numerically using FEM method for different needle elec-

Table 2: Quantification of electric field strength for plate electrodes models – calculated Ett_{min}, Ett_{max} and E_{max} parameters.

2 plate electrode configuration	U/d = 1.15 V/cm			U/d = 1300 V/cm		
	Target tissue Ett_{max}(V/cm)	Target tissue Ett_{min}(V/cm)	Entire tissue E_{max}(V/cm)	Target tissue Ett_{max}(V/cm)	Target tissue Ett_{min}(V/cm)	Entire tissue E_{max}(V/cm)
(Fig. 3a)	U/d = 1.15	U/d = 1.15	U/d = 1.15	U/d = 1300	U/d = 1300	U/d = 1300
(Fig. 3b)	1.152	1.113	5.515	1297.0	1253.0	6209.0
(Fig. 3c)	1.081	0.691	5.533	1217.0	777.9	6229.2

Calculated minimal *E* (Ett_{min}) and maximal *E* (Ett_{max}) inside the target tissue and maximal *E* within the entire tissue E_{max} for different plate electrode configurations as defined in Fig. 1 are given. The results are given for applied voltage *U* = 1 V giving *U/d* = 1.15 V/cm and for applied voltage (scaled results) for *U* = 1125.83 V giving *U/d* = 1300 V/cm.

Table 3: Calculated values of U_c and corresponding Ett_{min}, Ett_{max} and E_{max} for plate electrodes.

2 plate electrode configuration	Target tissue Ett_{max}(V/cm)	Target tissue Ett_{min}(V/cm)	Entire tissue E_{max}(V/cm)	Needed voltage on the electrodes-U_c (V)
(Fig. 3a)	U/d = 1300	U/d = 1300	U/d = 1300	U = 1125.83
(Fig. 3b)	1345.8	U/d = 1300	6441.5	1168
(Fig. 3c)	2001	U/d = 1300	10242	1851

The needed voltage between the electrodes (U_c) was chosen in a way that the minimal electric field inside the target tissue exceeded U/d: $Ett_{min} \geq U/d$, thus assuring successful permeabilization of the entire target tissue.

trode configurations and polarities. In order to obtain the parameter U/d = 1.15 V/cm in all models we set the applied voltage $U = 1\,V(U/d = 1V/5\sqrt{3}$ mm for electrode configurations shown in Figs. 4a–4e and for models shown in Figs. 4f–4g for applied voltage U = 0.575 V (d = l = 5 mm) giving U/d = 1.15 V/cm.

As shown in Figs. 4d–4g, we obtained that by using several electrodes (six or seven electrodes in the circle) and changing the potential and polarity on the electrodes we can achieve better coverage of target tissue with adequate E. In the case of only two electrodes we can see that the E in the surrounding tissue can be too high and may cause irreversible damages (Fig. 4a). In the cases of two, four and six electrodes (Figs. 4a–4c) reversing the polarities does not change the electric field distribution. Nevertheless, reversing the polarity can improve electropermeabilization on the level of cell membrane since the orientation of the electric field determines which side of the cell will be more permeabilized [23,31,42-44].

In table 4 we compare different configurations of the needle electrodes. If we compare these values to the "electric field intensity" U/d, we can see that both maximal and minimal E deviate significantly from U/d value, which can

be seen also in Fig 4. The low values of Ett_{min} mean that some parts of the target tissue will not be permeabilized whereas some parts of the 0surrounding tissue might be exposed to too high values causing irreversible damage especially around the electrodes (too high E_{max}), which is most pronounced for the geometry with two needle electrodes. From Table 4 it can be seen that for four and six electrodes Ett_{min} increases while E_{max} decreases. We also calculated the needed voltage U_c (Table 5) which has to be applied on the electrodes in order to achieve the condition $Ett_{min} \geq U/d$ assuming target tissue permeabilization and as it can be seen from Table 5 the needed voltage U_c differs substantially for different needle electrode configurations. Namely, increasing the number of electrodes from two to six we can decrease the applied voltage U_c from 2467 V to 1427 V.

The effect of tissue inhomogeneities on the electric field distribution

In order to analyze possible effects of tissue inhomogeneities we made additional models where target tissue had increased conductivity which is based on the fact that the tumor tissue has in general higher conductivity than its surrounding tissue. Namely, from the literature [19,45] we determined that reasonable approximation for conductivity of the target (tumor) tissue is σtt = 0.4 S/m and

Table 4: Quantification of electric field strength for needle electrode models – calculated Ett_{min}, Ett_{max} and E_{max} parameters.

Needle electrode configuration	U/d = 1.15 V/cm			U/d = 1300 V/cm		
	Target tissue Ett_{max}(V/cm)	Target tissue Ett_{min}(V/cm)	Entire tissue E_{max}(V/cm)	Target tissue Ett_{max}(V/cm)	Target tissue Ett_{min}(V/cm)	Entire tissue E_{max}(V/cm)
2 (Fig. 4a)	0.804	0.527	6.618	905.4	591.7	7450.3
4 (Fig. 4b)	0.824	0.779	5.829	928.7	876.9	6562.5
6 (Fig. 4c)	1.049	0.911	5.166	1180.9	1025.2	5816.6
6 (Fig. 4d)	0.822	0.778	5.794	925.4	875.9	6523.1
6 (Fig. 4e)	1.064	0.835	7.443	1197.9	940.1	8379.6
7 (Fig. 4f)	0.21	~0	5.17	236.4	1.038	5820.8
7 (Fig. 4g)	8.1	0.84	8.1	9119.2	945.7	9119.2

The results for models shown in Figs. 4a – 4e were calculated for applied voltage U = 1 V ($d = 5\sqrt{3}$ mm) and for models shown in Figs. 4f – 4g for applied voltage U = 0.575 V ($d = l$ = 5 mm) giving U/d = 1.15 V/cm. Furthermore, by scaling the results we also calculated the parameters Ett_{min}, Ett_{max} and E_{max} for U/d = 1300 V/cm.

Table 5: Calculated values of U_c and corresponding Ett_{min}, Ett_{max} and E_{max} for needle electrodes.

Needle electrode Configuration	Target tissue Ett_{max}(V/cm)	Target tissue Ett_{min}(V/cm)	Entire tissue E_{max}(V/cm)	Needed voltage on the electrodes-U_c (V)
2 (Fig. 4a)	1983.3	U/d = 1300	16325.0	2466.8
4 (Fig. 4b)	1376.8	U/d = 1300	9727.4	1668.8
6 (Fig. 4c)	1496.9	U/d = 1300	7371.9	1427.0
6 (Fig. 4d)	1373.2	U/d = 1300	9625	1670.0
6 (Fig. 4f)	1653.7	U/d = 1300	11558.7	1557.0
7 (Fig. 4f) *	/	/	/	/
7 (Fig. 4g)	12536	U/d = 1300	12536	889.88

*With this specific configuration of polarities (Fig. 4f) we can not achieve Et_{min} = U/d (Et_{min}~0), since the electric field intensity inside the target tissue is almost zero (Et_{min}~0) and therefore is this configuration suitable only in a combination with the configuration as shown in Fig. 4g.

conductivity of the surrounding tissue σst = 0.2 S/m. In Fig. 6 we compare electric field distributions calculated numerically using FEM method for two, four needle electrodes and six needle electrodes taking into account higher conductivity of the target tissue compared to the surrounding tissue.

Figure 6
Calculated electric field distribution for in-homogeneous models. Numerical results of the electric field distribution for needle electrode configurations defined in Figs. 2a–2c: a) two needle electrodes, b) four needle electrodes, c) six needle electrodes in two rows taking into account two-times higher conductivity of the target tissue compared to surrounding tissue (conductivity of the target tissue is σtt = 0.4 S/m and conductivity of the surrounding tissue σst = 0.2 S/m). In all cases the applied voltage was set in such a way that U/d = 1.15 V/cm.

Comparing the results of the inhomogeneous models shown in Fig. 6 to the electric field distribution in homogeneous models (Figs. 4a–4c) we obtained that in the inhomogeneous model the electric field strength inside the target tissue is lower, while the larger portion of the surrounding tissue is exposed to the value exceeding U/d. However, similarly as in homogenous model we again obtained that with larger number of electrodes better coverage of the target tissue with adequate E is obtained, namely for larger number of electrodes Ett_{min} increases while E_{max} decreases (see Table 6). We also obtained that similarly as for homogeneous models the local electric field is significantly different from the value U/d, e.g. for the selected parameters the minimum electric field strength inside the target tissue can deviate from the U/d by more than factor 3, see the Table 6.
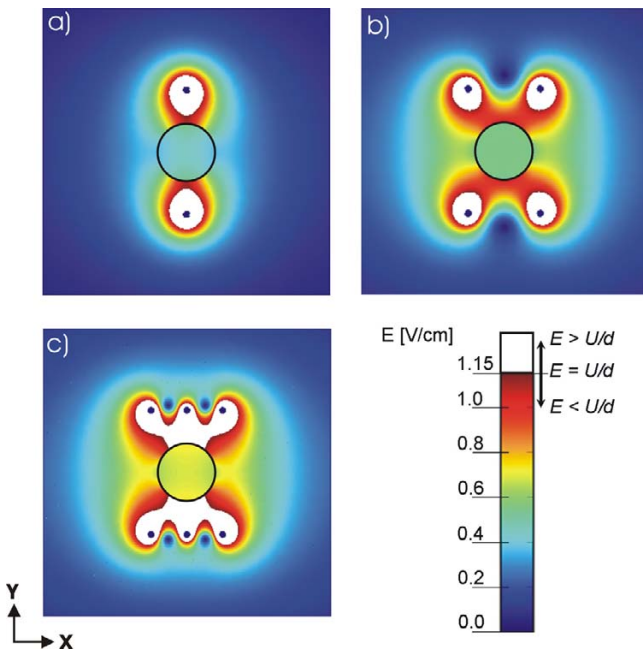
In Table 7 we give the results of the necessary voltage U_c in order to meet the condition Ett_{min}> U/d for inhomogeneous models where σtt is higher then σst. Our results show that U_c for given inhomogeneous model (σtt = 2 × σst) has to be higher compared to U_c in the homogeneous models in order to effectively treat the entire target tissue.

Discussion
In this study we numerically and analytically determined and compared the local electric field distribution in 2D for different electrode configurations which are used for in vivo electrochemotherapy and gene electrotransfer. We quantify and compare the local electric field by means of three parameters: the maximal in minimal local electric fields inside the treated tissue – Ett_{min}, Ett_{max} and maximal E over the entire treated tissue – E_{max}. Namely, the criteria for adequate or »optimal« local E distribution are the following: i) all the target tissue has to be exposed to the E above the threshold value for reversible electroporation (Ett_{min}> E_{rev}); ii) the maximal E inside the target tissue Ett_{max} has to be below the threshold value for irreversible electroporation (Ett_{max}< E_{irrev}), which is specially important in gene electrotransfer and iii) the surrounding tissue should not be exposed to excessively high electric field, therefore the maxi-

Table 6: Quantification of the electric field strength for in-homogeneousmodels – calculated Ett_{min}, Ett_{max} and E_{max} parameters.

Needle electrode configuration	U/d = 1.15 V/cm			U/d = 1300 V/cm		
	Target tissue Ett_{max}(V/cm)	Target tissue Ett_{min}(V/cm)	Entire tissue E_{max}(V/cm)	Target tissue Ett_{max}(V/cm)	Target tissue Ett_{min}(V/cm)	Entire tissue E_{max}(V/cm)
2 (Fig. 6a)	0.558	0.364	7.001	628.05	409.9	7887.1
4 (Fig. 6b)	0.572	0.539	6.104	643.4	606.2	6872.5
6 (Fig. 6c)	0.741	0.639	5.339	833.9	718.9	6011.2

Quantification of the electric field strength (E) for in-homogeneous models with needle electrode configurations which are defined in Fig. 2a-c. Conductivity of the target tissue is σtt = 0.4 S/m and the conductivity of the surrounding tissue σst = 0.2 S/m. Calculated minimal E (Ett_{min}) and maximal E (Ett_{max}) inside the target tissue and maximal E within the entire tissue E_{max} for different needle electrode configurations. The results for models shown in Figs. 6a-6c were calculated for applied voltage U = 1 V ($d = 5\sqrt{3}$ mm). Furthermore, by scaling the results we also calculated the parameters Ett_{min}, Ett_{max} and E_{max} for U/d = 1300 V/cm.

mal electric field in entire tissue E_{max} should be as low as possible, while meeting the first condition $Ett_{min} > E_{rev}$.

We further calculated the needed voltage U_c (Table 5) which has to be applied on the electrodes in order to subject the entire target tissue to the sufficiently high local electric field ($Ett_{min} \geq U/d$), where the value U/d was used in order to compare this parameter to the actual magnitude of E inside the treated tissue.

We showed that the electric field distribution in the tissue strongly depends on the number and position of the electrodes, as well as of the electric field orientation, as demonstrated in Fig. 4. As expected the highest values of E are obtained in the vicinity of the electrodes where E can exceed the irreversible threshold value E_{irrev} leading to the damage of the tissue. With increasing the number of electrodes the electric field strength inside the target tissue becomes higher for the same voltage applied, e.g. from the Table 4 it can be seen that Ett_{min} increases and E_{max} decreases for higher number of electrodes. Considering that Ett_{min} should be above E_{rev}, while keeping E_{max} as low as possible it can be seen (Table 4) that the six electrode configurations have the best ratio between Ett_{min} and E_{max}. Configurations with seven electrodes are reasonable only when combining the two polarities settings (Figs. 4f and

4f) on the electrodes in order to electropermeabilize the larger area of treated tissue.

We also demonstrate that if parameter U/d is used to select the applied voltage only smaller part of the tissue is exposed to $E \geq U/d$ (white region in Fig. 4), whereas in the other regions of tissue E is too small. We obtained that the ratio between minimal E inside the target tissue (Ett_{min}) and the value U/d can deviate for more than a factor of 2 (see Table 4). The higher local electric field can be achieved by increasing the applied voltage, therefore we further calculate the needed voltage U_c to fulfill the condition $Ett_{min} > U/d$ over the entire target tissue. We showed that the needed applied voltage U_c differs substantially for different needle electrode configurations (Table 5). Thus, the electric field distribution strongly depends on geometry and position of electrodes with respect to the target tissue therefore the needed voltage (U_c) requires its own calculation for each individual configuration. From Table 5 it can be seen that the U_c for two needle electrodes has to be about 2400 V compared to other configurations where U_c is in the range from 1400 V to 1700 V.

Another possibility to achieve better coverage of the target tissue with the adequate E with the same applied voltage is changing the electric field orientation as already experimentally and numerically demonstrated with two 90°

Table 7: Calculated values of U_c and corresponding Ett_{min}, Ett_{max} and E_{max} for in-homogeneous models (Figs. 6a-6c).

Needle electrode configuration	Target tissue Ett_{max}(V/cm)	Target tissue Ett_{min}(V/cm)	Entire tissue E_{max}(V/cm)	Needed voltage on the electrodes-U_c (V)
2 (Fig. 6a)	1991.87	U/d = 1300	25014.0	3570.6
4 (Fig. 6b)	1379.80	U/d = 1300	14738.4	2414.4
6 (Fig. 6c)	1508.0	U/d = 1300	10870.4	2035.9

Specific conductivity of the target tissue is σtt = 0.4 S/m and specific conductivity of the surrounding tissue σst = 0.2 S/m.

rotations of E using plate electrodes in [23] and experimentally in [26] with a sequence of 60° rotations of E using needle electrode configurations, as shown in Figs. 2d and 2e.

Moreover, changing the electric field orientation during the electric pulse delivery is also important for gene electrotransfer as it improves the efficiency of gene electrotransfer indirectly by also increasing the membrane area available for the transfer of plasmid DNA [46].

We used 2D numerical and analytical models in order to compare E for different electrode configurations in the central plane of a more general 3D model. The presented 2D results are good approximation of local electric field distribution in 3D models for needle electrodes since electrodes are usually long and deeply inserted in tissue.

The presented analytical solutions in 2D for the electric field around needle electrodes are extensions of the analytical expressions given by Dev et al. [31] for geometries given in Fig. 2 for arbitrary values of d and l, as well as for different polarities in case of six and seven electrodes. By comparing numerical and analytical calculations for given needle electrode configurations we obtained good agreement between the two methods. Thus we showed that the leading-order analytical approximation accurately describes the electric field distribution in the region between the needle electrodes. The presented analytical solutions can be used as a rapid pre-analysis of the electric field distribution for different needle electrode configurations.

Our models are approximation of more complex and in general time-dependent models where one has to take into account also the increase of the effective conductivity of the permeabilized region [18,19,47-51]. In our present study we assumed that tissue has a constant value of conductivity which represents the final stage of electropermeabilization. In most of the models we assumed homogeneous properties of the treated tissue which neglects the differences of the conductivities for different tissues. For plate electrodes, which are usually placed on the skin, this approximation is not adequate since the conductivity of the skin is few orders of magnitude lower [19]. However, for needle electrodes homogeneous models can be used to compare different configurations, since the treated tissues have roughly similar conductivities [45] and we can use the average conductivity.

In order to analyze possible effects of tissue inhomogeneities we made additional numerical models where target tissue had increased conductivity. The main conclusions of our study are independent of the electrical properties of tissues either homogenous or inhomogeneous. We

obtained that similarly as for homogeneous models electric field distribution significantly depends on the configuration and that the deviation of the value U/d approximation from local E inside the target tissue can be even more pronounced. Furthermore, also for inhomogeneous models six electrodes result in better local electric field distribution in terms of achieving high Ett_{min} and relatively low E_{max} compared to two or four needle electrodes models (Table 6).

Conclusion

The main objective of this paper was to provide the solutions of local electric field distribution and to visualize the local electric field inside the target tissue for most commonly used electrode configurations in electrochemotherapy and gene electrotransfer. In presented study we numerically and analytically quantify and compare electric field distribution in 2D for different electrode configurations which are used for in vivo electrochemotherapy and gene electrotransfer for the same value of parameter U/d. We demonstrate that the calculated local electric field inside the target tissue strongly depends on the chosen electrodes and electrode configuration and can be significantly different from a gross approximation U/d as usually used as an estimate of the local electric field in a number of different reports [8-10,12,15,32-36].

We show that electric field distribution strongly depends on geometry, position and polarity of the electrodes with respect to target tissue and that it requires its own calculation for each individual configuration, which is in agreement with previous reports [12,15,17,25,26,32,34,40,41, 52]. We present visualization of the electric field distribution and quantification of the maximal and minimal values of E inside the target tissue for frequently used electrode configurations. We also calculate the needed voltage for a specific configuration to meet the criterion that the local electric field over the entire target tissue exceeds the threshold value.

The results show that higher electric field inside the target tissue can be obtained by increasing the number of the electrodes, e.g. we obtained better electric field distribution with six electrodes compared to four or two electrodes (see Figs. 4a–4c). Namely, in this way the local electric field in the target tissue is increased while the electric field inside the surrounding tissue is reduced. We further show that changing the orientation of the electric field by changing electrodes' polarities leads to better coverage of the target tissue with desirable local electric field, which was already proven experimentally to improve electrochemotherapy efficiency and gene electrotransfer [23,34,43,46]. For example by consecutive changing the polarities of the electrodes (i.e. combining the polarity

configurations Fig. 4f and Fig. 4g) we electropermeabilize larger area with the same electrode configurations.

In addition we showed that for needle electrode configuration we can use the analytical solution as a rapid and simple method for visualizing electric field distribution inside the tissue without using special software for numerical modeling. But in case of more complex geometries and inhomogeneities of the tissue, numerical modeling is required to determine optimal parameters in order to achieve efficient tissue permeabilization [15-17,25,49,50,52].

To conclude, our numerical models and analytical calculations provide an estimate of actual local E inside the target tissue and can be used for comparison of different electrode configurations. They also enable more precise choice of applied voltage compared to using U/d approximation. Since optimal geometry, arrangement and position of the electrodes strongly depend on the position and geometry of the target tissue it is of crucial importance to design a system of electrodes, which could be easily adjustable according to each individual case and to develop software for numerical calculation which would enable optimization of parameters in order to render electrochemotherapy and gene electrotransfer as efficient as possible. An important step towards the optimization of local electric field for effective ECT has been made recently by IGEA company [53] currently providing the electroporator designed specifically to be used in the clinical practice for electrochemotherapy. They provide the voltage for different distances between electrodes taking into account also the differences in local electric field distribution for different electrode configurations. In order to improve the efficiency of the treatments training sessions should be also involved. The training sessions should also provide educational material about the knowledge and experiences that have already been acquired with electrochemotherapy and gene electrotransfer. This can be brought about by the web technology, as an easy and important way to collect and organize the information obtained from different clinical and research centers [54-56].

Appendix
In this section we present solutions of the Laplace equation for the coefficients C_n from Eq. 4 for different needle electrode configurations. We obtained the following result for two needle electrodes (Fig. 2a):

$$C_1 = -C_2 = \frac{V_0}{\log\left(d/a\right)}, \qquad (A.1)$$

for four electrodes (Fig. 2b):

$$C_1 = C_2 = -C_3 = -C_4 = \frac{V_0}{\log\left(\frac{\sqrt{d^2+l^2}}{l}\frac{d}{a}\right)}, \qquad (A.2)$$

for six electrodes (arranged in two parallel rows of three electrodes in each), as shown in Fig. 2c:

$$C_1 = C_3 = -C_4 = -C_6 = V_0 \frac{\log(d/a)-\log(\sqrt{d^2+l^2}/l)}{\log(d/a)\log(d\sqrt{d^2+4l^2}/2al)-2\left(\log(\sqrt{d^2+l^2}/l)\right)^2},$$

$$C_2 = -C_5 = \frac{V_0 - 2C_1\log(\sqrt{d^2+l^2}/l)}{\log(d/a)}, \qquad (A.3)$$

for six electrodes arranged in circle (Fig. 2e):

$$C_1 = C_5 = -C_2 = -C_4 = V_0\left[2\log(\sqrt{3})+\log(a/2d)\right],$$

$$-C_3 = C_6 = \frac{2C_1\log(\sqrt{3})-V_0}{\log(a/2d)}, \qquad (A.4)$$

for seven electrodes, as shown in Fig. 2f (six electrodes arranged in circle with additional placed in the center of this circle):

$$C_{1,3,5} = -C_{2,4,6} = \frac{V_0}{\log\left(2d/3a\right)}, \quad C_7 = 0. \quad (A.5)$$

In all configurations 2a–2f is the number of positive and negative electrodes equal, so we can set $C_0 = 0$.

For seven electrodes as shown in Fig. 2g we have one positive and six negative electrodes, so C_0 is not zero. To satisfy conservation of the current we have additional condition $C_7 = -6C_{1..6}$, and thus we obtain:

$$C_{1..6} = \frac{-2V_0}{6\log\left(a^5/6d^5\right)-12\log\left(a/d\right)}, \quad C_7 = -6C_{1..6}, \quad C_0 = V_0 - 6C_{1..6}\log\left(a/d\right). \qquad (A.6)$$

Competing interests
The author(s) declare that they have no competing interests.

Authors' contributions
All authors contributed equally to this work

All authors read and approved the final manuscript.

Acknowledgements

References

1. Zimermann U: **Electric field-mediated fusion and related electrical phenomena.** *Biochim Biophys Acta* 1982, **694:**227-277.
2. Neumann E, Sowers AE, Jordan CA: **Electroporation and Electrofusion in Cell Biology.** New York: Plenum Press; 1989.
3. Tsong TY: **Electroporation of cell membranes.** *Biophys J* 1991, **60:**297-306.
4. Weaver JC, Chizmadzhev YA: **Theory of electroporation: A review.** *Bioelectrochem Bioenerg* 1996, **41:**135-60.
5. Mir LM: **Therapeutic perspectives of in vivo cell electropermeabilization.** *Bioelectrochemistry* 2001, **53(1):**1-10.
6. Okino M, Mohri H: **Effects of a high-voltage electrical impulse and an anticancer drug on in vivo growing tumors.** *Jpn J Cancer Res* 1987, **78:**1319-1321.
7. Mir LM, Glass LF, Seřša G, Tessie J, Domenge C, Miklavčič D, Jaroszeski MJ, Orlowski S, Reintgen DS, Rudolf Z, Belehradek M, Gilbert R, Rols MP, Belehradek JJr, Bachaud JM, DeConti R, Štabuc B, Čemažar M, Coninx P, Heller R: **Effective treatment of cutaneous and subcutaneous malignant tumors by electrochemotherapy.** *Br J Cancer* 1998, **77:**2336-2342.
8. Barry BW: **Novel Mechanisms and devices to enable successful transdermal drug delivery.** *Eur J Pharm Sci* 2001, **14:**101-114.
9. Denet AR, Vanbever R, Préat V: **Skin electroporation for transdermal and topical delivery.** *Adv Drug Deliv Rev* 2004, **56(5):**659-674.
10. Mossop BJ, Barr RC, Henshaw JW, Zaharoff DA, Yuan F: **Electric fields in tumors exposed to external voltage sources: Implication for electric field-mediated drug and gene delivery.** *Annals of biomedical engineering* 2006, **34:**1564-1572.
11. Nishi T, Yoshizato K, Yamashiro S, Takeshima H, Sato K, Hamada K, Kitamura I, Yoshimura T, Saya H, Kuratsu J, Ushio Y: **High-efficiency in vivo gene transfer using intraarterial plasmid DNA injection following in vivo electroporation.** *Cancer Res* 1996, **56:**1050-1055.
12. Jaroszeski MJ, Heller R, Gilbert R: **Electrochemotherapy, electrogene therapy and transdermal drug delivery: electrically mediated delivery of molecules to cells.** Totowa, New Jersey: Humana Press; 1999.
13. Neumann E, Schaefer-Ridder M, Wang Y, Hofschneider PH: **Gene transfer into mause lyoma cells by electroporation in high electric fields.** *EMBO J* 1982, **1:**841-845.
14. Prud'homme GJ, Glinka Y, Khan AS, Draghia-Akli R: **Electroporation-enhanced nonviral gene transfer for the prevention or treatment of immunological, endocrine and neoplastic diseases.** *Current Gene Therapy* 2006, **6:**243-273.
15. Gehl J, Sorensen TH, Nielsen K, Reskmark P, Nielsen SL, Skovsgaard T, Mir LM: **In vivo electroporation of skeletal muscle: threshold, efficacy and relation to electric field distribution.** *Biochim Biophys Acta* 1999, **1428:**233-240.
16. Šemrov D, Miklavčič D: **Numerical Modelling for In Vivo Electroporation.** *Meth Mol Med* 2000, **37:**63-81.
17. Miklavcic D, Semrov D, Mekid H, Mir LM: **A validated model of in vivo electric field distribution in tissues for electrochemotherapy and for DNA electrotransfer for gene therapy.** *Biochim Biophys Acta* 2000, **1523(1):**73-83.
18. Šel D, Cukjati D, Batiuskaite D, Slivnik T, Mir LM, Miklavčič D: **Sequential finite element model of tissue electropermeabilization.** *IEEE Trans Biomed Eng* 2005, **52:**816-827.
19. Pavšelj N, Bregar Z, Cukjati D, Batiuskaite D, Mir LM, Miklavčič D: **The course of tissue permeabilization studied on a mathematical model of a subcutaneous tumor in small animals.** *IEEE Trans Biomed Eng* 2005, **52:**1373-1381.
20. Vernhes MC, Benichou A, Pernin P, Cabanes PA, Teissié J: **Elimination of free-living amoebae in fresh water with pulsed electric fields.** *Water Res* 2002, **36:**3429-3438.
21. Yeom HW, Streaker CB, Zhang QH, Min DB: **Effects of pulsed electric fields on the quality of orange juice and comparison**
22. Davalos RV, Mir LM, Rubinsky B: **Tissue ablation with irreversible electroporation.** *Ann Biomed Eng* 2005, **33:**223-231.
23. Seřša G, Čemažar M, Šemrov D, Miklavčič D: **Changing electrode orientation improves the efficacy of electrochemotherapy of solid tumors in mice.** *Bioelectrochem Bioenerg* 1996, **39:**61-66.
24. Miklavcic D, Semrov D, Mekid H, Mir LM: **A validated model of in vivo electric field distribution in tissues for electrochemotherapy and for DNA electrotransfer for gene therapy.** *Biochim Biophys Acta* 2000, **1523(1):**73-83.
25. Miklavčič D, Beravs K, Šemrov D, Čemažar M, Demšar F, Seřša G: **The importance of electric field distribution for effective in vivo electroporation of tissues.** *Biophys J* 1998, **74:**2152-2158.
26. Gilbert RA, Jaroszeski MJ, Heller R: **Novel electrode designs for electrochemotherapy.** *Biochim Biophys Acta* 1997, **1334(1):**9-14.
27. Sel D, Lebar AM, Miklavcic D: **Feasibility of employing model-based optimization of pulse amplitude and electrode distance for effective tumor electropermeabilization.** *IEEE Trans Biomed Eng* 2007, **54:**773-781.
28. Miklavčič D: **Electrodes and corresponding electric field distribution for effective in vivo electroporation.** *Proceedings of MEDICON-Mediterranean conference on medical engineering and computing, Pula, Croatia* 2001:5-9.
29. Schwan HP, Kay CF: **The conductivity of living tissues.** *Ann NY Acad Sci* 1957, **65:**1007.
30. Polk C, Postow E: **Dielectric Properties of Tissues.** In *Handbook of Biological Effects of Electromagnetics Fields* 2nd edition. Edited by: Polk C, Postow E. Florida: CRC Press; 2000:28-92.
31. Dev BS, Dhar D, Krassowska W: **Electric field of a six-needle array electrode used in drug and DNA delivery in vivo: analytical versus numerical solution.** *IEEE Trans Biomed Eng* 2003, **50(11):**1296-1300.
32. Heller R, Jaroszeski M, Atkin A, Moradpour D, Gilbert R, Wands J, Nicolau C: **In vivo gene electroinjection and expression in rat liver.** *FEBS Letters* 1996, **389:**225-228.
33. Puc M, Reberšek S, Miklavčič D: **Requirements for a clinical electrochemotherapy device-electroporator.** *Radiol Oncol* 1997, **31:**368-373.
34. Seřša G, Čemažar M, Rudolf Z: **Electrochemotherapy. "Advantages and drawbacks in treatment of cancer patients.** *Cancer Therapy* 2003, **1:**133-142.
35. Leroy-Willing A, Bureau MF, Scherman D, Carlier PG: **In vivo imaging evaluation of efficiency and toxity of gene electrotrensfer in rat muscle.** *Gene Ther* 2005, **12:**1434-1443.
36. Jaichandran S, Yap STB, Khoo ABM, Ho LP, Tien SL, Kon OL: **In Vivo Liver Electroporation: Optimization and Demonstration of Therapeutic Efficacy.** *Hum Gene Ther* 2006, **17:**362-375.
37. Marty M, Seřša G, J GarbayR, Gehl J, Collins CG, Snoj M, Billard V, Geertsen PF, Larkin JO, Miklavčič D, Pavlović I, Paulin-Košir SM, Čemažar M, Morsli N, Soden DM, Rudolf Z, Robert C, O'Sullivan GC, Mir LM: **Electrochemotherapy – An easy, highly effective and safe treatment of cutaneous and subcutaneous metastases: Results of ESOPE (European Standard Operating Procedures of Electrochemotherapy) study.** *Eur J Cancer Suppl* 2006, **4:**3-13.
38. Fagan MJ: **Finite element analysis-Theory and practice Longman Scientific Technical.** Harlow: Longman Scientific and Technical; 1992.
39. Puc M, Čorović S, Flisar K, Petkovsek M, Nastran J, Miklavčič D: **Techniques of signal generation required for electropermeabilization. Survey of electropermeabilization devices.** *Bioelectrochemistry* 2004, **64:**113-124.
40. Trezise AE: **In vivo DNA Electrotransfer.** *DNA Cell Biol* 2002, **21(12):**869-877.
41. Šemrov D, Miklavčič D: **Numerical modeling for in vivo electroporation.** *Meth Mol Med* 2000, **37:**63-81.
42. Tekle E, Astumian RD, Chock PB: **Electro-permeabilization of cell membranes: effect of the resting membrane potential.** *Biochem Biophys Res Commun* 1990, **172(1):**282-287.
43. Faurie C, Phez E, Golzio M, Vossen C, Lesbordes JC, Delteil C, Teissie J, Rols MP: **Effect of electric field vectoriality on electrically mediated gene delivery in mammalian cells.** *Biochim Biophys Acta* 2004, **1665:**92-100.

44.　Valic B, Pavlin M, Miklavcic D: **The effect of resting transmembrane voltage on cell electropermeabilization: a numerical analysis.** *Bioelectrochemistry* 2004, **63(1-2):**311-315.
45.　Miklavčič D, Pavšelj N, Hart FX: **Electric Properties of Tissues.** In *Wiley Encyclopedia of Biomedical Engineering* John Wiley & Sons, New York; 2006.
46.　Reberšek M, Faurie C, Kandušer M, Čorović S, Teissié J, Rols MP, Miklavčič D: **Electroporator with automatic change of electric field direction improves gene electrotransfer** *in vitro.* *Biomed Eng Online* 2007, **6:**25.
47.　Pavlin M, M Kandušer, Reberšek M, Pucihar G, Hart FX, Magjarević R, Miklavčič D: **Effect of cell electroporation on the conductivity of a cell suspension.** *Biophys J* 2005, **88:**4378-4390.
48.　Pavlin M, Leben V, Miklavčič D: **Electroporation in dense cell suspension – Theoretical and experimental analysis of ion diffusion and cell permeabilization.** *Biochim Biophys Acta* 2007, **1770:**12-23.
49.　Davalos RV, Huang Y, Rubinsky B: **Electroporation: bio-electrochemical mass transfer at the nano scale.** *Microscale Thermophys Eng* 2000, **4:**147-159.
50.　Davalos RV, Rubinsky B, Otten DM: **A feasibility study for electrical impedance tomography as a means to monitor tissue electroporation for molecular medicine.** *IEEE Trans Biomed Eng* 2002, **49(4):**400-403.
51.　Davalos RV, Otten DM, Mir LM, Rubinsky B: **Electrical impedance tomography for imaging tissue electroporation.** *IEEE Trans Biomed Eng* 2004, **51(5):**761-767.
52.　Šel D, Mazeres S, Teissie J, Miklavčič D: **Finite-element modeling of needle electrodes in tissue from the perspective of frequent model computation.** *IEEE Trans Biomed Eng* 2003, **50:**1221-1232.
53.　**IGEA S.r.l** [http://www.igea.it]
54.　Pavlović I, Kramar P, Čorović S, Cukjati D, Miklavčič D: **A web-application that extends functionality of medical device for tumor treatment by means of electrochemotherapy.** *Radiol Oncol* 2004, **38:**49-54.
55.　Pavlović I, Miklavcic D: **Web-based electronic data collection system to support electrochemotherapy clinical trial.** *IEEE Trans Inf Technol Biomed* 2007, **11(2):**222-230.
56.　Humar I, Sinigoj A, Bešter J, Hegler MO: **Integrated component web-based interactive learning systems for engeneering.** *IEEE Trans Educ* 2005, **8:**664-675.

Paper II

Numerical Modeling and Optimization of Electric Field Distribution in Subcutaneous Tumor Treated With Electrochemotherapy Using Needle Electrodes

Selma Corovic, Anze Zupanic, and Damijan Miklavcic

Abstract—Electrochemotherapy (ECT) is an effective antitumor treatment employing locally applied high-voltage electric pulses in combination with chemotherapeutic drugs. For successful ECT, the entire tumor volume needs to be subjected to a sufficiently high local electric field, whereas, in order to prevent damage, the electric field within the healthy tissue has to be as low as possible. To determine the optimum electrical parameters and electrode configuration for the ECT of a subcutaneous tumor, we combined a 3-D finite element numerical tumor model with a genetic optimization algorithm. We calculated and compared the local electric field distributions obtained with different geometrical and electrical parameters and different needle electrode geometries that have been used in research and clinics in past years. Based on this, we established which model parameters had to be taken into account for the optimization of the local electric field distribution and included them in the optimization algorithm. Our results showed that parallel array electrodes are the most suitable for the spherical tumor geometry, because the whole tumor volume is subjected to sufficiently high electric field while requiring the least electric current and causing the least tissue damage. Our algorithm could be a useful tool in the treatment planning of clinical ECT as well as in other electric field mediated therapies, such as gene electrotransfer, transdermal drug delivery, and irreversible tissues ablation.

Index Terms—Electrochemotherapy (ECT), electropermeabilization, finite element method, genetic algorithm, optimization, subcutaneous tumor.

I. INTRODUCTION

ELECTROCHEMOTHERAPY (ECT) is a nonthermal and local tumor treatment, clinically proven to be effective, safe, and well tolerated by patients [1], [2]. ECT standard operating procedures have been defined for the treatment of cutaneous and subcutaneous tumor nodules of different histologies. Numerous published research and clinical reports have shown that it can be used as an efficient local tumor treatment for various tumor types [3]–[8].

ECT is performed using either intravenous or intratumoral chemotherapeutic injection, followed by the application of high-voltage electric pulses locally delivered to the target tissue via appropriate sets of electrodes. Electric pulses induce a local electric field (E) within the treated tissue, which depends on the tissue's electrical and geometrical properties. Namely, for efficient ECT, it is necessary that the entire tumor tissue is subjected to a local electric field in the range between reversible and irreversible electropermeabilization threshold values ($E_{rev} < E < E_{irrev}$), which causes transient structural changes in cell membranes (termed reversible electropermeabilization) and allows for increased entrance of chemotherapeutics into target tissues. This increased membrane permeabilization potentiates the effect of chemotherapeutic drugs, thus significantly lowering the required dose and improving the effectiveness of the treatment [9]. Other requirements for efficient ECT are that the healthy tissue volume subjected to $E > E_{rev}$ has to be kept minimal so as not to expose the healthy tissue to an E higher than necessary and to prevent the excessive irreversible tissue damage ($E > E_{irrev}$). At the same time, the electric current through the tissue has to be as low as possible due to the technical limitations of the high voltage pulse generator.

The magnitude and distribution of local electric field and thus the degree of tissue electropermeabilization can be controlled by electrode configuration and polarity and the amplitude of electric pulses [10], [11]. Local electric field, however also depends on the geometrical and electrical properties of treated tissues; therefore, both have to be taken into account when planning the treatment. Electrode types currently most often used for therapeutic and research purposes are external parallel plate electrodes and different geometries of needle electrode arrays [6], [12]–[14]. External plate electrodes are suitable for the treatment of protruding cutaneous tumors as the local electric field can be easily controlled by the contact surface between electrodes and the treated tissue, the interelectrode distance, and the amplitude of the applied electric pulses. If the target tissue cannot be fixed between the electrodes or is seated in deeper tissue, an array of needle electrodes is more effective as it can penetrate into the tissue to assure the necessary magnitude of electric field within the deeper parts of the tumor. The choice of the suitable electrode type and geometry can be determined by means of a numerical model [13], [15]. Numerical modeling can therefore serve as a vital component in ECT treatment planning; moreover, it can predict the treatment outcome for each tumor type with its specific electrical and geometrical properties, as has already been demonstrated [16].

The authors are with the Faculty of Electrical Engineering, University of Ljubljana, 1000 Ljubljana, Slovenia (e-mail: selma.corovic@fe.uni-lj.si; anze.zupanic@fe.uni-lj.si; damijan.miklavcic@fe.uni-lj.si).

Color versions of one or more of the figures in this paper are available online at http://ieeexplore.ieee.org.

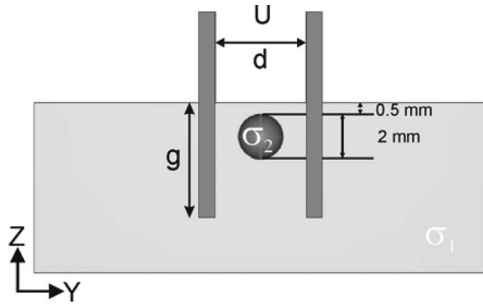Digital Object Identifier 10.1109/TPS.2008.2000996

Fig. 1. Central YZ view across the subcutaneous tumor model, where U is the applied voltage between the electrode rows, g is the depth of needle insertion, d is the distance between the electrodes as shown in Fig. 3, and σ_1 and σ_2 are the healthy and tumor tissue conductivities, respectively. The tumor is positioned 0.5 mm below the surface of the model.

In this paper, we used finite element method and genetic algorithm to investigate and optimize the local electric field distribution within a given 3-D model of a subcutaneous tumor. The electric properties of the modeled tissues are based on the fact that the tumor tissue is more conductive than its surrounding healthy tissue [16], [17]. We investigated the influence of the number of needle electrodes, depth of electrode insertion, configuration of electrodes with respect to the treated tissue, and amplitude of electric pulses. We quantified local electric field distribution inside the tumor and its surrounding healthy tissue obtained with four needle electrode geometries that have been used in clinics and research in past years [1], [14], [18]. Based on the calculated distributions of electric field, we established which model parameters had to be taken into account for the optimization of the local electric field distribution and included them in the genetic optimization algorithm that we developed in order to determine the optimum electrode configuration in the target tissue. As the output of the algorithm, we obtained the optimum solution of the analyzed treatment parameters. Our algorithm can be used in local electric field optimization and thus in ECT treatment planning for arbitrary tumor geometries and electrical properties. Our optimization approach can be beneficial also in the treatment planning of other electric field mediated treatments, such as gene electrotransfer [19], transdermal drug delivery [20], and tissue ablation treatments [21].

II. METHODS

A. Tissue Properties and Model Geometry

Our model of a subcutaneous tumor consisted of two tissues, the target tumor tissue (a sphere with a diameter of 2 mm), and its surrounding healthy tissue (Figs. 1–3). Both tissues were considered isotropic and homogeneous, the assigned conductivity values being 0.4 S/m for the tumor and 0.2 S/m for the healthy tissue. These values describe the conductivity at the end of the electropermeabilization process. The values were chosen in accordance with previous measurements of tumor and tissue conductivity and models of subcutaneous tumor and skin electropermeabilization [16], [17], [19].

The electric field distribution was calculated for four different electrode geometries: three different parallel needle electrode arrays [Fig. 2(a)–(c)] and a hexagonal electrode array
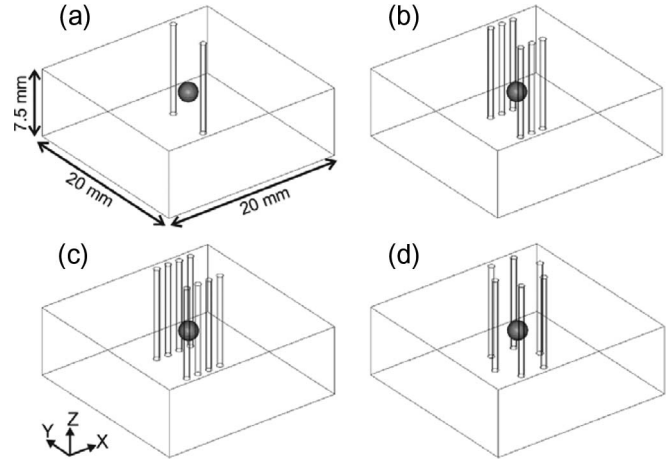

Fig. 2. Three-dimensional geometry of subcutaneous tumor with four needle electrode geometries analyzed: (a) One needle electrode pair, (b) three needle electrode pairs, (c) four needle electrode pairs, and (d) hexagonal needle electrode array.
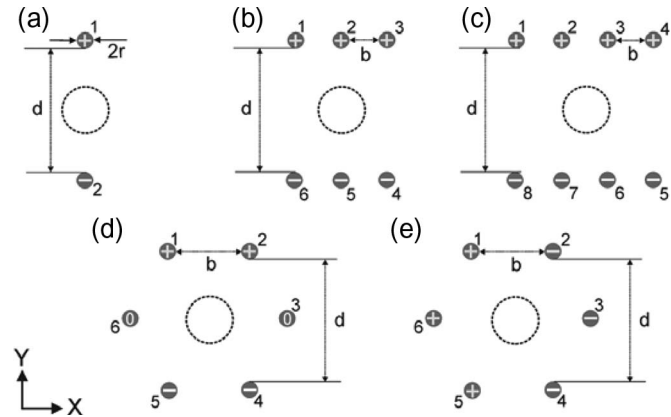

Fig. 3. XY view of the model with electrode geometries, polarities, and arrangement with respect to (the circled region) the target/tumor tissue: (a) One needle electrode pair, (b) three needle electrode pairs, (c) four needle electrode pairs, (d) 2 × 2 hexagonal needle electrode array (two electrodes on positive potential, two on negative potential, and two grounded), and (e) 3 × 3 hexagonal needle electrode array (three electrodes on positive potential and three on negative potential). d and b stand for the distance between opposite sets of electrodes and distance between electrodes of the same row (parallel needle electrode arrays) or distance between neighboring electrodes (hexagonal needle electrode array), respectively.

[Fig. 2(d)], and five electrode polarities: three for the parallel needle electrode arrays [Fig. 3(a)–(c)] and two for the hexagonal electrode array [Fig. 3(d) and (e)]. These geometries and polarities were chosen as they are the most often used in ECT research and therapy.

B. Numerical Modeling

All numerical calculations were performed with a commercial finite element software package COMSOL Multiphysics 3.3a (COMSOL AB, Sweden) and run on a desktop PC (Windows XP, 3.0-GHz Pentium 4, 1-GB RAM). Electric field distribution in the tissue, caused by an electric pulse, was determined by solving the Laplace equation for static electric currents

$$-\nabla \cdot (\sigma \cdot \nabla \varphi) = 0 \qquad (1)$$

where σ and φ stand for the electric conductivity of the tissue and electric potential, respectively. The boundary conditions used in our calculations were a constant potential on the surface of the electrodes (Fig. 3) and electric insulation on all outer boundaries of the model. Results were controlled for numerical errors by increasing the size of our model and increasing the mesh density, until the electric insulation condition and error due to meshing irregularities were insignificant—a further increase in domain size or mesh density only increased the computation time; however, the results changed less than 0.5%.

The electric field distributions obtained in our models were displayed in the range from the reversible $E_{\text{rev}} = 400$ V/cm to the irreversible electropermeabilization threshold value $E_{\text{irrev}} = 900$ V/cm. These values were taken from a previously published study, in which we estimated them by comparing *in vivo* measurements and the numerical modeling of the electropermeabilization of a subcutaneous tumor [16], [22]. Namely, E_{rev} was estimated to be the same for the tumor and skin tissue (400 V/cm), whereas the E_{irrev} values were estimated to be 800 and 1000 V/cm for the tumor and skin, respectively. The E_{irrev} in our model was set as the average of these two values (900 V/cm) in the tumor and healthy tissue.

C. Optimization

The genetic algorithm [23] was written with MATLAB 2007a (Mathworks, USA) and run together with the numerical calculation using the link between MATLAB and COMSOL. The initial population of chromosomes (vectors of real numbers: $X = (x_1, x_2, \ldots, x_n)$) was generated randomly, taking into account the following model constraints: range of distances between electrodes, range of depth of electrode insertion into tissue, and range of voltages between the electrodes. These constraints were chosen so that the calculation domain size, COMSOL meshing capabilities, and oncology experts' demands for a safety margin [24], when treating solid tumors, were all respected. Chromosomes for reproduction were selected proportionally to their fitness, according to the fitness function

$$F = 12 + 100 \cdot V_{\text{Trev}} - 10 \cdot V_{\text{Hirrev}} - V_{\text{Hrev}} - V_{\text{Tirrev}} \quad (2)$$

where F stands for fitness, V_{Trev} and V_{Tirrev} stand for tumor volume subjected to the local electric field above E_{rev} and E_{irrev}, respectively, and V_{Hrev} and V_{Hirrev} stand for the volume of healthy tissue subjected to local electric field above E_{rev} and E_{irrev}, respectively. The weights in the fitness function were set accordingly to the importance of the individual parameters for efficient ECT. Namely, V_{Trev} is crucial for efficient ECT; therefore, its weight is largest (100) in comparison to the weight of V_{Hirrev} (10), which was in turn larger than the weights of V_{Hrev} and V_{Tirrev}, as their significance for successful ECT is still debated. Other weight values that kept a similar ratio gave similar results. The integer 12 is present only to assure that the fitness function is always positive.

The selected chromosomes reproduced by crossover or mutation. When crossover takes place, each new chromosome

TABLE I
GENETIC ALGORITHM PARAMETERS

Size of initial population	Number of generations	Fraction of elite chromosomes [%]	Probability of cross-over	Probability of mutation
20 - 30	100	10	0.95	0.05

$Z = (z_1, z_2, \ldots, z_n)$ is a random linear combination of parent chromosomes X and Y

$$z_i = a_i \cdot x_i + (1 - a_i) \cdot y_i, \qquad a_i \in [0, 1]. \quad (3)$$

When mutation takes place, each new chromosome $M = (m_1, m_2, \ldots, m_n)$ is a random variation of one parent chromosome X

$$m_i = x_i + b_i \cdot x_i, \qquad b_i \in [-0.3, 0.3]. \quad (4)$$

Crossover and mutation were chosen according to the probabilities in Table I, with the exception that the top ranking solutions (elite) could not be subjected to mutation. The genetic algorithm was terminated after 100 generations, when the fitness of the highest ranking solution usually reached a plateau. The algorithm always converged to a possible optimum solution. The average computation time of the algorithm was two hours. Other genetic algorithm parameters can be found in Table I.

D. Protocol

To select the optimum electrode configuration for ECT of the subcutaneous tumor model, we first analyzed the local electric field distribution inside the tissue model for several discrete values of applied voltage between electrodes for all electrode geometries and polarities (Fig. 3). Distance between opposite sets of electrodes d and distance between electrodes of the same row b (parallel needle electrode arrays) or distance between neighboring electrodes b (hexagonal needle electrode array) were kept constant, at $b = 0.65$ mm (parallel arrays), $b = 4/\sqrt{3}$ mm (hexagonal array), and $d = 4$ mm, in all simulations. For each electrode geometry and two electrode depths ($g = 3$ mm—as deep as the bottom of the tumor; $g = 5$ mm—double the depth of the tumor), we calculated the minimum voltage U_c (critical voltage) that had to be applied between the electrodes so that the minimum electric field over the entire tumor volume exceeded E_{rev}. This was done by a sequence of calculations, in which we decreased the voltage by increments of 10 V, until the lowest needed amplitude was reached. We then selected the calculated critical voltage U_c that resulted in the lowest calculated values of reversibly electropermeabilized volume of healthy tissue V_{Hrev} and total electric current I and applied it to each electrode configuration. We examined the influence of the depth of insertion on the local electric field distribution within the target tumor tissue and its surrounding healthy tissue by visualization of the electric field and by quantification of electric distribution by calculating V_{Trev}, V_{Hrev}, V_{Hirrev}, and I.

TABLE II

CALCULATED VALUES OF CRITICAL VOLTAGE U_C, TOTAL ELECTRIC CURRENT I, REVERSIBLY ELECTROPERMEABILIZED TUMOR VOLUME V_{Trev}, AND REVERSIBLY AND IRREVERSIBLY ELECTROPERMEABILIZED HEALTHY TISSUE V_{Hrev} AND V_{Hirrev}, RESPECTIVELY, ARE GIVEN FOR ALL ANALYZED ELECTRODE GEOMETRIES AND POLARITIES AND FOR DEPTHS OF ELECTRODE INSERTIONS $g = 3$ mm AND $g = 5$ mm. ALL VOLUME VALUES ARE NORMALIZED BY THE TUMOR VOLUME V_T. DISTANCE BETWEEN OPPOSITE SETS OF ELECTRODES d AND DISTANCE BETWEEN ELECTRODES OF THE SAME ROW b (NEEDLE ELECTRODE ARRAYS) OR DISTANCE BETWEEN NEIGHBORING ELECTRODES b (HEXAGONAL NEEDLE ELECTRODE ARRAY) WERE KEPT CONSTANT AT $b = 0.65$ mm (PARALLEL NEEDLE ELECTRODE ARRAYS), $b = 4/\sqrt{3}$ mm (HEXAGONAL NEEDLE ELECTRODE ARRAY), AND $d = 4$ mm, IN ALL SIMULATIONS

Electrode configuration and polaririty	g [mm]	U_C [V]	I [A]	$\dfrac{V_{Trev}}{V_T}$	$\dfrac{V_{Hrev}}{V_T}$	$\dfrac{V_{Hirrev}}{V_T}$
one-needle pair	5	400	0.248	1	29.96	6.14
	3	440	0.175	1	21.00	5.14
three-needle pairs	5	260	0.270	1	31.86	1.71
	3	290	0.198	1	24.86	2.35
four-needle pairs	5	240	0.294	1	43.78	2.43
	3	280	0.234	1	29.21	2.14
2x2 hexagonal array	5	290	0.301	1	38.36	3.64
	3	350	0.234	1	30.64	4.92
3x3 hexagonal array	5	280	0.463	1	42.43	9.71
	3	310	0.330	1	31.4	8.07

TABLE III

CALCULATED VALUES OF TOTAL ELECTRIC CURRENT I, REVERSIBLY ELECTROPERMEABILIZED TUMOR VOLUME V_{Trev}, AND REVERSIBLY AND IRREVERSIBLY ELECTROPERMEABILIZED HEALTHY TISSUE V_{Hrev} AND V_{Hirrev}, RESPECTIVELY, ARE GIVEN FOR ALL ANALYZED ELECTRODE GEOMETRIES AND POLARITIES AND FOR DEPTHS OF ELECTRODE INSERTIONS $g = 3$ mm AND $g = 5$ mm. ALL VOLUME VALUES ARE NORMALIZED BY THE TUMOR VOLUME V_T. DISTANCE BETWEEN OPPOSITE SETS OF ELECTRODES d AND DISTANCE BETWEEN ELECTRODES OF THE SAME ROW b (NEEDLE ELECTRODE ARRAYS) OR DISTANCE BETWEEN NEIGHBORING ELECTRODES b (HEXAGONAL NEEDLE ELECTRODE ARRAY) WERE KEPT CONSTANT AT $b = 0.65$ mm (PARALLEL NEEDLE ELECTRODE ARRAYS), $b = 4/\sqrt{3}$ mm (HEXAGONAL NEEDLE ELECTRODE ARRAY), AND $d = 4$ mm, IN ALL SIMULATIONS. VOLTAGE WAS SET TO $U = 290$ V IN ALL SIMULATIONS

Electrode configuration and polaririty	g [mm]	U [V]	I [A]	$\dfrac{V_{Trev}}{V_T}$	$\dfrac{V_{Hrev}}{V_T}$	$\dfrac{V_{Hirrev}}{V_T}$
one-needle pair	5	290	0.180	0.08	17.21	2.71
	3	290	0.115	0.03	10.42	2.00
three-needle pairs	5	290	0.301	1.00	37.21	2.79
	3	290	0.198	1.00	24.86	2.36
four-needle pairs	5	290	0.354	1.00	45.86	2.86
	3	290	0.236	1.00	30.64	2.42
2x2 hexagonal array	5	290	0.291	1.00	36.86	3.29
	3	290	0.190	0.41	22.93	2.71
3x3 hexagonal array	5	290	0.471	1.00	44.07	10.57
	3	290	0.308	0.99	29.07	7.00

Erev<E   Erev<E<Eirrev   E>Eirrev

Fig. 4. False color legend used in Figs. 5–7, indicating the local electric field E distribution within the tissue models (i.e., the degree of tissue electropermeabilization). The white region represents insufficiently electropermeabilized regions of tissue ($E < E_{\text{rev}}$), and the patterned region represents irreversibly electropermeabilized regions of tissue ($E > E_{\text{irrev}}$).

Because the first part of our study showed that voltage (U), distances between electrodes (b and d), and depth of electrode insertion (g) are all relevant for the distribution of electric field in the model, all four parameters were chosen for the optimization procedure. We ran the genetic algorithm for all electrode geometries and polarities in two distinct stages. In the first stage, ten runs of the algorithm were performed using a random initial population. To calculate solutions closer to the true optimum, the ten best solutions acquired from the first stage were "seeded" into the initial population of the second stage and five more solutions were calculated, all being of better fitness than the first-stage solutions. However, the difference between the best first- and second-stage solutions was less than 1% (if compared by V_{Hirrev}); therefore, no third stage was required, and the best second stage solution was considered to be the optimum.

III. RESULTS

The calculated critical voltage U_c needed to cover the entire tumor tissue with electric field above reversible electropermeabilization threshold E_{rev} for each electrode geometry and polarity is given in Table II. The shallower insertion of the electrodes generally increased the necessary U_C; however, the total current I through the model decreased. Increasing the number of the electrodes had the opposite effect: Lower U_C and higher I were calculated. Both observations can be explained by the size of contact surface between electrodes and treated tissue—larger contact surface increases I and decreases the necessary U_C.

When we applied the same voltage (290 V) to all electrode configurations, complete electropermeabilization of the tumor was not obtained in all cases. Namely, one needle electrode pair was completely unsuccessful, whereas both hexagonal geometries did not provide adequate coverage at $g = 3$ mm [Table III, Figs. 4, 5(a) and (b), and 6(b) and (d)]. Figs. 5 and 6 show a definite influence of electrode configuration on electric field distribution in the tumor and healthy tissue. This influence is most clearly seen by comparing electric field distributions of both hexagonal needle electrode arrays—electric field penetrates deeper for 3×3 geometry and V_{Hirrev} is considerably larger than in 2×2 geometry (Fig. 6). It can also be observed that deeper insertion of electrodes ($g = 5$ mm) and insufficient voltage applied on the electrodes cause the electric field to be higher within the healthy tissue below the tumor compared to
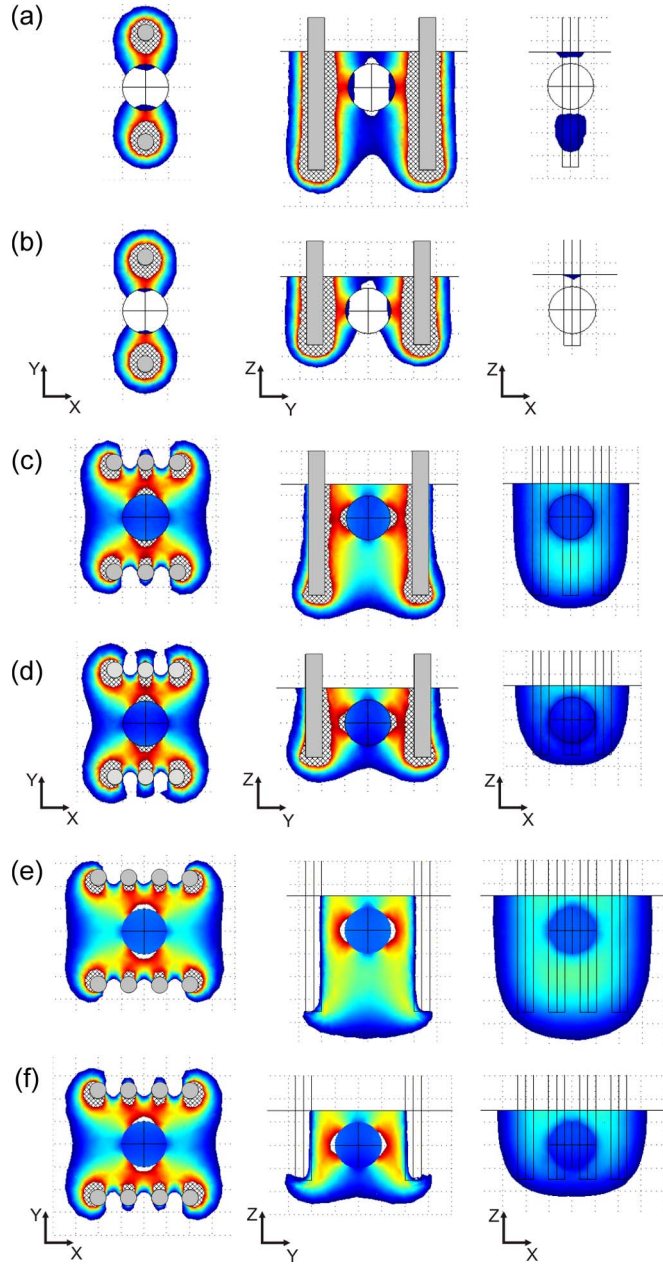
Fig. 5. Local electric field distribution for the models of (a) and (b) one needle electrode pair, (c) and (d) three needle electrode pairs, and (e) and (f) four needle electrode pairs is shown for two depths of electrodes' insertion $g = 5$ mm [(a), (c), (e)] and $g = 3$ mm [(b), (d), (f)]. Electric field distribution is shown in three central perpendicular planes: XY, YZ, and XZ all passing through the center of the tumor. Distance between opposite sets of electrodes d, distance between electrodes of the same row b (needle electrode arrays) or distance between neighboring electrodes b (hexagonal needle electrode array) and voltage U are given in the caption of Table III.

Fig. 6. Local electric field distribution for the models of (a) and (b) 2×2 hexagonal needle electrode array and (c) and (d) 3×3 hexagonal needle electrode array is shown for two depths of electrodes' insertion $g = 5$ mm [(a), (c)] and $g = 3$ mm [(b), (d)]. Electric field distribution is shown in three central perpendicular planes: XY, YZ, and XZ all passing through the center of the tumor. Distance between opposite sets of electrodes d, distance between electrodes of the same row b (needle electrode arrays) or distance between neighboring electrodes b (hexagonal needle electrode array) and voltage U are given in the caption of Table III.

the electric field inside the tumor (Fig. 5(a), (c), and (e) in ZX orientation).

To assure complete electropermeabilization of the tumor and with the least healthy tissue damage in our model, all geometrical and electrical parameters have to be accounted for. When all parameters were optimized simultaneously, the required U_C was significantly lower (Table IV) than when determining the U_C for only two depths of needle insertion (Table II). At the same time, I, V_{Hrev}, and V_{Hirrev} were also
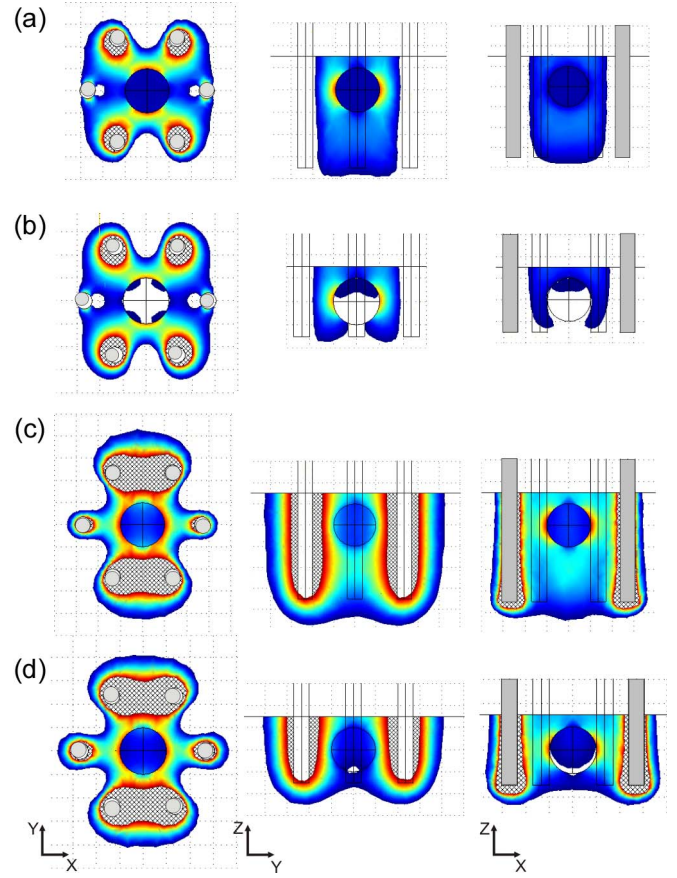
decreased, thus minimizing healthy tissue damage and required electric energy. Interestingly, the optimum depth of insertion depended very much on the electrode geometry, i.e., at similar applied voltages, the 2×2 hexagonal needle electrode array has to be inserted deeper than the 3×3 needle electrode array to achieve similar coverage of the target tumor tissue. The results of optimization using our algorithm are shown in Table IV and Fig. 7.

IV. DISCUSSION AND CONCLUSION

The aim of our study was to investigate and optimize the local electric field within a simple 3-D model of a subcutaneous tumor. We report the results of optimization of the geometrical and electrical parameters (voltage, distances between electrodes, depth of electrode insertion: U, b, d, and g; Figs. 1 and 3) of various needle electrode geometries used in research and clinical ECT for a 3-D numerical model of a subcutaneous tumor (Fig. 2). We show by using our optimization algorithm, how the local electric field distribution depends on the number, arrangement, depth of electrodes' insertion, and the amplitude

TABLE IV
OPTIMIZED VALUES OF DISTANCE BETWEEN ELECTRODES OF THE SAME ROW b (NEEDLE ELECTRODE ARRAYS), DISTANCE BETWEEN NEIGHBORING ELECTRODES b (HEXAGONAL NEEDLE ELECTRODE ARRAY), DISTANCE BETWEEN OPPOSITE SETS OF ELECTRODES d, DEPTH OF ELECTRODES' INSERTION g, AND CRITICAL VOLTAGE U_C FOR ALL ANALYZED ELECTRODE GEOMETRIES AND POLARITIES ARE GIVEN. CALCULATED VALUES OF TOTAL ELECTRIC CURRENT I, REVERSIBLY ELECTROPERMEABILIZED TUMOR VOLUME V_{Trev}, REVERSIBLY AND IRREVERSIBLY ELECTROPERMEABILIZED HEALTHY TISSUE V_{Hrev} AND V_{Hirrev}, RESPECTIVELY, ARE GIVEN FOR ALL OPTIMUM SOLUTIONS. ALL VOLUME VALUES ARE NORMALIZED BY THE TUMOR VOLUME V_T

Electrode configuration and polaririty	b [mm]	d [mm]	g [mm]	U_C [V]	I [A]	$\dfrac{V_{Trev}}{V_T}$	$\dfrac{V_{Hrev}}{V_T}$	$\dfrac{V_{Hirrev}}{V_T}$
three-needle pairs	0.70	4.04	3.15	272	0.20	1	23.64	1.86
four-needle pairs	0.67	4.10	3.20	265	0.25	1	28.29	1.65
2x2 hexagonal array	1.71	3.47	3.57	256	0.24	1	21.86	2.34
3x3 hexagonal array	1.71	3.47	2.90	246	0.32	1	21.64	5.14

of electric pulses (Figs. 5–7, Tables II–IV). The complete coverage of the target tumor tissue with the local electric field magnitude required for successful ECT ($E_{\mathrm{rev}} < E < E_{\mathrm{irrev}}$) was achieved, whereas the volumes of healthy tissue exposed to the magnitude of the local electric field above reversible and irreversible thresholds were minimized (thus minimizing healthy tissue damage) for all analyzed electrode geometries.

Our study was built on previous research works done by our group and others, in which the usefulness of numerical modeling in predicting electropermeabilization outcomes was demonstrated. Already, the early numerical plate and needle electrode models in combination with *in vivo* experiments showed great promise in analysis of tissue electropermeabilization *in vivo* [18], [25]. However, only after the experimental validation of a numerical model was performed by comparing the numerical calculations to histological examinations of electropermeabilized tissue did numerical modeling gain ground in ECT research [11]. Different geometries of needle electrodes have been since then compared by [14], [26], and [27]; however, none of these included optimization and only Sel *et al.* [28] used a 3-D model. In our study, three needle electrode pairs, four needle electrode pairs, and 2×2 hexagonal needle electrode array all gave similar results, whereas the 3×3 hexagonal needle electrode array was significantly worse than the others. We examined the adequacy of needle electrode geometries by calculating values of total electric current through the model and volumes of reversibly and irreversibly electropermeabilized (damaged) healthy tissue. By analyzing all three measures, we can conclude that three needle electrode pairs gave the best results—they required the lowest total electric current, which caused a small volume of healthy tissue to be reversibly and even less to be irreversibly electropermeabilized (Fig. 7(a), Table IV). Four needle electrode pairs caused the
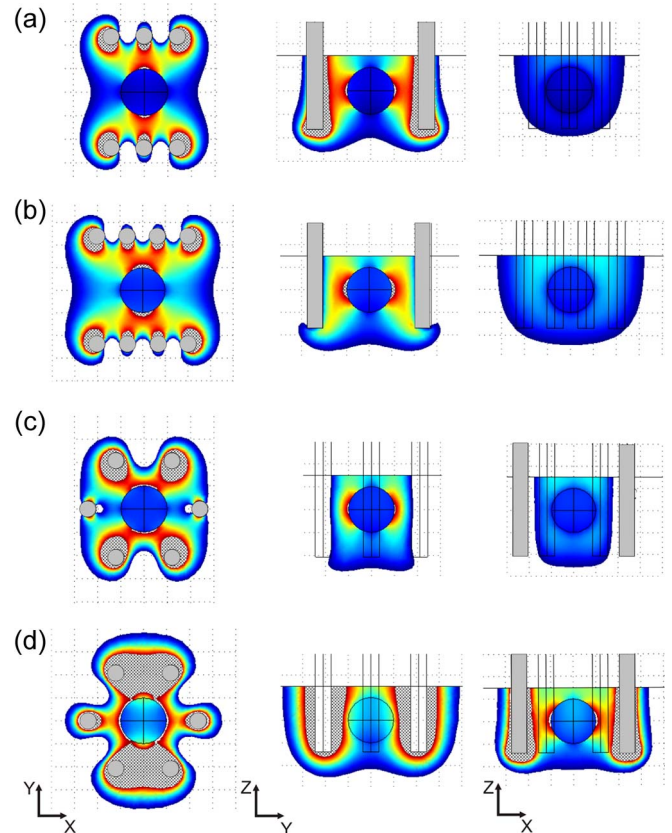

Fig. 7. Local electric field distribution for the optimized models of (a) three needle electrode pairs, (b) four needle electrode pairs, (c) 2×2 hexagonal needle electrode array, and (d) 3×3 hexagonal needle electrode array is shown. The electric field distribution is shown in three central perpendicular planes: XY, YZ, and XZ all passing through the center of the tumor. Corresponding optimized parameters which are distance between electrodes of the same row b (needle electrode arrays), distance between neighboring electrodes b (hexagonal needle electrode array), distance between opposite sets of electrodes d, depth of electrodes' insertion g, and critical voltage U_C are given in Table IV.

least healthy tissue damage; however, they required more current and more healthy tissue to be reversibly electropermeabilized (Fig. 7(b), Table IV), confirming previous results of our group—more electrodes mean a more invasive procedure, higher needed current, and lower needed voltage to obtain the same target tissue coverage [11], [26]. The 2×2 hexagonal needle electrode array caused the least volume of healthy tissue to be reversibly electropermeabilized and more to be irreversibly electropermeabilized (Fig. 7(c), Table IV). The 3×3 hexagonal needle electrode array optimization lead to the highest values of total electric current and the largest area of irreversibly permeabilized healthy tissue (Fig. 7(d), Table IV). The preference for three needle electrode pairs is also in agreement with our previous 2-D study [27].

The only other ECT optimization study was performed by Sel *et al.* who optimized the distance and voltage between electrodes for a realistic brain tumor using four pairs of needle electrodes as a proof of principle [28]. In our study, we used a simpler tumor model; however, we took the optimization one step further by optimizing for four different electrode geometries and polarities and for four different parameters, one of them being the depth of needle insertion, which turned

out to be significant. We demonstrated that inserting needle electrodes deeper than necessary, using inadequate electrode geometries, polarities, and arrangement with respect to the target tumor tissue, and applying insufficient voltage can result in unsuccessful electropermeabilization ($E < E_{\text{rev}}$) of the tumor. Moreover, the electric field within the healthy tissue below the tumor can be higher compared to the electric field inside the tumor [Figs. 5(a) and 6(d)]. This effect can be even more pronounced if the tumor is much more conductive than the surrounding tissue, because the electric field is then lower in the tumor and higher in the surrounding tissue [27]. The importance of insertion depth can also be seen if we compare the optimum depth for hexagonal needle electrode arrays—deeper insertion is required for the 2×2 needle electrode array, although all other geometrical parameters are the same for both configurations.

Even though our algorithm gives good results, significant challenges remain before it can be used for the optimization of *in vivo* ECT of large tumors. Our study does not analyze the possibility of changing electric field orientation in consecutive pulses, which can lead to less tissue damage, because such protocols can require lower voltage and total current [14]. Unfortunately, increasing the number of pulses can increase the unpleasantness of the treatment [29]. We also did not take into account the dynamic changes in tissue conductivities due to the tissue electropermeabilization [19], [28], [30] because this would significantly increase the computation time and would not considerably contribute to the results. Instead, we incorporated the change in conductivity into our model by choosing conductivity values at the end of the electropermeabilization process. Stratum corneum was not added to the model, as needle electrodes penetrate the skin and thus bypass its high resistivity [13]; however, if plate electrodes were to be used, we would most probably have to take into account also the stratum corneum and the skin conductivity changes due to electropermeabilization.

We chose the genetic algorithm as our optimization method, as it is relatively easy to develop and, unlike classical optimization methods, it does not require the fitness function to be differentiable. Linear and nonlinear constraints, such as the realistic technical limitations of high-voltage electric pulse generator (maximum output voltage and current), can be easily implemented into the algorithm, and it also allows optimization of a large number of continuous, discrete, and categorical parameters, e.g., type of electrodes. The drawbacks of the method are that it gives only an approximate solution to the optimization problem and requires a relatively long computation time. However, because the solutions of the algorithm are very close to the true optimum and computation times can be shortened by using a more powerful computer, we do not consider these to be significant drawbacks and believe that the suggested approach is well suited to the problem being addressed.

Numerical modeling and optimization can be efficiently combined to control the extent of tissue electropermeabilization in ECT and to produce the optimum electrode configuration for different types of tumors taking into account their electric properties. Our algorithm is a step forward to an effective treatment planning, not only in clinical ECT, but also in other electroporation-based treatments, such as gene electrotransfer [19], transdermal drug delivery [20], and irreversible tumor ablation [21].

References

[1] M. Marty, G. Sersa, J. R. Garbay, J. Gehl, C. G. Collins, M. Snoj, V. Billard, P. F. Geertsen, J. O. Larkin, D. Miklavcic, I. Pavlovic, S. M. Paulin-Kosir, M. Cemazar, N. Morsli, Z. Rudolf, C. Robert, G. C. O'Sullivan, and L. M. Mir, "Electrochemotherapy—An easy, highly effective and safe treatment of cutaneous and subcutaneous metastases: Results of ESOPE (European Standard Operating Procedures of Electrochemotherapy) study," *Eur. J. Cancer, Suppl.*, vol. 4, no. 11, pp. 3–13, Nov. 2006.

[2] G. Sersa, "The state-of-the-art of electrochemotherapy before the ESOPE study; advantages and clinical uses," *Eur. J. Cancer, Suppl.*, vol. 4, no. 11, pp. 52–59, Nov. 2006.

[3] R. Heller, R. Gilbert, and M. J. Jaroszeski, "Clinical applications of electrochemotherapy," *Adv. Drug Deliv. Rev.*, vol. 35, no. 1, pp. 119–129, Jan. 1999.

[4] A. Gothelf, L. M. Mir, and J. Gehl, "Electrochemotherapy: Results of cancer treatment using enhanced delivery of bleomycin by electroporation," *Cancer Treat. Rev.*, vol. 29, no. 5, pp. 371–387, Oct. 2003.

[5] B. M. Tijink, R. De Bree, G. Van Dongen, and C. R. Leemans, "How we do it: Chemo-electroporation in the head and neck for otherwise untreatable patients," *Clin. Otolaryngol.*, vol. 31, no. 5, pp. 447–451, Oct. 2006.

[6] L. M. Mir, J. Gehl, G. Sersa, C. G. Collins, J. R. Garbay, V. Billard, P. F. Geertsen, Z. Rudolf, G. C. O'Sullivan, and M. Marty, "Standard operating procedures of the electrochemotherapy: Instructions for the use of bleomycin or cisplatin administered either systemically or locally and electric pulses delivered by the Cliniporator by means of invasive or non-invasive electrodes," *Eur. J. Cancer, Suppl.*, vol. 4, no. 11, pp. 14–25, Nov. 2006.

[7] M. Snoj, Z. Rudolf, M. Cemazar, B. Jancar, and G. Sersa, "Successful sphincter-saving treatment of anorectal malignant melanoma with electrochemotherapy, local excision and adjuvant brachytherapy," *Anti-Cancer Drugs*, vol. 16, no. 3, pp. 345–348, Mar. 2005.

[8] G. Sersa, M. Cemazar, D. Miklavcic, and Z. Rudolf, "Electrochemotherapy of tumours," *Radiol. Oncol.*, vol. 40, no. 3, pp. 163–174, 2006.

[9] C. Domenge, S. Orlowski, B. Luboinski, T. De Baere, G. Schwaab, J. Belehradek, and L. M. Mir, "Antitumor electrochemotherapy: New advances in the clinical protocol," *Cancer*, vol. 77, no. 5, pp. 956–963, Mar. 1996.

[10] D. Miklavcic, K. Beravs, D. Semrov, M. Cemazar, F. Demsar, and G. Sersa, "The importance of electric field distribution for effective in vivo electroporation of tissues," *Biophys. J.*, vol. 74, no. 5, pp. 2152–2158, May 1998.

[11] D. Miklavcic, D. Semrov, H. Mekid, and L. M. Mir, "A validated model of in vivo electric field distribution in tissues for electrochemotherapy and for DNA electrotransfer for gene therapy," *Biochim. Biophys. Acta*, vol. 1523, no. 1, pp. 73–83, Sep. 2000.

[12] M. Puc, S. Corovic, K. Flisar, M. Petkovsek, J. Nastran, and D. Miklavcic, "Techniques of signal generation required for electropermeabilization. Survey of electropermeabilization devices," *Bioelectrochemistry*, vol. 64, no. 2, pp. 113–124, Sep. 2004.

[13] D. Miklavcic, S. Corovic, G. Pucihar, and N. Pavselj, "Importance of tumour coverage by sufficiently high local electric field for effective electrochemotherapy," *Eur. J. Cancer, Suppl.*, vol. 4, no. 11, pp. 45–51, Nov. 2006.

[14] R. A. Gilbert, M. J. Jaroszeski, and R. Heller, "Novel electrode designs for electrochemotherapy," *Biochim. Biophys. Acta*, vol. 1334, no. 1, pp. 9–14, Feb. 1997.

[15] J. F. Edd, L. Horowitz, R. V. Davalos, L. M. Mir, and B. Rubinsky, "In vivo results of a new focal tissue ablation technique: Irreversible electroporation," *IEEE Trans. Biomed. Eng.*, vol. 53, no. 7, pp. 1409–1415, Jul. 2006.

[16] N. Pavselj, Z. Bregar, D. Cukjati, D. Batiuskaite, L. Mir, and D. Miklavcic, "The course of tissue permeabilization studied on a mathematical model of a subcutaneous tumor in small animals," *IEEE Trans. Biomed. Eng.*, vol. 52, no. 8, pp. 1373–1381, Aug. 2005.

[17] D. Miklavcic, N. Pavselj, and F. X. Hart, "Electric properties of tissues," in *Wiley Encyclopedia of Biomedical Engineering*. New York: Wiley, 2006.

[18] J. Gehl, T. H. Sorensen, K. Nielsen, P. Raskmark, S. L. Nielsen, T. Skovsgaard, and L. M. Mir, "In vivo electroporation of skeletal muscle:

Threshold, efficacy and relation to electric field distribution," *Biochim. Biophys. Acta*, vol. 1428, no. 2, pp. 233–240, Aug. 1999.

[19] D. Cukjati, D. Batiuskaite, F. Andre, D. Miklavcic, and L. M. Mir, "Real time electroporation control for accurate and safe in vivo non-viral gene therapy," *Bioelectrochemistry*, vol. 70, no. 2, pp. 501–507, May 2007.

[20] U. F. Pliquett, R. Vanbever, V. Preat, and J. C. Weaver, "Local transport regions (LTRs) in human stratum corneum due to long and short "high voltage" pulses," *Bioelectrochem. Bioenerg.*, vol. 47, no. 1, pp. 151–161, Nov. 1998.

[21] B. Al-Sakere, C. Bernat, E. Connault, P. Opolon, B. Rubinsky, R. Davalos, and L. M. Mir, "Tumor ablation with irreversible electroporation," *PLoS ONE*, vol. 2, no. 11, p. e1 135, 2007.

[22] D. Semrov and D. Miklavcic, "Calculation of the electrical parameters in electrochemotherapy of solid tumours in mice," *Comput. Biol. Med.*, vol. 28, no. 4, pp. 439–448, Jul. 1998.

[23] J. H. Holland, *Adaptation in Natural and Artificial Systems: An Introductory Analysis With Applications to Biology, Control, and Artificial Intelligence*. Cambridge, MA: MIT Press, 1992.

[24] J. Gehl and P. F. Geertsen, "Palliation of haemorrhaging and ulcerated cutaneous tumours using electrochemotherapy," *Eur. J. Cancer, Suppl.*, vol. 4, no. 11, pp. 35–37, Nov. 2006.

[25] G. Sersa, M. Cemazar, D. Semrov, and D. Miklavcic, "Changing electrode orientation improves the efficacy of electrochemotherapy of solid tumors in mice," *Bioelectrochem. Bioenerg.*, vol. 39, no. 1, pp. 61–66, Feb. 1996.

[26] D. Sel, S. Mazeres, J. Teissie, and D. Miklavcic, "Finite-element modeling of needle electrodes in tissue from the perspective of frequent model computation," *IEEE Trans. Biomed. Eng.*, vol. 50, no. 11, pp. 1221–1232, Nov. 2003.

[27] S. Corovic, M. Pavlin, and D. Miklavcic, "Analytical and numerical quantification and comparison of the local electric field in the tissue for different electrode configurations," *Biomed. Eng. Online*, vol. 6, no. 1, p. 37, 2007.

[28] D. Sel, A. M. Lebar, and D. Miklavcic, "Feasibility of employing model-based optimization of pulse amplitude and electrode distance for effective tumor electropermeabilization," *IEEE Trans. Biomed. Eng.*, vol. 54, no. 5, pp. 773–781, May 2007.

[29] A. Zupanic, S. Ribaric, and D. Miklavcic, "Increasing the repetition frequency of electric pulse delivery reduces unpleasant sensations that occur in electrochemotherapy," *Neoplasma*, vol. 54, no. 3, pp. 246–250, 2007.

[30] R. V. Davalos, B. Rubinsky, and D. M. Otten, "A feasibility study for electrical impedance tomography as a means to monitor tissue electroporation for molecular medicine," *IEEE Trans. Biomed. Eng.*, vol. 49, no. 4, pp. 400–403, Apr. 2002.

Selma Corovic was born in 1976. She received the B.Sc. and M.Sc. degrees in electrical engineering from the University of Ljubljana, Ljubljana, Slovenia. She is currently working toward the Ph.D. degree at the Faculty of Electrical Engineering, University of Ljubljana and at the Paris University-Sud XI, Châtenay-Malabry 92 296, France.

She is an Assistant Researcher with the Faculty of Electrical Engineering, University of Ljubljana. Her main research interests are multiphysics numerical modeling and *in vivo* studies of electroporation process in biological tissues and web-based e-learning application development for electroporation-based treatments.

Anze Zupanic was born in 1981. He received the B.Sc. degree in electrical engineering from the University of Ljubljana, Ljubljana, Slovenia, where he is currently working toward the Ph.D. degree in electrical engineering in the Faculty of Electrical Engineering.

He is a Young Researcher with the Faculty of Electrical Engineering, University of Ljubljana. His main research interests are multiphysics numerical modeling and optimization of electroporation-based treatments.

Damijan Miklavcic was born in Ljubljana, Slovenia, in 1963. He received the Ph.D. degree in electrical engineering from the University of Ljubljana, Ljubljana.

He is a Professor with the Faculty of Electrical Engineering, University of Ljubljana, and the Head of the Laboratory of Biocybernetics. He is active in the field of biomedical engineering. His interest in the last years focuses on electroporation-assisted drug and gene delivery, including cancer treatment by means of electrochemotherapy, tissue oxygenation, modeling of biological processes, and hardware development.

Paper III

Importance of Contact Surface Between Electrodes and Treated Tissue in Electrochemotherapy

www.tcrt.org

Electrochemotherapy is an effective antitumor treatment employing locally applied high voltage electric pulses delivered through conductive electrodes to the tumor in combination with chemotherapeutic drugs. The efficiency of electrochemotherapy strongly depends on the local electric field distribution inside the target tissue. For successful therapy the entire target tissue has to be exposed to the local electric field strength above the reversible threshold. The aim of this study is to demonstrate the influence of the contact surface between electrode and treated tissue on the coverage of the tumor tissue by sufficiently high local electric field. The electric field distribution is calculated by means of numerical modeling using finite element method. Numerical results are confirmed with *in vivo* experiments. We demonstrated that the placement of electrodes giving larger electrode-tissue contact surface leads to improved electrochemotherapy outcome. Our results provide guidance on electrochemotherapy for treatment of protruding cutaneous tumors using parallel plate electrodes.

Key words: Electroporation; Electropermeabilization; Electrochemotherapy; Cutaneous tumor; Numerical modeling; Electrodes; DNA electrotransfer; Gene electrotransfer; Electric field distribution.

Selma Čorović, M.Sc.[1,2,3,§]
Bassim Al Sakere, MD, M.Sc.[1,2,§]
Vincent Haddad, M.Sc.[4]
Damijan Miklavčič, D.Sc.[3]
Lluis M. Mir, D.Sc.[1,2,*]

[1]CNRS UMR 8121
Institut Gustave-Roussy
Villejuif, France
[2]University Paris-Sud
UMR 8121
[3]University of Ljubljana
Faculty of Electrical Engineering
Ljubljana, Slovenia
[4]Service of Biostatistics and Epidemiology
Institute Gustave-Roussy
Villejuif, France

§Both authors contributed equally.

Introduction

Electrochemotherapy (1) (ECT) is a non-thermal antitumor treatment employing locally applied high voltage electric pulses (EP) in combination with either sistemic or local injection of chemotherapeutic drugs, such as bleomycin and cisplatin. ECT has been proven to be highly efficient in treatment of solid tumors regardless of their histological origin (1-7). The ECT Standard Operating Procedures are presently defined for cutaneous and subcutaneous tumors (8).

ECT is based on the reversible increase of cell membrane permeability that follows cell exposure to appropriate EP, termed electropermeabilization or electroporation (EPN). These EP, alone, do not kill the cells and have no antitumor effect. Indeed they just allow cytotoxic drugs, which otherwise do not easily penetrate cell membrane to enter and the target tumor cells and to kill them (9, 10).

An important advantage of ECT is that it results in the complete response (CR) of the tumors with drug doses that by themselves have minimal or no antitumor effect and no toxicity on the patients. After ECT good cosmetic effects are obtained due to a selective cell death mechanism that primarily affects the dividing tumor cells (9, 11).

*Corresponding Author:
Lluis M. Mir, D.Sc.
Email : luismir@igr.fr

Abbreviations: ECT, Electrochemotherapy; EP, Electroporation pulses; EPN, Electropermeabilization; CR, Complete response.

In order to obtain a good antitumor effect it is mandatory to electropermeabilise the whole tumor. When a tissue is exposed to EP, an electric field strength is established within the tissue volume. To electropermeabilize the whole tumor in a reversible and safe way, each of the tumor cells have to be subjected to a local electric field (E) above reversible value E_{rev} (which causes transient and reversible perturbations in the cell membrane) and below irreversible value E_{irrev} (which causes permanent damages of the cells). E distribution depends on EP parameters (*i.e.*, amplitude of the pulses, duration, number, repetition frequency, and shape), number, shape, and position of electrodes with respect to the treated tissue, structure of target/tumor tissue, and its surrounding tissues (12-15). It was also previously shown, by combining numerical modeling and experimental approaches, that the ECT treatment efficacy, at a given electrode configuration and pulse amplitude, depends on the magnitude of E within the whole of the target/tumor tissue (10, 12-14, 16-18).

In our present study, we numerically and experimentally analyzed the effect of two different ways of parallel plate electrode placement on the electric field distribution and on the efficacy of ECT treatment of cutaneous tumor with parallel plate electrodes. In the first situation, the electrodes were placed in such a way that very small contact with tissue was formed, while in
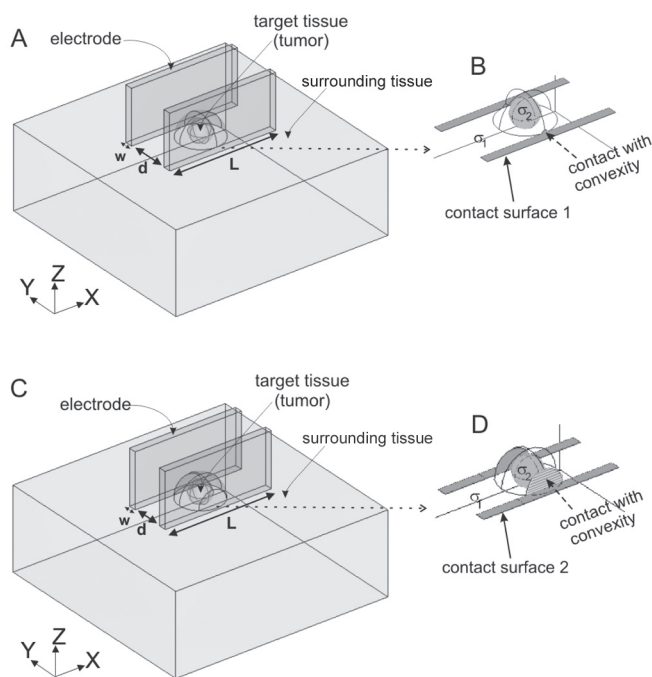
the second one the tissue was placed between two electrodes so that a large surface of contact between electrode and tissue was formed. Predictions on ECT efficacy were made according to the numerical results and they were confronted to the results of the *in vivo* ECT of mice tumors obtained by the two different electrode placements. We demonstrate that the placement of electrodes giving larger electrode-tissue contact surface results in better effectiveness of ECT outcome and in the lower effects on the surrounding normal tissue, a result important for the physicians applying ECT to their patients.

Materials & Methods

Numerical Modeling

The 3D model is based on the numerical solution of partial differential equations for steady electric current in isotropic conductive media. The numerical calculations were performed by means of finite element method using COMSOL Multiphysics 3.3 software package in the 3D Conductive Media DC application mode on a PC running Windows XP with a 3.00 GHz Pentium D processor and 1 GB of RAM.

The model of cutaneous tumor consisted of two tissues: the tumor and its surrounding skin tissue. The input to the model was constant voltage applied to the electrodes and corresponds to the amplitude of the EPN pulses generated by a high voltage generator. The output of the model was the electric field distribution within the treated tissues.

Two distinct model geometries representing two different parallel plate electrode placement situations were built (Fig. 1a and Fig. 1c). The convexity of the tumor and skin is modeled as a 4 mm-diameter hemisphere and the tumor as a 2 mm-diameter sphere.

The results of numerical simulations were controlled by refining the mesh until the difference in numerical solutions was negligible (less than 0.5%) when the number of finite elements (*i.e.*, mesh density) is increased. The mesh of the models with contact surface 1 and contact surface 2 [models 1 (Fig. 1a) and 2 (Fig. 1c)] consisted of 176,419 and 158,760 elements, respectively.

The calculated electric field distribution in our numerical models is shown in the range between the critical values E_{rev} = 400 V/cm and E_{irrev} = 1500 V/cm. The E_{rev} is chosen based on our previous study (16), while the E_{irrev} is chosen based on the latest study on irreversible EPN (18).

Contact Surface Definition

Model 1 (Fig. 1a) describes the treatment situation where electrodes are placed perpendicularly with respect to the sur-

Figure 1: Panels **A** and **B**: Model of cutaneous tumor with d = 4mm, U = 520V and contact surface 1; (**A**) *3D* model with electrodes and (**B**) zoomed convexity of the treated tissue with highlighted contact surface 1. Panels **C** and **B**: Model of cutaneous tumor with d = 3mm, U = 390V and contact surface 2: (**C**) *3D* model with electrodes and (**D**) zoomed convexity of the treated tissue with highlighted contact surface 2. In both models w = 0.7mm, L = 10mm, σ_1 is surrounding tissue conductivity and σ_2 is tumor tissue conductivity.

face of the cutaneous tumor touching the skin tissue just at the limit of the tumor convexity. Model 2 (Fig. 1c) describes the situation where the same cutaneous tumor is placed in between two electrodes touching also the surface of the volume convexity (see patterned region of the contact surface 2, Fig. 1d). In model 1 contact is obtained on a small surface of the treated volume convexity, pointed to by the dashed arrow in Figure 1b, corresponding to 2% of the contact surface in model 2. The distances between electrodes (d) were 4 mm and 3 mm, respectively. The voltage delivered to the tissue from the EP generator was modeled as a constant potential set to the entire surface between electrodes and treated tissue. In both models the applied voltage was set so that the ratio $U/d = 1300$ V/cm was obtained, setting the voltage to 520V and 390V, respectively, in model 1 and 2. Based on this the Direchlet boundary condition was defined. The Neumann boundary condition, *i.e.*, the electric-insulation condition was set to the rest of the outer boundaries of the models.

Material Properties of the Modeled Tissues

Since we modeled the tumor and surrounding skin layers at the end of the EPN process (to numerically evaluate the outcome of the treatment), the conductivity values of tumor and its surrounding tissue were selected considering both data obtained with direct current measurements of tissue conductivities of electropermeabilized tissues (19) and the conductivity data obtained in *in vivo* experiments and numerical analysis in (16). Namely, conductivities of 0.4S/m and 0.2S/m were assigned, respectively, to the regions representing the electropermeabilized tumor and the electropermeabilized surrounding tissue (which describes the average conductivity of the skin tissue, not considering the high resistance of the stratum corneum that is almost immediately broken after the beginning of the first EP) (20). Thus, both tissues in our model were considered to be isotropic and homogeneous, not taking into account the changes in conductivity of tissues due to electropermeabilization. These changes would require an additional more complex analysis of functional dependency of tissue conductivity on electric field distribution, while not contributing to the demonstration of the influence of the contact surface on the ECT outcome.

In Vivo Experiments

The LPB cells, a methylcholanthrene-induced C57Bl/6 mouse sarcoma cell line, was cultured using standard procedures and minimum essential medium (Gibco BRL, Cergy-Pontoise, France) supplemented with 100U/ml penicillin, 100mg/ml streptomycin (Sarbach, France), and 8% foetal calf serum (Gibco). C57Bl/6 female mice, 6-8 weeks old, were inoculated subcutaneously in the left flank with 1×10^6 cells, producing cutaneous tumors of the same dimensions as those of the numerical models in about nine days.

The two longest orthogonal diameters of the cutaneous tumor a and b (with $a > b$), were measured using callipers. At the day of treatment, average tumor diameter, including the skin tissue was 3.85 ± 0.21 mm. The range of the tumor diameters $(a + b)/2$ was 3.5-4.25 mm and the maximal individual diameter a was 4.3 mm. The volume V of the tumors was determined using the Equation [1]:

$$V = (\pi/6) \cdot a \cdot b^2 \qquad [1].$$

Animals were housed and handled according to recommended guidelines (21).

Tumor Treatment and Follow-up

Mice were anaesthetised with 12.5 mg/kg xylazine (Bayer Pharma, Puteaux, France) and 125 mg/kg ketamine (Parke Davis, Courbevoie, France) injected intraperitoneally in 150 µl saline before the ECT.

ECT treatment consisted in an intravenous injection of 10 µg bleomycin (Roger Bellon, Neuilly, France) followed, 4 minutes after the injection, by 8 rectangular, 100 µs long EP at a repetition frequency of 5000 Hz (2, 22). The EP were generated by a Cliniporator™ (Igea, Carpi, Italy) and delivered directly to the tissue using 3 mm and 4 mm apart stainless-steel parallel plate electrodes (10 mm long and 0.7 mm wide). The electrodes were placed in direct contact to the previously shaved skin on both sides of the cutaneous tumors. No conductive gel was used, to fully respect the geometry and contact area between the skin and the electrodes. As in the models described before, the amplitude of voltage pulses applied between the two parallel electrodes 3 and 4 mm apart were 390V and 520V, respectively. The ECT outcomes obtained with these two electrode placements were followed in two groups of 15 mice for 27 days after the ECT, by means of measurements of the perpendicular diameters a and b every second day. A control group of 13 mice, not treated with ECT, was similarly followed. Response to ECT was qualified as CR if tumor completely disappeared at the end of the follow-up. For ethical reasons all the mice bearing tumor were sacrificed at the end of the follow-up, while those having no palpable or visible tumor were observed up to day 100. No tumor recurrence was observed at the end of the observation period. In addition very good cosmetic healing scar was obtained in the mice which responded with CR.

Statistical Analysis

The normal distribution of the individual tumor volumes was verified by the test of Shapiro-Wilk and a linear model was then used to determine the significance of the differences between the evolutions of the tumor volumes in the various experimental groups. The Fisher's exact test was

used to compare differences in CR rates between each individual group treated with ECT and the control group of mice and between the two groups treated by ECT.

Results

Numerical Results

The comparison of the numerically calculated E distribution between the two *3D* models of cutaneous tumor in *XY* (Z=0), *ZY* (X=0), and *ZX* (Y=0) planes is shown in Figure 2. The contact surfaces 1 and 2 are given in Figures 2a and b, respectively. The *XY*, *ZY*, and *ZX* planes are three orthogonal cross-sections along the center of the tumor geometry. The electric field distribution within model 1 is shown in Figure 2a1-3 and within model 2 in Figure 2b1-3. The values of E are displayed in the range from $E_{rev} = 400$ V/cm to $E_{irrev} = 1500$ V/cm value (scale bar, Fig. 2). The patterned region represents the part of tissue with electric field strength exceeding the E_{irrev}.

The comparison of E presented in Figures 2a1 and 2a2 and in Figures 2b1 and 2b2 shows that E within the tumor inside model 2 is higher and more restrained within the tissue area situated between electrodes.

Comparing the *XY* cross-sections, E exceeds E_{rev} (400 V/cm) in a very small part of the tumor in model 1 (Fig. 2a1), while the entire tumor in the model 2 is subjected to $E > 400$ V/cm (Fig. 2b1). The highest E within the tumor surrounding tissue is in the close proximity to the electrode, decreasing toward the center of the tumor in *Y* direction. In the *X* direction E decreases symmetrically towards the two marginal tissue regions.

Comparing the *ZY* cross-sections, E inside model 1 (Fig. 2a2) only exceeds the E_{rev} value in the deepest part of the tumor, while the upper part remains below E_{rev}. In model 2 the entire tumor tissue is covered by $E > E_{rev}$ (Fig. 2b2). E is higher in the region of the surrounding tissue below the tumor than the E inside the tumor.

In the *ZX* cross-section parallel to the electrodes, E only exceeds the E_{rev} in the deepest part in of the tumor tissue inside model 1 (see E distribution in direction Z in Fig. 2a3), while whole tumor volume inside model 2 is exposed to E above E_{rev} (Fig. 2b3).

We also calculated minimum and maximum electric field magnitudes $Etumor_{min}$ and $Etumor_{max}$ over the region representing the tumor, and the percentage of the tumor volume ($Vtumor_{E \geq Erev}$) exposed to the reversible electric field above $E > E_{rev} = 400$ V/cm, for both electrode placements analyzed (Table I).

Table I

$Etumor_{max}$ and $Etumor_{min}$ inside the tumor and percentages of tumor volumes $Vtumor_{E \geq Erev}$ subjected to E above $E_{rev} = 400$V/cm, calculated for both models.

Model	$Etumor_{max}$ [V/cm]	$Etumor_{min}$ [V/cm]	$Vtumor_{E \geq Erev}$
1	516	207	32%
2	1119	610	100%

In addition we calculated the percentage of healthy tissue volume exposed to E above E_{rev} ($Vsurr_{E \geq Erev}$) and E_{irrev} ($Vsurr_{E \geq Eirrev}$) over the entire volume of surrounding tissue in both models (Table II). Further, in order to more precisely investigate the local E within the healthy surrounding tissue in the close vicinity of electrodes we calculated the average E ($Esurr$) below the electrodes over the tissue exposed to $E > Eirrev$ (Table II).

Experimental Results

The comparison between tumor regression obtained in the two groups of mice treated with ECT (Fig. 3) demonstrates

Table II

Average E within surrounding tissue in close vicinity of electrodes ($Esurr$) and percentages of healthy tissue volumes $Vsurr_{E \geq Erev}$ and $Vsurr_{E \geq Eirrev}$ subjected to E above $E_{rev} = 400$V/cm and $Eirrev = 1500$V/cm, respectively.

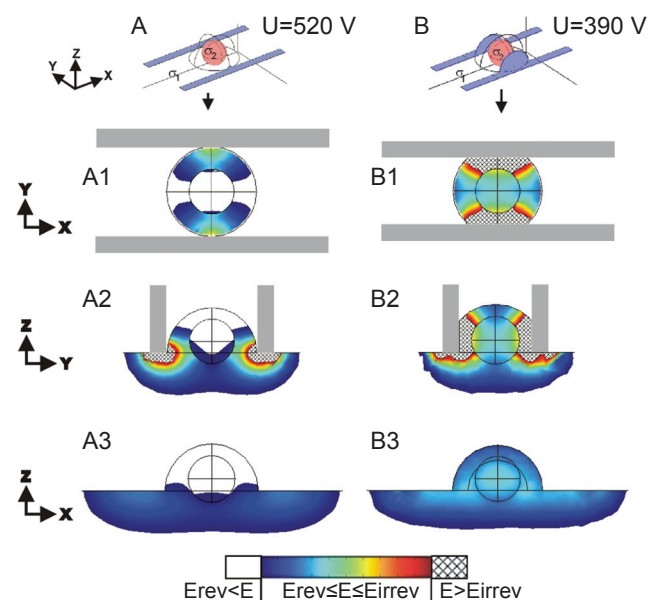| Model	$Esurr$ [V/cm]	$Vsurr_{E \geq Erev}$	$Vsurr_{E \geq Eirrev}$
1	2130	4.79%	0.37%
2	1760	3.40%	0.35%

Figure 2: Comparison of results obtained between model 1 [(**A**) 3D model geometry with highlighted contact surface 1; (**A1**) E in *XY* cross section; (**A2**) E in *ZY* cross section; and (**A3**) E in *ZX* cross section] and model 2 [(**B**) 3D model geometry with highlighted contact surface 2; (**B1**) E in *XY* cross section; (**B2**) E in *ZY* cross section; and (**B3**) E in *ZX* cross section], ($\sigma_1 = 0.2$S/m, $\sigma_2 = 0.4$S/m, $E_{rev} = 400$V/cm, and $E_{irrev} = 1500$V/cm).

that ECT performed with electrode placement with larger electrode-tissue contact surface (contact surface 2, U = 390 V, d = 3 mm) resulted in significantly better anti-tumor effectiveness compared to the ECT with electrode placement with the smaller electrode tissue contact surface (contact surface 1, U = 520 V, d = 4 mm) (p = 0.0002). The average tumor volumes obtained at the end of the follow-up (on day 27) were 2697 mm^3 and 648 mm^3 for the groups of tumors treated with ECT with contact surfaces 1 and 2, respectively, while it was 4528 mm^3 in the control group (statistically significant, p = 0.006 and p < 0.0001, respectively).

The ECT of tumors performed with electrode placement with contact surface 2 resulted in 7 CR out of 15 treated mice (47%) and in only 1 CR in the group of 15 mice (7%) treated with electrode placement with electrode contact tissue 1 (Table III). According to the Fisher's exact test, the difference between control group and the group treated with ECT (contact surface 2) is statistically significant (p = 0.007), while the difference between control group and the group of animals treated with ECT (contact surface 1) was not statistically significant (p = 1). Further, the result of Fisher's exact test evaluation between the group treated with ECT (contact surface 2) and the group treated with ECT (contact surface 1) is significant (p = 0.04).

Table III

Number of CR in the three experimental groups. There were statistically significant differences between the ECT - contact surface 2 group and the two other groups (p = 0.007 with the control group and p = 0.004 with the ECT - contact surface 1 group). There was no significant difference between the control and the ECT - contact surface 1 groups.

Groups	Number of mice	Number of CR	Percentage of CR
Control	13	0	0%
ECT – contact surface 1	15	1	7%
ECT – contact surface 2	15	7	47%

Discussion

In this study we numerically and experimentally analyzed the consequences of the effects of two different ways to place parallel plate electrodes for the treatment of cutaneous tumors by electrochemotherapy. These two situations differ by the contact surface between the electrodes and the tissue. The aim was to show which of the two electrode placements meets better the requirements for effective ECT, which means to achieve high electropermeabilization efficiency of target/tumor tissue but at the same time spare normal tissue and avoid side effects. In terms of local electric field distribution the requirements are the following: (i) all the target tissue has to be exposed to the electric field E above the threshold value for reversible electroporation ($E > E_{rev}$) and (ii) the surrounding tissue should not be exposed to excessively high E, meaning that the local electric field in the surrounding healthy tissue should be as low as possible.
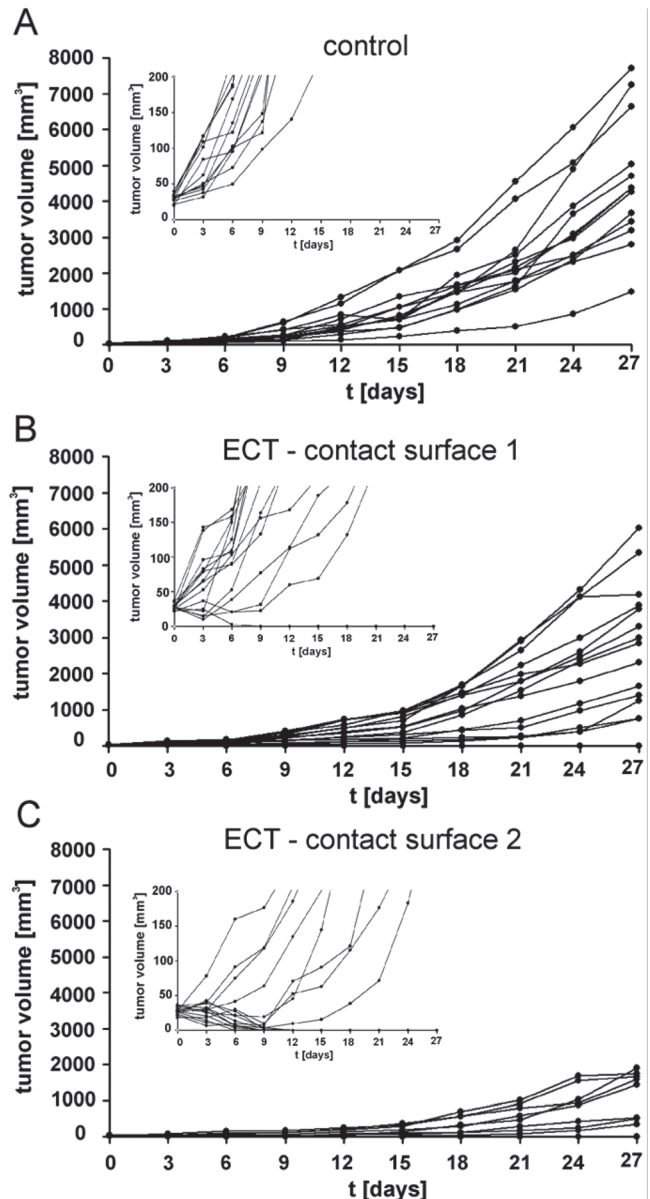

Figure 3: Evolution of the tumor volume: (**A**) in the control group (n = 13); (**B**) in the mice treated with ECT (U = 520V, d = 4 mm, and contact surface 1) (n = 15); and (**C**) in the mice treated with ECT (U = 390V, d = 3 mm, and contact surface 2) (n = 15). Each curve corresponds to an individual tumor growth. Differences are statistically significant (p = 0.0002 between the two treated groups and p = 0.006 and p < 0.0001 between the control group and, respectively, the groups treated with ECT using d = 4 mm and contact surface 1 and d = 3 mm and contact surface 2). Inserts in each panel show the growth of the tumors for sizes not larger than 200 mm^3, displaying the initial tumor volume evolution and the regression of one and seven tumors, respectively, in the group treated with ECT using U = 520V, d = 4 mm, and contact surface 1 and in the group treated with ECT using U = 390V, d = 3 mm, and contact surface 2.

The two 3D numerical models and the experiments with *in vivo* cutaneous tumors were carried out with the same input parameter as the voltage to distance ratio U/d was set to 1300 V/cm, a parameter usually applied in clinical end ex-

perimental ECT (1, 2, 8). By means of numerical modeling we examined the influence of the dimensions of electrode-tissue contact surface on the electric field strength inside the target tumor tissue (Tables I and II). The results show that the larger the electrode-tissue contact surface, the higher the local electric field strength inside the tumor and the lower local electric field in the surrounding tissue.

These numerical results were confirmed by *in vivo* ECT of mice tumors having similar dimensions as those numerically modeled. In the first electrode placement, the electrodes were 4 mm apart and just a point contact with the tumor convexity was obtained (corresponding to the point defined by the arrow in Fig. 1b). In the second electrode placement the electrodes were 3 mm apart. By "squeezing" the tissue in between the electrodes a larger electrode-tissue contact surface with cutaneous tumor convexity was obtained (corresponding to the patterned surface in Fig. 1d).

We obtained better results with the larger electrode-tissue contact surface 2, due to the fact that in this electrode placement the entire volume of the tumor was subjected to E in the range $E_{rev} \leq E < E_{irrev}$. Indeed, the complete EPN of the tumor allowed the bleomycin to enter and kill all the tumor cells, resulting in tumor CR in 7 out of 15 treated tumors. In contrast, the smaller electrode-tissue contact surface resulted in only one CR out of 15 tumors, due to the residual untreated tumor cells, in the region of the tumor where the value of the local electric field strength was below E_{rev}.

It is interesting to note that the best antitumor (thus electropermeabilizing) effects in situation 2 are reached by the lowest voltage set ($U = 390$V instead of $U = 520$V), just because in situation 2 the contact surface is the largest. This is in agreement with our previously published data where the local E distribution in liver tissue was determined based on results of biological observations and numerical calculations obtained with needle electrodes of different diameters (14). The applied voltage at which reversible and irreversible tissue electropermeabilization was obtained was lower, and the local E distribution was more homogeneous, using the electrodes of largest diameter, the needles of the largest diameter having of course the largest electrode tissue contact surface. Similarly, in this paper we show that in the larger electrode-tissue contact surface lower voltage ($U = 390$V) results in higher local E inside the tumor (Table I), while lower value of E in the close vicinity of the electrodes was found and less healthy tissue was electropermeabilized compared to the results obtained with the smaller contact surface (Tables I and II).

In conclusion, the experimental results presented herein are in good agreement with numerical models. By appropriate placement of electrodes on the surface of the treated tissue, a better coverage by sufficiently high electric field ($E \geq Erev$)

can be achieved over the entire target tissue and minimized in the surrounding tissues and thus better therapy outcome. Recommendations can be given to researchers and physicians to choose electrodes geometry and placement in the way assuring the largest electrode-tissue contact surface. Another important consequence is that the needed parameters for successful ECT of each individual type of tumor can be determined, and thus the needed treatment planning carried out, by means of numerical modeling, as previously suggested in (17). Moreover, the electrode placement in a way to increase the electrode-tissue contact surface, described in this paper, can be beneficial also in other electropermeabilization mediated therapies such as gene electrotransfer (23), transdermal drug delivery (20), and irreversible tumor ablation (24-27).

Acknowledgements

References

1. Mir, L. M., Orlowski, S., Belehradek, J. Jr., Paoletti, C. Electrochemotherapy Potentiation of Antitumor Effect of Bleomycin by Local Electric Pulses. *Eur J Cancer 27*, 68-72 (1991).
2. Marty, M., Sersa, G., Garbay, J. R., Gehl, J., Collins, C. G., Snoj, M., Billard, V., Geertsen, P. F., Larkin, J. O., Miklavcic, D., Pavlovic, I., Paulin-Kosir, S. M., Cemazar, M., Morsli, N., Soden, D. M., Rudolf, Z., Robert, C., O'Sullivan, G. C., Mir, L. M. Electrochemotherapy - An Easy, Highly Effective and Safe Treatment of Cutaneous and Subcutaneous Metastases: Results of ESOPE (European Standard Operating Procedures of Electrochemotherapy) Study. *Eur J Cancer Supplements 4*, 3-13 (2006).
3. Snoj, M., Rudolf, Z., Paulin-Kosir, S. M., Cemazar, M., Snoj, R., Sersa, G. Long Lasting Complete Response in Melanoma Treated by Electrochemotherapy. *Eur J Cancer Supplements 4*, 26-28 (2006).
4. Garbay, J. R., Billard, V., Bernat, C., Mir, L. M, Morsli, N., Robert, C. Successful Repetitive Treatments by Electrochemotherapy of Multiple Unresectable Kaposi Sarcoma Nodules. *Eur J Cancer Supplements 4*, 29-31 (2006).
5. Whelan, M. C., Larkin, J. O., Collins, C. G., Cashman, J., Breathnach, O., Soden, D. M., O'Sullivan, G. C. Effective Treatment of an Extensive Recurrent Breast Cancer Which Was Refractory to Multimodal Therapy by Multiple Applications of Electrochemotherapy. *Eur J Cancer Supplements 4*, 32-34 (2006).
6. Gehl, J., Geertsen, P. F. Palliation of Heamorraging and Ulcerated Cutaneous Tumors Using Electrochemotherapy. *Eur J Cancer Supplements 4*, 35-37 (2006).
7. Sersa, G. The State-of-the-art of Electrochemotherapy Before the ESOPE Study; Advantages and Clinical Uses. *Eur J Cancer Supplements 4*, 52-9 (2006).
8. Mir, L. M, Gehl, J., Sersa, G., Collins, C. G., Garbay, J. R., Billard V., Geertsen, P. F., Rudolf, Z., O'Sullivan, G. C., Marty, M. Standard Operating Procedures of Electrochemotherapy: Instructions for the Use of Bleomycin or Cisplatin Administered either Systemically or Locally and Electric Pulses Delivered by CliniporatorTM by Means of Invasive or Non-invasive Electrodes. *Eur J Cancer Supplements 4*, 14-25 (2006).

9. Mir, L. M., Orlowski, S. Mechanisms of Electrochemotherapy. *Adv Drug Deliv Rev 35*, 107-118 (1999).

10. Miklavcic, D., Corovic, S., Pucihar, G., Pavselj, N. Importance of Tumor Coverage by Sufficiently High Local Electric Field for Effective Electrochemotherapy. *Eur J Cancer Supplements 4*, 45-51 (2006).

11. Mir, L. M. Bases and Rationale of Electrochemotherapy. *Eur J Cancer Supplements 4*, 38-44 (2006).

12. Gehl, J., Sorensen, T. H., Nielsen, K., Raskmark, P., Nielsen, S. L., Skovsgaard, T., Mir, L. M. *In vivo* Electroporation of Skeletal Muscle: Threshold, Efficacy and Relation to Electric Field Distribution. *Biochim Biophys Acta 1428*, 233-240 (1999).

13. Corovic, S., Pavlin, M., Miklavcic, D. Analytical and Numerical Quantification and Comparison of the Local Electric Field in the Tissue for Different Electrode Configurations. *BioMedical Engineering OnLine 6*, 1-14 (2007).

14. Miklavcic, D., Semrov, D., Mekid, H., Mir, L. M. A Validated Model of *In vivo* Electric Field Distribution in Tissues for Electrochemotherapy and for DNA Electrotransfer for Gene therapy. *Biochim Biophys Acta 1523*, 73-83 (2000).

15. Pavlin, M., Pavselj, N., Miklavcic, D. Dependence of Induced Transmembrane Potential on Cell density, Arrangement, and Cell Position Inside a Cell System. *IEEE Trans Biomed Eng 49*, 605-612 (2002).

16. Pavselj, N., Bregar, Z., Cukjati, D., Batiuskaite, D., Mir, L. M., Miklavcic, D. The Course of Tissue Permeabilization Studied on a Mathematical Model of a Subcutaneous Tumor in Small animals. *IEEE Trans Biomed Eng 52*, 1373-1381 (2005).

17. Sel, D., Lebar, A. M., Miklavcic, D. Feasibility of Employing Model-Based Optimization of Pulse Amplitude and Electrode Distance for Effective Tumor Electropermeabilization. *IEEE Trans Biomed Eng 54*, 773-781 (2007).

18. Ivorra, A., Rubinsky, B. *In vivo* Electrical Impedance Measurements During and After Electroporation of Rat Liver. *Bioelectrochemistry 70*, 287-295 (2007).

19. Miklavcic, D., Pavselj, N., Hart, X. F. Electric Properties of Tissues. *Wiley Encyclopedia of Biomedical Engineering*, John Wiley & Sons, New York (2006).

20. Pliquett, U. F., Vanbever, R., Preat, V., Weaver, J. C. Local Transport Regions (LTRs) in Human Stratum Corneum Due to Long and Short 'high voltage' Pulses. *Bioelectrochem Bioenerg 47*, 151-161 (1998).

21. (UKCCCR) Guidelines for Welfare of Animals in Experimental Neoplasia (Second Edition). *Br J Cancer 77*, 1-10 (1998).

22. Zupanic, A., Ribaric, S., Miklavcic, D. Increasing the Repetition Frequency of Electric Pulse Delivery Reduces Unpleasant Sensations that Occur in Electrochemotherapy. *Neoplasma 54*, 246-250 (2007).

23. Cukjati, D., Batiuskaite, D., Andre, F., Miklavcic, D., Mir, L. M. Real Time Electroporation Control for Accurate and Safe In vivo Nonviral Gene Therapy. *Bioelectrochemistry 70*, 501-507 (2007).

24. Al-Sakere, B., Bernat, C., Connault, E., Opolon, P., Rubinsky, B., Davalos, R., Mir, L. M. Tumor Ablation with Irreversible Electroporation. *PLoS ONE 2*, 11 (2007).

25. Al-Sakere, B., Bernat C., André, F., Connault, E., Opolon, P., Davalos, R. V., Mir, L. M. A Study of the Immunological Response to Tumor Ablation with Irreversible Electroporation. *Technol Cancer Res Treat 6*, 301-306 (2007).

26. Onik, G., Mikus, P., Rubinsky, B. Irreversible Electroporation: Implications for Prostate Ablation. *Technol Cancer Res Treat 6*, 295-300 (2007).

27. Bertacchini, C., Margotti, P. M., Bergamini, E., Lodi, A., Ronchetti, M., Cadossi, R. Design of an Irreversible Electroporation System for Clinical Use. *Technol Cancer Res Treat 6*, 313-320 (2007).

Paper IV

BioMedical Engineering OnLine

Research

An e-learning application on electrochemotherapy

Selma Corovic†, Janez Bester† and Damijan Miklavcic*†

Address: University of Ljubljana, Faculty of Electrical Engineering, Trzaska 25, 1000 Ljubljana, Slovenia

Email: Selma Corovic - selma.corovic@fe.uni-lj.si; Janez Bester - janez.bester@fe.uni-lj.si; Damijan Miklavcic* - damijan.miklavcic@fe.uni-lj.si

* Corresponding author   †Equal contributors

Abstract

Background: Electrochemotherapy is an effective approach in local tumour treatment employing locally applied high-voltage electric pulses in combination with chemotherapeutic drugs. In planning and performing electrochemotherapy a multidisciplinary expertise is required and collaboration, knowledge and experience exchange among the experts from different scientific fields such as medicine, biology and biomedical engineering is needed. The objective of this study was to develop an e-learning application in order to provide the educational content on electrochemotherapy and its underlying principles and to support collaboration, knowledge and experience exchange among the experts involved in the research and clinics.

Methods: The educational content on electrochemotherapy and cell and tissue electroporation was based on previously published studies from molecular dynamics, lipid bilayers, single cell level and simplified tissue models to complex biological tissues and research and clinical results of electrochemotherapy treatment. We used computer graphics such as model-based visualization (i.e. 3D numerical modelling using finite element method) and 3D computer animations and graphical illustrations to facilitate the representation of complex biological and physical aspects in electrochemotherapy. The e-learning application is integrated into an interactive e-learning environment developed at our institution, enabling collaboration and knowledge exchange among the users. We evaluated the designed e-learning application at the International Scientific workshop and postgraduate course (Electroporation Based Technologies and Treatments). The evaluation was carried out by testing the pedagogical efficiency of the presented educational content and by performing the usability study of the application.

Results: The e-learning content presents three different levels of knowledge on cell and tissue electroporation. In the first part of the e-learning application we explain basic principles of electroporation process. The second part provides educational content about importance of modelling and visualization of local electric field in electroporation-based treatments. In the third part we developed an interactive module for visualization of local electric field distribution in 3D tissue models of cutaneous tumors for different parameters such as voltage applied, distance between electrodes, electrode dimension and shape, tissue geometry and electric conductivity. The pedagogical efficiency assessment showed that the participants improved their level of knowledge. The results of usability evaluation revealed that participants found the application simple to learn, use and navigate. The participants also found the information provided by the application easy to understand.

Conclusion: The e-learning application we present in this article provides educational material on electrochemotherapy and its underlying principles such as cell and tissue electroporation. The e-learning application is developed to provide an interactive educational content in order to simulate the "hands-on" learning approach about the parameters being important for successful therapy. The e-learning application together with the interactive e-learning environment is available to the users to provide collaborative and flexible learning in order to facilitate knowledge exchange among the experts from different scientific fields that are involved in electrochemotherapy. The modular structure of the application allows for upgrade with new educational content collected from the clinics and research, and can be easily adapted to serve as a collaborative e-learning tool also in other electroporation-based treatments such as gene electrotransfer, gene vaccination, irreversible tissue ablation and transdermal gene and drug delivery. The presented e-learning application provides an easy and rapid approach for information, knowledge and experience exchange among the experts from different scientific fields, which can facilitate development and optimisation of electroporation-based treatments.

Background

Electrochemotherapy is an effective approach in tumor treatment employing locally applied high-voltage electric pulses in combination with chemotherapeutic drugs which enter tumor cells after their membrane has been electroporated [1,2]. Electroporation is a phenomenon of cell membrane permeability increase due to local delivery of short and sufficiently intense voltage pulses via appropriate electrodes to the target cells and tissues [3,4]. In addition to electrochemotherapy, other medical applications of electroporation are emerging at an increasing rate, such as gene electrotransfection [5,6], cell fusion [7] and irreversible tissue ablation [8] and transdermal gene and drug delivery [9]. The effectiveness of cell and tissue electroporation, and thus the effectiveness of electroporation-based therapies, depends on one hand on the parameters of the applied pulses such as amplitude, duration, number and repetition frequency and type of electrodes used and on the other hand on the characteristics of the cell and tissues to be electroporated. Depending on the

electric pulse parameters used, electroporation can be reversible or irreversible. Namely, when the electric pulses are applied, local electric field (E) is established within the treated tissue. In order to cause structural changes in cell membrane magnitude of local electric field need to achieve the critical reversible threshold value ($Erev$). The phenomenon is reversible until the magnitude of local electric field reaches the irreversible threshold value $Eirrev$, which causes permanent damages of the cell membrane. The reversible electroporation regime has to be assured in all applications in which the viability of cells has to be preserved, such as electrochemotherapy and particularly gene therapy [4]. On the other hand, in some medical and biotechnological applications such as irreversible tumour tissue ablation, liquid food sterilization or water treatment, the irreversible electroporation is used as a nonthermal method for efficient cell killing [10]. The key role in electroporation effectiveness plays the local electric field, which can be directly modified by the amplitude of delivered electric pulses and electrodes used for electric pulse

Table 1: Scientific fields and the corresponding expertise needed in electrochemotherapy

Field	Expertise
- Oncology:	Tumor cells and tissues, cancer
- Biology:	Cells, normal tissue
- Biophysics:	Physics of biological cells and tissues
- Physical chemistry:	Chemistry
Electrical engineering:	Devices, electrodes
- Biophysical engineering:	Application of physics in medicine and biology
- Computer engineering:	Database systems, interactive web applications

delivery [11]. Thus, for controlled use of the method in each particular electroporation-based application electric pulse parameters and electrodes' shape and placement with respect to the target tissue need to be specifically optimized [12].

Knowledge exchange and collaboration among the experts involved in electroporation-based therapies

In development of electroporation-based therapies (e.g. electrochemotherapy), a multidisciplinary expertise is required. In electrochemotherapy a close collaboration, knowledge and experience exchange among experts in the fields of oncology, biology, biophysics, physical chemistry and electrical, biomedical engineering and informatics is needed (Table 1). The efficacy of electrochemotherapy can be assured with the knowledge of parameters of the local electric field (i.e. pulse parameters and electrode geometry and their positioning), being crucial for successful tissue electroporation and subsequently for the best electrochemotherapy treatment outcome. Realistic mathematical models validated by corresponding experimental observations are valuable tool in designing and optimization of local electric field distribution. To develop a good mathematical model allowing for therapy outcome prediction the engineers need to posses knowledge about biological mechanisms involved in electrochemotherapy. To make the therapy as efficient as possible it is of great importance to transfer the knowledge from basic science to the field of biomedical engineering and to the practicing clinicians who performs the treatment.

Information and communication technology is necessary for efficient interdisciplinary collaboration and knowledge exchange. Internet technology has already been successfully used to support clinical trials of electrochemotherapy by establishing a central database and the Web application system for electronic collection of data (such as treatment parameters used and treatment efficiency follow up) submitted by users from distant medical centres across Europe [13-15]. Based on a comprehensive analysis of collected data, performed by the developed system the standard operating procedures for clinical electrochemotherapy of cutaneous and subcutaneous tumor in patients have been defined [2,16-18]. The clinical trials showed and numerous other studies demonstrated, that electrochemotherapy is an efficient antitumor treatment regardless of tumor histology and its location. In order to further improve the treatment planning methods also for other electroporation-based therapies, to develop the needed equipment (i.e. generators, electrodes, software) and to broaden the clinical electrochemotherapy to other types of tumours, numerous international and multidisciplinary scientific projects are being conducted.

A collaborative e-learning in electrochemotherapy

The objective of our study was to develop an e-learning application to support collaboration, knowledge and experience exchange among experts involved in electrochemotherapy and to also apply the acquired knowledge to other electroporation-based technologies such as gene electrotransfection, irreversible tissue ablation and transdermal gene and drug delivery. The target users of our application are biomedical engineers, biologists involved in research and other application development, the clinicians, oncologists and medical personnel involved in choosing and performing the treatment, but also patients and all those who want to learn about electrochemotherapy. The target audience is therefore mixed [19] (i.e. coming from scientific areas, different fields of expertise, and with different level of experiences) and dispersed [20] (i.e. geographically located in different research centres spread around Europe/World). In order to consider the users involved in electrochemotherapy our e-learning application was designed to provide educational material for collaborative and flexible learning.

Computer-supported learning of various types i.e. e-learning based educational trainings such as web-based learning, CD-contents or virtual instruments play an important roll in sharing learning content and educational materials, which brings new potential for interdisciplinary and international co-operation among experts from different fields [21]. The e-learning programs that incorporate computer based simulations and visualization tools enable educationally effective and enjoyable learning and teaching methods compared to the conventional learning methods such as learning through listening to spoken words [22,23]. The use of computer based simulation techniques are particularly important in developing active e-learning environments and "hands-on" e-learning activities, which is proven to be important component in electromagnetic engineering, biomedical engineering and medical education [24-26]. In designing the e-learning content when the target users are coming from different professional backgrounds and with different levels of knowledge it is essential to develop an adaptive interface which can be suitable for different categories of users: novices, intermediates or expert users. In order to more clearly represent the underling mechanisms from the engineering, biological, chemical and medical sciences, scientific and information visualization concepts based on computer graphics software are necessary [27,28]. Furthermore, collaboration, learning, networking, communication of scientific ideas and knowledge and experience exchange, among the mixed and dispersed audience can be facilitated by computer-supported collaborative visualization [29,30].

The web based technologies facilitate flexible learning by providing a choice of learning modalities (i.e. in local, near or remote conditions), which is particularly important when the dispersed audience is concerned [20]. Accordingly, we used web-based technologies to collect, organize and transfer the acquired knowledge among the target audience in electrochemotherapy. We used computer graphics such as model-based visualization and simple 2D and 3D computer animations and graphical illustrations to facilitate the representation of complex biological and physical mechanisms involved in electrochemotherapy. The educational content is based on previously published results from molecular dynamics, lipid bilayers, single cell level and simplified tissue models to complex biological tissues [3,4,11,31-43].

The e-learning application is integrated into an interactive e-learning environment E-CHO [44] developed at our institution. The e-learning application on electrochemotherapy was introduced to the participants at the International Scientific workshop and postgraduate course (Electroporation Based Technologies and Treatments) that took place at the University of Ljubljana in November 2007 [45]. The pedagogical efficiency of the application was analyzed by participant evaluation on the presented educational content at the beginning and at the end of the e-learning training session. We also present the results of a simple usability evaluation of the application we performed by asking the participants to answer to a usability questionnaire and to provide users opinion/comments on the application and suggestions on its possible improvement.

Methods
The e-learning web application is based on HTML, JavaScript, ASP and Macromedia Flash web technologies. Graphical illustrations and 3-dimensional visualizations of the electroporation process on the levels of cell membrane, cell and tissues were done by using a software package 3D Studio Max. Based on the numerical calculations of electric filed distribution carried out with software packages FEMLAB and Matlab, more simple 2-dimensional and 3-dimensional illustrations were designed using software packages 3D StudioMax, Macromedia Flash, PhotoShop and CorelDraw. The educational content (textual and graphical information) is published using Hypertext Markup Language (HTML). The designed e-learning application is integrated into E-CHO e-learning system developed by the Laboratory of telecommunications [44] (University of Ljubljana) at the Faculty of Electrical Engineering. The E-CHO e-learning environment enables the use of various types of communications among users, such as forums, e-mail correspondence and videoconferencing as well as authentication of users, statistical analysis, network traffic measurement, and support for video streaming [46].

Evaluation
We introduced the designed e-learning application at the International Scientific workshop and postgraduate course (Electroporation Based Technologies and Treatments) [45] in order to evaluate its pedagogical and usability efficiency. The participants were a mixed audience of 17 participants with heterogeneous knowledge and experience in the field of electrochemotherapy and other electroporation-based technologies. The mixed audience was composed of participants coming from different research institutions across Europe and World:

- Denmark (University of Copenhagen: 1 biologist (PhD student) and 1 medical physician (PhD researcher) from Herlev Hospital and 1 from Gentofte Hospital);

- France (1 physicist (PhD student) from doctoral school École normale supérieure de Cachan; 1 biologist (Post-Doc researcher) from Institut Gustave Roussy, Villejuif; 2 biologists (1 PhD student and 1 PostDoc researcher) from IPBS (Institut de Pharmacologie et de Biologie Structurale) - Research Unit of CNRS/UMR 5089 and University Paul Sabatier, Toulouse);

- Egypt (University of Cairo: 1 physicist (PhD student) from Biophysics Department, Faculty of Science); and

- Slovenia (University of Ljubljana: 8 electrical engineers (PhD students) from Faculty of Electrical Engineering and 1 biologist (PhD student) from Faculty of Pharmacy).

In order to statistically analyze the obtained results we divided the mixed audience/participants into two groups:

first group of 11 engineers (by gathering electrical engineers and physicists) and second group of 7 biologists (by gathering biologists and the medical physician).

The participants were gathered in a computer-based classroom providing each participant with a computer. Each of the participants was provided with a username and password to log on to the E-CHO system. Before the start of the e-learning session a Power Point presentation was presented to the participants by the instructor giving instructions on the course of studying the educational content and on the evaluation testing. In order to create a collaborative e-learning environment the participants were encouraged to collaborate (i.e. discuss between each other and with the instructor) while studying the educational content.

The participants were given the instruction to execute the e-learning session according to the linear sequence of studying steps [30] by starting at the beginning of the e-learning content and by concluding with the final evalua-

tion tests. The evaluation tests were taken by each of the participants only once.

We evaluated the e-learning application by testing the pedagogical efficiency of the presented educational content and by performing the usability study of the application. All the participants were asked to provide their agreement on the use of the results of pedagogical efficiency and usability study for the research purposes. Each of the participants individually completed the evaluation tests and submitted them to the E-CHO system for further statistical analysis. The time sequence of the steps performed during our study is given by a flow chart in Fig. 1.

1) Pedagogical efficiency study
In order to evaluate the pedagogical efficiency of the educational content on electrochemotherapy the participants were asked to answer to the same test before and at the end of the e-learning session. The questions were targeted so as to give 50% to 100% success. The exact questions asked in the pre and post e-learning session test are given in Additional file 1.

2) Usability study
The usability evaluation was conducted at the end of the e-learning session after the pedagogical efficiency evaluation was completed. The participants were asked to complete a usability questionnaire related to the user satisfaction with the developed e-learning application, in order to allow the authors (i.e. developers and instructors) to detect possible errors or to obtain the users feedback on further upgrades/improvements. The questionnaire consisted of thirteen usability related questions (see Additional file 2). The participants were asked to express their opinion on a seven point Likert scale (LS) ranging from 1 (disagree - LS (1)) to 7 (strongly agree (LS - (7)) statement or to remain neutral by checking neither agree nor disagree (NA) statement, which we considered as negative evaluation result (Additional file 2). After completing the usability questionnaire the participants were encouraged to provide their opinion/comments on the application and suggestions for its improvement.

Results
The structure of the e-learning content
The e-learning content presents three different levels of knowledge on electroporation-based treatment (i.e. elec-
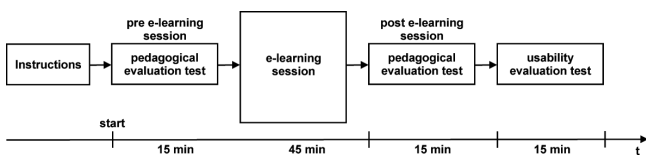

Figure 1
A flow chart representing the time sequence of the steps performed during the study.

trochemotherapy) and cell and tissue electroporation. The e-learning content particularly emphasizes the importance of local electric field for successful cell and tissue electroporation. The main structure of the e-learning content is given in Fig. 2.

The first part of our e-learning application (Basics of electroporation process) brings the educational material on basic mechanisms underlying electroporation process on the levels of: cell membrane, cell and tissue as a composite of cells. Electroporated cell in a local electric field exceeding reversible threshold value $E > Erev$ is represented by a simple graphical illustration in Fig. 3a. The electroporation of cell membrane first occurs within the cell area facing the electrodes (dashed line in Fig. 3a), since the induced transmembrane potential is maximal at the poles of the cell in accordance Schwan's equation: $U_{TI} = -1.5\ r\ E \cos(\phi)$, where r is the radius of the cell, E is the strength of applied electric field, and ϕ is the angle between the direction of the electric field and the selected point on the cell surface. Possible applications of electroporation process, depending on parameters of the electric pulses applied, are illustrated in Fig. 3b: the introduction of small molecules, macromolecules and cells' electrofusion require reversible electroporation regime ($Erev < E < Eirrev$), while the permanent cell damaging requires irreversible electroporation thus local electric field exceeding irreversible threshold $E > Eirrev$.

The value of induced transmembrane voltage and thus the cell electroporation depends on the cell size, shape, and the position of the cell with respect to the direction of applied electric field, which we represented in Figs. 4a, b, c and 4d. For a spheroidal cell, maximum induced transmembrane potential strongly depends on its orientation with the respect to the electric field. It is the highest when the spheroidal cell is parallel to the applied electric field. In Fig. 4e we illustrated that increasing the pulse amplitude results in larger area of membrane with smaller extent of electroporation, while increase in pulse number or duration does not affect the membrane area but increases the extent of electroporation.

In order to visualize the electroporation process as animations in three dimensions we used 3D Studio Max software. We visualized the introduction of small molecules through an electroporated cell membrane, into an electroporated cell and into all successfully electroporated cells within an exposed tissue (i.e. a composite of cells), as shown in Fig. 5.

The second part of the e-learning content (Modelling and visualization of local electric field) provides educational content about the importance of modelling and visualization of local electric field in electroporation-based treatments. The user is warned about possible errors that can

Figure 2
The structure of the e-learning application on electrochemotherapy.

be made while performing cell or tissue electroporation, such as insufficient amplitude of electric pulses or inadequate electrode geometry or electrode positioning. This part of e-learning content is particularly intended as guidance to the practitioners who perform electrochemotherapy treatment of solid tumours. Namely, for successful tumour treatment all the tumor cells have to be destroyed, otherwise the tumour cell can re-grow due to the insufficient magnitude of local electric field $E < Erev$. This was demonstrated in our e-learning application with an exam-

ple of an unsuccessful subcutaneous tumour treatment performed on a nude mouse shown in Fig. 6. The Fig. 6a shows the electrode position and the tumour geometry just before the treatment, while Fig. 6b shows the regrowth of two tumours after initial disappearance: two new tumours regrew in the regions (marked with numbers 1 and 2) where the tumour tissue was not exposed to the sufficient electric field $E > Erev$. Simple graphical illustration of the tumor and its surrounding tissue position between two plate electrodes is shown in Fig. 6c. In Fig. 6d
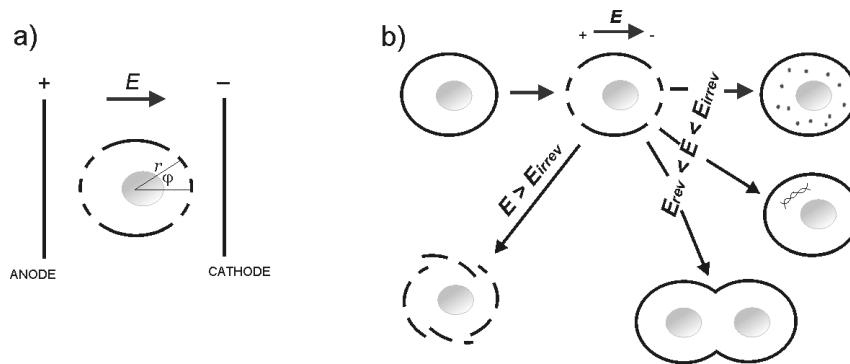

Figure 3
Single cell electroporation and different electroporation regimes. (a) The electroporation of cell membrane first occurs within the cell area facing the electrodes and (b) Different electroporation regimes: reversible $Erev < E < Eirrev$ and irreversible $E > Eirrev$. (Redrawn from [10]).
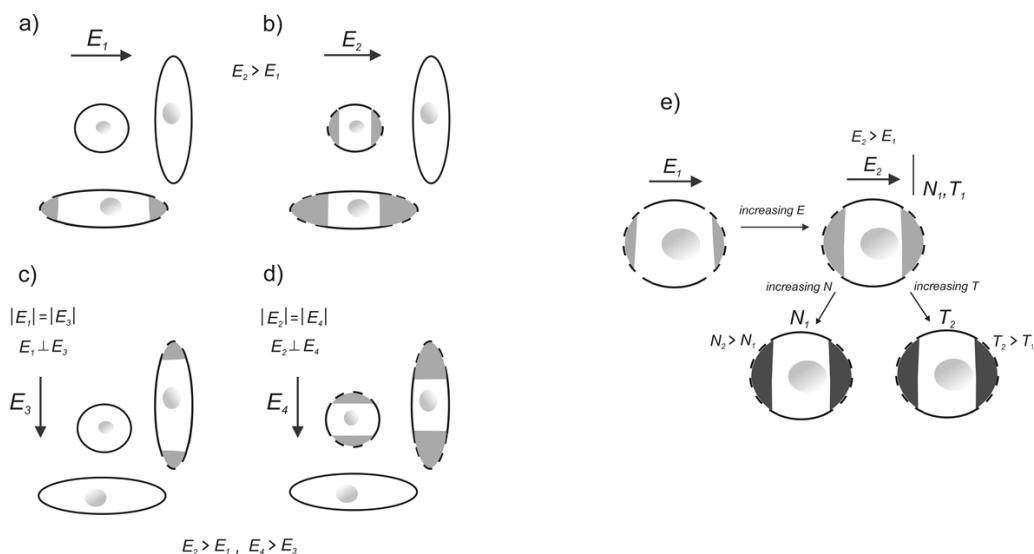
Figure 4
Influence of different parameters on cell electroporation. (a) Electric field parallel to elongated cell, (b) electric pulse amplitude is increased, (c) orientation of electric field is changed, (d) electric pulse amplitude is increased and (e) increasing the pulse amplitude results in larger area of membrane with smaller extent of electroporation, while increase in pulse number or duration does not affect the membrane area but increases the extent of electroporation. (Redrawn from [10]).

calculated local electric field distribution: the reversibly electroporated tissue is marked with colours (from blue to red), the tissue exposed to $E > Erev$ is marked white and the patterned region represents the irreversibly electroporated tissue $E > Eirrev$.

By using simple graphical illustration we pointed out that the effectiveness of electrochemotherapy can be improved by: optimizing the applied voltage, changing electrode dimension or changing electrode orientation and their position, which we previously predicted by means of numerical modelling. We further provide a list of important parameters of the local electric field in electropora-

tion-based treatments, such as: electrode geometry (needle or plate electrodes), dimension of the particular electrode (width, length, diameter), distance between electrodes, electrode position with respect to the target tissue, electrode orientation with respect to the target tissue, geometry of the target tissue, geometry of the tissue surrounding the target tissue, the contact surface between the electrode and the tissue, electric properties of the target tissue i.e. tissue conductivity, electric properties of the surrounding tissue, the voltage applied to the electrodes and threshold values of the tissue $Erev$ and $Eirrev$. Using mathematical modelling and graphical illustrations we showed that the local electric field within the treated tissue is not
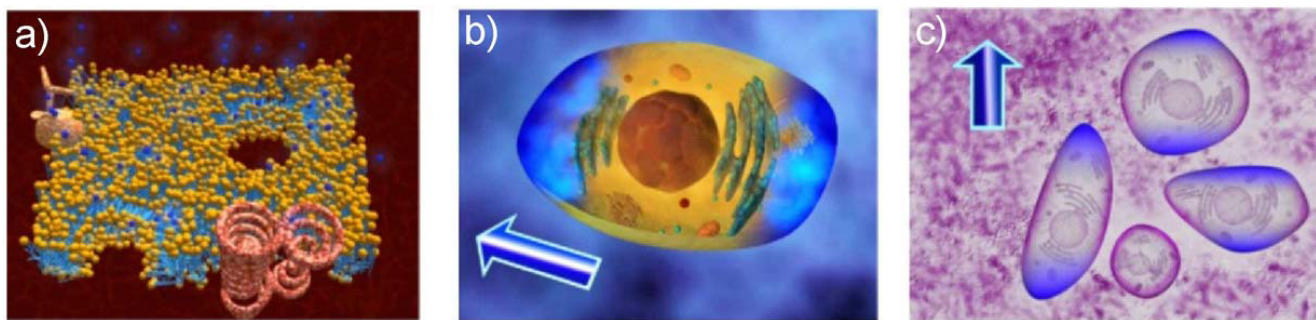

Figure 5
Administration of small molecules by electroporation. Administration of small molecules (blue molecules) through an electroporation cell membrane (a) into an electroporated cell (b) and into the successfully electroporated cells within an exposed tissue (i.e. composite of cells) (c).
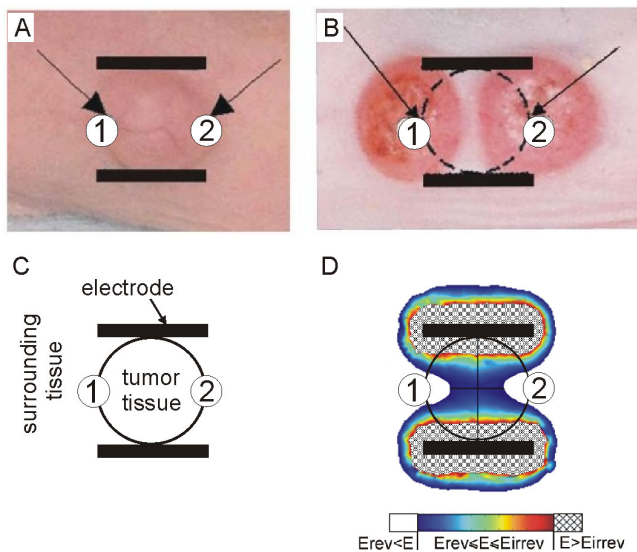
Figure 6
In vivo electrochemotherapy performed on a nude mouse -- tumour regrowth after initial disappearance. In vivo electrochemotherapy of tumour performed on a nude mouse: a) The electrode position and the tumour geometry just before the treatment, b) after the treatment two new tumours regrew in the regions (marked with numbers 1 and 2) where the tumour tissue was not exposed to $E > Erev$, c) graphical illustration of the tumour and its surrounding tissue position between electrodes and d) calculated local electric field distribution: the reversibly electroporated tissue is marked with colours (from blue to red), the tissue exposed to $E > Erev$ is marked white and the patterned region represents the irreversibly electroporated tissue $E > Eirrev$.

homogeneous due to the specific structure and electric properties of the tissues (particularly of the target tumour tissue that usually has higher electric conductivity than its surrounding tissues).

In the third part of the e-learning application (Local electric field in 3D tissue models) we developed an interactive module for visualization of local electric field distribution in tissues for different parameters such as voltage applied, distance between electrodes, electrode' dimension and shape, tissue geometry and electric conductivity. The module provides 3D animations we developed by using 3D Studio Max, which were based on previously calculated local electric field distribution in 3D realistic tissue models. For the numerical calculations we used COMSOL Multiphysics software.

The module allows for local electric field visualization in cutaneous (protruding tumours) and subcutaneous tumours (tumours more deeply seeded in the tissue). Users can appreciate the local electric field distribution

within the treated tissue when electroporated directly or through the skin by using plate or needle electrodes. The module also provides a guideline on how to overcome a highly resistive skin tissue in order to permeabilize more conductive underlying tissues.

The objective of this part of the e-learning application is to provide an interaction with the educational content in order to simulate the "hands-on" learning approach about the parameters of the local electric field. By varying different parameters (such as amplitude of electric pulses, electrodes' dimensions and shape and distance between electrodes) in the navigation bar users have the possibility to shape the electric field distribution within the models (see the navigation bar in Fig. 7). The local electric field distribution can be viewed in 2D model cross-sections or played as a 3D animation. The E is displayed in the range between $Erev$ to $Eirrev$. In Figure 7 the local electric field distribution inside the cutaneous protruding tumour obtained with two different amplitudes of applied voltage (Fig. 7a: $U = 300$ V and Fig. 7b: $U = 600$ V) using two parallel plate electrodes is shown as example. By increasing the applied voltage (for the same tissue geometry, electrode size and position) the stronger local electric field is obtained. Similar effect can be achieved by increasing the electrode dimensions (electrode width), while by increasing the distance between electrodes the tumor is exposed to a lower local electric field intensity, as shown in Figs. 7c and 7d.

The model of subcutaneous tumour gives the user an insight into the local electric field within the target tissue when electroporated through the skin. This model is composed of two layers; the upper layer representing skin tissue with lower specific conductivity compared to the underlying layer which is more conductive. The electric field distribution is presented in two models with two different thicknesses of the skin layer: 1 mm (Fig. 8a) and 3 mm (Fig. 8b). Thus, the user can appreciate the presence of the skin and its poor electric conductivity on the local electric field distribution within the target tumour and its surroundings.

The key messages that the interactive module provides are:

1) in order to successfully electroporate the target tumour through the skin layer a higher voltage needs to be applied compared to the tumour electroporation, which further depends also on skin thickness. The user is offered a guideline on how to overcome the highly resistive skin tissue in order to permeabilize more conductive underlying tissues using plate electrodes (Fig. 8);

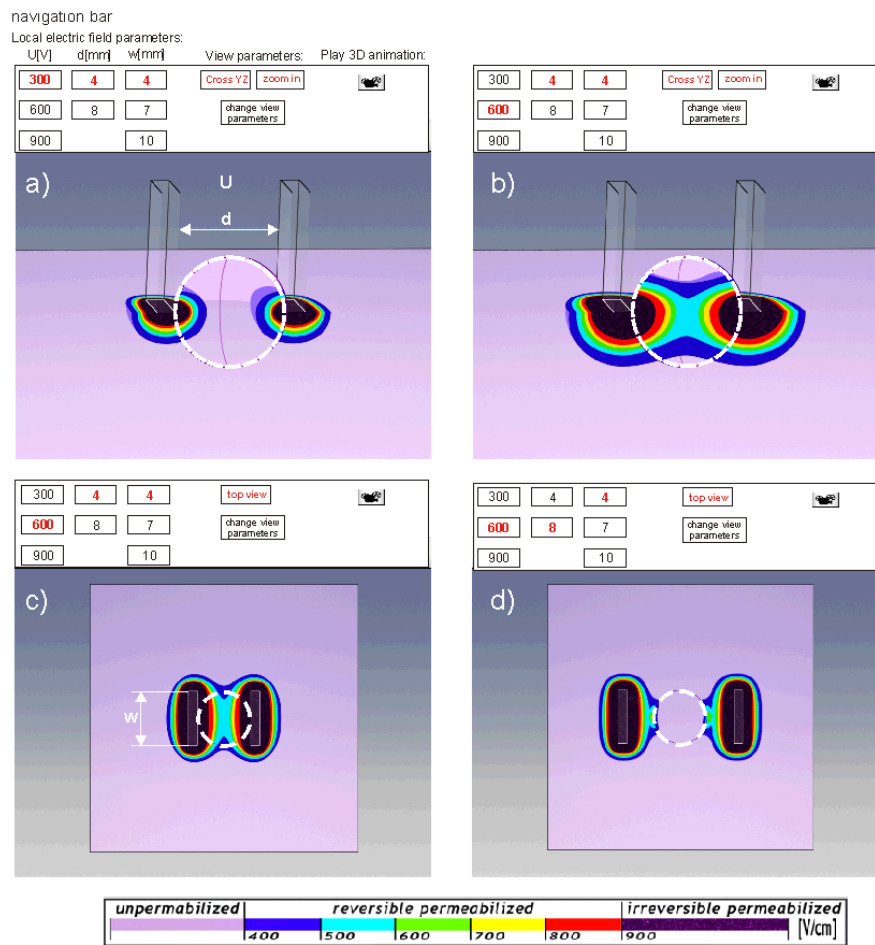2) plate electrodes are more suitable for treatment of protruding cutaneous tumours, while for situations when the

Figure 7
Local electric field distribution within a model of cutaneous (protruding) tumour. Local electric field distribution inside the protruding tumour model for two different applied voltages on the electrodes: a) U = 300 V and b) U = 600 V. The electrodes are 4 mm wide and 4 mm apart in both cases. Electric field distribution inside the models for two distances between electrodes: c) d = 4 mm and d) d = 8 mm. The electrodes are 4 mm wide with the applied voltage U = 600 V in both cases.

tumour is seeded more deeply in the tissue needle electrodes are to be used (Fig. 9a and 9b), and;

3) by increasing the number of needle electrodes stronger local electric field in the tissue can be achieved (Fig. 9c).

The educational web pages are concluded by a test (see Additional file 1) that gives the user an opportunity to test the acquired knowledge, while allowing the teacher and the web-developer to follow the efficacy of the constructed pages and their educational success.

Results of the pedagogical efficiency evaluation
The results of the pedagogical efficiency evaluation are shown in Fig. 10. The evolution of the scores obtained from the test before and after the e-learning session was analyzed on the basis of each question (listed in Additional file 1), which allowed for testing the participants' knowledge improvement for each question and the perti-

nence of the questions. The results of percentage rate analysis of correct answers to each question of the pre and post e-learning session test given by all participants, (both participant groups i.e. engineers and biologists), is shown in Fig. 10a. The results of the percentage rate analysis done for biologists and engineers separately are shown in Figs. 10b and 10c, respectively.

The percentage rate of correct answers for all participants (mixed population) obtained after the e-learning session was above 50% for all questions in the test (Fig. 10a). The results in Fig. 10a show that the level of knowledge of all participants was improved after the e-learning session compared to the knowledge shown before the session. The results in Fig. 10b show that before the e-learning session the knowledge of biologists was more heterogeneous compared to the knowledge possessed by engineers as shown in Fig. 10c.:
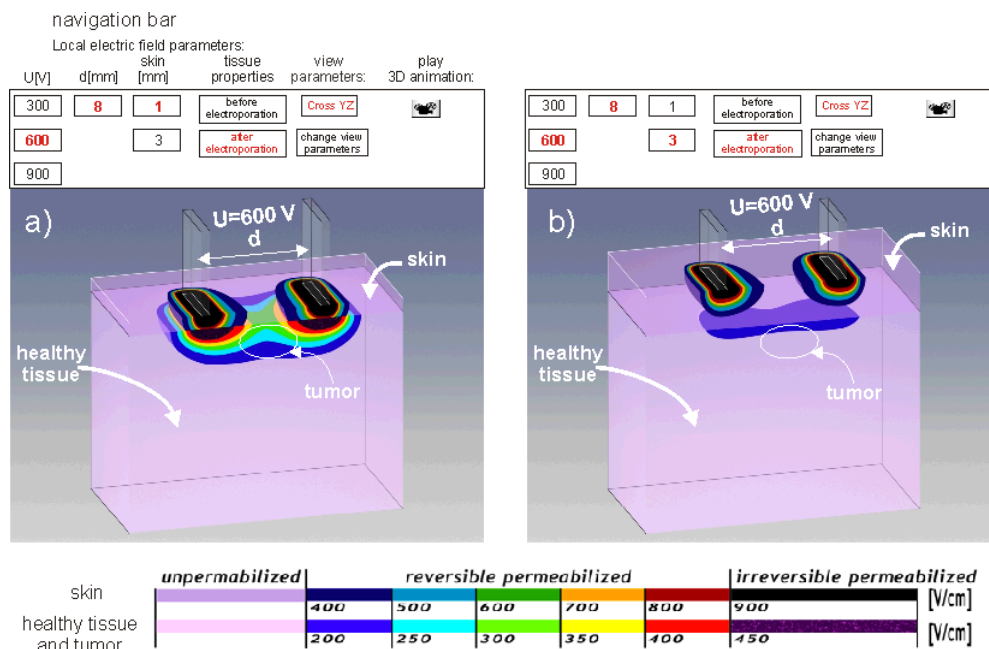
Figure 8
Local electric field distribution within a model of subcutaneous tumor. Local electric field distribution within a model of subcutaneous tumour seeded below: 1 mm thick skin layer (a) and 3 mm thick skin layer (b).

1) for biologists the average percentage rates of correct answers changed from 73% before e-learning session to 87% after e-learning session, with a large dispersion depending on the question (for example - question 4: from 0% before to 43% after e-learning session; question 9 from 86% before to 100% after e-learning session), Fig. 10b.

2) for engineers the average percentage rates of correct answers changed from 89% before e-learning session to 95% after e-learning session, Fig. 10c.

Nevertheless, increase in percentage rate of correct answers, after the e-learning session, to each of the questions was obtained for both groups i.e. biologists and engineers (Figs. 10b and 10c).

Results of the usability evaluation
The results of the usability evaluation of the e-learning application are shown in Fig. 11. The participants expressed their opinion for all 13 usability related questions with 6 or 7 agree statements in the seven point Likert scale (LS (6) and LS (7)) and with neutral neither agree nor disagree statement (NA). None of the questions was evaluated with statements from 1 to 5 in the Likert scale (LS (1-5)), as shown in Fig. 11.

The participants evaluated the statement that the information provided by the system is easy to understand (ques-

tion 9) with the highest percentage of agree statements in the Likert scale (58.3% of LS (7) and 25% of LS (6)). Participant were most neutral (41.7% of NA) regarding question 12 (The system covers all the areas I expected to cover). However, the same question was evaluated with 50% of LS (6) and 8.3% of LS (7) statements. The participants were neutral with 33% for questions 6 (I believe I became more confident with the system) (with 50% of LS (6)) and for question 11 (The interface of system is pleasant) (with 41.67% of LS (6)). Overall, the participants were satisfied with the developed e-learning application (question 13) with 41.6% of the highest percentage of agree statements in the Likert scale (LS (7)) and with only 8.3% of neutral statements (NA). The results of the usability evaluation (Fig. 11) also revealed that the participants were satisfied with how easy it was to use the system (question 1: 33.3% of LS (7) and 50% of LS (6)). The participants were comfortable using the system (question 4: 33.33% of LS (7) and 50% of LS (6)) and found the system simple to use (question 2: 41. 67% of both LS (7) and LS (6)), to learn to use (question 5: 41.67% of LS (7) and 50% of LS(6)) and to be effectively navigated (question 3: 25% of LS (7) and 66.67% of LS (6)). The users also found the information provided with system (such as online help, on-screen messages, and other documentation) clear (question 7: 33.3% of LS (7) and 50% of LS (6)), easy to find (question 8: 25% of LS (7) and 50% of LS (6)) and effective and complete (question 10: 16.67% of LS (7) and 66.67% of LS (6)) (Fig. 11).
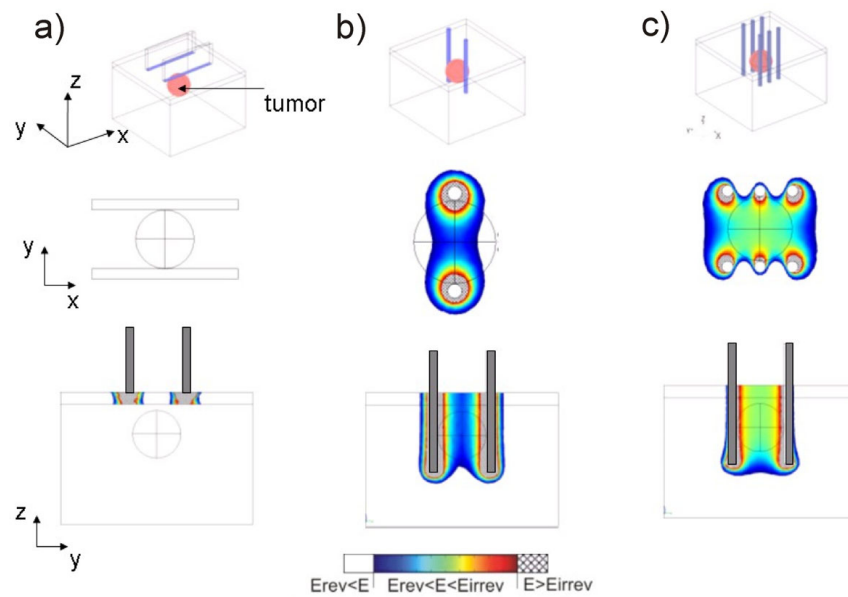
Figure 9
Local electric field in subcutaneous tumour model obtained by using different electrode configurations. Local electric field distribution in subcutaneous tumour model using plate electrodes (a), a pair of needles (b) and three pairs of needles (d). The applied voltage in all cases was U = 300 V.

After completing the usability questionnaire the participants provided their opinion/comments on the application and suggestions on its improvement. Most of participants provided the comment that they liked the idea to present the knowledge on electrochemotherapy in the form of e-learning application. The participants particularly found interesting the interactive visualization of local electric field in tissues for different parameters such as voltage applied, distance between electrodes, electrode' dimension, which for the time being can not be visualized while performing the electrochemotherapy treatment. The engineers, who are not familiar with chemical and biological processes during electroporation of cells and tissues, suggested that more of biological and chemical background should be also added to the existing educational material. On the other hand the biologists suggested that it would be interesting to have a possibility to visualize the distribution of local electric field and changes in electric properties for different cell types such as muscle fibers, hepatocytes, blood vessels, while being electroporated and which are potential target cells for gene transfer.

Discussion

We developed, implemented and evaluated an e-learning application on electroporation-based therapies such as electrochemotherapy. This is the first e-learning application developed to support collaboration, knowledge and experience exchange among the experts from different scientific fields involved in electrochemotherapy and other electroporation-based therapies and in order to organize and to transfer the acquired knowledge and experience to the users (such as clinicians, medical personnel, students, patients and all those who want to learn about electroporation-based therapies).

The educational content on electrochemotherapy and cell and tissue electroporation is based on previously published studies from molecular dynamics, lipid bilayers, single cell level and simplified tissue models to complex biological tissues and research and clinical results of electrochemotherapy treatment [3,4,11,31-43].

The e-learning content presents three different levels of knowledge on cell and tissue electroporation. In the first part of the e-learning application we explain basic mechanisms underlying electroporation process. Based on simple graphical illustrations we demonstrated the influence of each of the pulse parameters, such as pulse amplitude, pulse number and duration, on electroporation of cells with different sizes, shapes and orientations with respect to the applied electric field. By using 3D animation we visualized the aqueous pore formation in cell membrane, which is most widely accepted model, among different theoretical models that describe cell membrane electroporation.

Electrochemotherapy treatment outcome is directly related to the local electric field distribution within the target tumour tissue and its surrounding tissues
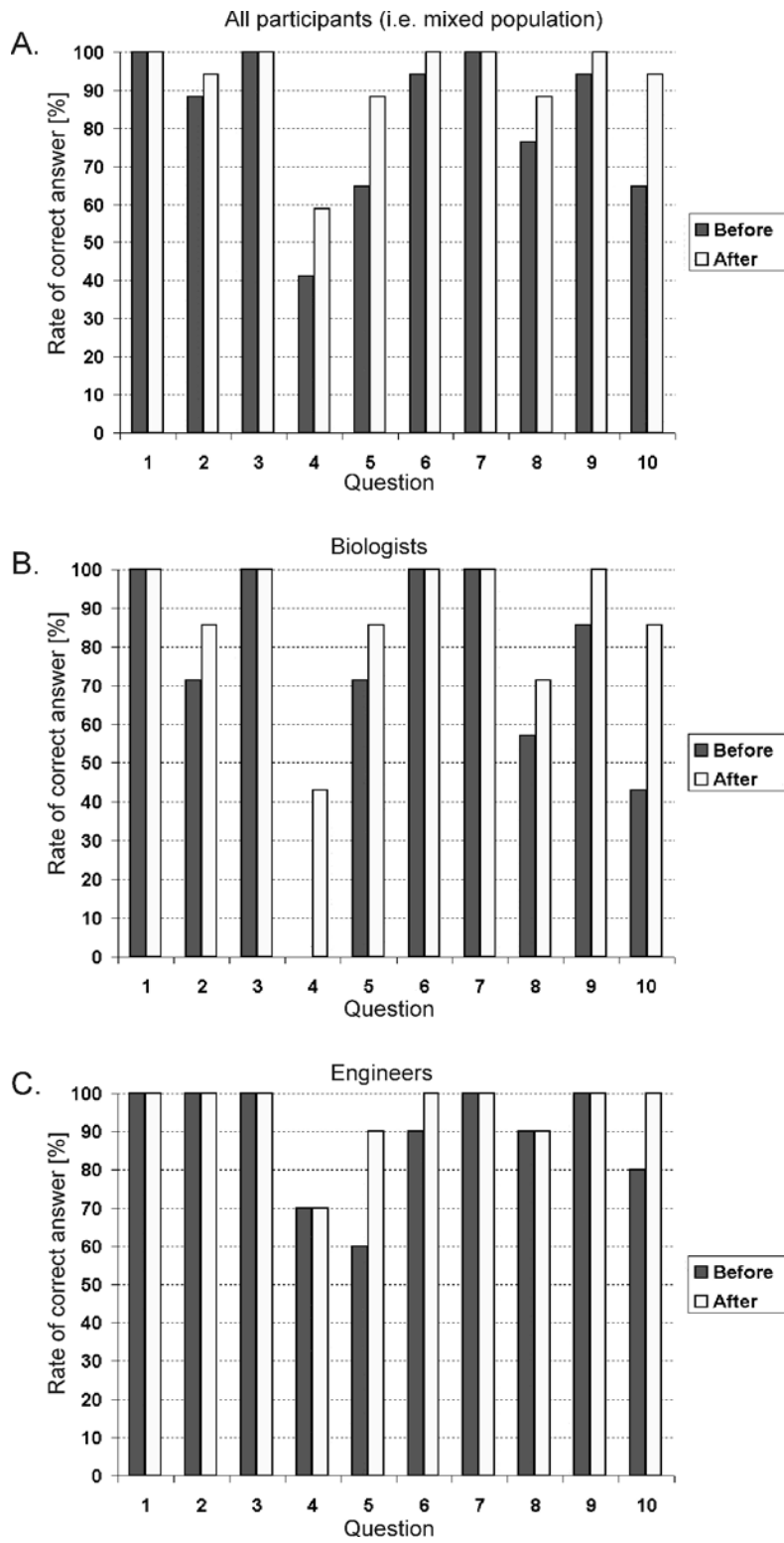
Figure 10
Results of the pedagogical efficiency evaluation. Percentage rate of correct answers for each question analyzed for: a) all participants (i.e. mixed population); b) biologists and c) engineers. The questions' numbering corresponds to the question' numbering in the test given in Additional file 1.
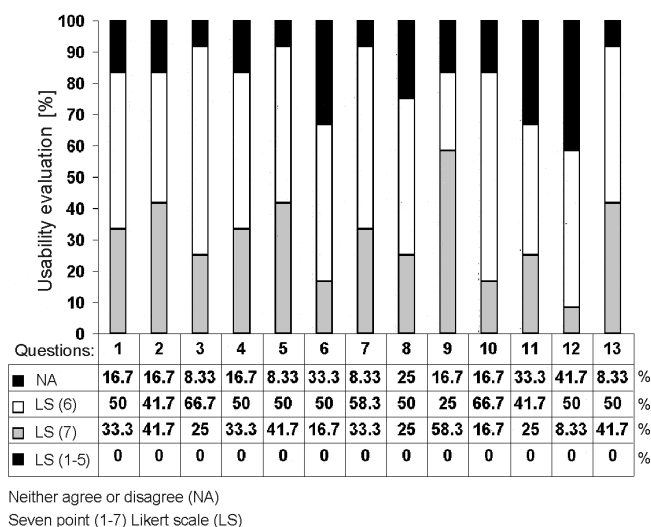
Questions:	1	2	3	4	5	6	7	8	9	10	11	12	13	
■ NA	16.7	16.7	8.33	16.7	8.33	33.3	8.33	25	16.7	16.7	33.3	41.7	8.33	%
□ LS (6)	50	41.7	66.7	50	50	50	58.3	50	25	66.7	41.7	50	50	%
▨ LS (7)	33.3	41.7	25	33.3	41.7	16.7	33.3	25	58.3	16.7	25	8.33	41.7	%
■ LS (1-5)	0	0	0	0	0	0	0	0	0	0	0	0	0	%

Neither agree or disagree (NA)
Seven point (1-7) Likert scale (LS)

Figure 11
Results of the usability evaluation.

[11,12,40,47-49]. The second part of the e-learning content was thus developed in order to provide the educational material about the parameters of local electric field being crucial to make the tumor treatment as efficient as possible. For this purpose we used combination of numerical calculations by means of mathematical modelling and simple graphical illustrations. We demonstrated how the pulse amplitude, electrode shape and electrode positioning influence on the local electric field distribution within the treated cells and tissues. We also demonstrated how the electric properties of a treated sample (i.e. its geometry and electric conductivity) can modify the local electric field distribution. Namely, when the voltage is applied, the electric field distributes within the complex tissue with different electric properties as in voltage divider. The latter means that the electric field is the highest in the layer with the highest electric resistivity (lowest conductivity) [43], which is particularly important when electroporating the skin and/or its underlying tissues.

In the third part of the e-learning application, we developed an interactive module for visualization of local electric field distribution in tissues for different parameters such as voltage applied, distance between electrodes, electrode' dimension, tissue geometry and electric conductivity. The interactive module is aimed at hands-on learning on how the above-mentioned parameters can modify the local electric field distribution within the treated tissue. The module allows for local electric field visualization in cutaneous and subcutaneous tumours. Users can appreciate the local electric field distribution within the treated tissue when electroporated directly or through the skin by using plate or needle electrodes. The module also provides guidelines on how to overcome a highly resistive

skin tissue in order to permeabilize more conductive underlying tissues. Since, for the time being the local electric field in the treated tissue can not be visualized while performing the electrochemotherapy treatment, the interactive visualization approach we provide in our e-learning application can serve as an important tool in selection of the appropriate electric pulses amplitude, electrode shape and their placement with respect to the tissue geometry and its electric conductivity, which is needed for best electrochemothertapy treatment outcome.

Good collaboration among the participants and with the instructor was established during the e-learning session. Namely, the participants assisted each other while studying the educational content and several discussions were initiated between physicists and biologists and between the participants and the instructor. The e-learning application was concluded by a test on the presented educational material and by a questionnaire on usability of the developed application.

We evaluated the designed e-learning application at the International Scientific workshop and postgraduate course (Electroporation Based Technologies and Treatments) [45]. The evaluation was carried out by testing the pedagogical efficiency of the presented educational content and by performing the usability study of the application. The pedagogical efficiency assessment showed that the participants improved their level of knowledge (Fig. 10).

The percentage rate of correct answers for all participants (mixed population) obtained after the e-learning session was above 50% for all test questions (Fig. 10a). The results in Fig. 10b show that before the e-learning session the knowledge of biologists was more heterogeneous compared to the knowledge possessed by engineers as shown in Fig. 10c. This is in part because the level of knowledge possessed by biologists (compared to the engineers) was lower before the e-learning session, since the test and the e-learning content was about electrical parameters. However, the increase in percentage rate of correct answers, after the e-learning session compared to the results obtained before the e-learning session, to each of the questions was obtained for both biologists and engineers (Figs. 10b and 10c). Only for question 4 the percentage of correct answers given by biologist after the e-learning session was slightly below 50% (i.e. 43% of success rate after e-learning session compared to 0% before e-learning session). In order to further improve the success rate of question 4 we concluded that: 1. question 4 should be more clearly formulated by developers and 2. more of e-learning content on the voltage applied between electrodes (U) and on electroporation threshold of local electric field (E) should be provided in the e-learning application. The

same question answered by engineers was 70% of success rate before and after e-learning session.

The results of usability evaluation revealed that participants found the application simple to learn to use and navigate (Fig. 11). Overall, the participants were satisfied with the e-learning application. The participants found the information provided by system easy to understand (question 9 with the highest percentage of agree statements in the Likert scale (58.3% of LS (7)) and 25% of LS (6)). The participants were most neutral regarding the statement that the e-learning application covered all the areas they expected to cover (question 12 evaluated with 41.7% of NA). However, the same question was evaluated with 50% of LS (6) and 8.3% of LS (7) statements. The modular structure of the application allows for upgrade with new educational content collected from the clinics and research, and for the integration of new application modules including computer-supported collaborative visualization being an important component in remote collaboration among the experts [29]. The e-learning application can be used as an education form at both levels: either as a completely independent e-learning form or as an integral part of a blended learning form. The e-learning session can be executed by the users in a linear sequence of studying steps according to the program flow model (i.e. by starting at the beginning of the e-learning content and by concluding with the final evaluation tests) or in a studying sequence which is not previously defined, which can serve as an additional e-learning module of blended learning [30].

Conclusion
The e-learning application together with E-CHO system is available to the users to provide collaborative and flexible learning in order to facilitate knowledge exchange among the experts from different scientific fields that are involved in electrochemotherapy. The e-learning application is developed to provide an interactive educational content in order to simulate the "hands-on" learning approach about the parameters being important for successful therapy. The e-learning application on electrochemotherapy can be easily adapted to serve as a collaborative e-learning tool also in other electroporation-based treatments such as gene electrotransfer, irreversible tissue ablation or transdermal gene and drug delivery [6,8,9,50]. The presented e-learning application provides an easy and rapid approach for information, knowledge and experience exchange among the experts from different scientific fields, which can facilitate development and optimisation of electroporation-based treatments.

Competing interests
The authors declare that they have no competing interests.

Authors' contributions
All authors read and approved the final manuscript.

Additional material

Additional file 1
Pedagogical efficiency questionnaire. The file provides the test on the educational content completed by the participants before and at the end of the e-learning session.
Click here for file
[http://www.biomedcentral.com/content/supplementary/1475-925X-8-26-S1.PDF]

Additional file 2
Usability efficiency questionnaire. The file provides usability questions related to the user satisfaction with the developed e-learning application.
Click here for file
[http://www.biomedcentral.com/content/supplementary/1475-925X-8-26-S2.PDF]

References
1. Mir LM: **Therapeutic perspectives of in vivo cell electropermeabilization.** *Bioelectrochemistry* 2001, **53:**1-10.
2. Marty M, Sersa G, Garbay JR, Gehl J, Collins CG, Snoj M, Billard V, Geertsen PF, Larkin JO, Miklavcic D, Pavlovic I, Paulin-Kosir SM, Cemazar M, Morsli N, Soden DM, Rudolf Z, Robert C, O'Sullivan GC, Mir LM: **Electrochemotherapy-An easy, highly effective and safe treatement of cutaneous and subcutaneous metastases: Results of ESOPE (European Standard Operating Procedures of Electrochemotherapy) study.** *Eur J Cancer Suppl* 2006, **4:**3-13.
3. Mir LM, Bureau M, Gehl J, Rangara R, Rouy D, Caillaud J, Delaere P, Branellec D, Schwartz B, Scherman D: **High-efficiency gene transfer into skeletal muscle mediated by electric pulses.** *Proc Natl Acad Sci USA* 1999, **96:**4262-4267.
4. Miklavcic D, Semrov D, Mekid H, Mir LM: **A validated model of in vivo electric field distribution in tissues for electrochemotherapy and for DNA electrotransfer for gene therapy.** *Biochim Biophys Acta* 2000, **1523:**73-83.
5. Prud'homme G, Glinka Y, Khan A, Draghia-Akli R: **Electroporation-enhanced nonviral gene transfer for the prevention or treatment of immunological, endocrine and neoplastic diseases.** *Curr Gene Ther* 2006, **6:**243-273.
6. Andre F, Gehl J, Serša G, Préat V, Hojman P, Eriksen J, Golzio M, Cemazar M, Pavselj N, Rols MP, Miklavcic D, Neumann E, Teissie J, Mir LM: **Efficiency of high- and low-voltage pulse combinations for gene electrotransfer in muscle, liver, tumor, and skin.** *Human Gene Ther* 2008, **19:**1261-1271.
7. Trontelj K, Reberšek M, Kanduser M, Curin-Serbec V, Sprohar M, Miklavcic D: **Optimization of bulk cell electrofusion in vitro for production of human-mouse heterohybridoma cells.** *Bioelectrochemistry* 2008, **74:**124-129.
8. Rubinsky J, Onik G, Mikus P, Rubinsky B: **Optimal parameters for the destruction of prostate cancer using irreversible electroporation.** *Journal of Urology* 2008, **180:**2668-2674.
9. Pavselj N, Miklavcic D: **A numerical model of permeabilized skin with local transport regions.** *IEEE Trans Biomed Eng* 2008, **55:**1927-1930.

10. Kanduser M, Miklavcic D: **Electroporation in biological cell and tissue: an overview.** In *Electrotechnologies for Extraction from Food Plants and Biomaterials* Edited by: Vorobiev E, Lebovka N. New York, Springer Science; 2008:1-37.
11. Miklavcic D, Beravs K, Semrov D, Cemazar M, Demsar F, Sersa G: **The importance of electric field distribution for effective in vivo electroporation of tissues.** *Biophys J* 1998, **74:**2152-2158.
12. Zupanic A, Corovic S, Miklavcic D: **Optimization of electrode position and electric pulse amplitude in electrochemotherapy.** *Radiol Oncol* 2008, **42:**93-101.
13. Pavlovic I, Kramar P, Corovic S, Cukjati D, Miklavcic D: **A web-application that extends functionality of medical device for tumor treatment by means of electrochemotherapy.** *Radiol Oncol* 2004, **38:**49-54.
14. Pavlovic I, Miklavcic D: **Web-based electronic data collection system to support electrochemotherapy clinical trial.** *IEEE Trans Inf Technol Biomed* 2007, **11:**222-230.
15. Pavlovic I, Kern T, Miklavcic D: **Comparison of paper-based and electronic data collec-tion process in clinical trials: Costs simulation study.** *Contemp Clin Trials* 2009, **30:**300-316.
16. Mir LM, Gehl J, Sersa G, Collins CG, Garbay JR, Billard V, Geertsen P, Rudolf Z, O'Sullivan GC, Marty M: **Standard operating procedures of the electrochemotherapy: instructions for the use of bleomycin or cisplatin administered either systemically or locally and electric pulses delivered by the CliniporatorTM by means of invasive or non-invasive electrodes.** *Eur J Cancer Suppl* 2006, **4:**14-25.
17. Sersa G, Miklavcic D: **Electrochemotherapy of tumours (Video Article).** *J Visual Exp* 2008, **22:**1038.
18. Colombo GL, Di Matteo S, Mir LM: **Cost-effectiveness analysis of electrochemotherapy with the Cliniporator™ vs other methods for the control and treatment of cutaneous and subcutaneous tumors.** *Therapeutics and Clinical Risk Management* 2008, **2:**541-548.
19. Godfrey M: **Teaching software engineering to a mixed audience.** *Information and Software Technology* 1998, **40:**229-232.
20. Gillet D, Nguyen Ngoc AV, Rekik Y: **Collaborative web-based experimentation in flexible engineering education.** *IEEE Trans Educ* 2005, **48:**696-703.
21. Holbert KE, Karady GG: **Strategies, challenges and prospects for active learning in computer-based classroom.** *IEEE Trans Educ* 2009, **52:**31-38.
22. Dale E: *Audio-Visual methods in teaching* 3rd edition. New York, Holt, Rinehart, and Winston; 1969.
23. Day AJ, Foley DJ: **Evaluating a web lecture intervention in a human-computer interaction course.** *IEEE Trans Educ* 2006, **49:**420-431.
24. Buret F, Muller D, Nicolas L: **Computer-aided education for magnetostatics.** *IEEE Trans Educ* 1999, **42:**45-49.
25. Guerrero JF, Bataller M, Soria E, Magdalena R: **BioLab: An educational tool for signal processing training in biomedical engineering.** *IEEE Trans Educ* 2007, **50:**34-40.
26. **Biomedical sciences teaching modules** [http://www.virtualcampus.ch/display.php?lang=1&pname=discipline_4]
27. Telea AC: *Data visualization - principles and practice* Wellesley, Massachusetts, AK Peters Ltd; 2008.
28. Assaad RS, Silva-Martinez J: **A graphical approach to teaching amplifier design at the undergraduate level.** *IEEE Trans Educ* 2009, **52:**39-45.
29. Teyseyre AR, Campo MR: **An overview of 3D software visualization.** *IEEE Trans Vis Comput Graphics* 2009, **15:**87-105.
30. Hoic-Bozic N, Mornar V, Boticki I: **A blended learning approach to course design and implementation.** *IEEE Trans Educ* 2009, **52:**19-30.
31. Neumann E, Rosenheck K: **Permeability changes induced by electric impulses in vesicular membranes.** *J Membr Biol* 1972, **10:**279-290.
32. Tsong TY: **Electroporation of cell membranes.** *Biophys J* 1991, **60:**297-306.
33. Weaver JC, Chizmadzhev YA: **Theory of electroporation: a review.** *Bioelectrochem Bioenerg* 1996, **41:**135-160.
34. Teissie J, Eynard N, Gabriel B, Rols MP: **Electropermeabilization of cell membranes.** *Adv Drug Deliver Rev* 1999, **35:**3-19.
35. Kotnik T, Miklavcic D: **Analytical description of transmembrane voltage induced by electric fields on spheroidal cells.** *Biophys J* 2000, **79:**670-679.
36. Valic B, Pavlin M, Miklavcic D: **The effect of resting transmembrane voltage on cell electropermeabilization: a numerical analysis.** *Bioelectrochemistry* 2004, **63:**311-315.
37. Pavlin M, Kanduser M, Rebersek M, Pucihar G, Hart FX, Magjarevic R, Miklavcic D: **Effect of cell electroporation on the conductivity of a cell suspension.** *Biophys J* 2005, **88:**4378-4390.
38. Tarek M: **Membrane electroporation: a molecular dynamics simulation.** *Biophys J* 2005, **88:**4045-4053.
39. Sel D, Cukjati D, Batiuskaite D, Slivnik T, Mir LM, Miklavcic D: **Sequential finite element model of tissue electropermeabilization.** *IEEE Trans Biomed Eng* 2005, **52:**816-827.
40. Pavselj N, Bregar Z, Cukjati D, Batiuskaite D, Mir LM, Miklavcic D: **The course of tissue permeabilization studied on a mathematical model of a subcutaneous tumor in small animals.** *IEEE Trans Biomed Eng* 2005, **52:**1373-1381.
41. Kotnik T, Miklavcic D: **Theoretical evaluation of voltage inducement on internal membranes of biological cells exposed to electric fields.** *Biophys J* 2006, **90:**480-491.
42. Teissié J, Escoffre JM, Rols MP, Golzio M: **Time dependence of electric field effects on cell membranes. A review for a critical selection of pulse duration for therapeutical applications.** *Radiol Oncol* 2008, **42:**196-206.
43. Pavselj N, Miklavcic D: **Numerical modeling in electroporation-based biomedical applications.** *Radiol Oncol* 2008, **42:**159-168.
44. **Interactive e-learning system (E-CHO), Laboratory of telecommunications, Faculty of Electrical Engineering, University of Ljubljana** [http://www.ltfe.org]
45. **International Scientific workshop and postgraduate course (Electroporation Based Technologies and Treatments), Faculty of Electrical Engineering, University of Ljubljana** [http://www.cliniporator.com/ect]
46. Humar I, Sinigoj A, Bester J, Hegler OM: **Integrated component web-based interactive learning systems for engineering.** *IEEE Trans Educ* 2005, **8:**664-675.
47. Corovic S, Zupanic A, Miklavcic D: **Numerical modeling and optimization of electric field distribution in subcutaneous tumor treated with electrochemotherapy using needle electrodes.** *IEEE Trans Plasma Sci* 2008, **36:**1665-1672.
48. Corovic S, Al Sakere B, Haddad V, Miklavcic D, Mir LM: **Importance of contact surface between electrodes and treated tissue in electrochemotherapy.** *Technol Cancer Res Treat* 2008, **7:**393-399.
49. Corovic S, Mojca P, Miklavcic D: **Analytical and numerical quantification and comparison of the local electric field in the tissue for different electrode configurations.** *Biomed Eng Online* 2007, **37:**1-14.
50. Al-Sakere B, Bernat C, Andre F, Connault E, Opolon P, Davalos R, Mir LM: **A study of the immunological response to tumor ablation with irreversible electroporation.** *Technol Cancer Res Treat* 2007, **6:**301-305.

Paper V

In vivo muscle electroporation threshold determination-realistic numerical models and *in vivo* experiments

Selma Čorović[a,b,c], Lluis M. Mir[b,c] and Damijan Miklavčič[a*]

[a] University of Ljubljana, Faculty of Electrical Engineering, SI-1000 Ljubljana, Slovenia
[b] UMR 8121 CNRS, Institute Gustave-Roussy, F-94805 Villejuif Cedex, France
[c] University Paris-Sud, UMR 8121

* Corresponding author:
damijan.miklavcic@fe.uni-lj.si

Abstract

In vivo electroporation is used as an effective technique for the delivery of therapeutic agents such as chemotherapeutic drugs or DNA into target tissue cells for different biomedical purposes. In order to successfully electroporate a target tissue it is essential to know the local electric field distribution produced by an application of electroporation voltage pulses. In this study three-dimensional finite element models were built in order to analyze local electric field distribution and corresponding tissue conductivity changes in rat muscle electroporated either transcutaneously or directly (i.e. two plate electrodes were either placed on the skin or directly on the skeletal muscle after removing the skin). Numerical calculations of electroporation thresholds and conductivity changes in skin and muscle were validated with *in vivo* measurements.

1. Introduction

Tissue electroporation (EP) (also termed electropermeabilization) is a transient electrical increase of cell membrane permeability by means of local delivery of short and sufficiently intense voltage pulses (i.e. electroporation pulses) to the target tissue cells via properly selected electrodes [Miklavcic et al., 2000]. *In vivo* electroporation is used as an effective technique for the delivery of a variety of therapeutic agents such as chemotherapeutic drugs, DNA or other molecules, which in normal conditions do not cross the cell membrane, into many different target tissue cells [Mir et al., 1995, Prud'homme et al., 2006]. Skeletal muscle tissue is one of the most promising tissues for DNA delivery by electroporation for either local or systemic gene therapy and gene vaccination [Mir et al., 1999, Mathiesen 1999, Umeda et al., 2004, Perez et al., 2004, Hojman et al., 2007, Hojman et al., 2008, Tevz et al., 2008]. Investigating *in vivo* muscle tissue electroporation is relevant to both clinical electrochemotherapy [Marty et al., 2006] and transdermal drug delivery [Denet et al., 2004] for providing knowledge on the sensitivity of underlying muscle tissue to the electroporation procedure [Zupanic et al., 2007, Mali et al., 2008], as well as in various physiological and developmental studies [Dev et al., 2000, Prud'homme et al., 2006].

The key parameter in effective tissue electroporation is local electric field distribution (*E*) established within the treated tissue due to the delivered EP pulses. The target tissue cells can be electroporated in a reversible and safe way only within the tissue regions subjected to the local electric field *E* of a magnitude of between reversible E_{rev} and irreversible electroporation thresholds E_{irrev} [Miklavcic et al., 2000]. The magnitude of *E* can be controlled by carefully chosen EP pulses' amplitude and electrode configuration, given that the electroporation thresholds E_{rev} and E_{irrev} and the tissue's electrical and geometrical properties are known [Sel et al., 2005, Sel et al., 2007, Zupanic et al., 2008, Corovic et al., 2008]. An important prerequisite for the determination of E_{rev} and E_{irrev} thresholds is the visualization of the local electric field distribution with numerical calculations in realistic tissue models which are validated with corresponding experimental observations, and thus they take into account realistic geometrical and electrical properties of the tissues to be modeled [Miklavcic et al., 1998, Gehl et al., 1999, Miklavcic et al., 2000]. Since the electroporation thresholds (and thus the induced transmembrane potentials at these thresholds) are related to the cell size, cell density and orientation with respect to the electric field, and to the parameters of EP pulses, they have to be determined for each cell and tissue type [Pavlin et al., 2002, Valic et al., 2003]. Theory and experiments also showed that when the cells are electroporated, their electrical properties change due to the increase in the cell membrane's conductivity, which is reflected in the bulk conductivity increase [Pavlin et al., 2003]. It was previously suggested that tissue conductivity changes, as an indicator of the tissue electroporation level, can also be assessed by *in vivo* measurements of changes in tissue conductance [Davalos et al., 2002, Davalos et al., 2004] and of the total current flowing through the treated tissues [Cukjati et al., 2007].

The protocols for *in vivo* muscle electroporation, both for muscle electroporated either transcutaneously or directly (i.e. without skin), were established based on the ratio of the amplitude of applied EP pulses relative to the distance between the electrodes; very few studies investigated the local electric field distribution in the muscle and its surrounding tissues [Gehl et al., 1999, Pavselj et al., 2005].

The aim of our study was to develop realistic numerical models in order to investigate the E_{rev} and E_{irrev} thresholds and electroporation process between these thresholds in skeletal muscle tissue electroporated either transcutaneously or directly. We numerically and experimentally investigated

the local electric field distribution, geometrical and electrical properties of skin and muscle tissue electroporated separately and of muscle electroporated through the skin. From the obtained results we observed an influence on electroporation efficiency in muscle tissue due to the presence of skin. We built three separate realistic numerical models of skin fold, muscle and muscle with skin. Changes in electrical properties resulting from electroporation were modelled by determining the functional dependency of tissue conductivity σ [S/m] on local electric distribution (E) above the reversible electroporation threshold E_{rev} in each of the examined tissues. By using finite element methods we calculated local electric field distribution and total electric current at voltages of equal amplitudes as the EP pulses that were applied in *in vivo* experiments.

In order to validate our numerical models we mathematically interpreted the data collected during an extensive *in vivo* study on the response of the skin, muscle and muscle with skin to the EP pulses [Cukjati et al., 2007]. We compared the results of our numerical simulations to the *in vivo* total current measurement and ^{51}CrEDTA uptake results. From the numerical models validated on the experimentally obtained results we determined electroporation parameters such as reversible and irreversible electroporation threshold values E_{rev} and E_{irrev}, the initial tissue conductivity (before the EP pulses were applied) σ_0, the conductivity of the same tissue modified due to the electroporation σ_1, and the functional dependency of tissue conductivity on local electric field distribution $\sigma(E)$ between the thresholds.

The same electroporation threshold values E_{rev} and E_{irrev} were found, as expected, for both muscle electroporated transcutaneously and directly, since the electroporation threshold is a property of the tissue and cannot be affected by neighboring tissues. However, in order to electrically overcome the skin barrier a higher voltage between the electrodes (i.e. amplitude of EP pulses applied) was required when the muscle was electroporated through the skin in contrast to the electroporation directly on the muscle.

2. Experimental considerations

2.1 *In vivo* experiments

Animals: Female Wistar rats purchased from Janvier (France) were used for the experiments. The rats were anesthetized by means of the intraperitoneal administration of Ketamine (100 mg/kg; Panpharma) and Xylazine (10 mg/kg; Bayer). The animals were handled according to recommended good practices and standard institutional ethics rules for animal experimentation [UKCCCR, 1998].

^{51}**Cr-EDTA:** To determine the electropermeabilization level of skin and muscle tissue when applying EP pulses directly or transcutaneously *in vivo*, we performed the quantitative uptake method using ^{51}Cr-EDTA as the indicator [Cukjati et al., 2007]. The animals were given 200 μl of ^{51}Cr-EDTA (Amersham, U.K.) with a specific activity of 3.7 MBq/ml intravenously 5 minutes before the delivery of the electric pulses. The injected ^{51}Cr-EDTA distributes freely in the vascular and extracellular compartments and can enter the intracellular compartments only if access is provided (e.g. by electroporation). The animals were euthanized 24 hours after injection, and tissues exposed to electric pulses were removed, weighed and counted in a Cobra 5002 gamma counter (Packard Instrument, Meriden, CT). The net ^{51}Cr-EDTA uptake as a result of electropermeabilization was calculated as the measured activity (converted to nanomoles of ^{51}Cr-

EDTA) per gram of the tissue exposed to the electric pulses. ^{51}Cr-EDTA uptake values were then used to calculate mean values of uptake (± SEM) as a function of the ratio of the applied voltage to the electrodes' distance in the rat skeletal muscle electroporated transcutaneously and directly.

Electroporation protocol: Electroporation pulses consisted of a train of eight square-wave and 100 µs long pulses, delivered at a repetition frequency of 1 Hz. In all experiments the electric pulses were generated by a PS 15 electropulse generator (Jouan, St. Herblain, France) and delivered to the tissue through two parallel plate stainless steel electrodes. The electrode dimensions used in our experiments are shown in Figure 1a. The following three experiments were carried out: electroporation of skin tissue only (a skin fold is formed and placed between the electrodes, as shown in Figure 1b), direct muscle electroporation (the skin was previously removed and the plate electrodes were placed directly on the muscle surface – Figure 1c) and transcutaneous muscle electroporation − Figure 1d. The electrodes were positioned on the tissue so that the electric field was perpendicular to the muscle fibers. We treated the triceps brachi muscle of the hind limb and the gastrocnemius medialis muscle of the forelimb. The electrodes were separated by 5.7 mm for the muscles electroporated directly and transcutaneously and by 2.8 mm for the electroporation of the skinfold. Good contact between the electrodes and tissue was assured by the use of a gel (EKO-GEL, Camina, ultrasound transmission gel, Egna, Italy). During the EP pulses' delivery the applied voltage and the actual current delivered were monitored and collected using a digital oscilloscope (Waverunner, LeCroy).
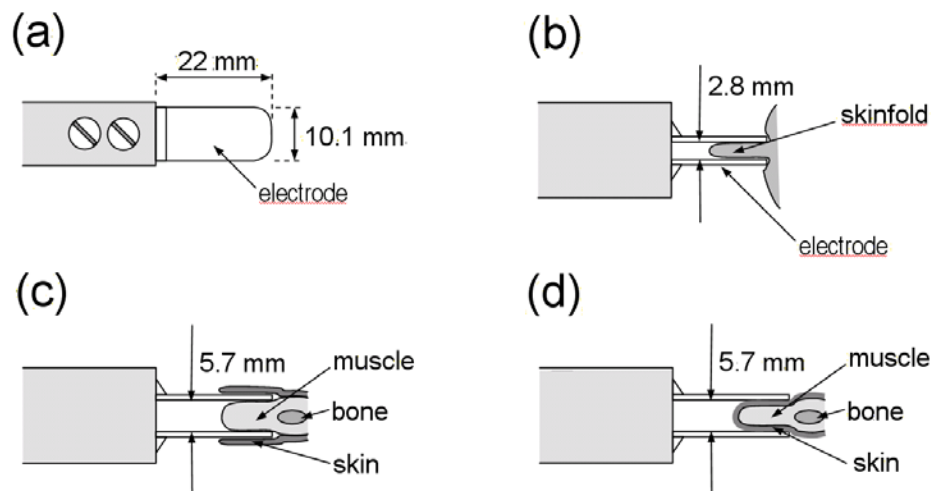

Fig. 1: The electrode dimensions used in experiments (a) and the geometry of the measurement setup for the skin fold electroporation (b) and the muscle electroporated directly (c) and transcutaneously (d)

2.2. Numerical modeling

The experimentally treated tissues were mathematically modeled as passive volume conductors in a quasi-stationary electric current field. Electric field distribution in the tissue models caused by EP pulses was determined by numerically solving Laplace's equation:

$$- \nabla \cdot (\sigma \cdot \nabla \varphi) = 0 ,$$

where σ and φ represent tissue conductivity [S/m] and electric potential [V], respectively. Total electric current flowing through the 3D modeled tissues was then calculated according to Ohm's law. In the first stage of numerical modeling we built 3D models of the skin fold (Fig. 2), muscle tissue electroporated directly (Fig. 3) and muscle tissue electroporated transcutaneously (Fig. 4) using the commercial software package EMAS (ANSOFT Corporation) [EMAS, 1997]. Taking into account the fact that electric field distribution and total electric current flowing through the tissue depend strongly on the tissue geometry, we designed the geometry of our numerical models as accurately as possible. Applied voltage (model input) was modeled as Dirichlet's boundary condition on the contact surface between electrode and tissue geometry. For the model input values we used the amplitudes of the EP pulses applied *in vivo* [Cukjati at al., 2007]. We mathematically separated the conductive segment from its surroundings by applying Neuman's boundary condition ($J_n = 0$, where J_n is the normal electric current density [A/m^2]) on all outer boundaries of the model. Results of the calculated model outputs (total electric current I and local electric field distribution E) were controlled for numerical errors by increasing the size of our model and increasing the mesh density until the electric insulation condition and error due to meshing irregularities were insignificant – a further increase in domain size or mesh density only increased the computation time, however the results changed by less than 0.5 %. The resulting models − mesh of skin fold, muscle and muscle electroporated transcutaneously − consisted of 4173, 7546 and 10074 tetrahedral finite elements, respectively.
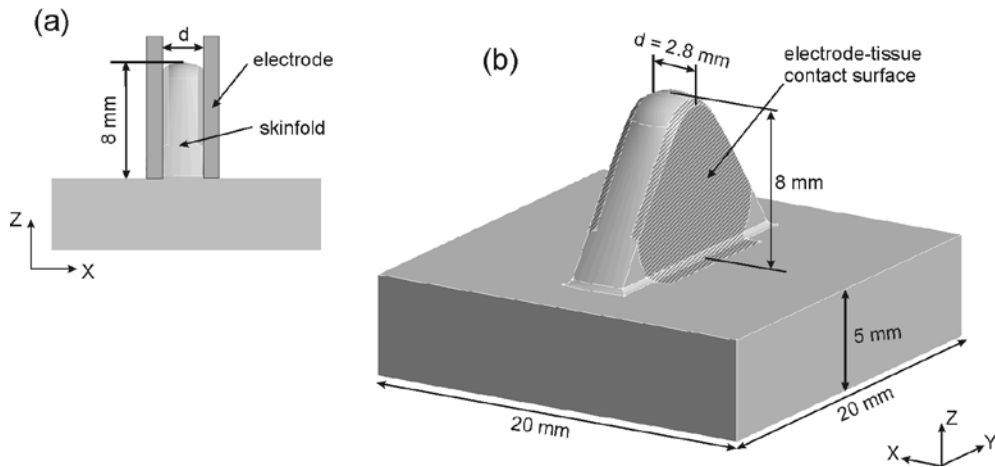

Fig. 2: Geometry of the skin fold finite element model in the ZX cross-sectional plane (a) and in 3D (b). The patterned region represents the contact surface between the electrode and tissue geometry (i.e. electrode-tissue contact surface).
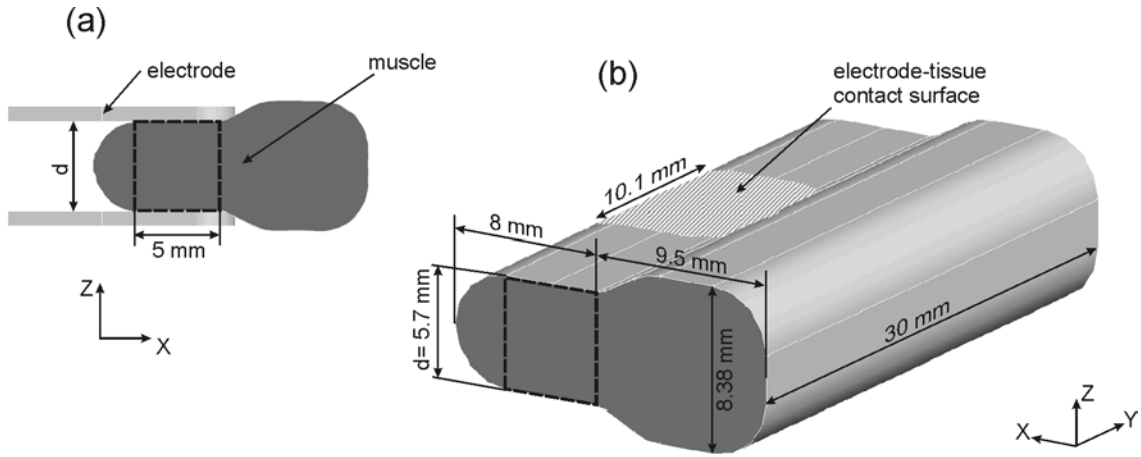
Fig. 3: Geometry of the muscle tissue finite element model (electroporated directly) in the ZX cross-sectional plane (a) and in 3D (b). The patterned region represents the contact surface between the electrode and tissue geometry (i.e. electrode-tissue contact surface).

.

Fig. 4: Geometry of the muscle electroporated transcutaneously in the ZX cross-sectional plane (a) and in 3D (b). The patterned region represents the contact surface between the electrode and tissue geometry (i.e. electrode-tissue contact surface).
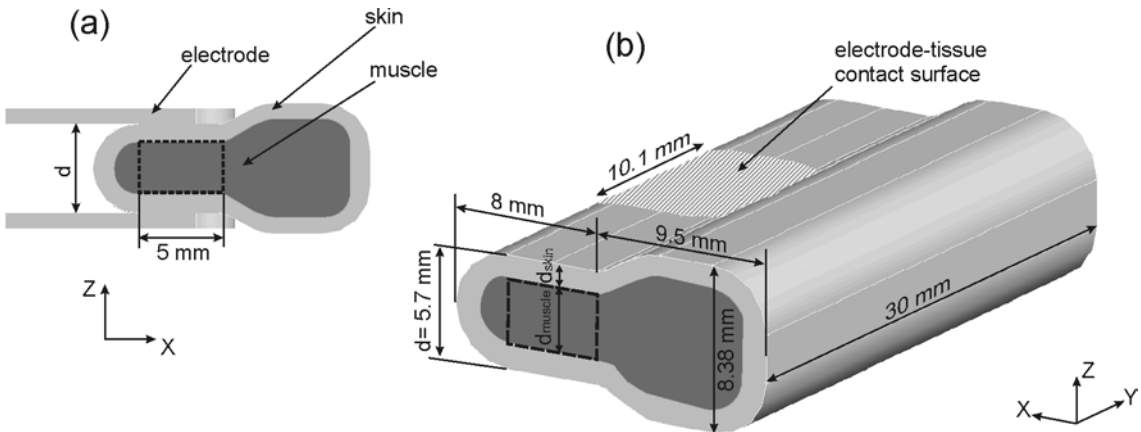
2.2.1 Electric properties of the modeled tissues and electroporation process modeling

In our numerical models, ohmic tissue behavior was analyzed (i.e. skin and muscle conductivities σ [S/m]). Before applying EP pulses or if the amplitude of the applied EP pulses was too low to produce a local electric field above the reversible electroporation threshold ($E < E_{rev}$), the tissues were modeled as linear conductors with linear current-voltage $I(U)$ relationships due to the constant tissue conductivities. The initial pre-pulse values of conductivities (σ_0 corresponding to the $E < E_{rev}$ condition) used in numerical models were selected from the available literature [Miklavcic et al.,

2006]: muscle tissue was considered an anisotropic conductor, being more conductive along the muscle fibers in the *Y axis* compared to the two other perpendicular *X* and *Z axes* (Table 1), while skin tissue was considered isotropic and homogeneous. Since the skin tissue was not the primary target of our investigation, different layers of skin were not modeled, thus the average value for conductivity was assigned to skin tissues in our models (Table 1). Namely, large differences in skin layers' geometries would unnecessarily increase the computational time of numerical simulations while not contributing to the accuracy of the electric field distribution in the muscle tissue [Pavšelj et al., 2005].

If the local electric field in the tissues exceeded the E_{rev} value, the tissue electric properties change (i.e. tissue conductivity increases due to the electroporation process). During the application of EP pulses, tissue conductivity increases according to the functional dependency of the tissue conductivity on the local electric field distribution $\sigma(E)$, which in our study describes the dynamics of the electroporation process. This subsequently results in nonlinear electric current of the applied voltage $I(U)$. Due to the change of σ, we detected the threshold electroporation E_{rev} as a result of the deviation of $I(U)$ from the linear relationship $I = U / R$ (where R [Ohm] is tissue electric resistance). The tissue electroporation dynamics were modeled based on the sequential permeabilization model proposed by Šel et al., 2005, where changes in tissue conductivity were used as an indicator of tissue permeabilization. For this purpose a sequence analysis subprogram (as an extension of EMAS) was developed to model the dynamics of electroporation as a discrete process with the sequence of static FEM models, where each of them describes the process at one discrete interval (each of the discrete intervals relates to a real, discrete, but undetermined time interval). In each static model in sequence, the tissue conductivity was determined based on the electric field distribution from the previous model in the sequence, as described in the equation:

$$\sigma(k) = f(E(k\text{-}1)), \qquad\qquad (\text{Eq. 2})$$

where k stands for the number of static FEM models in sequence.

Model input is the applied voltage pulse, and model outputs are the electric field distribution E and total electric current I in each specific sequence k. The modeled tissue behavior during the electroporation pulse delivery is illustrated in Fig. 5. The increase in electrical current I from I_0 to I_k simulates the tissue response during the delivery of the electroporation pulses U in each discrete interval k (static FEM model in sequence) to the tissue electroporation (i.e. due to the functional dependency of σ on the electric field distribution E). If the electroporation does not occur, σ remains constant, thus $I = I_0$. The sequence analysis subprogram gives us a choice of five different $\sigma(E)$ relationships given by Equations 3-7.
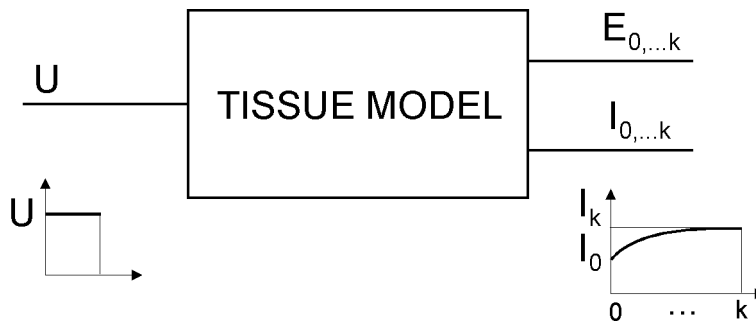

Fig. 5: The modeled tissue behavior during the electroporation pulse delivery, where *U* is the amplitude of the electroporation pulses delivered to the tissues. *E* is the electric field strength and *I* is the total electric current calculated in each sequence, where *k* is the number of the sequences corresponding to the duration of the electroporation pulses.

$$\sigma(E) = \begin{cases} \sigma_0, E < E_{rev} \\ \sigma_1, E \geq E_{irrev} \end{cases} \quad \text{(Eq.3)} \qquad \sigma(E) = \begin{cases} \sigma_0, E < E_{rev} \\ \dfrac{\sigma_1 - \sigma_0}{E_{irrev} - E_{rev}} \cdot E + \sigma_0, E_{rev} \leq E < E_{irrev} \\ \sigma_1, E \geq E_{irrev} \end{cases} \quad \text{(Eq.4)}$$

$$\sigma(E) = \begin{cases} \sigma_0, E < E_{rev} \\ A \cdot (1 - \exp(-(\dfrac{E - E_{rev}}{B}))) + \sigma_0, E_{rev} \leq E < E_{irrev} \\ \sigma_1, E \geq E_{irrev} \end{cases} \quad \text{(Eq.5)} \qquad \sigma(E) = \begin{cases} \sigma_0, E < E_{rev} \\ A \cdot (\exp(\dfrac{E - E_{irrev}}{B}) - 1) + \sigma_1, E_{rev} \leq E < E_{irrev} \\ \sigma_1, E \geq E_{irrev} \end{cases} \quad \text{(Eq.6)}$$

$$\sigma(E) = \begin{cases} \sigma_0, E < E_{rev} \\ \sigma_0 + \dfrac{\sigma_1 - \sigma_0}{(1 + \exp(-\dfrac{E - a}{B}))}, E_{rev} \leq E < E_{irrev} \\ \sigma_1, E \geq E_{irrev} \end{cases} \quad \text{(Eq.7), where} \quad A = \dfrac{\sigma_0 - \sigma_1}{\exp(\dfrac{E_{rev} - E_{irrev}}{B}) - 1} \quad \text{and} \quad a = \dfrac{E_{rev} - E_{irrev}}{2}$$

Parameters σ_0 and σ_1 represent the initial prepulse tissue conductivity and the conductivity of electroporated tissue, respectively; parameters E_{rev} and E_{irrev} stand for reversible and irreversible electroporation thresholds of the local electric field, respectively; and parameter B defines the shape of the exponential and sigmoid functions.

2.2.2. Single tissue models − skin and muscle tissue models

First we modeled the electroporation process in each of the tissue models separately: skin fold (Fig. 2) and muscle tissue model (Fig. 3). The same values of applied voltages *in vivo* were applied to the contact surfaces of the single muscle and skin models as model inputs. A comparison of the current-voltage $I(U)$ to the measured ones *in vivo* was used to determine which of the functional dependencies given by equations Eq. 2-6 best described the dynamics of the electroporation process in each of the tissues analyzed. Namely, in order to tune our single tissue models for *in vivo* electroporation of skin fold (Fig. 1b) and for direct *in vivo* muscle electroporation (Fig. 1c) measurement, we varied different functional relationships (step function (Eq. 2), exponent (Eq. 3 and Eq. 4), linear (Eq. 5) and sigmoid (Eq. 6)) with different reversible and irreversible electroporation threshold values (E_{rev} and E_{irrev}) until good agreement between $I(U)$ obtained numerically and the $I(U)$ characteristic measured *in vivo* was established.

From the resulting numerical models, we collected the initial prepulse tissue conductivity σ_0, the conductivity of the electroporated tissues σ_1, and the $\sigma(E)$ relationships between the reversible and irreversible threshold values E_{rev} and E_{irrev} (with the corresponding parameters a, A and B).

2.2.3. Complete muscle tissue model − model of muscle electroporated transcutaneously

The $\sigma(E)$ relationships with E_{rev} and E_{irrev} obtained from single models of the skin (Fig. 2) and muscle (Fig. 3) were applied to the skin and muscle composing the complete model (model of muscle electroporated transcutaneously) (Fig.4). The same values of voltages of transcutaneous muscle electroporation *in vivo* (Fig. 1d) were applied to the contact surfaces of the complete muscle with skin model (Fig. 4). In order to tune the intricate muscle model with the transcutaneously electroporated muscle *in vivo,* we also varied the thickness of the skin (d_{skin} parameter in Fig. 4) until the *I(U)* relationship matched the measured one. In such a way we numerically detected the complete muscle tissue geometry that corresponded to realistic muscle with a skin layer treated in our experiments *in vivo,* and we validated the model parameters σ_0, the conductivity of the σ_1 and $\sigma(E)$ relationships with E_{rev} and E_{irrev} collected from the single tissue electroporation modeling. In order to compare the conductivity change and geometry of skin layer numerically found in the intricate muscle model to the data from the published literature, we also calculated the complete muscle model resistance R [Ohm] for each of the voltages applied.

2.2.4. Analysis of the influence of skin presence on muscle electroporation

In order to analyze the influence of the skin layer on muscle electroporation, we compared the local electric field distribution in muscle electroporated directly (Fig.3) with the local electric field distribution obtained only in the muscle inside the intricate muscle model with skin (Fig.4). For this purpose, we wrote a program with Matlab7a to calculate the average local electric field E at the end of the electroporation process (i.e. the final sequence FEM model for each voltage applied).

The average electric field intensities were calculated in the volumes between two plate electrodes (the regions between electrodes marked with a dashed square in Fig. 3 and Fig. 4), where the local electric field (E) was the most homogeneous (i.e. equal to the applied voltage to the interelectrode distance ratio ($E = U/d$)). In this way we virtually removed the skin layer from the complete muscle model with skin shown in Fig.4. The numerical results of E in the muscle from the complete model were then compared to the numerical results of E calculated in the numerical model of directly electroporated muscle.

3. Results and discussion

The aims of our study were to develop realistic numerical models in order to investigate the electroporation process in skeletal muscle tissue electroporated directly and transcutaneously and to examine the influence of the presence of the skin on the electroporation process in muscle tissue. For this purpose, we numerically and experimentally investigated the local electric field, geometrical and electrical properties of electroporated skin fold and muscle tissue electroporated directly and transcutaneously. Numerical calculations of the local electric field were performed by means of the finite element method and sequential modeling of tissue electroporation [Šel et al., 2005] taking into account realistic geometry and electrical properties of the examined tissues. Local electric field distribution was experimentally examined by the total current measurement and the [51]CrEDTA uptake assessment *in vivo*. The three-dimensional realistic models of skin fold and muscle electroporated directly and transcutaneously were then developed (based on good agreement between numerical calculations and experimental observations).

It has been previously demonstrated that tissue electroporation can be modeled as a conductivity (σ [S/m]) change due to the tissue permeabilization [Šel et al., 2005]. Accordingly, in our numerical models we took into consideration changes in skin and muscle conductivities as the mathematical relationship between the tissue conductivity σ and the local electric field intensity E in the following manner: a magnitude of E below the reversible threshold E_{rev} does not permeabilize the cell membranes and therefore no changes in conductivity are expected (σ is constant); when the local electric field intensity exceeds the E_{rev} reversible threshold the cell membrane is electropermeabilized and tissue conductivity increases according to the function $\sigma(E)$. In order to numerically study the electroporation process in a complete model that is composed of different tissues, the electroporation parameters σ_0, σ_1, E_{rev}, E_{irrev} and $\sigma(E)$ between the thresholds need to be determined in each of the single tissue models separately as previously demonstrated by Pavselj et al., 2005. Similarly, in order to numerically study the electroporation of muscle tissue electroporated transcutaneously, we first built single models of skin folds (Fig. 2) and muscle tissue (Fig. 3) separately and determined the electroporation parameters for each of the tissues analyzed in our study based on a sequence permeabilization analysis [Sel et al., 2005]. The electroporation parameters for each of the tissues were determined based on criteria that the output of the models best fit the experimental data (i.e. the electroporation parameters were varied until good agreement between the computed and measured current-voltage $I(U)$ relationship was obtained). We found that $\sigma(E)$ in the skin fold model was exponential (Eq. 6 with $B = 50000$), while in the skeletal muscle model the function $\sigma(E)$ was sigmoid (Eq. 7 with $B = 10000$). The electroporation parameters calculated for each of the tissues are listed in Table 1. The $\sigma(E)$ was chosen so that the parameters such as E_{rev}, E_{irrev}, σo and $\sigma 1$ were as close as possible to the experimentally determined values. By varying all the functions of $\sigma(E)$ we noticed that $\sigma(E)$ can also be described with all the functions through proper adjustment of the electroporation parameters, which may be too far from the biologically justifiable values determined in the experiments, as previously suggested by [Pavšelj et al., 2005].

Table 1: The electroporation parametes σ_o, σ_1, E_{rev}, E_{irrev} calculated in single models of skin fold and muscle tissue.

Tissue	σ_o [S/m]	σ_1 [S/m]	E_{rev} [V/cm]	E_{irrev} [V/cm]
Skin	0.008	20 σ_o	480	1050
Muscle	in X and Y axes 0.135 in the Z axis* 0.75	3.5 σ_o	240	450

* The numerical calculations showed that varying the factor σ_{1/σ_o} in Z axis did not significantly change the $I(U)$ characteristic

Different functions of $\sigma(E)$ are needed to describe the propagation of tissue electroporation in our models of muscle and skin tissue. This is probably due to the differences in the biological properties (i.e. cell size and distribution, electrical properties of intra and extracellular media…) of the tissues analyzed.

The $\sigma(E)$ functions with E_{rev} and E_{irrev} found in single models of skin (Fig. 2) and muscle (Fig. 3) were applied to the individual skin and muscle models composing the complete muscle model (Fig.4). The same values of voltages of transcutaneous muscle electroporation *in vivo* (Fig. 1d) were applied to the contact surfaces of the complete muscle model (Fig. 4). In order to fine-tune the

complete muscle model for the transcutaneously electroporated muscle *in vivo*, we also varied the thickness of the skin (d_{skin} parameter in Fig. 4) until the *I(U)* relationship matched the measured one. Since electric current gives quantitative information about tissue geometry and electric properties (i.e. tissue conductivity changes), good agreement between calculated and measured electric current at the end of electroporation process for the corresponding applied voltages validated our three-dimensional finite element models. The agreement between calculated and measured current-voltage relationship obtained for the skin fold analysis is shown in Fig. 6a. The comparison of agreements between calculated and measured current-voltage relationships obtained for muscle and muscle with skin is shown in Fig. 6b.
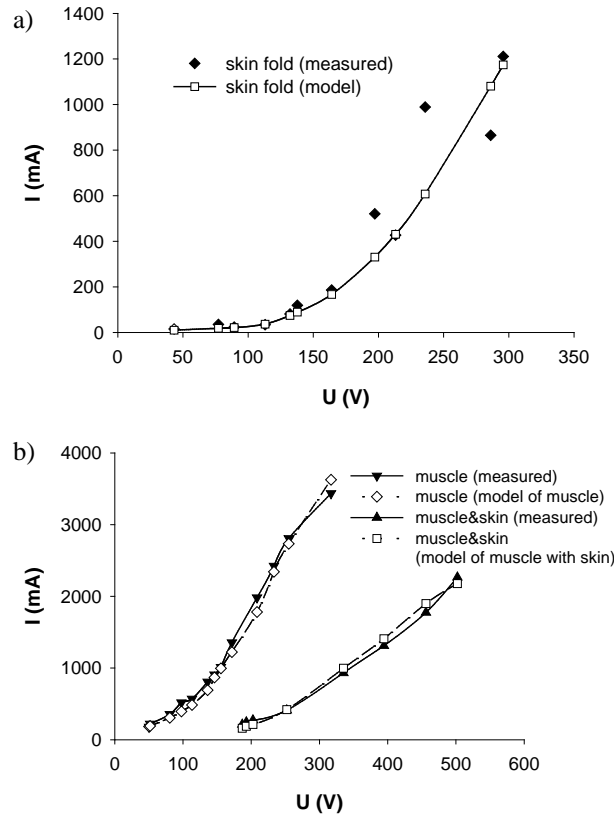

Fig. 6: Calculated and *in vivo* measured current-voltage relationships for a) skin fold and b) muscle and muscle with skin

At lower voltages the slope of the *I(U)* curve is low and linear, meaning that electroporation does not yet occur. The value of *U* at which the *I(U)* relationship starts to diverge from its linear curve indicates that the reversible threshold value of the local electric field for tissue electroporation has been obtained. The threshold value E_{rev} in the directly electroporated muscle model was obtained at 136 V and in the muscle model electroporated transcutaneously at 252 V. The local electric field distribution in both muscle models is displayed in *XY* cross-sectional plane in the middle of two plate electrodes in Fig. 7. To more precisely analyze the local electric field distribution around the reversible threshold obtained with sequence analysis ($E_{rev} = 240$ V/cm), we visualized *E* in the range 0 V/cm - 250 V/cm for the first four applied voltages. The reversible threshold for muscle electroporation is obtained at a lower value of applied voltage (*U* = 136 V) in the model of directly electroporated muscle (Fig. 7a) than in the model of muscle electroporated through the skin (*U* =

252 V) (Fig. 7b) due to the high resistance of the skin layer must be overcome by a higher U in order to target the underlying muscle tissue with $E > E_{rev}$. The reversible threshold value in muscle with skin was obtained at a higher U because the skin tissue needed to be permeabilized first. Namely, when U is applied, the electric field is distributed within the complex tissue according to its specific electric properties (acting as a voltage divider), meaning that the electric field is highest in the layer with the highest electric resistivity (i.e. lowest conductivity) [Pavselj et al., 2008]. When the skin becomes permeabilized, its conductivity increases according to the function $\sigma(E)$, which leads to the electric field redistribution in the skin and its underlying more conductive tissues (in our case muscle tissue). If U is too low, the highest electric field remains in the skin layer and does not reach the muscle. Due to the skin electroporation, an increase of skin conductivity reduces its electric resistance and consequently reduces electric field intensity in the skin which results in increased electric field intensity in the muscle, as shown in Fig. 7b.

Non-uniform propagation of tissue permeabilization also occurs in a single tissue (in our case muscle tissue) due to an inhomogeneous E distribution. The increase in tissue conductivity, thus tissue permeabilization, first occurs in close proximity to the electrodes (i.e. the region with the highest E). The conductivity increase causes a modification in E distribution according to $\sigma(E)$, which consequently causes another change in tissue conductivity and the propagation of muscle permeabilization away from the electrodes towards the regions with lower E between the electrodes, as shown in Fig. 7a.
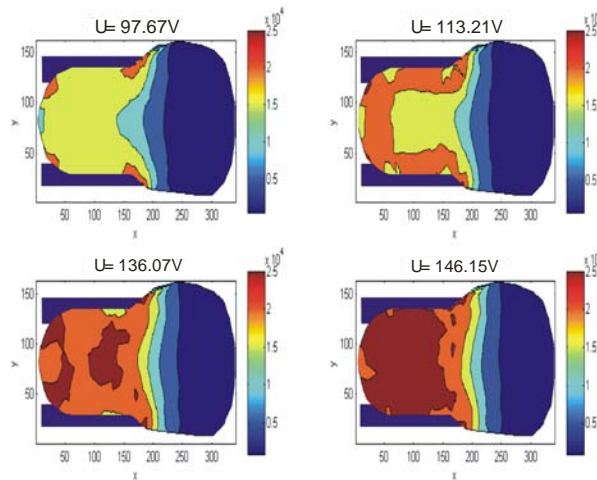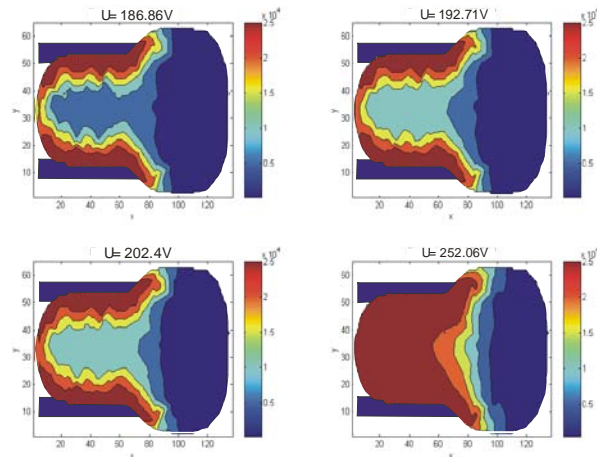
Fig. 7: Distribution of E in model of muscle alone (A) and in the muscle model with the skin (B)

In most of the studies on skin electroporation [Prausnitz et al., 1993, Pliquett et al., 1995], a pronounced change in skin resistance R [Ohm] was observed above 50 V for the experiments done through a single skin tissue layer. In order to compare our analysis on changes in electric properties in the skin layer in the complete muscle model to the data from the literature, we also calculated the resistance R [Ohm] of the complete muscle model for each of the voltages applied and added additional voltages ($U < 186.86$ V) that were not applied during *in vivo* experiments. The calculated resistance-voltage relationship $R(U)$ is shown in Fig. 8. From the $R(U)$ curve it can be observed that a visible drop in skin resistance was obtained at $U > 100$ V which is in agreement with abovementioned studies, proven by our study on electroporating the double skin layer. The increase in skin conductivity, thus the drop in skin resistance, in our skin fold (double skin layer) model was also observed at $U > 100$ V, as shown in Fig. 6a. In a similar experimental and numerical study on cutaneous tumor electroporation, pronounced changes in skin conductivity were also observed at 100 V of applied voltage [Pavselj et al., 2005]. Therefore, the conductivity change and the geometry of the skin layer numerically found in our complete muscle model are in agreement with previous studies on skin.
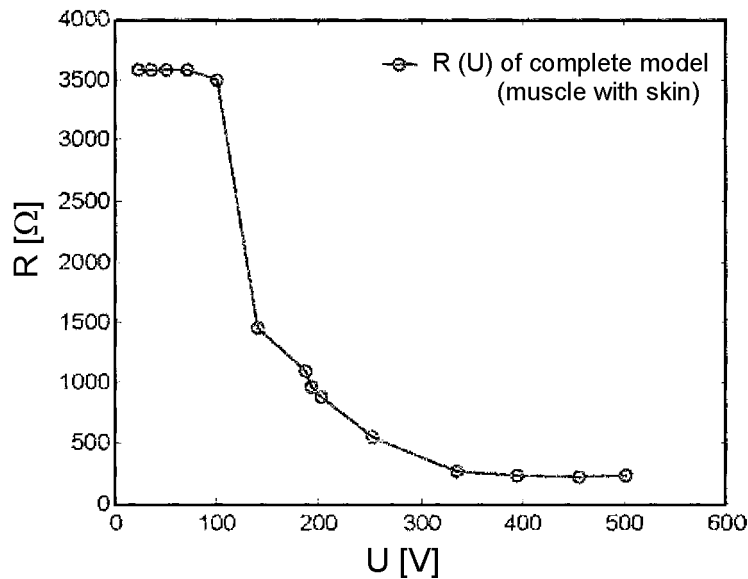

Fig. 8: Calculated resistance-voltage relationship for the complete model from Fig. 4 (muscle with skin)

In order to analyze the influence of the skin layer on muscle electroporation, we used *in vivo* experimental data of ^{51}Cr-EDTA uptake measured in muscle electroporated directly and transcutaneously. The ^{51}Cr-EDTA molecules from the extracellular compartments could enter only the electroporated cells. Both measurements were done at the same applied voltages as in the total current measurement *in vivo*. The experimentally obtained ^{51}Cr-EDTA (U/d) relationships for muscle electroporated directly and transcutaneously are shown in Fig. 9a. The start of the ^{51}Cr-EDTA uptake increase should correspond to the start of reversible electroporation, while the peak and more importantly, the start of uptake decline should correspond to the point of irreversible electroporation.

We then analyzed the electroporation parameters of muscles electroporated directly and transcutaneously by comparing the local electric field distribution in the model of muscle without skin (Fig. 3) with the local electric field distribution obtained only in the muscle inside the complete muscle model with skin (Fig. 4). The local electric field was analyzed at the end of the electroporation process (i.e. at the end of the sequence analysis). Namely, the average electric field intensities were calculated in the space between the two plate electrodes (the regions between electrodes marked with the dashed square in Fig. 3 and Fig. 4) where the electric field was the most homogeneous (i.e. where the electric field approaches U/d). In this way we virtually removed the skin layer from the complete muscle model with skin shown in Fig.4. The numerical results of E in the muscle from the complete model were then compared to the average E in the muscle electroporated directly, as shown in Fig. 9b. The ^{51}CrEDTA uptake values were normalized to the maximum uptake ^{51}CrEDTAmax obtained in the directly electroporated muscle.
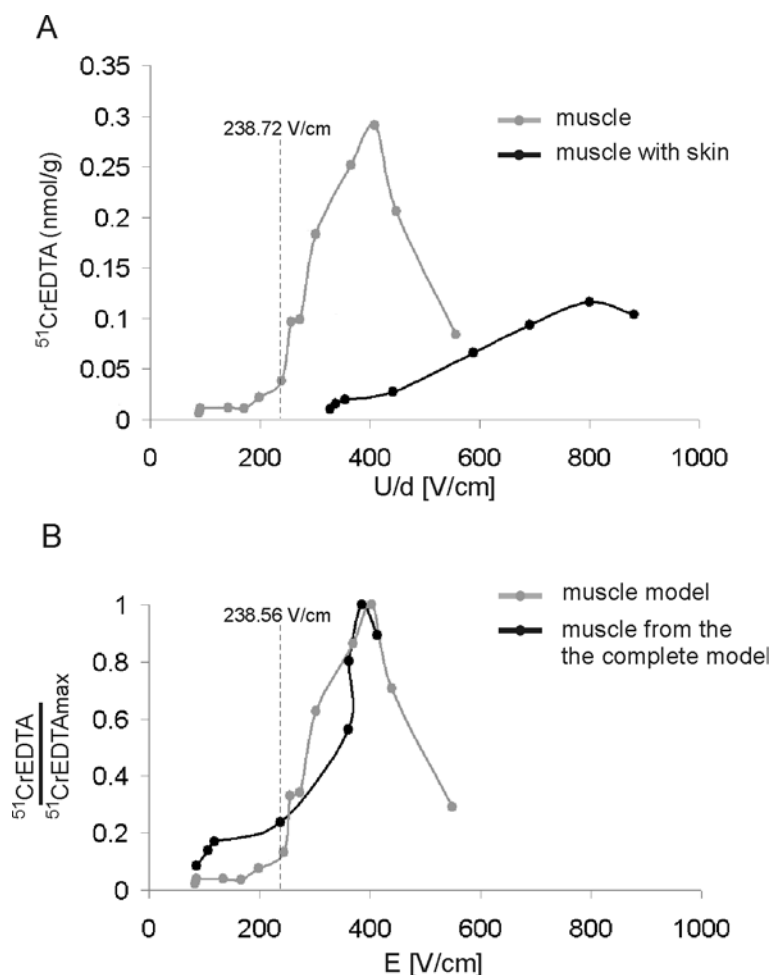

Fig. 9: a) Measured ^{51}CrEDTA uptake in muscle electroporated directly and transcutaneously at different applied voltages U (U values are normalized to the interelectrode distance ratio (U/d). The interelectrode distance used in all experiments was $d = 5.7$ mm) and b) ^{51}CrEDTA at calculated average local electric field intensity E at the applied voltages U.

The average value of E in the model of muscle alone calculated at $U = 136$ V ($U/d = 238.72$ V/cm) was $E_{rev} = 242$ V/cm, whereas the average E in muscle inside the complete model with skin at the higher applied voltage $U = 252$ V ($U/d = 442$ V/cm) was calculated to be almost the same as in muscle without skin $E_{rev} = 238.56$ V/cm, as shown in Fig. 9b. Similarly, the irreversible threshold values calculated as average local E for muscle alone and the muscle with skin were $E_{irrev} = 443$ V/cm (at applied $U = 255$ V) and $E_{irrev} = 414$ V/cm (at applied $U = 456$ V), respectively. Based on these calculations we can conclude that the skin layer has, as expected, no influence on the thresholds of the local electric field needed to successfully electroporate muscle tissue. We did however find that the presence of skin affects the [51]CrEDTA uptake into the muscle while being electroporated through the skin which can be explained by the dependency of the electroporation level on the duration and the number of EP pulses. Namely, due to the presence of the skin the effective duration of the EP pulses can be shorter, which consequently results in a lower ^{51}Cr-EDTA uptake in the muscle tissue. It is well known that the molecular flux through the permeabilized membrane depends on the duration and number of electroporation pulses [Puc et al., 2003, Pucihar et al., 2008].

The threshold values calculated in both the model of muscle alone and the complete model with skin are similar to the threshold values obtained with sequence analysis in the model of muscle alone $E_{rev} = 240$ V/cm and $E_{irrev} = 450$ V/cm. From Fig. 9 it can be seen that in the muscle electroporated directly the average local electric field in the region between the electrodes (gray curve in Fig. 9b), where the tissue is (region marked with dashed square in Fig. 3), is almost equal to the voltage over the interelectrode distance ratio U/d (gray curve in Fig. 9a), and is thus almost homogeneous. Consequently, the error we make using U/d values to approximately determine threshold value of local electric field to successfully electroporate muscle without skin is acceptably small. However, for precise determination of the local electric field threshold value needed only for electroporation of muscle inside a complex tissue, a realistic numerical model that takes into account realistic geometries, electric properties and electric field non-homogeneties due to the tissue permeabilization of all composing tissues needs to be used in combination with corresponding *in vivo* experiments.

Our results are comparable with data obtained in a similar numerical and *in vivo* study for the same type of pulses as used in our study (eight pulses, 100 μs, 1Hz) [Pavšelj et al., 2005], where the E_{rev} and E_{irrev} for muscle electroporated directly are estimated to be 200 V/cm and 450 V/cm, respectively. In Gehl et al., 1999, the combination of *in vivo* experiments (transcutaneous muscle electroporation using plate electrodes with $d = 4$ mm) and 2D numerical models resulted in a higher electroporation threshold (450 V/cm) compared to the one obtained in our study ($E_{rev} = 238$ V/cm), since in their study the tissue between electrodes was considered homogeneous in two dimensions, showing the differences in skin and muscle electric conductivity and geometry were not taken into account.

4. Conclusion

In this study we present the realistic numerical models of electroporated skin fold and skeletal muscle tissue electroporated directly and transcutaneously which we developed in order to analyze the electroporation process in skin and muscle tissue *in vivo*. The models are developed by validating numerical calculations on *in vivo* experimental results. We determined how to map electropermeabilization by identifying the local electric field distribution in skin and muscle tissue. Namely, we found the functional dependency of tissue conductivity on electric field intensity $\sigma(E)$ to be exponential for skin with electroporation thresholds $E_{rev} = 480$ V/cm and $E_{irrev} = 1050$ V/cm and sigmoid for muscle tissue with $E_{rev} = 240$ V/cm and $E_{irrev} = 430$ V/cm. The same electroporation threshold values E_{rev} and E_{irrev} were found for both muscle electroporated directly and transcutaneously. We thus conclude that the skin layer has, as expected, no influence on the thresholds of the local electric field intensity itself needed for successful muscle tissue electroporation, but it does require higher voltage to be applied between the electrodes when muscle is electroporated transcutaneously.

We also showed that the error of an approximate estimation of electroporation threshold values in *in vivo* experiments by calculating the *U/d* ratio, without numerical calculations of local electric field distribution, is small enough only if the plate electrodes are used and only for one type of tissue placed between the electrodes. For more complex tissues with different geometric and electrical properties, a combination of realistic numerical modeling and *in vivo* experiments approach needs to be used for the precise determination of electroporation threshold values.

It is also important to note that the thresholds of the local electric field for tissue electroporation depend on the type of molecules used for detection of *in vivo* tissue permeabilization [Kotnik et al., 2000] and electroporation pulse characteristics (i.e. duration and number of pulses as well as pulse repetition frequency). Thus, the threshold values determined in our study are relevant for the setting of eight pulses of 100 μs duration at a frequency of 1 Hz. For precise electroporation threshold determination for the other pulse parameters, our numerical models remains valid, but additional experiments need to be done and the obtained results must be included in the models.

The findings of our study carry important practical information for treatment planning in electroporation mediated therapies such as gene electrotransfer into the muscle, transdermal drug and gene delivery and clinical electrochemotherapy.

Acknowledgement

References

Al-Sakere B, Bernat C, Connault E, Opolon P, Rubinsky B, Davalos R, Mir LM. **Tumor ablation with irreversible electroporation.** *PLoSONE* 2:135, 2007.

Batiuskaite D, Cukjati D, Mir LM. **Comparison of in vivo electropermeabilization of normal and malignant tissue using the ^{51}Cr-EDTA uptake test**. *Biologija* 2003: 45-47, 2003.

Corovic S, Zupanic A, Miklavcic D. **Numerical modeling and optimization of electric field distribution in subcutaneous tumor treated with electrochemotherapy using needle electrodes**. *IEEE Trans. Plasma Sci.* 36: 1665-1672, 2008.

Cukjati D, Batiuskaite D, André F, Miklavcic D, Mir LM. **Real time electroporation control for accurate and safe *in vivo* non-viral gene therapy**. *Bioelectrochemistry* 70: 501-507, 2007.

Davalos R, Rubinsky B, Otten DM. **A feasibility study for electrical impedance tomography as a means to monitor tissue electroporation for molecular medicine.** *IEEE Trans. Biomed. Eng*. 49: 400–403, 2002.

Davalos RV, Otten DM, Mir LM, Rubinsky B. **Electrical impedance tomography for imaging tissue electroporation.** *IEEE Trans.Biomed. Eng.* 51: 761–767, 2004.

Denet AR, Vanbever R, Pre´at V. **Skin electroporation for transdermal and topical delivery**. *Adv. Drug Deliv. Rev.* 56: 659–674, 2004.

Dev SB, Rabussay DP, Widera G, Hofmann GA. **Medical applications of electroporation.** *IEEE Trans. Plasma Sci.* 28: 206-223, 2000.

EMAS User's Manual, Ansoft Corp., Jul. 1997.

Gehl J, Sorensen TH, Nielsen K, Raskmark P, Nielsen SL, Skovsgaard T, Mir LM. **In vivo electroporation of skeletal muscle: Threshold, efficacy and relation to electric field distribution.** *Biochim. Biophys. Acta* 1428: 233–240, 1999.

Leroy-Willig A, Bureau MF, Scherman D, Carlier PG. **In vivo NMR imaging evaluation of efficiency and toxicity of gene electrotransfer in rat muscle.** *Gene Ther*,12(19):1434-43, 2005

Hojman P, Zibert JR, Gissel H, Eriksen J, Gehl J. **Gene expression profiles in skeletal muscle after gene electrotransfer.** *BMC Mol Biol.* 8: 56, 2007.

Hojman P, Gissel H, Andre F, Cournil-Henrionnet C, Eriksen J, Gehl J, Mir LM. **Physiological effects of high and low voltage pulse combinations for gene electrotransfer in muscle.** *Hum Gene Ther.* 2008

Kotnik T, Maček-Lebar A, Miklavčič D, Mir LM. **Evaluation of cell membrane electropermeabilization by means of nonpermeant cytotoxic agent**. *Biotechniques* 28: 921-926, 2000.

Marty M, Sersa G, Garbay JR, Gehl J, Collins CG, Snoj M, Billard V, Geertsen PF, Larkin JO, Miklavcic D, Pavlovic I, Paulin-Kosir SM, Cemazar M, Morsli N, Soden DM, Rudolf Z, Robert C, O'Sullivan GC, Mir LM. **Electrochemotherapy – An easy, highly effective and safe treatment of cutaneous and subcutaneous metastases: Results of ESOPE (European Standard Operating Procedures of Electrochemotherapy) study**. *Eur. J. Cancer Suppl.* 4: 3-13, 2006.

Mathiesen I. **Electropermeabilisation of skeletal muscle enhances gene electrotransfer in vivo.** *Gene Therapy*. 6: 508-514, 1999.

Mir LM, Orlowski S, Belehradek JJr, Teissié J, Rols MP, Sersa G, Miklavcic D, Gilbert R, Heller R. **Biomedical applications of electric pulses with special emphasis on antitumor electrochemotherapy.** *Bioelectrochem.* 38: 203-207, 1995.

Mir LM, Bureau MF, Gehl, Rangara R, Rouy D, Caillaud JM, Delaere P, Branellec D, Schwartz B, Scherman D. **High-efficiency gene transfer into skeletal muscle mediated by electric pulses**. *Proc Natl Acad Sci USA*, 74: 4262-4267, 1999.

Miklavcic D, Beravs K, Semrov D, Cemazar M, Demsar F, Sersa G. **The importance of electric field distribution for effective in vivo electroporation of tissues**. *Biophys. J*. 74: 2152-2158, 1998.

Miklavcic D, Semrov D, Mekid H, Mir LM. **A validated model of in vivo electric field distribution in tissues for electrochemotherapy and for DNA electrotransfer for gene therapy**. *Biochim. Biophys. Acta* 1523: 73-83, 2000.

Miklavcic D, Pavselj N, Hart FX. **Electric Properties of Tissues**. *Wiley Encyclopedia of Biomedical Engineering*, John Wiley & Sons, New York, 2006.

Pavselj N, Bregar Z, Cukjati D, Batiuskaite D, Mir LM, Miklavcic D. **The course of tissue permeabilization studied on a mathematical model of a subcutaneous tumor in small animals.** *IEEE Trans. Biomed. Eng*. 52: 1373-1381, 2005.

Pavselj N, Miklavcic D. **Numerical modeling in electroporation-based biomedical applications**. *Radiol. Oncol.* 42: 159-168, 2008.

Pavlin M, Pavselj N, Miklavcic D. **Dependence of induced transmembrane potential on cell density, arrangement, and cell position inside a cell system**. *IEEE Trans. Biomed. Eng*. 49: 605-612, 2002.

Pavlin M, Miklavcic D. **Effective conductivity of a suspension of permeabilized cells: a theoretical analysis**. *Biophys. J.*, 85:. 719–729, 2003.

Perez N, Bigey P, Scherman D, Danos O, Piechaczyk M, Pelegrin M. **Regulatable systemic production of monoclonal antibodies by in vivo muscle electroporation.** *Genetic Vaccines and Therapy*, 2: 2, 2004.

Pliquett U, Langer R, Weaver JC. **Changes in the passive electrical properties of human stratum corneum due to electroporation.** *BBA*, 1239: 111–121, 1995.

Prausnitz MR, Lau BS, Milano CD, Conner S, Langer R, Weaver JC. **A quantitative study of electroporation showing a plateau in net molecular transport.** *Biophys. J.,* 65: 414-422, 1993.

Prud'homme GJ, Glinka Y, Khan AS, Draghia-Akli R. **Electroporation enhanced nonviral gene transfer for the prevention or treatment of immunological, endocrine and neoplastic diseases.** *Current Gene Therapy*, 6: 243-273, 2006.

Puc M, Kotnik T, Mir LM, Miklavčič D. **Quantitative model of small molecules uptake after in vitro cell electropermeabilization**. *Bioelectrochemistry* 60: 1-10, 2003.

Pucihar G, Kotnik T, Miklavčič D, Teissié J. **Kinetics of transmembrane transport of small molecules into electropermeabilized cells**. *Biophys. J.* 95: 2837-2848, 2008.

Mali B, Jarm T, Corovic S, Paulin-Kosir MS, Cemazar M, Serša G, Miklavcic D. **The effect of electroporation pulses on functioning of the heart**. *Med. Biol. Eng. Comput.* 46: 745-757, 2008.

Sel D, Cukjati D, Batiuskaite D, Slivnik T, Mir LM, Miklavcic D. **Sequential finite element model of tissue electropermeabilization**. *IEEE Trans. Biomed. Eng.* 52: 816-827, 2005.

(UKCCCR) **Guidelines for Welfare of Animals in Experimental Neoplasia (Second Edition)**. *Br. J. Cancer 77*, 1-10 (1998).

Umeda Y, Marui T, Matsuno Y, Shirahashi K, Iwata H, Takagi H, Matsumoto K, Nakamura T, Kosugi A, Mori Y, Takemura H. **Skeletal muscle targeting in vivo electroporation-mediated HGF gene therapy of bleomycin-induced pulmonary fibrosis in mice.** *Laboratory investigation*, 84: 836-844, 2004.

Tevz G, Pavlin D, Kamensek U, Kranjc S, Mesojednik S, Coer A, Sersa G, Cemazar M. **Gene Electrotransfer into Murine Skeletal Muscle: A Systematic Analysis of Parameters for Long-term Gene Expression.** *TCRT,* 7, 2: 91-154, 2008.

Valic B, Golzio M, Pavlin M, Schatz A, Faurie C, Gabriel B, Teissie J, Rols MP, Miklavcic D. **Effect of electric field induced transmembrane potential on spheroidal cells: theory and experiments**. *Eur. Biophys. J.* 32: 519–528. 2003.

Zupanič A, Corović S, Miklavcic D. **Optimization of electrode position and electric pulse amplitude in electrochemotherapy**. *Radiol. Oncol.* 42: 93-101, 2008.

Paper VI

ORIGINAL ARTICLE

The influence of skeletal muscle anisotropy on electroporation: in vivo study and numerical modeling

Selma Čorović · Anže Županič · Simona Kranjc ·
Bassim Al Sakere · Anne Leroy-Willig ·
Lluis M. Mir · Damijan Miklavčič

Abstract The aim of this study was to theoretically and experimentally investigate electroporation of mouse tibialis cranialis and to determine the reversible electroporation threshold values needed for parallel and perpendicular orientation of the applied electric field with respect to the muscle fibers. Our study was based on local electric field calculated with three-dimensional realistic numerical models, that we built, and in vivo visualization of electroporated muscle tissue. We established that electroporation of muscle cells in tissue depends on the orientation of the applied electric field; the local electric field threshold values were determined (pulse parameters: 8×100 μs, 1 Hz) to be 80 V/cm and 200 V/cm for parallel and perpendicular orientation, respectively. Our results could be useful electric field parameters in the control of skeletal muscle electroporation, which can be used in treatment planning of electroporation based therapies such as gene therapy, genetic vaccination, and electrochemotherapy.

1 Introduction

In vivo electroporation (also termed electropermeabilization) is an effective method for administration of therapeutic drugs (such as chemotherapeutic agents) and one of the most efficient and simple nonviral methods for gene transfer into target tissue, provided appropriate electrical parameters are chosen [19, 21, 22]. In vivo electroporation is successfully applied in clinics for electrochemotherapy of solid tumors [16]. Gene transfer by means of electroporation (gene electrotransfer) has also been performed in humans and it seems likely it could be applied clinically for nonviral gene therapy. Efficient in vivo gene electrotransfer has been shown in a wide range of tissues [2, 4, 27, 33]. Skeletal muscle is one of the most attractive tissues for administration of therapeutic genes by electroporation for both local and systemic gene therapy, for genetic vaccination against infectious agents (e.g. hepatitis B virus, human immunodeficiency virus-1) as well as for basic research of muscle physiology, due to a number of its biological properties such as relatively easy access the skeletal muscles, long term stable transgene expression and excellent vascularisation [13, 17, 26, 35].

In order to assure optimal conditions for gene therapy and genetic vaccination, the electrical parameters (such as applied voltage, electrode shape, and position) need to be chosen to assure reversible muscle electroporation just above the reversible threshold value. After the application of electric pulses the electroporated cell membrane needs to be resealed in order to obtain efficient DNA transfer.

S. Čorović · A. Županič · D. Miklavčič (✉)
Faculty of Electrical Engineering, University of Ljubljana,
Trzaska 25, SI-1000 Ljubljana, Slovenia
e-mail: damijan.miklavcic@fe.uni-lj.si

S. Čorović · B. Al Sakere · L. M. Mir
Institute Gustave-Roussy, CNRS, UMR 8121, 39 Rue C.
Desmoulins, 94805 Villejuif, France

S. Čorović · B. Al Sakere · L. M. Mir
Univ Paris-Sud, UMR 8121, Paris, France

S. Kranjc
Institute of Oncology, Zaloška 2, SI-1000 Ljubljana, Slovenia

A. Leroy-Willig
Univ Paris-Sud, UMR 8081, U2R2M, Batiment 220, 91405
Orsay Cedex, France

This can be assured with appropriate pulse parameters that induce reversible muscle electroporation, otherwise the viability of the target muscle fibers is lost, due to the irreversible membrane electroporation (i.e. leading to cell death). The reversible electroporation is required also in electrochemotherapy, so as to avoid exposure of healthy tissues to high electric field (above irreversible threshold) and possible ulceration and wound appearance.

Electroporation pulses establish a local electric field (E) within the treated tissue, which depends on the amplitude of the applied electroporation pulses, electrodes' shape and placement, and tissue geometrical and physical properties [18, 24]. In order to obtain reversible tissue electroporation, the target tissue has to be subjected to the local electric field inducing reversible electroporation (E between reversible and irreversible electroporation thresholds $E_{rev} < E < E_{irrev}$) [19], while the magnitude of E above E_{irrev} induces irreversible tissue electroporation [29].

By combination of numerical modeling and optimization algorithms, the level and extent of the tissue electroporation can be controlled by appropriate amplitude of electroporation pulses and electrodes shape and placement, provided that the electroporation thresholds, E_{rev} and E_{irrev}, for each tissue type are known [5, 31, 38]. In a study on liver tissue electroporation, Miklavcic et al. [19] showed that electroporation thresholds of local electric field and electroporated-tissue extent can be efficiently determined by comparing experimental observations (i.e. visualization of electroporated tissue region) to the local electric field distribution obtained by three-dimensional numerical simulations on realistic mathematical models that take into account electric properties of the involved tissues. Since muscle tissue exhibits anisotropic electric properties, its sensitivity to electroporation is expected to be electric field orientation dependent. Thus, determination of electroporation thresholds for different electric field orientations with respect to the muscle fibers is of great importance for optimization of local electric field distribution and for control of electroporation process in the target tissue. Most of in vivo studies on skeletal muscle electroporation have been done for the direction of the electric field perpendicular to the long axis of the fibers [3, 7, 10, 11, 14, 25]. Only, Aihara and Miyazaki [1] experimentally examined also the influence of parallel electric field orientation on gene electrotransfer in skeletal muscle using two needle electrodes. Analytical solution for the electric potential and activating function in two dimensions established by needle electrodes in anisotropic tissue was reported by [12].

Our study was based on the comparison of local electric field calculated using three-dimensional realistic numerical models and in vivo visualization of electroporated target tissue, which for skeletal muscle tissue has not been performed before. The aim of our study was to (1) investigate electroporation of mouse tibialis for parallel and perpendicular orientation of the applied electric field with respect to the muscle fibers and (2) determine the electroporation thresholds of mouse tibialis cranialis muscle using both electric field orientations; theoretically and experimentally using two plate electrodes.

2 Methods

2.1 Animals

Female C57B1/6 mice were housed and handled according to recommended guidelines [34] and French legislation concerning animal welfare. Prior to all procedures, mice were anesthetized by administrating 12.5 mg/kg xylazine (Bayer Pharma, Puteaux, France) and 125 mg/kg ketamine (Parke Davis, France) by intraperitoneal injection in 150 µl saline.

2.2 Electroporation protocol and electrodes

Electroporation was performed by applying eight rectangular monophasic 100 µs electroporation pulses at a repetition frequency of 1 Hz. The electroporation pulses were delivered through two stainless-steel parallel plate electrodes (10 mm long and 0.7 mm wide), which were in direct contact with the tibialis muscle after skin incision (Fig. 1). We carefully controlled the electrode placement by marking its position on the muscle and contact surface formed between the electrode and muscle surface (Fig. 1). Namely, we carefully measured the position of electrodes on the muscle during the in vivo experiments. Those measurements were then taken into account when modeling the geometry of the muscle and the contact surface between the electrodes and the muscle. We aligned the images obtained in in vivo measurements with the images from numerical models by using graphical software (i.e. CorelDraw). Electrode tissue set-ups were examined for perpendicular and parallel orientation of electric field with respect to the long axis of the muscle fibers, as illustrated in Fig. 1a, b, respectively.

Electroporation pulses of amplitude $U < 60$ V were generated by a PS 15 electropulsator (Jouan, St. Herblin, France), while the pulses of amplitude $U \geq 60$ V were generated by a Cliniporator (Igea, Carpi, Italy).

2.3 Magnetic resonance imaging (MRI) experiments

For the detection of the electroporated muscle volume by means of MRI we used Gd-DOTA (Dotarem, Guerbet, Aulnay-sous-Bois, France), contrast agent. The assessment of reversibly electroporated muscle volume was based on
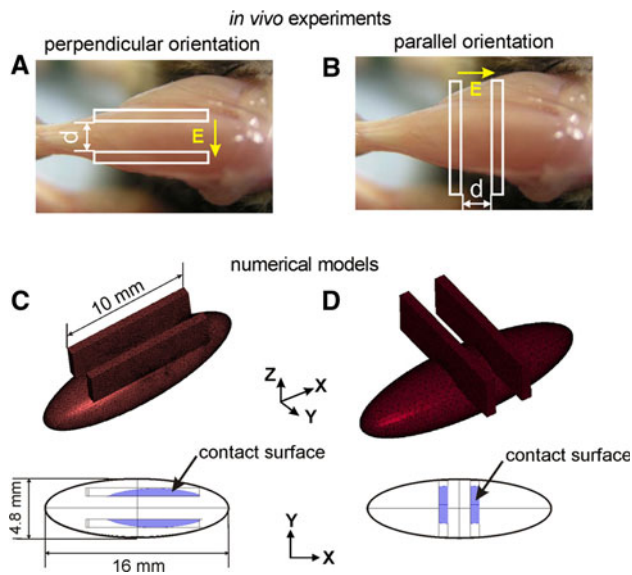
Fig. 1 Experimental electrode tissue set-up for **a** perpendicular and **b** parallel orientation of electric field with respect to the long axis of muscle fibers and the corresponding three-dimensional finite element model geometries for **c** perpendicular and **d** parallel electric field orientation. The corresponding contact surfaces between the electrodes and muscle model are depicted below the three-dimensional models in **a** and **d** for perpendicular and parallel orientation, respectively

T1 relaxation time weighted images. The T1 weighted images were expected to show the muscle areas where the Gd-DOTA molecules were trapped inside the reversibly electroporated muscle cells. T2 relaxation time weighted images were used to detect the irreversibly electroporated muscle areas by detecting the signs related to the cell damage, such as leakage of Gd-DOTA molecules out of the cells and edema [14] (in the absence of these signs the images showed reversible muscle electroporation).

Twenty mice were anesthetised and Gd-DOTA was injected intraperitoneally at the dose 10 ml/kg of a diluted solution isoosmotic to plasma (1 ml of Dotarem and 2.77 ml of water). It was previously demonstrated that after slow transperitoneal passage to the blood flow, the contrast agent remained in the extracellular space at a roughly constant concentration between 15 and 120 min after the injection [23]. In our experiments, skin was incised and electroporation pulses were delivered directly to the muscle (Fig. 1) 20 min after the injection.

The amplitudes of the in vivo delivered electroporation pulses were selected based on a preliminary numerical analysis of electric field orientation with respect to the muscle fibers. For the perpendicular orientation of applied electric field (Fig. 1a) 18 muscles were treated with electroporation pulses ranging from 30 to 164 V (voltage to electrodes distance ratio ranging from 150 to 820 V/cm).

For the parallel orientation (Fig. 1b), 20 muscles were treated with electroporation pulses ranging from 8 to 160 V (voltage to electrodes distance ratio ranging from 20 to 400 V/cm). Distances between electrodes (d) were $d = 2$ mm for perpendicular (Fig. 1a) and $d = 4$ mm for parallel orientation (Fig. 1b). Two injected muscles were not electroporated and served as controls.

After electroporation, skin incisions were sewed up. The signal increase corresponding to the uptake of contrast agent by the reversibly electroporated cells was measured by MRI 3 days later, since complete elimination of the contrast agent located within the extracellular space is reached at day 3 after the injection [23].

2.3.1 MRI acquisition

MRI examinations were performed using a 4.7 Tesla system equipped with a Tecmag spectrometer with a home built bird-cage coil (inner diameter 32 mm). Mice were positioned with legs extended inside a cylindrical holder fitting inside the coil.

T1-weighted magnetic resonance images were obtained using a T1-weighted spin-echo sequence with the following parameters: TR 644 ms, TE 7.1 ms, spectral width 80 kHz, 4 accumulations, in-plane spatial resolution 120 μm × 150 μm, slice thickness 2 mm, and slice spacing 2 mm. Eleven successive axial slices perpendicular to the long leg axis and thus to the muscle fibers (i.e. MR images of YZ cross-sections (Fig. 1)) were obtained in 11 min.

Figure 2 shows T1-weighted images of mice legs treated at voltages producing E above the reversible threshold values (Fig. 2a for perpendicular and Fig. 2b for parallel orientation) and below the reversible thresholds (Fig. 2c for perpendicular and Fig. 2d for parallel orientation). The dotted white lines in Fig. 2 mark the corresponding electrode positions on the treated mice legs. The zones of increased muscle signal (i.e. electroporated muscle regions, where the contrast agent remained inside cells 3 days after the electroporation increased the muscle water signal by shortening its relaxation time T1) are indicated by arrows in Fig. 2a, b.

T2-weighted MR images were obtained using a T2-weighted spin-echo sequence with the following parameters: TR 2250 ms TE 50 ms, two averages, in-plane resolution 400 μm × 400 μm, and slice thickness 2 mm. Five successive axial slices perpendicular to the muscle fibers (i.e. MR images of YZ cross-sections (Fig. 1)) were obtained in 10 min.

Images were reconstructed with zero-filling to improve in plane spatial resolution and analyzed using a home written algorithm (MATLAB 2007a, The MathWorks, Natick, USA).
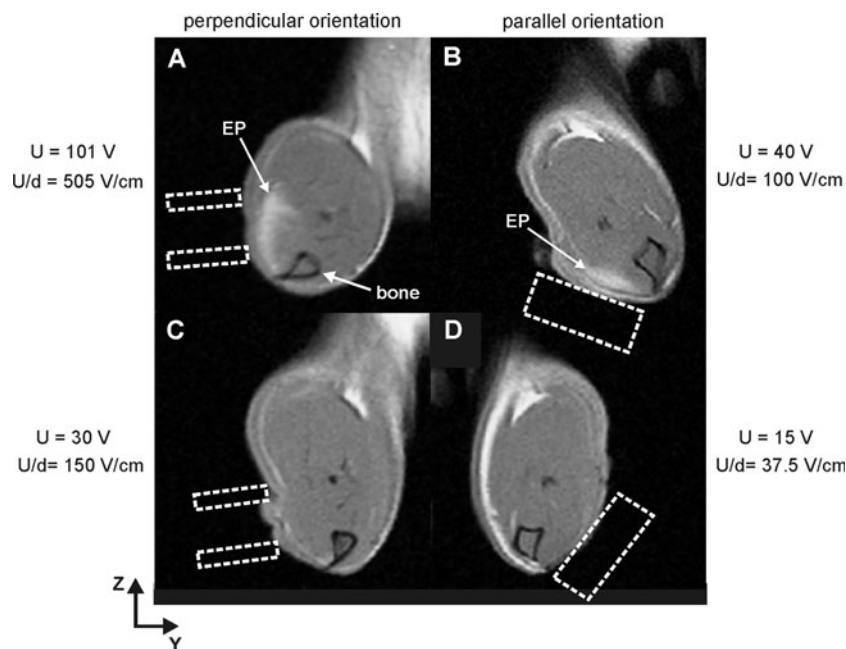
Fig. 2 T1-weighted MRI images of four examined mice legs in *ZY* cross-section: **a** $U = 101$ V, perpendicular, **b** $U = 40$ V, parallel, **c** $U = 30$ V, perpendicular, and **d** $U = 15$ V, parallel orientation. **a** and **b** show the successfully electroporated muscles where the zones of increased muscle signal (electroporated region EP) are indicated by *arrows*. **c** and **d** show the muscles with the *E* below the reversible electroporation threshold ($E < E_{rev}$). The electrode placements are illustrated with *dashed squares*. Distances between electrodes for perpendicular and parallel orientations are 2 and 4 mm, respectively. In **b** and **d** (parallel orientation); the *box* corresponds to the position of the two electrodes, one lying 2 mm above the image and the other 2 mm below

2.3.2 MRI image analysis

All slices (i.e. MRI images) where a zone of increased signal was detected were taken into account for the analysis (electroporation volume detection). The number of analyzed slices for the perpendicular orientation was 1 (2 mm leg extent at lower voltages applied) to 5 (10 mm, which corresponds to the electrode length). The number of slices analyzed for the parallel orientation was 1 (2 mm) to 3 (6 mm leg extent—distance between the electrodes was 4 mm). The area with increased signal indicating the successfully electroporated area of tibialis cranialis muscle was analyzed by determination of two regions of interest (ROI—ROI_1 and ROI_2, as marked in Fig. 3) in each magnetic resonance image obtained. Figure 3 shows an example of the marked ROI in the MRI image obtained with $U = 101$ V (the corresponding position of electrodes is marked in Fig. 2a).

The first region of interest (ROI_1), as marked in Fig. 3 with dotted black line, was carefully drawn by an expert around the zone with increased signal indicating the successfully electroporated area of the tibialis cranialis muscle, after windowing the image to increase the contrast. The number of pixels within the drawn ROI_1 region in each of the magnetic resonance images was determined and the obtained sum of the pixels from all magnetic resonance images was converted to the labeled volume by its multiplication with the elementary volume corresponding to one pixel $V = 9.0 \ 10^{-3}$ mm^3.
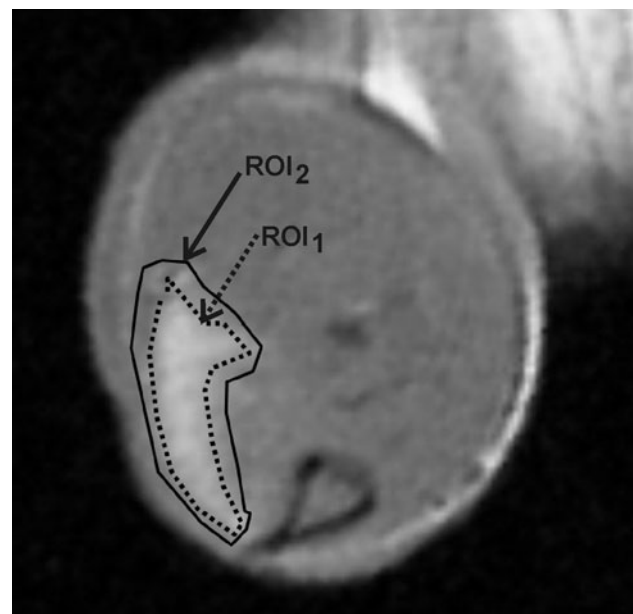
Fig. 3 T1-weighted MRI image of examined mice leg in *ZY* cross-section obtained at applied $U = 101$ V in perpendicular orientation. Regions of interest ROI_1 is marked with *dotted black line*. Region of interest ROI_2 is marked with *solid black line*. The corresponding electrode position for this experiment is shown in Fig. 2a

The second region of interest ROI_2 (as marked in Fig. 3 with solid black line), slightly larger than the previous one, was manually drawn around the ROI_1 in each of the

magnetic resonance images. The mean signal, S, inside this zone was computed. A reference zone, where muscle was not affected by electroporation pulses, was drawn in another unaffected muscle and its mean reference signal, S_0, was computed.

In the larger zone with increased signal (ROI$_2$), the signal of each pixel (i, j) is $S(i, j)$ and S_0 is the estimation of the signal $S_0(i, j)$ that would correspond to the local value in the absence of modification due to electroporation.

An index of integrated muscle signal increase was determined from the following relation (Eq. 1):

$$I = \sum i,j \left((S(i,j) - S_0(i,j)) / S_0(i,j) \right) \tag{1}$$

The determined index, I, is robust compared to the delimitation of the ROI where the signal increase is determined, since the same sum is obtained in a larger region of interest, ROI$_2$, than in a closely drawn ROI$_1$. The index, I, evaluates the sum of local signal increase that is related to the total amount of contrast agent inside muscle cells as long as the relation between contrast agent concentration and signal is linear [14], which is the case at the dose injected in our experiments.

2.4 Propidium iodide (PI) uptake experiments

In order to visualize the extent of muscle electroporation in XY cross sections of the examined muscles (Fig. 1), a fluorescent dye, PI, (Sigma, Saint Louis, USA) was used. The dye is essentially membrane impermeant, but can enter the cells being electroporated. Because its fluorescence increases several fold upon binding to DNA or mRNA, it can be used to detect cell electroporation within the treated tissue [28].

Eleven mice were anesthetized, the skin facing the muscle was removed and 20 µl (10 mM) of PI was slowly injected into the tibialis cranialis (injection duration = 30 s). The muscle was electroporated immediately after the injection. The amplitudes of the electroporation pulses delivered to the examined muscles were selected based on a preliminary numerical analysis of electric field orientation with respect to the muscle fibers. The muscle electroporation was investigated for pulse amplitudes $U = 50, 60, 70, 80,$ and 100 V ($U/d = 250, 300, 350, 400,$ and 500 V/cm) for perpendicular orientation and $U = 10, 20, 30, 40, 50$ V ($U/d = 50, 100, 150, 200, 250,$ and 300 V/cm) for the parallel orientation. In order to assess the reproducibility of the fluorescence patterns we repeated the measurements 2–3 times for each of the voltages applied. Two injected muscles were not electroporated and served as controls. Distance between electrodes (d) was 2 mm for both perpendicular (Fig. 1a) and parallel orientation (Fig. 1b). The PI fluorescence was observed under

the stereomicroscope (Leica MZFLIII, Germany) and photographed with a digital camera (Olympus® Camedia C-5050 Zoom) 15 min after the electroporation. The obtained PI fluorescence displayed the total sum of the signal obtained within the entire muscle observed under the microscope (from the top view). Mice were killed after the experiment while still anesthetized.

2.5 Numerical modeling

The three-dimensional model of muscle tissue is based on the numerical solution of partial differential equation for steady electric current in anisotropic conductive media, Eq. 2.

$$\nabla \cdot (\sigma \cdot (-\nabla u)) = 0, \tag{2}$$

where σ is conductivity tensor [S/m] describing anisotropic electric properties of the muscle (Eq. 3), and the negative gradient of the potential u [V] in the tissue volume defines vector of electric field intensity $\vec{E}$ [V/m].

The numerical calculations were performed by means of finite element method using COMSOL Multiphysics 3.4 software package in the 3D Conductive Media DC application mode on a PC running Windows XP with a 3.00 GHz Pentium D processor and 2 GB of RAM.

2.5.1 Model geometry and electric properties of muscle tissue

In our numerical model, the muscle tissue geometry is represented as an ellipsoid (Fig. 1c, d), with radii 8 mm and 2.4 mm along X- and Y-axis, respectively, and the radius 2 mm along Z-axis. The model is oriented in the orthogonal Cartesian system so that the long axis of the muscle fibers is aligned with the axis X. The contact surfaces between the electrode and muscle were modeled to be as similar as possible to the contact surfaces obtained in in vivo experiments.

2.5.2 Electric properties of the modeled tissues and electroporation process modeling

Before applying electroporation pulses or if the amplitude of the applied electroporation pulses was too low to produce the local electric field above the reversible electroporation threshold ($E < E_{rev}$), the muscle was modeled with constant electric conductivity σ[S/m]. The muscle tissue was considered anisotropic, having higher conductivity along the muscle fibers ($\sigma_{xx} = 0.75$ S/m) compared to the conductivities perpendicular to the fibers ($\sigma_{yy} = \sigma_{zz} = 0.135$ S/m), as represented with a diagonal conductivity matrix, Eq. 3.

$$\sigma = \begin{bmatrix} \sigma_{xx} & 0 & 0 \\ 0 & \sigma_{yy} & 0 \\ 0 & 0 & \sigma_{zz} \end{bmatrix}. \tag{3}$$

These values were selected considering both our previous numerical and in vivo electroporation studies [7, 25] and the measurements of muscle tissue conductivity found in the available literature [20].

If the local electric field in the tissues exceeded the value E_{rev} ($E > E_{rev}$) the tissue conductivity changed according to the function $\sigma(E)$. Namely, the dynamics of the electroporation process (i.e. the conductivity changes during the eight pulses) in the treated tissue was modeled with a sequence static finite element models according to a sequential permeabilization model, proposed by Sel et al. [30]. In each step in sequence (i.e. static finite element model k) the tissue conductivity was determined based on electric field distribution calculated in the previous step in sequence (i.e. static finite element model $k - 1$), as described in equation Eq. 4

$$\sigma(k, E) = f(E(k-1)), \tag{4}$$

where σ is electric conductivity of the modeled tissue, k is number of static finite element models in sequence, and E is local electric field distribution calculated in each of the steps k. In our models the $\sigma(E)$ function was considered to be sigmoid and electric conductivity at the end of the pulse delivery increased by a factor of 3.5 in parallel direction and by a factor of 0.135 in perpendicular direction compared to the initial electric conductivity values (σ_{xx} and $\sigma_{yy} = \sigma_{zz}$, respectively). The sigmoid shape of the $\sigma(E)$ function and the electric conductivity values at the end of the pulse delivery were determined based on comparison of the electric current measured in vivo and the electric current calculated in realistic numerical model in our previous study (Corovic et al., 2010, submitted to Comptes Rendus Physiques).

2.5.3 Boundary conditions and mesh parameters

Dirichlet boundary condition was defined by applying constant voltages, U, between the electrodes. The Neumann boundary condition, i.e., the insulation condition, was set to the rest of the outer boundaries of the model. The electric field distribution was calculated for each of the applied voltage. The results of numerical simulations were controlled by refining the mesh until the difference in numerical solutions was negligible (less than 0.5%) when the number of finite elements (i.e. mesh density) increased. The resulting three-dimensional finite element muscle models illustrated in Fig. 1c, d, consisted of 90,213 and 89,420 elements, respectively.

2.5.4 Analysis of the local electric field distribution

Experimentally determined reversible thresholds $E_{rev\parallel} = 80$ V/cm and $E_{rev\perp} = 200$ V/cm for parallel and perpendicular electric field orientation, respectively, were included in the numerical muscle models (Fig. 1c, d) to calculate the volume (V) of the muscle tissue exposed to the local electric field above the thresholds. The calculations of V were performed with an algorithm, which was written in MATLAB 2007a and run together with the numerical calculation using the link between MATLAB and COMSOL. The numerically calculated volumes for each of the applied voltages for parallel and perpendicular electric field orientation were then compared to the experimentally obtained labeled volumes of the muscles examined by using MRI.

3 Results

3.1 MRI results and numerical calculations

The experimentally obtained labeled volume that corresponds to the successfully eletroporated area of tibialis cranialis muscle (i.e. the detection of signal increase in T1-weighted images), obtained in all examined extremities with electric fields parallel and perpendicular to the long axis of muscle fibers are shown in Fig. 4a. The labeled volume is negligible at low voltages applied $U/d \leq 75$ V/cm for parallel orientation and $U/d \leq 195$ V/cm for perpendicular orientation. The comparison of labeled volume determined in vivo and numerically calculated volume above reversible threshold values for parallel and perpendicular orientations is shown in Fig. 4b, c, respectively. General agreement was obtained. Based on this the electric field threshold values $E_{rev\parallel}$ and $E_{rev\perp}$ were determined to be 80 V/cm and 200 V/cm for parallel and perpendicular orientation, respectively. The labeled volume in Fig. 4 exhibits a plateau at about 35 mm^3 both with perpendicular electric field (from 250–300 V/cm to 800 V/cm), and with the parallel electric field (from 200 to 400 V/cm).

The detection of signal increase in T2-weighted images showed muscle edema in two legs (at 800 V/cm, perpendicular orientation, data not shown), which corresponds to the irreversibly electroporated muscle, as previously demonstrated [23]. The muscle edema was not observed at electric field lower than 800 V/cm (which indicated that at $U/d < 800$ V/cm the treated muscle tissue was not irreversibly electroporated).

Figure 5 shows the index of signal increase inside the tibialis cranialis muscle obtained in all examined
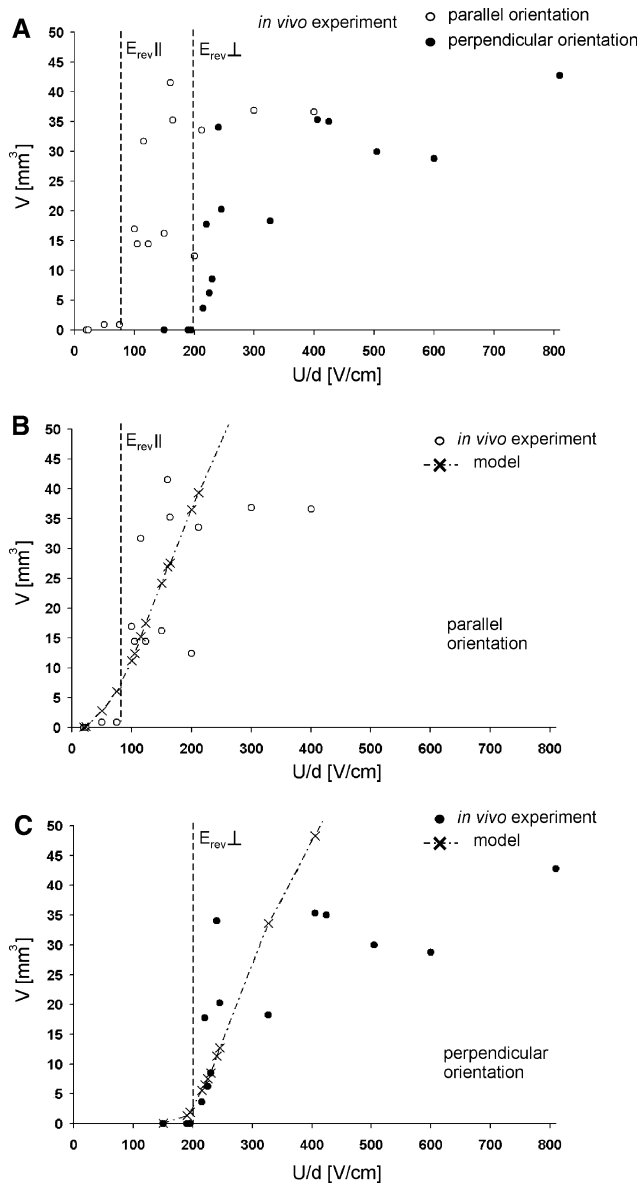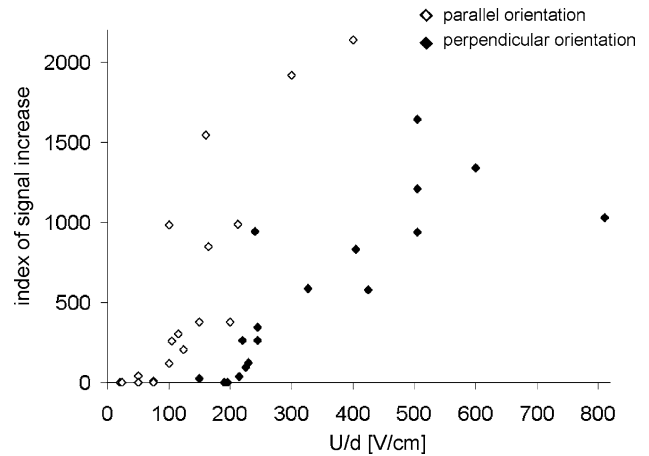
Fig. 5 Index of MRI signal increase within the tibialis cranialis muscle obtained in all examined extremities for parallel and perpendicular electric field

### 3.2 PI fluorescence and numerical modeling

3.2.1 Parallel orientation of the electric field vs. muscle fibers

Experimentally visualized PI fluorescence within the *parallelly* electroporated muscles for the applied $U = 10, 20, 30,$ and 40 V (i.e. $U/d = 50, 100, 150,$ and 200 V/cm) is shown in Fig. 5a). The corresponding electric field distribution calculated at the beginning (step 1 of sequence analysis) and at the end (step 5 of sequence analysis) of each of the voltage pulses of the same amplitude as applied in in vivo experiments is shown in Fig. 6b, c. The reversible electroporation threshold value $E_{rev\parallel} = 80$ V/cm, previously determined experimentally by means of MRI, was included in the numerical muscle model as a parameter of sigmoid $\sigma(E)$ function for all the voltages applied. The electric field is displayed in the range from the reversible threshold value $E_{rev\parallel} = 80$ to 800 V/cm. In order to compare the shapes of experimentally and numerically detected electroporated muscle regions, the numerically obtained contour of local electric field strength, corresponding to the reversible electroporation threshold ($E_{rev\parallel} = 80$ V/cm), calculated at the end of permeabilization (Fig. 6c), was added to the experimentally visualized images (white solid line in Fig. 6a). The dotted white lines in Fig. 6 correspond to the contact line formed between the electrodes and muscle surface.

3.2.2 Perpendicular orientation of the electric field versus muscle fibers

Experimentally visualized PI fluorescence within the perpendicularly electroporated muscles for the applied

Fig. 4 In vivo MRI determined labeled volume within the tibialis cranialis muscle, determined in all examined extremities with parallel and perpendicular electric field (**a**) and the comparison of labeled volume determined in vivo and numerically calculated volume above reversible threshold values for parallel (**b**) and perpendicular electric field orientation (**c**)

extremities for parallel and perpendicular electric field. This index, defined by Eq. 1, is roughly proportional to the quantity of contrast agent inside the treated zone. In contrast to the labeled volumes in Fig. 4, however, the index of signal increase in Fig. 5 does not exhibit the plateau but continues to increase with the applied voltage U, except at the highest value of U ($U/d = 800$ V/cm) where the signal decreases.

Fig. 6 Measured propidium iodide fluorescence of in vivo electroporated tibialis cranialis (a) and local electric field distribution E (displayed in XY plane 0.3 mm below electrodes) for applied U = 10, 20, 30 and 40 V (i.e. U/d = 50, 100, 150, and 200 V/cm) calculated: b at the beginning of the pulse and c at the end of the pulse. The calculated E is displayed in the range from reversible threshold value $E_{rev\parallel}$ = 80 to 800 V/cm. The dotted white line corresponds to the contact line formed between the electrodes and muscle surface. The solid white line in a denotes to the contour of local electric field strength, corresponding to the reversible electroporation threshold ($E_{rev\parallel}$ = 80 V/cm), calculated at the end of permeabilization. The dotted and solid white lines from the numerical models were aligned with the fluorescence images by using graphical software (i.e. CorelDraw)
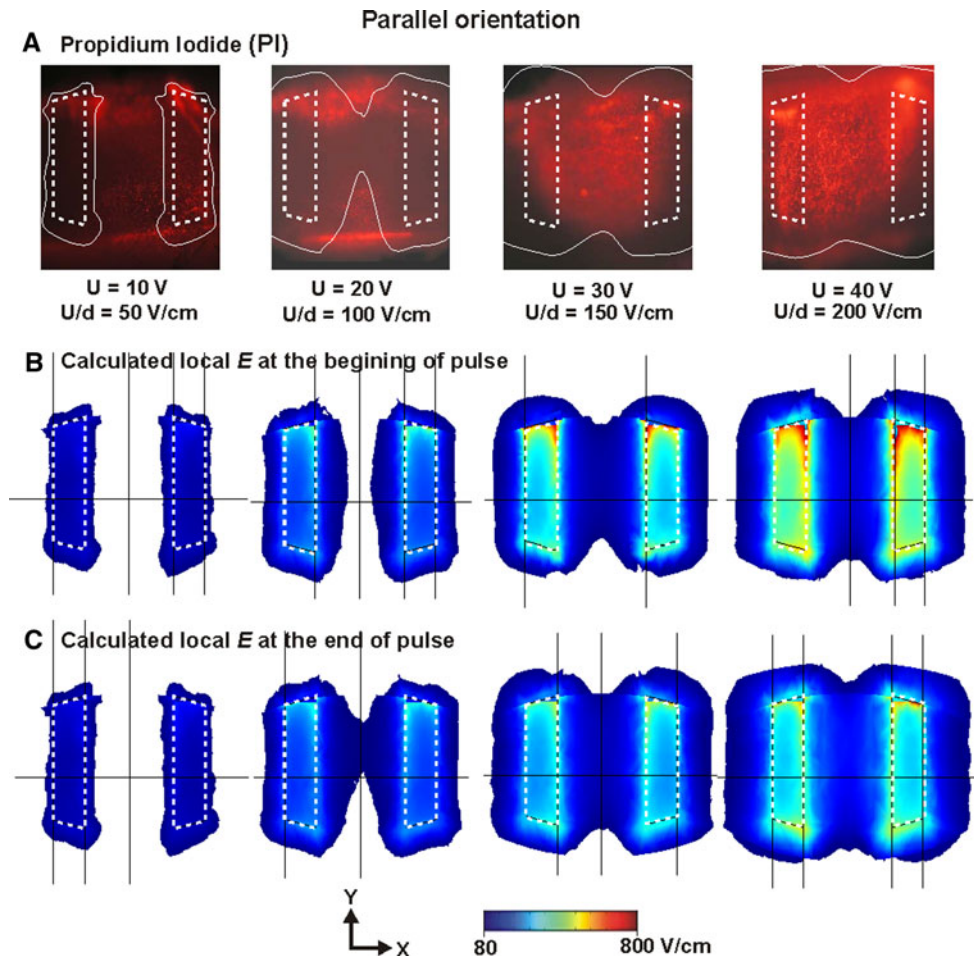
U = 60, 70, 80, and 100 V (i.e. U/d = 300, 350, 400 and 500 V/cm) is shown in Fig. 7a. The corresponding electric field distribution calculated at the beginning and at the end of each of the voltage pulse, U, of the same amplitude as applied in in vivo experiments is shown in Fig. 7b, c. The reversible electroporation threshold value $E_{rev\perp}$ = 200 V/cm, previously determined experimentally by means of MRI, was included in the numerical muscle model as a parameter of sigmoid $\sigma(E)$ function for all the voltages applied. The local electric field is also displayed in the range from the reversible threshold value 80 to 800 V/cm. The contour of electric field strength corresponding to the reversible threshold for perpendicular orientation ($E_{rev\perp}$ = 200 V/cm) is drawn by a solid white line. The same numerically obtained contour at the end of pulse (Fig. 7c) was added to the experimentally visualized images in order to compare the shapes of experimentally and numerically detected electroporated muscle regions (white solid line in Fig. 7a). The dotted white lines in Fig. 7 correspond to the contact line formed between the electrodes and muscle surface.

The obtained PI fluorescence in Figs. 6a and 7a displays the total sum of the signal obtained within the entire muscle observed under the microscope (from the top view). The local electric field is more pronounced (i.e. the fluorescence is more intense) within the muscle region where the electrodes are more pressed against the muscle due to better contact obtained between the electrodes and the muscle surface. The numerically calculated electric field distribution is displayed in Figs. 6 and 7 in the largest XY cross section plane of the muscle volume exposed to the $E > E_{rev}$. The electric field in Figs. 6b and 7b shows the conditions describing the electric properties of muscle at the beginning of the electroporation process (i.e. first step in sequence analysis) when small changes in tissue conductivity due to the muscle electroporation were expected [25, 30].

From the Figs. 6b and 7b it can be seen that at the beginning of the pulse the highest local electric field is distributed around the electrodes. In the course of voltage pulse the muscle region exposed to the highest local E is being electroporated first, thus its conductivity increases according to the $\sigma(E)$ function and subsequently reduces the local E in the muscle around the electrodes. During the same voltage pulse applied, as in a voltage divider, the electric field redistributes towards the tissue region with
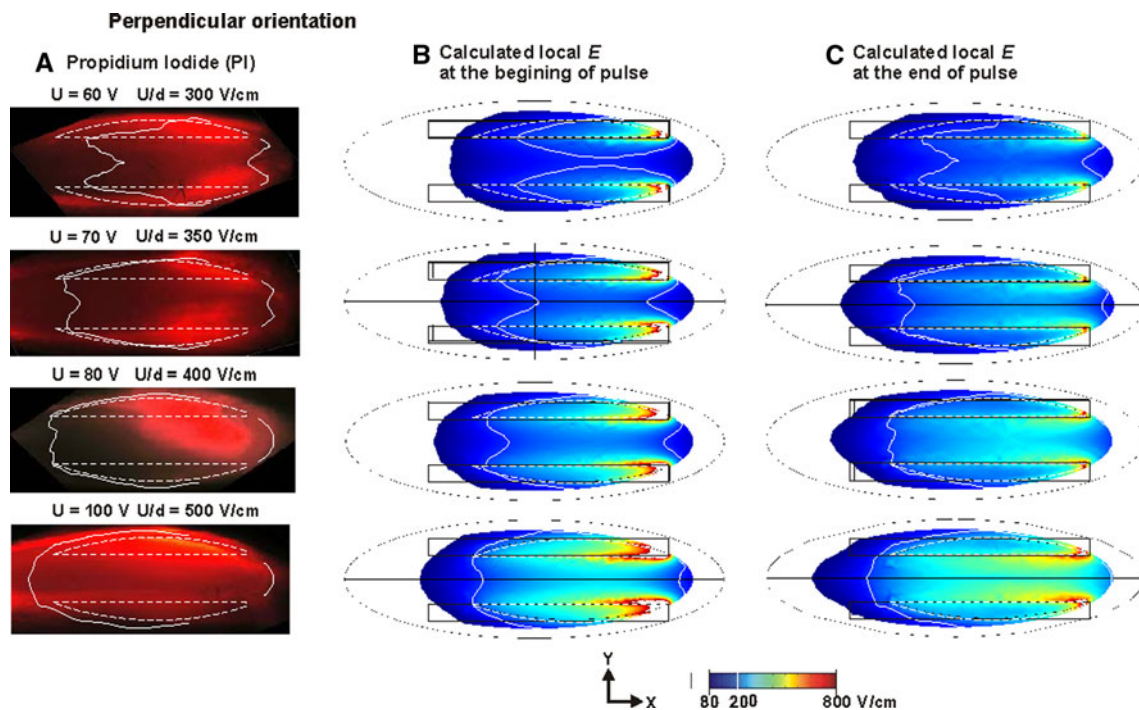
Fig. 7 Measured propidium iodide fluorescence of in vivo electroporated tibialis cranialis (**a**) and local electric field distribution E (displayed in XY plane 0.3 mm below electrodes) for applied $U = 60$, 70, 80, and 100 V (i.e. $U/d = 300$, 350, 400, and 500 V/cm) calculated: **b** at the beginning of the pulse and **c** at the end of pulse. The calculated E is also displayed in the range from 80 to 800 V/cm. The contour of local electric field strength corresponding to the reversible electroporation threshold for perpendicular orientation ($E_{rev\perp} = 200$ V/cm) is drawn by a *solid white line*. The *dotted white line* corresponds to the contact line formed between the electrodes and muscle surface. The dotted and solid white lines from the numerical models were aligned with the fluorescence images by using graphical software (i.e. CorelDraw)

lower conductivity in the middle between electrodes [24]. Accordingly, at the end of the pulse we obtained higher electric field in the middle between electrodes and lower electric field in the muscle around electrodes (Figs. 6c, 7c) compared to the electric field distribution obtained at the beginning of the same pulse applied (Figs. 6b, 7b). From the comparison of in vivo experiments and corresponding electric field distribution calculated at the beginning and at the end of pulse we showed that the visualized PI fluorescence corresponding to the in vivo electroporated muscle (Figs. 6a, 7a) comprises both components: the electroporated region obtained at the beginning (Figs. 6b, 7b) and at the end of pulse (Figs. 6c, 7c).

By comparing experimental and numerical results we thus detected successfully electroporated area of the muscle obtained for each of the applied voltages. In this way we also detected the shape of the local electric field distribution above the electroporation thresholds ($E > 80$ V/cm for parallel and $E > 200$ V/cm for perpendicular orientation) inside the muscle for each of the applied voltages. As expected, muscle electroporation was detected at lower voltages for parallel orientation of electric field versus long axis of the muscle fibers ($U = 10$ V) compared to the perpendicular orientation ($U = 60$ V).

4 Discussion

In our present study, we numerically and experimentally: (1) determined the electroporation thresholds of mouse tibialis cranialis muscle in vivo for parallel and perpendicular orientation of the applied electric field with respect to the muscle fibers (at given pulse parameters, i.e., eight pulses, 100 μs, frequency 1 Hz) and (2) analyzed the difference in successfully electroporated muscle volume and extent using both electric field orientations. Our study was based on the comparison of local electric field calculated with three-dimensional realistic numerical models and in vivo visualization of electroporated target tissue, which for skeletal muscle tissue (mouse tibialis cranialis) has not been performed before.

The numerical calculations were performed using the finite element method, which has proven to be effective in numerical modeling and optimization of electric field distribution in cells and tissues exposed to electric pulses [6, 24]. The in vivo electroporation detection was performed by means of two different in vivo tests: MRI detecting the electrotransfer of a strictly extracellular contrast agent Gd-DOTA [14, 23] and fluorescence visualization of PI binding to DNA or mRNA of the electroporated cells [9, 28].

Both tests allowed for visualization of the level and the extent of muscle electroporation and thus indirect determination of the local electric field distribution in the examined muscles. We used parallel plate electrodes, thus the error of an approximate estimation of local electric field by calculating U/d ratio is small enough since the muscle tissue was electroporated without skin, i.e., only for one type of tissue placed between electrodes [7]. The in vivo results were than compared to the numerical calculations. Good agreement between numerical calculations and experimental observations was obtained (Figs. 4, 6, 7). The agreement between numerically calculated results and experimental observations validated our three-dimensional model. The main purpose of our study was to directly compare the results of numerical calculations to the experimental observations [i.e. muscle volume exposed to the $E > E_{rev}$ in the model to in vivo electroporated muscle volume detected by MRI (Fig. 4) and by PI fluorescence measurements (Figs. 6, 7)]. However, for a detailed statistical analysis more experimental data would be needed.

We demonstrated that the local electric field distribution in muscle tissue strongly depends on the orientation of the electric field with respect to the muscle fibers and thus on electrode placement. A lower magnitude of local electric field was needed to electroporate muscle tissue when the electric field was oriented parallel to the long axis of the muscle fibers compared to the perpendicular orientation, indicating lower electroporation threshold for electric field parallel to the muscle fibers. By direct comparison of calculated electric field distribution with the PI fluorescent regions of the muscle we found that muscle electroporation occurs at lower applied voltage when the electric field is parallel to the muscle fibers for the same distance between electrodes.

The electric field threshold values for the specific pulse parameters $E_{rev\parallel}$ and $E_{rev\perp}$ were determined to be 80 and 200 V/cm for parallel and perpendicular orientation of the applied electric field with respect to the long axis of the muscle fibers, respectively (Fig. 2). As the electroporation thresholds depend on pulse characteristics, for other pulse durations and frequencies it will be necessary to determine corresponding threshold values experimentally and include them in the model. It is to be noted that the labeled volume exhibits a plateau at about 35 mm^3 both with perpendicular electric field (from 250–300 V/cm to 800 V/cm), and with the parallel electric field (from 200 to 400 V/cm) (Fig. 4), while the index of the signal increase in this volume does not show such a plateau (Fig. 5). Actually, the plateau indicates the maximum volume of tissue that can be permeabilized with the electrodes used in our experiments while the integral shows that the level of reversible electroporation of the muscle fibers continues to increase with increasing values of the voltage to electrode distance ratio

[except at the highest value (800 V/cm), where integral decreases, probably due to the fact that irreversible electroporation occurred]. The plateau is obtained at approximately one half of total mouse tibialis cranialis volume (which is approximately 60 mm^3). A larger area of the muscle could be treated with different shape and placement of electrodes.

The behavior at 800 V/cm is coherent with the occurrence of muscle cell damage that causes the leakage of the contrast agent out of the cells and the edema observed on T2 weighted images [14]. Based on this we can conclude that the irreversible threshold value $E_{irrev\perp}$ should be near 800 V/cm for transversal orientation of E with respect to the long axis of the muscle fiber, while $E_{irrev\parallel}$ (for parallel orientation of E) cannot be determined from the data reported in Fig. 4, but is higher than 400 V/cm (i.e. maximum E at which the measurements were done).

The findings of our study on skeletal muscle tissue are in agreement with recently published study on electric field effects on isolated ventricular myocytes by [8], where the myocytes were found to be more sensitive to the electric field when it was applied parallel (versus perpendicular) to the cell major axis. Also, the electroporation threshold values determined in our study are consistent with other studies on muscle tissue electroporation using electric field perpendicular to the long axis of the muscle fibers, either in vivo [7, 23] or in vivo and in silico [25]. The results of our numerical modeling are in agreement also with findings of numerical studies by [32] and [36] demonstrating that the induced transmembrane potential in ellipsoidal cells oriented parallel to the electric field is minimal, while it is maximal for ellipsoidal cells that lie perpendicular to the applied electric field. However, we found the electroporation threshold for perpendicular orientation to be lower compared to the voltage over distance between electrodes ratio in muscle tissue reported by Gehl et al. [11], since in our study the muscle electroporation was experimentally and numerically (in three-dimensional models) examined based on local electric field distribution without presence of the skin. The E_{rev} in our study is also significantly lower compared to the ratio U/d (1,000–1,300 V/cm), which was empirically determined for the electrochemotherapy of cutaneous tumors, due to the fact that the electroporation threshold value depends also on the type of the tissue.

In conclusion, the determined local electric field thresholds of electroporation enable better control of muscle tissue electroporation, and can be used to predict the optimal window for gene electrotransfer, which can facilitate the translation of gene therapy and genetic vaccination into the clinical practice. Results of our study can also be of interest for clinical electrochemotherapy and transdermal drug and gene delivery, since it provides insight into sensitivity of underlying muscle tissue to the

electroporation procedure [15, 37]. The findings of our study can furthermore significantly contribute to the understanding of electroporation process of other tissues that exhibits anisotropic electric properties.

References

1. Aihara H, Miyazaki J (1998) Gene transfer into muscle by electroporation in vivo. Nat Biotechnol 16:867–870
2. Andre F, Gehl J, Sersa G, Preat V, Hojman P, Eriksen J, Golzio M, Cemazar M, Pavselj N, Rols M, Miklavcic D, Neumann E, Teissie J, Mir LM (2008) Efficiency of high- and low-voltage pulse combinations for gene electrotransfer in muscle, liver, tumor, and skin. Hum Gene Ther 19:1261–1271
3. Batiuskaite D, Cukjati D, Mir LM (2003) Comparison of in vivo electropermeabilization of normal and malignant tissue using the ^{51}Cr-EDTA uptake test. Biologija 2:45–47
4. Bettan M, Ivanov M, Mir LM, Boissiere F, Delaere P, Scherman D (2000) Efficient DNA electrotransfer into tumors. Bioelectrochemistry 52:83–90
5. Corovic S, Zupanic A, Miklavcic D (2008) Numerical modeling and optimization of electric field distribution in subcutaneous tumor treated with electrochemotherapy using needle electrodes. IEEE Trans Plasma Sci 36:1665–1672
6. Corovic S, Al Sakere B, Haddad V, Miklavcic D, Mir LM (2008) Importance of contact surface between electrodes and treated tissue in electrochemotherapy. Technol Cancer Res Treat 7:393–399
7. Cukjati D, Batiuskaite D, Andre F, Miklavcic D, Mir LM (2007) Real time electroporation control for accurate and safe in vivo non-viral gene therapy. Bioelectrochemistry 70:501–507
8. de Oliveira P, Bassani R, Bassani J (2008) Lethal effect of electric fields on isolated ventricular myocytes. IEEE Trans Biomed Eng 55:2635–2642
9. Gabriel B, Teissie J (1997) Direct observation in the millisecond time range of fluorescent molecule asymmetrical interaction with the electropermeabilized cell membrane. Biophys J 73:2630–2637
10. Gehl J, Mir LM (1999) Determination of optimal parameters for in vivo gene transfer by electroporation, using a rapid in vivo test for cell permeabilization. Biochem Biophys Res Commun 261:377–380
11. Gehl J, Sorensen T, Nielsen K, Raskmark P, Nielsen S, Skovsgaard T, Mir LM (1999) In vivo electroporation of skeletal muscle: threshold, efficacy and relation to electric field distribution. Biochim Biophys Acta 1428:233–240
12. Guo L, Cranford JP, Neu JC, Neu WK (2009) Activating function of needle electrodes in anisotropic tissue. Med Biol Eng Comput 47:1001–1010
13. Hojman P, Zibert J, Gissel H, Eriksen J, Gehl J (2007) Gene expression profiles in skeletal muscle after gene electrotransfer. BMC Mol Biol 8:56
14. Leroy-Willig A, Bureau M, Scherman D, Carlier P (2005) In vivo NMR imaging evaluation of efficiency and toxicity of gene electrotransfer in rat muscle. Gene Ther 12:1434–1443
15. Mali B, Jarm T, Corovic S, Paulin-Kosir M, Cemazar M, Sersa G, Miklavcic D (2008) The effect of electroporation pulses on functioning of the heart. Med Biol Eng Comput 46:745–757
16. Marty M, Sersa G, Garbay J, Gehl J, Collins C, Snoj M, Billard V, Geertsen P, Larkin J, Miklavcic D, Pavlovic I, Paulin-Kosir S, Cemazar M, Morsli N, Rudolf Z, Robert C, O'Sullivan G, Mir LM (2006) Electrochemotherapy—an easy, highly effective and safe treatment of cutaneous and subcutaneous metastases: Results of ESOPE (European Standard Operating Procedures of Electrochemotherapy) study. Eur J Cancer Suppl 4:3–13
17. Mathiesen I (1999) Electropermeabilization of skeletal muscle enhances gene transfer in vivo. Gene Ther 6:508–514
18. Miklavcic D, Beravs K, Semrov D, Cemazar M, Demsar F, Sersa G (1998) The importance of electric field distribution for effective in vivo electroporation of tissues. Biophys J 74:2152–2158
19. Miklavcic D, Semrov D, Mekid H, Mir LM (2000) A validated model of in vivo electric field distribution in tissues for electrochemotherapy and for DNA electrotransfer for gene therapy. Biochim Biophys Acta 1523:73–83
20. Miklavcic D, Pavselj N, Hart XF (2006) Electric properties of tissues. In: Akay M (ed) Wiley encyclopedia of biomedical engineering. Wiley, New York
21. Mir LM (2001) Therapeutic perspectives of in vivo cell electropermeabilization. Bioelectrochemistry 53:1–10
22. Mir LM, Bureau M, Gehl J, Rangara R, Rouy D, Caillaud J, Delaere P, Branellec D, Schwartz B, Scherman D (1999) High-efficiency gene transfer into skeletal muscle mediated by electric pulses. Proc Natl Acad Sci USA 96:4262–4267
23. Paturneau-Jouas M, Parzy E, Vidal G, Carlier P, Wary C, Vilquin J, de Kerviler E, Schwartz K, Leroy-Willig A (2003) Electrotransfer at MR imaging: tool for optimization of gene transfer protocols—feasibility study in mice. Radiology 228:768–775
24. Pavselj N, Miklavcic D (2008) Numerical modeling in electroporation-based biomedical applications. Radiol Oncol 42:159–168
25. Pavselj N, Bregar Z, Cukjati D, Batiuskaite D, Mir LM, Miklavcic D (2005) The course of tissue permeabilization studied on a mathematical model of a subcutaneous tumor in small animals. IEEE Trans Biomed Eng 52:1373–1381
26. Perez N, Bigey P, Scherman D, Danos O, Piechaczyk M, Pelegrin M (2004) Regulatable systemic production of monoclonal antibodies by in vivo muscle electroporation. Genet Vaccines Ther 2:2
27. Prud'homme G, Glinka Y, Khan A, Draghia-Akli R (2006) Electroporation-enhanced nonviral gene transfer for the prevention or treatment of immunological, endocrine and neoplastic diseases. Curr Gene Ther 6:243–273
28. Rols MP, Teissie J (1990) Electropermeabilisation of mammalian cells. Quantitative analysis of the phenomenon. Biophys J 58:1089–1098
29. Rubinsky J, Onik G, Mikus P, Rubinsky B (2008) Optimal parameters for the destruction of prostate cancer using irreversible electroporation. J Urol 180:2668–2674
30. Sel D, Cukjati D, Batiuskaite D, Slivnik T, Mir LM, Miklavcic D (2005) Sequential finite element model of tissue electropermeabilization. IEEE Trans Biomed Eng 52:816–827
31. Sel D, Macek-Lebar A, Miklavcic D (2007) Feasibility of employing model-based optimization of pulse amplitude and electrode distance for effective tumor electropermeabilization. IEEE Trans Biomed Eng 54:773–781
32. Susil R, Semrov D, Miklavcic D (1998) Electric field-induced transmembrane potential depends on cell density and organization. Electro Magnetobiol 17:391–399
33. Tevz G, Pavlin D, Kamensek U, Kranjc S, Mesojednik S, Coer A, Sersa G, Cemazar M (2008) Gene electrotransfer into murine

skeletal muscle: a systematic analysis of parameters for long-term gene expression. Technol Cancer Res Treat 7:91–101

34. UKCCCR (1998) Guidelines for welfare of animals in experimental neoplasia (Second Edition). Br J Cancer 77:1–10

35. Umeda Y, Marui T, Matsuno Y, Shirahashi K, Iwata H, Takagi H, Matsumoto K, Nakamura T, Kosugi A, Mori Y, Takemura H (2004) Skeletal muscle targeting in vivo electroporation-mediated HGF gene therapy of bleomycin-induced pulmonary fibrosis in mice. Lab Invest 84:836–844

36. Valic B, Golzio M, Pavlin M, Schatz A, Faurie C, Gabriel B, Teissie J, Rols M, Miklavcic D (2003) Effect of electric field induced transmembrane potential on spheroidal cells: theory and experiment. Eur Biophys J 32:519–528

37. Zupanic A, Ribaric S, Miklavcic D (2007) Increasing the repetition frequency of electric pulse delivery reduces unpleasant sensations that occur in electrochemotherapy. Neoplasma 54:246–250

38. Zupanic A, Corovic S, Miklavcic D (2008) Optimization of electrode position and electric pulse amplitude in electrochemotherapy. Radiol Oncol 42:93–101

Paper VII

Optimization of electrode position and electric pulse amplitude in electrochemotherapy

Anže Županič, Selma Čorović and Damijan Miklavčič

University of Ljubljana, Faculty of Electrical Engineering, Ljubljana, Slovenia

Background. *In addition to the chemotherapeutic drug being present within the tumor during electric pulse delivery, successful electrochemotherapy requires the entire tumor volume to be subjected to a sufficiently high electric field, while the electric field in the surrounding healthy tissue is as low as possible to prevent damage. Both can be achieved with appropriate positioning of the electrodes and appropriate amplitude of electric pulses.*

Methods. *We used 3D finite element numerical models and a genetic optimization algorithm to determine the optimum electrode configuration and optimum amplitude of electric pulses for treatment of three subcutaneous tumor models of different shapes and sizes and a realistic brain tumor model acquired from medical images.*

Results. *In all four tumor cases, parallel needle electrode arrays were a better choice than hexagonal needle electrode arrays, since their utilization required less electric current and caused less healthy tissue damage. In addition, regardless of tumor geometry or needle electrode configuration, the optimum depth of electrode insertion was in all cases deeper than the deepest part of the tumor.*

Conclusions. *Our optimization algorithm was able to determine the best electrode configuration in all four presented models and with further improvement it could be a useful tool in clinical electrochemotherapy treatment planning.*

Key words: electrochemotherapy; electroporation; subcutaneous tumor; finite element method; numerical modeling; optimization

Introduction

Electrochemotherapy (ECT) is an effective local tumor therapy performed by the administration of chemotherapeutic drugs followed by the application of local high-voltage electric pulses.[1, 2] The electric

pulses cause transient structural changes (electroporation) of tumor cell membranes and thus increase the entrance of the chemotherapeutic drugs. This potentiates the chemotherapeutic effect and lowers the required drug dose.[3] Numerous studies have demonstrated ECT to be a very efficient treatment in various tumor types; in recent years, it has become a treatment of choice for cutaneous and subcutaneous tumor nodules of different histologies.[4-9]

Two conditions have to be met for ECT to be efficient: 1) a sufficient amount of chemotherapeutic drug has to be present in the
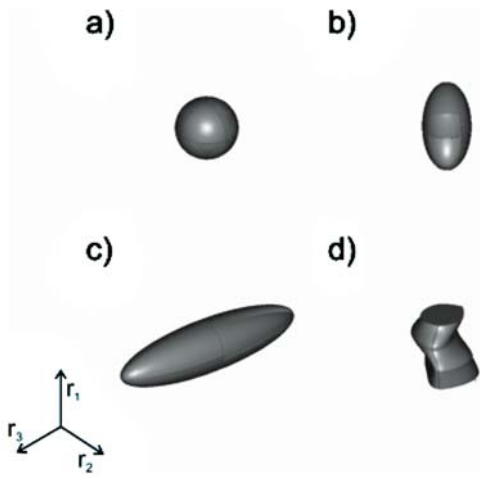
Figure 1. 3D subcutaneous tumor geometries. a) sphere (r_{1-3} = 2 mm); b) ellipsoid positioned deeper in tissue (r_1 = 4 mm, $r_{2,3}$ = 2 mm); c) ellipsoid ($r_{1,2}$ = 2 mm, r_3 = 8 mm); d) realistic tumor geometry from medical images (r_1 = 3.8 mm, r_2 = 2.4 mm, r_3 = 2.6 mm).

Figure 2. Electrode geometries and polarities: a) three needle electrode pairs (3 pairs); b) four needle electrode pairs (4 pairs); c) hexagonal needle electrode array with two electrodes on positive potential, two on negative and two neutral (2x2); d) hexagonal needle electrode array with three electrodes on positive potential and three on negative potential (3x3). Distances between electrodes d_{1-3} were among the optimized parameters in our optimization process. Diameter of all electrodes was 0.7 mm.

target tissue, when the electric pulses are applied; 2) the electric pulses have to reversibly electroporate the entire tumor volume, which means that the electric field established by the pulses should be of a magnitude between the reversible and irreversible electroporation threshold ($E_{rev} < E < E_{irrev}$). The optimal ECT protocol should thus destroy all tumor cells, while minimising electrically induced damage to healthy tissue due to irreversible electroporation. This can be achieved by choosing the most suitable electrode configuration and the lowest amplitude of electric pulses that guarantees whole tumor electroporation.[10,11] Finding the optimum treatment parameters is often difficult, since it requires a complete understanding of the treatment mechanisms. Since the electric field is one of the most important factors in ECT efficiency, modeling the electric field distribution is not only necessary for understanding the treatment, but is also a crucial step towards treatment planning.[12-14] This study presents the first use of an ECT optimization algorithm on several different tumor geometries.

The goal of our study was to optimize the electric field distribution in four different 3D subcutaneous tumor models (Figure 1) by optimizing the electrode configuration around the tumor tissue and the amplitude of the electric pulses for each of the four different electrode geometries that have been used in clinics in recent years (Figure 2).[1,15] Optimization was performed using a combination of finite element numerical modeling and a genetic algorithm. All tumor/electrode cases were optimized for the following parameters: distances between electrodes (Figure 2), depth of electrode insertion and amplitude of electric pulses. Our optimization algorithm successfully found the best parameters in all cases and with some further improvement it could be a useful tool in clinical ECT treatment planning as well as in treatment planning of other electroporation based treatments.[16-18]

Materials and methods

Tissue properties and model geometry

Each model of a subcutaneous tumor consisted of two tissues: the target/tumor tissue and the surrounding healthy tissue. Four different tumor geometries were chosen, a small sphere, an ellipsoid positioned deeper in the tissue, an elongated ellipsoid and a realistic tumor geometry taken from a previous study and scaled for better comparison with the other tumor geometries (Figure 1).[14] All tissues were considered isotropic and homogeneous, the assigned conductivity values being 0.4 S/m for the tumors and 0.2 S/m for the healthy tissue. These values describe the conductivity at the end of the electroporation process.[19] The values were chosen in accordance with previous measurements of tumor and tissue conductivity and models of subcutaneous tumor and skin electroporation.[13,16,20] The electric field distribution was calculated for three different electrode geometries: two different parallel needle electrode arrays (Figure 2a,b) and a hexagonal electrode array with two different electrode polarities (Figure 2c,d). These geometries and polarities were chosen because they are frequently used in ECT research and therapy.

Numerical modeling

Numerical calculations were performed with the commercial finite element software package COMSOL Multiphysics 3.4 (COMSOL AB, Sweden). The electric field distribution in the tissue, caused by the electroporative pulse, was determined by solving the Laplace equation for static electric currents:

$$-\nabla \cdot (\sigma \cdot \nabla \varphi) = 0 \ ,$$

where σ and ϕ are the conductivity of the tissue and electric potential, respectively. The boundary conditions used in our cal-
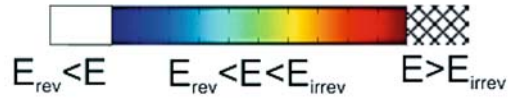
Figure 3. False color legend of Figs. 4, 5 indicating the degree of tissue permeabilization. The white region represents insufficiently permeabilized regions of tissue ($E < E_{rev}$) and the patterned region represents irreversibly permabilized regions of tissue ($E \geq E_{irrev}$).

culations were a constant potential on the surface of the electrodes and electric insulation on all outer boundaries of the model.

The electric field distributions obtained in our models were displayed in the range from the reversible $E_{rev} = 400$ V/cm to the irreversible electroporation threshold value $E_{irrev} = 900$ V/cm (Figure 3). These values were taken from a previously published study, in which we estimated them by comparing *in vivo* measurements and numerical modeling of electroporation of a subcutaneous tumor.[13,21]

Optimization

The genetic algorithm[22] was written in MATLAB 2007a (Mathworks, USA) and was run together with the finite element model using a link between MATLAB and COMSOL. The initial population of possible solutions was generated randomly, taking into account the following model constraints: range of distances between electrodes (d_1: 0.7-4.0 mm; d_2: 3.4-5.0 mm; d_3: 1.3-5.0 mm), range of depths of electrode insertion into tissue (-1.0-5.0 mm below the tumor) and range of amplitudes of electric pulses (1-1200 V). These constraints were chosen so that the calculation domain size, COMSOL meshing capabilities and oncology experts' demands for a safety margin[23] when treating solid tumors, were all respected. Solutions for reproduction were selected proportionally to their fitness, according to the fitness function:

Table 1. Optimized distances between electrodes (d_{1-3}), depth of electrode insertion below the tumor and amplitude of electric pulse (U) are given for all analyzed tumor models and electrode geometries. Qualities of individual optimized solutions are described by the calculated values of total electric current through tissue (I), fraction of reversibly permeabilised target tissue (V_{Trev}/V_T) and normalized volume of damaged healthy tissue (V_{Hirrev}/V_{sph}).

Tumor	Electrode geometry	d_1 [mm]	d_2 [mm]	d_3 [mm]	Insertion depth [mm]	U [V]	I [A]	V_{Trev}/V_T	V_{Hirrev}/V_{sph}
	3 pairs	0.70	3.4		1.1	210	0.45	1	1.00
	4 pairs	0.70	3.4		0.9	210	0.52	1	1.03
	3x3			1.3	0.3	200	0.55	1	3.58
	2x2x2			1.3	0.3	220	0.32	1	1.77
	3 pairs	0.70	3.4		0.9	220	0.65	1	1.59
	4 pairs	0.70	3.6		0.9	220	0.75	1	1.39
	3x3			1.3	0.3	210	0.89	1	6.31
	2x2x2			1.3	0.7	220	0.47	1	2.51
	3 pairs	2.60	3.4		0.9	320	0.88	1	7.40
	4 pairs	1.60	3.4		0.7	320	0.96	1	7.08
	3x3			4.3	0.5	550	1.19	1	15.84
	2x2x2			4.6	0.1	1160	1.25	1	31.22
	3 pairs	0.75	3.4		0.9	270	0.65	1	3.17
	4 pairs	0.70	3.4		0.7	270	0.70	1	3.39
	3x3			1.8	1.1	320	1.07	1	11.44
	2x2x2			1.6	0.9	320	0.55	1	5.45

$$F = 12 + 100 \cdot V_{Trev} - 10 \cdot V_{Hirrev} - V_{Hrev} - V_{Tirrev} ,$$

where F stands for fitness, V_{Trev} and V_{Tirrev} stand for the tumor volume subjected to the local electric field above E_{rev} and above E_{irrev}, and V_{Hrev} and V_{Hirrev} stand for the volume of healthy tissue subjected to the local electric field above E_{rev} and above E_{irrev}, respectively. The weights in the fitness function were set according to the importance of the individual parameters for efficient ECT. Namely, V_{Trev} is crucial for efficient ECT, so its weight is largest (100) in comparison to the weight of V_{Hirrev} (10), which was in turn larger than the weights of V_{Hrev} and V_{Tirrev}, since their significance for successful electrochemotherapy is still debated. Other weight values that kept a

similar ratio gave similar results. The integer 12 is present only to ensure that the fitness function is always positive.

The selected solutions reproduced by cross-over or by mutation. The genetic algorithm was terminated after 100 generations, when the fitness of the highest ranking solution usually reached a plateau. The average computation time of the algorithm was two hours on a standard desktop PC (Windows XP, 3.0 GHz, 1 GB RAM).

Results

The optimized parameters of electrochemotherapy (ECT) for all tumor/electrode cases are given in Table 1. The optimum distance
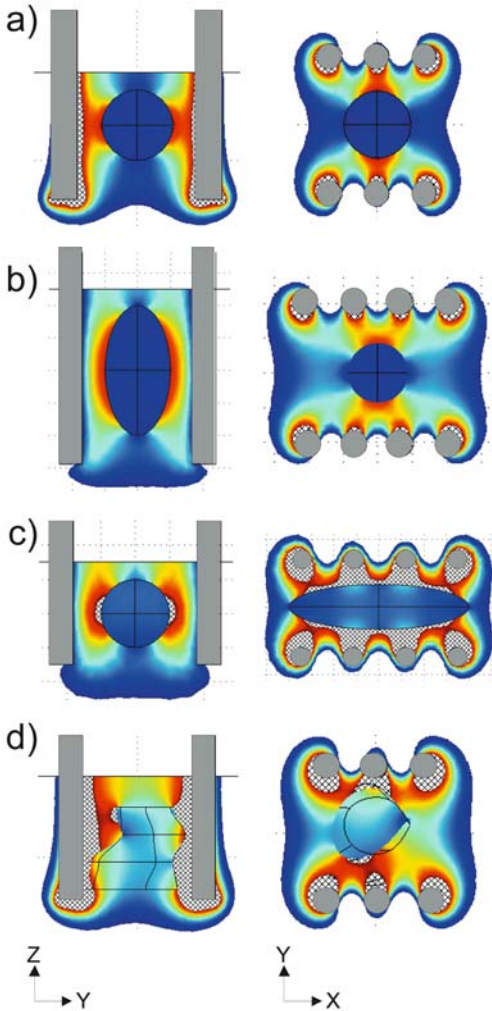
Figure 4. Electric field distribution for the optimized models of subcutaneous tumors is shown. In each case, only the best electrode configuration is given: a) three needle pairs for the spherical tumor; b) four needle pairs for the ellipsoid; c) four needle pairs for the ellipsoid deeper in tissue; d) three needle pairs for the realistic tumor. The electric distribution is shown in two central perpendicular planes: YZ and XY both passing through the center of the tumor. Corresponding values of parameters are given in Table 1.

between electrodes in a parallel row (d_1) was similar for all tumor models, except, due to its size, for the elongated ellipsoid tumor geometry, for which successful electroporation required the electrodes to be

further apart. The electrodes were as close to each other as possible considering the parameter constraints, which guaranteed that the electric field distribution in the target tissue was homogeneous as possible (comparison of Figure 4b and Figure 4c). The optimum distance between electrode rows (d_2) was also similar for all tumor geometries and as small as possible, the reason being that small inter-electrode distances required a lower voltage to ensure electroporation, thus also requiring less electric energy and causing less damage to tissue. The same is true for the distance between electrodes in a hexagonal array (d_3), the reason this time being a combination of both homogeneity of the local electric field and lower required voltage. In contrast, the optimum depth of electrode insertion varied with the tumor and electrode geometry. Nevertheless, the optimum position for the electrodes was in all cases below the tumor. The optimum electric pulse amplitude did not differ much in cases of a spherical tumor and ellipsoid tumor deep in tissue but in other tumor geometries, parallel electrode arrays required considerably lower amplitudes than their hexagonal counterparts.

We compared the quality of the optimized solution in terms of total electric current through the tissue and extent of healthy tissue damage (Table 1 – V_{Hirrev}/V_{sph}). We normalized the volumes of irreversibly electroporated tumor with the volume of a spherical tumor better to compare the amount of tissue damage between individual treatment cases. Parallel electrode arrays gave better results for all four tumor geometries. Three needle pairs always resulted in less total electric current. However, four needle pairs produced a more homogeneous field, which, in combination, caused three needle pairs to be a slightly better choice (less healthy tissue damage) for the spherical and the realistic
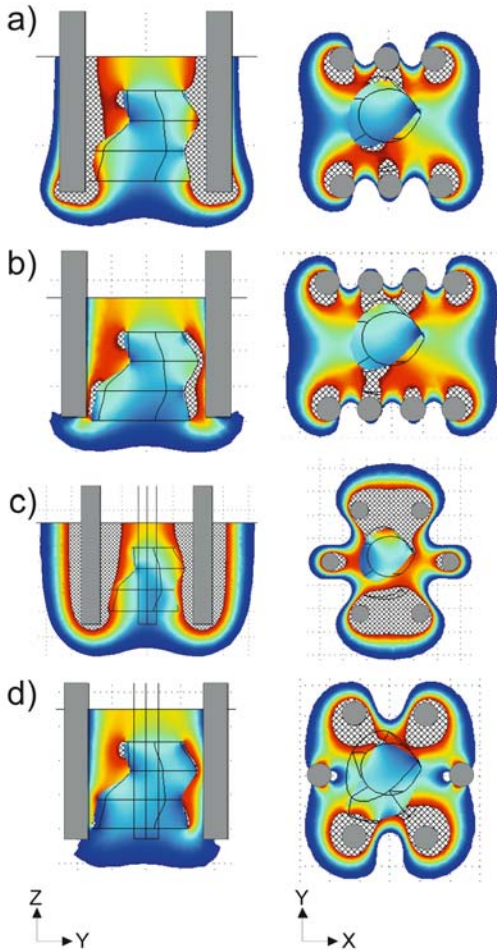
Figure 5. Electric field distribution for the optimized model of the realistic tumor with a) three needle pairs; b) four needle pairs; c) 3x3 hexagonal needle electrode array; d) 2x2x2 hexagonal needle electrode array is shown. The electric distribution is shown in two central perpendicular planes: YZ and XY both passing through the center of the tumor. Corresponding values of parameters are given in Table 1.

tumor geometry and four needle pairs to be slightly better for the other two geometries. The best electrode configurations for all tumor geometries and the corresponding electric field distributions are shown in Figure 4. Hexagonal electrodes caused considerably more healthy tissue damage ($E > E_{irrev}$) than parallel electrodes, which can be seen

in Figure 5 for the realistic tumor geometry. The 3x3 hexagonal electrode array caused more healthy tissue damage than the other three geometries and also required the highest total electric current, mostly because the electric current ran between the closest positive and negative electrodes, instead of through the target tissue (Figure 5).

Discussion

The aim of our study was to optimize the electrode configuration around the target tissue and electric pulse amplitude for ECT of four 3D models of subcutaneous tumors treated with four different needle electrode array geometries. In all 16 cases, the optimization resulted in reversible electroporation of the entire tumor (Table 1: $V_{Trev}/V_T = 1$), which was the parameter with the highest weight in our fitness function. At the same time, the damage to healthy tissue was minimal. When treating a spherical tumor, only a volume of healthy tissue equal to the tumor volume was irreversibly electroporated (Table 1: V_{Hirrev}/V_{sph}). Treatment of larger tumors caused more healthy tissue damage.

The usefulness of numerical modeling in predicting electroporation outcomes has already been demonstrated.[14,15,19,24-26] We examined the adequacy for ECT of needle electrode array geometries by calculating the values of total electric current through the model (must be as low as possible to avoid nerve stimulation[27] and not exceed the capacities of the electric pulse generator[28]) and volumes of reversibly and irreversibly electroporated tumor tissue and healthy tissue. Three-needle electrode pairs were best for the spherical and the realistic tumor geometry; they required the lowest total electric current and caused only a small volume of healthy tissue to be irreversibly electroporated (healthy tissue damage) (Figure 4).

Four-needle electrode pairs caused the least healthy tissue damage in the other tumor geometries, but they required more electric current (Figure 4), confirming previous results of our group - more electrodes mean a more invasive procedure, higher required current and lower required voltage to obtain the same target tissue coverage. Parallel electrode arrays gave much better results than the 2x2 and 3x3 hexagonal needle electrode arrays, mostly because they induced a much more homogeneous field and, consequently, a lower electric current density.

Our work built on a previous study by our group that optimized the distance and voltage between electrodes for a realistic brain tumor (the same tumor geometry that we used in a scaled form in this study).[14] Our present study took optimization one step further by optimizing for four different electrode geometries and for two additional parameters, *i.e.* distance between electrodes in a row and depth of electrode insertion, which lead to perhaps the most important practical result. It is very difficult to guess the best possible insertion depth, since it depends in complex ways on tumor geometry, electrode geometry, electroporation thresholds and the conductivities of tumor and healthy tissue. However, based on our results, electrodes should always be inserted deeper than the deepest part of the tumor (Table 1).

We chose a genetic algorithm as the optimization method, since different linear and non-linear constraints, such as the technical limitations of the high-voltage electric pulse generator (maximum output voltage and current) can be easily taken into account. A genetic algorithm also allows optimization of a large number of continuous, discrete and categorical parameters, *e.g.* type of electrodes and can give as a result many solutions of similar quality, which can nevertheless be topologically very different. This gives the treating physician more alternatives for the positioning of electrodes, which can be very valuable if some of them are not easy to access. The major drawback of a genetic algorithm is the relatively long computation time. However, since it can be considerably shortened by using a more powerful computer or by making the optimization parameters discrete instead of continuous, we do not consider this to be a significant issue and believe that this approach is well suited to the problem being addressed.

Even though our algorithm gives good results, several challenges remain to be addressed before it can be used for treatment planning of ECT. We must determine the most appropriate level of complexity of our numerical models. In this study, we did not take into account changes to tissue conductivity due to electroporation, the possibility of several consecutive pulses being used, of changing the electric field orientation or of moving the electrodes during treatment of a larger tumor; all of which options must be considered in the future.[13,15,25] Another crucial development would be an algorithm that would convert medical images of the treatment area into 3D structures ready to import into numerical modeling software.

In conclusion, we demonstrated that numerical modeling and optimization can be efficiently combined to control the extent of tissue electroporation in ECT and to produce the optimum electrode configuration and amplitude of electric pulses. Our algorithm is a step towards effective treatment planning, not only in clinical ECT, but also in other electroporation based treatments, such as gene electrotransfer, transdermal drug delivery and irreversible tumor ablation.[16-18]

Acknowledgements

References

1. Marty M, Sersa G, Garbay JR, et al. Electrochemotherapy - An easy, highly effective and safe treatment of cutaneous and subcutaneous metastases: Results of ESOPE (European Standard Operating Procedures of Electrochemotherapy) study. *Eur J Cancer Suppl* Nov 2006; **4:** 3-13.

2. Sersa G. The state-of-the-art of electrochemotherapy before the ESOPE study; advantages and clinical uses. *Eur J Cancer Suppl* 2006; **4:** 52-9.

3. Domenge C, Orlowski S, Luboinski B, DeBaere T, Schwaab G, Belehradek J, et al. Antitumor electrochemotherapy - New advances in the clinical protocol. *Cancer* 1996; **77:** 956-63.

4. Heller R, Gilbert R, Jaroszeski MJ. Clinical applications of electrochemotherapy. *Adv Drug Deliv Rev* 1999; **35:** 119-29.

5. Gothelf A, Mir LM, Gehl J. Electrochemotherapy: results of cancer treatment using enhanced delivery of bleomycin by electroporation. *Cancer Treat Rev* 2003; **29:** 371-87.

6. Tijink BM, De Bree R, Van D, Leemans CR. How we do it: Chemo-electroporation in the head and neck for otherwise untreatable patients. *Clin Otolaryngol* 2006; **31:** 447-51.

7. Mir LM, Gehl J, Sersa G, et al. Standard operating procedures of the electrochemotherapy: Instructions for the use of bleomycin or cisplatin administered either systemically or locally and electric pulses delivered by the Cliniporator (TM) by means of invasive or non-invasive electrodes. *Eur J Cancer Suppl* 2006; **4:** 14-25.

8. Snoj M, Rudolf Z, Cemazar M, Jancar B, Sersa G. Successful sphincter-saving treatment of anorectal malignant melanoma with electrochemotherapy, local excision and adjuvant brachytherapy. *AntiCancer Drugs* 2005; **16:** 345-8.

9. Sersa G, Cemazar M, Miklavcic D, Rudolf Z. Electrochemotherapy of tumours. *Radiol Oncol* 2006; **40:** 163-74.

10. Miklavcic D, Beravs K, Semrov D, Cemazar M, Demsar F, Sersa G. The importance of electric field distribution for effective in vivo electroporation of tissues. *Biophys J* 1998; **74:** 2152-8.

11. Miklavcic D, Semrov D, Mekid H, Mir LM. A validated model of in vivo electric field distribution in tissues for electrochemotherapy and for DNA electrotransfer for gene therapy. *Biochim Biophys Acta* 2000; **1523:** 73-83.

12. Miklavcic D, Corovic S, Pucihar G, Pavselj N. Importance of tumour coverage by sufficiently high local electric field for effective electrochemotherapy. *Eur J Cancer Suppl* 2006; **4:** 45-51.

13. Pavselj N, Bregar Z, Cukjati D, Batiuskaite D, Mir LM, Miklavcic D. The course of tissue permeabilization studied on a mathematical model of a subcutaneous tumor in small animals. *IEEE Trans Biomed Eng* 2005; **52:** 1373-81.

14. Sel D, Lebar AM, Miklavcic D. Feasibility of employing model-based optimization of pulse amplitude and electrode distance for effective tumor electropermeabilization. *IEEE Trans Biomed Eng* 2007; **54:** 773-81.

15. Gilbert RA, Jaroszeski MJ, Heller R. Novel electrode designs for electrochemotherapy. *Biochim Biophys Acta* 1997; **1334:** 9-14.

16. Cukiati D, Batiuskaite D, Andre F, Miklavcic D, Mir LM. Real time electroporation control for accurate and safe in vivo non-viral gene therapy. *Bioelectrochemistry* 2007; **70:** 501-7.

17. Pliquett UF, Vanbever R, Preat V, Weaver JC. Local transport regions (LTRs) in human stratum corneum due to long and short 'high voltage' pulses. *Bioelectrochem Bioener* 1998; **47:** 151-61.

18. Al Sakere B, Bernat C, Connault E, Opolon O, Rubinsky B, Davalos R, et al. Tumour ablation with irreversible electroporation. *PLoS ONE* 2007:11.

19. Corovic S, Pavlin M, Miklavcic D. Analytical and numerical quantification and comparison of the local electric field in the tissue for different electrode configurations. *Biomed Eng Online* 2007; **6.**

20. Miklavcic D, Pavselj N, Hart FX. Electric properties of tissues. *Wiley Encyclopedia of Biomedical Engineering.* New York: John Wiley & Sons; 2006.

21. Semrov D, Miklavcic D. Calculation of the electrical parameters in electrochemotherapy of solid tumours in mice. *Comput Biol Med* 1998; **28:** 439-48.

22. Holland JH. *Adaptation in Natural and Artificial Systems: An Introductory Analysis with Applications to Biology, Control, and Artificial Intelligence.* Cambridge: MIT Press; 1992.

23. Gehl J, Geertsen PF. Palliation of haemorrhaging and ulcerated cutaneous tumours using electrochemotherapy. *Eur J Cancer Suppl* 2006; **4:** 35-7.

24. Gehl J, Sorensen TH, Nielsen K, Raskmark P, Nielsen SL, Skovsgaard T, et al. In vivo electroporation of skeletal muscle: threshold, efficacy and relation to electric field distribution. *Biochim Biophys Acta* 1999; **1428:** 233-40.

25. Sersa G, Cemazar M, Semrov D, Miklavcic D. Changing electrode orientation improves the efficacy of electrochemotherapy of solid tumors in mice. *Bioelectrochem Bioener* 1996; **39:** 61-6.

26. Sel D, Mazeres S, Teissie J, Miklavcic D. Finite-element modeling of needle electrodes in tissue from the perspective of frequent model computation. *IEEE Trans Biomed Eng* 2003; **50:** 1221-32.

27. Zupanic A, Ribaric S, Miklavcic D. Increasing the repetition frequency of electric pulse delivery reduces unpleasant sensations that occur in electrochemotherapy. *Neoplasma* 2007; **54:** 246-50.

28. Puc M, Corovic S, Flisar K, Petkovsek M, Nastran J, Miklavcic D. Techniques of signal generation required for electropermeabilization. Survey of electropermeabilization devices. *Bioelectrochemistry* 2004; **64:** 113-24.

Paper VIII

Electrode commutation sequence for honeycomb arrangement of electrodes in electrochemotherapy and corresponding electric field distribution

Matej Reberšek [a], Selma Čorović [a], Gregor Serša [b], Damijan Miklavčič [a,*]

[a] University of Ljubljana, Faculty of Electrical Engineering, Tržaška 25, SI-1000 Ljubljana, Slovenia
[b] Institute of Oncology, Department of Experimental Oncology, Zaloška 2, SI-1000 Ljubljana, Slovenia

ARTICLE INFO

ABSTRACT

Electrochemotherapy is a treatment based on combination of chemotherapeutic drug and electroporation. It is used in clinics for treatment of solid tumours. For electrochemotherapy of larger tumours multiple needle electrodes were already suggested. We developed and tested electrode commutation circuit, which controls up to 19 electrodes independently. Each electrode can be in one of three possible states: on positive or negative potential or in the state of high impedance. In addition, we tested a pulse sequence using seven electrodes for which we also calculated electric field distribution in tumour tissue by means of finite-elements method. Electrochemotherapy, performed by multiple needle electrodes and tested pulse sequence on large subcutaneous murine tumour model resulted in tumour growth delay and 57% complete responses, thus demonstrating that the tested electrode commutation sequence is efficient.

© 2008 Elsevier B.V. All rights reserved.

1. Introduction

Electroporation is a phenomenon that occurs in cell membranes when cells are exposed to sufficiently high electric field [1–4]. Molecules, such as some drugs or nucleic acids, which otherwise are unable to cross cell membrane may then enter cells. This phenomenon is used in combination with some chemotherapeutic drugs e.g. bleomycin and cisplatin for tumour treatment, which is known as electrochemotherapy [5–7]. It is used in clinics for transfer of chemotherapeutic drugs in tumour cells by means of short high voltage electric pulses applied to the tumour [8,9].

Generators of electrical pulses for electroporation are named electroporators. For small tumours electric pulses are delivered to the tissue usually via two metal (plate) electrodes [10,11]. Electrochemotherapy of small tumours is already well investigated and good results are obtained with a single pair of electrodes. To achieve good electrochemotherapy the entire volume of the tumour needs to be effectively permeabilized [12]. On larger tumours pair of electrodes should be repositioned or higher voltage should be used [13]. However, repositioning of electrodes is not practical since positions and amplitudes should be pre-calculated to achieve effective permeabilization over the whole tumour. Moreover, electroporators certified for clinical use do not generate electric pulses with amplitudes over a few kV [14]. Therefore, multiple needle electrodes were

suggested for effective tissue permeabilization in electrochemotherapy, i.e. to cover the whole tumour with sufficiently high electric field. Such electrodes allow for treatment of larger tumours and at the same time using lower pulse voltages [15,16].

Electronic circuits which commutate electric pulses between the electrodes are named electrode commutation circuits. Honeycomb and square arrangements of electrodes were mainly suggested proposed as multiple needle arrangements, which theoretically enable the use of infinite arrays of needle electrodes with finite electrode commutation circuit [17]. Therefore the design of electrode commutation circuit does not depend on the number of electrodes but only on the maximum voltage applied and current to be delivered through the electrodes.

The aim of our study was to develop electrode commutation circuit and test its efficiency *in vivo* by performing electrochemotherapy with multiple needle electrodes on larger tumours, which with a single pair of electrodes cannot be achieved. For this we developed an electrode commutation circuit, which commutates the usual electroporation single output signal from an electroporator to multiple electrodes. We used seven-needle electrodes, for which we suggested and tested an effective electrode commutation sequence for tissue electroporation. We also calculated the corresponding electric field distribution in tumour tissue by means of finite elements method (FEM) in 3D model taking into account the increase of tissue conductivity due to electroporation in order to demonstrate also theoretically that the entire tumour volume is exposed to sufficiently high electric field leading to tissue permeabilization and efficient electrochemotherapy.

---

* Corresponding author. Tel.: +386 1 4768 456; fax: +386 1 4264 658.
 E-mail address: damijan.miklavcic@fe.uni-lj.si (D. Miklavčič).

2. Materials and methods

2.1. Electroporator (EP-GMS 7.1) with embedded electrode commutation circuit

Both electroporator (EP-GMS 7.1) and embedded electrode commutation circuit for multiple electrodes were developed at the University of Ljubljana, Faculty of Electrical Engineering. The EP-GMS 7.1 electroporator was already used in previously reported studies [18–20]. The main advantage of this electroporator is the ability to automatically commutate electrical pulses between electrodes with embedded electrode commutation circuit.

The user defines electrical parameters of applied electric pulse through the interface of the electroporator (EP-GMS 7.1) on a personal computer (PC). These parameters are then transferred to the executive part of the electroporator. After this transfer the electroporator is ready to generate defined electric pulses in defined sequence.

Electroporator (EP-GMS 7.1) generates square electric pulses from 80 to 530 V, duration from 10 to 1000 μs, repetition frequency from 0.1 to 5000 Hz and from 1 to 32 pulses. Particularity of this electroporator is an embedded electrode commutation circuit which consists of controlling part and executive part (Fig. 1).

The commutation control (Fig. 1) is compatible with external bus interface of microprocessor MCF5204 (FreeScale, USA) or with any other similar 16-bit bus interfaces. Computer board based on microprocessor MCF5204 is a part of EP-GMS 7.1 and it can be controlled by personal computer (PC) via serial port (RS-232). The commutation control works like parallel input–output unit (PIO), which can control up to 38 relays in the executive part of the electrode commutation circuit which corresponds to 19 electrodes. The commutation control registers the time of last command and thus estimates the position of relays. This is necessary due to relatively long switching time of relays. Commutation control functions are designed on Field Programmable Gate Array (FPGA, XCS30-VQ100, Xilinx, USA).

Each executive module (Fig. 1) consists of fourteen relays TRK1703 (Iskra, Slovenia), which with their positions define states of seven electrodes. The first half of relays defines the polarity of electrodes, while the second part defines the impedance state of the electrodes. Each of the electrodes can thus be in one of three possible states: positive, negative or in high impedance. Positive state means that electrode is connected to positive potential of electroporator, negative state means that electrode is connected to negative potential of electroporator and high impedance state means that electrode is disconnected from electroporator. This concept and design of commutating the electroporation signal allows no possibility to short-circuit electroporator.

Maximal voltage of electroporation signal which can be connected to the executive module is 1 kV. Maximal continuous current is 3 A per executive module and 2 A per electrode. Maximal pulse current of maximum duration 10 ms and more than nine times longer pause is 30 A per executive module and 10 A per electrode. Electric (galvanic) separation between the commutation control and electroporation signal is more than 4 kV.

Because of the presence of high voltage and high electric current in the executive module the distance between the contacts and the weight of the anchor in relays is very large. Therefore the switching time of such a relay is relatively long. With proper selection of relays and especially with adequate driving circuit we achieved switching time of 6 ms (Fig. 2). The relay is driven by high voltage Darlington transistors and paralleled by a zener diode. This allowed for optimization of the relay turning off time. The fastest would be without the diode but sooner or later this would result in the transistors break down. Due to ageing and variations in elements, the time reserved for switching was extended to 12 ms. Embedded electrode commutation circuit can therefore automatically commutate electrical pulses between electrodes with frequencies up to 83 Hz.

2.2. Electric field in tumour tissue during the electroporation process

A three-dimensional finite-elements model of tumour tissue (cylinder; diameter: 15 mm, length: 6 mm; Fig. 3) with inserted seven-needle electrodes (honeycomb arrangement; diameter of needles: 0.5 mm, distance between two neighbouring needles: 5.5 mm) was built according to specifications of *in vivo* electrochemotherapy experiment using software package EMAS (ANSOFT Corporation, USA). Applied voltage (±265 V) was modelled as Dirichlet's boundary condition on the surface which presents the cross-section of electrode and

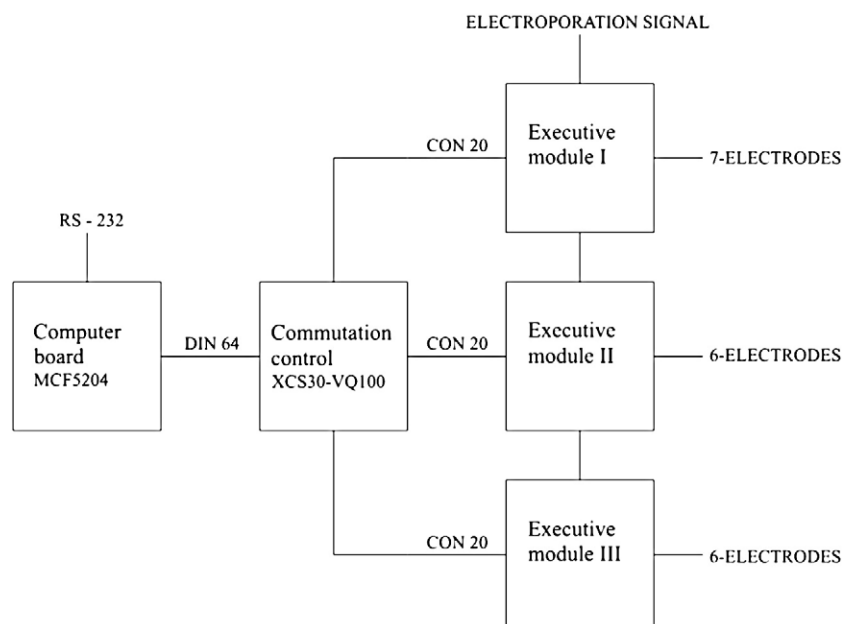**Fig. 1.** Block scheme of electrode commutation circuit, which commutates electroporation single output signal from an electroporator to up to 19 independent electrodes. Electrode commutation circuit consists of controlling part (Commutation control XCS30-VQ100) and executive part (three Executive modules) and it can be controlled by personal computer (PC) over serial port (RS-232) on computer board MCF5204.
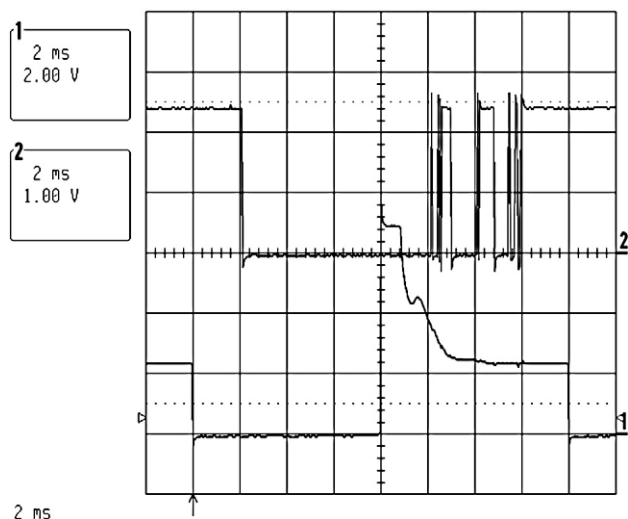
Fig. 2. Switching time of relay Iskra TRK1703. Signal 1 represents negative driving voltage for relay and signal 2 represents the commutation of relay. Signal 2 shows us that coil releases or pulls the anchor in 2 ms and that the anchor then bounces on the contact for 4 ms. Therefore the whole switching time is about 6 ms.

tumour tissue. Dirichlet's boundary condition was also set on the surface of disconnected (high impedance) electrodes to satisfy the conditions, that electrodes are a lot more conductive then tumour tissue. Electropotential of disconnected electrodes was defined as zero, because our model is symmetrical and disconnected electrodes were always in the middle between the connected electrodes. Tumour tissue was mathematically separated from surrounding area by Neuman's boundary condition:

$$J_N = 0, \tag{1}$$

where J_N is the normal electric current density [A/m^2]. The distribution of the electric field intensity in tumour tissue for given electrode geometry was calculated numerically by means of finite-elements method [21]. Tumour tissue was modelled as a quasi-stationary passive and isotropic volume conductor in the quasi-stationary electric current field. A condition in such structure is described by Laplace's equation:

$$\Delta \phi = 0, \tag{2}$$

where ϕ is the electric field potential [V].

Due to a functional dependency of tumour tissue conductivity on electric field intensity, a sequence analysis application for modelling of electrical properties changes during electroporation process was used. In each static model of the sequence analysis tissue conductivity was determined based on electric field distribution in previous model of the sequence analysis:

$$\sigma(k) = f(E(k-1)), \tag{3}$$

where σ is the tissue conductivity [S/m], E is the electric field intensity [V/m], k is the sequential number of static model in the sequence analysis and f functional dependency of tumour tissue conductivity on electric field intensity, which was obtained from previously reported studies [22,23].

In *in vivo* electrochemotherapy experiment we used an electrode commutation sequence as presented on Fig. 4. In the commutation sequence used first (Fig. 4b) all outer electrodes were activated and neighbouring needles were of the opposite polarity (±265 V), while the middle electrode was in high impedance state (0 V in the finite-elements model). After the commutation the second part (Fig. 4c) was delivered in which all outer electrodes were positive (+265 V) and the inner electrode was negative (−265 V).
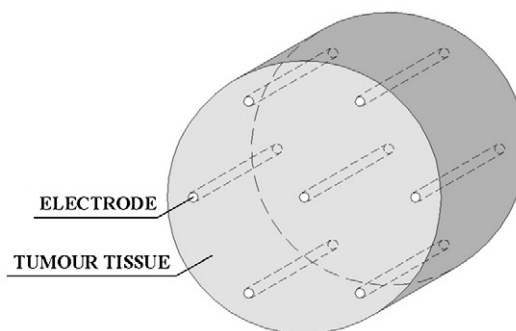

Fig. 3. A geometry of 3D-model of multiple needle electrodes inserted into the tumour tissue. Tumour tissue is in the shape of a cylinder with a diameter of 15 mm and length of 6 mm. Inserted seven-needle electrodes are in honeycomb arrangement with a diameter of 0.5 mm and the distance between two neighbouring needles is 5.5 mm.

The course of electrical conductivity changes inside the model of the tumour tissue due to electroporation is presented in Fig. 5b, with corresponding distribution of electric field intensity presented in Fig. 5a. The electric field intensity and the specific conductivity are given in *XY* cross-section (*Z*=2 mm plane) of the three-dimensional finite-elements model. First part of electric field intensity and electrical conductivity is presented on Fig. 5a1-3 and b1-3, while second part of electrode commutation sequence is presented on Fig. 5a4 and b4.

2.3. Electrochemotherapy

In vivo electrochemotherapy experiment was performed at the Department of Experimental Oncology, Institute of Oncology, Ljubljana, Slovenia in accordance with ethical provisions for research on animals.

In experiment subcutaneous SA-1 fibrosarcoma syngeneic to A/J mice was initiated by injection of 5×10^5 cells into the left flank of the animal. SA-1 cell suspension was cultivated in Eagle Minimal Essential Media with 10% of Foetal Calf Serum (MEM, FCS; Sigma, ZDA). Ten days after subcutaneous injection of cells, the tumours were large enough (volume ≈ 300 mm^3, diameter ≈ 12 mm) for electroporation with multiple needle electrodes.

During the electrochemotherapy animals were anaesthetized with ketamin and rompun (2 μl of ketamin + 8 μl of 0.9% physiological solution and 0.5 μl of rompun + 9.5 μl of 0.9% physiological solution per gram of mouse). Animals were divided into four experimental groups: control, chemotherapy (CT), electric pulses (EP) and electrochemotherapy (ECT). In each experimental group 7 mice were treated independently. In all experimental groups multiple needle electrodes were inserted into the tumour. Animals in CT and ECT experimental
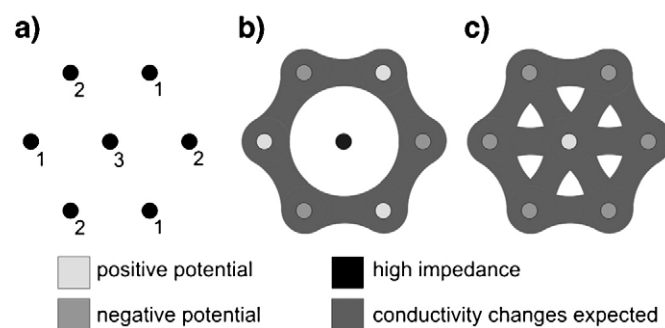

Fig. 4. Electrode commutation sequence of two parts for honeycomb arrangement of electrodes. Position of the electrodes and its numeration (a). States of the electrodes in the first part of electrode commutation sequence (b). States of the electrodes in the second part of electrode commutation sequence (c).
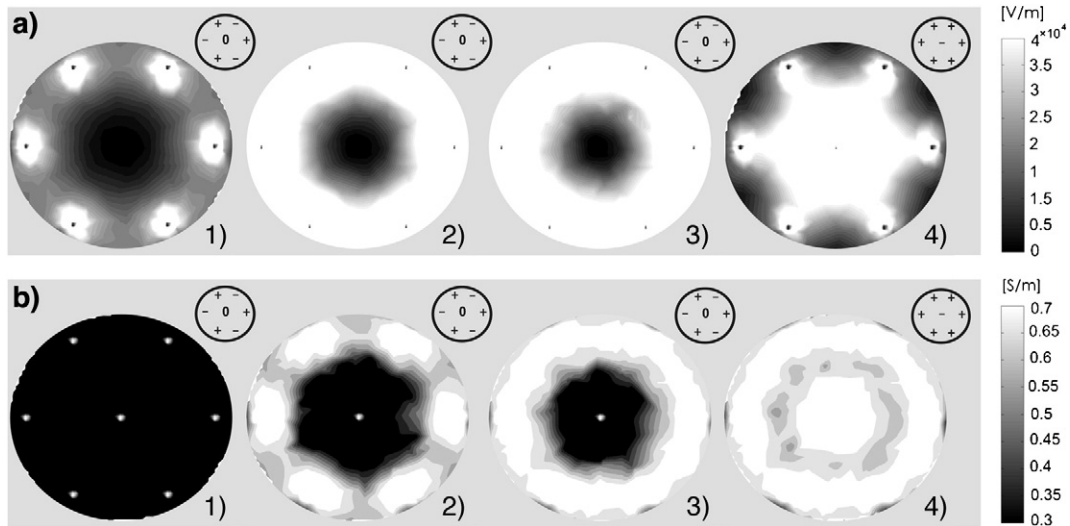
Fig. 5. Electric field intensity [V/m] (a) and electrical conductivity [S/m] (b): the sequence analysis was not applied (1), the first static model in the first part (2), the final static model in the first part (3) and the final static model in the second part of the electrode commutation sequence (4).

groups were injected intravenously with 100 μg of bleomycin. Tumours in experimental groups EP and ECT were exposed to electric pulses (2 intervals × 8 square pulses, duration 100 μs, amplitude 530 V and pulse repetition frequency of 100 Hz). Pulses in the ECT group were delivered 3–4 min after the bleomycin injection.

Each day after the treatment on day 0 cranial/caudal, dorsal/ventral and medial/lateral diameters of the tumours were measured. Volumes of tumours were then modelled and calculated as spheroids. Results are given in form of scatter graphs (SigmaPlot 9.0, Systat, USA), where each point represents the mean volume of tumours in each experimental group and the error bars indicate the standard error of the mean (Fig. 6).

3. Results

Electric field intensity (Fig. 5a) in tumour tissue and consecutive tumour tissue conductivity changes (Fig. 5b) were calculated for suggested electrode commutation sequence (Fig. 4) by means of finite-elements method. In Fig. 5a1 and b1 sequence analysis was not yet applied. Fig. 5a2 and b2 represents first static model of sequence

analysis. And Fig. 5a3,4 and b3,4 represents final static model of sequence analysis. In the first part of electrode commutation sequence (all outer electrodes are activated and neighbouring needles are of the opposite polarity, while the middle electrode is in high impedance state; Fig. 4b) when sequence analysis was not yet applied electric field intensity was strong only around outer electrodes (Fig. 5a1). When sequence analysis was applied electric field intensity (Fig. 5a2) and tumour tissue conductivity (Fig. 5b2) quickly iterated to its final value, which was obtained with insignificant numerical error in only four steps (Fig. 5a3 and b3). Strong electric field intensity around outer electrodes distributed around all outer part of tumour tissue (Fig. 5a3). We can see that after the first part of electrode commutation sequence all outer part of tumour tissue changed its conductivity which can also be considered as it was electroporated while the tumour tissue around the middle electrode remained unchanged i.e. not porated (Fig. 5b3). In the second part of electrode commutation sequence (all outer electrodes are positive and the inner electrode is negative; Fig. 4c) electric field intensity was particularly strong around inner electrode (Fig. 5a4) also because outer tumour tissue was already electroporated.

After completed electrode commutation sequence tumour tissue was thus well electroporated (Fig. 5b4), which was demonstrated also by electrochemotherapy effectiveness (Fig. 6). The suggested electrode

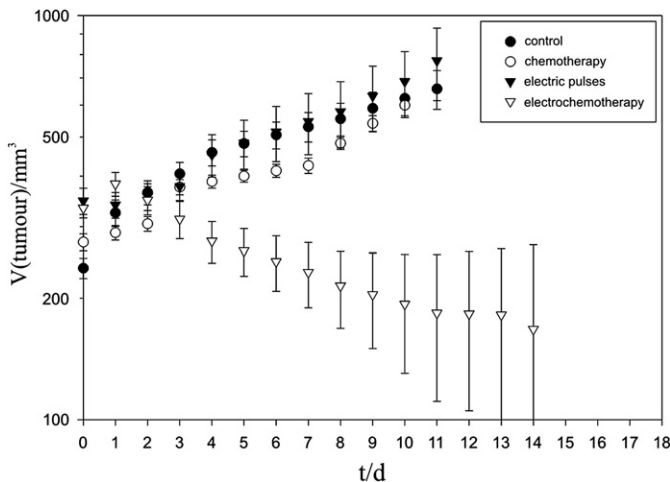**Fig. 6.** Tumour growth after electrochemotherapy (ECT) on day 0 and three standard control groups for ECT: control, chemotherapy (CT) and electric pulses (EP). Each symbol represents an average tumour volume and standard error in specific experimental group.
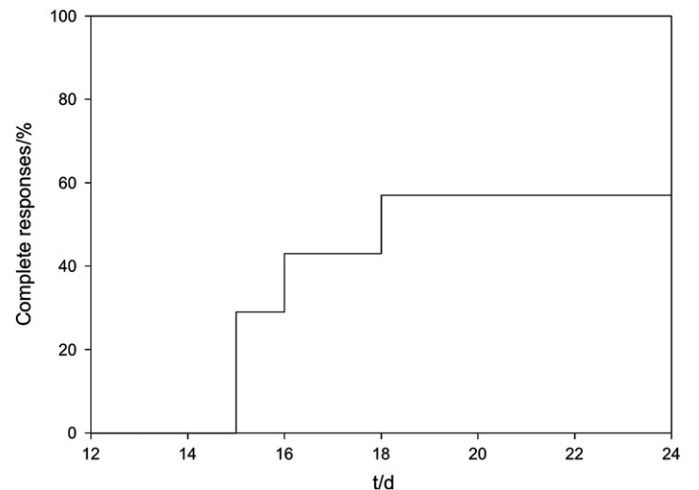

Fig. 7. Complete responses of tumour treatment on A/J mice after electrochemotherapy (ECT) on day 0. Tumours were observed for 3 months after day 0.

commutation sequence for honeycomb arrangement of seven-needle electrodes was evaluated in *in vivo* electrochemotherapy (ECT) experiment on larger tumours. Three standard experimental groups for evaluating ECT were used: control, chemotherapy (CT) and electric pulses (EP). Tumours in these experimental groups were not retarded in growth and animals were sacrificed after 10 days due to large tumours. In ECT group where tumours were subjected to the electrochemotherapy on day 0, tumours were however significantly reduced in volume and delayed in growth. In addition, 57% (4/7) complete responses were obtained (Fig. 7).

4. Discussion and conclusion

The aim of our study was to develop and test an effective *in vivo* electrochemotherapy on larger tumours by means of multiple needle electrodes. We thus developed and tested an electrode commutation circuit, which commutates the usual single output electroporation signal between the seven-needle electrodes used in our study. We suggested and tested experimentally by performing electroche- motherapy an effective electrode commutation sequence for tissue electroporation. Results of electrochemotherapy show a significant reduction in tumour volume, delay in growth and 57% complete responses (Fig. 6 and 7). We also calculated corresponding electric field distribution in tumour tissue taking into account an increase of tissue conductivity due to electroporation. Results of calculations show that large volume of tumour tissue is successfully electroporated by using suggested electrode commutation sequence (Fig. 5b4).

Electroporation is a dynamic process, meaning that tissue proper- ties are changing during the constant voltage pulse from 0.3 to 0.7 S/m [22,23]. Electric field intensity below the reversible threshold value does not permeabilize the cell membranes and therefore no changes in conductivity are expected. When the electric field intensity exceeds reversible threshold cell membrane is permeabilized and tissue conductivity increases. The membrane permeabilization is reversible for electric field intensities below irreversible threshold.

The main purpose of the modelling was to foresee electroporated tissue in treated tumours. We thus had to take into account the influence of electric field intensity on tumour tissue conductivity and that changes in tumour tissue conductivity retroact on electric field distribution. Therefore sequence analysis was used to take into account such retroactivity. Results obtained with this application describe a sequence of static models, where each of them describes the process at one discrete interval. Each discrete interval relates to a real yet undetermined time interval. If we compare first (Fig. 5b2) and the last (Fig. 5b3) result of sequence analysis iteration we can see such retroactivity in results of tumour tissue conductivity. These results demonstrate that larger volume of electroporated tumour tissue is expected if sequence analysis is applied. Such expectations are in agreement with electrochemotherapy results (Figs. 6 and 7).

In *in vivo* electrochemotherapy experiment multiple needle electro- des in honeycomb arrangement were used, because such arrangement of electrodes is preferable in electrochemotherapy as better coverage of tumour tissue with electric field distribution can be achieved with single amplitude of electric pulses. For such electrodes an effective and short pulse electrode commutation sequence for electroporation is required. In our study we used a combination of two parts, which are presented on Fig. 4. Such sequence of voltage pulses application is quick, because it is delivered in only two parts and therefore suitable for clinical use where patients are subjected to muscle contraction and painful sensations. It is also effective as the conductivity changes expected due to tissue permeabilization are favouring electric field distribution through all the area between the electrodes.

Embedded electrode commutator, which was developed and used in our study, has been proven to be effective and was therefore built in the Cliniporator device [24]. Moreover, such electrode commutator is relatively easy to construct due to simple design and can be used for any other single output electroporator. On the basis of our experi- mental and numerical results we can conclude that suggested elec- trode commutation sequence for honeycomb arrangement of electrodes can be efficiently used in electrochemotherapy. Given out- put amplitude allows for treatment of larger tumours using multiple needle electrodes without repositioning of electrodes.

Acknowledgments

Appendix A. Supplementary data

Supplementary data associated with this article can be found, in the online version, at doi:10.1016/j.bioelechem.2008.03.001.

References

[1] E. Neumann, M. Schaefer-Ridder, Y. Wang, P.H. Hofschneider, Gene transfer into mouse lynoma cells by electroporation in high electric fields, EMBO J. 7 (1982) 841–845.
[2] E. Neumann, S. Kakorin, K. Toensing, Fundamentals of electroporative delivery of drugs and genes, Bioelectrochem. Bioenerg. 48 (1999) 3–16.
[3] L.M. Mir, Therapeutic perspectives of *in vivo* cell electropermeabilization, Bioelectrochemistry 53 (2001) 1–10.
[4] J. Teissie, M. Golzio, M.P. Rols, Mechanisms of cell membrane electropermeabiliza- tion: a minireview of our present (lack of?) knowledge, BBA — General Subjects Special Issue: Biophysics Complex Systems, vol. 1724, 2005, pp. 270–280.
[5] L.M. Mir, S. Orlowski, Mechanisms of electrochemotherapy, Adv. Drug Deliv. Rev. 35 (1999) 107–118.
[6] J. Gehl, Electroporation: theory and methods, perspectives for drug delivery, gene therapy and research, Acta Physiol. Scand. 177 (2003) 437–447.
[7] G. Sersa, The state-of-the-art of electrochemotherapy before the ESOPE study; advantages and clinical uses, Eur. J. Cancer Suppl. 4 (2006) 52–59.
[8] R. Heller, R. Gilbert, M.J. Jaroszeski, Clinical applications of electrochemotherapy, Adv. Drug Deliv. Rev. 35 (1999) 119–129.
[9] L.M. Mir, J. Gehl, G. Sersa, C.G. Collins, J.R. Garbay, V. Billard, P.F. Geertsen, Z. Rudolf, G.C. O'Sullivan, M. Marty, Standard operating procedures of the electrochemother- apy: Instructions for the use of bleomycin or cisplatin administered either systemically or locally and electric pulses delivered by the Cliniporator™ by means of invasive or non-invasive electrodes, Eur. J. Cancer Suppl. 4 (2006) 14–25.
[10] L.M. Mir, L.F. Glass, G. Sersa, J. Teissie, C. Domenge, D. Miklavcic, M.J. Jaroszeski, S. Orlowski, D.S. Reintgen, Z. Rudolf, M. Belehradek, R. Gilbert, M.P. Rols, J. Jr Belehradek, J.M. Bachaud, R. DeConti, B. Stabuc, M. Cemazar, P. Coninx, R. Heller, Effective treatment of cutaneous and subcutaneous malignant tumours by electrochemotherapy, Br. J. Cancer 77 (1998) 2336–2342.
[11] J. Gehl, L.M. Mir, Determination of optimal parameters for *in vivo* gene transfer by electroporation, using a rapid *in vivo* test for cell permeabilization, Biochem. Biophys. Res. Commun. 261 (1999) 337–380.
[12] D. Miklavcic, S. Corovic, G. Pucihar, N. Pavselj, Importance of tumour coverage by sufficiently high local electric field for effective electrochemotherapy, Eur. J. Cancer Suppl. 4 (2006) 45–51.
[13] M. Cemazar, D. Miklavcic, L. Vodovnik, T. Jarm, Z. Rudolf, R. Stabuc, T. Cufer, G. Sersa, Improved therapeutic effect of electrochemotherapy with cisplatin by intratumoral drug administration and changing of electrode orientation for electropermeabili- zation on EAT tumor model in mice, Radiol. Oncol. 29 (1995) 121–127.
[14] M. Puc, S. Corovic, K. Flisar, M. Petkovsek, J. Nastran, D. Miklavcic, Techniques of signal generation required for electropermeabilization. Survey of electropermea- bilization devices, Bioelectrochemistry 64 (2004) 113–124.
[15] R.A. Gilbert, M.J. Jaroszeski, R. Heller, Novel electrode designs for electroche- motherapy, Biochim. Biophys. Acta 1334 (1997) 9–14.
[16] L.H. Ramirez, S. Orlowski, D. An, G. Bindoula, R. Dzodic, P. Ardouin, C. Bognel, J. Belehradek, J.N. Munck, L.M. Mir, Electrochemotherapy on liver tumours in rabbits, Br. J. Cancer 77 (1998) 2104–2111.
[17] G.A. Hoffman, Methods in molecular medicine, Ch. Instrumentation and electrodes for *in vivo* electroporation, Humana Press, New York, 2000, pp. 37–61.
[18] T. Kotnik, G. Pucihar, M. Rebersek, L.M. Mir, D. Miklavcic, Role of pulse shape in cell membrane electropermeabilization, Biochim. Biophys. Acta 1614 (2003) 193–200.
[19] M. Pavlin, M. Kanduser, M. Rebersek, G. Pucihar, F.X. Hart, R. Magjarevic, D. Miklavcic, Effect of cell electroporation on the conductivity of a cell suspension, Biophys. J. 88 (2005) 4378–4390.
[20] M. Rebersek, C. Faurie, M. Kanduser, S. Corovic, J. Teissie, M.P. Rols, D. Miklavcic, Electroporator with automatic change of electric field direction improves gene electrotransfer in vitro, Biomed. Eng. Online 6 (2007) 1–11.

[21] D. Semrov, D. Miklavcic, Numerical modeling for *in vivo* electroporation, Meth. Mol. Med. 37 (2000) 63–81.

[22] D. Sel, D. Cukjati, D. Batiuskaite, T. Slivnik, L.M. Mir, D. Miklavcic, Sequential finite element model of tissue electropermeabilization, IEEE Trans. Biomed. Eng. 52 (2005) 816–827.

[23] N. Pavselj, Z. Bregar, D. Cukjati, D. Batiuskaite, L.M. Mir, D. Miklavcic, The course of tissue permeabilization studied on a mathematical model of a subcutaneous tumor in small animals, IEEE Trans. Biomed. Eng. 52 (2005) 1373–1381.

[24] M. Marty, G. Sersa, J.R. Garbay, J. Gehl, C.G. Collins, M. Snoj, V. Billard, P.F. Geertsen, J.O. Larkin, D. Miklavcic, I. Pavlovic, S.M. Paulin-Kosir, M. Cemazar, N. Morsli, D.M. Soden, Z. Rudolf, C. Robert, G.C. O'Sullivand, L.M. Mir, Electrochemotherapy — an easy, highly effective and safe treatment of cutaneous and subcutaneous metastases: results of ESOPE (European Standard Operating Procedures of Electrochemotherapy) study, Eur. J. Cancer Suppl 4 (2006) 3–13.

Paper IX

Nataša Pavšelj[1], David Cukjati[2], Selma Čorović[3], Tomaž Jarm[4], Gregor Serša[5], Damijan Miklavčič[6]

Spremljanje, modeliranje in analiza dogajanja med elektroporacijo celičnih membran *in vivo* ter njena uporaba

Assessment, Modeling and Analysis of Cell Membrane Electroporation In Vivo and Its Applications

IZVLEČEK

KLJUČNE BESEDE: celična membrana, elektroporacija, gensko zdravljenje, zdravilo sistemi sproščanja

Membrana biološke celice v splošnem ni prepustna za večje molekule. Dovolj visoko električno polje pa povzroči elektroporacijo celične membrane in začasno poveča njeno prepustnost, tako da molekule, kot so zdravilne učinkovine večjih molekulskih mas ali DNA, lahko vstopijo v celično notranjost. Najbolj razširjene biomedicinske uporabe elektroporacije so elektrokemoterapija, vnos genov v celice in vnos zdravilnih učinkovin v telo skozi kožo. Pri vseh teh metodah je zelo pomembno, da dosežemo učinkovito elektroporacijo in obenem ne poškodujemo tkiva s previsokim električnim poljem. Uspešnost elektroporacije lahko zaznamo šele po koncu dovajanja pulzov (pri nekaterih metodah *in vitro* lahko že po nekaj minutah, *in vivo* pa ponavadi po 24 ali več urah), z merjenjem spremembe prevodnosti permeabiliziranega tkiva pa bi bilo mogoče potek elektroporacije spremljati že med dovajanjem pulzov. Poleg tega pa opis elektroporacije v celicah in tkivih s pomočjo analitičnih in numeričnih metod predstavlja pomembno orodje za analizo in razlago kompleksnih dogajanj, načrtovanje poskusov *in vivo*, oblik in postavitev elektrod ter novih protokolov. Pri tem moramo biti pozorni na lastnosti tkiv, ki jih opisujemo z modeli, spremembe njihove prevodnosti med elektroporacijo in na nekatere pozitivne ali negativne sekundarne in stranske učinke. V članku predstavljamo najpomembnejše vidike eksperimentalne elektroporacije *in vivo* in načine, ki so nam na voljo za spremljanje in analizo dogajanja, naš cilj pa je kasnejša uporaba metode v klinične namene.

ABSTRACT

KEY WORDS: cell membrane, electroporation, gene therapy, drug delivery systems

Cell membrane is, in general, impermeable to larger molecules. However, the application of electric pulses to cells, either in suspension or as tissue, causes the electroporation of the cell

[1] Dr. Nataša Pavšelj, univ. dipl. el., Laboratorij za biokibernetiko, Fakulteta za elektrotehniko, Univerza v Ljubljani, Tržaška 25, 1000 Ljubljana.

[2] Doc. dr. David Cukjati, univ. dipl. el., Laboratorij za biokibernetiko, Fakulteta za elektrotehniko, Univerza v Ljubljani, Tržaška 25, 1000 Ljubljana.

[3] Mag. Selma Čorović, univ. dipl. el., Laboratorij za biokibernetiko, Fakulteta za elektrotehniko, Univerza v Ljubljani, Tržaška 25, 1000 Ljubljana.

[4] Doc. dr. Tomaž Jarm, univ. dipl. el., Laboratorij za biokibernetiko, Fakulteta za elektrotehniko, Univerza v Ljubljani, Tržaška 25, 1000 Ljubljana.

[5] Prof. dr. Gregor Serša, univ. dipl. biol., Onkološki inštitut Ljubljana**,** Zaloška cesta 2, 1000 Ljubljana.

[6] Prof. dr. Damijan Miklavčič, univ. dipl. el., Laboratorij za biokibernetiko, Fakulteta za elektrotehniko, Univerza v Ljubljani, Tržaška 25, 1000 Ljubljana.

membrane, increasing its permeability and making it possible for larger molecules which otherwise cannot cross the membrane, such as drug molecules or the DNA, to enter cells. The most widely used electroporation-based biomedical applications are electrochemotherapy, gene electrotransfer and transdermal drug delivery. A high level of cell membrane electroporation is the objective of all applications. However, caution should be exercised in order not to damage the tissue with excessively strong electric fields. The outcome of electroporation-based treatments can be assessed by various methods a certain time after treatment. The course of tissue permeabilization can be evaluated by measuring tissue conductivity changes during pulse delivery. Furthermore, cell and tissue electroporation can be described by means of analytical methods or numerical modeling which offers useful insight into the understanding of the underlying biological processes and can help us plan future experiments and develop new electrodes and protocols.

UVOD

Membrana biološke celice v splošnem ni prepustna za večje molekule. Že kratkotrajni visokonapetostni električni pulz pa lahko prepustnost celične membrane poveča. S tem omogočimo molekulam, kot so nekatere zdravilne učinkovine večjih molekulskih mas in molekule DNA, za katere je sicer celična membrana neprepustna ali slabo prepustna, neposreden vstop v celično notranjost. Metodo imenujemo elektroporacija celične membrane in je običajno reverzibilna, ob dovolj visokem električnem polju in njegovem dovolj dolgem trajanju pa je lahko tudi ireverzibilna, kar povzroči celično smrt. Z elektroporacijo lahko v celice vnašamo DNA, citotoksična zdravila, olajšamo vstop specifičnim zaviralcem znotrajcelične encimske aktivnosti ali pa v celično membrano vstavljamo beljakovine. Prav tako lahko preučujemo nekatera dogajanja, kot sta aktivnost encimov *in vivo* ali celična signalizacija preko nadzora koncentracije ionov v citosolu. Nadalje lahko s pomočjo elektroporacije celice tudi zlivamo med seboj *(1)*. Najpomembnejše in najpogosteje uporabljane biomedicinske elektroporacijske aplikacije so elektrokemoterapija, vnos genov v celice in vnos zdravilnih učinkovin v telo skozi kožo *(2–5)*. Obstajajo različne razlage za povečanje prepustnosti celične membrane, ena od njih temelji na nastanku tako imenovanih por, od tod tudi izraz elektroporacija, ki se med raziskovalci na tem področju najpogosteje uporablja. Posledica dovajanja dovolj visokih električnih pulzov pa je prav gotovo povečanje prepustnosti celične membrane, zato se namesto besede elektroporacija pogosto uporablja izraz elektropermeabilizacija. Slednjega bomo v nadaljevanju uporabljali predvsem takrat, ko bomo želeli izpostaviti povečano prepustnost – (elektro)permeabilnost – membran celic.

Elektropermeabilizacija celic je odvisna od različnih dejavnikov: prevodnosti medija, parametrov električnih pulzov ter od velikosti, oblike, orientacije in gostote celic. Parametri električnih pulzov ter oblika in postavitev elektrod so edini dejavniki elektroporacije celic v pogojih *in vivo*, na katere lahko vplivamo. Prav zato so bile objavljene številne raziskave, katerih cilj je bil razviti najbolj uspešne elektroporacijske protokole za različne vrste celic, tkiv in aplikacij. Poskusi so pokazali, da tako število pulzov kot tudi njihova amplituda in trajanje vplivajo na uspešnost elektroporacije. Nekateri predlagani protokoli zato združujejo električne pulze različnih amplitud in trajanj *(6)*.

V klinični praksi je zelo pomembno, da se doseže učinkovita elektroporacija ob čim manjši poškodbi tkiva. Celična membrana se permeabilizira pri pragovni vrednosti transmembranske napetosti, le-ta pa nastopi pri pragovni vrednosti jakosti zunanjega električnega polja. Pri tem moramo paziti, da celic zaradi previsokega električnega polja ne poškodujemo. Zato želimo, da je njegova jakost med reverzibilnim in ireverzibilnim pragom permeabilizacije. To je še posebej pomembno za gensko transfekcijo *in vivo*, kjer želimo doseči visoko stopnjo prepustnosti celičnih membran in obenem preživetje premeabiliziranih celic. Žal učinke elektroporacije zaznamo

šele po določenem času, zaželeno pa bi bilo spremljanje poteka elektroporacije in s tem napovedovanje njenih učinkov med samim dovajanjem električnih pulzov. Možna načina sta meritev spremembe prevodnosti tkiva ali pa električna impedančna tomografija. Na tem področju so bile narejene študije, ki kažejo na morebitno uporabnost impedančne tomografije za spremljanje elektroporacije v realnem času, vseeno pa bo do njene uporabe v klinični praksi potrebno še nekaj dela *(7–8)*.

Potek elektropermeabilizacije tkiva in vpliv spremembe parametrov na porazdelitev električnega polja v tkivu in tokove skozenj med elektroporacijo in po njej lahko preučujemo tudi z numeričnimi modeli. Teoretična razlaga dogajanja nam namreč nudi pomemben vpogled v proces elektropermeabilizacije celic, tkiv in organov, pri čemer si lahko pomagamo z analitičnimi izračuni in numeričnim modeliranjem. Predvsem slednje se je izkazalo za nepogrešljivo pri izračunih porazdelitve električne poljske jakosti v tkivih in organih, kjer so obravnavane geometrije preveč zapletene za uporabo analitičnih metod.

Poznavanje mehanizmov elektroporacije celic v tkivih v pogojih *in vivo* razširja osnovno znanje o delovanju električnih polj na celice v pogojih *in vitro*. Teorijo elektroporacije celične membrane in opis poskusov *in vitro* smo v Medicinskih razgledih že opisovali *(9)*. Poskusi *in vitro* nam ne morejo podati optimalnih parametrov za uspešno elektroporacijo *in vivo*, saj je gostota celic in s tem njihova medsebojna interakcija mnogo večja v tkivu *(10–12)*. Prav tako v tkivu niso vse celice enakega tipa. Takšno nehomogeno sestavo tkiva je mnogo teže raziskati kot posamezne celice ali celice v suspenziji. Različne celice ne bodo elektroporirane pri istih vrednostih električnega polja, ki ga moramo prilagoditi na ciljno skupino celic. Za izboljšanje razumevanja elektroporacije v pogojih *in vivo* delamo poskuse na malih laboratorijskih živalih in tudi na večjih živalih.

Pri poskusih potrebujemo opremo za dovajanje elektroporacijskih pulzov. Oprema obsega generator visokonapetostnih pulzov in elektrode, preko katerih električne pulze dovedemo tkivu. Elektrode izberemo glede na ciljno tkivo in njegovo lokacijo in so lahko

invazivne (igelne) ali neinvazivne (ploščate) *(13)*. Naš cilj je, da je električno polje, ki se ustvari med elektrodama, višje od potrebnega za permeabilizacijo, da pokrije celotno prostornino ciljnega tkiva in je hkrati čimbolj homogeno *(14)*. Obenem pa bi radi v okoliškem tkivu dosegli čim nižjo vrednost električnega polja.

UPORABA ELEKTROPORACIJE *IN VIVO*

Elektrokemoterapija

Problem uničevanja tumorskih celic s kemoterapevtiki je velikokrat njihova nespecifična citotoksičnost, ki škoduje tudi zdravim celicam, ter rezistenca tumorskih celic zaradi genetskih sprememb. Za uspešno zdravljenje je potrebna dovolj velika koncentracija kemoterapevtika, ki običajno vpliva tudi na normalne celice in povzroča neželene stranske učinke. Poseben problem predstavljajo kemoterapevtiki, ki težko prehajajo celično membrano – v takih primerih so pri zdravljenju potrebni še večji odmerki zdravil. Elektrokemoterapija je metoda hkratne uporabe kemoterapevtikov in elektroporacije ciljnega tkiva. S to metodo se učinkovitost kemoterapevtikov, ki zaradi slabe prepustnosti celične membrane težko vstopajo v notranjost tumorskih celic (cisplatin, bleomicin), močno poveča. Obenem pa se zmanjšajo stranski učinki, ker za učinkovito zdravljenje zadoščajo nizki odmerki kemoterapevtikov. Prvi poskusi na področju elektrokemoterapije segajo v leti 1987 in 1988 *(15–17)*. Številne raziskave kažejo na večstokratno povečanje učinkovitosti kemoterapevtika bleomicin ter do 70-kratno povečanje učinkovitosti kemoterapevtika cisplatin *in vitro*, kadar ju uporabimo v kombinaciji z elektroporacijo ciljnega tkiva *(18–19)*. Elektrokemoterapijo vedno bolj uspešno uporabljajo tudi v klinični praksi za zdravljenje kožnih zasevkov tumorjev različnih histologij (slika 1). Glavnina z elektrokemoterapijo zdravljenih tumorjev so bili kožni zasevki malignega melanoma, kožnega bazalno celičnega karcinoma, zasevki adenokarcinomov vratu in glave, tumorjev dojke, pa tudi zasevki bolj redkih tumorjev, kot sta Kaposijev sarkom in hipernefrom *(2, 3, 13, 19–22)*. Trenutno se elektrokemoterapija

179
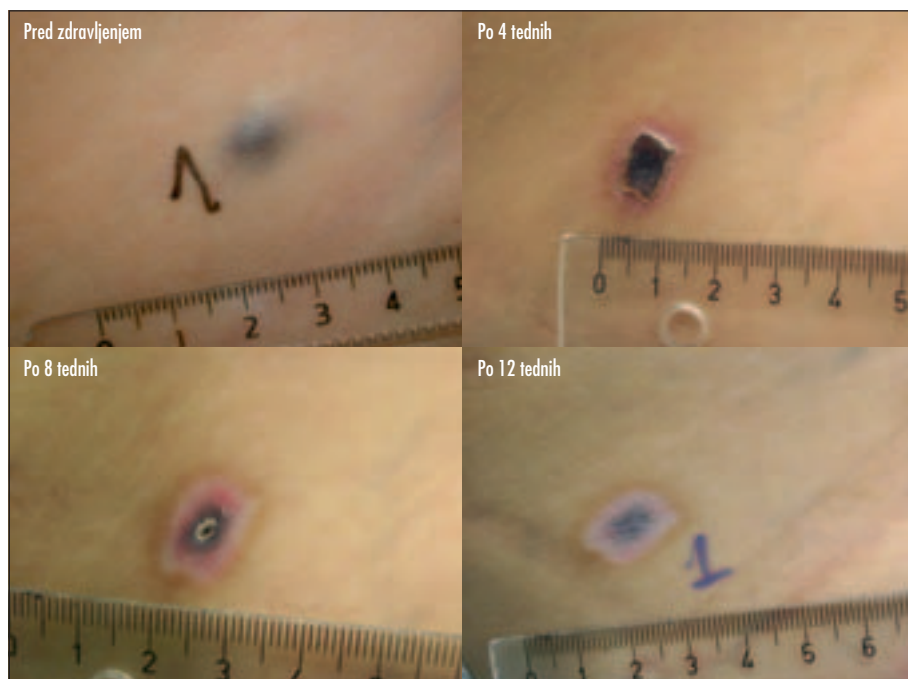
Slika 1. *Protitumorski učinek elektrokemoterapije na kožnem zasevku malignega melanoma. Elektrokemoterapija je bila izvedena ob intratumorskem injiciranju cisplatina. Po 12 tednih je viden popoln regres zdravljenega tumorskega nodula z rahlo pigmentacijo in dobrim kozmetičnim učinkom zdravljenega predela.*

uporablja za paliativne namene in v primerih, ko pride do ponovitve ali zasevanja predhodno zdravljenih tumorjev (kirurško, z obsevalno terapijo) in ti standardni pristopi niso več možni. Razvoj elektrokemoterapije gre v zdravljenje tumorjev tudi v notranjih organih, kar bo vsekakor povečalo nabor indikacij za elektrokemoterapijo.

Vnos genov v celice z elektroporacijo

Napredek na področju razkrivanja človeškega genoma je povzročil pravo evforijo v farmacevtskih in medicinskih znanstvenih krogih. Z vnašanjem genov namreč lahko zdravimo nekatere dedne in celo nalezljive bolezni. Pri genski terapiji gre za umestitev nove, delujoče kopije okvarjenega gena v genom. V splošnem tu ne moremo govoriti o zamenjavi gena, ki povzroča bolezen, z »zdravim« genom, temveč le dodamo delujočo kopijo, da bi nadomestila funkcijo okvarjenega gena. Za vnos nove kopije gena pa potrebujemo nek nosilec, tako

imenovani vektor, s katerim terapevtski gen vnesemo v pacientove ciljne celice. Poleg načrtovanja ustrezne učinkovite molekule nukleinskih kislin pa je še vedno problematičen prav uspešen vnos genov v ciljne celice in tkiva. Virusni vektorji, čeprav uspešni pri vnosu svojega genskega zapisa s terapevtskimi geni v ciljne celice, prinašajo mnogo vprašanj glede z virusi povezanega tveganja za zdravje ljudi *(23)*. Veliko raziskav je zato v zadnjem času posvečeno razvoju nevirusnih metod vnosa terapevtskih genov v ciljna tkiva in organe *(24–25)*. Ena od metod je tudi uporaba električnih pulzov za povečanje prepustnosti membrane, imenovana vnos genov z elektroporacijo *(5)*. Uspešen vnos dosežemo z različnimi protokoli, le-ti pa lahko vključujejo vlak enakih pulzov ali pa kombinacije pulzov različnih trajanj in amplitud. Poskusi kažejo tudi na dvojnost delovanja električnih pulzov za vnos genskega materiala v celice: z visokonapetostnimi pulzi povečamo prepustnost celične membrane (elektropermeabilizacija), s pomočjo daljšega nizkonapetostnega pulza

pa električno negativne molekule DNA potisnemo v bližino permeabilizirane membrane in v notranjost celice (elektroforeza) *(26–27)*. Pri vnosu genov v celice z elektroporacijo moramo biti še posebej pazljivi, da s previsokim električnim poljem ne ogrozimo celičnega preživetja. To pri elektrokemoterapiji predstavlja nekoliko manjši problem, saj je uničenje tumorskih celic pravzaprav naš cilj, paziti pa moramo seveda, da s previsokim električnim poljem ne poškodujemo okoliškega, zdravega tkiva.

Vnos zdravilnih učinkovin v telo preko kože

Zdravilne učinkovine lahko vnašamo v telo skozi kožo. Zaradi majhne prepustnosti kože si lahko pri tem pomagamo z različnimi metodami, kot so ultrazvok, iontoforeza (potisk električno nabitih molekul zdravilne učinkovine s pomočjo šibkega električnega toka iste polaritete) ali elektroporacija *(28–31)*. Takšen vnos zdravilnih učinkovin ima določene prednosti, saj je manj invaziven kot intravenski vnos, izognemo pa se tudi škodljivemu vplivu prebavnih encimov in nizkih pH vrednosti na učinkovine, kar je lahko problem, kadar dajemo zdravilo peroralno. Nadalje lahko s transdermalnimi terapevtskimi sistemi dosežemo postopen, konstanten vnos zdravilne učinkovine v telo namesto hitrega dajanja z intravensko injekcijo. Vendar pa je zaradi zaščitne funkcije kože in njene zelo nizke prepustnosti vnos molekul v kožo težaven. Elektroporacija je ena od metod, s katero začasno povečamo prepustnost kože brez škodljivih posledic, električni tok pa lahko dodatno pospeši prenos ionov in električno nabitih molekul v kožo *(30, 32–33)*.

Odstranjevanje tkiva

Pri odstranjevanju benignih ali malignih tumorjev je zelo pomembno, da to storimo na nadzorovan način, ob čim manjšem poškodovanju zdravega okoliškega tkiva. Z leti se je razvilo kar nekaj minimalno invazivnih metod, ki so alternativa invazivnim operacijam. Neželeno tkivo lahko odstranimo z vrsto načinov, kot so na primer radiofrekvenčna ablacija, kriokirurgija, ultrazvočna koagulacija, v zadnjem času pa raziskujejo tudi možnost

uporabe ireverzibilne elektroporacije. Pri ostalih zgoraj naštetih uporabah elektroporacije *in vivo*, npr. pri elektrokemoterapiji in elektrogenski terapiji, je naš cilj doseči električno polje, ki omogoča permeabilizacijo celic in obenem omogoča njihovo preživetje, pri ablaciji tkiva pa dovolj močno električno polje že samo povzroči nekrozo tkiva. Metoda ni zahtevna, je minimalno invazivna in ne zahteva uporabe dodatnih zdravilnih učinkovin *(34)*. Ireverzibilna elektroporacija je netermična metoda, s katero se izognemo denaturaciji proteinov, struktura tkiva ostane nepoškodovana, prav tako ob njeni uporabi ne pride do vnetja in brazgotinjenja. Metodo uspešno uporabljajo za odstranjevanje tumorskega tkiva pri raku prostate in tkiva srčne mišice pri zdravljenju nekaterih srčnih aritmij *(34–35)*. Postopki so v začetni fazi klinične rabe, v literaturi tako še ne zasledimo poročil o neželenih stranskih učinkih in slabostih.

BIOLOŠKO TKIVO IN NJEGOVE ELEKTRIČNE LASTNOSTI

Za uspešno uporabo zgoraj opisanih načinov uporabe elektroporacije moramo najprej teoretično in praktično raziskati dogajanje v tkivu med elektroporacijo *in vivo*. *In vitro* običajno izvajamo poskuse na prostornini 50–100 μl, kjer 1 do 2 % prostornine zasedajo celice, 98 do 99 % pa gojišče. V pogojih *in vivo* celice zasedajo od 10 do 80 % prostornine. Tako v običajnih pogojih *in vitro* posamezna celica nima vpliva na permeabilizacijo ostalih celic, razen v posebnih izredno gostih celičnih suspenzijah. V pogojih *in vivo* pa načeloma že permeabilizacija ene same celice spremeni prevodnost tkiva v okolici in s tem lokalno porazdelitev električnega polja, kar lahko vpliva na permeabilizacijo sosednjih celic.

Zaradi različnih oblik celic in različnih načinov njihove namestitve v tkivu ter različnih električnih lastnosti medceličnega prostora je namreč dogajanje v tkivih na mikro nivoju precej kompleksno *(36)*.

Razlike zaradi nehomogenosti tkiv

Biološko tkivo je zelo nehomogen material. Celice v tkivih so različnih velikosti in imajo

181

različne funkcije. Med vrednostmi električnih prevodnosti tkiv zasledimo velike razlike: zaradi tekočega tkiva, ki teče po žilah, mielinskih ovojnic, ki kot izolatorji ovijajo aksone živčnih celic, veznega tkiva, ki mora prenesti mehanski stres, kosti, zob, mišic, mrtvih delov kože, plinov v pljučnem tkivu itn. Kri je zelo dober prevodnik, jetra in vranica manj. Možgani prevajajo bolje, mišica slabše. Med najslabšimi prevodniki v telesih toplokrvnih živali so pljuča (zaradi visoke vsebnosti plinov), maščoba (zaradi nizke vsebnosti elektrolitov), koža (zaradi neprevodne zunanje plasti *stratum corneum*) in kosti (ker so zgrajene pretežno iz nizkoprevodnega kalcijevega fosfata). Od vseh tkiv v človeškem telesu je prevodnost kosti tudi najbolj spremenljiva. To ni presenetljivo, saj je kost po svoji strukturi zelo nehomogena. Lobanja npr. je iz dveh gostih, slabo prevodnih kosov, spužvasto tkivo med njima pa je polno krvi, ki je dober prevodnik. Podobno so tudi dolge kosti v resnici slabo prevodni votli valji, napolnjeni z visoko prevodnim žilnatim kostnim mozgom.

Anizotropnost tkiv

Nekateri biološki materiali imajo izrazite anizotropne lastnosti, kar pomeni, da so njihove fizikalne lastnosti v različnih smereh različne. Takšna je recimo mišica *(37)*. Mišične celice so zaradi krčenja mišice usmerjene, zaradi česar so električne lastnosti odvisne od smeri merjenja. Prevodnost v smeri vzdolž mišičnih vlaken je tako večja kot prečna prevodnost, vendar pa se ta razlika z višanjem frekvence zmanjšuje.

Ostali fiziološki dejavniki

Tkiva se med seboj razlikujejo tudi v odvisnosti od živalske vrste, kateri pripadajo. Vseeno pa lahko iz literature s primerjavo meritev pri različnih živalskih vrstah ugotovimo, da te razlike niso sistematične in so lahko dosti večje znotraj iste vrste kot med različnimi vrstami *(38)*. Vpliv na električne lastnosti tkiva imajo tudi sezonske spremembe, dejavniki okolja, starost osebka in morebitna bolezenska stanja *(39)*.

SPREMEMBA PREVODNOSTI TKIVA MED ELEKTROPORACIJO

Spremljanje permeabilizacije tkiva v realnem času je želja mnogih raziskovalcev in uporabnikov. Povratno informacijo o poteku elektropermeabilizacije tkiva bi lahko uporabili za prilagajanje električnih parametrov med samo terapijo, kar bi izboljšalo učinek terapije. V nasprotju s tem se danes še vedno uporablja vnaprej določene parametre pulzov, ki so se izkazali za najučinkovitejše. Med in po elektroporaciji se električne lastnosti tkiva spremenijo. Najbolj pomembna merljiva posledica je povečanje specifične prevodnosti tkiva, podvrženega elektroporaciji. Ob dosegu praga električne poljske jakosti, ki povzroči permeabilizacijo tkiva, steče skozenj višji tok, porazdelitev električnega polja pa je drugačna kot na začetku *(40–41)*. Pri tem se moramo spopasti s problemom različnih električnih lastnosti tkiv, ki jih elektroporiramo. Dovedena električna napetost se bo v tkivih porazdelila po principu napetostnega delilnika, ki pravi, da se bo pri zaporedni vezavi elementov (tkiv) z različno električno upornostjo napetost po elementih (tkivih) porazdelila v razmerju vrednosti upornosti, tako da bo napetost največja na elementu (tkivu) z največjo upornostjo. Največji padec napetosti bo torej v tkivu z najvišjo specifično upornostjo, kjer bo tudi električno polje najvišje. Električne pulze dovedemo tkivom preko elektrod, ki so lahko neinvazivne, zunanje, kjer pulze dovajamo preko kože (ploščate elektrode), ali pa invazivne, igelne, s katerimi predremo kožo in tako dosežemo globlje ležeča tkiva *(42)*.

Za primer vzemimo elektrokemoterapijo podkožnega tumorja, kjer električne pulze dovedemo z zunanjimi ploščatimi elektrodami. Ob dovajanju električnih pulzov praktično celoten padec napetosti prevzame koža, ki je v okolici podkožnega tumorja tkivo z najvišjo specifično upornostjo. Ob uporabi dovolj visoke napetosti pulzov povzročimo permeabilizacijo kože, saj je električna poljska jakost v njej nad kritičnim pragom permeabilizacije. Električna upornost kože se med permeabilizacijo zato močno zmanjša, kar spremeni porazdelitev električne poljske jakosti tudi v podkožnih tkivih. Tako dovolj močno elek-
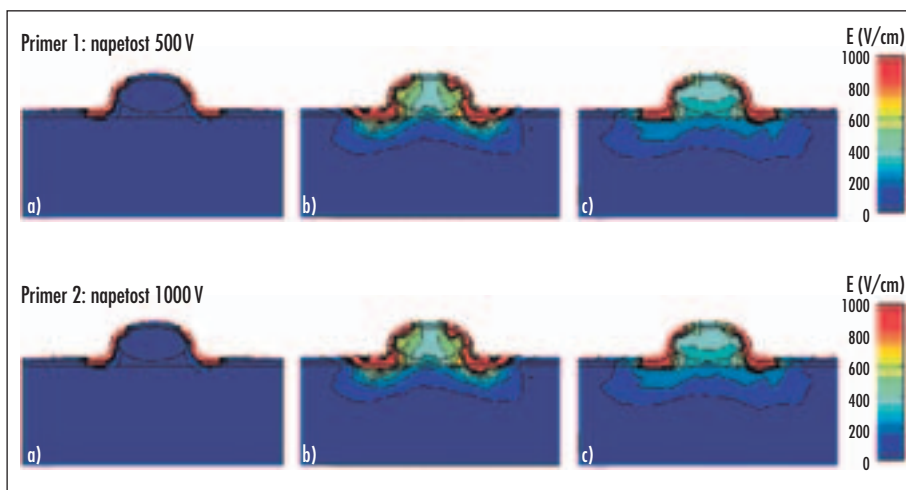
Slika 2. *Numerični model elektropermeabilizacije podkožnega tumorja in okoliških tkiv. Pulzi so dovedeni preko ploščatih elektrod z razmikom 8 mm, napetost med njima je v prvem primeru 500 V, v drugem pa 1000 V. Elektrode so modelirane kot robni pogoj. Slike prikazujejo porazdelitev električnega polja (E) a) pred permeabilizacijo tkiv; b) med procesom elektropermeabilizacije, ko se specifične prevodnosti tkiv spremenijo; c) v končnem stanju procesa elektropermeabilizacije. Opis postopka numeričnega izračunavanja je opisan (40).*

trično polje »doseže« tumor, s čimer povzročimo uspešno elektropermeabilizacijo tumorskih celic in s tem vnos kemoterapevtika *(40)*.

Slika 8 prikazuje numerični izračun porazdelitve električnega polja v podkožnem tumorju in okoliških tkivih med elektroporacijo za dve različni napetosti med ploščatima elektrodama: 500 V in 1000 V.

Če pogledamo končno stanje procesa elektropermeabilizacije pri 500 V, ugotovimo, da je električno polje v večjem delu ciljnega tkiva – tumorja – še vedno pod reverzibilnim pragom permeabilizacije (le-ta znaša približno 400 V/cm). Z uporabo napetosti 1000 V pa je električno polje v tumorju zadosti visoko za uspešno permeabilizacijo, v nekaterih področjih pa celo preseže ireverzibilni prag (nad 800 V/cm). Ti rezultati se ujemajo tudi z eksperimentalnimi rezultati elektrokemoterapije podkožnega tumorja na živalskem tumorskem modelu *(19)*.

NUMERIČNO MODELIRANJE ELEKTROPORACIJE TKIV *IN VIVO*

Za razumevanje poteka elektroporacije v tkivu in načrtovanje poskusov *in vivo* je torej pomembna teoretična analiza dogajanja v tki-

vu, pri čemer uporabljamo analitične in numerične metode. Določiti želimo porazdelitev vektorskih in skalarnih električnih veličin v tkivu oziroma organizmu kot posledico dovedenih električnih pulzov. Na področju bioelektromagnetike predstavljajo numerični izračuni porazdelitev električnih tokov in elektromagnetnih polj znotraj bioloških sistemov pomembno orodje za analizo in razlago kompleksnih dogajanj v bioloških sistemih. Z numeričnimi izračuni porazdelitve električnih tokov in elektromagnetnih polj lahko ovrednotimo različne električne pogoje, kot so velikosti tokov oz. napetosti, velikosti in smeri polj, geometrijo elektrod, ipd. *(43–44)*. Eksperimentiranje na modelih je namreč lažje kot na realnih bioloških sistemih, kjer v nekaterih primerih sploh ni mogoče ali dopustno. Seveda pa moramo numerične modele ovrednotiti, tako da jih primerjamo z eksperimenti na realnih bioloških sistemih.

Spreminjanje električnega vzbujanja je poenostavljeno, saj gre le za spremembe robnih oziroma začetnih pogojev na istem modelu; le začetna faza – izgradnja modela – zahteva precej časa, natančnosti in izkušenj. Analitični izračun porazdelitve elektromagnetnih polj je enostaven le takrat, ko lahko geometrijo, nehomogenosti in anizotropnosti

183

materialov ter robne pogoje opišemo v izbranem koordinatnem sistemu (npr. pravokotnem, valjnem ali krogelnem). V nasprotju s tem numerične metode reševanja večinoma omogočajo približevanje dejanskim oblikam in robnim pogojem. Pri večini numeričnih metod je mogoče materialom pripisati nehomogenost in pri nekaterih tudi anizotropnost. Za večino bioloških sistemov je značilna zapletena in nepravilna geometrija ter nehomogenost in anizotropnost materialov, kar kaže na nujnost uporabe numeričnih metod v tovrstnih raziskavah.

Numerična metoda končnih elementov se je izkazala za zelo učinkovito pri analizi porazdelitve električnega polja znotraj bioloških struktur. Bistvo metode je v razdelitvi geometrije na manjše sestavne dele – končne elemente. Iskane veličine se znotraj elementov spreminjajo kot funkcije polinomov nižjega reda, odvisno od vrste elementa. Snovne lastnosti pa so znotraj elementov homogene. V področjih, kjer pričakujemo dinamično spreminjanje računanih veličin, moramo ponavadi postaviti gostejšo mrežo, prav tako tudi v področjih, kjer nas porazdelitve električnega polja še posebej zanimajo. Mreža mora biti gostejša tudi v mejnih področjih med dvema materialoma, katerih snovne lastnosti se močno razlikujejo. Slabo zgrajena mreža končnih elementov je najpogostejši vzrok za slab izračun, zato je treba gradnji mreže posvetiti še posebno pozornost. Eden najosnovnejših postopkov preverjanja modela, ki ga običajno opravimo na samem začetku raziskave, je gostitev mreže v opazovanih področjih (na primer znotraj tumorja ali v okolici elektrod). Če se pri gostejši mreži rezultati bistveno ne spremenijo, je mreža dovolj gosta. Gradnja mreže je močno poenostavljena pri modelih, katerih geometrija je pravilne ali simetrične oblike. Z določitvijo osi oziroma ravnin simetrije se zmanjša tudi potrebno število končnih elementov in s tem močno poenostavi in skrajša izračun.

DOLOČANJE ELEKTRO-PERMEABILIZACIJE CELIC V POGOJIH *IN VIVO*

Dober model, potrjen z rezultati meritev, nam omogoča razlago dogajanja v tkivu med elektroporacijo, načrtovanje poskusov *in vivo* ter geometrij elektrod. Kljub temu se moramo zavedati dejstva, da so modeli zelo poenostavljena slika realnih razmer. Numerični izračuni zato ne morejo nadomestiti eksperimentalnega dela, ampak služijo kot vir dodatnih informacij za osvetlitev dogajanj in načrtovanje eksperimentov in terapije. Zato morajo teoretičnemu modeliranju slediti poskusi, najprej v pogojih *in vitro*, kasneje neizogibno tudi poskusi *in vivo* na laboratorijskih živalih.

S poskusi *in vivo* zato želimo določiti uspešnost elektroporacije oziroma stopnjo permeabiliziranosti celic v tkivu. V pogojih *in vivo* je zaznavanje permeabilizacije celic oteženo. Markerji ali ciljne molekule namreč niso porazdeljeni enakomerno in v bližini celic, kot so to v pogojih *in vitro*, temveč nehomogeno in zaradi ovir (druge celice, ekstracelularni matriks, membrane kot je mišična ovojnica v mišici) tudi ne nujno v primerni bližini. Vnos markerjev ali ciljnih molekul je možen z lokalnim ali znotrajžilnim vnosom. Slednje je možno le, če ima močno razredčena molekula še vedno biološki učinek (npr. bleomicin) oz. če molekulo še vedno lahko zasledimo. V nadaljevanju bomo na kratko opisali nekaj metod, ki jih uporabljamo za določanje elektropermeabilizacije celic v pogojih *in vivo*.

Večina metod za določanje permeabilizacije membran celic v tkivu temelji na lastnostih markerskih molekul in na dejstvu, da z elektroporacijo membrane začasno povečamo njeno prepustnost za te molekule. Markerji ali ciljne molekule ne smejo prehajati celične membrane v običajnih razmerah, v primeru permeabilizacije celične membrane pa molekule vstopijo v membrano. Takšne molekule so npr. bleomicin, EDTA, DTPA. Njihova značilnost je, da jih po določenem času v telesu ne zasledimo, razen v primeru njihove akumulacije v celicah po elektropermeabilizaciji membrane. Če označimo molekule z radioaktivnim izotopom, jih lahko v tkivu po določenem času zaznamo z gama kamero *in situ* ali pa *ex vivo*. Učinek neoznačenega bleomicina pa lahko opazujemo na histoloških preparatih, kjer ugotavljamo spremembe v celični morfologiji. V drugi sklop molekul, ki jih lahko uporabimo za detekcijo permeabilizacije membran celic *in vivo*, sodijo npr. fluo-

rescentne molekule propidijev jodid, GFP in encim luciferaza, ki katalizira reakcijo luminiscence. Vse te molekule nam omogočajo določitev tako reverzibilnega kot tudi ireverzibilnega praga. Prisotnost teh molekul pa lahko z ustrezno opremo za detekcijo opazujemo tako *in situ* kot tudi *ex vivo*. V tretji sklop metod za določitev elektropermeabilizacije celičnih membran *in vivo* pa sodi merjenje električnih lastnosti tkiva: impedančna spektrometrija in merjenje toka in napetosti ter določitev dinamične prevodnosti tkiva med samim dovajanjem elektroporacijskih električnih pulzov. Merjenje električnih lastnosti tkiva nam omogoča detekcijo praga reverzibilne elektroporacije, ne pa tudi ireverzibilne. Ireverzibilni prag elektroporacije lahko določimo tudi samo z opazovanjem pojava nekroze, vendar pa moramo tu najprej določiti optimalni čas opazovanja po elektroporaciji *(44)*.

1. Bleomicin. Metoda temelji na spoznanju, da bleomicin prehaja plazmalemo z receptorsko posredovano endocitozo, z elektroporacijo pa se prepustnost membrane za bleomicin izrazito poveča *(44–45)*. Bleomicin povzroči pri majhnih znotrajceličnih koncentracijah mitotično celično smrt, pri velikih pa sproži procese, ki so značilni za apoptozo. Bleomicin po vstopu v celico namreč tvori enojne in dvojne prelome DNK vijačnice. Če je teh prelomov relativno malo, celična smrt nastopi šele takrat, ko se celica deli. Kadar pa je teh prelomov veliko, pride do sprožanja apoptoze. Bleomicin lahko v večjih količinah vstopi le v permeabilizirane celice. Že v nekaj minutah po vstopu bleomicina postanejo jedra apoptotična. Opazovanje karakterističnih morfoloških sprememb celic je možno na histoloških preparatih z mikroskopom. Ta metoda nam omogoča določevanje reverzibilnega praga elektropermeabilizacije tkiva, ne pa tudi ireverzibilnega praga *(44)*.

2. [57]Co-Bleomicin je stabilna mešanica kobalta in bleomicina z visoko specifično radioaktivnostjo *(46)*. Slabost metode je počasno odvajanje molekul iz telesa preko ledvic. Zato lahko dobimo rezultate šele po treh dneh, ko izmerimo stopnjo radioaktivnosti ciljnega tkiva in tako ocenimo uspešnost elektropermeabilizacije. Razpolovni cikel [57]Co je 270 dni, kar pomeni, da moramo radioaktivne živali in odpadke zelo dolgo hraniti v ustrezno zaščitenih prostorih.

3. ^{51}Cr-EDTA. Radioaktivna snov, katere razpolovni čas je le 27,7 dneva. Tipično damo 0,72 MBq v veno nekaj minut pred dovajanjem električnih pulzov. Vnešena snov se porazdeli v žilnem in medceličnem prostoru, vendar ne more vstopiti v celice, če ni zagotovljen dostop, npr. z elektroporacijo. V 24 urah se radioaktivna snov, ki ni ujeta v reverzibilno permeabiliziranih celicah, izloči iz organizma. Takrat živali usmrtimo, izrežemo ciljno tkivo, ga stehtamo in v gama števcu izmerimo stopnjo radioaktivnosti. Vsebnost substance, ki je rezultat reverzibilne elektroporacije tkiva, izračunamo iz meritev in izrazimo v nanomolih ^{51}Cr-EDTA na gram ciljnega tkiva. Z metodo lahko določamo oba praga elektroporacije, reverzibilnega in ireverzibilnega. Ob povečevanju amplitude dovedenih pulzov najprej zaznamo povečano zadrževanje ^{51}Cr-EDTA v vzorcih tkiva, ki narašča do amplitude pulzov, pri kateri se začenja ireverzibilna elektroporacija. Od te amplitude naprej se količina ^{51}Cr-EDTA v vzorcih ponovno začne zmanjševati. Prag reverzibilne elektroporacije je torej pri amplitudi pulzov, kjer zaznamo povečanje ^{51}Cr-EDTA v vzorcu, prag ireverzibilne elektroporacije pa pri amplitudi, kjer dosežemo maksimalno količino ^{51}Cr-EDTA v vzorcu *(42)*.

4. ^{99m}Tc-DTPA. Radiofarmacevtska snov, ki se uporablja v radionuklidni angiografiji, statičnih možganskih slikanjih ter raziskavah ledvic in sečnih poti. Farmakokinetsko je zelo podobna bleomicinu, saj se hitro izloči iz telesa s sečem. Obe snovi sta hidrofilni, kar pomeni, da ne prehajata skozi celično membrano. Snov vbrizgamo v veno pred elektroporacijo. Elektroporirano tkivo lahko slikamo z gama kamero šest ur kasneje in slike primerjamo s slikami tkiva pred postopkom ter tako dobimo podatek o reverzibilnem in ireverzibilnem pragu elektroporacije *(47)*.

5. PI (Propidijev jodid) je fluorescenčna molekula, ki lahko preide v notranjost celic le s povečano prepustnostjo membrane *(48)*. Propidijev jodid se v celici veže na DNA. Šele na DNA vezan propidijev jodid fluorescira z rdečo barvo. Rezultate uspešnosti

185

elektroporacije pridobimo sorazmerno hitro, ker fluorescenco lahko opazujemo že v prvih 15 minutah po dovajanju elektroporacijskih pulzov. Zanimivost te metode je tudi v tem, da med eksperimentom ohranimo geometrijo tkiva, kar nam omogoča, da na podlagi fluorescence tkiva izsledimo tudi obliko porazdelitve električnega polja oziroma reverzibilno in ireverzibilno pragovno vrednost elektroporacije tkiv.

6. GFP (angl. *green fluorescent protein*) je protein, ki fluorescira zeleno, ko ga osvetlimo z modro svetlobo. V *in vivo* pogojih v tkivo vnesemo gen, ki kodira protein GFP. Tkivu dovedemo elektroporacijske pulze, ki omogočijo vstop plazmida v celice. Izražanje gena GFP nekaj dni kasneje nam omogoči opazovanje elektropermeabiliziranega tkiva in določitev pragov reverzibilne in ireverzibilne elektroporacije. Fluorescenco lahko opazujemo pod konfokalnim mikroskopom in tako dobimo kvalitativen podatek o mestu izražanja gena, z opazovanjem moči fluorescence pa dobimo semikvantitativen podatek o količini prisotnega proteina GFP *(49–50)*.

7. Luciferaza je encim, ki katalizira reakcijo luminiscence in ga lahko tako kot GFP uporabljamo za merjenje uspešnosti elektroporacije *in vivo* in določitev pragovnih vrednosti elektroporacije. Luminiscenco tkiva merimo z napravo luminometer nekaj dni po vnosu plazmida, ki kodira protein luciferazo, kateremu je sledila elektroporacija. Podatek je kvantitativen in nam po umeritvi z referenčno vrednostjo pove vsebnost proteina v tkivu *(49)*.

8. Impedančna spektrometrija. Običajno merimo impedanco tkiva v območju 10 Hz do 200 kHz tik pred (Z_{pred}) in takoj po (Z_{po}) elektroporaciji tkiva. Nato izračunamo razmerje impedance pred in po elektroporaciji Z_{pred}/Z_{po}, kar korelira z uspešnostjo elektroporacije *(51)*. Uporabimo lahko dvoelektrodni ali štirielektrodni sistem. Pri dvoelektrodnem uporabimo iste elektrode za merjenje impedance in za dovajanje visokonapetostnih pulzov, pri štirielektrodnem sistemu pa en par elektrod uporabljamo za dovajanje pulzov, drugi par za merjenje napetosti, impedanco potem določimo iz meritev na obeh parih elektrod.

9. Merjenje karakteristike toka in napetosti (I/U metoda). Opazujemo potek toka v odvisnosti od napetosti na elektrodah. Permeabiliziranemu tkivu se namreč poveča prevodnost, skozenj steče večji tok, to pa se odraža v spremembi naklona poteka I/U odvisnosti. Na ta način lahko določamo predvsem reverzibilni prag elektroporacije, ireverzibilni je veliko manj izrazit. Rezultati so odvisni tudi od homogenosti porazdelitve električnega polja, torej od stopnje homogenosti tkiva in geometrije elektrod *(52)*.

Pri vseh naštetih metodah določanja reverzibilnega in ireverzibilnega praga elektroporacije *in vivo* pa je treba upoštevati porazdelitev električnega polja v tkivu, ki je odvisna od uporabljenih elektrod − njihove geometrije in postavitve glede na tkivo − in električne prevodnosti različnih tkiv. Zavedati pa se moramo tudi, da je določitev praga reverzibilne permeabilizacije tkiva odvisna tudi od uporabljenega markerja ali ciljne molekule, pa tudi od drugih uporabljenih parametrov električnih pulzov poleg amplitude − to je od trajanja, števila dovedenih pulzov in njihove ponavljalne frekvence.

SEKUNDARNI UČINKI ELEKTROPORACIJE

Uporaba visokonapetostnih elektroporacijskih pulzov ima poleg primarnega učinka permeabilizacije celične membrane tumorskih celic tudi sekundarne učinke. Glavni mehanizem delovanja terapij, ki vključujejo elektroporacijo, temelji na začasno močno povečani prepustnosti celične membrane za molekule, ki drugače membrano težko prehajajo ali pa je sploh ne. V primeru elektrokemoterapije tumorjev lahko na ta način močno povečamo vnos kemoterapevtika v notranjost tumorskih celic in s tem lokalno izražen protitumorski učinek. Poleg tega neposrednega učinka pa imajo elektroporacijski pulzi velik vpliv tudi na lokalni pretok krvi, tako v normalnih tkivih, kot je mišica, kot tudi v tumorjih *(3, 53)*. Hitre spremembe v pretoku krvi v tkivih na nivoju mikrocirkulacije lahko ovrednotimo z optično lasersko dopplersko metodo, pri kateri merimo spremembe v valovni dolžini laserske svetlobe, ko
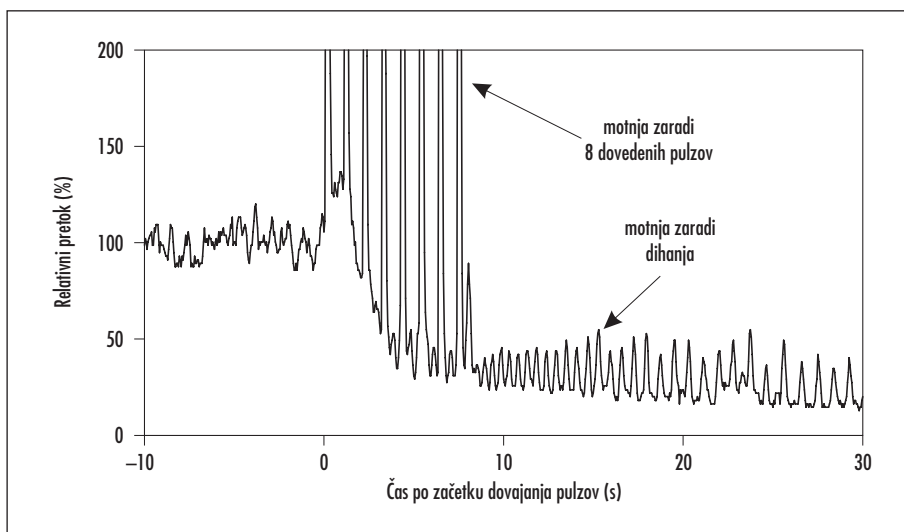
Slika 3. *Primer spremembe v nivoju mikrocirkulacije zaradi uporabe elektroporacijskih pulzov. Osnovni nivo pretoka predstavlja spodnji rob krivulje, vidimo pa tudi motnjo zaradi dihanja in mišičnih kontrakcij ob dovedenih pulzih. Izmerjeno z metodo laser Doppler v podkožnem tumorju Sa-1 pri miši seva A/J (60).*

se ta sipa na premikajočih se krvnih celicah v kapilarah, arteriolah in venulah. Na sliki 3 lahko vidimo, kako se lokalna tumorska mikrocirkulacija skoraj popolnoma zaustavi že med dovajanjem elektroporacijskih pulzov. Ta takojšnji učinek na pretok krvi je posledica močnega krčenja gladkih mišičnih celic v stenah krvnih žil zaradi električnega toka in pa tudi večje prepustnosti žil zaradi porušitve struktur celičnega skeleta *(54)*. Mikrocirkulacija se v tumorjih delno obnovi relativno hitro po aplikaciji pulzov, kljub temu pa je eno uro kasneje pretok krvi v tumorjih še vedno močno zmanjšan, kar je razvidno iz slike 4. Z metodama barvanja tkiva *in vivo* z barvilom patent modro ter merjenja vsebnosti radioaktivnega izotopa rubidija v tkivu smo ugotovili zmanjšano prekrvljenost tumorjev celo 48 ur po elektroporaciji *(55–56)*. V času, ko je zmanjšan pretok krvi v tumorjih, je povečano zadrževanje kemoterapevtika, kar je dodatni pozitivni dejavnik, saj je z daljšim delovanjem učinkovitost kemoterapevtikov povečana. Poleg tega je potrebno poudariti, da zmanjšani mikrocirkulaciji sledi tudi zmanjšana oksigenacija tkiv, kar ima vpliv na delovanje kemoterapevtikov in na izražanje vnešenih genov *(57)*.

Začetno zmanjšanje mikrocirkulacije in dogajanje v prvih minutah do nekaj ur po elektroporaciji lahko večinoma pripišemo učinku električnih pulzov na celice gladkih mišic in prepustnosti žilja. V kasnejšem obdobju po elektroporaciji pa je v primeru elektrokemoterapije zmanjšan pretok krvi posledica predvsem citotoksičnih učinkov kemoterapevtika na endotelne celice v stenah krvnih žil, ki so podobno kot tumorske celice izpostavljene elektroporacijskim učinkom. Na ta način prihaja do žilno ciljanega zdravljenja saj pri dolgotrajni zaustavitvi krvnega pretoka pride do odmiranja celic, ki jih oskrbujejo prizadete kapilare in s tem do posrednega delovanja na tumorske celice *(56, 58)*. To hipotezo podpirajo tudi rezultati študije učinka elektrokemoterapije na endotelne celice v pogojih *in vitro (59)*. Vedno več je torej dokazov, da moramo elektroporacijo obravnavati tudi s stališča njenega vpliva na lokalno žilje in na lokalni pretok krvi. S tem pa se odpirajo tudi nove možnosti za uporabo elektroporacije v zdravljenju.

STRANSKI UČINKI ELEKTROPORACIJE

Med elektrokemoterapijo in po njej se lahko pojavijo tudi nekateri neprijetni stranski

187
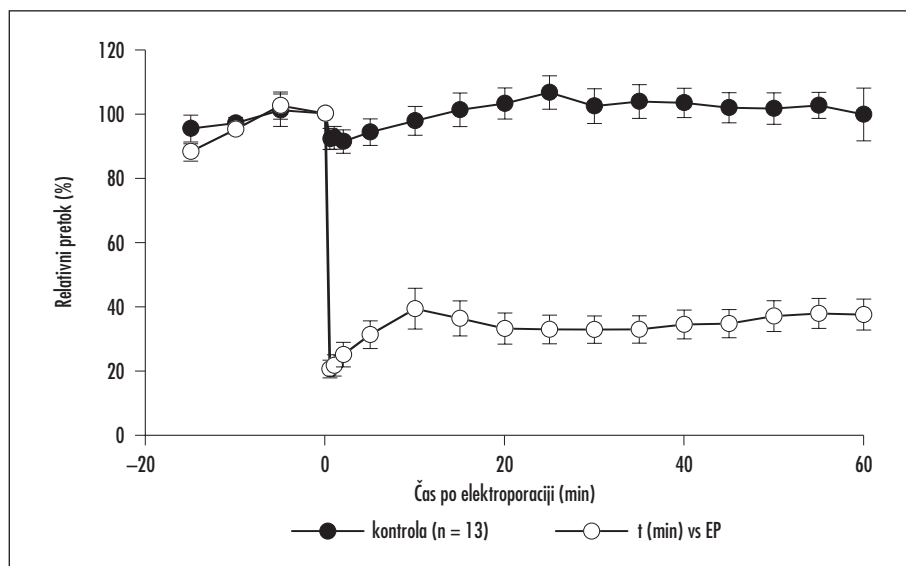
Slika 4. *Vpliv elektroporacije na pretok krvi v podkožnih tumorjih Sa-1 pri miš ih seva A/J. Prikazane so srednje vrednosti pretoka s standardno napako. Izmerjeno z metodo laser Doppler (60).*

učinki. Zaradi visokih lokalnih vrednosti tokovne gostote med dovajanjem pulzov lahko na koži neposredno pod mestom stika z elektrodami nastanejo lokalne opekline, ki pa običajno v kratkem času (v nekaj urah do enega dneva) izginejo *(61)*. Mogoč je tudi nastanek edema in bolj pogosto rdečice okrog mesta zdravljenja, vendar sta tudi ta pojava zgolj kratkotrajna. Za bolnike sta bolj neprijetni bolečina in nehoteno mišično krčenje, ki se pojavita med dovajanjem električnih pulzov. Vsak električni pulz ponavljalne frekvence 1 Hz namreč povzroči zelo kratko ostro bolečino in močno nehoteno mišično krčenje, kar je lahko za bolnika razmeroma neprijetno. Z uporabo višjih ponavljalnih frekvenc, npr. 5 kHz, se število bolečinskih zaznav in mišičnih krčenj zniža *(62–63)*. Protitumorski učinek obeh ponavljalnih frekvenc električnih pulzov je primerljiv, kar potrjujejo eksperimentalni podatki in klinični rezultati *(63–64)*.

ZAKLJUČEK

Elektroporacijo kot metodo vnosa lahko uporabljamo v različne biološke, biotehnološke in medicinske namene. Narejene so bile številne raziskave, s katerimi so poskušali določiti vpliv različnih parametrov celic, tkiv in električnih pulzov na izid elektroporacije. Želje, da bi elektroporacijske metode prišle tudi v klinično prakso, dvigujejo pomembnost teh raziskav, saj so učinkovitost, varnost in pacientovo sprejemanje neke terapevtske metode na prvem mestu. Kot pomembno dopolnilo eksperimentalnemu delu lahko s pomočjo numeričnih modelov teoretično opišemo in razložimo rezultate poskusov *in vivo*, optimiziramo parametre pulzov, napovedujemo izid terapije in načrtujemo nove pristope k protokolom električnih pulzov in geometrijam elektrod. Uporaba elektroporacije za vnos genskega materiala v celice ter uporaba za vnos snovi v kožo sta še v predklinični fazi. Kombinacija kemoterapevtikov in elektroporacije – elektrokemoterapija – pa se že uspešno uporablja v kliničnem okolju za zdravljenje kožnih in podkožnih tumorjev.

ZAHVALA

188

LITERATURA

1. Maček Lebar A, Serša G, Čemažar M, et al. Elektroporacija. Med Razgl 1998; 37: 339–54.
2. Gehl J. Electroporation: theory and methods, perspectives for drug delivery, gene therapy and research. Acta Physiol Scand 2003; 177: 437–47.
3. Serša G. The state-of-the-art of electrochemotherapy before the ESOPE study; advantages and clinical uses. Eur J Cancer Suppl 2006; 4: 52–9.
4. Zampaglione I, Arcuri M, Cappelletti M, et al. In vivo DNA gene electro-transfer: a systematic analysis of different electrical parameters. J Gene Med 2005; 7: 1475–81.
5. Čemažar M, Golzio M, Serša G, et al. Electrically-assisted nucleic acids delivery to tissues in vivo: Where do we stand? Curr Pharm Design 2006; 12: 3817–25.
6. Mir LM, Bureau MF, Rangara R, et al. Long-term, high level in vivo gene expression after electric pulse – mediated gene transfer into skeletal muscle. Medical Sciences 1998; 321: 893–9.
7. Davalos RV, Otten DM, Mir LM, et al. Electrical impedance tomography for imaging tissue electroporation. IEEE Trans Biomed Eng 2004; 51: 761–7.
8. Davalos R, Mir LM, Rubinsky B. Tissue ablation with reversible electroporation. Ann Biomed Eng 2005; 33 (2): 223–31.
9. Kotnik T, Maček Lebar A, Kandušer M, et al. Elektroporacija celične membrane: teorija ter poizkusi in vitro = Electroporation of the cell membrane: theory and experiments in vitro. Med razgl 2005; 44 (1): 81–90.
10. Šemrov D, Miklavčič D. Vsiljeni transmembranski potencial zaradi zunanjega električnega polja v odvisnosti od oblike in orientacije ter gostote celic. Elektrotehniški vestnik 1995; 62 (1): 35–42.
11. Susil R, Šemrov D, Miklavčič D. Electric field induced transmembrane potential depends on cell density and organization. Electro Magnetobiol 1998; 17: 391–9.
12. Pavlin M, Pavšelj N, Miklavčič D. Dependence of induced transmembrane potential on cell density, arrangement, and cell position inside a cell system. IEEE Trans Biomed Eng 2002; 49 (6): 605–12.
13. Miklavčič D, Čorović S, Pucihar G, et al. Importance of tumour coverage by sufficiently high local electric field for effective electrochemotherapy. Eur J Cancer Suppl 2006; 4: 45–51.
14. Puc M, Čorović S, Flisar K, et al. Techniques of signal generation required for electropermeabilization. Survey of electropermeabilization devices. Bioelectrochemistry 2004; 64: 113–24.
15. Okino M, Mohri H. Effects of high-voltage electrical impulse and an anticancer drug on in vivo growing tumors. Jpn J Cancer Res 1987; 78: 1319–21.
16. Mir LM, Banoun H, Paoletti C. Introduction of definite amounts of nonpermeant molecules into living cells after electropermeabilization: Direct access to the cytosol. Exp Cell Res 1988; 175: 15–25.
17. Mir LM, Orlowski S, Belehradek J, et al. Electrochemotherapy potentiation of antitumor effect of bleomycin by local electric pulses. Eur J Cancer 1991; 27 (1): 68–72.
18. Poddevin B, Orlowski S, Belehradek J, et al. Very high cytotoxicity of bleomycin introduced into the cytosol of cells in culture. Biochem Pharmacol 1991; 42: 67–75.
19. Serša G, Čemažar M, Miklavčič D. Antitumor effectivness of electrochemotherapy with cis-diamminedichloro-platinium (II) in mice. Cancer Res 1995; 55: 3450–55.
20. Heller R, Jaroszeski MJ, Reintgen DS, et al. Treatment of cutaneous and subcutaneous tumors with electrochemotherapy using intralesional bleomycin. Cancer 1998; 83: 148–57.
21. Heller R, Gilbert R, Jaroszeski MJ. Clinical application of electrochemotherapy. Adv Drug Deliv Rev 1999; 35: 119–29.
22. Serša G, Čemažar M, Rudolf Z. Electrochemotherapy: advantages and drawbacks in treatment of cancer patients. Cancer Therapy 2003; 1: 133–42.
23. Ferber D. Gene therapy: safer and virus-free? Science 2001; 294: 1638–42.
24. Parker AL, Newman C, Briggs S, et al. Nonviral gene delivery: techniques and implications for molecular medicine. Expert Rev Mol Med 2003; 5: 1–15.
25. Mehier-Humbert S, Guy RS. Physical methods for gene transfer: improving the kinetics of gene delivery into cells. Adv Drug Deliv Rev 2005; 57 (5): 733–53.
26. Šatkauskas S, Bureau M, Puc M, et al. Mechanisms of in vitro DNA electrotransfer: Respective contributions of cell electropermeabilization and DNA electrophoresis. Mol Ther 2002; 5 (2): 133–40.
27. Šatkauskas S, Andre F, Bureau MF, et al. Electrophoretic component of electric pulses determines the efficacy of in vivo DNA electrotransfer. Hum Gene Ther 2005; 16: 1194–201.
28. Barry BW. Novel mechanisms and devices to enable successful transdermal drug delivery. Eur J Pharm Sci 2001; 14: 101–14.
29. Prausnitz MR, Mitragotri S, Langer R. Current status and future potential of transdermal drug delivery. Nat Rev Drug Discov 2004; 3 (2): 115–24.
30. Prausnitz MR. The effects of electric current applied to skin: A review for transdermal drug delivery. Adv Drug Deliv Rev 1996; 18: 395–425.

189

31. Prausnitz MR. Reversible skin permeabilization for transdermal delivery of macromolecules. Crit Rev Ther Drug Carrier Syst 1997; 14 (4): 455–83.

32. Denet A-R, Préat V. Transdermal delivery of timolol by electroporation through human skin. J Control Release 2003; 88: 253–62.

33. Prausnitz MR. A practical assessment of transdermal drug delivery by skin electroporation. Adv Drug Deliv Rev 1999; 35: 61–76.

34. Lavee J, Onik G, Mikus P, et al. A Novel Nonthermal Energy Source for Surgical Epicardial Atrial Ablation: Irreversible Electroporation. The Heart Surgery Forum 2007; 10 (2): 96–101.

35. Onik G, Mikus P, Rubinsky B. Irreversible electroporation: Implications for prostate ablation. Technology in Cancer Research and Treatment 2007; 6 (4): 295–300.

36. Miklavčič D, Pavšelj N, Hart FX. Electric Properties of Tissues. In: Wiley Encyclopedia of Biomedical Engineering, John Wiley & Sons, New York, 2006.

37. Epstein BR, Foster KR. Anisotropy in the dielectric properties of skeletal muscle. Med Biol Eng Comput 1983; 21 (1): 51–5.

38. Gabriel C, Gabriel S, Corthout E. The dielectric properties of biological tissues: I. literature survey. Phys Med Biol 1996; 41: 2231–49.

39. Geddes LA, Baker LE. The specific resistance of biological material – a compendium of data for the biomedical engineer and physiologist. Med Biolog Eng 1967; 5: 271–93.

40. Pavšelj N, Bregar Z, Cukjati D, et al. The course of tissue permeabilization studied on a mathematical model of a subcutaneous tumor in small animals. IEEE Trans Biomed Eng 2005; 52: 1373–81.

41. Šel D, Cukjati D, Batiuskaite D, et al. Sequential finite element model of tissue electropermeabilization. IEEE Trans Biomed Eng 2005; 52: 816–27.

42. Gehl J, Sorensen TH, Nielsen K, et al. In vivo electroporation of skeletal muscle: threshold, efficacy and relation to electric field distribution. Biochim Biophys Acta 1999; 1428: 233–40.

43. Fear EC, Stuchly MA. Modeling assemblies of biological cells exposed to electric fields. IEEE Trans Biomed Eng 1998; 45 (10): 1259–71.

44. Miklavčič D, Šemrov D, Mekid H, et al. A validated model of in vivo electric field distribution in tissues for electrochemotherapy and for DNA electrotransfer for gene therapy. Biochim Biophys Acta 2000; 1523: 73–83.

45. Mir LM, Tounetki O, Orlowski S. Bleomycin: revival of an old drug. General Pharmacol 1996; 27: 745–48.

46. Pron G, Mahrour N, Orlowski S, et al. Internalisation of the bleomycin molecules responsible for bleomycin toxicity: a receptor-mediated endocytosis mechanism. Biochem Pharmacol 1999; 57 (1): 45–56.

47. Engstrom PE, Persson BR, Salford LG. Studies of in vivo electropermeabilization by gamma camera measurements of (99m)Tc-DTPA. Biochim Biophys Acta 1999; 1473: 321–8.

48. Gabriel B, Teissié J. Direct observation in the millisecond time range of fluorescent molecule asymmetrical interaction with the electropermeabilized cell membrane. Biophys J 1997; 73: 2630–7.

49. Pavšelj N, Préat V. DNA electrotransfer into the skin using a combination of one high- and one low-voltage pulse. J Control Release 2005; 106: 407–15.

50. Čemažar M, Wilson I, Dachs GU, et al. Direct visualization of electroporation-assisted in vivo gene delivery to tumors using intravital microscopy – spatial and time dependent distribution. BMC Cancer 2004; 4 (81): 1–7.

51. Ivorra A, Rubinsky B. In vivo electrical impedance measurements during and after electroporation of rat liver. Bioelectrochemistry 2007; 70 (2): 287–95.

52. Cukjati D, Batiuskaite D, André F, et al. Real time electroporation control for accurate and safe in vivo non-viral gene therapy. Bioelectrochemistry 2007; 70: 501–7.

53. Gehl J, Skovsgaard T, Mir LM. Vascular Reactions to in Vivo Electroporation: Characterization and Consequences for Drug and Gene Delivery. Biochim Biophys Acta 2002; 1569: 51–8.

54. Kanthou C, Kranjc S, Serša G, et al. The endothelial cytoskeleton as a target of electroporation based therapies. Mol Cancer Ther 2006; 5: 3145–52.

55. Serša G, Čemažar M, Parkins CS, et al. Tumor blood flow changes induced by application of electric pulses. Eur J Cancer 1999; 35: 672–7.

56. Serša G, Čemažar M, Miklavčič D, et al. Tumor blood flow modifying effect of electrochemotherapy with bleomycin. Anticancer Res 1999; 19: 4017–22.

57. Serša G, Čemažar M, Miklavčič D. Tumor blood flow modifying effects of electrochemotherapy: a potential vascular targeted mechanism. Radiol Oncol 2003; 37: 43–8.

58. Serša G, Kržič M, Šentjurc M, et al. Reduced blood flow and oxygenation in SA-1 tumours after electrochemotherapy with cisplatin. Br J Cancer 2002; 87: 1047–54.

59. čemažar M, Parkins CS, Holder AL, et al. Electroporation of human microvascular endothelial cells: evidence for an anti-vascular mechanism of electrochemotherapy. Br J Cancer 2001; 84: 565–70.

60. Serša G, Jarm T, Kotnik T, et al. Vascular disrupting action of electroporation and electroche-motherapy with bleomycin in murine sarcoma. Br J Cancer 2008; 98: 388–98.

61. Mir LM, Glass LF, Serša G, et al. Effective treatment of cutaneous and subcutaneous malignant tumours by electroc-hemotherapy. Br J Cancer 1998; 77: 2336−42.
62. Miklavčič D, Pucihar G, Pavlovec M, et al. The effect of high frequency electric pulses on muscle contractions and antitumor efficiency in vivo for a potential use in clinical electrochemotherapy. Bioelectrochemistry 2005; 65: 121−8.
63. Županič A, Ribarič S, Miklavčič D. Increasing the Repetition Frequency of Electric Pulse Delivery Reduces Unpleasant Sensations that Occur in Electrochemotherapy. Neoplasma 2007; 54: 246−50.
64. Marty M, Serša G, Garbay JR, et al. Electrochemotherapy − An easy, highly effective and safe treatment of cutaneous and subcutaneous metastases: Results of ESOPE (European Standard Operating Procedures of Electrochemot-herapy) study. Eur J Cancer Suppl 2006; 4: 3−13.

Prispelo 10. 1. 2008

Paper X

ORIGINAL ARTICLE

The effect of electroporation pulses on functioning of the heart

**Barbara Mali · Tomaz Jarm · Selma Corovic ·
Marija Snezna Paulin-Kosir · Maja Cemazar ·
Gregor Sersa · Damijan Miklavcic**

Abstract Electrochemotherapy is an effective antitumor treatment currently applied to cutaneous and subcutaneous tumors. Electrochemotherapy of tumors located close to the heart could lead to adverse effects, especially if electroporation pulses were delivered within the vulnerable period of the heart or if they coincided with arrhythmias of some types. We examined the influence of electroporation pulses on functioning of the heart of human patients by analyzing the electrocardiogram. We found no pathological morphological changes in the electrocardiogram; however, we demonstrated a transient RR interval decrease after application of electroporation pulses. Although no adverse effects due to electroporation have been reported so far, the probability for complications could increase in treatment of internal tumors, in tumor ablation by irreversible electroporation, and when using pulses of longer durations. We evaluated the performance of our algorithm for synchronization of electroporation pulse delivery with electrocardiogram. The application of this algorithm in clinical electroporation would increase the level of safety for the patient and suitability of electroporation for use in anatomical locations presently not accessible to existing electroporation devices and electrodes.

Keywords Electrochemotherapy · Electrocardiogram · QRS detection · Synchronization of electroporation pulse delivery with ECG

B. Mali · T. Jarm · S. Corovic · D. Miklavcic (✉)
Laboratory of Biocybernetics, Faculty of Electrical Engineering,
University of Ljubljana, Trzaska 25, 1000 Ljubljana, Slovenia
e-mail: damijan.miklavcic@fe.uni-lj.si
URL: http://lbk.fe.uni-lj.si/

B. Mali
e-mail: barbara.mali@fe.uni-lj.si

T. Jarm
e-mail: tomaz.jarm@fe.uni-lj.si

S. Corovic
e-mail: selma.corovic@fe.uni-lj.si

M. S. Paulin-Kosir · M. Cemazar · G. Sersa
Institute of Oncology Ljubljana, Zaloska 2,
1000 Ljubljana, Slovenia
e-mail: skosir@onko-i.si

M. Cemazar
e-mail: mcemazar@onko-i.si

G. Sersa
e-mail: gsersa@onko-i.si

1 Introduction

The combined treatment in which delivery of chemotherapeutic drug is followed by application of high-voltage electric pulses locally to the tumor has been termed electrochemotherapy. The effect of local electropermeabilization of the cell membrane (the disruption of the lipid matrix and creation of aqueous pathways [10, 38]), also termed electroporation, transiently enables the entry of anticancer drugs, such as bleomycin or cisplatin, into the cells and hence greater effectiveness of tumor treatment. Electrochemotherapy has been successfully used for treatment of cutaneous and subcutaneous tumors irrespective of their histological origin in different animal tumor models and in humans [19, 36, 51, 52]. In these studies, a typical electrochemotherapy protocol involved eight electroporation pulses (EP pulses) with amplitude of about 1,000 V, duration 100 μs, repetition frequency 1 Hz, and inter-electrode distance 8 mm. However, the protocol involving eight EP

pulses at repetition frequency of 5 kHz has been suggested and is currently replacing the 1-Hz protocol due to a lesser discomfort and pain inflicted to patients [31, 57]. Electrodes of three different configurations can be used for EP pulse delivery during electrochemotherapy. EP pulses applied by plate electrodes are used in case of superficial tumor nodules whereas EP pulses to deeper-seated tumors (subcutaneous nodules) are applied using needle row array electrodes (eight needle electrodes arranged in two rows) or needle hexagonal array electrodes (six hexagonally arranged electrodes with the seventh electrode in the centre) [31]. The number of applied EP pulses and pulse repetition frequency depend on the electrode type and define the duration of electroporation, which is 1.6 ms for plate and needle row array electrodes [31] and approximately 200 ms for needle hexagonal array electrodes [31, 45]. New protocols for delivery of EP pulses are either already in use or are being developed. For gene electrotransfer three different EP pulse protocols are in use: short high-voltage EP pulses, EP pulses of a much longer duration (in the order of milliseconds), or combination of short high-voltage EP pulses with very long low-voltage electrophoretic pulses (amplitude 50–100 V, duration 100 ms) [8, 18, 20, 40, 48]. Tumor ablation by irreversible electroporation is another recently developed application, where EP pulses with larger amplitudes (up to 3,000 V) and longer durations (up to 24 ms) are delivered [3, 14, 28, 35]. New applications using endoscopic or surgical means to access internal tumors are also being developed [21].

Electrochemotherapy is reported as an efficient and safe method. No adverse effects have been reported so far. Electrochemotherapy causes only minor side effects in the patients such as the transient lesions in areas in direct contact with the electrodes [37] and acute localized pain due to contraction of muscles in vicinity of the electrodes [36, 57]. The induced contraction could present a problem if provoked in the heart muscle [46]. There is very little chance that currently used electroporation protocols could interfere with functioning of the heart since there is no such practical evidence. However, this issue has not been systematically investigated yet. Given the increasing need for palliative treatment of internal tumors, the possibility of EP pulses interfering with functioning of the heart is emerging for tumors located close to the heart muscle. Among possible irregularities of functioning of the heart that the application of EP pulses could induce (e.g., atrial and ventricular flutter and fibrillation, premature heartbeats), the most dangerous is ventricular fibrillation [46]. Fibrillation can be induced if electrical stimulus is delivered during late atrial or ventricular systole, during the so-called vulnerable period of the heart [25, 46, 55] (Fig. 1). For ventricular myocardium, the vulnerable period coincides with the middle and terminal phases of the T wave [46], but higher shock strengths cause the vulnerable period to occur
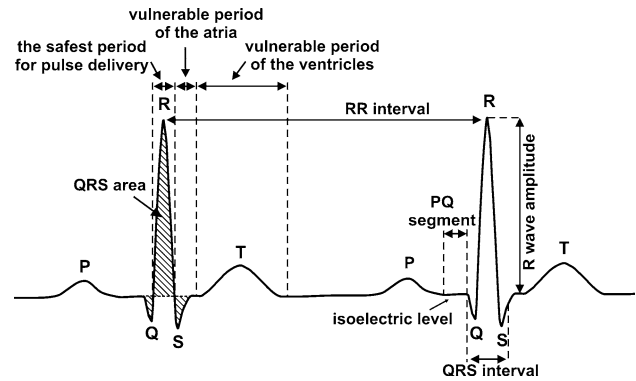
Fig. 1 The vulnerable period and characteristics of a typical heartbeat

several milliseconds earlier in the heartbeat [27]; therefore, the whole T wave can be considered to be within the vulnerable period of the ventricles. For the atria, the vulnerable period is somewhere in the S wave [46]. Externally applied electric pulses delivered outside the vulnerable period have extremely low probability of inducing ventricular fibrillation [46]. According to this fact the synchronization of EP pulse delivery with electrocardiogram (ECG) would increase safety of the patient. The likelihood of electroporation to influence functioning of the heart depends also on applied pulse voltage, duration, number and repetition frequency of EP pulses, and electric current pathway [46].

Although fibrillation can occur in normal and healthy hearts, it is more likely in hearts with structural or functional abnormalities [11]. Abnormalities of the heart rhythm (arrhythmias) are indicated by significant deviation of RR interval from its normal value [12, 46]. During some arrhythmias the heart becomes more susceptible to external stimuli due to a decreased threshold level for fibrillation. Therefore EP pulses coinciding with some arrhythmias could elicit fibrillation. This potential danger is most significant after premature heartbeat, the extrasystole [46].

The main purpose of this study was therefore to investigate the possible effects of EP pulses on functioning of the heart and to address the relevance of synchronization of EP pulse delivery with ECG. In this context we also evaluated the performance of our previously developed algorithm for QRS detection and synchronization of EP pulse delivery with ECG [30].

2 Methods and materials

2.1 Patients and electrochemotherapy

Fourteen human patients were included in this study. Before electrochemotherapy treatment a signed consent was obtained from each patient. Patients were treated

according to the electrochemotherapy protocols as described by Marty et al. [31] with the addition of ECG monitoring. Electrochemotherapy drugs (cisplatin or bleomycin) were administered locally to tumors. EP pulses were generated by the electric pulse generator Cliniporator^{TM} (IGEA S.R.L., Carpi, Italy). Altogether 93 applications of EP pulses were performed. Main characteristics of the patients, tumors and electrochemotherapy are presented in Table 1.

We recorded 16 ECG signals on 14 patients during electrochemotherapy at the Institute of Oncology in Ljubljana. Two patients were treated twice. Thus ECG signals number 1 and 2 belong to the same person as well as signals number 5 and 6 (Table 1). ECG signals were acquired at sampling frequency of 250 Hz using a BIOPAC data acquisition and measurement system (BIOPAC Systems, Inc., USA). To enable early detection of QRS complex we required an ECG lead, which results in a distinctive ascendant QR junction, high R wave amplitude and high dynamics within the QRS complex in comparison to other parts of the ECG signal. Typical standard ECG leads fulfilling these requirements include the chest lead V$_4$ and standard limb leads I, II and III. We recorded ECG signals from leads I and III by placing the electrodes (disposable soft cloth ECG electrodes, diameter 6 cm, 3M^{TM} Red Dot^{TM}) on wrists and ankles and computed the third limb lead II by summing the leads I and III. The lead with best dynamic characteristics was selected for the analysis individually for each patient (see Table 5).

2.2 Analysis of electrocardiograms

The primary analysis of ECG signals recorded during electrochemotherapy was made by using QRS detection algorithm based on the analysis of a single lead ECG, which enables EP pulse delivery prior to the vulnerable period of the heart [30]. This algorithm for synchronization of EP pulse delivery with ECG was developed and evaluated using records of the Long-term ST database (LTST DB database) [23] and was written in ANSI C programming language. The algorithm is described in detail elsewhere [30]. Briefly, it consists of two major components (the detection phase and the decision-making phase), which are preceded by the learning phase during which architecture parameters are estimated from the ECG signal. The detection phase is based on consideration of several ECG signal features: the QR interval, the R wave amplitude and the RR interval (see Fig. 1), in order to achieve a reliable QRS detector performance and to assure clear distinction between normal and abnormal individual heartbeats. For implementation of such a detector the peaks of Q and R waves and the isoelectric level are extracted from the ECG signal. During the decision-making phase, a

decision is made whether the EP pulse can be delivered or not based on evaluating deviations of R wave amplitude and RR interval of individual heartbeat from moving average values of these two parameters.

Further analysis of ECG signals recorded during electrochemotherapy was performed to estimate the effect of EP pulse delivery on ECG. For this purpose the peaks of S waves and ends of QRS complexes were determined using program routines written in Matlab. Since the longest normal duration of the QRS complex is 120 ms [22] and the R peak is located approximately at the centre of the QRS complex, it is reasonable to expect the S peak within an interval of 60-ms after the R peak. The algorithm calculates the first derivative of the ECG signal in this 60 ms interval and looks for the first occurrence of three successive samples with negative first derivative followed by a sample with nonnegative derivative. The S peak is assigned to the third of these four samples. Next, the algorithm searches for the flattest part of the ST segment in order to determine the end of the QRS complex. For this purpose an interval of 40 ms after the S peak is analyzed. The average value of five successive samples from this interval having the minimal total deviation from their average value is taken as the flattest part of the ST segment and the middle sample is considered as the end of QRS complex, i.e., the end of QRS interval. After this, the area under the QRS complex is estimated. A similar routine is used for localization of the end of T wave except that an interval of 130 ms after the T peak is analyzed; the flattest part is searched for and the middle sample of this flattest part is considered as the end of T wave. The corrected QT interval (QTc interval) is calculated as the QT interval divided by the square root of the corresponding RR interval.

For evaluation of the effects of EP pulse delivery on functioning of the heart we calculated the average values of RR interval, QRS interval, QTc interval, QRS area and R wave amplitude before and after the application of EP pulses. The length of the averaging interval (8.5 s) was chosen based on the minimum interval between two successive applications of EP pulses, which was 8.5 s.

Testing and evaluation of this newly developed part of the algorithm was performed by manual verification of automatically defined locations of S peak, T peak, the end of T wave, and duration of QRS interval on randomly selected sequences of ECG signals included in our study. In addition, since this was the first application of the newly developed part algorithm, we also manually verified the results of the algorithm on 8.5 s-long segments of ECG signals before and after all 93 applications of EP pulses.

All ECG signals were manually examined by two medical doctors (including a cardiologist), who classified all abnormal heartbeats present in the signals. Other heartbeats were considered as normal. They found no evidence of significant

Table 1 Main characteristics of the patients, tumors and electrochemotherapy pulses for individual ECG signal

Signal number	Patient				Tumor			Electrochemotherapy			
	Sex	Age	BMI	Pre-existing cardiac conditions	Type	Number of nodules	Location of nodules	Electrode type	Number of applications	Voltage (V)	Drug
1	F	78	35.3	None	Malignant melanoma	1	EX: left ankle	Hexagonal[a]	1	730	Cisplatin
2	F	78	35.3	None	Malignant melanoma	1	EX: left lower leg	Plate (6 mm)	1	680	Cisplatin
3	F	71	20.5	Mitral valve prolapse	Infiltrating lobular cancer	1	TR: parasternal right	Plate (8 mm)	4	960	Bleomycin
4	M	75	24.3	Arterial hypertension	Malignant melanoma	1	TR: lower abdomen	Plate (6 mm)	3	680	Bleomycin
5	F	60	24.8	Arterial hypertension	Malignant melanoma	5	EX: left upper leg	Plate (8 mm)	6	960	Bleomycin
6	F	60	24.8	Arterial hypertension	Malignant melanoma	1	EX: under left knee	Plate (8 mm)	1	960	Bleomycin
						5	EX: left upper leg	Plate (8 mm)	5	960	
7	F	48	21.7	None	Malignant melanoma	1	TR: thorax, right side	Plate (8 mm)	4	960	Bleomycin
						1	TR: back, right side	Plate (8 mm)	7	960	
8	F	68	23.2	None	Malignant melanoma	1	EX: left instep	Hexagonal[a]	3	730	Bleomycin
9	F	92	20.8	Arterial hypertension	Malignant melanoma	10	EX: left lower leg	Plate (6 mm)	10	680	Cisplatin
10	F	73	27.3	Arterial hypertension	Invasive ductal carcinoma	11	TR: thorax	Plate (6 mm)	11	680	Bleomycin
11	F	72	20.0	None	Malignant melanoma	1	EX: under right knee	Plate (6 mm)	1	680	Cisplatin
12	M	67	21.5	None	Malignant melanoma	1	TR: thorax left side	Plate (6 mm)	2	680	Cisplatin
						1	TR: thorax right	Plate (6 mm)	2	680	
						1	EX: left upper arm	Plate (6 mm)	4	680	
13	F	80	23.5	None	Malignant melanoma	3	EX: left lower leg	Plate (6 mm)	3	680	Cisplatin
						1	EX: left upper leg	Plate (6 mm)	1	680	
14	F	79	28.6	Arterial hypertension	Malignant melanoma	1	EX: under right knee	Plate (6 mm)	6	680	Cisplatin
						1	EX: right ankle-back	Plate (6 mm)	4	680	
15	F	81	NA	None	Malignant melanoma	6	EX: left lower leg	Plate (6 mm)	9	680	Cisplatin
16	F	52	32.4	None	Sarcoma	1	TR: left hip	Plate (6 mm)	5	680	Cisplatin

BMI body mass index, *NA* not available, *EX* location on extremities, *TR* location on trunk

[a] Penetration depth 3 and 2 mm, respectively

long-lasting heart arrhythmias (e.g., bradycardia, tachycardia). For evaluation of QRS complex detection, we calculated the following scores for each record: N_d, TP, FN and FP (for definitions see Table 5). Based on these scores obtained with a beat-by-beat comparison of the results of our algorithm [30] with the medical expert-defined annotations of the heartbeats, we calculated standard performance measures of the algorithm: the sensitivity (Se), the positive predictivity ($+P$) and the detection error rate (DER) for QRS detection (Eqs. 1–3, respectively). The performance measures for an ideal QRS detector would be $Se = 100\%$, $+P = 100\%$ and $DER = 0\%$.

$$Se(\%) = \frac{TP}{N_d} \times 100 \tag{1}$$

$$+P(\%) = \frac{TP}{TP + FP} \times 100 \tag{2}$$

$$DER(\%) = \frac{FP + FN}{N_d} \times 100 \tag{3}$$

For evaluation of EP pulse delivery we calculated the following scores for each record: N_p, TP_p, FN_p and FP_p (for definitions see Table 5). Based on these scores and in the absence of any standard performance metrics for EP pulse delivery, we calculated the performance measures analogous to QRS detection metrics: the sensitivity (Se_p), the positive predictivity ($+P_p$) and the delivery error rate (DER_p) for EP pulses. The performance measures for an ideal algorithm for EP pulse delivery would be $Se_p = 100\%$, $+P_p = 100\%$ and $DER_p = 0\%$.

The performance of our algorithm for QRS detection and EP pulse delivery has previously been evaluated on ECG signals from a standard LTST DB database [30]. The results were: $Se = 99.4\%$, $+P = 100.0\%$, $DER = 0.6\%$, $Se_p = 91.8\%$, $+P_p = 100.0\%$ and $DER_p = 8.3\%$ (median values).

2.3 Numerical modeling

We performed numerical calculations of electric field and current distribution for tissue models. The geometry of models and electrode configurations are shown in Fig. 2. The modeled conditions (needle row array, needle hexagonal array and plate electrode configurations and voltages applied) were the same as actually used in clinical electrochemotherapy (see Tables 3 and 4 for details). The modeled tissues (the target tumor tissue and the surrounding healthy tissue) are treated as isotropic materials with ohmic behavior (only conductivity of the tissues was taken into account). The assigned conductivity values were set to be 0.4 S/m for the tumor and 0.2 S/m for the healthy tissue according to previous measurements of tumor and tissue conductivity [34], models of subcutaneous tumor and skin electropermeabilization [43], a 3D finite element model of thorax, where the sensitivity of defibrillation

parameters to the variations in model inhomogeneity and approximation of skeletal muscle anisotropy was examined for different paddle placements [9], and average conductivity of tissues composing the thorax [26]. The conductivity of cardiac muscle was reported to be in the range between 0.17 and 0.25 S/m [9, 26]. The assigned conductivity values for target tumor tissue (0.4 S/m) and the surrounding healthy tissue (0.2 S/m) describe the conductivity at the end of the electropermeabilization process, thus incorporating the changes to tissue conductivity due to exposure to external electric pulses.

The critical depth for electric field of 200 and 450 V/cm (value for reversible and irreversible electroporation of the muscle, respectively [43]), by solving the Laplace equation, and the critical depth for current of 100 mA (threshold for ventricular fibrillation for 500 μs-long electrical stimulus [46]), were estimated by means of finite element method using COMSOL Multiphysics 3.3 software package (COMSOL AB, Sweden). Of the total electric current flowing through the tissue during the EP pulse delivery, no more than 100 mA (the threshold value for fibrillation) is allowed to flow through the heart. Therefore we defined the critical depth as a distance from the surface of the body (at the site of EP delivery) below which the total electric current flowing is equal to this threshold value. This is a very conservative approach in which it is assumed that the entire current flowing below the critical depth actually passes through the heart. The validity of the model is further discussed in the Sect. 4.1.

2.4 Statistical analysis

The performance of the algorithm and average values of heartbeat parameters were compared using either the Mann–Whitney Rank Sum or Wilcoxon Signed Rank test. In all tests, a p value of less than 0.05 was considered as indication of statistically significant difference. The statistical analysis was performed using SigmaStat 3.1 software package. Since the data were not normally distributed, we give statistical summary of the results using both the mean/standard deviation and the median/quartile values. However, when we say "on average" in the text we are referring to median values, which are more representative of the middle of the sample and population than the mean values.

3 Results

3.1 The effect of electroporation pulse delivery on electrocardiogram

Our program-based analysis of heartbeat characteristics (RR interval, QRS interval, QTc interval, R wave and QRS

Fig. 2 The geometry of tissue models with tumor for: **a** plate electrodes (length 7 mm, thickness 0.7 mm, distance between the electrodes d is 4, 6 or 8 mm, tumor diameter is 1 mm larger than distance between the electrodes); **b** needle row array electrodes (diameter 0.7 mm for each needle, distance between two rows of electrodes $d = 4$ mm, tumor radius $r = 4$ mm, tumor location 0.5 mm under the skin surface); **c** needle hexagonal array electrodes (diameter 0.7 mm for each needle, distance between two electrodes 8 mm, tumor radius $r = 15$ mm)
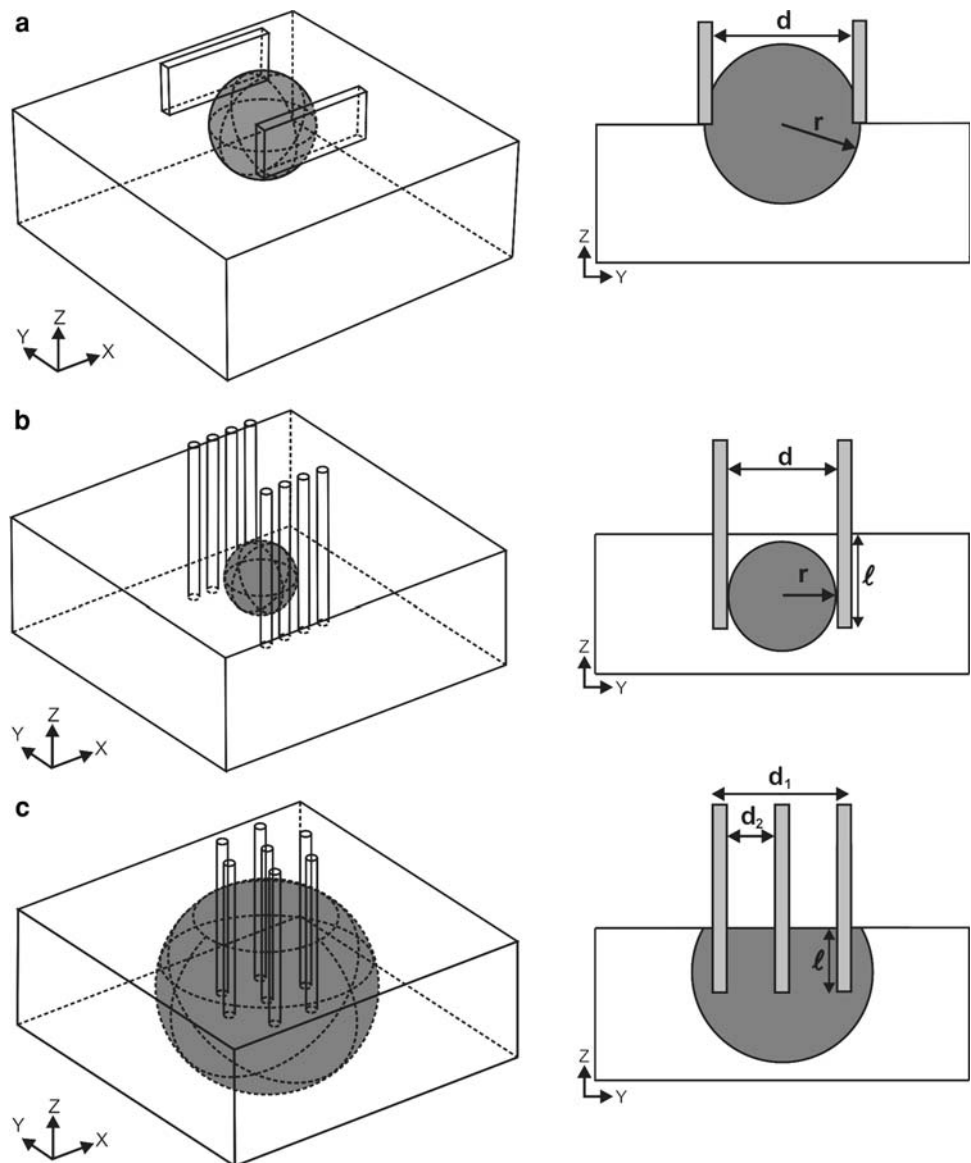
area) revealed no pathological morphological changes caused by EP pulses in patients subjected to electrochemotherapy. This finding was confirmed independently by two medical doctors. The significant change, however, was detected in RR and QRS interval duration after each application of EP pulses (see Table 2).

The medical doctors involved in the study confirmed that EP pulses induced no heart arrhythmias. Moreover, additional premature heartbeats were not triggered by EP pulses in the cases where premature heartbeats were present in ECG signal before the application of EP pulses.

The results of modeling the distribution of electric field and current in tissue models are presented in Tables 3 and 4. It can be seen that in the worst-case scenario (needle hexagonal array electrodes, 10 mm depth of insertion) the critical depth for current of 100 mA is 4.10 cm. The largest

Table 2 The change in heartbeat parameters after EP pulse delivery

Evaluated parameters	Median change	Percentile		Statistical significance (p)
		25%	75%	
RR interval (ms)	−5.43	−19.60	7.72	0.006
QRS interval (ms)	−1.25	−9.13	4.13	0.042
R wave amplitude (mV)	6.46	−28.50	35.20	0.414
QRS area (mV ms)	515	−671	2,010	0.091
QTc interval (ms)	1.89	−9.73	11.40	0.380

Wilcoxon Signed Rank test, $n = 93$

critical depths for reversible and irreversible electroporation are 1.30 and 1.07 cm, respectively, for needle row array electrodes at insertion depth 10 mm.

Table 3 Calculated critical depths for electric field and current in different plate electrode configurations

Distance between electrodes (d) (mm)	Tumor radius (r) (mm)	Applied voltage (V)	Critical depth for 100 mA (cm)	Critical depth for 200 V/cm (cm)	Critical depth for 450 V/cm (cm)
4	2.5	520	1.00	0.31	0.18
6	3.5	780	1.55	0.43	0.22
8	4.5	1,000	2.38	0.51	0.30

Table 4 Calculated critical depths for electric field and current in needle row array and needle hexagonal array electrode configurations

Depth of insertion (l) (mm)	Needle row array electrodes (400 V, tumor radius r = 2 mm)			Needle hexagonal array electrodes (730 V, tumor radius r = 15 mm)		
	Critical depth for 100 mA (cm)	Critical depth for 200 V/cm (cm)	Critical depth for 450 V/cm (cm)	Critical depth for 100 mA (cm)	Critical depth for 200 V/cm (cm)	Critical depth for 450 V/cm (cm)
2	1.55	0.43	0.26	2.23	0.43	–
4	2.37	0.68	0.46	2.65	0.64	0.30
6	2.94	0.90	0.70	3.20	0.87	0.54
8	3.40	1.10	0.90	3.69	1.04	0.70
10	3.79	1.30	1.07	4.10	1.25	0.93

3.2 The algorithm for synchronization of electroporation pulse delivery with electrocardiogram

The performance of the algorithm for QRS detection and synchronization of EP pulse delivery with ECG is summarized in Table 5. On average, the algorithm correctly detected 99.2% of all QRS complexes. The total number of erroneously detected QRS complexes was 15. On average, the algorithm would correctly deliver EP pulses in 94.6% of normal QRS complexes. The average positive predictivity for EP pulses ($+P_p$) was 100.0% and thus ideal.

A comparison of performance between 16 ECG signals recorded during electrochemotherapy and 42 ECG signals from the LTST DB database [30] was performed. The results showed that there is not a statistically significant difference in the median values between all compared performance measures (Se, +P, DER, Se_p, DER_p) ($0.142 < p < 0.924$) except for the positive predictivity for EP pulse delivery ($+P_p$) ($p = 0.026$, Mann–Whitney Rank Sum test). This performance measure was significantly better for ECG signals recorded during electrochemotherapy than for ECG signals from LTST DB database.

4 Discussion

4.1 The effect of electroporation pulse delivery on electrocardiograms

We found no heart arrhythmias or other pathological morphological changes of heartbeat as a consequence of applied EP pulses. No additional premature heartbeats were triggered even in cases when these were present in ECG signal before the first application of EP pulses (signals number 11, 12 and 16). This is in agreement with the results of the work by Al-Khadra et al. [2] that showed no arrhythmias in association with electroporation applied directly on the heart. According to the heart strength-duration curve a very large current would be required to cause a single premature heartbeat [7, 15, 46] for very short EP pulse duration (the microsecond range). Since no additional premature heartbeats were detected, it is highly improbable that EP pulses alone could create the inhomogeneity (altered states of depolarization–repolarization), which is a requisite for onset of fibrillation.

The computer-based analysis demonstrated no significant statistical change in the QTc interval but a significant statistical decrease in the RR and QRS interval after each application of EP pulses (Table 2). This transient effect disappeared within 10 s after each application of EP pulses. The RR and QRS intervals are tightly correlated because they are both dependent on the heartbeat frequency [46]. A significant change in QT interval is one of the most important indicators of arrhythmias [4]. However, its value is also dependent on the heart rate (the faster the heart rate, the shorter the QT interval) and has to be adjusted to aid interpretation. For this reason the QTc interval is used in practice. A significant change in the QTc interval would indicate a clinically relevant effect of electrochemotherapy. However, no such effect was observed in our study (1.89 ms median change of QTc interval after application of EP pulses, see Table 2).

Table 5 ECG signals, ECG lead used, number of heartbeats of particular type, the results of QRS detection and the results of EP pulse delivery

Signal number	Lead name	P	N_d	TP	FN	FP	Se (%)	+P (%)	DER (%)	N_p	TP_p	FN_p	FP_p	Se_p (%)	+P_p (%)	DER_p (%)
1	I	0	461	460	1	1	99.8	99.8	0.4	461	452	9	0	98.0	100.0	2.0
2	I	0	609	607	2	0	99.7	100.0	0.3	609	602	7	0	98.9	100.0	1.1
3[#]	I	0	462	455	7	2	98.5	99.6	1.9	462	415	47	0	89.8	100.0	10.2
4	I	0	354	351	3	2	99.2	99.4	1.4	354	334	20	0	94.4	100.0	5.7
5	I	0	1,716	1,714	2	0	99.9	100.0	0.1	1,716	1,702	14	0	99.2	100.0	0.8
6	II	0	1,822	1,819	3	0	99.8	100.0	0.2	1,822	1,809	13	0	99.3	100.0	0.7
7	II	0	1,635	1,622	13	1	99.2	99.9	0.9	1,635	1,548	87	0	94.7	100.0	5.3
8	I	0	415	415	0	0	100.0	100.0	0.0	415	412	3	0	99.3	100.0	0.7
9	I	1	1,405	1,397	8	2	99.4	99.9	0.7	1,404	1,359	45	0	96.8	100.0	3.2
10[#]	I	1	1,264	1,260	4	0	99.7	100.0	0.3	1,263	991	272	0	78.5	100.0	21.5
11[#]	III	131	795	664	131	0	83.5	100.0	16.5	664	422	242	0	63.6	100.0	36.4
12	II	17	1,348	1,330	18	0	98.7	100.0	1.3	1,331	1,307	24	0	98.2	100.0	1.8
13[#]	I	1	678	666	12	0	98.2	100.0	1.8	677	589	55	0	87.0	100.0	8.1
14[#]	I	0	1,009	1,001	8	6	99.2	99.4	1.4	1,009	540	469	0	53.5	100.0	46.5
15	I	8	798	784	14	0	98.2	100.0	1.8	790	746	44	0	94.4	100.0	5.6
16	I	18	1,384	1,358	26	1	98.1	99.9	2.0	1,366	1,291	75	0	94.5	100.0	5.5
Total	–	177	16,155	15,903	252	15	–	–	–	15,978	14,519	1,426	0	–	–	–
Min	–	0	354	351	0	0	83.5	99.4	0.0	354	334	3	0	53.5	100.0	0.7
25%	–	0	536	534	3	0	98.4	99.8	0.3	536	437	14	0	88.4	100.0	1.5
Median	–	0	904	893	8	0	99.2	100.0	1.1	900	674	45	0	94.6	100.0	5.4
75%	–	5	1,395	1,378	14	2	99.7	100.0	1.8	1,385	1,333	81	0	98.5	100.0	9.1
Max	–	131	1,822	1,819	131	6	100.0	100.0	16.5	1,822	1,809	469	0	99.3	100.0	46.5
Mean	–	11	1,010	994	16	1	98.2	99.9	1.9	999	908	89	0	90.0	100.0	9.7
St. dev.	–	33	501	504	32	2	4.0	0.2	3.9	505	516	129	0	13.6	0.0	13.6

P premature heartbeats of ventricular, supraventricular or ectopic origin; N_d total number of possible detected QRS complexes (normal and abnormal), the sum of TP and FN; TP true positive for QRS detection (the number of correctly detected QRS complexes); FN false negative for QRS detection (the number of missed QRS complexes); FP false positive for QRS detection (the number of false QRS detections); Se sensitivity for QRS detection; +P positive predictivity for QRS detection; DER detection error rate for QRS detection; N_p total number of normal QRS complexes (total number of possible delivered EP pulses), the sum of TP_p and FN_p; TP_p true positive for EP pulses (the number of EP pulses delivered at correctly detected normal QRS complexes); FN_p false negative for EP pulses (the number of correctly detected normal QRS complexes, where no EP pulse was delivered); FP_p false positive for EP pulses (the number of EP pulses delivered in the absence of correctly detected normal QRS complexes); Se_p sensitivity for EP pulses; +P_p positive predictivity for EP pulses; DER_p delivery error rate for EP pulses

[#] ECG signals with relatively poor values of performance metrics

Several studies suggested that there is a link between negative emotions (e.g., anxiety) and the oscillations of RR interval [1, 16, 24, 32, 53, 56]. The most frequently reported symptoms in panic attacks, which are characterized by episodes of intense anxiety, are heart pounding and tachycardia [16, 32]. Another possible reason for RR interval decrease is intrinsic sympathetic activation of the nervous system, occurring in response to stress, exercise, or heart disease [1, 53]. The applications of electrochemotherapy to internal tumors could also directly affect the cardiac tissue if tumors were located close to the heart muscle. However, this effect is highly unlikely for current applications of electrochemotherapy because of relatively large distance between treated tumors and the heart (at

least several centimeters) and due to small inter-electrode distances (8 mm or less). This assumption is further supported by the calculated critical depths for electric current threshold values discussed later in the text. Therefore, we suggest that the observed changes in RR interval can be largely if not completely attributed to anxiety and stress of the patient undergoing electrochemotherapy.

In our study almost one third (30.5%) of the 93 non-synchronized EP applications were delivered within the vulnerable period, which is in accordance with the fact that the duration of the vulnerable period is around one third of the duration of heart cycle [46]. The study of occurrence of ventricular fibrillation after atrial cardioversion performed with transthoracic electrodes pointed out that delivery of

electric pulse, which was not synchronized with the R wave consistently resulted in ventricular fibrillation if the pulse was delivered within the T wave, the vulnerable period of the ventricles [5]. The probability for ventricular fibrillation was decreased but not eliminated with the arrival of synchronized defibrillators for cardioversion [5]. A high percentage of EP pulses delivered during the vulnerable period in our study, when EP application is not synchronized with ECG, underlines the importance of synchronization.

The values of electric field and current in the heart muscle during electroporation are important for evaluation of the danger for inducing ventricular fibrillation. For tissue models (Fig. 2) we estimated critical depths by calculating threshold value of electric field for reversible and irreversible electroporation of the muscle (200 and 450 V/cm, respectively [43]), and threshold value of current for ventricular fibrillation (100 mA for 500 µs-long stimulus [46]) (see Tables 3 and 4). In the study by Galvão et al. [17] they showed that the threshold current that stimulates the heart strongly depends on the age of the animal (i.e., old animals have lower threshold levels). Due to the relatively old patients included in our study (median value 70.8 years) we can therefore assume that the current threshold value is lowered. On the other hand, the EP pulses used in electrochemotherapy are much shorter (100 µs) and therefore the threshold value should in theory be approximately five times greater than for the 500 µs-long stimulus [15, 46]. Furthermore, amplitude threshold for fibrillation for pulsed direct currents is considerably higher than for alternating currents [46]. Currently we have no conclusive information regarding the influence of the repetition frequency of pulsed direct currents on the threshold for fibrillation. Therefore we adopted the threshold value of 100 mA as an estimate of true threshold value. For the needle row array and needle hexagonal array electrodes the critical depth depends on the depth of insertion. The results showed that for the plate electrodes with 8 mm distance between the electrodes the critical depth for threshold current was 2.38 cm (see Table 3). For needle row array and needle hexagonal array electrodes at depth of insertion of 10 mm, the critical depths for threshold current were 3.79 and 4.10 cm, respectively (see Table 4). The critical depth for threshold current for plate electrodes is smaller in comparison to the needle row array or needle hexagonal array electrodes because most of the voltage drop occurs on the skin [33].

With electrodes positioned distantly from the heart (e.g., on a single limb), as in the majority of EP pulse delivery cases (see Table 1), the current traversing the heart is negligible and therefore a smaller risk of accidental cardiac stimulation exists [44]. EP pulses frequently provoke strong and painful muscle contractions [57]. In contrast to the heart muscle, the motor neurons innervating the skeletal muscles, which are located in relative proximity to the electrodes, are always stimulated by EP pulses.

In electrochemotherapy applications included in our study, plate electrodes with distances between the electrodes of 6 and 8 mm and needle hexagonal array electrodes with small depths of insertion (2 or 3 mm) were used (see Table 1). The majority of the EP pulses were delivered on extremities and even when delivered on the trunk they were delivered distantly from the heart. However, two applications of EP pulses were delivered on the chest relatively close to the heart (distance approximately 5 cm) with plate electrodes. Since the heart lies at least 3 cm beneath the skin surface [54], for the applications involved in our study the results of modeling indicated that it is highly unlikely that EP pulses even when applied on the trunk directly above the heart could affect functioning of the heart (critical depths 2.23 and 2.38 cm for needle hexagonal array and plate electrodes, respectively). Furthermore, the most vulnerable part of the heart, the apex, lies behind the breast and is thus additionally protected from the external stimulation by breast tissue. Additionally, if the electrodes were located above sternum or above a rib, the risk of affecting the heart would be further reduced due to low conductivity of bones (range from 0.01 to 0.06 S/m) [34] and larger dimension of sternum and ribs in comparison to the distance between the electrodes. However, if the electrodes were not located directly above the sternum or a rib, the critical depths would be larger due to higher conductivity of the underlying tissues. In this case according to the results of modeling there exists a theoretical chance to affect the functioning of the heart in case of deep insertion of either needle hexagonal or row array electrodes (approximately 4 cm for both types of electrodes at insertion depth of 10 mm). This should be considered in future applications of electrochemotherapy.

For the modeled tissues only the conductivity was taken into account. The capacitive behavior of the tissues was neglected since the transient effects are present only during the charging time of the cell membrane, which lasts around 1 µs [39]. The membrane charging time is much shorter compared to the EP pulse duration used in electrochemotherapy. It was also shown in several studies that static analysis of the electric field distribution during electroporation without taking into account the transient effects are adequate [43, 49, 50], since after the transient effect the tissue exhibits only ohmic behavior [13]. Using current-voltage measurements on cells in vitro [42] or tissues in vivo [13] it was shown that electroporation occurs after the transient time and that the dynamic behavior at the start of the pulses (that includes capacitive behavior of the tissue) is not crucial for the process of electroporation. On the other hand, this transient effect induces a rapid initial current increase followed by an exponential decrease and a

constant level. The applied current during electrochemotherapy is limited to 16 A. Since the transient effect lasts only 1 μs and according to the heart strength-duration curve it is very unlikely that the transient part of an EP pulse could induce ventricular fibrillation [7, 15, 46].

Since the electrode dimensions (electrode–tissue contact surface area) and distance between electrodes used in electrochemotherapy for tumors analyzed in our study are significantly smaller compared to the electrode dimensions and positions used for cardiac defibrillation, we can assume that the differences in thorax tissues conductivities should not change the electric field and current distribution calculated with our numerical models. Therefore, based on the previous studies [9, 26, 34, 43] we can conclude that our numerical models with chosen electrical properties can be used for the evaluation (rough estimate) of critical electric field and current for protruding cutaneous tumors or subcutaneous tumors, which are located immediately under the skin surface (0.5 mm under the skin surface in our study). However, for more deeply located tumors the exact conductivities of all tissues should be incorporated in the numerical model of the thorax.

Recently a new method of local and drug-free tissue ablation called irreversible electroporation has been developed for clinical use as a promising approach to solid tumor therapy [3, 14, 35], prostate ablation [41] and cardiac tissue ablation [28]. In these studies EP pulses with larger amplitudes (up to 3,000 V [11]) and longer durations (range from 100 to 24 ms) are used. The application of EP pulses during irreversible electroporation is therefore more likely to influence functioning of the heart than EP pulses usually applied in electrochemotherapy. However, the results of a recent study by Lavee et al. [28] using irreversible electroporation for epicardial atrial ablation for the treatment of atrial fibrillation showed that ablation pulses (amplitudes of 1,500–2,000 V, duration 100 μs, frequency 5 Hz) caused no permanent arrhythmia or any other rhythm disturbance apart from the rapid atrial pacing during the pulse sequence application. The immediate resumption of sinus rhythm following the ablation was recorded. Similarly, the results of study by Al-Khadra et al. [2] demonstrated lack of any evidence of spontaneous arrhythmias (reentrant or focal) associated with electroporation of the endocardium or the papillary muscles. In their study they presented experimental evidence suggesting that electroporation might even transiently reduce myocardial vulnerability to arrhythmias. But on the other hand, they pointed out that electric pulses of high energy are known to produce a permanent damage, perhaps associated with electroporation. This effect of electroporation may provide a substrate for arrhythmogenesis [2]. Our results of modeling showed

that the critical depths for irreversible electroporation of the muscle/heart (450 V/cm) are 1.07 and 0.93 cm for needle row array and needle hexagonal array electrodes, respectively, at insertion depth 10 mm (Table 3). The critical depth for the plate electrodes is smaller (0.30 cm for 8 mm distance between the electrodes). Since the heart lies at least 3 cm beneath the skin surface [54], for the applications involved in our study the results of modeling indicated that it is impossible to affect functioning of the heart by irreversible electroporation even when EP pulses were applied on the trunk directly above the heart. That would not be the case for electrochemotherapy treatment of internal tumors located close to the heart muscle.

Considering these facts, it is nevertheless advisable to incorporate synchronization of EP pulse delivery with ECG in medical equipment for electroporation in order to maximize safety of the patients especially in future clinical applications. Synchronization of EP pulse delivery with the refractory period of the cardiac cycle is always advisable whenever there is a possibility of EP pulses influencing the functioning of the heart.

4.2 The algorithm for synchronization of electroporation pulse delivery with electrocardiogram

The algorithm for QRS detection and EP pulse delivery reliably detected QRS complexes in all signals recorded during electrochemotherapy (see Table 5). The algorithm would allow for EP pulse delivery only for correctly identified heartbeats with no abnormalities. The performance of our algorithm for QRS detection is similar to that of some other detectors with comparably simple algorithms [6, 47]. The algorithm performed poorly (large *DER*, marked with # in Table 5) for ECG signals with either very unstable R wave amplitudes or RR intervals, or heavy contamination with high-frequency noise with amplitudes similar to R wave, or presence of premature heartbeats not satisfying the dynamic requirements within the QRS complex [12, 29]. In total we found 15 false positive detections (*FP*), which were caused by the occurrence of transient noise having the morphology and the time of appearance so similar to a normal QRS complex that the algorithm could not distinguish them. Many of the false negative detections (*FN*) were due to our self-imposed strict requirements for as few as possible false positive detections (*FP*).

The most appropriate time for EP pulse delivery is before the onset of the vulnerable period since the vulnerable period can sometimes be prolonged (e.g., after premature heartbeat) [46]. Thus delivery of EP pulses immediately after the R wave detection but within the QRS

complex is the most reasonable. The delivery of EP pulses during the vulnerable period of the atria does not present a serious threat for the patient's life. The hemodynamic effects of atrial flutter and fibrillation, which could be potentially caused by EP pulses during the vulnerable period of the atria, are slim and patients are frequently unaware of them [46]. The time reserve for safe EP pulse delivery after the R wave detection and before the onset of the vulnerable period of the ventricles is approximately 60 ms. This time reserve is long enough for safe EP pulse delivery by plate or needle row electrodes and even avoids the vulnerable period of the atria. The requirement for avoiding the delivery of EP pulses at the moments of potential danger for the patient would be fulfilled excellently as indicated by the ideal $+P_p$ values for all ECG signals (see Table 5). However, when using hexagonal electrodes the synchronization becomes irrelevant due to 200 ms-long EP pulse sequence which extends into the vulnerable period of the atria and ventricles. Therefore, a modification of the existing EP pulse delivery protocol for hexagonal electrodes would be needed for safer application in the immediate vicinity of the heart. The suggested solution is to delay the delivery of EP pulses by approximately one half of the current RR interval, which would result in EP pulses being delivered after the vulnerable period provided that the following heartbeat was normal. However, delayed EP pulses would be delivered exactly within the vulnerable period in case of the appearance of premature heartbeat. The other possibility is to synchronize the switching between the electrodes and partial pulse delivery with ECG.

The statistical comparison of performance of the algorithm between ECG signals recorded during electrochemotherapy and ECG signals from the LTST DB database [30] generally showed no statistically significant differences except for positive predictivity for EP pulse delivery ($+P_p$). This performance measure was significantly better for ECG signals recorded during electrochemotherapy than for ECG signals from LTST DB database thus showing that the algorithm was developed for worser conditions than encountered during clinical application of electroporation. In spite of numerous arrhythmias in some ECG signals from the LTST DB database the algorithm performed excellently [30]. The clinical electrochemotherapy was so far indicated only for patients without clinically significant or severe heart disease, which reflects in ideal value $+P_p = 100\%$ in all ECG signals recorded during electrochemotherapy. However, mostly old patients are included in electrochemotherapy treatment nowadays because of the emerging need for palliative treatment of tumors with electrochemotherapy. With the increasing age of the patients, the probability for encountering pathological ECG is also increasing,

therefore, the synchronization of EP pulse delivery with ECG would maximize safety of the patient.

5 Conclusions

Currently used electroporation protocols could interfere with functioning of the heart although no such practical evidence exists till now. Because no systematic study regarding this topic has been done yet, we examined in our study the effects of EP pulses on functioning of the heart. We measured ECG signals during electrochemotherapy and analyzed their characteristics. We found no arrhythmias or other pathological morphological changes due to application of EP pulses. The only demonstrated effect of EP pulses on ECG is a transient RR interval decrease. The facts contributing to a belief that EP pulse delivery during electrochemotherapy cannot affect functioning of the heart are: short EP pulse duration, use of direct current, application mainly on locations relatively distant from the heart (i.e., on extremities), and small inter-electrode distance. On the other hand, there are some open issues regarding electrochemotherapy that need to be considered, for example: EP pulses delivered by plate or needle row electrodes that are not synchronized with ECG could be delivered within the vulnerable period, EP pulses delivered by hexagonal electrodes mainly coincide within the vulnerable period, the threshold levels of the heart for elderly patients are lowered, possible use of electrochemotherapy on patients with clinically significant heart disease, new applications with longer durations and/or higher amplitudes of EP pulses as well as applications involving endoscopic or surgical means to access internal tumors are being developed. Even though no practical evidence for electroporation having an effect on functioning of the heart has been observed so far, we can still maximize safety of the patients by incorporating the algorithm for synchronization of EP pulse delivery with ECG in medical equipment for EP pulse delivery. The usual application of eight EP pulses with duration 100 μs each can benefit from synchronizing delivery of EP pulses with electrocardiogram but this is not the case for hexagonal electrodes or combination of high- and low-voltage EP pulses and pulses with higher amplitudes as used in tumor tissue ablation by irreversible electroporation.

References

1. Acharya UR, Joseph KP, Kannathal N, Lim CM, Suri JS (2006) Heart rate variability: a review. Med Biol Eng Comput 44:1031–1051

2. Al-Khadra A, Nikolski V, Efimov IR (2000) The role of electroporation in the fibrillation. Circ Res 87:797–804

3. Al-Sakere B, Bernat C, André F, Connault E, Opolon P, Davalos RV, Mir LM (2007) A study of the immunological response to tumor ablation with irreversible electroporation. Technol Cancer Res Treat 6:301–305

4. Anderson ME (2006) QT interval prolongation and arrhythmia: an unbreakable connection? J Intern Med 259:81–90

5. Ayers GM, Alferness CA, Ilina M, Wagner DO, Sirokman WA, Adams JM, Griffin JC (1994) Ventricular proarrhythmic effects of ventricular cycle length and shock strength in a sheep model of transvenous atrial defibrillation. Circulation 89:413–422

6. Benitez DS, Gaydecki PA, Zaidi A, Fitzpatrick AP, Laguna P (2000) A new QRS detection algorithm based on the Hilbert transform. IEEE Comput Cardiol 27:379–382

7. Bruner JMR, Leonard PF (1989) Electricity, safety, and the patient. Year Book Medical Publishers, Inc., Chicago

8. Bureau MF, Gehl J, Deleuze V, Mir LM, Scherman D (2000) Importance of association between permeabilization and electrophoretic forces for intramuscular DNA electrotransfer. Biochim Biophys Acta 1474:353–359

9. Camacho MA, Lehr JL, Eisenberg SR (1995) A three-dimensional finite element model of human transthoracic defibrillation: paddle placement and size. IEEE Trans Biomed Eng 42:572–578

10. Chen C, Smye SW, Robinson MP, Evans JA (2006) Membrane electroporation theories: a review. Med Biol Eng Comput 44:5–14

11. Clayton RH, Holden AV (2000) Re-entry in computational models of heterogenous and abnormal myocardium. Int J Bioelectromagn, available online: http://www.rgi.tut.fi/ijbem/volume2/number2/clayton/paper_ijbem.htm

12. Cuesta-Frau D, Biagetti MO, Quinteiro RA, Micó-Tormos P, Aboy M (2007) Unsupervised classification of ventricular extrasystoles using bounded clustering algorithms and morphology matching. Med Biol Eng Comput 45:229–239

13. Cukjati D, Batiuskaite D, André F, Miklavcic D, Mir LM (2007) Real time electroporation control for accurate and safe in vivo non-viral gene therapy. Bioelectrochemistry 70:501–507

14. Davalos RV, Mir LM, Rubinsky B (2005) Tissue ablation with irreversible electroporation. Ann Biomed Eng 33:223–231

15. Fish RM, Geddes LA, Babbs CF (2003) Medical and bioengineering aspects of electrical injuries. Lawyers and Judges Publishing Company, Arizona

16. Friedman BH, Thayer JF (1998) Autonomic balance revisited: panic anxiety and heart rate variability. J Psychosom Res 44:133–151

17. Galvão KM, Mateus EF, Gomes PAP (2001) Electric stimulation of isolated hearts: age dependance of the threshold electric field. Memorias II Congreso Latinoamericano de Ingeniería Biomédica 950-7132-57-5 (c)

18. Heller R, Jaroszeski M, Atkin A, Moradpour D, Gilbert R, Wands J, Nicolau C (1996) In vivo gene electroinjection and expression in rat liver. FEBS Lett 389:225–228

19. Heller R, Jaroszeski MJ, Reintgen DS, Puleo CA, DeConti RC, Gilbert RA, Glass LF (1998) Treatment of cutaneous and subcutaneous tumors with electrochemotherapy using intralesional bleomycin. Cancer 83:148–157

20. Heller LC, Heller R (2006) In vivo electroporation for gene therapy: review. Hum Gene Ther 17:890–897

21. Hofmann GA (2000) Instrumentation and electrodes for in vivo electroporation. In: Jaroszeski MJ, Heller R, Gilbert R (eds) Electrochemotherapy, electrogenetherapy, and transdermal drug delivery: electrically mediated delivery of molecules to cells. Humana, Totowa

22. Houghton AR, Gray D (1997) Making sense of the ECG: a hands-on guide. Arnold, London

23. Jager F, Taddei A, Moody GB, Emdin M, Antolic G, Dorn R, Smrdel A, Marchesi C, Mark RG (2003) Long-term ST database: a reference for the development and evaluation of automated ischaemia detectors and for the study of the dynamics of myocardial ischaemia. Med Biol Eng Comput 41:172–182

24. Johnsen BH, Thayer JF, Laberg JC, Wormnes B, Raadal M, Skaret E, Kvale G, Berg E (2003) Attentional and physiological characteristics of patients with dental anxiety. J Anxiety Disord 17:75–87

25. Jones M, Geddes LA (1977) Strength-duration curves for cardiac pacemaking and ventricular fibrillation. Cardiovasc Res Cent Bull 15:101–112

26. Karlon WJ, Lehr JL, Eisenberg SR (1994) Finite element models of thoracic conductive anatomy: sensitivity to changes in inhomogeneity and anisotropy. IEEE Trans Biomed Eng 41:1010–1017

27. Kirchhof PF, Fabritz CL, Zabel M, Franz MR (1996) The vulnerable period for low and high energy T-wave shocks: role of dispersion of repolarization and effect of D-sotalol. Cardiovasc Res 31:953–962

28. Lavee J, Onik G, Mikus P, Rubinsky B (2007) A novel non-thermal energy source for surgical epicardial atrial ablation: irreversible electroporation. Heart Surg Forum 10:96–101

29. Lin CH (2006) Classification enhancible grey relational analysis for cardiac arrhythmias discrimination. Med Biol Eng Comput 44:311–320

30. Mali B, Jarm T, Jager F, Miklavcic D (2005) An algorithm for synchronization of in vivo electroporation with ECG. J Med Eng Technol 29:288–296

31. Marty M, Sersa G, Garbay JR, Gehl J, Collins CG, Snoj M, Billard V, Geertsen PF, Larkin JO, Miklavcic D, Pavlovic I, Paulin-Kosir SM, Cemazar M, Morsli N, Soden DM, Rudolf Z, Robert C, O'Sullivan GC, Mir LM (2006) Electrochemotherapy—an easy, highly effective and safe treatment of cutaneous and subcutaneous metastases: results of ESOPE (European Standard Operating Procedures of Electrochemotherapy) study. Eur J Cancer Suppl 4:3–13

32. McCraty R, Atkinson M, Tomasino D, Stuppy WP (2001) Analysis of twenty-four hour heart rate variability in patients with panic disorder. Biol Psychol 56:131–150

33. Miklavcic D, Corovic S, Pucihar G, Pavselj N (2006) Importance of tumour coverage by sufficiently high local electric field for effective electrochemotherapy. Eur J Cancer Suppl 4:45–51

34. Miklavcic D, Pavselj N, Hart FX (2006) Electric properties of tissues. In: Wiley encyclopedia of biomedical engineering. Wiley, New York

35. Miller L, Leor J, Rubinsky B (2005) Cancer cells ablation with irreversible electroporation. Technol Cancer Res Treat 4:1–7

36. Mir LM, Glass LF, Sersa G, Teissie J, Domenge C, Miklavcic D, Jaroszeski MJ, Orlowski S, Reintgen DS, Rudolf Z, Belehradek M, Gilbert R, Rols MP, Belehradek J Jr, Bachaud JM, DeConti R, Stabuc B, Cemazar M, Coninx P, Heller R (1998) Effective treatment of cutaneous and subcutaneous malignant tumors by electrochemotherapy. Br J Cancer 77:2336–2342

37. Mir LM, Orlowski S (1999) Mechanisms of electrochemotherapy. Adv Drug Deliv Rev 35:107–118

38. Neumann E, Schaefer-Ridder M, Wang Y, Hofschneider PH (1982) Gene transfer into mouse lyoma cells by electroporation in high electric fields. EMBO J 1:841–845

39. Neumann E, Sowers AE, Jordan CA (1989) Electroporation and electrofusion in cell biology. Plenum Press, New York

40. Niu G, Heller R, Catlett-Falcone R, Coppola D, Jaroszeski M, Dalton W, Jove R, Yu H (1999) Gene therapy with dominant-negative Stat3 suppresses growth of the murine melanoma B16 tumor in vivo. Cancer Res 59:5059–5063

41. Onik G, Mikus P, Rubinsky B (2007) Irreversible electroporation: implications for prostate ablation. Technol Cancer Res Treat 6:295–300

42. Pavlin M, Kanduser M, Rebersek M, Pucihar G, Hart FX, Magjarevic R, Miklavcic D (2005) Effect of cell electroporation on the conductivity of a cell suspension. Biophys J 88:4378–4390

43. Pavselj N, Bregar Z, Cukjati D, Batiuskaite D, Mir LM, Miklavcic D (2005) The course of tissue permeabilization studied on a mathematical model of a subcutaneous tumour in small animals. IEEE Trans Biomed Eng 52:1373–1381

44. Prausnitz MR (1996) The effects of electric current applied to skin: a review for transdermal drug delivery. Adv Drug Deliv Rev 18:395–425

45. Rebersek M, Faurie C, Kanduser M, Corovic S, Teissié J, Rols MP, Miklavcic D (2007) Electroporator with automatic change of electric field direction improves gene electrotransfer in vitro. Biomed Eng Online 6:25

46. Reilly JP (1998) Applied bioelectricity: from electrical stimulation to electropathology. Springer, New York

47. Ruha A, Sallinen S, Nissilä S (1997) A real-time microprocessor QRS detector system with a 1-ms timing accuracy for the measurement of ambulatory HRV. IEEE Trans Biomed Eng 44:159–167

48. Satkauskas S, Bureau MF, Puc M, Mahfoudi A, Scherman D, Miklavcic D, Mir LM (2002) Mechanisms of in vivo DNA electrotransfer: respective contributions of cell electropermeabilization and DNA electrophoresis. Mol Ther 5:133–140

49. Sel D, Macek Lebar A, Miklavcic D (2007) Feasibility of employing model-based optimization of pulse amplitude and electrode distance for effective tumor electropermeabilization. IEEE Trans Biomed Eng 54:773–781

50. Sel D, Cukjati D, Batiuskaite D, Slivnik T, Mir LM, Miklavcic D (2005) Sequential finite element model of tissue electropermeabilization. IEEE Trans Biomed Eng 52:816–827

51. Sersa G, Cufer T, Cemazar M, Miklavcic D, Rebersek M, Rudolf Z (2000) Electrochemotherapy with bleomycin in the treatment of hypernephroma metastasis: case report and literature review. Tumori 86:163–165

52. Sersa G (2006) The state-of-the-art of electrochemotherapy before the ESOPE study; advantages and clinical uses. Eur J Cancer Suppl 4:52–59

53. Task Force of the European Society of Cardiology, the North American Society of Pacing and Electrophysiology (1996) Heart rate variability: standards of measurement, physiological interpretation, and clinical use. Eur Heart J 17:354–381

54. The visible human project. National Library of Medicine, United States, online: http://www.nlm.nih.gov/research/visible/visible_human.html

55. Wiggers CJ, Wégria R (1940) Ventricular fibrillation due to single, localized induction and condenser shocks applied during the vulnerable phase of ventricular systole. Am J Physiol 128:500–505

56. Yeragani VK, Balon R, Pohl R, Ramesh C, Glitz D, Weinberg P, Merlos B (1990) Decreased R-R variance in panic disorder patients. Acta Psychiatr Scand 81:554–559

57. Zupanic A, Ribaric S, Miklavcic D (2007) Increasing the repetition frequency of electric pulse delivery reduces unpleasant sensations that occur in electrochemotherapy. Neoplasma 54:246–250

Paper XI

Research

Electroporator with automatic change of electric field direction improves gene electrotransfer *in-vitro*

Matej Reberšek[1], Cécile Faurie[2], Maša Kandušer[1], Selma Čorović[1], Justin Teissié[2], Marie-Pierre Rols[2] and Damijan Miklavčič*[1]

Address: [1]University of Ljubljana, Faculty of Electrical Engineering, Tržaška 25, SI-1000 Ljubljana, Slovenia and [2]Institut de Pharmacologie et de Biologie Structurale du CNRS UMR 5089, 205, route de Narbonne, 31077 Toulouse cedex, France

Email: Matej Reberšek - matej.rebersek@fe.uni-lj.si; Cécile Faurie - faurie.cecile@laposte.net; Maša Kandušer - masa.kanduser@fe.uni-lj.si; Selma Čorović - selma.corovic@fe.uni-lj.si; Justin Teissié - justin.teissie@ipbs.fr; Marie-Pierre Rols - marie-pierre.rols@ipbs.fr; Damijan Miklavčič* - damijan.miklavcic@fe.uni-lj.si

* Corresponding author

Abstract

Background: Gene electrotransfer is a non-viral method used to transfer genes into living cells by means of high-voltage electric pulses. An exposure of a cell to an adequate amplitude and duration of electric pulses leads to a temporary increase of cell membrane permeability. This phenomenon, termed electroporation or electropermeabilization, allows various otherwise non-permeant molecules, including DNA, to cross the membrane and enter the cell. The aim of our research was to develop and test a new system and protocol that would improve gene electrotransfer by automatic change of electric field direction between electrical pulses.

Methods: For this aim we used electroporator (EP-GMS 7.1) and developed new electrodes. We used finite-elements method to calculate and evaluate the electric field homogeneity between these new electrodes. Quick practical test was performed on confluent cell culture, to confirm and demonstrate electric field distribution. Then we experimentally evaluated the effectiveness of the new system and protocols on CHO cells. Gene transfection and cell survival were evaluated for different electric field protocols.

Results: The results of *in-vitro* gene electrotransfer experiments show that the fraction of transfected cells increases by changing the electric field direction between electrical pulses. The fluorescence intensity of transfected cells and cell survival does not depend on electric field protocol. Moreover, a new effect a shading effect was observed during our research. Namely, shading effect is observed during gene electrotransfer when cells are in clusters, where only cells facing negative electro-potential in clusters become transfected and other ones which are hidden behind these cells do not become transfected.

Conclusion: On the basis of our results we can conclude that the new system can be used in *in-vitro* gene electrotransfer to improve cell transfection by changing electric field direction between electrical pulses, without affecting cell survival.

1. Background

Gene therapy is an experimental method used in clinics proven to be successful in *in-vitro* and *in-vivo* conditions. For gene therapy, DNA or RNA molecules are transferred into living cells to replace, change or silence gene expression. Consequently cells change their biological nature in therapeutical purposes [1,2]. Effective and potentially safe transfer of DNA molecules into living cells has been a goal of scientific research for many years. This research is now divided into two main fields: viral and non-viral gene delivery. Viral vectors are considered to provide the highest effectiveness of DNA transfer, but they are often associated with immune responses [3] and insertional mutagenesis [4-6]. That is why non-viral methods of DNA transfer are being sought for [7-9].

An exposure of a cell to adequate amplitude and duration of electric pulses leads to temporary increase of cell membrane permeability while preserving cell viability. This phenomenon, termed electroporation or electropermeabilization, allows various otherwise non-permeant molecules to cross the membrane and enter the cell. Both *in-vitro* and *in-vivo*, reversible electropermeabilization allows for internalization of a wide range of substances [10,11]. When DNA molecules are transferred into cells by electropermeabilization, this method is called gene electrotransfer. Gene electrotransfer is therefore a non-viral method used to transfer DNA molecules into living cells by means of high-voltage electric pulses [11-16]. Being extensively investigated, gene electrotransfer is becoming more and more effective and therefore gaining importance as a non-viral gene therapy method [7,9].

Electropermeabilization of the cell occurs in the area of cell membrane facing negative and positive electro-potential regarding intercellular potential [17,18]. However, DNA molecules do not spontaneously interact with mammalian cell membrane but are driven to the membrane by electrophoretic forces. Therefore, negative DNA molecules only interact with the cell membrane facing negative electro-potential. Thus, only one side of cell membrane is susceptible for transfer of DNA molecules. Any increase in the susceptible area for transfer of DNA molecules therefore increases the effectiveness of transfection [19,20].

Changing the electric field direction between electrical pulses presumably increases the area of successful electropermeabilization [21] and therefore increases susceptible area for transfer of DNA molecules. This method is especially effective for cells *in-vivo* and also for plated cells *in-vitro*, because their cell shapes and their orientations in the electric field are important for successful electropermeabilization [22-24]. Changing the polarity of electric field during the electric pulse delivery is also important for gene electrotransfer as it allows interaction of DNA mole-

cules on both sides of the cell membrane perpendicular to direction of electric field (changing the electric field polarity corresponds to changing the electric field direction for 180°). Changing the electric field direction between electrical pulses therefore improves the efficiency of gene electrotransfer indirectly by increasing the area of successful electropermeabilized membrane, or directly by interaction of DNA molecules with the cell membrane on both sides.

The protocol that defines changes of electric field direction between electrical pulses is referred to as the electric field protocol. Researchers who had already investigated influence of electric field protocol on the gene electrotransfer did not use any of the existing systems for automatic change of electric field direction between electrical pulses. That is because they did not have any electrodes which would allow delivery of electric field protocols with relatively homogeneous electric field intensity. Because of that they had to change the electric field direction by rotating the electrodes manually, which however is not always possible [20]. Nevertheless similar research, with or without such automatic system, had also been done in electrochemotherapy, but predominantly with the aim of improving electric field distribution including its homogeneity [21,25].

The aim of our research was to develop and test new system and protocol which would improve gene electrotransfer by automatic change of electric field direction between electrical pulses. For this we chose an electroporator, which can control at least four electrodes. In addition, we designed new electrodes made of four cylindrical rods that provides as homogeneous electric field distribution as possible. We calculated the distribution of electric field numerically for given electrode design and electric field protocol. New system and protocols were tested experimentally on Chinese Hamster Ovary cells. *In-vitro* gene transfection and cell survival were evaluated for different electric field protocols by fluorescence microscopy. A shading effect, previously not yet described in scientific literature was observed during our research.

2. Methods

A new system for gene electrotransfer was developed which consists of an electroporator (EP-GMS 7.1, Fig. 1a) and specially designed new electrodes (E-S 4.1, Fig. 1b). Both were developed at the University of Ljubljana, Faculty of Electrical Engineering. The EP-GMS 7.1 electroporator was already used and described in previously reported studies [26,27]. The main advantage of this electroporator is the ability to automatically change the electric field direction between electrical pulses at various frequencies, without rotation or movement of electrodes.
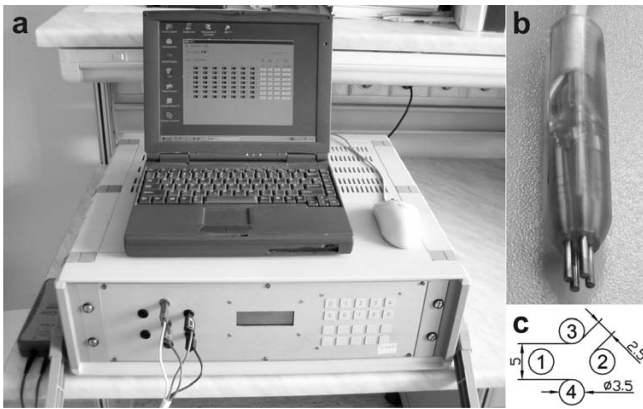
Figure 1
A new system for gene electrotransfer. Photograph of the electroporator EP-GMS 7.1 (a), photograph of the electrodes E-S 4.1 (b) and electrodes E-S 4.1 geometry design (c). Electrodes are numbered. Their diameter is 3.5 mm. Electrodes 1 and 2 or 3 and 4 are opposite electrodes and are 5 mm apart. Adjacent electrodes are 2.5 mm apart, which is a half distance between opposite electrodes.

2.1 Electroporator (EP-GMS 7.1) and electrodes (E-S 4.1)

The user defines electrical parameters of applied electric pulse through the interface of the electroporator (EP-GMS 7.1) on a personal computer (PC). Parameters are then transferred to the executive part of the electroporator. After this transfer the electroporator is ready to generate defined electric pulses in predefined directions.

Electroporator (EP-GMS 7.1) generates from 1 to 32 square electric pulses from 80 to 400 V, duration from 10 to 1000 µs and repetition frequency from 0.1 to 5000 Hz. Particularity of this electroporator is an embedded electrode commutator which controls up to seven electrodes. This commutator applies one of three possible states to each of the electrodes: positive, negative or high impedance state. Electrode state change is accomplished within 12 ms thus the electric field direction between the electrodes can be changed.

The electrodes (E-S 4.1) were designed as four cylindrical rods that allow delivery of electric field in different directions and at the same time providing relatively homogeneous electric field distribution. Delivery of electric field in all directions can be achieved by two sinusoidal signals phase shifted for 90°, which are delivered on two pairs of opposite electrodes (e.g. 1–2 and 3–4, Fig. 1c). However, for that different electroporator should be used, which allows delivery of such sinusoidal signals.

The electrodes are made of stainless steel; their diameter is 3.5 mm, adjacent electrodes are 2.5 mm apart, opposite electrodes are 5 mm apart, their length is 18 mm (Fig. 1c).

Electrodes are connected to 4-wire cable and fixed with polyester resin, which assures constant distance between the electrodes and also protects the user against high-voltage.

Four different electric field protocols were used with this new system (electroporator and electrodes) in our experiments: single polarity (SP), both polarities (BP), orthogonal single polarity (OSP) and orthogonal both polarities (OBP; Fig. 2). When SP electric field protocol is used, single polarity electric pulses are applied between two opposite electrodes (Fig. 2a). When BP electric field protocol is used, both polarities electric pulses are applied between two opposite electrodes (Fig. 2b). When OSP electric field protocol is used, single polarity electric pulses are applied alternately between two pairs of opposite electrodes (Fig. 2c). And when OBP electric field protocol is used, both polarities electric pulses are applied alternately between two pairs of opposite electrodes (Fig. 2d).

2.2 Electric field intensity

Electric field intensity between the electrodes during the electric pulse delivery was calculated numerically by means of finite-elements method (Fig. 3a–c) [28] and a quick practical test was performed to confirm the correct-
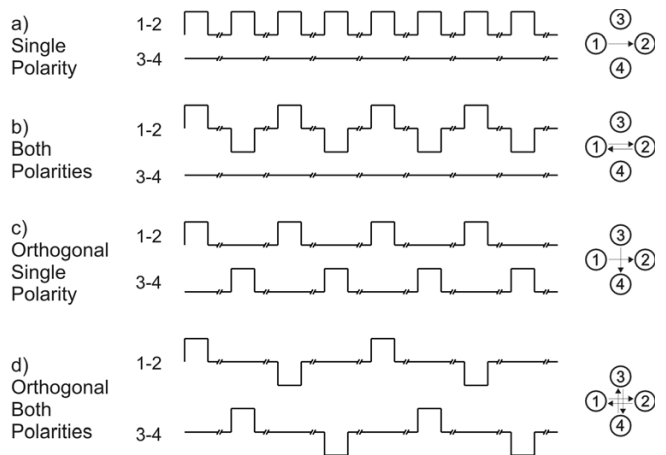

Figure 2
Electric field protocols. In single polarity (SP) electric field protocol direct electric pulses are applied between two opposite electrodes. While in both polarities (BP) electric field protocol alternating electric pulses are applied between two opposite electrodes. In orthogonal single polarity (OSP) electric field protocol direct electric pulses are applied between both opposite pairs of electrodes. While in orthogonal both polarities (OBP) electric field protocol alternating electric pulses are applied between both opposite pairs of electrodes. Signals in the middle represent applied voltage to the electrodes. Symbols on the right represent electric field protocols in which arrows represent directions of electric field in the centre between the electrodes.
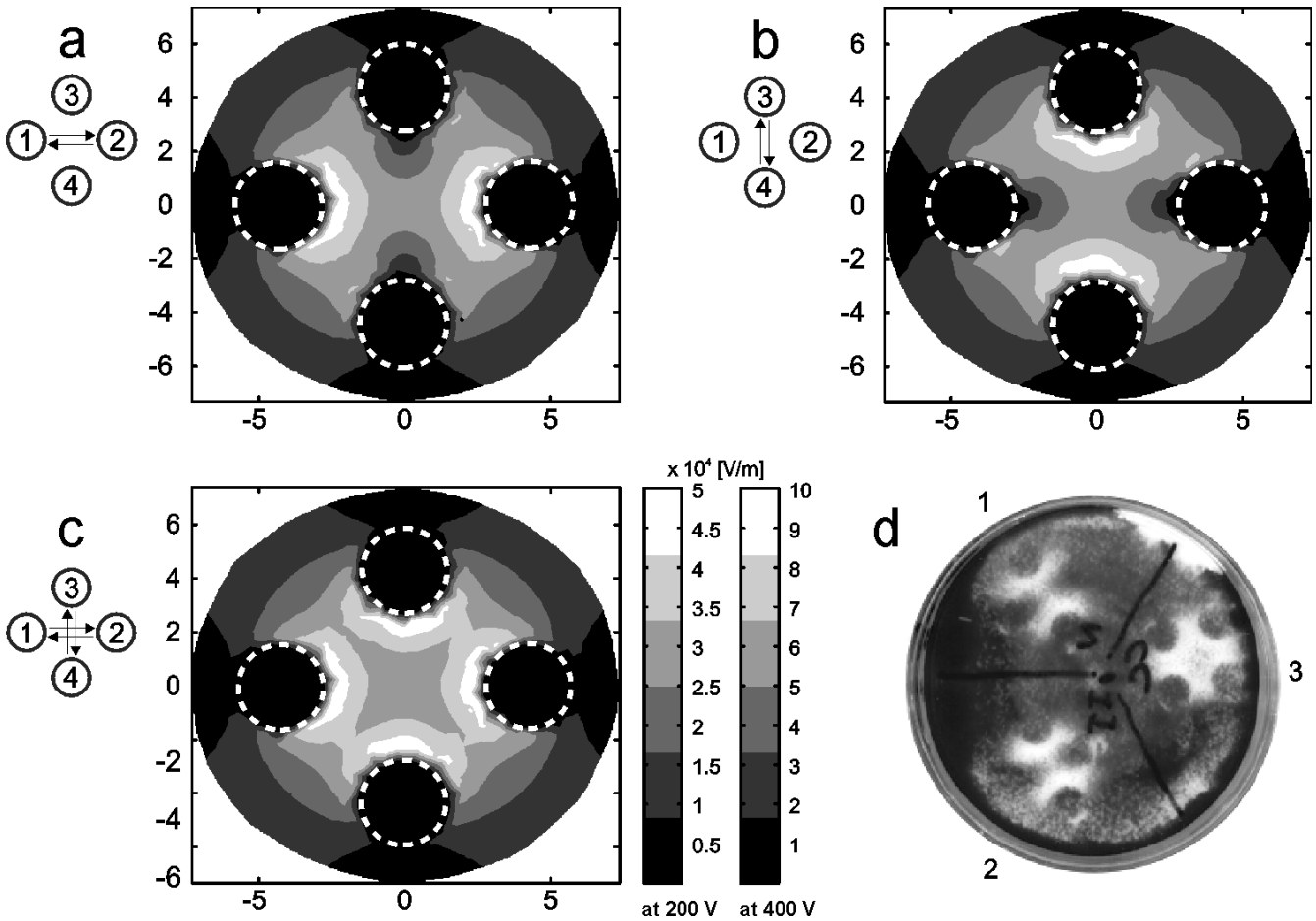
Figure 3
Calculated electric field intensity between the electrodes. Calculated electric field intensity between the electrodes during the electric pulse delivery of 200 V (+100 V, -100 V) and 400 V (+200 V, -200 V), when electrical pulses are applied between electrodes 1 and 2 (a) and when they are applied between electrodes 3 and 4 (b). Calculated local maxima of electric field intensity between the electrodes in orthogonal single polarity (OSP) and orthogonal both polarities (OBP) electric field protocol (c). Dashed circles represents position of electrodes. Symbols on the left represent electric field protocols. Electric field intensity scale is given for 200 V and 400 V. Experimental electric field intensity between the electrodes E-S 4.1 during the electric pulse delivery (d), when electrical pulses are applied between electrodes 1 and 2 (d1) and when they are applied between electrodes 3 and 4 (d2). Experimental local maxima of electric field intensity between the electrodes, when electrical pulses are applied between electrodes 1 and 2 and between electrodes 3 and 4 (d3). A train of eight electric pulses with amplitude of 400 V (+200 V, -200 V), duration 1 ms and repetition frequency 1 Hz was applied.

ness of calculations and demonstrate electric field intensity distribution (Fig. 3d).

A three-dimensional finite-elements model of an electroporation medium in culture dish with inserted electrodes (E-S 4.1) was designed using software package EMAS (ANSOFT Corporation, USA). Applied voltage was modelled as Dirichlet's boundary condition on the surface which presents the cross-section of electrode and cell suspension. Electro-potential of disconnected electrodes was defined as zero, because our model is symmetrical and disconnected electrodes are always in the middle between the connected electrodes. Electro-potential of disconnected electrodes was also defined as zero, to satisfy the conditions that electrodes are a lot more conductive then electroporation medium and that the sum of current through the entire surface to disconnected electrodes is always zero. Electroporation medium was mathematically separated from surrounding area by Neuman's boundary condition:

$$J_N = 0, \qquad\qquad (1)$$
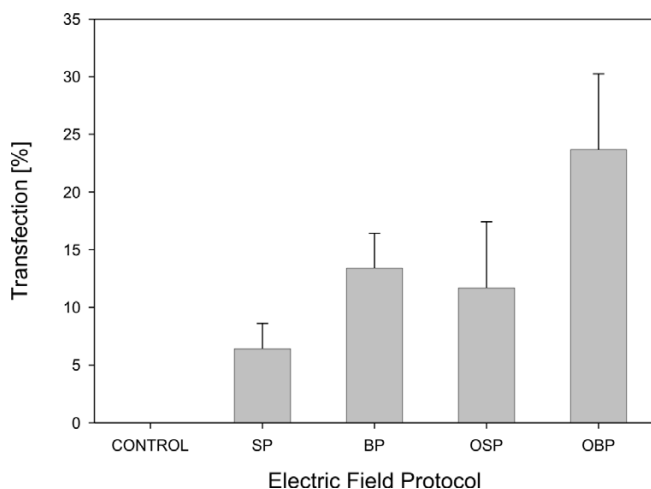
Figure 4
Fraction of transfected CHO cells. Fraction of transfected CHO cells after gene electrotransfer experiment in different electric field protocol. Cells were exposed to a train of eight pulses with amplitude of 200 V, duration 1 ms and repetition frequency 1 Hz. Results were obtained by means of fluorescence microscopy. Each value in the graph represent mean of four independent experiments, ± standard deviation. Electric field protocols result in different fraction of transfected cells (ANOVA: P = 0.002).

where J_N is the normal electric current density [A/m²]. Electroporation medium was modelled as a constant i.e. independent of electric field applied, passive, homogeneous and isotropic volume conductor in the quasi-stationary electric current field. A condition in such structure is described by Laplace's equation:

$$\Delta\phi = 0, \qquad (2)$$

where ϕ is electric potential [V]. Results of electric field intensity obtained by such linear model are scalable by applied voltage ratio (Fig. 3).

To calculate the electric field intensity, when electrical pulses are applied between electrodes 1 and 2 (Fig. 3a), boundary conditions on the surface of the electrode 1 were set to +100 V and on the electrode 2 to -100 V. Electrodes 3 and 4 were in this case set to 0 V and thus defined as disconnected. Calculation of electric field intensity, when electrical pulses are applied between electrodes 3 and 4 (Fig. 3b), was done in the similar way as calculation of electric field intensity, when electrical pulses are applied between electrodes 1 and 2. Local maxima of both electric field intensities (Fig. 3c) were calculated to evaluate effectiveness of OSP and OBP electric field protocol [29].

Results of calculations have shown that electric field intensity in the space between the electrodes is very homogeneous compared to electric field intensity between two cylindrical rods, because of the two additional rods, which are highly conductive with respect to electroporation medium, are equalizing the distances between the equipotential lines in the space between the electrodes.

Quick practical test was performed on confluent cell culture in plastic culture dish. To confirm and demonstrate electric field distribution, plastic culture dish was separated into three sections (Fig. 3d). A train of eight electric pulses with amplitude of 400 V (+200 V, -200 V), duration 1 ms and repetition frequency 1 Hz was applied to kill the cells exposed to highest electric field intensity. In the first section electric pulses were applied between electrodes 1 and 2 (Fig. 3d1). In the second section electric pulses were applied between electrodes 3 and 4 (Fig. 3d2). In the third section electric pulses were applied between electrodes 1 and 2 and between electrodes 3 and 4 (Fig. 3d3). After 24 hours, killed cells were washed out and living cells were fixed in plastic culture dish with methanol for 10 minutes and stained with crystal violet.

2.3 Cells, cell survival and gene electrotransfer
Chinese Hamster Ovary (CHO; European Collection of Cell Cultures, Great Britain) cells were used. Cells in suspension were cultured in Eagle's Minimum Essential Medium (MEM; Sigma, USA) supplemented with 10 % Foetal Calf Serum (FCS; Sigma, USA). When cell suspension density reached 2×10^6 cells/ml, it was diluted with culture medium. For experiments, 5×10^5 cells were plated in a plastic culture dish (growth surface: 9.2 cm², diameter: 40 mm, height: 11 mm; TPP, Switzerland) and grown in the incubator (37°C, 5% CO$_2$) for 24 hours. During that time they attached to the surface of the culture dish and started to divide.

For gene electrotransfer experiments, plasmid DNA pEGFP-C1 (Clontech, USA; 4649 base pairs), which expresses green fluorescent protein (GFP, excitation 488 nm, emission 507 nm) under promoter cytomegalovirus, was added in concentration 40 μg/ml to the electroporation medium (10 mM phosphate buffer K$_2$HPO$_4$/KH$_2$PO$_4$, 1 mM MgCl, 250 mM sucrose; pH: 7.4, conductivity: 0.14 S/m). Culture medium was removed and 100 μl drop of electroporation medium containing plasmids was placed between electrodes. A train of eight electric pulses with amplitude of 200 V (+100 V, -100 V), duration 1 ms and repetition frequency 1 Hz was applied according to previous results [19,20]. Four different electric field protocols were used as described previously in subsection 2.1: single polarity (SP), both polarities (BP), orthogonal single polarity (OSP) and orthogonal both polarities
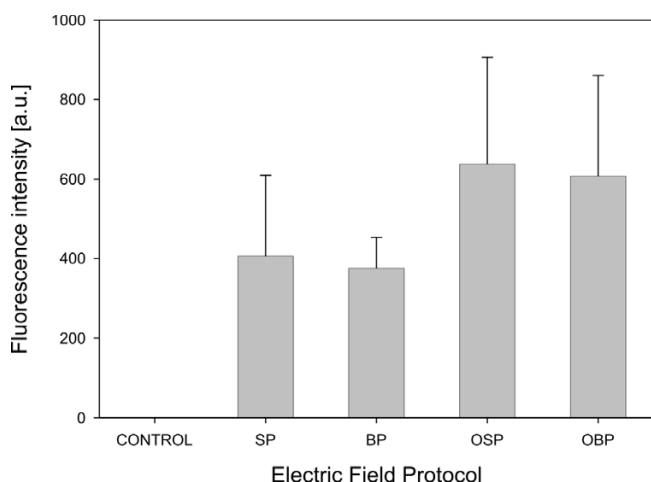
Figure 5
Fluorescence intensity of transfected CHO cells. Fluorescence intensity of transfected CHO cells after gene electrotransfer experiment in influence of electric field protocol. Cells were exposed to a train of eight pulses with amplitude of 200 V, duration 1 ms and repetition frequency 1 Hz. Results were obtained by means of fluorescence microscopy. Each value in the graph represent mean of four independent experiments, ± standard deviation. Different electric field protocols did not result in different level of fluorescence intensity (ANOVA: P = 0.246).

(OBP) (Fig. 2), to determine gene expression. In the control, cells were not exposed to electric pulses.

After electroporation, cells were left for 15 min at room temperature for cell membrane resealing. Then 2 ml of culture medium was added and culture dishes were then placed into incubator (37°C, 5% CO_2). 24 hours after electroporation, cells were investigated under inverted fluorescence microscope (Axiovert 200, Zeiss, Germany). Five photos of phase contrast and fluorescence images were taken per sample randomly in the area in the centre between the electrodes with cooled CCD camera (12 bit; VisiCam, Germany). Objective magnification was 20× and approximately 100 cells per image were observed. For fluorescence imaging, excitation wavelength 425 nm (Polycome IV, Visitron Systems, Germany), dichroic mirror (460 DCLP; Chroma, USA) and emission filter (D505/40 m; Chroma, USA) were used.

MetaMorph (Version 5.0r7, Universal Imaging Corporation, USA) was used for image analysis. The fraction of transfected cells was calculated as the ratio between transfected cells and all viable cells in a given treatment. The fluorescence intensity of transfected cells related to quantity of GFP inside the transfected cells was quantified on acquired images by MetaMorph. The fraction of cell survival was calculated as the ratio between viable cells in

treatment and viable cells in control, which were not treated with electric pulses. Independent experiments of gene electrotransfer were repeated four times. Results (the fraction of transfected cells, the fluorescence intensity of transfected cells and the fraction of cell survival) are given in a form of bar graphs (SigmaPlot 9.0, Systat, USA), where every point represents the mean of four independent experiments and the error bars indicate the standard deviation (Fig. 4, 5). Statistical tests One way analysis of variance (One Way ANOVA) were performed on all results (SigmaStat 3.1, Systat, USA). Bonferroni t-test was performed on results if there was indication of a statistically significant difference between different electric field protocols used.

To visualize interaction of DNA with cell membrane immediately after application of electric pulses, we stained plasmid DNA pEGFP-C1 with thiazole orange homodimer dye (TOTO-1, excitation 514 nm, emission 533 nm; Molecular Probes, USA). Plasmid DNA pEGFP-C1 was mixed with TOTO-1 by base pair to dye ratio of 5 and placed on ice for 1 hour [30]. Electropermeabilization procedure was the same as for gene electrotransfer, except that only two different electric field protocols were used as described previously in subsection 2.1: single polarity (SP) and both polarities (BP; Fig. 2), to determine areas of DNA interaction with cell membranes (Fig. 6a, b). Up to 5 minutes after electropermeabilization photos of phase contrast and fluorescence images of cells were taken under inverted fluorescence microscope (Fig. 7, 8). For fluorescence imaging excitation wavelength 480 nm (Polycome IV, Visitron Systems, Germany), dichroic mirror (Q505LP; Chroma, USA) and emission filter (HQ535/50m; Chroma, USA) were used.

3. Results
Effects of four different electric field protocols: single polarity (SP), both polarities (BP), orthogonal single polarity (OSP) and orthogonal both polarities (OBP) on *in-vitro* gene electrotransfer were evaluated by determining the fraction of transfected cells (Fig. 4) and the fluorescence intensity of transfected cells (Fig. 5). At the same time also the fraction of cell survival was determined.

The results of our *in-vitro* gene electrotransfer experiments show that the fraction of transfected cells increases by changing the electric field direction between electrical pulses. This increase is almost quadrupled at OBP electric field protocol with respect to SP electric field protocol. The largest fraction of transfected cells was observed at OBP electric field protocol and was 24 % (Fig. 4). One way ANOVA indicates that there is a statistically significant difference between different electric field protocols (P = 0.002). Bonferroni t-test indicates that there is a statistically significant difference in comparison of OBP ver-
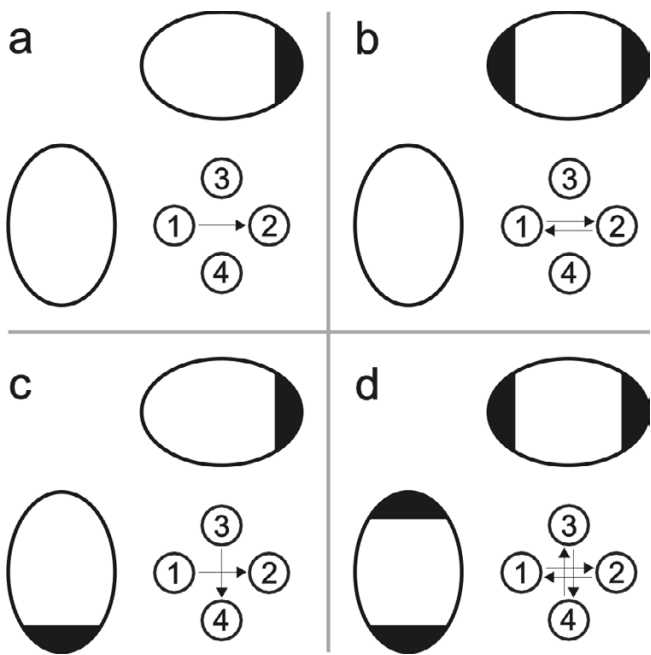
Figure 6
Schematic drawing of competent areas for DNA interaction with cell membrane. Schematic drawing of competent cell membrane areas for DNA interaction with cell membrane in influence of electric field protocols: single polarity (a), both polarities (b), orthogonal single polarity (c) and orthogonal both polarities (d). Black areas represent regions of permeabilized membrane where DNA interacts with cell membrane.

sus SP electric field protocol (P = 0.001) and OBP versus OSP electric field protocol (P = 0.023).

The fluorescence intensity of transfected cells does not however depend on electric field protocol (Fig. 5). One way ANOVA indicated that there is no difference between the electric field protocols (P = 0.246), although transfected cells exposed to orthogonal polarities show higher intensity.

Cell survival after electric pulses applied at 200 V is in the range 96 – 102 % at all four electric field protocols (data not shown). One way ANOVA indicated that there is no difference between the electric field protocols and control (P = 0.963).

Visualization of interaction between DNA and cell membrane showed that DNA molecules interact with the cell membrane facing negative electro-potential (Fig. 7). If SP electric field protocol is used, DNA interacts with cell membrane only from one side of the cell (Fig. 7a) whereas if BP electric field protocol is used, DNA interacts with cell membrane from two sides of the cell (Fig. 7b).

Shading effect is observed when cells are in clusters (Fig. 8). In such clusters we can observe that cells facing negative electro-potential are shading other cells so that DNA molecules can not interact with them (Fig. 8c). Therefore if SP electric field protocol is used the cells in clusters, which are exposed to one side of negative electro-potential during SP electric field protocol, interacts with DNA molecules (III and V, partially: I; Fig. 8c1) and the cells, which are hidden behind this cells in clusters, does not interact with DNA molecules (II and IV, partially: I; Fig. 8c1). And if BP electric field protocol is used the cells in clusters, which are exposed to one of both sides of negative electro-potential during BP electric field protocol, interacts with DNA molecules (VI and VIII, partially VII; Fig. 8c2) and the cells, which are hidden behind this cells in clusters from both sides, does not interact with DNA molecules (partially: VII; Fig. 8c2).

4. Discussion and Conclusion
The aim of our research was to develop and test new system and protocol which would improve gene electrotransfer by automatic change of electric field direction between electrical pulses. For this we chose electroporator with embedded electrode commutation circuit, which controls up to seven electrodes and applies one of three possible states to each of the electrodes: positive, negative or high impedance. Although any other electroporator could be used for such experiments. Since previous observations already demonstrated that homogeneity of electric field distribution affects the effectiveness of electropermeabilization [29,31], we developed electrodes that allow as homogeneous electric field distribution as possible.

An ideal homogeneous electric field distribution can only be achieved between two infinite flat electrodes. In practice we achieve a very close approximation to such electric field distribution if we use sufficiently large flat parallel electrodes that are relatively close to each other. But between two parallel electrodes only two directions of electric field are possible. To generate electric field in more that two directions we need to use more electrodes. We could use four plate electrodes, but in this case we get very inhomogeneous electric field distribution between the electrodes, since the current predominantly flows through the metal of the adjacent electrodes and less through the sample (cells suspension or tissue). That is why in the development of new electrodes (E-S 4.1) we focused on conductivity between opposite electrodes and between adjacent electrodes. Our hypothesis in the development of electrodes was that the most homogeneous electric field distribution between four cylindrical electrodes is achieved when conductivity between opposite electrodes is twice the sum of conductivity between adjacent electrodes (Fig. 1c).
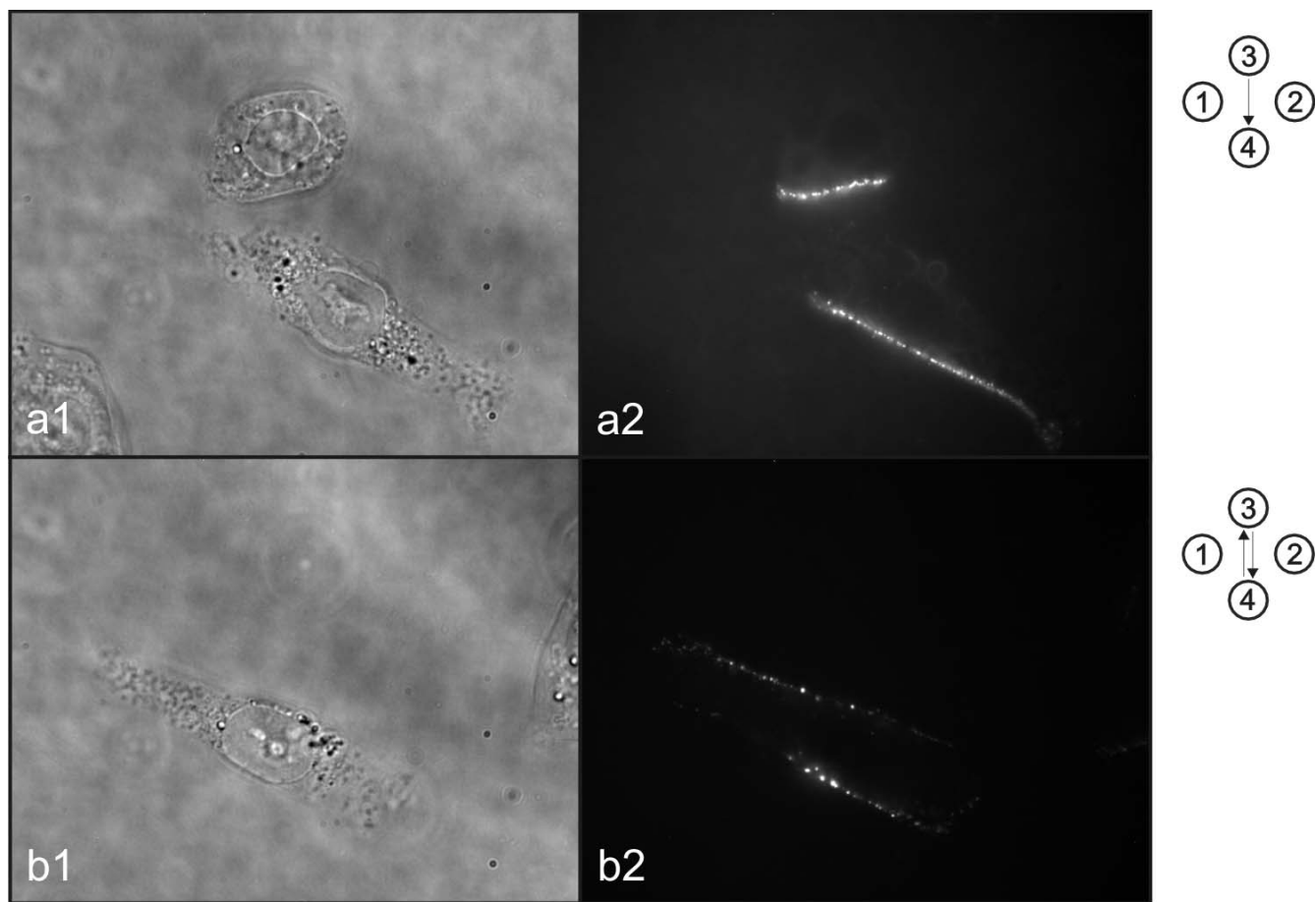
Figure 7
Visualization of interaction between DNA and cell membrane. Visualization of interaction between DNA and cell membrane after single polarity electric field protocol (a) and both polarities electric field protocol (b). Photos of phase contrast (1) and fluorescence (2) images were taken under inverted fluorescence microscope. Symbols on the right represent electric field protocol used.

To evaluate homogeneity of electric field between the electrodes, we designed a three-dimensional finite-elements model of an electroporation medium in culture dish with inserted electrodes. Calculations of electric field intensity in this model showed that the electric field distribution is relatively homogeneous between the electrodes for all four different electric field directions (Fig. 3). Results of calculations have also shown that orthogonal single polarity (OSP) and orthogonal both polarities (OBP) electric field protocols are efficient only in the space between the electrodes, because only there the electric field direction can be rotated for 90°. In addition, a quick practical test was performed to confirm the correctness of calculations and demonstrate electric field intensity distribution (Fig. 3d). In this test, cell survival was depended on electric field intensity. At highest electric field intensity all cells where killed and at low electric field

intensity all cells survived. Good agreement was obtained between calculated and experimental data.

In the next step we experimentally evaluated effectiveness of new system and electric field protocols to improve *in-vitro* gene electrotransfer on Chinese Hamster Ovary cells. Results show that changing the electric field direction between electrical pulses increases the fraction of transfected cells (Fig. 4), with no statistically significant influence on fluorescence intensity of transfected cells (Fig. 5) and cell survival. Therefore, the results obtained in our research support previous observations that changing the electric field direction between electrical pulses improves gene electrotransfer with no significant effect on cell survival [20,32].

Plated cells are of various shapes and often elongated. Because of this, their orientation in electric field is impor-
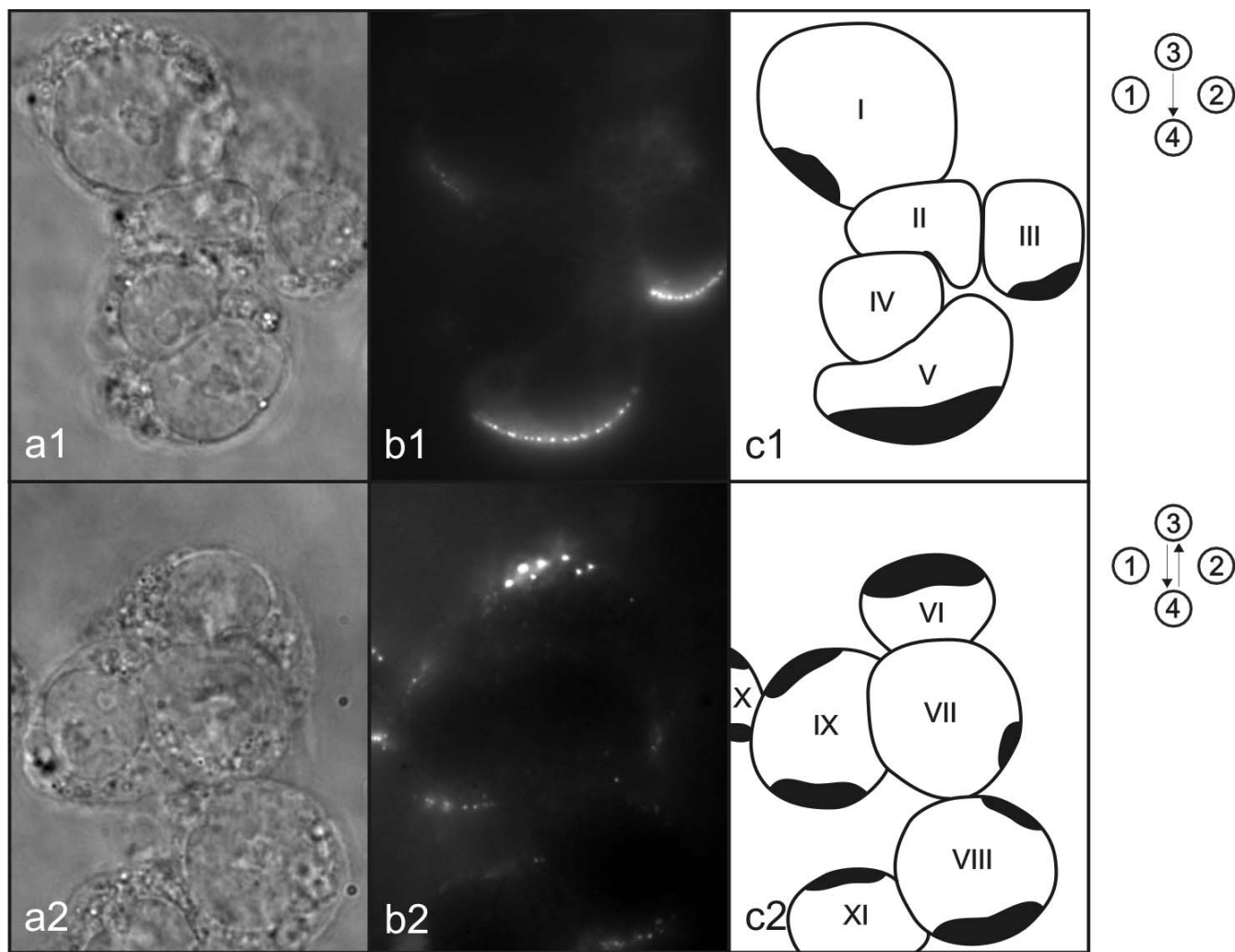
Figure 8
Shading effect. Photos of phase contrast (a) and fluorescence (b) images were taken under inverted fluorescence microscope. Symbolic picture (c) was made for better representation of the observed shading effect. Drawn shapes represent cells and black areas represent regions of permeabilized membrane where DNA interacts with cell membrane. Symbols on the right represent electric field protocol used.

tant [23]. If they are elongated in the direction of electric field, they have higher probability to be permeabilized and that DNA interacts with this part of the membrane (Fig. 6a, b). If we change the direction of electric field during electric pulse delivery, cumulatively more cells are elongated in the direction of electric field and therefore DNA interacts with the membranes of more cells (Fig. 6c, d). Consequently there are more transfected cells (Fig. 4).

We observed another effect during our research i.e. a shading effect, which is also important for efficient gene electrotransfer of plated cells. Shading effect is observed during gene electrotransfer when cells are in clusters, where only cells facing negative electro-potential in clusters become transfected and other ones which are hidden

behind these cells do not become transfected (Fig. 8c1). And if we change electric field direction between electrical pulses, cumulatively more cells face negative electro-potential (in case of inhomogeneous electric field distribution the direction of electric field is not always the same as direction towards electrodes, therefore the term facing electro-potential is used instead of the term facing electrodes) in cluster and more cells in cluster become transfected (Fig. 8c2). Therefore changing electric field direction between electrical pulses improves fraction of transfected cells in clusters, which is another reason why it is advisable to use orthogonal both polarities (OBP) electric field protocol instead of single polarity (SP) electric field protocol.

For each electric field protocol we used the same cumulative number of pulses (Fig. 2). Thus, if we used more directions of electric field during electric pulse delivery, fewer pulses were delivered in each direction. Therefore from each direction a lower "degree" of membrane permeabilization is obtained and less DNA interacts with the cell membrane. But overall, our results indicate that fluorescence intensity of transfected cells is not affected when using our protocols.

Cell survival was also not significantly affected by electric pulse application, which is important for gene transfection as damaged cells difficultly express genes [33]. This means that our protocol is also appropriate for cells which are valuable, such as human primary cells, which are taken directly from a donor or patient [34].

On the basis of our results we can conclude that although homogeneity of electric field distribution between the newly designed electrodes presented in this paper is not as good as between two parallel plate electrodes, the results of gene electrotransfer are improved. By automatic change of electric field direction, electric pulses can be delivered at precise frequencies, which enables new experiments for better understanding of DNA interaction with cell membrane. In addition, the new system can be used wherever manual rotating is not possible, like in case of multiple electrodes, when they are used with different electric field direction between electrical pulses. Such an embedded electrode commutator is being built in the Cliniporator device [35]. In conclusion, the main advantage of the new system and electric field protocol is that it can be used in *in-vitro* gene electrotransfer to improve fraction of transfected cells without affecting fluorescence intensity of transfected cells and cell survival by using automatic orthogonal both polarities electric field protocol.

Acknowledgements

References
1. Murphy DB, Epstein SL: **Guidance for industry: guidance for human somatic cell therapy and gene therapy.** CBER FDA, Rockville; 1998.
2. Cavazzana-Calvo M, Thrasher A, Mavilio F: **The future of gene therapy.** *Nature* 2004, **427**:779-781.
3. Lehrman S: **Virus treatment questioned after gene therapy death.** *Nature* 1999, **401**:517-518.
4. Williams DA, Baum C: **Gene therapy – new challenges ahead.** *Science* 2003, **302**:400-401.
5. Hacein-Bey-Abina S, Von Kalle C, Schmidt M, McCormack MP, Wulffrat N, Leboulch P, Lim A, Osborne CS, Pawliuk R, Morillon E, Sorensen R, Forster A, Fraser P, Cohen JI, de Saint Basile G, Alexander I, Wintergerst U, Frebourg T, Aurias A, Stoppa-Lyonnet D, Romana S, Radford-Weiss I, Gross F, Valensi F, Delabesse E, Macintyre E, Sigaux F, Soulier J, Leiva LE, Wissler M, Prinz C, Rabbitts TH, Le Deist F, Fischer A, Cavazzana-Calvo M: **LMO2-associated clonal T cell proliferation in two patients after gene therapy for SCID-X1.** *Science* 2003, **302**:415-419.
6. Davé UP, Jenkins NA, Copeland NG: **Gene therapy insertional mutagenesis insights.** *Science* 2004, **303**:333.
7. Ferber D: **Gene therapy: safer and virus-free?** *Science* 2001, **294**:1638-1642.
8. Herweijer H, Wolff JA: **Progress and prospects: naked DNA gene transfer and therapy.** *Gene Ther* 2003, **10**:453-458.
9. Prud'homme GJ, Glinka Y, Khan AS, Draghia-Akli R: **Electroporation-enhanced nonviral gene transfer for the prevention or treatment of immunological, endocrine and neoplastic diseases.** *Curr Gene Ther* 2006, **6**:243-273.
10. Neumann E, Sowers AE, Jordan CA: **Electroporation and electrofusion in cell biology.** Plenum Press, New York; 1989.
11. Mir LM: **Therapeutic perspectives of *in vivo* cell electropermeabilization.** *Bioelectrochemistry* 2000, **53**:1-10.
12. Neumann E, Schaefer-Ridder M, Wang Y, Hofschneider PH: **Gene transfer into mouse lynoma cells by electroporation in high electric fields.** *EMBO J* 1982, **7**:841-845.
13. Wolf H, Rols MP, Boldt E, Neumann E, Teissié J: **Control by pulse parameters of electric field-mediated gene transfer in mammalian cells.** *Biophys J* 1994, **66**:524-531.
14. Heller R, Jaroszeski M, Atkin A, Moradpour D, Gilbert R, Wands J, Nicolau C: ***In vivo* gene electroinjection and expression in rat liver.** *FEBS lett* 1996, **389**:225-228.
15. Neumann E, Kakorin S, Tœnsing K: **Fundamentals of electroporative delivery of drugs and genes.** *Biochem Bioenerg* 1999, **48**:3-16.
16. Gehl J: **Electroporation: theory and methods, perspectives for drug delivery, gene therapy and research.** *Acta Physiol Scand* 2003, **177**:437-447.
17. Kinosita K, Itoh H, Ishiwata S, Hirano K, Nishizaka T, Hayakawa T: **Dual-view microscopy with a single camera: real-time imaging of molecular orientations and calcium.** *J Cell Biol* 1991, **115**:67-73.
18. Gabriel B, Teissié J: **Time courses of mammalian cell electropermeabilization observed by millisecond imaging of membrane property changes during the pulse.** *Biophys J* 1999, **76**:2158-2165.
19. Golzio M, Teissie J, Rols MP: **Direct visualization at the single-cell level of electrically mediated gene delivery.** *Proc Natl Acad Sci USA* 2002, **99**:1292-1297.
20. Faurie C, Phez E, Golzio M, Vossen C, Lesbordes JC, Delteil C, Teissié J, Rols MP: **Effect of electric field vectoriality on electrically mediated gene delivery in mammalian cells.** *Biochim Biophys Acta* 2004, **1665**:92-100.
21. Serša G, Čemažar M, Šemrov D, Miklavčič D: **Changing electrode orientation improves the efficacy of electrochemotherapy of solid tumors in mice.** *Bioelectrochem Bioenerg* 1996, **39**:31-66.
22. Kotnik T, Miklavčič D: **Analytical description of transmembrane voltage induced by electric fields on spheroidal cells.** *Biophys J* 2000, **79**:670-679.
23. Valič B, Golzio M, Pavlin M, Schatz A, Faurie C, Gabrile B, Teisssié J, Rols MP, Miklavčič D: **Effect of electric field induced transmembrane potential on spheroidal cells: theory and experiment.** *Eur Biophys J* 2003, **32**:519-528.
24. Phez E, Faurie C, Golzio M, Teisssié J, Rols MP: **New insights in the visualization of membrane permeabilization and DNA/membrane interaction of cells submitted to electric pulses.** *Biochim Biophys Acta* 2005, **1724**:248-254.
25. Gilbert RA, Jaroszeski MJ, Heller R: **Novel electrode designs for electrochemotherapy.** *Biochim Biophys Acta* 1997, **1334**:9-14.
26. Kotnik T, Pucihar G, Reberšek M, Mir LM, Miklavčič D: **Role of pulse shape in cell membrane electropermeabilization.** *Biochim Biophys Acta* 2003, **1614**:193-200.
27. Pavlin M, Kandušer M, Reberšek M, Pucihar G, Hart FX, Magjarević R, Miklavčič D: **Effect of cell electroporation on the conductivity of a cell suspension.** *Biophys J* 2005, **88**:4378-4390.
28. Šemrov D, Miklavčič D: **Numerical modeling for *in vivo* electroporation.** *Meth Mol Med* 2000, **37**:63-81.
29. Šemrov D, Miklavčič D: **Calculation of the electrical parameters in electrochemotherapy of solid tumours in mice.** *Comput Bio Med* 1998, **28**:439-448.
30. Rye HS, Yue S, Wemmer DE, Quesada MA, Haugland RP, Mathies RA, Glazer AN: **Stable fluorescent complexes of double-stranded**

DNA with bis-intercalating asymmetric cyanine dyes: prop-
erties and applications.** *Nucleic Acids Res* 1992, **20:**1803-1812.

31. Miklavčič D, Beravs K, Šemrov D, Čemažar M, Demšar F, Serša G:
**The importance of electric field distribution for effective *in
vivo* electroporation of tissues.** *Biophys J* 1998, **74:**2152-2158.

32. Tekle E, Astumian RD, Chock PB: **Electroporation by using bipo-
lar oscillating electric field: an improved method for DNA
transfection of NIH 3Ts cells.** *Proc Natl Acad Sci USA* 1991,
88:4230-4234.

33. Rols MP, Delteil C, Golzio M, Teisssié J: **Control by ATP and ADP
of voltage-induced mammalian-cell-membrane permeabili-
zation, gene transfer and resulting expression.** *Eur J Biochem*
1998, **254:**382-388.

34. Grossman M, Raper SE, Kozarsky K, Stein EA, Engelhardt JF, Muller
D, Lupien PJ, Wilson JM: **Successful *ex vivo* gene therapy
directed to liver in a patient with familial hypercholestero-
laemia.** *Nat Genet* 1994, **6:**335-341.

35. Marty M, Serša G, Garbay JR, Gehl J, Collins CG, Snoj M, Billard V,
Geertsen PF, Larkin JO, Miklavčič D, Pavlović I, Paulin-Košir SM,
Čemažar M, Morsli N, Soden DM, Rudolf Z, Robert C, O'Sullivand
GC, Mir LM: **Electrochemotherapy – An easy, highly effective
and safe treatment of cutaneous and subcutaneous metas-
tases: Results of ESOPE (European Standard Operating Pro-
cedures of Electrochemotherapy) study.** *EJC supplements* 2006,
4:3-13.

Paper XII

Importance of tumour coverage by sufficiently high local electric field for effective electrochemotherapy

Damijan Miklavcic*, Selma Corovic, Gorazd Pucihar, Natasa Pavselj

Faculty of Electrical Engineering, University of Ljubljana, Tržaška 25, SI-1000 Ljubljana, Slovenia

ARTICLE INFO

ABSTRACT

Electrochemotherapy is an effective local treatment of solid tumours which combines delivery of chemotherapeutic drug and electric pulses. Electric pulses increase permeability of plasma membrane transiently and reversibly, leading to increased transport of the drug into the cell. As all clonogenic cells in the tumour need to be eradicated for effective treatment, all cells have to be permeabilised, i.e. all cells in the tumour have to be exposed to appropriate electric pulses. Electric pulses are delivered to tissue by electric pulses generator via electrodes. In general there are two types of electrodes, plate electrodes and needle electrodes. The target tissue, i.e. tumour, is to be positioned well in-between the electrodes. The electrodes should thus fit the size of the tumour for good electric field distribution. Plate electrodes which are noninvasive are better suited for tumours on the surface on the skin, whereas needle electrodes which are used invasively with appropriate and sufficient depth of their insertion are more appropriate for treating tumours seeded deeper in the skin.

1. Cell in electric field and electrochemotherapy

Electrochemotherapy is an effective local treatment of solid tumours which combines delivery of corresponding drug and electric pulses.[1–10] Drugs with hindered transmembrane transport and having intracellular target are good candidates for electrochemotherapy. Bleomycin and cisplatin proved to be the best candidates so far.[11–13] Electric pulses with appropriate parameters, amplitude, duration, number, repetition frequency and shape, will increase permeability of plasma membrane transiently and reversibly, leading to increased transport of the drug into the cell. This increased transport will thus allow the drug to enter the cell in sufficient amount and reach its intracellular target, consequently killing the cell. As all clonogenic cells in the tumour need to be eradicated for effective treatment, all cells have to be permeabi-

lised, i.e. all cells in the tumour have to be exposed to appropriate electric pulses. Effectiveness of electrochemotherapy thus depends on drug availability in the tumour and coverage of the whole area of the tumour by sufficiently high electric field/pulses.

When a cell is placed into electric field, its geometrical and material properties cause a transmembrane voltage to be induced and superimposed on the natural resting transmembrane voltage. The amplitude of the induced transmembrane voltage depends on the position on the membrane and is dictated by the following equation:

$$\Delta\Phi_{\mathrm{m}} = \frac{3}{2}ER\cos\theta, \tag{1}$$

where $\Delta\Phi_{\mathrm{m}}$ is the induced transmembrane voltage on the membrane, θ is the angle between the direction of the electric field E and radius vector R on the membrane[14] (see also Fig. 1).

* Corresponding author: Tel.: +386 1 4768 456; fax: +386 1 426 46 58.
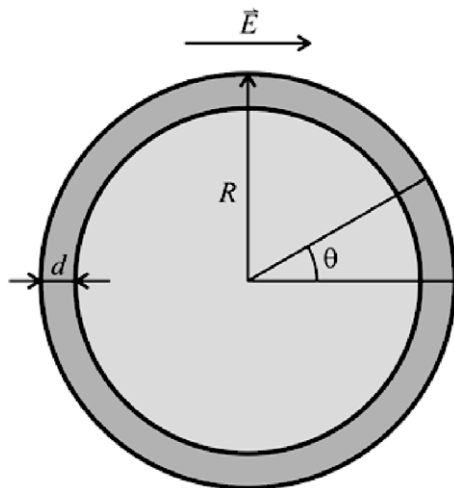 E-mail address: damijan.miklavcic@fe.uni-lj.si (D. Miklavcic).

Fig. 1 – A schematic presentation of a cell having diameter 2R, membrane thickness d, where θ is the angle between the direction of the electric field E and radius vector R on the membrane.
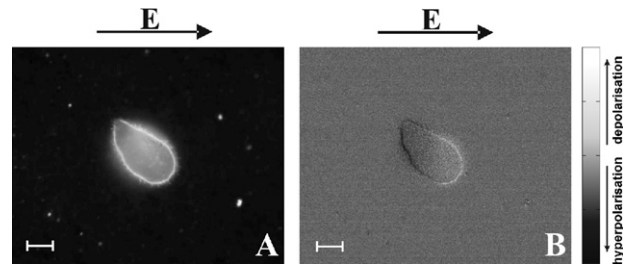

Fig. 2 – Induced transmembrane voltage (ITV) on an irregularly shaped CHO cell. Electric field E was directed from left to right. (a) The 8-bit fluorescence image of a cell stained with di-8-ANEPPS and acquired during the exposure to 40 V (100 V/cm), 100 ms rectangular pulse. The brightness of the image was automatically enhanced. Bar represents 10 μm. (b) Changes in fluorescence of cell obtained by subtracting the control image (not shown) from the image with pulse and shifting the greyscale range by 50%. The side of the cell coloured in white represents an increase in fluorescence (depolarisation), and the side of the cell coloured in black, a decrease in fluorescence (hyperpolarisation). The brightness of the image was automatically enhanced.

If the induced transmembrane voltage is sufficiently high,[15] the membrane permeability non-selectively increases and molecules which otherwise cannot cross the plasma membrane can now enter (or leave) the cell. The transport of small molecules like bleomycin and cisplatin across the membrane is predominantly diffusion-driven due to concentration gradient.[16] When electric pulses are applied, membrane permeability of cells in the tissue exposed to sufficiently high electric field will non-selectively increase. If the drug is present in the tumour (surrounding the tumour cells, but not being able to penetrate the cell through its membrane), this increased membrane permeability will allow entrance of the drug into the cells, increasing drug cytotoxicity.

Induced transmembrane voltage can easily be calculated for a spherical cell and it follows Eq. (1).[14] What we can see from this equation is that for a given cell the induced transmembrane voltage is proportional to the electric field; more precisely, it is proportional to the local electric field in which the cell is placed. The induced transmembrane voltage for non-spherical irregular shapes, such as cells are, can, however, be calculated by numerical methods or measured

(Fig. 2).[17] It is important to note that if the induced voltage is not sufficiently high, no flow will occur as the membrane will not become permeabilised. Nevertheless, the flux of the drug occurs only through parts of the membrane where the induced transmembrane voltage exceeds a critical threshold (Fig. 3). Thus the flux of the drug through the membrane is established through areas where sufficiently high induced transmembrane voltage was induced, but also depends on pulse duration and number of pulses.

If pulse parameters are selected appropriately, the cell membrane will become transiently permeabilised, and will reseal afterwards, thus preserving cell viability. This is termed reversible permeabilisation. However, if the amplitude of pulses, their number is too large and/or duration is too long, the membrane will not reseal and the cell will lose its viability. This is termed irreversible permeabilisation.

The electric field in a tissue and electric current passing through the tissue are coexisting and are connected by Ohm's law (Eq. 2)
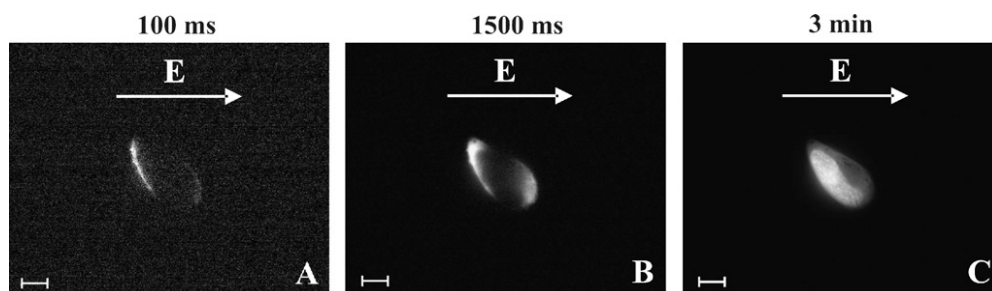
Fig. 3 – Electropermeabilisation of a CHO cell shown in Fig. 2. (A) Fluorescence of the cell 100 ms, (B) 1500 ms, and (C) 3 min after pulse delivery. The cell was exposed to a single 400 V (1000 V/cm) rectangular unipolar pulse (200 μs). The images were corrected for the background fluorescence and the brightness was automatically enhanced. Propidium Iodide (100 μM), which was here used as a marker of membrane permeabilisation, was added to suspension before the pulse was applied to visualize the permeabilised regions. Bar represents 10 μm.

$$j = \sigma \cdot E, \tag{2}$$

where j is current density, σ is tissue electric conductivity, and E the electric field. The corresponding integral values are electric current I, conductance G (which is the reverse of resistance R), and voltage U. The Ohm's law then takes the form of:

$$U = R \cdot I \quad \text{or} \quad I = G \cdot U. \tag{3}$$

Current passes through the tissue if voltage i.e. potential difference exists between two points in the tissue, and the current loop is closed. In practice, we generate the potential difference (voltage) on electrodes with an electric pulse generator. When both electrodes (one needs at least two electrodes to close the loop) are placed on/in the tissue (which is a conductive material where charge carriers are ions as in electrolyte solutions), the current loop is closed and the current passes through the tissue.

As the electric current passes through a biological tissue, it is distributed through different parts of the tissue, depending on their electrical conductivity. In general, better perfused tissues have higher conductivity. So blood is highly conductive, liver and muscles as well, whereas bone and fatty tissue have low conductivity. The current will flow easier and for the same voltage in higher proportion through more conductive tissues (e.g. muscles, liver). On the contrary, the electric field in these tissues will be lower than in tissues with low conductivity for the same current. Since the same voltage in higher conductive media will give higher currents and because conductivity of the tissue increases as it becomes permeabilised, rather high currents pass through the tissue during electrochemotherapy.[18,19]

Nevertheless, as the electric current takes the shortest and easiest path through the tissue, the current will be contained predominantly between the electrodes if they are close enough to each other. This property allows for relatively good control and containment of electric field distribution predominantly between the electrodes.[20]

Solid tumours usually have somewhat higher conductivity than the surrounding tissue due to its rich, irregular and fenestrated vasculature. This causes electric current to pass mainly through the tumour, but the electric field will be somewhat lower than in its surroundings. Nevertheless,

when the tissue becomes permeabilised (i.e. plasma membrane becomes permeable) its conductivity also increases, which leads to electric field redistribution in the tumour and its surroundings. This phenomenon is most obvious in subcutaneous tumours.[21] Namely, the skin, serving as a natural barrier protecting internal tissues from exposure to chemical and physical trauma and bacteria, has an extremely low electric conductivity. When two electrodes are placed on the skin, practically the entire voltage drop rests on the skin (on its outermost layer, the *stratum corneum*, being the least conductive skin layer), where the electric field is by far the highest. The electric field, when applying high voltage pulses as in the case of electrochemotherapy, "breaks through" the skin, forming structures known as Local Transport Regions that make skin more conductive.[22] Now the current can pass through the skin more easily and the voltage drop and electric field in the skin are lowered (Fig. 4). Consequently, other skin layers and tissues under the skin are exposed to higher electric fields.

In conclusion, cells in tissues which are exposed to sufficiently high electric field will become permeabilised, rendering electrochemotherapy effective. If pulse parameters are selected correctly and sufficiently high (but not too high – see below) local field is assured and cells will become reversibly permeabilised, i.e. allowing for the uptake of cytotoxic drug and resealing of the membrane. This will allow the drug to exert its cytotoxic activity selectively to tumour cells and not to normal cells. If, however, the cells are exposed to too high an electric field (at given pulse parameters), cells will be killed nonselectively and instantly, *losing* selectivity and therapeutic index of electrochemotherapy, leading to localised tissue necrosis. Electric field associated *with* reversible permeabilisation is noted as E_{rev}, whereas the electric field associated *with* irreversible permeabilisation is noted as E_{irrev} in Figs. 6 and 7.

2.　Selection and positioning of electrodes

In general there are two types of electrodes, plate electrodes and needle electrodes[23,24] (Fig. 5). Plate electrodes are noninvasive, usually parallel and separated by a distance d. The
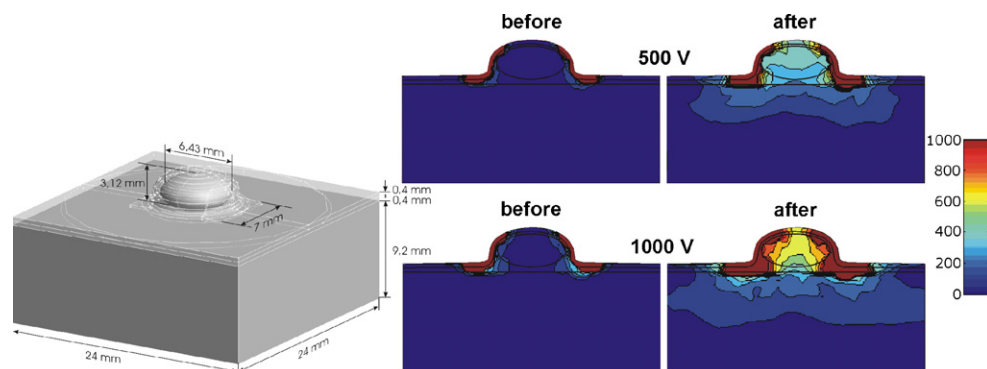

Fig. 4 – Modelled electric field distributions in the subcutaneous tumour and the surrounding tissues before and after tissue electropermeabilisation at 500 and 1000 V between two plate electrodes of 8 mm distance. The electric field distributions are shown in V/cm. The geometry of the numerical model is shown on the left. The electrodes are modelled as a boundary condition.
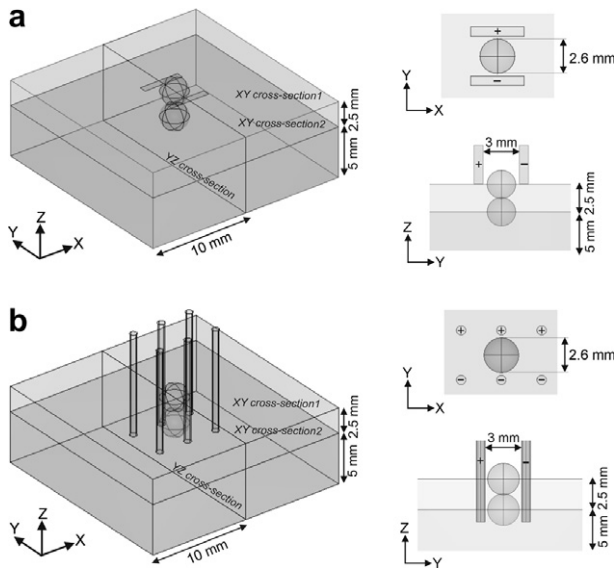
Fig. 5 – Geometry of tissue models with the given electrode configurations: (a) 3D model of cutaneous and subcutaneous tumour with two parallel plate electrode configuration and corresponding XY and YZ cross-sections across the target tissue i.e. tumour geometry and (b) 3D model of cutaneous and subcutaneous tumour with needle electrode configurations and corresponding XY and YZ cross-sections across the target tissue i.e. tumour geometry. Tumour was for demonstration purposes placed at two different positions in the model: as cutaneous and subcutaneous tumour. Each time only one tumour was considered in calculations and explanations.

Fig. 6 – The comparison of electric field distribution for different electrode configurations shown in XY cross-section of cutaneous and subcutaneous 3D models from Fig. 5: (a) two parallel plate electrodes – cutaneous tumour including the electric field distribution within the gel layer surrounding the target tissue; (b) two parallel plate electrodes – subcutaneous tumour; (c) two parallel needle electrodes – cutaneous tumour; (d) two parallel needle electrodes – subcutaneous tumour; (e) six parallel needle electrodes – cutaneous tumour and (f) six parallel needle electrodes – subcutaneous tumour. In all cases the applied voltage $U = 300$ V. Black circle represents the target tissue and the patterned region represents part of tissue where $E \geqslant E_{irrev}$.

target tissue, i.e. tumour, is to be somehow placed in-between these two plates. The tumour is pinched or pushed between electrodes. The electrodes should fit the size of the tumour for good electric field distribution. Electrodes "too far" from the tumour will not allow for efficient electropermeabilisation. Either fixed distance electrodes (most often) or variable distance electrodes are used. In both cases it is important to assure good electrical contact between metal electrodes and tissue – this is usually assured by using conductive gel (see Figs. 6a and 7a) and exerting sufficient pressure to create and maintain good contact even in the case of tissue movement due to muscle contractions provoked by the electric pulses. Also, the applied voltage needs to be determined/calculated with respect to the distance between electrodes, their shape and tissue-electrode geometry, as well as tissue anatomy.

Needle electrodes are used invasively. In this way good electrical contact is assured. However, the electric field distribution is more inhomogeneous and depends on the electrode diameter, number of electrodes, distance between the electrodes and depth of their insertion (Figs. 6 and 7)[25,26]. In principle, thinner electrodes, larger distance and shallower insertion lead to more inhomogeneous electric field distribution. This causes extremely high current density and high electric fields in immediate vicinity of the needle electrode. But at even a short distance from the needle electrode the field amplitude is already very low – possibly too low to cause

cell membrane permeabilisation. Furthermore, the effective electric field between the electrodes occurs at a lesser depth than needle electrode insertion. Thus needle electrodes generally need to be inserted deeper than the deepest part of the tumour.

For improving electric field homogeneity and local field distribution using needle electrodes at least two strategies can be proposed. More needle electrodes positioned in parallel rows improve the homogeneity, whereas multiple needle electrodes arranged into a matrix allow larger volumes of the target tissue to be treated.[25,27] Such an array of electrodes connected to an electroporator through a commutation/switching device can deliver well designed sequences of pulses that increase the probability for cell membrane permeabilisation. Usually electrodes are used in pairs and pulses are delivered in more than one direction to the same cells, which increases the probability of a cell to become permeabilised.[28] Also, improved coverage of tumour with a sufficiently high electric field can be achieved. The same can be done with plate electrodes.[29,30]
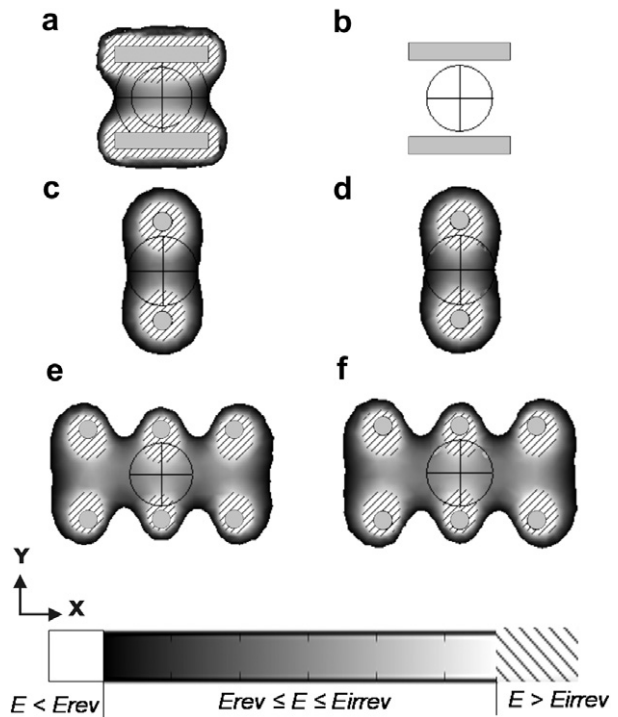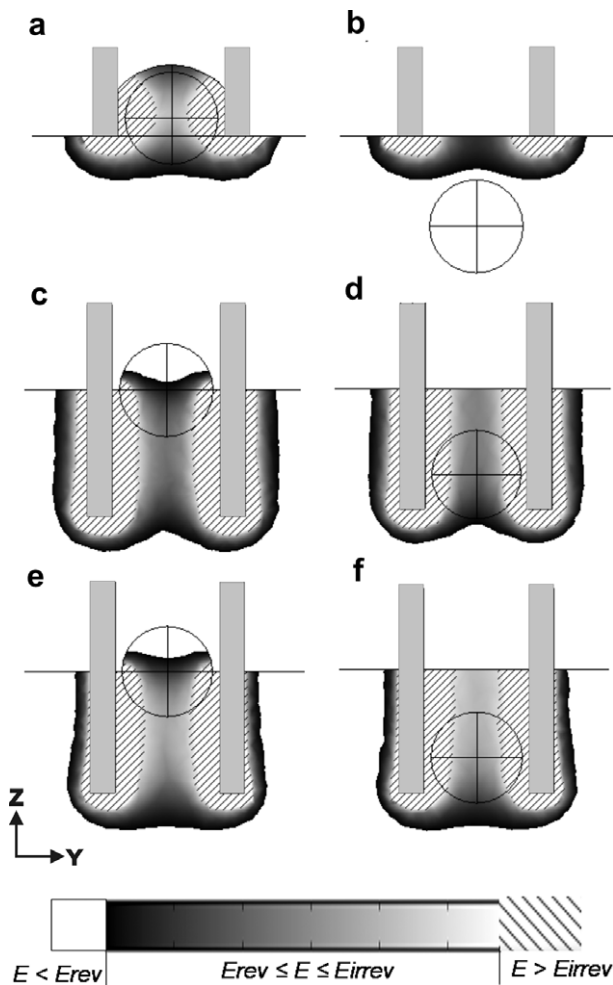
Fig. 7 – The comparison of electric field distribution for different electrode configurations shown in YZ cross-section of cutaneous and subcutaneous 3D models: (a) two parallel plate electrodes – cutaneous tumour including the electric field distribution within the gel layer surrounding the target tissue; (b) two parallel plate electrodes – subcutaneous tumour; (c) two parallel needle electrodes – cutaneous tumour; (d) two parallel needle electrodes – subcutaneous tumour; (e) six parallel needle electrodes – cutaneous tumour and (f) six parallel needle electrodes – subcutaneous tumour. In all cases the applied voltage $U = 300$ V. Black circle represents the target tissue and the patterned region represents part of tissue where $E \geqslant E_{irrev}$.

Adequate pulse amplitudes, set and delivered by a pulse generator, were initially and are all too often still determined empirically. Now they can be calculated by means of numerical models and tested.[15,26,30,31] The electric pulses voltage that needs to be applied depends on electrode type, number of electrodes and electrode geometry. Next necessary step is correct positioning of the electrodes into/onto the tumour, which will assure sufficiently high electric field in the whole tumour as to cause membrane permeabilisation of all clonogenic cells. In principle, after visualising the tumour, determining the size and position, the best suited electrode type has to be selected and plan has to be made as to where and

how the electrodes need to be placed with respect to the tumour. Most of the time, however, physicians can be very rapidly trained to use the electrodes appropriately. Especially in treatment of cutaneous and subcutaneous tumours, a single training session is sufficient. Moreover, the electrical coverage of the vicinity of the tumour is recommended, particularly when the drug used is the bleomycin injected intravenously, due to the absence of toxic effects on the neighbouring normal tissue (see L.M. Mir, this issue).

3.   Possible pitfalls and side effects of electrical nature

As in every treatment, there are number of possible mistakes that can be made. It is the procedures that have to be defined to minimize the risk of making mistakes,[32] which is why the Standard Operating Procedures for the Electrochemotherapy were prepared and reported in this issue. In addition, to be used in Europe, an electroporator has to be certified as a CE medical device, which assures safety of patients, physicians and members of medical staff performing the treatment. Besides the CE mark, the minimal requirement of a clinical electroporator, the equipment used to deliver the pulses *can* also include features allowing detecting potential mistakes of the operator. Indeed, after injecting the drug into the tumour or systemically, and allowing for distribution of the drug in the tumour, one selects and positions the electrodes and applies the appropriate electric pulses. It is of utmost importance to have a possibility to monitor and control the current and the voltage of the pulses being delivered.[24] This can either be achieved by using external oscilloscope, which can be difficult if not impossible in a clinical setting, or by using an electroporator that has such monitoring of pulses built in.

In addition, since high voltage electric pulses are delivered, they usually provoke muscle contraction. If, as it was often the case in the past, a 1 Hz repetition frequency is used, each single pulse leads to a twitch, which may result in losing electrical contact if insufficient pressure is exerted by the operator. This happens momentarily and is difficult to notice without proper monitoring of pulse delivery (as mentioned in the previous paragraph). Too high a pressure may on the other hand lead to large contact area, which requires high electric current – too high for the comfort of the patient and/or for the electroporator to deliver. Namely, some electroporators will, for security reasons, discontinue pulse delivery if the current exceeds a given level (e.g. 12 A). This kind of protection will prevent damage of the electroporator. Such discontinuation of pulse delivery may pass unnoticed and will result in lower or nonexistent electropermeabilisation, causing electrochemotherapy to fail. The undesired consequences of the twitch, caused by the first pulse in the train of "standard" eight electric pulses most often delivered to achieve a good cell permeabilisation, can also be completely avoided using a 5000 Hz pulse repetition frequency, instead of the classical 1 Hz frequency. When using this high pulse repetition frequency, the whole train of pulses is then delivered in 1.5 ms, that is before the twitch is provoked and the electrode displacement can occur. This high repetition frequency thus ensures the quality of the treatment and reduces patient discomfort. Moreover, in the

ESOPE study using the Cliniporator™ we have demonstrated good clinical results of electrochemotherapy, irrespective of pulse repetition frequency.

Finally, when plate electrodes are used, burn marks can appear on the skin where electrodes were in contact with it. This can be due to an insufficient electrical contact during pulse delivery. Good electrical contact can be assured by using conductive gel and exerting more pressure to the electrodes to avoid sparking and very local high current leaving burn marks on the skin, especially if the electrodes are placed perpendicularly to the skin, having small contact area. However, we have to be careful not to use too much conductive gel. Filling the gap between the electrodes with an excess of conductive gel may shunt the electrical path through the tissue, rendering electrochemotherapy inefficient. Hairy skin may cause sparking and give rise to unpleasant smell of burning hair. Thus it may be appropriate to shave and clean the skin above the tumour if possible.

In conclusion, the target tissue, i.e. tumour, is to be positioned well in-between the electrodes. The electrodes should fit the size of the tumour for good electric field distribution. Noninvasive plate electrodes are better suited for tumours on the surface on the skin, whereas needle electrodes, which are used invasively, with appropriate and sufficient depth of their insertion, are more appropriate for treating subcutaneous tumours seeded deeper in the skin.

Acknowledgements

REFERENCES

1. Allegretti JP, Panje WR. Electroporation therapy for head and neck cancer including carotid artery involvement. *Laryngoscope* 2001;**111**:52–6.
2. Rols MP, Bachaud JM, Giraud P, Chevreau C, Roche H, Teissie J. Electrochemotherapy of cutaneous metastases in malignant melanoma. *Melanoma Res* 2000;**10**:468–74.
3. Sersa G, Stabuc B, Cemazar M, Miklavcic D, Rudolf Z. Electrochemotherapy with cisplatin: clinical experience in malignant melanoma patients. *Clin Cancer Res* 2000;**6**:863–7.
4. Sersa G, Cemazar M, Rudolf Z. Electrochemotherapy: advantages and drawbacks in treatment of cancer patients. *Cancer Therapy* 2003;**1**:133–42.
5. Gothelf A, Mir LM, Gehl J. Electrochemotherapy: results of cancer treatment using enhanced delivery of bleomycin by electroporation. *Cancer Treatment Rev* 2003;**29**:371–87.
6. Rodriguez-Cuevas S, Barroso-Bravo S, Almanza-Estrada J, Cristobal-Martinez L, Gonzalez-Rodriguez E. Electrochemotherapy in primary and metastatic skin tumours: Phase II trial using intralesional bleomycin. *Arch Med Res* 2001;**32**(4):273–6.

7. Domenge C, Orlowski S, Luboinski B, et al. Antitumour electrochemotherapy. New advances in clinical protocol. *Cancer* 1996;**77**:956–63.
8. Heller R, Gilbert R, Jaroszeski MJ. Clinical application of electrochemotherapy. *Adv Drug Delivery Rev* 1999;**35**:119–29.
9. Heller R, Jaroszeski MJ, Glass LF, et al. Phase I/II trial for the treatment of cutaneous and subcutaneous tumours using electrochemotherapy. *Cancer* 1996;**77**:964–71.
10. Jaroszeski MJ, Gilbert R, Heller R. Electrochemotherapy: an emerging drug delivery method for the treatment of cancer. *Adv Drug Delivery Rev* 1997;**26**:185–97.
11. Pendas S, Jaroszeski MJ, Gilbert R, et al. Direct delivery of chemotherapeutic agents for the treatment of hepatomas and sarcomas in rat models. *Radiol Oncol* 1998;**32**:53–64.
12. Mir LM, Tounekti O, Orlowski S. Bleomycin: revival of an old drug. *General Pharmacol* 1996;**27**:745–8.
13. Sersa G, Cemazar M, Miklavcic D. Antitumour effectivness of electrochemotherapy with *cis*-diamminedichloroplatinium (II) in mice. *Cancer Res* 1995;**55**:3450–5.
14. Kotnik T, Bobanovic F, Miklavcic D. Sensitivity of transmembrane voltage induced by applied electric fields – a theoretical analysis. *Bioelectrochem Bioenerg* 1997;**43**:285–91.
15. Miklavcic D, Semrov D, Mekid H, Mir LM. A validated model of in vivo electric field distribution in tissues for electrochemotherapy and for DNA electrotransfer for gene therapy. *Biochim Biophys Acta* 2000;**1523**:73–83.
16. Puc M, Kotnik T, Mir LM, Miklavcic D. Quantitative model of small molecules uptake after in vitro cell electropermeabilization. *Bioelectrochemistry* 2003;**60**:1–10.
17. Pucihar G, Kotnik T, Valic B, Miklavcic D. Numerical determination of transmembrane voltage induced on irregularly shaped cells. *Ann Biomed Eng* 2006;**34**:642–52.
18. Pavlin M, Miklavcic D. Effective conductivity of a suspension of permeabilized cells: a theoretical analysis. *Biophys J* 2003;**85**:719–29.
19. Pavlin M, Kanduser M, Rebersek M, et al. Effect of cell electroporation on the conductivity of a cell suspension. *Biophys J* 2005;**88**:4378–90.
20. Miklavcic D, Beravs K, Semrov D, Cemazar M, Demsar F, Sersa G. The importance of electric field distribution for effective in vivo electroporation of tissues. *Biophys J* 1998;**74**:2152–8.
21. Pavselj N, Bregar Z, Cukjati D, Batiuskaite D, Mir LM, Miklavcic D. The course of tissue permeabilization studied on a mathematical model of a subcutaneous tumour in small animals. *IEEE Trans Biomed Eng* 2005;**52**:1373–81.
22. Pliquett UF, Vanbever R, Preat V, Weaver JC. Local transport regions (LTRs) in human stratum corneum due to long and short 'high voltage' pulses. *Bioelectrochem Bioenerg* 1998;**47**:151–61.
23. Gilbert R, Jaroszeski MJ, Heller R. Novel electrode designs for electrochemotherapy. *Biochim Biophys Acta* 1997;**1334**:9–14.
24. Puc M, Corovic S, Flisar K, Petkovsek M, Nastran J, Miklavcic D. Techniques of signal generation required for electropermeabilization. Survey of electropermeabilization devices. *Bioelectrochemistry* 2004;**64**:113–24.
25. Sel D, Mazeres S, Teissié J, Miklavcic D. Finite-element modeling of needle electrodes in tissue from the perspective of frequent model computation. *IEEE Trans Biomed Eng* 2003;**50**:1221–32.
26. Gehl J, Sorensen TH, Nielsen K, et al. In vivo electroporation of skeletal muscle: threshold, efficacy and relation to electric field distribution. *Biochim Biophys Acta* 1999;**1428**:233–40.

27. Ramirez LH, Orlowski S, An D, et al. Electrochemotherapy on liver tumours in rabbits. *Br J Cancer* 1998;**77**:2104–11.

28. Valic B, Golzio M, Pavlin M, et al. Effect of electric field induced transmembrane potential on spheroidal cells: theory and experiment. *Eur Biophys J* 2003;**32**:519–28.

29. Sersa G, Cemazar M, Semrov D, Miklavcic D. Changing electrode orientation improves the efficacy of elecrochemotherapy of solid tumours in mice. *Bioelectrochem Bioenerg* 1996;**39**:61–6.

30. Semrov D, Miklavcic D. Calculation of the electrical parameters in electrochemotherapy of solid tumours in mice. *Comput Biol Med* 1998;**28**:439–48.

31. Dev SB, Dhar D, Krassowska W. Electric field of a six-needle array electrode used in drug and DNA delivery in vivo: analytical versus numerical solution. *IEEE Trans Biomed Eng* 2003;**50**:1296–300.

32. Kern T. Organizational structure without hierarchy. *Strojarstvo* 2003;**45**:101–10.

Paper XIII

UDK: 615.38:537.212

Selma Ćorović,[1] Ivan Pavlović,[1] Gregor Serša,[2] Damijan Miklavčič[1]

ELEKTROPORACIJA ĆELIJE I NJENA PRIMENA U MEDICINI

Sazetak: Kada se biološko tkivo izloži vrlo kratkim naponskim impulsima visoke amplitude nastaje električno polje. Ukoliko se intenzitet nastalog električnog polja poveća iznad odgovarajuće kritične vrednosti ćelijska membrana postaje propustljivija za jone i molekule, koji inače ne mogu da pređu u ćeliju. Ovakva modulacija propustljivosti ćelijske membrane pod uticajem električnog polja naziva se *elektroporacija* (takođe poznata i pod imenom elektropermeabilizacija) i omogućava pojačan transport jona i molekula u ćeliju. Ovaj fenomen ima široku *in vivo* i *in vitro* biološku i medicinsku primenu u cilju da olakša transfer raznih lekova u ćeliju, kao što su hemoterapeutici i DNA. U ovom radu predstavljamo sledeće oblike primene ćelijske elektroporacije u medicini: elektrohemoterapija, elektrogeni transdermalni transport lekovitih supstanci.

Ključne reči: elektropermeabilizacija, elektroporacija, elektrohemoterapija, matematičko modeliranje.

CILJ RADA: Cilj rada je predstaviti i istaći mogućnost upotrebe elektroporacije za povećanje propustljivosti ćelijske membrane kako bi se olakšao transport lekovitih supstanci u ćeliju. Ova metoda, koju nazivamo i elektropermeabilizacija, je u mnogim istraživačkim studijama pokazala velik potencijal za primenu u medicini. Ovim radom istaknućemo nekoliko osnovnih dostignuća u primeni elektroporacije u elektrohemoterapiji, elektrogenskoj terapiji i transportu lekovitih supstanci transdelmalnim putem.

UVOD

Elektropermeabilizacija, poznata i pod imenom elektroporacija, ćelijske membrane je metoda za povećanje propustljivosti ćelijske membrane pod uticajem električnog polja [Neumann *et al.*, 1989, Weaver *et al.*, 1996, Gehl *et al.*, 2003, Miklavcic and Kotnik, 2004].

Ovom metodom olakšava se transport većih molekula kroz ćelijsku membranu, što inače membrana u stabilnom stanju sprečava. Tako se elektropermeabilizacijom olakšava transport mnogih lekovitih supstanci kao i molekula DNK. Zato je ova metoda veoma popularna istraživačka tema, a njena upotreba je pored drugih područja dokazana i na području humane medicine. Na primer u onkologiji se elektroporacijom selektivno povećava transport citostatika u tumorske ćelije, u biotehnologiji se na ovaj način olakšava transport molekula DNK za modifikaciju ćelija, a počela je i primena ove metode u terapiji genima (elektrogenska terapija). Jedan od glavnih faktora u postizanju optimalnih rezultata elektropermeabilizacijom predstavlja električno polje. Zato vrlo bitnu ulogu u razvoju ove metode igra rešavanje mnogih inženjerskih problema, naročito na području elektrotehnike. Tako je jedna od istraživačkih aktivnosti kojom se bave autori ovog rada upravo optimizacija elektropermeabilizacije ćelija i tkiva. Između ostalog istraživanje obuhvata eksperimentalnu optimizaciju u *in vitro* i *in vivo* uslovima, kompjutersku simulaciju pomoću numeričkih modela i razvoj elektronskih komponenata za proizvođenje električnog polja [http://lbk.fe.uni-lj.si].

Definicija elektroporacije (elektropermeabilizacije)

1. Ćelijska membrana je selektivno propustljiva, što ćeliji omogućava da kontroliše razmenu materije i da na, taj način, obavlja svoje funkcije i očuva svoj unutrašnji sastav.

2. Pod uticajem dovoljno jakog električnog polja dolazi do promena u strukturi lipidnog dvosloja i do promene transmembranskog napona, odnosno razlike površinskog i potencijala mirovanja na membrani. Ovo posledično utiče na način na koji ćelija obavlja razmenu materija sa neposrednim okruženjem.

1 Elektrotehnički fakultet, Univerzitet u Ljubljani, Slovenija.
2 Onkološki institut u Ljubljani, Slovenija.

3. Sa elektrotehničkog vidika ćelijska membrana pod uticajem električnog polja ispoljava karakteristike električnog izolatora. Njena specifična provodljivost (S/m) je milion puta manja od provodljivosti izvanćelijskog i unutarćelijskog prostora. Zato je potrebno proizvesti jako električno polje dovoljnog intenziteta da bi se ova barijera prevazišla.
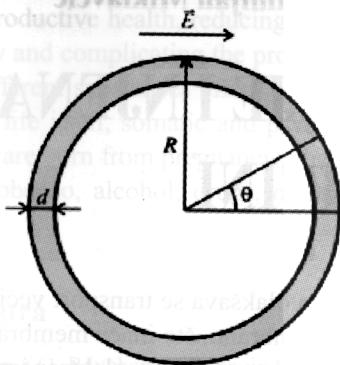
Slika 1: Grafički prikaz ćelije prečnika 2R, debljine membrane d i ugla θ između električnog polja E i vektora poluprečnika R

Električno polje potrebno za elektropermeabilizaciju postiže se vrlo kratkim naponskim impulsima (trajanja oko 100 μs) visoke amplitude (high-voltage HV pulses). Ovakve pulseve ćelijama ili tkivu treba dopremiti preko elektroda iz provodnog materijala odgovarajućeg oblika.

Pod uticajem električnog polja, između unutrašnjeg i spoljašnjeg dela membrane indukuje se razlika potencijala, odnosno formira se indukovani transmembranski napon. Ako je posmatrana ćelija okruglog oblika, kao što to prikazuje Slika 1, indukovani transmembranski napon (ΔΦ) određuje se prema sledećoj formuli (1):

$$\Delta\phi = \frac{3}{2} \cdot E \cdot R \cos\theta \qquad (1)$$

U navedenoj formuli E je amplituda električnog polja, R je poluprečnik ćelije, a θ je ugao između pravca električnog polja i vektora poluprečnika R koji povezuje centralnu tačku ćelije sa proizvoljnom tačkom na površini membrane. Vrednost indukovanog transmembranskog napona je, dakle, srazmerna intenzitetu električnog polja E i dimenzijama ćelije, i zavisi od pozicije posmatrane tačke na membrani (srazmerno kosinusu θ).

Indukovani transmembranski napon formira se u vrlo kratkom vremenskom intervalu (nekoliko μs), a kada prevaziđe određenu kritičnu vrednost struktura ćelijske membrane se menja formirajući proširenja, takozvane pore, u lipidnom dvosloju membrane [Šemrov *et al.*, 1995, Pavlin *et al*, 2002]. Otuda ovaj proces dobija ime elektroporacija. Prema podacima iz litera-

ture, kritični transmembranski napon koji električnim poljem treba obezbediti ćeliji kako bi se membrana elektropermeabilizovala kreće se u rasponu od 200 mV do 1 V. Najzanimljivija činjenica u procesu elektroporacije je ta da je preko ovako nastalih pora moguće preneti bilo koju vrstu jona ili molekula u unutrašnjost ćelije. Upravo zbog ove činjenice elektroporacija ima veliki potencijal na područjima kao što su medicina, biotehnologija i farmacija.

U nastavku uvodnog dela ovog rada predstavićemo značaj elektropermeabilizacije i raspodele električnog polja za elektrohemoterapiju, EGT i transport lekovitih supstanci transdelmalnim putem. Detaljnije ćemo opisati elektrohemoterapiju, jer se ova metoda već primenjuje na čoveku, odnosno u klinici, kao palijativna metoda za lečenje kožnih i potkožnih tumora različitih histologija.

Elektrohemoterapija

Zahvaljujući elektropermeabilizaciji tkiva hemoterapija može postati lokalna metoda za selektivno odstranjivanje tumora. U tom slučaju citostatik deluje samo na deo tkiva koji je izložen delovanju električnog polja, a to je tkivo između elektroda.

Osnove hemoterapije

Hemoterapija, kao metoda za lečenje rakastih oboljenja, predstavlja korišćenje određenih lekova koji obično deluju na celo telo kako bi se uništile ćelije raka koje su metastazirale ili su se raširile u one delove tela koji se nalaze daleko od primarnog tumora. Postoji više vrsta lekova koji se koriste u hemoterapiji. Iako se svaki od njih može koristiti pojedinačno u lečenju raka, poznato je da je njihovo dejstvo snažnije kada se koristi kombinovano, jer se na taj način uništava više kancerogenih ćelija, a ujedno se i smanjuje verovatnoća da pacijent postane rezistentan na određenu vrstu leka. Iz tog razloga, lekar obično propisuje određenu kombinaciju lekova kao i dužinu trajanja tretmana, koje su za pacijenta najprimerenije. Sve odluke u vezi sa hemoterapijskim lečenjem zavise od tipa raka, njegove lokacije, stadijuma razvoja, kao i od toga kako utiče na normalne telesne funkcije i opšte zdravlje pacijenta.

Sve odluke u vezi lečenja hemoterapijom zavise od tipa raka, njegove lokacije, stadijuma razvoja, kao i toga kako utiče na normalne telesne funkcije i generalno zdravlje pacijenta.

Osnovni princip delovanja lekova koji se koriste u hemoterapiji je takav da uništavaju ćelije koje se brzo razvijaju. Međutim, pošto ovi lekovi putuju kroz celo telo, oni mogu da utiču i na normalne, zdrave, ćelije koje se takođe prirodno brzo dele. Ovakve su, na primer, ćelije koštane srži, ćelije korena kose i ćelije ga-

trično polje u celoj zapremini tumora mora prekoračiti kritičnu, odnosno, reverzibilnu, vrednost kojom se postiže elektropermeabilizacija. Ova vrednost električnog polja u literaturi se označava kao E_{rev}. U slučaju kada vrednost električnog polja u tkivu prekorači ireverzibilnu vrednost (u literaturi označenu kao E_{irev}) nastupe permanentna oštećenja u ćelijskoj membrani što dovodi do nekroze ćelije.

Na Slici 3 prikazana je raspodela električnog polja, kao rezultat dovođenja impulsa pločastim (Slika 3A) i igličastim elektrodama (Slika 3B) koje se najčešće koriste u kliničnoj elektrohemoterapiji. Intenzitet električnog polja u tkivu označen je skalom koja se nalazi u donjem delu Slike 3. Mnogim *in vivo* i *in vitro* studijama je dokazano da je efikasnost elektropermeabilizacije ćelija u korelaciji sa vrednošću električnog polja, na osnovu čega tvrdimo da i uspešnost elektrohemoterapije zavisi od raspodele električnog polja u tumoru [Gehl *et al.* 1999, Miklavčič *et al.*, 2000, Pavšelj *et al.*, 2005, Miklavčič *et al.*, 2006]. Vrednost električnog polja u tretiranom tkivu može se regulisati parametrima koji određuju njegovu jačinu, a to su dimenzije, orijentacija i oblik upotrebljenih elektroda, kao i amplituda dovedenih električnih impulsa. Pomenuti parametri moraju se odrediti u skladu sa električnim karakteristikama i geometrijom tumorskog tkiva, kao i zdravog tkiva u njegovoj neposrednoj blizini, kako bi se u tumoru postiglo odgovarajuće lokalno električno polje ($E > E_{rev}$), a ujedno i zaštitilo zdravo tkivo. Za dizajniranje odgovarajućih elektroda i ektričnih impulsa za tretman elektrohemoterapijom veliki značaj predstavljaju matematičke numeričke simulacije. U Laboratoriji za biokibernetiku, na Elektrotehničkom fakultetu u Ljubljani, bavimo se dizajnom i takozvanim predtretmanskim (pre-treatment) planiranjem. U saradnji sa Onkološkim institutom u Ljubljani i drugim istraživačkim centrima razvijamo optimizacijske metode kako bi elektrohemoterapija bila što efikasnija i prihvaćena kao uobičajena metoda u lečenju rakastih oboljenja [Miklavčič *et al.*, 2006, Šel *et al.*, 2007]. Matematičko modeliranje koristi se takođe, za optimizaciju elektromermeabilizacije u elektrogenskoj terapiji i transportu lekovitih supstancija transdermalnim putem. U modeliranju za numeričko rešavanje bioloških problema najčešće koristimo metodu konačnih elemenata [Šel *et al.*, 2005]. Validacija matematičkih modela vrši se na osnovu usklađivanja rezultata numeričkih simulacija sa odgovarajućim *in vivo* ili *in vitro* eksperimentima [Miklavčič *et al.*, 2000].

Kao što je pokazano na Slici 3 jačina električnog polja određuje stepen, odnosno režim, elektropermeabilizacije u tkivu: električno polje slabije od E_{rev} (područje na slici označeno kao $E < E_{rev}$) ne povećava propusnost ćelijske membrane; polje jačine između E_{rev} i

A. PLOČE:

B. IGLE:

Raspodela električnog polja kao rezultat aplikacije HV impulsa:

Skala koja označava jačinu električnog polja u tkivu:

$E < Erev$ $Erev \le E \le Eirev$ $E > Eirev$

- E < Erev – tkivo nije elektropermeabilizovano
- Erev ≤ E < Eirev – tkivo je reverzibilno elektropermeabilizovano
- E ≥ Eirev – tkivo je ireverzibilno elektropermeabilizovano
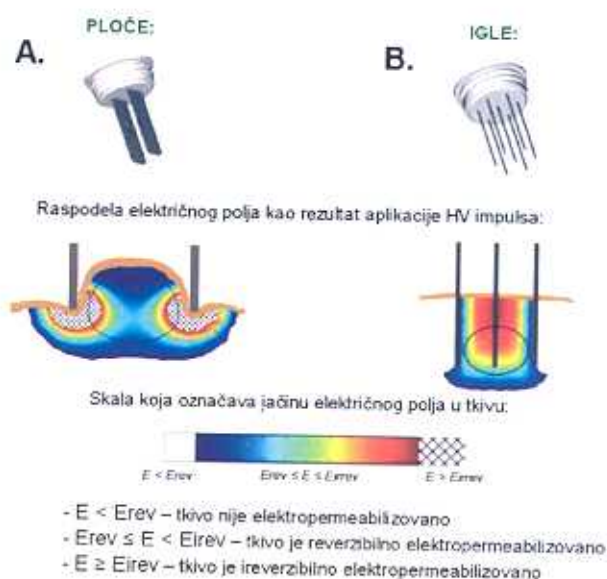
Slika 3: Jačina električnog polja — stepen odnosno režim elektropermeabilizacije: A. Pločaste (plate) electrode; B. Igličaste (needle) electrode.

E_{irev} reverzibilno elektropermeabilizuje ćelije tako da su nakon prestanka električnih impulsa sposobne da se oporave; dok električno polje nad ireverzibilnim pragom E_{irev} (šrafirano područje) prouzrokuje ablaciju ćelija. U elektrohemoterapiji je poželjno da se električni parametri dizajniraju tako da na ćelije tumora deluje električno polje reverzibilne elektropemeabilizacije, jer se na taj način obezbeđuje da tumorske ćelije umiru usled delovanja citostatika. Reverzibilnom elektropermeabilizacijom i citostaticima tj. elektrohemoterapijom postiže se vrlo brzo zarastanje tkiva i dobar kozmetički efekat, dok se ireverzibilno električno polje bez primene citostatika koristi za ablaciju tkiva kao alternativa hirurškim metodama odstranjivanja tumora [Davalos *et al.*, 2005].

Treba istaći da je kod korišćenja električnog polja u terapiji genima i transdermalnom transportu lekova obavezna primena reverzibilne elektropermeabilizacije, jer nam je cilj da sve elektropermeabilizovane ćelije prežive.

DISKUSIJA

1. Primena elektrohemoterapije u klinici

Prva klinička studija elektrohemoterapije objavljena je 1991 godine [Mir *et al.*, 1991]. Nakon toga sledile su brojne kliničke studije faze I i II, koje su pokazale vrlo pozitivnu kliničku primenu elektrohemoterapije bleomicinom i cisplatinom. U tim studijama lečeni su kožni i potkožni tumorski noduli pacijenata sa mnogim napredovanim malignitetima, kao što su sarkomi, karcianomi, a najčešće maligni melanomi. Tako je ovom metodom lečeno ukupno 247 pacijenata u svim

strointestalnog trakta. Sporedni efekti se javljaju upravo usled oštećenja zdravih tkiva, koji nestaju nakon završetka tretmana kada se zdrave ćelije oporave.

Konvencionalne kliničke metode za lokalno odstranjivanje glavnog tumora i obližnjeg zaraženog tkiva su hirurgija i radioterapija. Često se nakon operacije glavnog tumora hemoterapija koristi kao metoda za odstranjivanje preostalih ćelija raka u telu. Hemoterapija se primenjuje i kao metoda za smanjivanje tumora, kako bi hirurgu bilo lakše da ga odstrani, isto tako ova metoda se u klinici primenjuje i za olakšavanje simptoma za pacijente čiji je rak neizlečiv.

Osnove elektrohemoterapije:

Za lokalno odstranjivanje kožnih i potkožnih tumora u klinici koristi se i elektrohemoterapija — metoda koja predstavlja kombinaciju tretmana hemoterapijom i električnim poljem [Serša et al., 2003, Serša et al., 2006]. Radi se o odstranjivanju tumora lekovima koji se i inače upotrebljavaju u hemoterapiji, a čija se citotoksičnost može znatno povećati primenom električnog polja. U elektrohemoterapiji se kao citostatici trenutno koriste bleomicin i cisplatin. Pod uticajem električnog polja citotoksičnost cisplatina može se povećati do 80 puta, dok se citotoksičnost bleomicina na ovaj način može povećati čak i do 8000 puta [Serša et al., 1995, Orlowski et al., 1988]. Zato je jedna od najznačajnijih prednosti elektrohemoterapije ta, da je za uspešan tretman dovoljna vrlo mala koncentracija antitumorskog leka, koja bez aplikacije električnog polja nema nikakvog citotoksičnog efekta, što je činjenica koja je dokazana brojnim studijama [Serša at al., 2000]. Na ovaj način, značajno se mogu redukovati sporedni efekti koji mogu biti izazvani delovanjem antitumorskih lekova na zdrave ćelije. Isto tako, dokazano je da jačina električnog polja koja se koristi u elektrohemoterapiji bez delovanja hemoterapeutika nema efekta u lečenju tumora. Dakle, dok primenom samo hemoterapije ili samo električnog polja nema nikakvog antitumorskog efekta, kombinacijom ta dva tretmana mogu se postići izuzetno dobri rezultati.

Kako se primenjuje elektrohemoterapija?

Tretman elektrohemoterapijom izvodi se kombinacijom ubrizgavanja antitumorskog leka, odnosno citostatika, koje se može sprovesti sistemskim intravenoznim ili lokalnim intratumorskim putem i primenom električnih (HV-high voltage pulses) impulsa. Kao što je već rečeno, citostatici koji se koriste u elektrohemoterapiji su bleomicin i cisplatin, a njihova antitumorska efikasnost znatno se povećava aplikacijom električnih impulsa. Aplikacija električnih impulsa, proizvedenih generatorom napona, na tumorsko tkivo vrši se preko

provodničkih elektroda. Oblik elektrode zavisi od oblika i lokacije tumora. Elektrohemoterapija kožnih tumora koji su locirani na površini kože, i zato lako dostupni za neinvazivne elektrode, sprovodi se pločastim elektrodama, dok za tretman potkožnih tumora koji su se razvili daleko od površine kože, koristimo invazivne, odnosno, igličaste elektrode [Miklavčič et al., 2006].

Električni impulsi koji se primenjuju u elektrohemoterapiji pravougaonog su oblika, a protokol pod kojim se ovaj tretman izvodi sastoji se iz niza od 8 pravougaonih impulsa širine 100 μs, frekvencije 1 Hz ili 5 kHz, dok je proporcija između amplitude impulsa (U) i razdaljine između elektroda (d) obično u opsegu od 1300 V/cm do 1500 V/cm. Ovaj protokol je određen u okviru prekliničkih i kliničkih in vivo studija [Marty et al., 2006].

Na Slici 2 ilustrovan je redosled postupaka pri izvođenju elektrohemoterapije; broj jedan (1.) na slici označava injekciju antitumorskog leka (bleomicina ili cisplatina) i njegovu raspodelu u vanćelijskom prostoru, broj dva (2.) označava aplikaciju pravougaonih električnih impulsa i ulazak leka u tumorsku ćeliju kroz elektropermeabilizovanu ćelijsku membranu, dok je brojem tri (3.) ilustrovano vraćanje ćelijske membrane u prvobitno stanje nakon prestanka električnih impulsa. Citostatik ostaje u ćeliji i, aktivirajući proces mitotičke ćelijske smrti, uništava je [Mir et al., 1996].
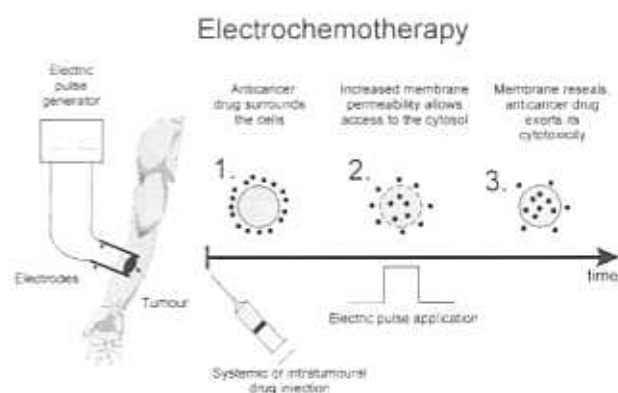
Slika 2: Ilustracija primene elektrohemoterapije (po S. B. Dev, Cancer Watch, 1994): 1. injekcija antitumorskog leka (bleomicina ili cisplatina), 2. aplikacija električnih impulsa na tkivo i ulazak leka u tumorsku ćeliju kroz elektropermeabilizovanu ćelijsku membranu i 3. povratak ćelijske membrane u prvobitno stanje nakon prestanka impulsa.

Raspodela električnog polja i elektropermeabilizacija

U cilju uspešnog lečenja tumora elektrohemoterapijom, potrebno je postići uspešnu elektropermeabilizaciju svih ćelija tumorskog tkiva, što znači da elek-

objavljenim kliničkim studijama od 1991. do 2003. godine (ukupno je bilo lečenih 1009 tumorskih nodula). U svim tim studijama je pokazano da je elektrohemoterapija praktična, jednostavna i efikasna metoda za lokalno lečenje kožnih i potkožnih tumorskih nodula, pri čemu su nepoželjni efekti uglavnom zanemarljivi [Gothelf *et al.*, 2003, Serša *et al.*, 2003, Burian *et al.*, 2003, Byrne *et al.*, 2005].

Ovi tretmani sprovođeni su prema protokolima koji su bili posebno prilagođeni za svaki od pojedinačnih onkoloških centara, što znači da se elektrohemoterapija u svakom od njih izvodila upotrebljavajući različite citostatike, različite parametre električnih impulsa (frekvencija i amplituda), različite generatore električnih impulsa, kao i različite konfiguracije elektroda [Puc *et al.*, 2004]. 2003. godine pokrenut je evropski projekat (ESOPE — European Standard Operating procedures of Electrochemotherapy) u cilju određivanja standardnog protokola za sprovođenje elektrohemoterapije. Ovim projektom izvršila se procena i potvrdila efikasnost i bezbednost elektrohemoterapije kožnih i potkožnih tumorskih nodula primenom bleomicina i cisplatina na pacijentima sa različitim malignim melanomima i drugim malignitetima u četiri onkološka istraživačka centra primenjujući jednake protokole. U kliničkoj studiji učestvovali su sledeći onkološki centri: Institut Gustave-Roussy (IGR), Villejuif, Francuska; Onkološki institut u Ljubljani, Slovenija; Univerzitet u Kopenhagenu Harlev bolnica, Herlev, Danska i Bolnica univerziteta Mercy (National University of Irland (CCRC), Cork, Irland.

Glavni ciljevi kliničke studije bili su sledeći: odrediti objektivni i kompletan odgovor na lečenje (objective OR and complete responce rate) nakon samo jednog tretmana; ispitati efikasnost bleomicina i cisplatina, kao i optimalan način njihove primene; odrediti rezultat terapije u odnosu na histologiju tumora, konfiguraciju primenjenih elektroda, frekvenciju i amplitudu električnih impulsa; odrediti rezultat terapije u odnosu na centar u kome se terapija sprovodila kao i oceniti toksičnost i bezbednost elektrohemoterapije.

Svi onkološki centri koristili su jednak generator električnih impulsa koji je u okviru projekta Cliniporator (koji je prethodio projektu ESOPE) bio posebno dizajniran za primenu elektrohemoterapije u klinici. Generator je nazvan istim imenom, dakle Cliniporator^{TM}, a sada ga komercijalno proizvodi italijansko preduzeće IGEA S.r.l., u Karpiju, Italija.

Za potrebe ESOPE projekta razvijen je centralizovani elektronski sistem za sakupljanje podataka o pacijentima koji su učestvovali u kliničkoj studiji. (Web--based electronic data collection system [Pavlović *et al.*, 2007]). Sakupljeni podaci su uključivali informacije o stanju pacijenta pre tretmana, opis tretmana, kao i

podatke o rezultatima elektrohemoterapije u periodu (follow-up period) 60 dana nakon terapije. Dimenzije tumorskih nodula pre tretmana i tokom follow-up-a merene su i praćene prema kriterijumima propisanim u WHO Handbook for Reporting Results of Cancer Treatement [WHO Handbook].

Na kraju follow-up perioda stanje svakog od tretiranih tumorskih nodula određeno je prema pomenutim WHO kriterijumima: CR — complete response rate za potpuni nestanak nodula; PR — partial responce rate za redukciju nodula za više od 50%; NC — no change za uvećanje nodula do 25% ili PD — progressive disease za uvećanje nodula za više od 25%.

Unos podataka iz svakog pojedinačnog centra u elektronski sistem vršio se preko elektronskih formulara (case report forms — CRF) dostupnih na Internetu. Informacije iz svih onkoloških centara sakupljane su u centralnoj bazi podataka, što je omogućilo neprekidno praćenje toka studije, kao i ažurnu statističku obradu sakupljenih podataka tokom same studije i po završetku studije. Struktura i sadržaj CRF formulara su interaktivni. Oni, na primer, sadrže interaktivnu mapu tela čoveka na kojoj je moguće označiti lokaciju tumorskog nodula i uneti odgovarajuće podatke o karakteristikama tumora (Slika 4). U obrasce je takođe moguće dodati digitalne fotografije tumorskih nodula, podatke o načinu tretmana i postignutim rezultatima tokom follow-up-a.
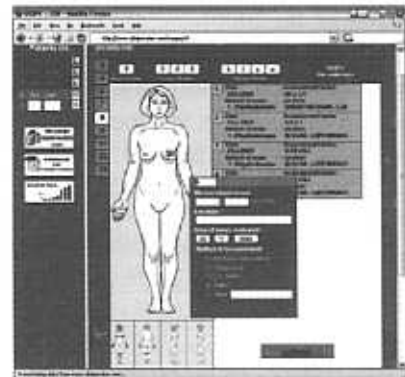
Slika 4: Interaktivna mapa čoveka urađena u Macromedia Flash-u. Označivši lokaciju tumorskog nodula lekaru se automatski nudi mogućnost za unos odgovarajućih podataka u digitalnu mapu.

Kao i u prethodnim sličnim studijama i u toku ESOPE studije takođe lečeni su, takođe, kožni i potkožni tumorski noduli pacijenata sa mnogim napredovanim malignitetima različite histologije: maligni melanomi, sarkomi i karcianomi. Projekat je trajao od 31. marta 2003. do 20. aprila 2005. godine.

U određivanje efikasnosti elektrohemoterapije (overall treatement response), u skladu sa definisanim protokolom, uključen je bio 41 pacijent, što ukupno iz-

nosi 171 tumorski nodul. Od toga je odgovor na elektrohemoterapiju postignut u tretmanu 145 nodulova (84.8%), pri čemu je potpuno ozdravljenje (complete response) postignuto kod 73.7% nodula, a delimično ozdravljenje (partial responce) kod 11.1%. Negativan odgovor (negative response) imalo je 15.2% nodula, a procenat napredovanih tumora bio je 4.7%. Opisani rezultati prikazani su grafikonom na Slici 5.
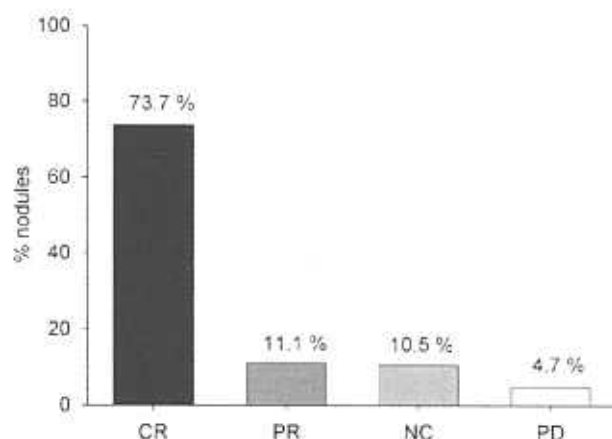
Slika 5: Efikasnost elektrohemoterapije kožnih i potkožnih tumora različitih histologija: CR — complete response rate; PR — partial responce rate; NC — no change and PD — progressive disease

Rezultati postignuti u toku ESOPE projekta potvrdili su prethodna dostignuća na području elektrohemoterapije [Marty et al., 2006].

Broj pacijenata i broj lečenih tumorskih nodula u objavljenim studijama pre ESOPE studije kao i onih lečenih tokom ESOPE studije, te uspešnost lečenja elektrohemoterapijom dati su u tabeli 1.

Rezultati tretmana elektrohemioterapijom	Broj Pacijenata	Broj tumorskih nodula	Rezultat (Response rate) %				
			OR	CR	PR	NC	PD
Pre ESCOPE studija	247	1009	83	64	19	11	6
ESCOPE studija	41	171	85	74	11	10	5

Tabela 1: Efikasnost elektrohemijoterapije u objavljenim studijama pre ESOPE projekta i tokom ESOPE projekta

Na osnovu postignutih rezultata tokom ovog projekta, uzimajući u obzir znanje i iskustvo postignuto pre ove studije propisani su protokoli (Standard Operating Prosedures SOP) za primenu elektrohemoterapije u klinici. Ovim protokolima precizno su definisani parametri kao što su primena anestezije, koncentracija i način davanja citostatika (bleomicina ili cisplatina), izbor odgovarajućih elektroda, amplituda i frekvencija električnih impulsa u odnosu na karakteristike tumorskih nodula (dimenzije pojedinačnog tumora, broj tumora i njihova lokacija), kao i propisi u vezi sa praće-

njem toka lečenja (follow-up period). Protokol je detaljno definisan u [Mir et al., 2006].

Na osnovu iskustva stečenog u elektrohemoterapiji do sada, obuhvatajući rezultate ESOPE studije, prednosti koje ovaj tretman pruža mogu se rezimirati na sledeći način [Serša et al., 2006, Marty et al., 2006]:

— CR — complete response rezultat lečenja tumora moguće je postići nakon samo jednog tretmana elektrohemoterapijom.

— Efikasnost metode ne zavisi od histologije tumora: terapijom melanoma, kao i tretmanom karcinoma i sarcoma postignuti su jednaki rezultati u efikasnosti elektrohemoterapije (OR — objective response 81%).

— Minimalni sporedni efekti: usled primene vrlo niske doze citostatika i lokalnog delovanja električnog polja ne dolazi do sistemskih sporednih efekata, nakon tretmana nije potrebna posebna nega pacijenta, prema rezultatima evaluacijskog testa o bolnosti ovog tretmana 93% ispitanih pacijenata ponovilo bi ovaj tretman ako bi to bilo potrebno.

— Jednostavna primena: elektrohemoterapija se uglavnom primenjuje pod lokalnom anestezijom i nije potrebna hospitalizacija, primena je kratkotrajna (trajanje: do 25 min) i daleko jednostavnija u poređenju sa radijoterapijom ili metodama isolated extremity perfusion i infusion (prema SOP protokolu obuka medicinskog osoblja može se izvesti u toku jednog dana).

— Moguće je ponavljanje terapije sa jednakom efikasnošću u lečenju tumora većih dimenzija kao i većeg broja tumora. U ovom slučaju tumor se može ponovo pojaviti u marginalnim područjima koja nisu bila dovoljno elektropermeabilizovana usled upotrebe elektroda čije dimenzije su manje od dimenzija tumora. I u ovakvim slučajevima, kada je tretman trebalo ponoviti, rezultat terapije bio je pozitivan, što takođe znači da pacijent usled ponavljanja tretmana ne postaje rezistentan na citostatik [Mir et al., 1998], [Serša et al., 2000]. Navedimo i slučaj efikasnosti tretmana nodula Kaposi sarkoma ponavljajućom elektrohemoterapijom [Garbay et al., 2006].

— Metoda je efikasna i u tretmanu tumora koji su se pojavili nakon tretmana konvencionalnim metodama. Naime, elektrohemoterapija primenjena na pacijenatima (u terminalnoj fazi), naročito u slučaju kada su se tumori pojavili nakon hirurgije [Mir et al., 1998] i radioterapije [Serša et al., 1998], pokazala se vrlo efikasnom u odstranjivanju tumorskih nodula. Na osnovu ovih rezultata može se zaključiti da se elektrohemoterapijom može uspešno intervenisati u slučajevima kada ostale konvencionalne metode više nije moguće primeniti i na taj način doprineti u olakšavanju simptoma pacijentima kod kojih je rak neizlečiv.

Prema do sada postignutim rezultatima možemo zaključiti da elektrohemoterapija u klinici može biti izuzetno korisna u sledećim slučajevima [Serša et al., 2006]:

— kao palijativni tretman (paliative treatement) poodmakle bolesti (melanom u fazi IV), naročito kod starijih osoba.

— kao neoadjuvantni tretman (neoadjuvant treatement), odnosno citoreduktivna terapija pre hirurške intervencije, kako bi se očuvao što veći deo organa, a ujedno i njegova funkcionalnost. Navedimo primer uspešnog odstranjivanja analnog melanoma, gde je kombinacijom elektrohemoterapije i hirurgije sačuvan sfinkter [Snoj et al., 2005]. Isto tako, kombinacijom elektrohemoterapije i hirurgije postižu se dobri rezultati digital chondrosarcoma, gde se prst spasava od amputacije, koja bi bez primene elektrohemoterapije bila neizbežna [Shimizu et al., 2003].

— u očuvanju organa i njihove funkcije (organ and function sparing), budući da je elektrohemoterapiju moguće primeniti na bilo kojem delu tela uključujući lobanju, lice, usnu duplju, kao i analno područje. Za terapiju tumora na pomenutim delovima tela elektrohemoterapija bila bi adekvatnija od radioterapije ili hirurgije. Navedimo primer uspešne elektrohemoterapije bazalnih karcinoma na području lica [Heller at al., 1998].

— kao tretman hemoragičnih i bolnih tumorskih nodula. Pod uticajem električnog polja dolazi do vaskulatornih promena u tkivu, odnosno dolazi do redukcije protoka krvi u tumoru. Usled ovog fenomena, takozvanog »vascular lock«-a, produžava se delovanje citostatika, zaustavlja krvarenje i ublažava bol. Navedimo primer efikasnog paliativnog tretmana hemoragičnih kožnih metastaza, gde je elektrohemoterapijom zaustavljeno krvarenje [Ghel et al., 2000] i slučaj pacijenta (sa vrlo bolnim squamous carcinoma of supraglotis) kome je elektrohemoterapijom ublažen bol [Serša et al., 1998].

Opšti zaključak: Elektrohemoterapija je jednostavna, bezbedna i efikasna metoda koja može dati vrlo dobre rezultate nakon jednog samog tretmana. Trenutno se u klinici koristi kao palijativna metoda za odstranjivanju kožnih maligniteta različitih histologija. Razvojem endoluminarnih elektroda u kombinaciji sa hirurškom intervencijom ova metoda trebala bi da počne da se primenjuje i za lečenje tumora na unutrašnjim organima. Očekuje se da će se budućim razvojem, kao i širenjem stečenog znanja i iskustva, indikacije za primenu elektrohemoterapije u klinici raširiti.

2. Elektroporacija u trasnferu DNK:

Sa dešifrovanjem ljudskog genoma dolazi do revolucionarnog napretka u istraživanjima na području farmacije i medicine, jer se transferom gena, pruža mogućnost za lečenje mnogih naslednih i infektivnih bolesti. Uprkos obećavajućim rezultatima postignutih uspešnom terapijom genima koji su unešeni pomoću virusnih vektora, postoji još mnogo nerešenih pitanja u vezi sa neželjenim efektima koji mogu nastupiti usled negativnog odgovora imunskog sistema. Zato se u nauci puno pažnje posvećuje nevirusnim metodama transfera terapijskih gena u ciljna tkiva i organe [Parker et al., 2003; Mehier-Humbert and Guy, 2005]. Jedno od mogućih nevirusnih rešenja za transfer gena u ćelije je primena električnih impulsa, odnosno električnog polja, kako bi se povećala propustljivost membrane. Ovu metodu nazivamo *elektrogenska terapija* [Čemažar et al., 2006]. Eksperimenti potvrđuju da se najbolji rezultati transfera genetskog materijala kroz ćelijsku membranu mogu postići kombinacijom kratkih impulsa visoke amplitude i dugotrajnih impulsa niske amplitude. Na taj način, prvim impulsom postižemo povećanje propustljivosti ćelijske membrane, odnosno njenu elektropermeabilizaciju. Naredni, duži impuls manjeg intenziteta, vrši elektroforezu, pri čemu negativno naelektrisani molekuli DNK bivaju potisnuti prema prethodno elektropermeabilizovanoj membrani i unutrašnjosti ćelije [Šatkauskas et al., 2002; Šatkauskas et al., 2005]. Pri unosu gena ovom metodom moramo biti jako oprezni kod dizajniranja električnog polja koje ne sme da bude previsoko kako bi reverzibilno elektropermeabiliziovali ćelijske membrane, i time očuvali ćelije. Sa druge strane, ireverzibilna elektropermeabilizacija pri elektrohemoterapiji nije naročito opasna, jer je uništavanje tumorskih ćelija cilj ove terapije.

Prva klinička ispitivanja (odnosno kliničke studije faze I i II) za primenu elektropermeabilizacije u genskoj terapiji već su u toku.

3. Elektroporacija u transdermalnom transportu lekovitih supstanci

Lekovite supstance moguće je unositi u telo i transdermalnim putem, koji u odnosu na primenu lekova invazivnim intravenoznim putem ima određene prednosti među kojima su sprečavanje nepoželjnog delovanja probavnih encima na supstance koje se unose, kao i postepen, konstantan unos lekovite supstance u telo, nasuprot brzom intravenoznom unosu. Za unos lekova transdermalnim putem koriste se sledeće metode: ultrazvuk, iontoforeza i elektropermeabilizacija (elektroporacija) [Prausnitz, 1997; Barry, 2001; Denet and Préat, 2003; Prausnitz et al., 2004]. Zbog svoje zaštitne funkcije i velikog električnog otpora, koža predstavlja veliku barijeru za transdermalni transport supstanci. Pod uticajem električnog polja, odnosno procesom elektropermeabilizacije, moguće je privremeno smanjiti električni otpor kože i na taj način privremeno povećati propustljivost kože kako bi se omogućio transport leka u telo. Elektropermeabilizacija kože može se postići bez nastanka nepoželjnih i štetnih efekata, a treba istaknuti da električna struja tokom ovog procesa dodatno ubrza transdermalni prenos jona i naelektrisanih molekula [Prausnitz, 1996; Prausnitz, 1999].

Summary

APPLICATION OF CELL ELECTROPORATION IN MEDICINE

Selma Ćorović,[1] Ivan Pavlović,[1] Gregor Serša,[2] Damijan Miklavčič[1]

1 — School of Electrical Engineering, University of Ljubljana; 2 — Institute of Oncology, in Ljubljana

When a biological tissue is exposed to the high voltage pulses a local electric field distribution within its volume is created. If the magnitude of the local electric field exceeds a critical threshold value the cell membranes become more permeable for ions and molecules, which otherwise can not enter the cell. Such a modality of cell membrane permeabilization by means of electric field is named electroporation (also termed electropermeabilization) and allows for increased entrance of any type of ions and molecules into the cell. This phenomenon is being widely used in many in vivo and in vitro biological and medical applications in order to facilitate the transfer of diverse therapeutic into cells, such as chemotherapeutics and DNA. In this paper we present the following medical applications of cell electroporation process: electrochemotherapy, electrogene transfection and transdermal drug delivery.

Literatura

Barry BW. Novel mechanisms and devices to enable successful transdermal drug delivery. Eur J Pharm Sci 2001; 14: 101–114.

Burian M, Formanek M, Regele H. Electroporation therapy in head and neck cancer. Acta Otolaryngol 2003; 123 : 264–8.

Byrne CM, Thompson JF, Johnston H, et al. Treatement of metastatic melanoma using electroporation therapy with bleomycin (electrochemotherapy). Melanoma Res 2005; 15 : 45–51.

Čemažar M, Golzio M, Serša G, Rols MP, Teissie J. Electrically-assisted nucleic acids delivery to tissues in vivo: Where do we stand? Curr Pharm Design 2006; 12 : 3817–25.

Davalos R, Mir LM, Rubinsky B. Tissue ablation with reversible electroporation. Ann Biomed Eng 2005; 33(2) : 223–231.

Denet A-R, Préat V. Transdermal delivery of timolol by electroporation through human skin. J Control Release 2003; 88 : 253–262.

Garbay J, Billard V, Bernat C, Mir LM, Morsli N, Robert C. Successful repetitive treatements by electrochemotherapy of multiple unresectable Kaposi sarcoma nodules. Eur J Cancer Suppl 2006; 4 : 29–31.

Gehl J, Sorensen TH, Nielsen K, Reskmark P, Nielsen SL, Skovsgaard T, Mir LM. In vivo electroporation of skeletal muscle: threshold, efficacy and relation to electric field distribution. Biochim Biophys Acta 1999; 1428 : 233–240.

Gehl J, Geertsen PF. Efficient palliation of heamorrhaging malignant melanoma skin metastasis by electrochemotherapy. Melanoma Res 2000; 10 : 585–9.

Gehl J. Electroporation: theory and methods, perspectives for drug delivery, gene therapy and research. Acta Physiol Scand 2003; 177 : 437–447.

Gothelf A, Mir L M, J. Mir. Electrochemotherapy: results of cancer treatement using enhanceddelivery of bleomycin by electroporation. Cancer Treatement Rev 2003; 29 : 371–87.

Heller R, Jaroszeski MJ, Reintgen DS, Puleo CA, DeConti RC, Gilbert R, Glass LF. Treatment of cutaneous and subcutaneous tumors with electrochemotherapy using intralesional bleomycin. Cancer 1998; 83 : 148–157.

Marty M, Serša G, Garbay JR, Gehl J, Collins CG, Snoj M et al. Electrochemotherapy — An easy, highly effective and safe treatment of cutaneous and subcutaneous metastases: Results of ESOPE (European Standard Operating Procedures of Electrochemotherapy) study. Eur J Cancer Suppl 2006; 4 : 3–13.

Mehier-Humbert S, Guy RS. Physical methods for gene transfer: improving the kinetics of gene delivery into cells. Adv Drug Deliv Rev 2005; 57(5) : 733–753.

Miklavčič D, Ćorović S, Pucihar G, Pavšelj N. Importance of tumour coverage by sufficiently high local electric field for effective electrochemotherapy. Eur J Cancer Suppl 2006; 4 : 45–51.

Miklavčič D, Pucihar G, Pavlovec M, Ribarič S, Mali M, Maček-Lebar A, Petkovšek M, Nastran J, Kranjc S, Čemažar M, Serša G. The effect of high frequency electric pulses on muscle contractions and antitumor efficiency in vivo for a potential use in clinical electrochemotherapy. Bioelectrochemistry 2005; 65 : 121–128.

Miklavčič D, Šemrov D, Mekid H, Mir LM. A validated model of in vivo electric field distribution in tissues for electrochemotherapy and for DNA electrotransfer for gene therapy. Biochim Biophys Acta 2000; 1523 : 73–83.

Miklavčič D, Kotnik T. Electroporation for Electrochemotherapy and Gene Therapy. Bioelectromagnetic Medicine, Marcel Dekker, New York 2004; 637–656.

Mir LM, Banoun H, Paoletti C. Introduction of definite amounts of nonpermeant molecules into living cells after electropermeabilization: Direct access to the cytosol. Exp Cell Res 1988; 175 : 15–25.

Mir LM, Glass LF, Serša G, Teissie J, Domenge C, Miklavčič D et al., Effective treatment of cutaneous and subcutaneous malignant tumours by electrochemotherapy. Br J Cancer 1998; 77 : 2336–2342. OK

Mir LM, Orlowski S, Belehradek J, Paoletti C. Electrochemotherapy potentiation of antitumor effect of bleomycin by local electric pulses. Eur J Cancer 1991; 27(1) : 68–72.

Mir LM, Tounetki O, Orlowski S. Bleomycin: revival of an old drug. General Pharmacol 1996; 27 : 745–748.

Mir LM, Gehl J, Serša G et al. Standard operating procedures of the electrochemotherapy : Instructions for the use of bleomycin or cisplatin administrated either systemically or lo-

cally and electric pulses delivered by CliniporatorTM by means of invasive or non-invasive electrodes. Eur J Cancer Suppl 2006; 4 : 14–25.

Neumann E, Sowers A E, Jordan C A. Electroporation and Electrofusion in Cell Biology. Plenum Press, New York 1989.

Okino M, Mohri H. Effects of high-voltage electrical impulse and an anticancer drug on in vivo growing tumors. Jpn J Cancer Res 1987; 78 : 1319–1321.

Orlowski S, Belehradek Jr J, Paoletti C, Mir LM. Transient electropermeabilisation of cells in culture. Increase in the cytotoxicity of anticancer drugs. Biochem Pharmacol 1998; 37 : 4724–33.

Parker AL, Newman C, Briggs S, Seymour L, Sheridan PJ. Nonviral gene delivery: techniques and implications for molecular medicine. Expert Rev Mol Med 2003; 5: 1–15. OK

Pavlin M, Pavšelj N, Miklavčič D. Dependence of induced transmembrane potential on cell density, arrangement, and cell position inside a cell system. IEEE Trans Biomed Eng 2002; 49(6) : 605–612

Pavlovic I, Miklavcic D. Web-based electronic data collection system to support electrochemotherapy clinical trial. IEEE Trans. Inform. Tech. Biomed. 11 : 222–230, 2007.

Pavšelj N, Bregar Z, Cukjati D, Batiuskaite D, Mir LM, Miklavčič D. The course of tissue permeabilization studied on a mathematical model of a subcutaneous tumor in small animals. IEEE Trans Biomed Eng 2005; 52 : 1373–1381.

Prausnitz MR, Mitragotri S, Langer R. Current status and future potential of transdermal drug delivery. Nat Rev Drug Discov 2004; 3(2) : 115–124.

Prausnitz MR. A practical assessment of transdermal drug delivery by skin electroporation. Adv Drug Deliv Rev 1999; 35 : 61–76.

Prausnitz MR. Reversible skin permeabilization for transdermal delivery of macromolecules. Crit Rev Ther Drug Carrier Syst 1997; 14(4) : 455–483.

Prausnitz MR. The effects of electric current applied to skin: A review for transdermal drug delivery. Adv Drug Deliv Rev 1996; 18 : 395–425.

Puc M, Ćorović S, Flisar K, Petkovšek M, Nastran J, Miklavčič D. Techniques of signal generation required for electropermeabilization. Survey of electropermeabilization devices. Bioelectrochemistry 2004; 64 : 113–124.

Šatkauskas S, Andre F, Bureau MF, Scherman D, Miklavčič D, Mir LM. Electrophoretic component of electric pulses determines the efficacy of in vivo DNA electrotransfer. Hum Gene Ther 2005; 16 : 1194–1201.

Šatkauskas S, Bureau M, Puc M, Mahfoudi A, Scherman D, Miklavčič D, Mir LM. Mechanisms of in vitro DNA electro-transfer: Respective contributions of cell electropermeabilization and DNA electrophoresis. Mol Ther 2002; 5(2) : 133–140.

Šel D, Cukjati D, Batiuskaite D, Slivnik T, Mir LM, Miklavčič D. Sequential finite element model of tissue electropermeabilization. IEEE Trans Biomed Eng 2005; 52 : 816–827.

Šemrov D, Miklavčič D. Vsiljeni transmembranski potencial zaradi zunanjega električnega polja v odvisnosti od oblike in orientacije ter gostote celic. Elektrotehniški vestnik 1995; 62(1) : 35–42.

Serša G, Čemažar M, Miklavčič D, Chaplin DJ. Tumor blood flow modifying effect of electrochemotherapy with bleomycin. Anticancer Res 1999; 19(5B) : 4017–22.

Serša G, Čemažar M, Miklavčič D. Antitumor effectivness of electrochemotherapy with cis-diamminedichloroplatinium (II) in mice. Cancer Res 1955; 55 : 3450–3455.

Serša G, Čemažar M, Miklavčič D. Tumor blood flow modifying effects of electrochemotherapy: a potential vascular targeted mechanism. Radiol Oncol 2003; 37 : 43–8.

Serša G, Štabuc B, Čemažar M, Jančar B, Miklavčič D, Rudolf Z. Electrochemotherapy with cisplatin: potentiation of local cisplatin antitumor effectivness by application of electric pulses in cancer patients. Eur J Cancer 1998; 34 : 1213–8.

Serša G, Čemažar M, Parkins CS, Chaplin DJ. Tumor blood flow changes induced by application of electric pulses. Eur J Cancer 1999; 35 : 672–677.

Serša G, Čemažar M, Rudolf Z. Electrochemotherapy: advantages and drawbacks in treatment of cancer patients. Cancer Therapy 2003; 1 : 133–142.

Serša G, Kržič M, Šentjurc M, Ivanuša T, Beravs K, Kotnik V, Coer A, Swartz HM, Čemažar M. Reduced blood flow and oxygenation in SA-1 tumours after electrochemotherapy with cisplatin. Br J Cancer 2002; 87 : 1047–54.

Serša G, Štabuc B, Čemežar M, Miklavčič D, Rudolf Z. Electrochemotherapy with cisplatin: Clinical experience in malignant melanoma patients. Clinical Cancer Research 2000; 6 : 863–867.

Serša G. The state-of-the-art of electrochemotherapy before the ESOPE study; advantages and clinical uses. Eur J Cancer Suppl 2006; 4 : 52–59.

Shimizu T, Nikaido T, Gomyo H et al. Electrochemotherapy for digital Chondrosarcoma. J Orthop Sci 2003; 8 : 248–51.

Snoj M, Rudolf Z, Cemazar M, Jancar B, Sersa G. Successful sphincter-saving treatment of anorectal malignant melanoma with electrochemotherapy, local excision and adjuvant brachytherapy. Anti-Cancer Drugs 2005;16 : 345–348.

Weaver J C, Chizmadzhev Y A. Theory of electroporation: A review. Bioelectrochem. Bioenerg. 1996; 41 : 135–60.

WHO Handbook for Reporting Results of Cancer Treatement, vol. 48. Geneva; 1997. p. 22–7.

Paper XIV

A web-application that extends functionality of medical device for tumor treatment by means of electrochemotherapy

Ivan Pavlović, Peter Kramar, Selma Čorović, David Cukjati, Damijan Miklavčič

Faculty of Electrical Engineering, University of Ljubljana, Slovenia

Electrochemotherapy (ECT) is a novel method for efficient tumor treatment in clinical environment. It combines local drug delivery and application of short high voltage pulses, which permeabilize the plasma membrane by electroporation. Drug can enter only the cells with permeabilzed membrane. Recently, medical device Cliniporator™ for controlled electroporation was developed. Here, we present a web-application that extends the functionality of this medical device. The aim of the application is to collect, store and to allow the analysis of every ECT application using this medical device. The application helps transferring data collected by device during the electroporation process to the central database, and enables filling of medical records through the web-forms. The application is based on technologies ASP, HTML, Flash, JavaScript, XML and others. The application main advantages are easy and rapid data access, scalability and independence of client computer operating system as well as easy application debugging and upgrading.

Key words: neoplasms-drug therapy; drug delivery systems; electroporation-instrumentation; internet

Introduction

In the cooperation with the European partners, the medical device called Cliniporator™ (IGEA s.r.l., Carpi, Italy) was developed, in the frame of the *Cliniporator* project (2000-03) funded by European Community. This device was designed for controlled *in vivo* cell permeabilization by electroporation. Electroporation is used to provide access to molecules distributed freely in the vascular and extracellular compartments that normally do not enter the intracellular compartments.[1,2,3] This technique is already used clinically to deliver cytotoxic molecules like bleomycin and cisplatin to solid tumors by *electrochemotherapy* (ECT).[4,5]

For a successful cell electroporation a voltage applied for a given electrode tissue geometry, pulse duration and number of pulses should always be in the range between reversible and irreversible threshold value. If the voltage applied exceeds the irreversible threshold value, a change in a cell membrane becomes permanent and destroys the cell. The most commonly very short (100 µs) high-voltage pulse or a sequence of such pulses are delivered. Pulses are generated in the high-voltage generator of Cliniporator™ and deliv-

ered through the needle or plate electrodes to the tissue. By measuring both current and voltage simultaneously the device is monitoring electrical property changes of tissue in real time.

Cliniporator™ is also the first medical device designed for *in vivo* DNA electrotransfer in clinical applications. The two key steps of DNA electrotransfer are the electroporation of the target cells and the electrophoresis of the DNA within the tissue. Therefore, the device delivers to the target cells a combination of short high-voltage pulse(s) that permeabilize the cells without substantial DNA transfer/transport, and a long low-voltage pulse(s) that do not cause permeabilization but facilitate DNA transfer into the cells. This non viral gene therapy method is called *electrogenetherapy* (EGT) and has many advantages with respect to viral methods.[6]

Indeed, the medical device Cliniporator™ is already used in clinical trials. They are performed in four approved medical centers in Europe, funded by European Community in a frame of ESOPE project (2003-2004). The aim of the project is to define Standard Operating Procedures (SOP) for electrochemotherapy and electrogenetherapy. Definition of the SOP can only be based on the wide study of ECT and EGT efficiency. Therefore, it is necessary to carefully follow and collect outcomes of ECT and EGT clinical trials.

For collection of data acquired in ECT clinical trials a standard paper forms (Clinical Report Forms - CRF) were prepared. The CRF consists of a number of subforms, of which extent depends on the number of treated tumors and number of sessions required to treat the tumor. The CRF include patient's general data, his/her medical history, tumor treatment data and response data. A tumor treatment can be repeated if necessary. The melanoma nodules can efficiently be treated by ECT, therefore patients with this type of tumors were included in the study. For every patient, medical personnel has to fill in 40

pages of forms on average. Since all forms are predefined and same for all patients, we decided to set up a unified database (*central database*) for collection of data from all four medical centers involved in the study. For submission of relatively high number of data into the central database we developed a web-application, which enables access to the central database and filling of forms from any computer connected to the World Wide Web.

Cliniporator™

Cliniporator™ is a medical device for electrochemotherapy and electrogenetherapy. It consists of two parts: a console (industrial PC compatible computer) for local collection of treatment data and user friendly interface; and an electroporator. Electroporator consists of a control unit, high voltage amplifier and low voltage amplifier. Control unit consists of a processor board, a measurement card for current and voltage measurement, a control card for driving voltage amplifiers and a control-relay card for switching between the electrodes.

A user controls the electroporator through graphical display and a keyboard of the console unit. He/she can enter relevant patient data, choose appropriate electrodes, and define pulse parameters such as number (e.g. 8 pulses), amplitude (up to 1000 V), duration (e.g. 100 μs), and repetition frequency (e.g. 1 Hz) of pulses. All users' presets are stored in a local database, which is integrated into the console. By pressing a foot switch, the user triggers pulse generation. Square-shaped pulses are delivered. During the pulse delivery, the control unit measures voltage and current through the load (a cell suspension or a tissue). After the pulse application voltage and current measurements are stored into the local database. User can use the local database for later analysis of performed treatments. Based on collected data we intend to

develop an algorithm, which will allow device to adjust pulse voltage according to the current and voltage measurements in the real time and thus prevent irreversible changes in the cell membranes.

Central database

The central database (Microsoft SQL Server) stores following data collected from all the medical centers involved in study:

- patient data (demography, medical history, physical examination,...etc.),
- treatment data (sessions, evaluation visits, follow-ups,...etc.),
- data submitted from local databases of Cliniporator™ medical devices,
- images of tumor nodules in a different phases of treatment.

A backup copy of central database is automatically generated once per week.

Each medical center has limited data access. Users from one medical center cannot read or modify data entered by other centers. Entered data are protected by username and password. Every medical center can have more authorized users, who all have access to the same data. Users can lock selected data, so they cannot be accidentally modified (it is like signing medical forms).

Web-application

Since medical centers that share data in the central database are spread all over Europe, we had to develop an application for user interaction with the database, which is easy to install, debug and upgrade. It also had to be very intuitive for using, so the users (a medical personnel) should not require any computer knowledge background or excessive training. It had to involve functionalities like: filling the clinical report forms (CRF), interactive human map for marking location of nod-

ules, uploading images to the central database, image gallery, uploading local databases to the central database, and review of already submitted data. In order to follow the progress of individual centers the application also involves statistical representation of the submitted data. An important prerequisite, common in research studies, was that the system has to be upgradeable.

A client-server application would be costly to maintain and upgrade, therefore such solution was not acceptable. Therefore, we developed a web-application (*called Cliniporator Web-Recorder*), which is in our opinion an optimal solution. Such solution does not need any installations on a client computer. Clients can access the central database through the web-application from any computer connected to the World Wide Web and installed internet browser (Internet Explorer, Netscape, Mozzila,...). The web-application is executing on a web-server. The application speed depends only on the web-server capabilities and the internet communication bandwidth while the client computer does not affect the application speed. By submitting username and password users can access all the application functionalities according to their level of authorization.

Cliniporator Web-Recorder maintenance and upgrade is performed exclusively on the web-server. This is the quickest and the most effective and inexpensive way for debugging and upgrading the system. During the application development users have a possibility to participate in testing, which is very important for timely detection of irregularities in the system.

Cliniporator Web-Recorder functionalities are:
- web-forms (digital clinical report file (CRF));
- interactive human map for marking location of tumor nodules;
- image upload;
- local database upload;

- basic statistics (statistical processing of the submitted data).

   Web-forms (digital CRF) are form-like web pages (Figure 1). Through digital CRF users submit patient and treatment data to the central database. Digital CRF have the same form as the paper-based CRF. They are organized in the following sections: pre-study visit, sessions, adverse events, concomitant medications, follow-up and end of study. The particular section is divided into several pages. *Pre-study visit* consists of few pages where users enter patient's demography data, medical history (history of cancer, previous treatments and history of chronic non malignant diseases), vital signs, physical examinations, tumor lesions, laboratory results, inclusion criteria and exclusion criteria. Users can add any

number of *sessions* (most usually two sessions). For every session users have to mark treated nodules and fill several pages with the following data: the time of the begin and the end of the session, vital signs, physical examination, post procedure data (memory from the procedure and pain assessment), and, later, day 15 and day 30 evaluation visit data (response to the treatment and memory from the procedure). Users can create one or more *follow-up* sections and enter data like date of the visit and lesion measurements. In the *end of study* section users should enter the reason for study termination. According to the already submitted data, some form-like web pages are dynamically generated, (e.g. if a patient has more tumor nodules, each nodule requires few form-like web pages for its description).

Figure 1. A digital CRF page.

An important advantage of the digital CRF is an automatic data checking. The web-application warns a user if he/she mistypes or enters erroneous data. The other advantage is a simple navigation through numbered forms.

At the end of every section users have an opportunity to »digitally sign« the completed section. By signing a section the corresponding forms are »locked« and all further modifications are disabled.

The purpose of the **interactive human map** is a visual representation of the tumor locations. According to the patient's sex, appropriate body map is displayed. Users can switch between four views: front, rear, left and right. By simply clicking on the map, user can »add« a tumor, and then submit some principal data about the tumor (location, measurement lesion, date and method of examination) and corresponding images. During the sessions, users can select on the map which of the pre-registered tumors are treated. The interactive human map is shown on the Figure 2.

Image upload enables storing of tumor images into the central database. Images, captured by a digital camera, can be uploaded in the original size. A smaller image, suitable for displaying, as well as a thumbnail of the image, are dynamically generated and also stored in the database. Users can add a caption and a description to every image. Images can be added in every phase of the treatment (pre-study, sessions, follow-up,...). In the *image gallery* (Figure 3) users can review all the uploaded images of one patient, or only the pictures of a particular phase of the treatment. This is very useful for the visual observation of tumor changes.

Local database upload is also performed trough the internet browser. The user simply selects the local database file and fills in comments. The rest of the process is automatic: application saves uploaded file on the server, records some upload information (date and time, user id, name of the file,...), and then copy data from the uploaded file to the central database. Application takes care of a duplicate data and their overwriting - the newer data will overwrite the older ones. At the end of the upload process user is informed about the upload success. In the list of the uploaded data user can check all the data uploaded from his/her center.
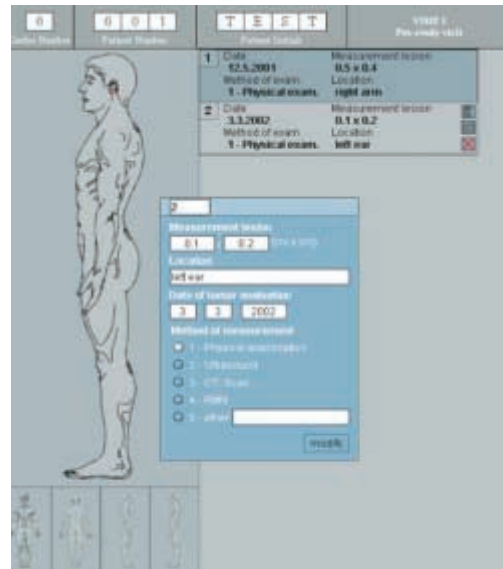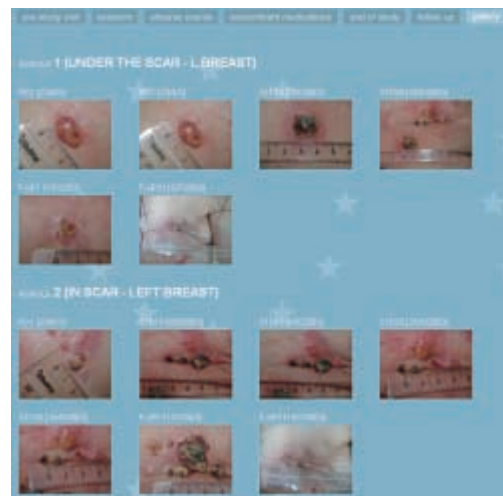

Figure 2. Interactive human map.

Figure 3. Image gallery: images are grouped by nodule and sorted by time.

Basic statistics, which allow the follow-up of the project progress, are dynamically generated from the data in the central database. Therefore, it offers information about the number of treated patients per center as well as number of ended therapies, number of tumor sessions and uploaded corresponding local databases, distributions of applications of different electrode types and different drugs. Every center has access to these statistics and can compare its activities with others. Some statistics (usually local statistics) can be dedicated to a particular center and therefore hidden from other users.

Conclusion

We have developed a web-application, *Cliniporator Web-Recorder*, for user interaction with the database of medical records collected during the testing period of medical device Cliniporator™. It also supports central collection of data stored in local databases of Cliniporator™ medical devices. This is important for fast detecting of possible device malfunctions and for following the single-use electrode stocks. The amount of data collected in the central database gives us an opportunity to perform a wide analysis of clinical trial results. The results of analysis will contribute to establish standard operating procedures (SOP) for electrochemotherapy and later for electrogenetherapy. These results will also help us in improving the Cliniporator™ medical device and determining algorithms for intelligent pulse delivery. A large collection of medical records can also be helpful to clinicians in choosing optimal treatment protocol for a particular tumor lesion. Our aim is to build a decision making system that will be able to suggest an optimal therapy for a particular tumor.

The advantage of the *Cliniporator Web-Recorder* is that the system can easily be upgraded without any users' disturbance. Due to the web-application and database centralization all system modifications are implemented locally on the server, while users are just informed about the improvements.

References

1. Maček Lebar A, Serša G, Čemažar M, Miklavčič D. Electroporation. *Med Razgl* 1998; **37:** 339-54.

2. Neumann E, Kakorin S, Toensing K. Fundamentals of electroporative delivery of drugs and genes. *Bioelectrochem Bioenerg* 1999; **48:** 3-16.

3. Satkauskas S, Bureau MF, Puc M, Mahfoudi A, Scherman D, Miklavčič D, et al. Mechanisms of in vivo DNA electrotransfer: respective contributions of cell electropermeabilization and DNA electrophoresis. *Mol Ther* 2002; **5:** 133-40.

4. Serša G, Čemažar M, Rudolf Z. Electrochemotherapy: advantages and drawbacks in treatment of cancer patients. *Cancer Therapy* 2003; **1:** 133-42.

5. Mir LM, Orlowski S. Mechanisms of electrochemotherapy. *Adv Drug Deliv Rev* 1999; **35:** 107-18.

6. Ferber D. Gene Therapy. Safer and virus-free? *Science* 2001; **294:** 1638-42.

Paper XV

Review

Techniques of signal generation required for electropermeabilization. Survey of electropermeabilization devices

Marko Puc, Selma Čorović, Karel Flisar, Marko Petkovšek, Janez Nastran, Damijan Miklavčič*

Damijan Miklavčič, University of Ljubljana, Faculty of Electrical Engineering, Tržaška 25, SI-1000 Ljubljana, Slovenia

Abstract

Electropermeabilization is a phenomenon that transiently increases permeability of the cell plasma membrane. In the state of high permeability, the plasma membrane allows ions, small and large molecules to be introduced into the cytoplasm, although the cell plasma membrane represents a considerable barrier for them in its normal state. Besides introduction of various substances to cell cytoplasm, permeabilized cell membrane allows cell fusion or insertion of proteins to the cell membrane. Efficiency of all these applications strongly depends on parameters of electric pulses that are delivered to the treated object using specially developed electrodes and electronic devices— electroporators. In this paper we present and compare most commonly used techniques of signal generation required for electropermeabilization. In addition, we present an overview of commercially available electroporators and electroporation systems that were described in accessible literature.
© 2004 Elsevier B.V. All rights reserved.

Keywords: Electroporation; Electropermeabilization; Instrumentation; Electrochemotherapy; Gene transfection

1. Introduction

The use of high voltage electric pulse technology, electropermeabilization, in cell biology, biotechnology and medicine has attracted significant interest ever since first reports were published several decades ago [1–3]. Electropermeabilization is a transient phenomenon that increases permeability of the cell plasma membrane. In the state of high permeability, the plasma membrane allows ions, small and large molecules to be introduced into the cytoplasm, although the cell plasma membrane in its normal state represents a considerable barrier for them. Besides introduction of different substances to the cytoplasm, the permeabilized cell membrane allows cell fusion or insertion of proteins into cell membrane (Fig. 1) [4–7]. Efficacy of electropermeabilization and its applications strongly depends on many parameters that can be divided into parameters of the electric field (i.e. pulse amplitude, pulse duration, pulse repetition frequency, number of pulses and pulse shape) [8–13], and parameters that define the state of

cells, their surroundings and cell geometry (i.e. temperature, osmotic pressure, cell size and shape, etc.) [7,14]. With properly chosen values of the electric field parameters, the process of electropermeabilization is reversible and cells return into their normal physiological state. If these parameters exceed certain values (e.g. amplitude of pulses is too high or duration of pulses is too long), cells are irreversibly permeabilized and lose their viability (Fig. 1) [5–7].

Permeabilization of cell plasma membrane is achieved by exposure of the cell to a short but intense electric field. The basic quantity underlying this process is presumably the induced transmembrane potential difference, which is in the first approximation proportional to the product of the applied electric field strength E and cell radius R [7,16]. Furthermore, it has been shown that electric field controls the permeabilization of cell membrane in two ways. (1) Electric field initiates permeabilization of cell membrane in the regions where transmembrane potential difference exceeds the threshold value (between 200 and 300 mV) [7,9]. (2) Electric field strength defines the size of permeabilized area of cell membrane [7,9,11]. This means that permeabilization of cell membrane will occur only if the applied electric field is larger than the threshold value. Since the induced transmembrane potential difference is also proportional to the cell radius, it is

---

* Corresponding author. Tel.: +386-1-4768-456; fax: +386-1-4264-658.

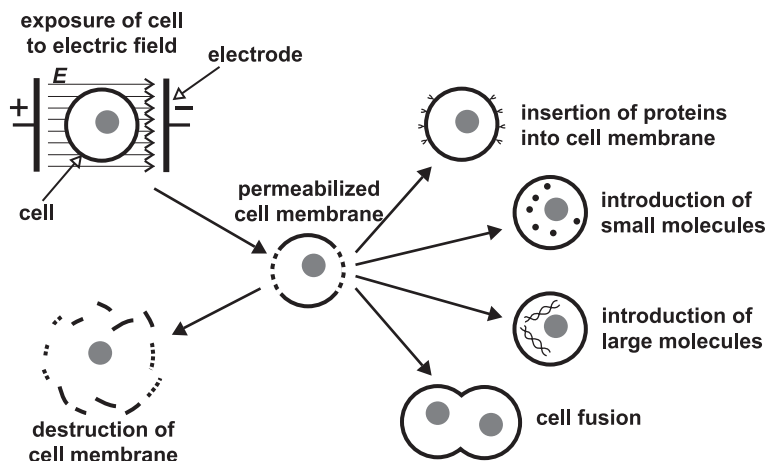*E-mail address:* damijan@svarun.fe.uni-lj.si (D. Miklavčič).

Fig. 1. Exposure of a cell to an electric field may result either in permeabilization of cell membrane or its destruction. In this process the electric field parameters play a major role. If these parameters are within certain range, the permeabilization is reversible, therefore it can be used in applications such as introduction of small or large molecules into the cytoplasm, insertion of proteins into cell membrane or cell fusion.

evident that threshold value of electric field varies with cell size. This means that large cells are more sensitive to lower electric field strengths than small cells [7,9]. Moreover, it has been shown that induced transmembrane potential difference also depends on cell density, arrangement and cell position [17–19]. Considering this, it is very difficult to generalize the electric field parameters for different experimental conditions (i.e. single cell permeabilization, in vitro, in vivo, etc.), or for different cell types (i.e. animal, plant, fungi, prokaryotic). In addition, different applications require different time variation of electric fields (i.e. exponentially decaying, square wave, etc.) and different exposure times.

It is not an aim of this paper to focus on further description of electric field parameters that are required in different applications of electropermeabilization. Instead, we would like to present and compare advantages and drawbacks of the existing and most commonly used concepts of electric signal generation and available devices that fulfill electrical requirements of applications such as: electrochemotherapy, electrotransfection, insertion of proteins into cell membrane, cell fusion and transdermal drug delivery [5–7,15,20–23].

2. Techniques of signal generation required for electropermeabilization

Effectiveness of electropermeabilization in either in vitro, in vivo or clinical environment depends on the distribution of electric field inside the treated sample [24–26]. To achieve this, we have to use an appropriate set of electrodes (e.g. needle, parallel plates, cuvettes, etc.) and an electropermeabilization device—electroporator that generates required voltage or current signals. Although both parts of the mentioned equipment are equally important for effectiveness of electropermeabilization, electroporator has substantially more important role since it has to be able to deliver

the required signal to its output loaded by impedance of sample between electrodes.

Probably the major problem that every engineer faces during the design of electroporator is characterization of the load, which in principle has resistive and capacitive component. The value of each component is defined by geometry and material of electrodes and by electrical and chemical properties of the treated sample. In in vitro conditions these parameters that influence on impedance of load can be well controlled since size and geometry of sample is known especially if cuvettes are used, furthermore by using specially prepared cell mediums electrical and chemical properties are defined or can be measured [27–30]. On the other hand, in in vivo or clinical conditions, size and geometry can still be controlled to a certain extent but electrical and chemical properties can only be estimated. But what is practically impossible to predict during the development of the device are changes in the electrical and chemical properties of the sample due to exposure to high-voltage electric pulses. Besides electropermeabilization of cell membranes which increases electrical conductivity of the sample [31–33,38,39], electric pulses also cause at least two known side effects: heating and electrolytic contamination of the sample [10,34–37]. Furthermore, there are several other side effects that evolve from interactions between electrodes and treated sample, but we will not explain their influence on electrical and chemical properties of the sample because this is beyond the scope of this paper.

When most of the electrical parameters that electroporator should provide are determined, engineer has to choose the type of electroporator he is going to design. In principle, electroporators can be divided in several groups depending on the biological applications, but from the electrical point of view only two types of electroporators exist: devices with voltage output (output is voltage signal $U(t)$) and devices with current output (output is current signal $I(t)$). Both types of devices have their advantages and disadvantages, but one

point definitely speaks in favor of devices with voltage output. For example, if we perform in vitro experiments with stainless steel parallel plate electrodes with plate sides substantially larger than the distance between them, the electric field strength E that is applied to the sample can be approximated by the voltage-to-distance ratio U/d, where d is the electrode distance and U the amplitude of applied signal obtained from an electroporator with voltage output. On the other hand, if an electroporator with current output is used, the same approximation could be used only if additional measurement of voltage difference between electrodes is performed or if the impedance Z of the sample is known, measured or approximated and voltage difference between electrodes is estimated using Ohm's law $U = IZ$. This example shows that if an electroporator with voltage output is used, estimation of applied electric field strength can be made without additional measurements or knowledge of samples passive electrical properties.

Since electroporators with voltage output are much more widespread than the electroporators with current output, we will concentrate on most commonly used techniques to generate voltage signals required for electropermeabilization.

2.1. Discharge of a capacitor

This is the oldest technique used to generate signals for electropermeabilization primarily in in vitro environment. The device consists of: high voltage power supply, capacitor, switch, and optionally resistance (Fig. 2). The device operates in two phases, charge and discharge, and generates exponentially decaying pulses. During the charge phase, the switch (S) is in the position 1 and variable high voltage power supply (V) charges the capacitor (C) to the preset voltage. In the discharge phase, the switch is in the position 2, and the capacitor discharges through the load connected to the output. Time constant of discharge τ can be approximated by product $Z_L C$, where C is the capacitance of capacitor and Z_L is the absolute value of the load impedance. But most commercially available devices have built-in resistances that are connected in parallel to the load. Their main purpose is to define exactly the time
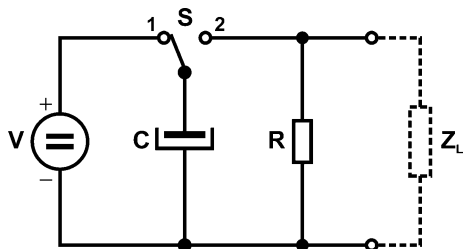

Fig. 2. Discharge of a capacitor (generator of exponentially decaying pulses). The basic setup comprises: variable high-voltage power supply (V), capacitor (C), switch (S), and optionally resistance (R). The device operates in two phases: charge (switch is in position 1 and capacitor charges to the preset voltage) and discharge (switch is in position 2 capacitor discharges through the load connected to the electrodes).
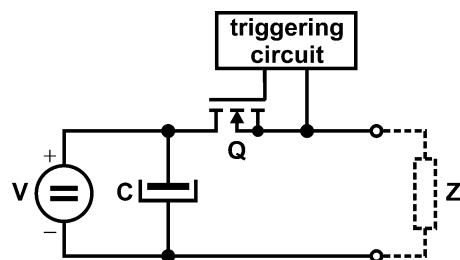
Fig. 3. Switching high voltage power supply with power transistors (generator of square wave pulses). The device consists of power supply part and pulse generator. The variable high-voltage power supply (V) continuously charges the capacitor (C) that stores energy required during the pulse. To deliver the pulse to the electrodes, the triggering circuit generates low-voltage pulse, usually around 10 V, that opens transistor (Q) (e.g. fast power MOSFET or IGBT) for the duration of the low-voltage pulse.

constant of discharge, since the impedance of load (e.g. cell suspension) varies [38–40]. If additional resistors are connected in parallel to the output the time constant of discharge is defined by: $(R \| Z_L) C$, where R is resistance of the internal resistor. If absolute value of the impedance of load Z_L is at least 10 times larger than the resistance R $(Z_L \geq 10R)$, the time constant can be approximated by the RC product.

The presented concept is very simple and the generated pulse could be used even for gene transfection since it includes the high voltage part for permeabilization and low voltage electrophoretic part [54]. Although the transition from high voltage to low voltage is smooth, the respective lengths of each part is ill-defined. Definition of electric field parameters is probably the major drawback of the presented technique. Moreover, repetition frequency of signal delivery is low due to a long charge phase, and the flexibility of electric field parameters is in general poor. Besides this, the presented technique usually requires additional circuits to prevent sparking that might be caused during the change of switch position.

2.2. Square wave generators

For better control of electric field parameters, square wave pulse generator has been introduced. The device still comprises a variable high voltage power supply (V) and a capacitor (C) for energy storage, yet the switch is replaced with a fast power MOSFET (metal oxide silicon field effect transistor) or IGBT (insulated gate bipolar transistor) (Q) and a triggering circuit (Fig. 3). In principle, such a device can continuously deliver square wave pulses to the output, provided that the high voltage power supply is able to recharge the capacitor during the delay between two consecutive pulses. The output amplitude of pulses is defined by amplitude of variable power supply, while pulse duration, pulse repetition frequency and possibly number of pulses are programmed by a computer that also comprises triggering circuit.

Despite improved control over the electric field parameters, this technique still has drawbacks that limit flexibility and accuracy of pulse parameters available to the user. The main problem lies in limited power capabilities of high voltage power supply. The charging current of capacitor that is delivered from power supply is usually much smaller than the discharging current that flows through the load during the pulse. Since more charge is taken from the capacitor than delivered, the voltage on capacitor decreases, which results in a decrease of pulse amplitude. The decrease of voltage can be limited by increasing capacitance of the capacitor, or it can be totally eliminated by using power supply that meets power requirements of the load. Because the first solution to the problem is more common, the accuracy of pulse amplitude of delivered pulses is within the range of few percent of the maximum value. In addition, limited power supply also influences the limitation of pulse duration and pulse repetition frequency. If consecutive pulses are generated, it is usually required that each pulse has the same amplitude as the first one that was generated. Due to the decrease of voltage on the capacitor during the pulse, next pulse can be delivered only after the capacitor is recharged to the preset voltage.

Despite these drawbacks, square wave pulse generators are still very often used to generate pulses especially in combination with pulse transformers (Fig. 4). This technique requires a square wave generator that generates low voltage pulses, while pulse transformer (T) outputs a high voltage pulse due to translation function that is defined by its properties. Furthermore, this configuration provides great safety margin because by using pulse transformer, the output floats and pulse transformer can be built to saturate if the pulse length exceeds the maximum pulse length [41,42].

Improved safety reduces the flexibility of pulse parameters, and while amplitude of pulses can be as high as 3 kV, pulse duration and pulse repetition frequency are limited by the characteristics of the pulse transformer. Despite the safety feature of the pulse transformer, it has to be stressed that development of such a transformer is
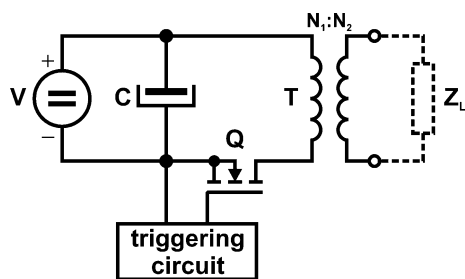
Fig. 5. Simplified circuit of an analogue generator of arbitrary signal. The signal generated by function generator F_G is delivered through the unity gain amplifier to the voltage stage, where the amplitude of signal is increased. The amplitude of signal delivered from driving stage (i.e. function generator and unity gain amplifier) defines the output amplitude of voltage stage. The signal then enters the current stage, which ensures the power required by the load Z_L.

complex due to nonlinear relationship between magnetic field density (B) and magnetic field strength (H) in the core of transformer. Beside this, additional output circuits are usually necessary to demagnetize the transformer after the end of the pulse. With no additional circuit at the output, demagnetization is carried out through the load, and consequently the shape of the signal is distorted (i.e. quasi bipolar pulses are produced).

2.3. Analogue generator of unipolar arbitrary signals

Although square wave and exponentially decaying pulses were and probably still are most frequently used signals for electropermeabilization, in some experiments pulses of different shape (e.g. trapezoidal pulses with possibility of control of rise and fall time or square wave pulses modulated with high-frequency sinusoidal signals) have been used [13,43].

For generation of arbitrary unipolar signals, technique requires at least two amplification stages (voltage and current) and appropriate driving stage (Fig. 5) [44]. The driving stage consists of a signal generator (F_G), which is usually a computer with a digital-to-analog converter, and a unity-gain amplifier (A_D) that meets power and impedance requirements at the input of a voltage stage. The voltage stage in the presented case is composed of a MOSFET (Q_V) and a resistor network connected to the source of the transistor. The signal delivered to the input of the voltage stage opens the transistor according to the transfer function, thus the output voltage changes (e.g. input of 4 V results in 200 V at the output). The major drawback of such voltage stage is that the ground of voltage stage must be electrically isolated from the ground of the driving stage. The signal is then delivered to the current stage, which is a classical source follower made of power MOSFETs connected in

Fig. 4. Square wave pulse generator with pulse transformer. Similarly to the previous technique (see Fig. 3) the device comprises power supply and pulse generator, but between the load Z_L and pulse generator there is also pulse transformer (T) that additionally increases the amplitude of pulses.
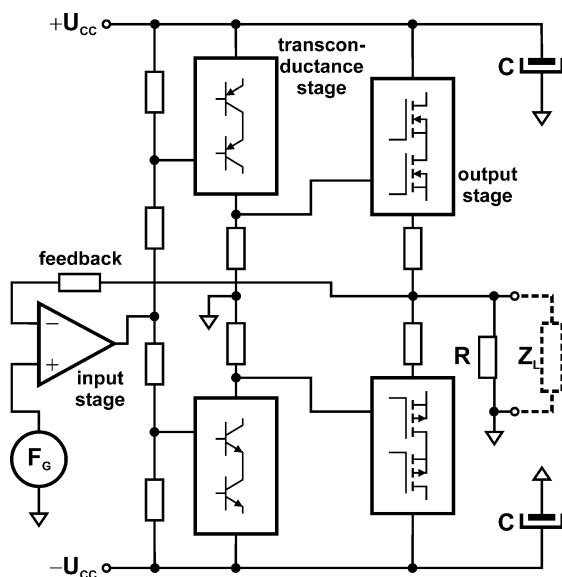
Fig. 6. Simplified circuit of an analogue generator of bipolar arbitrary signal. The signal generated by an arbitrary signal source (F_G) is delivered to the input stage where the signal is subtracted from attenuated output signal delivered through the feedback network. The differential signal is delivered to the inputs of two transconductance stages that increase voltage of signal (upper stage for positive signal and lower stage for negative signal). The two signals from each transconductance stage are then delivered to two output stages, where signals are recombined and amplified to meet power requirements required by load Z_L [47].

parallel. This last stage meets the power requirements determined by the impedance of load (Z_L) between the electrodes [45].

This design allows wide flexibility of all electrical parameters, yet some drawbacks still exist. The driving stage is much more complex than in previously described techniques, and besides this, it must have electrically isolated power supplies. With this design it is possible to generate signals with maximal amplitudes that are approximately 20 to 30 V lower than supply voltage ($+U_{CC}$). Probably the major problem remains general limitation of output voltage and current due to limitations of semiconductor technology (SOA-safe operation area of transistors).

2.4. Analogue generator of bipolar arbitrary signals

Until now we presented techniques that are only able to deliver unipolar signals. But some researchers in the field of electropermeabilization tend to utilize bipolar signals [9,10,46]. Today probably one of the best techniques that have been evaluated is a class AB bipolar amplifier, in other words the closed-loop push–pull amplifier (Fig. 6) [47].

The signal generated by an arbitrary signal source (F_G) is delivered to the input stage where the signal is subtracted from appropriately reduced output signal delivered through the feedback network. The difference of the two signals is delivered to the input of a bipolar voltage amplifier that comprises two transconductance stages, one for the positive and one for the negative period of the signal. Each amplifying stage is composed of two bipolar transistors (PNP-

Fig. 7. Simplified circuit of modular high-voltage source. Operation of the device is based on a principle of digital-to-analogue converter, thus the device comprises several (N) individually controlled electrically isolated DC voltage modules, where the amplitude of the particular voltage source V_N is twice as high as in the preceding module. With an appropriate control of output transistors $Q_1 – Q_N$ the modules are connected in series and a total of 2^N different output voltage levels with the resolution of V_1 are obtained [48].

Table 1
Comparison of presented techniques of signal generation for electro-permeabilization

Technique	Advantages	Disadvantages
Discharge of capacitor	−simple and inexpensive construction	−poor flexibility of parameters
Square wave generator (power transistors)	−simple construction −better control of pulse parameters	−limitation of output parameters due to semiconductor technology
Square wave generator (pulse transformer)	−very safe (possibility to use in clinical environment) −very high pulse amplitudes	−limitations of pulse duration and repetition frequency −complex design of pulse transformer
Analogue generator of unipolar arbitrary signals	−wide flexibility of pulse parameters −arbitrary signal shape	−limitation of output current and voltage due to semiconductor technology
Analogue generator of bipolar arbitrary signals	−genuine bipolar arbitrary signals −arbitrary signal shape	−limitation of bandwidth, output current and voltage due to semiconductor technology
Modular high voltage source	−high dynamics −high currents and voltages	−price

Table 2
List of commercially available electroporators with their parameters, biological applications and possible signal generation technique

Company/product	Output characteristics	Voltage range	Time constant (τ)/pulse length (T)	Charge time (t_c)/pulse repetition frequency (f)	Biological application	Possible signal generation technique
ADITUS MEDICAL http://www.aditusmedical.com						
CythorLab	Arbitrary	LV: 0 V–600 Vpp, HV: 0 V–3000 Vpp	LV: T = 400 ms HV: T = 5 ms	NA	*in vitro, in vivo*	NA
AMAXA Biosystems http://www.amaxa.com						
Nucleofector	NA	NA	NA	NA	*in vitro* transfection	NA
BIORAD http://www.biorad.com						
Micro Pulser	Exponential	200–3000 V	τ = 1–4 ms	t_c = 5 s	bacterial, yeast	Capacitor discharge
Gene Pulser Xcell	Exponential Square wave	10–3000 V	τ = 0.5 ms–3.3 ms T = 0.05–10 ms	t_c = 5 s f = 0.1–10 Hz	all cell type, eukaryotic and prokaryotic cells	Capacitor discharge
BTX http://www.btxonline.com						
ECM 399	Exponential	LV: 2–500 V HV: 10–2500 V	LV: τ = 157 ms HV: τ = 5.4 ms	t_c < 5 s	bacterial, yeast, mammalian	Capacitor discharge
ECM 630	Exponential	LV: 10–500 V HV: 50–2500 V	LV: τ = 25 μs–5 s HV: τ = 625 μs–78 ms	t_c < 5 s	bacterial, yeast, mammalian, plant, *in vivo*	Capacitor discharge
ECM 830	Square wave	LV: 5–500 V HV: 30–3000 V	LV: T = 10 μs–10 s HV: T = 10–600 μs	f = 0.1–10 Hz	bacterial, yeast, mammalian, plant, *in vivo, in ovo*	LV: square wave generator HV: pulse transformer
ECM 2001	Square wave Sinus (AC)	LV: 10–500 V HV: 10–3000 V 0 V–150 Vpp	LV: T = 10 μs–99 ms HV: T = 1–99 μs f_{AC} = 1 MHz	NA NA	mammalian, plant, electrofusion	LV: square wave generator HV: pulse transformer AC: NA
HT 3000	Square wave	LV: 0–500 V HV: 0–3000 V	LV: T = 10 ms–1 s HV: T = 10–600 ms	f = 0.1–10 Hz	*in vitro*	LV: square wave generator HV: pulse transformer
CLONAID http://www.clonaid.com						
RMX2010	Square wave	5–200 V	T = 10 μs–990 ms	f = 1–10 Hz	gene transfection	Square wave generator
CYTO PULSE SCIENCES http://www.cytopulse.com						
PA-2000	Square wave	5–1000 V	T = 1 μs–2 ms	f < 8 Hz	*in vitro, in vivo, ex vivo*	Square wave generator
PA-4000	Square wave	5–1100 V	T = 1 μs–2 ms	f < 8 Hz	*in vitro, in vivo, ex vivo*	Square wave generator
PA-101	Sinus (AC)	10–150 Vpp	f_{AC} = 0.2–2 MHz		dielectrophoresis	AC: NA
EPPENDORF SCIENTIFIC http://www.eppendorf.com						
Electroporator 2510	Exponential	200–2500 V	τ = 5 ms	t_c < 8s	bacterial, yeast	Capacitor discharge
Multiporator:						
Eukaryotic module	Exponential	20–1200 V	τ = 15–500 μs	t_c < 30s	mammalian, plant, oocytes	Capacitor discharge
Bacterial module	Exponential	200–2500 V	τ = 5 ms	t_c < 30 s	bacterial, yeast	Capacitor discharge
Fusion module	Square wave sinus (AC)	0–300 V 2–20 Vpp	T = 5–300 μs f_{AC} = 2 MHz	f = 1 Hz	mammalian, plant	Square wave generator AC: NA
EQUIBIO http://www.equibio.com						
Easyjec T Plus	Exponential	100–3500 V	τ = 10 μs–7 s	NA	all cell types	Capacitor discharge
Easyjec T Optima	Exponential	20–2500 V	τ = 1.5 ms–7 s	NA	all cell types	Capacitor discharge
Easyjec T Prima	Exponential	1800–2500 V	τ = 5 ms	NA	bacterial	Capacitor discharge
GENETRONICS http://www.genetronics.com						
MEDPULSER	Square wave	NA	NA	NA	electrochemotherapy, clinical device	NA
IGEA http://www.igea.it						
Cliniporator	Square wave	LV: 20–200 V HV: 50–1000 V	LV: T = 10 μs–20 ms HV: T = 30–200 μs	f = 1 Hz–10 kHz	electrochemotherapy, gene therapy, clinical device	unipolar arbitrary generator

Table 2 (*continued*)

Company/product	Output characteristics	Voltage range	Time constant (τ)/pulse length (T)	Charge time (t_c)/pulse repetition frequency (f)	Biological application	Possible signal generation technique
JOUAN						
Electropulsator PS10	Square wave	0–1000 V	$T = 5$ μs–24 ms	$f = 1$–10 Hz	bacterial, yeast, mammalian, plant	Square wave generator
Electropulsator PS15	Square wave	0–1500 V	$T = 5$ μs–24 ms	$f = 1$–10 Hz	bacterial, yeast, mammalian, plant	Square wave generator
PROTECH INTERNATIONAL http://www.protechinternational.com						
CUY-21	Square wave	LV: 0.1–199 V HV: 200–500 V	LV: $T = 0.1$–999 ms HV: $T = 0.1$–100 ms	$f = 0.1$–10 Hz	*in vitro*, *in vivo*, *in ovo*, *in utero*	Square wave generator
LF101	Square wave	0–999 V	$T = 5$–99 ms	$f = 0.1$–10 Hz	mammalian, plant, electrofusion	Square wave generator
TRITECH RESEARCH http://www.tritechresearch.com						
Mammo Zapper	Exponential	NA	NA	$t_c = 15$ s	mammalian	Capacitor discharge
Bacto Zapper	Exponential	<2000 V	$\tau < 10$ ms	$t_c = 5$ s	Bacterial	Capacitor discharge
THERMO ELECTRON CORPORATION http://www.savec.com						
CelljecT Uno	Exponential	1800 or 2500 V	$\tau = 5$ ms	NA	bacterial, yeast	Capacitor discharge
CelljecT Duo	Exponential	20–2500 V	$\tau = 1.5$ ms–7 s	NA	all cell type, eukaryotic and prokaryotic cells	Capacitor discharge
CelljecT Pro	Exponential	20V–3500V	$\tau = 10$ μs–7 s	$t_c < 30$ s	bacterial, yeast, mammalian, plant	Capacitor discharge

Signal generation techniques that are given for each device were anticipated according to the output characteristic. During our investigation we did not have access to the electrical schemas of the devices nor had we any of the listed device in our hands.
NA stands for not available.

type for positive and NPN-type for negative period) connected in cascade and a resistor network necessary for normal operation. At this point it has to be stressed that complementary transistors have to be used (i.e. NPN and PNP type which are close match) otherwise symmetry between positive and negative part of amplifier cannot be achieved. The two signals amplified in each transconductance stage are delivered to two output stages, again one for positive and one for negative period of signal. The output stages are composed of power MOSFETs, if possible complementary (N-type for positive and P-type for negative period), that are connected in cascade as source followers. These last two stages recombine two signals from voltage amplifier and meet the power requirements defined by the impedance of the load between electrodes [47].

Although, the design by itself has no problems and is given as an example in any electronic design book, the major problem originates in poor availability of semiconductor components (i.e. high voltage and high power complementary transistors) necessary to build each of the amplifying stage. Since those transistors exist only up to 250 V, undesired cascades that gradually reduce dynamics have to be used to generate signals required for electropermeabilization.

2.5. Modular high voltage source

Another possible improvement of a square wave generator is a modular high voltage source that consists of several (N) individually controlled and electrically isolated DC voltage modules (Fig. 7). Its operation is based on a principle of a digital-to-analog converter, thus the amplitude of the particular source V_N is twice as high as the predecessor ($V_N = 2V_{N-1}$). The voltage of the individual source is constant and can participate in a generation of a common output pulse at any time. With an appropriate control of output transistors $Q_1 - Q_N$ that operate as switches and connect the modules in series, a total of 2^N different output voltage levels with the resolution of V_1 are obtained [48]. Although the design of each individual source is similar to the design of previously described square wave pulse generator, the individual source used in this concept has no problems with the shortage of power. For correct operation, each source (even the smallest one) must be able to produce and sustain the maximum possible current during the pulse generation. If this is not ensured, the pulse amplitude will decrease.

The presented modular topology has many advantages due to very high dynamics and high power that can be delivered to its output. Furthermore, with a supplemented single-phase transistor bridge on the output, bipolar pulses can be generated as well. Besides the electrode polarity change, the transistor bridge also increases the incorporated safety measures of the device in case of malfunction, which could result in a delivery of huge power to the output. Namely, for any given pulse amplitude at least three power transistor switches have to be turned ON (two for the selection of the pulse polarity and at least one for the selection of the desired output pulse amplitude). The modular solution and consequently the increased number of

Table 3

List of commercially available electrodes with their properties and biological applications suggested by manufacturer

Company/product	Number of electrodes	Electrode distance	Needle length (L)/electrode size (shape)/Volume (V)	Electrode material	Biological application
BIORAD http://www.biorad.com					
CUVETTES: Compatible with Micro pulser, Gene Pulser Xcell					
	2	1 mm	$V = 100$ μl	Aluminum	in vitro
	2	2 mm	$V = 400$ μl	Aluminum	in vitro
	2	4 mm	$V = 800$ μl	Aluminum	in vitro
BIOSMITH http://www.biosmith.com					
CUVETTES: Compatible with electroporation devices from all major manufacturers					
72001	2	1 mm	$V = 100$ μl	Aluminum	in vitro
72002	2	2 mm	$V = 400$ μl	Aluminum	in vitro
72004	2	4 mm	$V = 800$ μl	Aluminum	in vitro
BTX http://www.btxonline.com					
2-NEEDLE ARRAY: Compatible with: ECM 830, 630, 395, 399, 600, T820					
Model 531	2	10 mm	$L = 200$ mm	Stainless steel	in vivo
Model 532	2	5 mm	$L = 200$ mm	Stainless steel	in vivo
GENETRODES: Compatible with: ECM 630, 830, 2001, 600, T820					
Model 508	2	1–10 mm	$L = 5$ mm	Gold plating	in vivo
Model 510	2	1–10 mm	$L = 10$ mm	Gold plating	in vivo
Model 512	2	0–13 mm	$L = 5$ mm (L-shaped)	Gold plating	in ovo
Model 514	2	0–13 mm	$L = 3$ mm (L-shaped)	Gold plating	in ovo
Model 516	2	0–13 mm	$L = 1$ mm (L-shaped)	Gold plating	in ovo
CALIPER: Compatible with: ECM 830, 600, 630, 2001, T820					
Model 384	2	1–130 mm	10×10 mm (square)	Stainless steel	in vivo
Model 384L	2	1–130 mm	20×20 mm (square)	Stainless steel	in vivo
TWEZERTRODES: Compatible with: ECM T820, 630, 830, 2001					
Model 520	2	1–20 mm	7 mm diameter (disk)	Stainless steel	in vivo
Model 522	2	1–20 mm	10 mm diameter (disk)	Stainless steel	in vivo
GENEPADDLES: Compatible with: ECM 830, 2001, 630, 600, T820					
Model 542	2	1–10 mm	3×5 mm (rectangle)	Gold plating	in vitro, in vivo
Model 543	2	1–10 mm	5×7 mm (rectangle)	Gold plating	in vitro, in vivo
PETRI PULSER: Compatible with: ECM 830, 630, 600, 399, 395, T820					
PP35-2P	13	2 mm	$V = 0.5–30$ ml	Gold plating	in vitro
PETRI DISH ELECTRODES: Compatible with:ECM 830, 630, 2001, 600, T 820					
	24	2 mm	$V = 10–50$ ml	Stainless steel	in vitro
BTX http://www.btxonline.com					
MICROSLIDE: Compatible with: ECM 630, 830, 395, 399, 2001, 600, T820					
Model 450	2	0.5 mm	$V = 20$ μl	Stainless steel	in vitro, fusion
Model 450-1	2	1 mm	$V = 40$ μl	Stainless steel	in vitro, fusion
Model 453	2	3.2 mm	$V = 0.7$ ml	Stainless steel	in vitro, fusion
Model 453-10	2	10 mm	$V = 2.2$ ml	Stainless steel	in vitro, fusion
FLAT ELECTRODE CHAMBER: Compatible with: ECM 630, 830, 2001, 600, T820					
Model 484	2	1 mm	$V = 0.5$ ml	Stainless steel	in vitro, fusion
Model 482	2	2 mm	$V = 1$ ml	Stainless steel	in vitro, fusion
MEANDER FUSION CHAMBER: Compatible with: ECM 630, 830, 2001, 200, 600, T820					
	2	0.2 mm	–	Silver	in vitro, fusion
Electroporation plates:					
Model HT-P96-2B/W	96	2 mm	$V = 150$ μl	Gold plating	in vitro
Model HT-P96-4B/W	96	4 mm	$V = 300$ μl	Gold plating	in vitro
Model HT-P384-2B/W	384	2 mm	$V = 700$ μl	Gold plating	in vitro
MULTI-WELL COAXIAL ELECTRODES: Compatible with: ECM 630, 830, 2001, 600, T820					
Model 491-1	1	1.6 mm	$V = 0.3$ ml (circular)	Gold plating	in vitro
Model 747	8	1.6 mm	$V = 0.3$ ml (circular)	Gold plating	in vitro
Model 840	96	1.6 mm	$V = 0.3$ ml (circular)	Gold plating	in vitro
Flatpack chambers:					
Model 485	2	1.83 mm	$V = 1.5$ ml	Stainless steel	in vitro

Table 3 (continued)

Company/product	Number of electrodes	Electrode distance	Needle length (L)/electrode size (shape)/Volume (V)	Electrode material	Biological application
Model 486	2	0.56 mm	$V = 85$ μl	Stainless steel	in vitro
Cuvettes:					
Model 610	2	1 mm	$V = 20–90$ μl	Aluminum	in vitro
Model 620	2	2 mm	$V = 40–400$ μl	Aluminum	in vitro
Model 640	2	4 mm	$V = 80–800$ μl	Aluminum	in vitro
EPPENDORF http://www.eppendorf.com					
CUVETTES: Compatible with Multiporator, Electroporator 2510					
	2	1 mm	$V = 100$ μl	Aluminum	in vitro
	2	2 mm	$V = 400$ μl	Aluminum	in vitro
	2	4 mm	$V = 800$ μl	Aluminum	in vitro
CYTOPULSE http://www.cytopulse.com					
COAXIAL ELECTRODES: Compatible with PA-101					
Model FE-C25/400	2	2.5 mm	$V = 350$ ml	NA	in vitro, fusion
Model FE-C25/800	2	2.5 mm	$V = 750$ ml	NA	in vitro, fusion
Model FE-C20/1000	2	2 mm	$V = 1000$ ml	NA	in vitro, fusion
Tweezers:					
TE-5-10	2	Adjustable	5×10 mm (rectangular)	NA	in vivo
TE-5R	2	Adjustable	5 mm diameter (circular)	NA	in vivo
2-row needle array:					
NE-4-4	8	4 mm		NA	in vivo
NE-4-6	12	4 mm		NA	in vivo
NE-6-4	8	6 mm		NA	in vivo
NE-6-6	12	6 mm		NA	in vivo
Cuvettes:					
CUV-01	2	1 mm	$V = 100$ μl	NA	ex vivo
CUV-02	2	2 mm	$V = 400$ μl	NA	ex vivo
CUV-04	2	4 mm	$V = 800$ μl	NA	ex vivo
Electrode array:					
96W-A	96 wells	5.5 mm	$V = 300$ μl/well	NA	ex vivo
EUROGENTEC http://www.eurogentec.com					
CUVETTES: Compatible with most existing electroporation systems					
	2	1 mm	NA	Aluminum	in vitro
	2	2 mm	NA	Aluminum	in vitro
	2	4 mm		Aluminum	in vitro
ICHOR http://www.ichorms.com					
Trigrid					
	multiple	NA	NA	NA	in vivo
IGEA http://www.igea.it.					
TYPE I: Compatible with Cliniporator					
Plate electrodes	2	6–8 mm	10×30 mm (rectangular)	Stainless steel	clinical applications
TYPE II: compatible with cliniporator					
Needle rows	8	4 mm	$L = 20–30$ mm	Stainless steel	clinical applications
TYPE III: Compatible with Cliniporator					
Hexagonal needle array	7	8 mm	$L = 20–30$ mm	Stainless steel	clinical applications

NA stands for not available.

assembly parts (isolated DC modules, IGBT driver circuitry, etc.), on the other hand, increase the costs of the device, which is a subject of optimization during the design stage.

3. Discussion

Nowadays electropermeabilization is widely used in various biological, medical, and biotechnological applications such as electrochemotherapy, gene transfer, electroinsertion of proteins into cell plasma membrane, electrofusion of cells, transdermal drug delivery, water treatment and food preservation [5–7,15,20–23,55–57]. Efficiency of all these applications strongly depends on parameters of electric pulses, which are delivered to the treated object using specially developed electrodes and electronic devices—electroporators. Both parts of equipment play equally important role in process of electropermeabilization, but in this paper we

have focused exclusively on electroporators and advantages and disadvantages of techniques used for generating required signals (Table 1). At this point we did not discuss how each of the presented techniques can solve different problems like tissue burning, electrolytic contamination, etc., since this would require additional analysis of electrode designs and materials.

Besides reviewing known techniques of signal generation, we also investigated the world market of electroporators. A list of existing commercially available electroporators with their parameters, biological applications and possible signal generation technique are given in Table 2. Devices are grouped by manufacturer and each device is presented with the following parameters: output characteristics, voltage range, time constant (τ)/pulse length (T), and charge time (t_c)/pulse repetition frequency (f). The value of last two parameters depends on output characteristic if the device produces exponentially decaying pulses, time constant and charge time are given as parameters. On the other hand, if the device generates square wave pulses, pulse length and pulse repetition frequency are given as parameters. Since some of manufacturers also offer different electrodes for different applications we have also made a list that is given in Table 3. Electrodes are grouped by manufacturers and each electrode is presented with the following parameters: electrode type, electrode distance and biological applications.

We can see that it is practically impossible to compare the listed devices due to difference in their characteristics. Even if we compare devices with identical output characteristic (e.g. exponential, square wave, arbitrary) we see that either their voltage range or their time constant/pulse length vary in incomparable range. We believe that with each of the listed devices adequate experimental results can be achieved, yet some questions still remain. Do we need any special buffers for electropermeabilization of cells? How can we set the required parameters for electropermeabilization (i.e. user friendliness of the device)? Is the device modular or non-modular type (i.e. with addition of new module we extend working parameters)? From this we can conclude that manufacturers of the electroporators have to standardize electrical parameters of devices, which would also include list of required buffers that have to be used for efficient electropermeabilization. This has already been done by some manufacturers (Eppendorf, BioRad, BTX, etc.) who supply protocols and standardized buffers for different procedures.

Besides standardization of parameters of devices, manufacturers should also start offering a built-in module for current and voltage monitoring. It is very important that researcher has an immediate feedback about the electropermeabilizing signal that has been delivered to the electrodes. Monitoring of voltage and current can be performed by use of an oscilloscope, but this requires additional space for another electronic device in already overstuffed laboratory and also additional wiring for signal measurements. In addition, researcher must also be able to set the oscilloscope before the experiments, which requires additional training. Probably there are many more drawbacks (e.g. expensive high voltage probes and current probes) of using the oscilloscope that could be overcome by built in current and voltage monitors.

Although today we can find several new studies showing biological effects of nanosecond pulsed electric fields [51,52], we did not review the parameters and technologies used, since this has already been done by Mankowski et al. [49]. In this review, they have presented several short pulse generator technologies such as discharge of capacitor, pulse forming line (PFL), Marxx-generator, etc. Besides this they also offer a list of commercially available short pulse generators.

In conclusion we can say that even though manufacturers offer a brand variety of electroporators and electroporation systems, these devices still have specific limitations. This was probably the main reason why many researchers have developed their own custom-designed devices or systems. Since many of these custom-built devices are poorly described in the articles, we were unable to explore their parameters in details. What we offer instead is a list of articles describing the devices (see Refs. [43,44,47–57]).

Acknowledgements

References

[1] K. Kinosita, T.Y. Tsong, Formation and resealing of pores of controlled sizes in human erythrocyte membrane, Nature 268 (1977) 438–441.

[2] J. Teissie, T.Y. Tsong, Electric field induced transient pores in phospolipid bilayer vesicles, Biochemistry 20 (1981) 1548–1554.

[3] E. Neumann, M.S. Ridder, Y. Wang, P.H. Hofschneider, Gene transfer into mouse lyoma cells by electroporation in high electric fields, EMBO J. 1 (1982) 841–845.

[4] E. Neumann, A.E. Sowers, C.A. Jordan, Electroporation and Electrofusion in Cell Biology, Plenum, New York, 1989.

[5] L.M. Mir, Therapeutic perspectives of in vivo cell electropermeabilization, Bioelectrochemistry 53 (2000) 1–10.

[6] E. Neumann, S. Kakorin, K. Toensing, Fundamentals of electroporative delivery of drugs and genes, Bioelectrochem. Bioenerg. 48 (1999) 3–16.

[7] J. Teissie, N. Eynard, B. Gabriel, M.P. Rols, Electropermeabilization of cell membranes, Adv. Drug Deliv. Rev. 35 (1999) 3–19.

[8] M.P. Rols, J. Teissie, Electropermeabilization of mammalian cells to macromolecules: control by pulse duration, Biophys. J. 75 (1998) 1415–1423.

[9] T. Kotnik, L.M. Mir, K. Flisar, M. Puc, D. Miklavčič, Cell membrane electropermeabilization by symmetrical bipolar rectangular pulses: Part I. Increased efficiency of permeabilization, Bioelectrochemistry 54 (2001) 83–90.

[10] T. Kotnik, L.M. Mir, D. Miklavčič, Cell membrane electropermeabilization by symmetrical bipolar rectangular pulses: Part II. Reduced electrolytic contamination, Bioelectrochemistry 54 (2001) 91–95.

[11] M. Puc, T. Kotnik, L.M. Mir, D. Miklavčič, Quantitative model of small molecules uptake after in vitro cell electropermeabilization, Bioelectrochemistry 60 (2003) 1–10.

[12] G. Pucihar, L.M. Mir, D. Miklavčič, The effect of pulse repetition frequency on the uptake into electropermeabilized cells in vitro with possible analysis and it application, Bioelectrochem. Bioenerg. 57 (2002) 167–172.

[13] T. Kotnik, G. Pucihar, M. Reberšek, D. Miklavčič, L.M. Mir, Role of pulse shape in cell membrane electropermeabilization, Biochim. Biophys. Acta 1614 (2003) 193–200.

[14] M. Golzio, M.P. Mora, C. Raynaund, C. Delteil, J. Teissie, M.P. Rols, Control by osmotic pressure of voltage-induced permeabilization and gene transfer in mammalian cells, Biophys. J. 74 (1998) 3015–3022.

[15] J. Teissie, Transfer of foreign receptors to living cell surfaces: the bioelectrochemical approach, Bioelectrochem. Bioenerg. 46 (1998) 115–120.

[16] T. Kotnik, F. Bobanović, D. Miklavčič, Sensitivity of transmembrane voltage induced by applied electric fields: a theoretical analysis, Bioelectrochem. Bioenerg. 43 (1997) 285–291.

[17] P.J. Canatella, J.F. Karr, J.A. Petros, M.R. Prausnitz, Quantitative study of electroporation-mediated molecular uptake and cell viability, Biophys. J. 80 (2001) 755–764.

[18] M. Pavlin, N. Pavšelj, D. Miklavčič, Dependence of induced transmembrane potential on cell density, arrangement, and cell position inside a cell system, IEEE Trans. Biomed. Eng. 49 (2002) 605–612.

[19] B. Valič, M. Golzio, M. Pavlin, A. Schatz, C. Faurie, B. Gabriel, J. Teissie, M.P. Rols, D. Miklavčič, Effect on electric field induced transmembrane potential on spheroidal cells: theory and experiments, Eur. Biophys. J. 32 (2003) 519–528.

[20] M.R. Prausnitz, V.G Bose, R. Langer, J.C. Weaver, Electroporation of mammalian skin: a mechanism to enhance transdermal drug delivery, P. Natl. Acad. Sci. U. S. A. 90 (1993) 10504–10508.

[21] M.R. Prausnitz, A practical assessment of transdermal drug delivery by skin electroporation, Adv. Drug Deliv. Rev. 35 (1999) 61–67.

[22] S.B. Dev, D.P. Rabussay, G. Widera, G.A. Hofmann, Medical applications of electroporation, IEEE Trans. Plasma Sci. 28 (2000) 206–223.

[23] J. Gehl, Electroporation: theory and methods, perspectives for drug delivery, gene therapy and research, Acta Physiol. Scand. 177 (2003) 437–447.

[24] D. Miklavčič, K. Beravs, D. Šemrov, M. Čemažar, G. Serša, The importance of electric field distribution for effective in vivo electroporation of tissue, Biophys. J. 74 (1998) 2152–2158.

[25] J. Gehl, T.H. Sorensen, K. Nielsen, P. Raskmark, S.L. Nielsen, T. Skovsgaard, L.M. Mir, In vivo electroporation of skeletal muscle: threshold, efficacy and relation to electric field distribution, Biochim. Biophys. Acta 1428 (1999) 233–240.

[26] G. Serša, M. Čemažar, D. Šemrov, D. Miklavčič, Changing electrode orientation improves the efficacy of electrochemotherapy of solid tumors in mice, Bioelectrochem. Bioenerg. 39 (1996) 61–66.

[27] M.P. Rols, J. Teissie, Ionic-strength modulation of electrically induced permeabilization and associated fusion of mammalian cells, Eur. J. Biochem. 179 (1989) 109–115.

[28] E. Neumann, Membrane electroporation and direct gene transfer, Bioelectrochem. Bioenerg. 28 (1992) 247–267.

[29] C.S. Djuzenova, U. Zimmermann, H. Frank, V.L. Sukhorukov, E. Richter, G. Fuhr, Effect of medium conductivity and composition on the uptake of propidium iodide into electropermeabilized myeloma cells, Biochim. Biophys. Acta 1284 (1996) 143–152.

[30] G. Pucihar, T. Kotnik, M. Kandušer, D. Miklavčič, The influence of

[31] medium conductivity on electropermeabilization and survival of cells in vivo, Bioelectrochemistry 54 (2001) 107–115.

[31] I.G. Abidor, A.I. Barbul, D.Z. Zhev, P. Doinov, I.N. Bandarina, E.M. Osipova, S.I. Sukharev, Electrical properties of cell pallet and cell fusion in centrifuge, Biochim. Biophys. Acta 152 (1994) 207–218.

[32] I.G. Abidor, L.-H. Li, S.W. Hui, Studies of cell pallets: II. Osmotic properties, electroporation and related phenomena: membrane interactions, Biophys. J. 67 (1994) 427–435.

[33] R.V. Davalos, B. Rubinsky, D.M. Otten, A feasibility study for electrical impedance tomography as a means to monitor tissue electroporation for molecular medicine, IEEE Trans. Biomed. Eng. 49 (2002) 400–403.

[34] U. Pliquett, E.A. Gift, J.C. Weaver, Determination of the electric field and anomalous heating caused by exponential pulses with aluminum electrodes in electroporation experiments, Bioelectrochem. Bioenerg. 39 (1996) 39–53.

[35] U. Friderich, N. Stachowicz, A. Simm, G. Fuhr, K. Lucas, U. Zimmermann, High efficiency electrotransfection with aluminum electrodes using microsecond controlled pulses, Bioelectrochem. Bioenerg. 47 (1998) 103–111.

[36] F. Loste, N. Eynard, J. Teissie, Direct monitoring of the field strength during electropulsation, Bioelectrochem. Bioenerg. 47 (1998) 119–127.

[37] T. Tomov, I. Tsoneva, Are the stainless steel electrodes inter? Bioelectrochemistry 51 (2000) 207–209.

[38] M. Pavlin, T. Slivnik, D. Miklavčič, Effective conductivity of cell suspensions, IEEE Trans. Biomed. Eng. 49 (2002) 77–80.

[39] M. Pavlin, D. Miklavčič, Effective conductivity of a suspension of permeabilized cells: a theoretical analysis, Biophys. J. 85 (2003) 719–729.

[40] R.D. Fomekong, U. Pliquett, F. Pliquett, Passive electrical properties or RBC suspensions: changes due to distribution of relaxation times in dependence on the cell volume fraction and medium conductivity, Bioelectrochem. Bioenerg. 47 (1998) 81–88.

[41] G.A. Hofmann, S.B. Dev, G.S. Nanda, Electrochemotherapy: transition from laboratory to clinic, IEEE Eng. Med. Biol. Mag. 15 (1996) 124–132.

[42] M. Okino, H. Tomie, H. Kanesada, M. Marumoto, K. Esato, H. Suzuki, Optimal electric conditions in electrical impulse chemotherapy, Jpn. J. Cancer Res. 83 (1992) 1095–1101.

[43] D.C. Chang, Cell poration and cell fusion using an oscillating electric field, Biophys. J. 56 (1989) 641–652.

[44] M. Puc, K. Flisar, S. Reberšek, D. Miklavčič, Electroporator for in vitro cell permeabilization, Radiol. Oncol. 35 (2001) 203–207.

[45] M. Puc, S. Reberšek, D. Miklavčič, Requirements for a clinical electrochemotherapy device—electroporator, Radiol. Oncol. 31 (1997) 368–373.

[46] E. Tekle, R.D. Astumian, P.B. Chock, Electroporation by using bipolar oscillating electric field: an improved method foe DNA transfection of NIH 3T3 cell, P. Natl. Acad. Sci. U. S. A. 88 (1991) 4230–4234.

[47] K. Flisar, M. Puc, T. Kotnik, D. Miklavčič, A system for in vitro cell membrane electropermeabilization with arbitrary pulse waveforms, IEEE Eng. Med. Biol. Mag. 22 (2003) 77–81.

[48] M. Petkovšek, J. Nastran, D. Vončina, P. Zajec, D. Miklavčič, G. Serša, High voltage pulse generation, Electron. Lett. 38 (2002) 680–682.

[49] J. Mankowski, M. Kristiansen, A review of short pulse generator technology, IEEE Trans. Plasma Sci. 28 (2000) 102–108.

[50] Y.C. Lin, C.M. Jen, M.Y. Huang, C.Y Wu, X.Z. Lin, Electroporation microchips for continuous gene transfection, Sens. Actuators, B, Chem. 79 (2001) 137–143.

[51] S.J. Beebe, P.M. Fox, L.J. Rec, K. Somers, R.H. Stark, K.H. Schoenbach, Nanosecond pulsed electric field (nsPEF) effects on cells and tissues: apoptosis induced and tumor growth inhibition, IEEE Trans. Plasma Sci. 30 (2002) 286–292.

[52] K.H. Schoenbach, S. Katsuki, R.H. Stark, E.S. Buescher, S.J. Beebe,

Bioelectrics—new applications for pulsed power technology, IEEE Trans. Plasma Sci. 30 (2002) 293–300.

[53] A.C. Durieux, R. Bonnefoy, C. Manissolle, D. Freyssenet, High-efficiency gene electrotransfer into skeletal muscle: description and physiological applicability of a new pulse generator, Biochem. Biophys. Res. Commun. 296 (2002) 443–450.

[54] S. Šatkauskas, M.F. Bureau, M. Puc, A. Mahfoudi, D. Scherman, D. Miklavčič, L.M. Mir, Mechanisms of in vivo DNA electrotransfer: respective contributions of cell electropermeabilization and DNA electrophoresis, Molec. Ther. 5 (2002) 133–140.

[55] K. Uemura, S. Isobe, Developing a new apparatus for inactivating *Escherichia coli* in saline water with high electric field AC, J. Food Eng. 53 (2002) 203–207.

[56] J. Teissie, N. Eynard, M.C. Vernhes, A. Benichou, V. Ganeva, B. Galutzov, P.A. Cabanes, Recent biotechnological developments of electropulsation. A prospective review, Bioelectrochemistry 55 (2002) 107–112.

[57] K. Uemura, S. Isobe, Developing a new apparatus for inactivating bacillus subtilis spore in orange juice with a high electric field AC under pressurized conditions, J. Food Eng. 56 (2003) 325–329.

3. Conclusions and future prospects

Development of realistic mathematical models (i.e. numerical models of biological tissues validated by corresponding *in vivo* experiments) plays an important role in the prediction of the successful outcome of an electroporation-based therapy, treatment or experiment.

The general conclusion of our study is that calculation and visualization of local electric field distribution in realistic numerical models allows for the selection of parameters, such as electrode configuration, electrode positioning and amplitude of electroporation pulses, so that the optimal permeabilisation of a treated tissue is achieved (i.e. electroporation of all cells within the target tissue by exposing them to the local electric field between reversible and irreversible threshold values *($E_{rev} < E < E_{irrev}$)*, while minimizing the total electric current flowing through the tissue and the electrically-induced damage to the healthy tissue) .

Our results can significantly contribute to more efficient tissue electroporation used in electroporation based therapies and treatments (e.g. clinical electrochemotherapy of tumors and gene electrotransfer) by the selection of electric parameters based on calculation and visualization of local electric field. Realistic numerical models are also useful tool in experiment planning in order to precisely determine the parameters to be tested and to reduce the number of animals used in experiments and to help understanding underlying *in vivo* mechanisms in tissues being electroporated.

To summarize our main conclusions and describe future prospects:

i) *Calculations and visualization of the local electric field distribution in numerical models of cutaneous and subcutaneous tumors*

- We performed 2D analytical and numerical analysis in order to determine relevant parameters that have to be taken into account for development of 3D realistic tissue models and optimization of local electric field. We systematically quantified and compared local electric field in the tissue of different most widely used electrode configurations (plate and needle) in electrochemotherapy and gene electrotransfer in past years. We analytically and numerically calculated and visualized local electric field distribution inside an example of modeled treated tissue (a spherical target tissue and its surroundings) in 2D for the plate and needle electrode configurations and compared the local electric field distribution to parameter *U/d*, which is widely used parameter in currently defined electroporation protocols. We show that the parameter *U/d* can differ significantly from the actual calculated values of the local electric field inside both homogeneous tissue and in tissue with more conductive target tissue compared to its surroundings. We showed dependency of local electric field distribution on the electrical parameters such as applied voltage on the electrodes, electrode placement with respect to the target tissue, electrode shape (plate or needle), number of electrodes, and distance between electrodes. We demonstrated that the local electric field in the treated tissue can be successfully controlled by the aforementioned electrical parameters. Furthermore, our results also demonstrate that local electric field is influenced by electric properties of the target tissue and its surroundings. We also presented analytical solutions, which provide a convenient, rapid, but an approximate method for a pre-analysis of electric field distribution in treated tissue [**Paper I**].

- We extended 2D numerical study to a 3D numerical study i.e. calculation, visualization and optimization of local electric field distribution in spherical subcutaneous tumors treated with needle electrodes' configurations used in clinics and research in past years. Higher electric conductivity was considered for tumor tissue with respect to the conductivity of the surrounding healthy tissue. The results show that voltage applied, distances between electrodes and depth of electrode insertion are all relevant for the control of local electric field distribution in the model and were thus chosen for optimization procedure. By using a genetic optimization algorithm developed in our institution we examined the adequacy of the needle electrode geometries by calculating electric current through the model and volumes of reversibly and irreversibly electroporated tissue. Based on the optimization analysis, we concluded that parallel array electrodes (three electrode pairs) gave the best results: they assured local electric field in tumor tissue to be above E_{rev} and required the lowest total electric current and caused a small volume of healthy tissue to be reversibly and even less to be irreversibly electropermeabilised.

Based on visualization of local electric field distribution we also demonstrated that inserting needle electrodes deeper than necessary, using inadequate electrode geometries, polarities and arrangement with respect to the target tumor tissue can result in unsuccessful tumor permeabilisation ($E < E_{rev}$). Moreover, the local electric field within the healthy tissue below the tumor can be higher compared to the local electric field inside the tumor. This effect can be even more pronounced if the tumor is much more conductive than the surrounding tissue, because the local electric field is then lower in the tumor and higher in the surrounding tissue [**Paper II**].

- In addition to the spherical subcutaneous tumor models, we performed the same 3D numerical calculation and visualization analysis and the genetic algorithm optimization to

determine the optimum electrode configuration and optimum voltage amplitude for subcutaneous tumor models of different shapes and sizes (spheres and ellipsoids) and for a realistic brain tumor model acquired from medical images. In all tumor cases, parallel needle electrode arrays were a better choice than hexagonal needle electrode arrays, since their utilization required less electric current and caused less healthy tissue damage. [**Paper VII**]

- We demonstrated numerical calculation and visualization of local electric field distribution in 3D can be successfully used in electrode design for *in vitro* and *in vivo* settings. The results obtained with our numerical modeling supported the design of new electrodes for *in vitro* gene electrotransfection integrated into the new system allowing for automatic changing of electric field direction [**Paper VIII**]. The new system can be used in *in vitro* gene electrotransfer to improve cell transfection by changing electric field direction between electrical pulses, without affecting cell survival. The results of our numerical modeling were useful in development and testing of the new multiple electrode commutation circuit, suggested for *in vivo* electrochemotherapy of larger tumors. Namely, we tested a pulse sequence using seven electrodes for which we also calculated local electric field distribution in tumour tissue by means of finite elements method. Electrochemotherapy, performed by multiple needle electrodes and tested pulse sequence on large subcutaneous murine tumour model resulted in tumour growth delay and 57% complete responses, thus demonstrating that the tested electrode commutation sequence is efficient [**Paper XI**].

- We demonstrated numerically and experimentaly *in vivo* the influence of the contact surface between electrode and treated tissue on the coverage of the tumor tissue by sufficiently high local electric field ($E > E_{rev}$). We demonstrated that the placement of electrodes giving larger electrode-tissue contact surface leads to improved electrochemotherapy outcome. These

results provide guidance on electrochemotherapy for treatment of protruding cutaneous tumors using parallel plate electrodes [**Paper III**]. We also observed that the electrode placement with smaller contact surface resulted in deeper penetration of local electric field distribution in the tissue below electrodes, compared to the electrode placement with larger contact surface. This observation also supports clinical findings reported by Sersa and colleagues [Sersa *et al.*, 2003] that pain can be avoided by lifting the treated tumor nodule while applying electric pulses through parallel plate electrodes. In addition, it was observed that obese patients had less sensation and less muscle contractions, because adipose tissue prevented electric field distribution deeper into the underlying tissue.

- We built 3D numerical models of cutaneous and subcutaneous tumors and calculated local electric field and total electric current considering safety level of electoporation when electrochemotherapy is performed on tumors localized on the trunk close to the cardiac muscle. The modeled conditions (i.e. needle row array, needle hexagonal array and plate configurations and voltages applied) were the same as those actually used in clinical electrochemotherapy. We proposed safety protocols of depth of insertion of needle electrodes and distance between plate electrodes for reversible and irreversible electroporation and fibrillation of cardiac muscle. For the safety limits of local electric field distribution between reversible and irreversible electroporation thresholds we used values determined in our realistic models (E_{rev} = 200 V/cm and E_{irrev} = 450 V/cm), while for the safety limit for cardiac muscle fibrillation we considered threshold current (100 mA) for ventricular fibrillation taken from the literature. We concluded that the results of our models can provide safety protocols for electrodes and voltages currently used in electrochemotherapy of cutaneous and subcutaneous tumors. However for internal (orthotopic) tumors located close to the heart safe

and precise electrochemotherapy requires treatment planning that includes optimization of the electrode and voltage applied [**Paper X**].

Our findings can already be used in guiding to practitioners in how to choose the most suitable electric parameters (such as the amplitude of electroporation pulses and electrode configuration – plate or needle, electrode placement, number and insertion) in order to perform the treatment as efficiently as possible: to target the tumor with $E > E_{rev}$ and destroy all tumor cells, while minimizing electrically induced damage to the healthy tissue and avoiding pain sensations. Selection of electric parameters based on calculation and visualization of local electric field distribution can be useful for refinement of the currently used protocols for clinical electrochemotherapy in order to even further improve the complete response rate of cutaneous and subcutaneous tumors. An important step towards the optimization of local electric field for effective ECT has been made recently by IGEA Company [www.igea.it] currently providing the electroporator designed specifically to be used in the clinical practice for electrochemotherapy. They recomend the voltage for different distances between electrodes (for plate electrode configuration) which was provided based on calculation and vizualization of local electric field distribution in our models.

ii) *Calculations and visualization of the local electric field distribution in numerical models of muscle tissue*

- We developed realistic numerical models of skeletal muscle tissue electroporated directly and transcutaneously in order to investigate the influence of skin on muscle electroporation. The numerical calculations were validated on *in vivo* experimental results using [51]CrEDTA indicator. We found the functional dependency of tissue conductivity on electric field intensity $\sigma(E)$ to be exponential for skin with electroporation thresholds $E_{rev} = 480$ V/cm and

E_{irrev} = 1050 V/cm and sigmoid for muscle tissue with E_{rev} = 240 V/cm and E_{irrev} = 430 V/cm. The same electroporation threshold values E_{rev} and E_{irrev} were found irrespective of whether muscle was electroporated directly (i.e. whitout skin) or transcutaneously. We thus conclude that the skin layer has no influence on the thresholds of the local electric field intensity itself needed for successful muscle tissue electroporation, but it does require higher voltage to be applied between the electrodes when muscle is electroporated transcutaneously.

- We also showed that the error of an approximate estimation of electroporation threshold values in *in vivo* experiments by calculating the *U/d* ratio, without numerical calculations of local electric field distribution, is small enough only if the plate electrodes are used and only for one type of tissue placed between the electrodes. For more complex tissues with different geometric and electrical properties, a combination of realistic numerical modeling and *in vivo* experiments needs to be used for the precise determination of electroporation threshold values. It is also important to note that the thresholds of the local electric field for tissue electroporation depend on the type of molecules used for detection of *in vivo* tissue permeabilization and electroporation pulse characteristics (i.e. duration and number of pulses as well as pulse repetition frequency). Thus, the threshold values determined in our study are relevant for the setting of eight pulses of 100 μs duration at a frequency of 1 Hz. For precise electroporation threshold determination for the other pulse parameters, our numerical models remains valid, but additional experiments need to be done and the obtained results must be included in the models.

- We also developed a realistic 3D numerical model of the mouse tibialis cranialis muscle (electroporated directly (i.e.with skin removed)) in order experimentally and numerically investigate muscle electroporation for parallel and perpendicular orientation of the applied

electric field with respect to the muscle fibers by using parallel plate electrodes. The agreement between numerically calculated results and experimental observations validated our 3D model. The electroporated muscle regions were visualized with two *in vivo* methods: magnetic resonance (Gd-DOTA) and fluorescence imaging (propidium iodide). We established that electroporation of muscle cells in tissue depends on the orientation of the applied electric field; the local electric field reversible threshold values were determined (pulse parameters: 8 x 100 μs, 1 Hz) to be 80 V/cm and 200 V/cm for parallel and perpendicular orientation, respectively. We present the first results of different electroporation thresholds with respect to electrode vs. tissue orientation for the tissue with anisotropic electric properties [**Paper VI**].

- The findings of our study carry important practical information on the voltage to be applied to the electrodes, and on how to orient the electric field with respect to the muscle fibers in order to reversibly electroporate the target area of the muscle. The determination of local electric field electroporation thresholds enables control of muscle tissue electroporation, and can be used to predict the optimal window for gene electrotransfer.

In addition to gene electrotransfer, our findings on electroporation thresholds and on influence of the skin on muscle electroporation can be of interest also for planning of other eletroporation based therapies and treatments (e.g. electrochemotherapy and trandermal drug and gene delivery) so as to avoid:

1. an invasive procedure when it is not necessary, by using plate electrodes;

2. painful sensations (unnecessary anesthesia) due to the electrode or electric field penetration deeper than necessary;

3. the irreversible damage of underlying or surrounding healthy muscle tissue and

4. fibrillation of cardiac muscle

iii) *Development of a web-based learning application on electroporation based therapies and treatments such as electrochemotrapy and gene electrotransfer*

- We developed an e-learning application to provide an interactive educational content in order to simulate the "hands-on" learning approach about the parameters being important for successful electroporation based therapies and treatments as electrochemotrapy and gene electrotransfer. The presented e-learning application provides an easy and rapid approach for information, knowledge and experience exchange among the experts from different scientific fields, which can facilitate development and optimization of electroporation based treatments [**Paper IV**].

Future prospects

-Future prospects using a presented approach can be treatment planning of electrochemotherapy for precise and safe therapy of orthotopic tumors that are located close to vital organs (for example tumors localized in deep brain which can not be treated whtout appropriate treatment planning).

-Similarly to the numerical model we developed for *in vitro* settings [**Paper XI**], further improvement of the realistic models for *in vivo* therapy and treatments could include the possibility to change the electric field orientation during the electroporation pulse in order to successfully control the electroporation with lower local electric field and lower electric current. For larger tumors the realistic models could include also the possibility to calculate, visualize and optimize the local electric field for an arbitrarily applied sequence of

electroporation pulses to the electrodes (as already shown in our study for a pulse sequence using seven electrodes [**Paper VIII**]) or moving the electrodes during the treatment.

-Another important development would be development of a realistic numerical model based on an algorithm that would convert medical images and *in vivo* measurements of electric conductivity of the treatment area into 3D structures ready to import into numerical software for calculation, visualization and optimization of local electric distribution.

Further development of our realistic numerical models of muscle and muscle with skin could include optimization of local electric field distribution and design of new plate electrodes for noninvasive *in vivo* gene electrotransfection by automatic change of electric field orientation in order to obtain precise delineation of the muscle region to be transfected with a local electric field as low as possible in both the target tissue and its surroundings, as the efficient gene electrotransfection requires an E just above E_{rev}. Similar system for muscle electroporation control could be developed also for invasive gene electrotransfection by using needle electrodes.

The modular structure of the web based e-learning application allows for upgrade with new educational content collected from the clinics and research, and can be easily adapted to serve as a collaborative e-learning tool also in other electroporation-based treatments.

4. References

Abidor IG, Barbul AI, Zhelev DV, Doinov P, Bandarina IN, Osipova EM, Sukarev SI. Electrical properties of cell pellet and cell fusion in a centrifuge. *Biochimica et Biophysica Acta*, 1152: 207-218, 1993.

Andre F, Gehl J, Sersa G, Preat V, Hojman P, Eriksen J, Golzio M, Cemazar M, Pavselj N, Rols MP, Miklavcic D, Neumann E, Teissie J, Mir LM. Efficiency of high- and low-voltage pulse combinations for gene electrotransfer in muscle, liver, tumor, and skin. *Human Gene Therapy,* 19: 1261-1271, 2008.

Aihara H, Myazaki J. Gene electrotransfer into muscle by electroporation *in vivo. Nature Biotechnology,* 16: 867-870, 1998.

Al-Sakere B, Bernat C, Connault E, Opolon P, Rubinsky B, Davalos R, Mir LM. Tumor ablation with irreversible electroporation. *PLoSONE,* 2:135, 2007.

Belehradek J, Orlowski S, Poddevin B, Paoletti C, Mir LM. Electrochemotherapy of spontaneous mammary tumors in mice. *European Journal of Cancer,* 27: 73-76, 1991.

Batiuskaite D, Cukjati D, Mir LM. Comparison of *in vivo* electropermeabilization of normal and malignant tissue using the ^{51}Cr-EDTA uptake test. *Biologija,* 2003: 45-47, 2003.

Bettan M, Ivanov MA, Mir LM, Boissiere F, Delaere P, Scherman D. Efficient DNA electrotransfer into tumors. *Bioelectrochemistry,* 52:83-90, 2000.

Campana LG, Mocellin S, Basso M, Puccetti O, De Salvo GL, Chiarion-Sileni V, Vecchiato A, Corti L, Rossi CR, Nitti D: Bleomycin-Based Electrochemotherapy: Clinical Outcome from a Single Institution's Experience with 52 Patients. *Annals of Surgical Oncology*, Online, 2008.

Curatolo P, Mancini M, Ruggiero A, Clerico R, Di Marco P, Calvieri S: Successful Treatment of Penile Kaposi's Sarcoma with Electrochemotherapy. *Dermatologic Surgery,* 34: 1–5, 2008.

Chazal M, Benchimol D, Baque P, Pierrefite V, Milano G, Bourgeon A. Treatment of hepatic metastases of colorectal cancer by electrochemotherapy: an experimental study in the rat. *Surgery* 124: 536-540, 1998.

Corovic S, Zupanic A, Miklavcic D. Numerical modeling and optimization of electric field distribution in subcutaneous tumor treated with electrochemotherapy using needle electrodes. *IEEE Tranactions on Plasma Science*, 36: 1665-1672, 2008.

Colombo GL, di Matteo S, Mir LM: Cost-effectiveness analysis of electrochemotherapy with the Cliniporator™ vs other methods for the control and treatment of cutaneous and subcutaneous tumors. *Therapeutics and Clinical Risk Management*, 4: 1–8, 2008.

Cukjati D, Batiuskaite D, André F, Miklavcic D, Mir LM. Real time electroporation control for accurate and safe in vivo non-viral gene therapy. *Bioelectrochemistry,* 70: 501-507, 2007.

Daud AI, DeConti RC, Andrews S, Urbas P, Riker AI, Sondak VK, Munster PN, Sullivan DM, Ugen KE, Messina JL, Heller R. Phase I trial of interleukin-12 plasmid electroporation in patients with metastatic melanoma. *Journal of clinical oncology*, 26: 896-903, 2008.

Davalos RV, Huang Y, Rubinsky B: Electroporation: bio-electrochemical mass transfer at the nano scale. *Microscale Thermophys Eng,* 4:147-159, 2000.

Davalos R, Rubinsky B, Otten DM. A feasibility study for electrical impedance tomography as a means to monitor tissue electroporation for molecular medicine. *IEEE Transactions on Biomedical Engineering,* 49: 400–403, 2002.

Davalos RV, Otten DM, Mir LM, Rubinsky B. Electrical impedance tomography for imaging tissue electroporation. *IEEE Transactions on Biomedical Engineering,* 51: 761–767, 2004.

Davalos R, Mir LM, Rubinsky B. Tissue ablation with irreversible electroporation. *Annals of Biomedical Engineering*, 33: 223-231, 2005.

Denet AR, Vanbever R, Preat V. Skin electroporation for transdermal and topical delivery. *Advanced Drug Delivery Reviews,* 56: 659–674, 2004.

Dev SB, Rabussay DP, Widera G, Hofmann GA. Medical applications of electroporation. *IEEE Transactions on Plasma Science,* 28: 206-223, 2000.

Dev SB, Dhar D, Krassowska W. Electric Field of a Six-Needle Array Electrode Used in Drug and DNA Delivery In Vivo: Analytical Versus Numerical Solution. *IEEE Transactions on Biomedical Engineering,* 50: 1296-1300, 2003.

Fantini F, Gualdi G, Cimitan A, Giannetti A. Metastatic Basal Cell Carcinoma With Squamous Differentiation. *Archives of Dermatology,* 144: 1186-1188, 2008.

Ferber D. Gene therapy: safer and virus-free? *Science,* 294:1638-1642, 2001.

Gabriel B, Teissie J. Direct observation in the millisecond time range of fluorescent molecule asymmetrical interaction with the electropermeabilized cell membrane. *Biophysical journal*, 73: 2630-2637, 1997.

Gehl J, Sorensen TH, Nielsen K, Raskmark P, Nielsen SL, Skovsgaard T, Mir LM. In vivo electroporation of skeletal muscle: Threshold, efficacy and relation to electric field distribution. *Biochimica et Biophysica Acta,* 1428: 233–240, 1999.

Gehl J. Electroporation: theory and methods, perspectives for drug delivery, gene therapy and research. *Acta Physiological Scandinavia,* 177:437-447, 2003.

Golzio M. DNA vaccine by electrotransfer. EBTT workshop 2009, www.cliniporator.com\ect\proceedings, pp. 57, 2009.

Gothelf A, Mir LM, Gehl J. Electrochemotherapy: results of cancer treatment using enhanced delivery of bleomycin by electroporation. *Cancer Treatment Reviews,* 29: 371-387, 2003.

Haemmerich D, Schutt1 DJ, AW Wright, Webster JG, Mahvi DM. Electrical conductivity measurement of excised human metastatic liver tumours before and after thermal ablation. *Physiological Measurement,* 30: 459–466, 2009.

Hamilton WA, Sale AJH. Effects of high electric fields on microorganisms: II. Mechanism and action of the lethal effect. *Biochimica et Biophysica Acta,* 148:789-800, 1967.

Heinz V, Alvarez I, Angersbach A, Knorr D. Preservation of liquid foods by high intensity pulsed electric field - basic concepts for process design. *Trends in food science and technology*, 12, 103-111, 2002.

Heller R, Jaroszeski M, Leo-Messina J, Perrot R, Van Voorhis N, Reintgen D, Gilbert R. Treatment of B16 mouse melanoma with the combination of electropermeabilization and chemotherapy. *Bioelectrochemistry and Bioenergetics* 36: 83-87, 1995.

Heller R, Jaroszeski M, Atkin A, Moradpour D, Gilbert R, Wands J, Nicolau C. In vivo gene electroinjection and expression in rat liver. *Federation of European Biochemical Societies Letters,* 389: 225-228, 1996.

Heller R, Jaroszeski MJ, Reintgen DS, Puleo CA, DeConti RC, Gilbert R, Glass LF. Treatment of cutaneous and subcutaneous tumors with electrochemotherapy using intralesional bleomycin. *Cancer,* 83: 148-157, 1998.

Heller R, Gilbert R, Jaroszeski MJ. Clinical application of electrochemotherapy. *Advanced Drug Delivery Reviews,* 35: 119-129, 1999.

Heller LC, Heller R. *In vivo* electroporation for gene therapy. *Human Gene Therapy,* 17: 890-897, 2006.

Hibino M, Shigemori M, Itoh H, Nagayama K, Kinosita K Jr. Membrane conductance of an electroporated cell analyzed by submicrosecond imaging of transmembrane potential. *Biophysical Journal,* 59: 209-220, 1991.

Hojman P, Zibert JR, Gissel H, Eriksen J, Gehl J. Gene expression profiles in skeletal muscle after gene electrotransfer. *BMC Molecular Biology,* 8: 56, 2007.

Hojman P, Gissel H, Andre F, Cournil-Henrionnet C, Eriksen J, Gehl J, Mir LM. Physiological effects of high and low voltage pulse combinations for gene electrotransfer in muscle. *Human Gene Therapy,* 2008.

Jaroszeski M, Gilbert RA, Heller R. *In vivo* antitumor effects of electrochemotherapy in a hepatoma model. *Biochimica et Biophysica Acta,* 1334: 15-18, 1997.

Jaroszeski M, Illingworth P, Pottinger C, Hyacinthe M, Heller R. Electrically mediated drug delivery for treating subcutaneous and orthotopic pancreatic adenocarcinoma in a hamster model. *Anticancer Research,* 19: 989-994, 1999a.

Jaroszeski M, Gilbert R, Nicolau C, Heller R. *In vivo* gene delivery by electroporation. *Advanced Drug Delivery Reviews* 35:131-137, 1999.

Kanduser M, Miklavcic D. Electroporation in biological cell and tissue: an overview. In Vorobiev E, Lebovka N (eds.), Electrotechnologies for Extraction from Food Plants and Biomaterials, Springer Science, New York, 1-37, 2008.

Kinosita K, Tsong 1979. Voltage induced conductance in human erythrocyte. *Biochimica et Biophysica Acta,* 554: 479-497, 1979.

Kotnik T, Bobanovic F, Miklavcic D. Sensitivity of transmembrane voltage induced by applied electric fields – a theoretical analysis. *Bioelectrochemistry and Bioenergetics,* 43: 285-291, 1997.

Kotnik T. Doctoral thesis: Influence de la dinamique du champ electrique sur l'efficacite de l'electropermeabilisation de la membrane cellulaire, 2000.

Kotnik T, Miklavcic D. Analytical description of transmembrane voltage induced by electric fields on spheroidal cells. *Biophysical Journal,* 79:670-679, 2000a.

Kotnik T, Macek-Lebar A, Miklavčič D, Mir LM. Evaluation of cell membrane electropermeabilization by means of nonpermeant cytotoxic agent. *Biotechniques,* 28: 921-926, 2000b.

Leroy-Willig A, Bureau MF, Scherman D, Carlier PG. *In vivo* NMR imaging evaluation of efficiency and toxicity of gene electrotransfer in rat muscle. *Gene Therapy*, 12: 1434-43, 2005.

Mali B, Jarm T, Corovic S, Paulin-Kosir MS, Cemazar M, Serša G, Miklavcic D. The effect of electroporation pulses on functioning of the heart. *Medical and Biological Engineering and Computing,* 46: 745-757, 2008.

Marty M, Sersa G, Garbay JR, Gehl J, Collins CG, Snoj M, Billard V, Geertsen PF, Larkin JO, Miklavcic D, Pavlovic I, Paulin-Kosir SM, Cemazar M, Morsli N, Soden DM, Rudolf Z, Robert C, O'Sullivan GC, Mir LM. Electrochemotherapy – An easy, highly effective and safe treatment of cutaneous and subcutaneous metastases: Results of ESOPE (European Standard Operating Procedures of Electrochemotherapy) study. *European Journal of Cancer Supplement,* 4: 3-13, 2006.

Mathiesen I. Electropermeabilisation of skeletal muscle enhances gene electrotransfer *in vivo*. *Gene Therapy,* 6: 508-514, 1999.

Mir LM, Banoun H, Paoletti C. Introduction of definite amounts of nonpermeant molecules into living cells after electropermeabilization: direct access to the cytosol. *Experimental Cell Research,* 175: 15-25, 1988.

Mir LM, Orlowski S, Belehradek J, Paoletti C. Electrochemotherapy potentiation of antitumor effect of bleomycin by local electric pulses. *European Journal of Cancer,* 27: 68-72, 1991.

Mir LM, Orlowski S, Belehradek JJr, Teissie J, Rols MP, Sersa G, Miklavcic D, Gilbert R, Heller R. Biomedical applications of electric pulses with special emphasis on antitumor electrochemotherapy. *Bioelectrochemistry,* 38: 203-207, 1995.

Mir LM, Bureau MF, Rangara R, Schwartz B, Scherman D. Long - term, high level *in vivo* gene expression after electric pulse - mediated gene transfer into skeletal muscle. *Medical sciences,* 321:893-899, 1998.

Mir LM, Bureau MF, Gehl, Rangara R, Rouy D, Caillaud JM, Delaere P, Branellec D, Schwartz B, Scherman D. High-efficiency gene transfer into skeletal muscle mediated by electric pulses. *The Proceedings of the National Academy of Sciences Online PNAS*, 74: 4262-4267, 1999.

Mir LM, Moller PH, Andre F, Gehl J. Electric-pulse mediated gene delivery to various animal tissues. *Advances in Genetics*, 83-114, 2005.

Miklavcic D, Beravs K, Semrov D, Cemazar M, Demsar F, Sersa G. The importance of electric field distribution for effective *in vivo* electroporation of tissues. *Biophysical Journal,* 74: 2152-2158, 1998.

Miklavcic D, Semrov D, Mekid H, Mir LM. A validated model of *in vivo* electric field distribution in tissues for electrochemotherapy and for DNA electrotransfer for gene therapy. *Biochimica et Biophysica Acta,*1523: 73-83, 2000.

Miklavcic D, Corovic S, Pucihar G, Pavselj N. Importance of tumour coverage by sufficiently high local electric field for effective electrochemotherapy. *European Journal of Cancer Supplement,* 4: 45-51, 2006a.

Miklavcic D, Pavselj N, Hart FX. Electric Properties of Tissues. Wiley Encyclopedia of Biomedical Engineering, John Wiley & Sons, New York, 2006.

Neumann E, Schaefer-Ridder M, Wang Y, Hofschneider PH. Gene transfer into mouse lyoma cells by electroporation in high electric fields. *European Molecular Biology EMBO Journal*, 1: 841-845, 1982.

Neumann E, Sowers AE, Jordan CA. Electroporation and Electrofusion in Cell Biology. New York: Plenum Press, 1989**.**

Nishi T, Yoshizato K, Yamashiro S, Takeshima H, Sato K, Hamada K, Kitamura I, Yoshimura T, Saya H, Kuratsu JI, Ushio Y. High - efficiency *in vivo* gene transfer using intraarterial plasmid DNA injection following *in vivo* electroporation. *Cancer Research,* 56: 1050-1055, 1996.

Okino M, Mohri H. Effects of a high-voltage electrical impulse and an anticancer drug on in vivo growing tumors. *Japanese Journal of Cancer Research,* 78: 1319-21, 1987.

Pavlovic I, Kramar P, Corovic S, Cukjati D, Miklavcic D. A web-application that extends functionality of medical device for tumor treatment by means of electrochemotherapy. *Radiology and Oncology*, 38: 49-54, 2004.

Pavlovic I, Miklavcic D. Web-based electronic data collection system to support electro-chemotherapy clinical trial. *IEEE Transactions on Information Technology in Biomedicine,* 11: 222-230, 2007.

Pavlovic I, Kern T, Miklavcic D. Comparison of paper-based and electronic data collec-tion process in clinical trials: Costs simulation study. *Contemporary Clinical Trials,* 30: 300-316, 2009.

Pavselj N, Bregar Z, Cukjati D, Batiuskaite D, Mir LM, Miklavcic D. The course of tissue permeabilization studied on a mathematical model of a subcutaneous tumor in small animals. *IEEE Transactions on Biomedical Engineering*, 52: 1373-1381, 2005.

Pavselj N, Miklavcic D. Numerical modeling in electroporation-based biomedical applications. *Radiology and Oncology,* 42: 159-168, 2008.

Pavlin M, Pavselj N, Miklavcic D. Dependence of induced transmembrane potential on cell density, arrangement, and cell position inside a cell system. *IEEE Transactions on Biomedical Engineering*, 49: 605-612, 2002.

Pavlin M, Miklavcic D. Effective conductivity of a suspension of permeabilized cells: a theoretical analysis. *Biophysical Journal*, 85:719–729, 2003.

Perez N, Bigey P, Scherman D, Danos O, Piechaczyk M, Pelegrin M. Regulatable systemic production of monoclonal antibodies by *in vivo* muscle electroporation. *Genetic Vaccines and Therapy*, 2: 2, 2004.

Pliquett U, Langer R, Weaver JC. Changes in the passive electrical properties of human stratum corneum due to electroporation. *Biochimica et Biophysica Acta*, 1239: 111–121, 1995.

Prausnitz MR, Lau BS, Milano CD, Conner S, Langer4 R, Weaver JC. A quantitative study of electroporation showing a plateau in net molecular transport. *Biophysical Journal*, 65: 414-422, 1993.

Prud'homme GJ, Glinka Y, Khan AS, Draghia-Akli R. Electroporation enhanced nonviral gene transfer for the prevention or treatment of immunological, endocrine and neoplastic diseases. *Current Gene Therapy*, 6: 243-273, 2006.

Poddevin B, Orlowski S, Belehradek J, Mir LM. Very high cytotoxicity of bleomycin introduced into the cytosol of cells in culture. *Biochemical Pharmacology,* 42: 67-75, 1991.

Puc M, Kotnik T, Mir LM, Miklavcic D. Quantitative model of small molecules uptake after *in vitro* cell electropermeabilization. *Bioelectrochemistry,* 60: 1-10, 2003.

Puc M, Corovic S, Flisar K, Petkovsek M, Nastran J, Miklavcic D. Techniques of signal generation required for electropermeabilization. Survey of electropermeabilization devices. *Bioelectrochemistry,* 64: 113-124, 2004.

Pucihar G, Kotnik T, Valic B, Miklavcic D. Numerical determination of transmembrane voltage induced on irregularly shaped cells. *Annals of Biomedical Engineering,* 34: 642-652, 2006.

Pucihar G, Kotnik T, Miklavcic D, Teissie J. Kinetics of transmembrane transport of small molecules into electropermeabilized cells. *Biophysical Journal,* 95: 2837-2848, 2008.

Ramirez LH, Orlowski S, An D, Bindoula G, Dzodic R, Ardouin P, Bognel C, Belehradek J, Munck JN, Mir LM. Electrochemotherapy on liver toumors in rabbits. *British Journal of Cancer,* 77: 2104-2111, 1998.

Rebersek M, Cufer T, et al. Electrochemotherapy with cisplatin of cutaneous tumors lesions in breast cancer. *Anticancer drugs*, 15:593-597, 2004.

Rols MP, Teissie J. Ionic-strength modulation of electrically induced permeabilisation and associated fusion mammalian cells. *European Journal of Biochemistry*, 179: 109-115, 1989.

Rols MP, Teissie J. Electropermeabilization of mammalian cells: quantitative analysis of the phenomenon. *Biophysical Journal,* 58: 1089–1098, 1990.

Rols MP, Delteil C, Golzio M, Dumond P, Cros S, Teissié J. *In vivo* electrically mediated protein and gene transfer in murine melanoma. *Nature Biotechnology,* 16: 168-171, 1998.

Rols MP, Bachaud JM, Giraud P, Chevreau C, Roche H, Teissie J. Electrochemotherapy of cutaneous metastases in malignant melanoma. *Melanoma Research,* 10: 468-474, 2000.

Rodriguez-Cuevas S, Barroso-Bravo S, Almanza-Estrada J, Cristobal-Martinez L, Gonzales-Rodriguez E. Electrochemotherapy in primary and metastatic skin tumors: Phase II trial using intralesional bleomycin. *Archives of Medical Research*, 32: 273-276, 2001.

Rudolf Z, Stabuc B, Cemazar M, Miklavcic D, Vodovnik L, and Sersa G. Electrochemotherapy with bleomycin: the first clinical experience in malignant melanoma patients. *Radiology and Oncology,* 29: 229 –235, 1995.

Sale AJH, Hamilton WA. Effects of high electric fields on microorganisms: I. Killing of bacteria and yeasts. *Biochimica et Biophysica Acta,* 148: 781-788, 1967.

Sale AJH, Hamilton WA. Effects of high electric fields on microorganisms: III. Lysis of erythrocytes and protoplasts. *Biochimica et Biophysica Acta,* 163:37-43, 1968.

Salford LG, Persson RBR, Brun A, Ceberg CP, Kongstad PC, Mir LM. A new brain tumor therapy combining bleomycin with in vivo electropermeabilisation. *Biochemical and Biophysical Research Communications,* 194: 938-943, 1993.

Sampedro F, Rivas A, Rodrigo A, Martinez A, Rodrigo M. Pulsed electric fields inactivation of Lactobacilus plantarum in an orange juice – milk based beverage: Effect of process parameters. *Journal of Food Engineering*, 80: 931-938, 2007.

Schwan HP, Kay CF: The conductivity of living tissues. *Annals of the New York Academy of Sciences*, 65: 1007, 1957.

Sel D, Cukjati D, Batiuskaite D, Slivnik T, Mir LM, Miklavcic D. Sequential finite element model of tissue electropermeabilization. *IEEE Transactions on Biomedical Engineering*, 52: 816-827, 2005.

Semrov D, Miklavcic D. Numerical Modelling for In Vivo Electroporation. *Methods in Molecular Medicine*, 37:63-81, 2000.

Sersa G, Cemazar M, Miklavcic D. Antitumor effectivness of electrochemotherapy with cis-diamminedichloroplatinium (II) in mice. *Cancer Research,* 55: 3450-3455, 1995.

Sersa G, Cemazar M, Parkins CS, Chaplin DJ. Tumour blood flow changes induced by application of electric pulses. *European Journal of Cancer,* 35: 672-677, 1999.

Sersa G, Cemazar M, Rudolf Z. Electrochemotherapy: advantages and drawbacks in treatment of cancer patients. *Cancer Therapy,* 1: 133-142, 2003.

Sersa G and Miklavcic D. Electrochemotherapy of Tumours. Jorunal of Visualized Experiments. JoVE. 22. 2008. http://www.jove.com/index/Details.stp?ID=1038, doi: 10.3791/1038].

Sixou S, Teissie J. Exogenous uptake and release of molecules by electroloaded cells: a digitized videomicroscopy study. *Bioelectrochemistry and Bioenergetics,* 31: 237-257, 1993.

Snoj M, Rudolf Z, Cemazar M, Jancar B, Sersa G. Succsessful sphincter-saving treatment of anorectal malignant melanoma with electrochemotherapy, local excision and adjuvant brachytherapy. *Anti-Cancer Drugs*, 16: 345-348, 2005.

Snoj M, Cemazar M, et al. Limb sparing treatment of bleeding melanoma recurrence by electrochemotherapy. *Tumori,* 95: 398-402, 2009.

Sinigoj AR, Elektromagnetno polje, Zalozba Fakultete za elektrotehniko, Ljubljana, Slovenia, 1996.

Susil R., Šemrov D., Miklavčič D.; Electric field induced transmembrane potential depends on cell density and organization; *Electro and Magnetobiology,* 17:391-399, 1998.

Smith SR, Foster KR, Wolf GL. Dielectric properties of VX-2 carcinoma versus normal liver tissue. *IEEE Transactions on Biomedical Engineering*, 33: 522–524, 1986.

Surowiec AJ, Stuchly S, Barr JR, Swarp A. Dielectric properties of breast carcinoma and the surrounding tissues. *IEEE Transactions on Biomedical Engineering*, 35:257–263, 1988.

Suzuki T, Shin B, Fujikura K, Matsuaki T, Takata K. Direct gene transfer into rat liver cells by in vivo electro oration. *Federation of European Biochemical Societies FEBS Letters,* 425: 436-440, 1998.

Teissie J, Rols MP. An experimental evaluation of the critical potential difference inducing cell membrane electropermeabilization. *Biophysical Journal,* 65: 409-413, 1993.

Teissie J, Eynard N, Vernhes MC, Benichou A, Ganeva V, Galutzov B, Cabanes PA. Recent biotechnological developments of electropulsation: A prospective review. *Bioelectrochemistry,* 55: 107–112, 2002.

Tevz G, Pavlin D, Kamensek U, Kranjc S, Mesojednik S, Coer A, Sersa G, Cemazar M. Gene Electrotransfer into Murine Skeletal Muscle: A Systematic Analysis of Parameters for Long-term Gene Expression. *Technology in Cancer Research and Treatment*, 7, 2: 91-154, 2008.

Titomirov AV, Sukharev S, Kistanova E. *In vivo* electroporation and stable transformation of skin cells of newborn mice by plasmid DNA. *Biochimica et biophysica acta*, 1088: 131-134, 1991.

Tsong TY. Electroporation of cell membranes. *Biophysical Journal,* 60:297–306, 1991.

Quaglino P, Mortera C, Osella-Abate S, Barberis M, Illengo M, Rissone M, Savoia P, Bernengo MG. Electrochemotherapy with Intravenous Bleomycin in the Local Treatment of Skin Melanoma Metastases. *Annals of Surgical Oncology*, Online, 2008.

Umeda Y, Marui T, Matsuno Y, Shirahashi K, Iwata H, Takagi H, Matsumoto K, Nakamura T, Kosugi A, Mori Y, Takemura H. Skeletal muscle targeting in vivo electroporation-mediated HGF gene therapy of bleomycin-induced pulmonary fibrosis in mice. *Laboratory investigation*, 84: 836-844, 2004.

Valic B, Golzio M, Pavlin M, Schatz A, Faurie C, Gabriel B, Teissie J, Rols MP, Miklavcic D. Effect of electric field induced transmembrane potential on spheroidal cells: theory and experiments. *European Biophysics Journal,* 32: 519–528. 2003.

William TJ, Zhang Y, Li C, Jirtle RL. The measured properties of normal and malignant human tissues from 50 to 900 MHz. *Medical Physics*, 21: 4–7, 1994.

Weaver JC, Chizmadzhev YA: Theory of electroporation: A review. *Bioelectrochemistry and Bioenergetics,* 41:135-60, 1996.

Zimmerman U, Pilwat G, Reimann F. Dielectric breakdown of cell membranes. *Biophysical Journal*, 14 881-899, 1974.

Zimermann U. Electric field-mediated fusion and related electrical phenomena. *Biochimica et biophysica acta*, 694:227-277, 1982.

Zupanic A, Corovic S, Miklavcic D. Optimization of electrode position and electric pulse amplitude in electrochemotherapy. *Radiology and Oncology,* 42: 93-101, 2008.

Web links:

http://en.wikipedia.org/wiki/File:BreastCancer.jpg

http://igea.it

http://clinicaltrials.gov

http://cliniporator.com\ect\proceedings

5. Original contributions to the scientific area

Based on results in this doctoral dissertation I claim for the recognition of the following original scientific contributions to the research area:

- We developed 3D realistic numerical model of cutaneous tumor and demonstrated the influence of contact surface between electrodes and treated tissue for electrochemotherapy outcome of cutaneous tumors. The larger the contact surfaces the more homogeneous the local electric field in the target tissue and the better treatment outcome. These results can significantly contribute to more efficient and safe electrochemotherapy of protruding cutaneous tumors and can be used as a protocol for the positioning of plate electrodes on the treated tissue. Our suggestion can prevent painful sensations due to electric field penetration deeper than necessary while more precisely targeting the tumor and avoiding damages in the surrounding healthy tissue.

- Based on calculation and visualization of local electric field distribution in our 3D numerical models we conclude that the treated tissue (e.g. tumour) is to be positioned well in-between the electrodes. The electrodes should thus fit the size of the tumour for good coverage of tumor tissue with sufficiently high electric field. Plate electrodes which are noninvasive are better suited for tumours on the surface on the skin, whereas needle electrodes which are used invasively with appropriate and sufficient depth of their insertion are more appropriate for treating tumours seeded deeper in the skin.

- We systematically compared and quantified the local electric field distribution in tissue model for different electrode configurations used in research and clinics in the past years.

Based on our analytical (in 2D) and numerical models (in both 2D and 3D) we calculated and visualized the local electric field distribution for the electrode configurations used. We have shown that the electric parameters (such as amplitude of the voltage applied, electrode geometry and position with respect to the target tissue, electrode number, distance between electrodes and depth of electrode insertion) need to be chosen specifically for each individual case of treated tissue and are relevant parameters for an optimization procedure. Realistic numerical modeling of the local electric field distribution can be used to optimize the appropriate electrode configuration and adequate voltage for each individual case of target tissue (taking into account its geometry, position and electric properties) in order to predict optimal level of permeabilization. Selection of suitable electric parameters based on calculation and visualization of local electric field distribution in realistic numerical models is thus a step forward towards the treatment and experiment planning in the electroporation-based therapies.

 - We have shown that numerical calculation and visualization of local electric field distribution in 3D can be successfully used in electrode design for *in vitro* and *in vivo* settings for prediction of the needed permeabilization level of the treated sample. The results obtained with our numerical modeling support design of new electrodes for *in vitro* gene electrotransfection integrated into the new system allowing for automatic changing of electric field direction. The new system can be used in *in vitro* gene electrotransfer to improve cell transfection by changing electric field direction between electrical pulses, without affecting cell survival. The results of our numerical modeling were useful in development and testing of the new multiple electrode commutation circuit, suggested for *in vivo* electrochemotherapy of larger tumors. Electrochemotherapy, performed by multiple needle electrodes and validated pulses sequence on large subcutaneous murine tumours resulted in tumour growth delay and

57% complete responses, thus demonstrating that the tested electrode commutation sequence is efficient**.**

- We developed 3D realistic models of muscle tissue and determined electroporation thresholds for muscle for two different orientations of electric field with respect to the muscle fibers: parallel and perpendicular. We present the first results of different electroporation thresholds with respect to electrode vs. tissue orientation for skeletal muscle. The determination of local electric field thresholds for electroporation enables control of the muscle tissue level electroporation and can be used to predict the optimal window for gene electrotransfer. These results carry important information for defining protocols (i.e. selection of suitable electrical parameters) needed for successful gene electrotransfer, which can facilitate the translation of gene therapy and genetic vaccination into the clinical practice.

The findings of our study on muscle tissue carry important practical information for further development of gene electrotransfer into the muscle, and subsequently for development of local and systemic gene therapy and genetic vaccination. Since the electroporation based gene therapy and vaccination are cost-effective and easily implementable methods of administration they can be useful for treatment of chronic diseases where patients must be treated for years of even for their whole lifetime. Translation of these two methods into clinical settings might potentially be of great help in developing countries also for treatment of severe viral diseases such as HIV or HCV and malaria infections.

- We developed realistic numerical models of skeletal muscle tissue electroporated directly and transcutaneously in order to investigate influence of skin on muscle electroporation. The same electroporation threshold values E_{rev} and E_{irrev} were found for both muscle electroporated directly (i.e. with skin removed) and transcutaneously (i.e. skin present). We

thus conclude that the skin layer has, no influence on the thresholds of the local electric field intensity itself needed for successful muscle tissue electroporation, but it does require higher voltage to be applied between the electrodes when muscle is electroporated transcutaneously. In addition to gene electrotransfer, our study can be of interest also for the planning of clinical electrochemotherapy of cutaneous and subsutaneous tumors and transdermal drug and gene delivery, since it provides knowledge on sensitivity of underlying muscle tissue to the electroporation procedure.

- Based on our numerical models we proposed safe protocols (i.e. taking into account critical depth of insertion and distance between electrodes for needle and plate configurations and voltage amplitudes currently used in clinical electrochemoterapy for cutaneous and subcutaneous tumors) in order to avoid fibrillation and reversible and irreversible electroporation of cardiac muscle. However for internal (orthotopic) tumors located close to the heart, safe and precise electrochemotherapy requires treatment planning that includes optimization of the electrodes and voltages applied.

- We also showed that the error of an approximate estimation of electroporation threshold values in *in vivo* experiments by calculating the *U/d* ratio, without numerical calculations of local electric field distribution, is small enough only if the plate electrodes are used and only for a single type of tissue placed between the electrodes. For more complex tissues with different geometric and electrical properties, a combination of realistic numerical modeling and *in vivo* experiments needs to be used for the precise determination of electroporation threshold values.

- We developed an e-learning application on electroporation based therapies and treatments. The presented e-learning application provides an easy and rapid approach for information, knowledge and experience exchange among the experts from different scientific fields, which can facilitate development and optimization of electroporation based therapies and treatments.

Declaration

The author herewith declares that the content of the thesis is a result of her own research work supervised by supervisors prof. Damijan Miklavcic Ph.D and Lluis M. Mir, Ph.D. The results which were done in collaboration with other colleagues are published in presented papers; other assistance from colleagues is stated in the acknowledgments. The published results of other authors are presented in the literature.

Selma Corovic

◆ Résumé de la thèse en français

**Modélisation et visualisation de l'électroperméabilisation
dans des tissues biologiques exposés aux impulsions électriques d'haute voltage**

L'efficacité des traitements médicaux, tel que électrochimiothérapie et la thérapie génique non-virale par électrotransfer d'ADN, est due à l'électroperméabilisation des cellules constituant le tissue ciblé par un champ électrique local d'intensité supérieure à une valeur seuil réversible. Une cellule électropermeabilisée est ainsi plus sensible à un médicament cytotoxique (e.g. la bléomycine) aussi bien qu'aux molécules de l'ADN. La première partie de la thèse s'est intéressée aux modèles mathématiques des tissues ciblés afin de visualiser la distribution du champ électrique local par des simulations numériques, ce qui permet d'optimiser le choix du type d'électrodes à utiliser et l'amplitude du voltage à appliquer de telle sorte qu'une thérapie basée sur l'électroperméabilisation soit la plus efficace possible. La deuxième partie expérimentale a consisté à valider les modelés mathématiques par des expériences in vivo chez les animaux. La dernière troisième partie de la thèse concerne le développement d'une application internet pour la formation à distance sur les mécanismes de l'électroperméabilisation au niveau des cellules et des tissus.
Mots clés: Electroporation, électroperméabilisation, impulsions électriques, modélisation mathématique, expériences in vivo, muscle, tumeur

◆ Résumé de la thèse en anglais

Modeling and visualization of electropermeabilization of biological tissues exposed to high-voltage electric pulses

In vivo electroporation is used as an effective and safe tool for administration of a variety of extracellular agents such as chemotherapeutic drugs (e.g. bleomycin), DNA or other molecules, which in normal conditions do not cross the cell membrane, into many different target tissue cells. The main focus of the present doctoral theses is the analysis of *in vivo* electroporation and corresponding local electric field distribution used in electrochemotherapy and electroporation based gene therapy and vaccination. The aims of this doctoral thesis cover three important issues in the development of electroporation based technologies and treatments: development of realistic numerical models of different tissues (i.e. muscle, tumor and skin) and calculations and visualization of local electric field distribution in the models; validation of the realistic numerical models by in vivo experiments and development of a web-based interactive e-learning application on electroporation of cells and tissues and on electroporation based therapies and treatments. (e.g. clinical electrochemotherapy of tumors and gene electrotransfer).
Key words: Electroporation, electropermeabilisation, electrical pulses, mathematical modeling, in vivo experiments, muscle, tumor

◆ Le nom du laboratoire de rattachement

Laboratoire de Vectorologie et Thérapeutiques Anticancéreuses
UMR 8203 CNRS Université Paris-Sud
Institut Gustave-Roussy
114 rue Edouard Vaillant
94805 VILLEJUIF Cédex FRANCE

PÔLE : PHARMACOTECHNIE ET PHYSICO-CHIMIE

UNIVERSITÉ PARIS-SUD 11
UFR «FACULTÉ DE PHARMACIE DE CHATENAY-MALABRY »
5, rue Jean Baptiste Clément
92296 CHÂTENAY-MALABRY Cedex FRANCE